A Study of Novel Ferrocenyl-Phosphorus Compounds

The University of Waikato
Te Whare Wānanga o Waikato

A thesis
submitted in partial fulfilment
of the requirements for the degree of

Doctor of Philosophy in Chemistry

at the
University of Waikato
by

Nicholas James Goodwin

University of Waikato
1998

It is the glory of God to conceal a matter;
to search out a matter is the glory of kings.

- Solomon

...since the creation of the world God's invisible qualities - his eternal power and divine nature - have been clearly seen, being understood from what has been made...

- St Paul

Abstract

The intent of this investigation was to use the distinctive characteristics of hydroxymethylphosphine chemistry in order to create new ferrocenyl-phosphorus compounds, as well as carry out investigations into both their electrochemistry and their potential for the production of ferrocene-containing polymers.

The compound $FcCH_2P(CH_2OH)_2$ **1** (Fc = ferrocenyl) was prepared by the reaction of $P(CH_2OH)_3$ with $[FcCH_2NMe_3]I$, and $FcCH_2PPh_2$ **2** was prepared by a similar reaction. The compounds $FcCH_2P(O)(CH_2OH)_2$ **3**, $FcCH_2P(S)(CH_2OH)_2$ **4**, $FcCH_2P(CH_2CH_2CN)_2$ **5**, $FcCH_2P(CH_2NEt_2)_2$ **6**, $FcCH_2P(O)(CH_2NEt_2)_2$ **7**, $[FcCH_2P(Me)(CH_2OH)_2]I$ **8**, $FcCH_2P(Me)CH_2OH$ **9**, $[(FcCH_2)_2P(CH_2OH)_2]Cl$ **10**, $(FcCH_2)_2PCH_2OH$ **11**, $FcCH_2P(H)PPh_2$ **14** and $FcCH_2P(O)PPh_2$ **15** were prepared and characterised, and the compounds $[FcCH_2P(Bz)(CH_2OH)_2]Br$ (Bz = benzyl) **12** and $FcCH_2P(Bz)CH_2OH$ **13** were investigated though not fully characterised. The ferrocenylphosphine complexes *cis*-$PtCl_2[FcCH_2P(CH_2OH)_2]_2$ **16**, $PdCl_2[FcCH_2P(CH_2OH)_2]_2$ **17**, $[Au\{FcCH_2P(CH_2OH)_2\}_2]Cl$ **18**, $RuCl_2(\eta^6\text{-}C_{10}H_{14})[FcCH_2P(CH_2OH)_2]$ **19** and $RuCl_2(\eta^6\text{-}C_{10}H_{14})(FcCH_2PPh_2)$ **20** were also prepared. X-ray crystal structure determinations were carried out for the compounds **1**, **2**, **4**, **8**, **18** and **20**, and the solid-state hydrogen-bonding interactions present in the case of **1**, **4**, **8** and **18** were deduced.

Hydrogen-bonding in the crystal structures of compounds $Ph_2P(O)CH_2OH$ **21**, $Ph_2P(S)CH_2OH$ **22** and $Ph_2P(Se)CH_2OH$ **23** was also investigated. Results were explained in terms of the positioning of hydrogen bonds in line with the direction of lone-pairs on the phosphine chalcogenide heteroatoms

The reaction of **1** with sodium metabisulfite in varying amounts was used to produce the compounds $FcCH_2PH_2$ **24**, $FcCH_2P(H)CH_2OH$ **25** and $FcCH_2P(O)(OH)CH_2OH$ **26**. The primary phosphine **24** was found to be remarkably air-stable, and was used to prepare the

complexes $Mo(CO)_5(FcCH_2PH_2)$ **27**, $Mo(CO)_4(FcCH_2PH_2)_2$ **28**, $RuCl_2(\eta^6\text{-}C_{10}H_{14})(FcCH_2PH_2)$ **29**, $Ru_3(\mu^2\text{-}H)_2(CO)_9(\mu^3\text{-}PCH_2Fc)$ **30** and $Ru_4(CO)_{10}(\mu^2\text{-}CO)(\mu^3\text{-}PCH_2Fc)_2$ **31**. Confirmation of the structures of **24**, **27**, **28** and **30** was obtained using X-ray crystallography.

Cyclic voltammetric analysis of the electrochemical behaviour of **1**, **2**, **5**, **24**, **25** and $FcCH(Me)P(CH_2OH)_2$ **32** showed that these compounds exhibit a reversible one-electron oxidation followed by a chemical reaction, which leads to formation of a product which undergoes another reversible one-electron oxidation at higher potential. The rate-determining step for the reaction is intermolecular. BE (bulk electrolysis) of **1**, **2** and **5** gave similar results in each case, with one-electron oxidation appearing to initially oxidise the ferrocene centre; in the case of **2** and **5** a green colour characteristic of ferrocenium species is seen during BE, but disappears with time. The conclusion was reached that this initial ferrocenium charge is transferred to another part of the molecule. Evidence from NMR and electrospray mass spectrometric analysis of BE products for **1** and **2** suggests the formation of unusual dimeric species is the end result of oxidation. The ferrocenylphosphine **11** shows simpler electrochemical behaviour consistent with previous literature. Compounds **3**, **4**, **8**, **10**, **14**, **15**, **16**, **17**, **18** and **30** showed very simple electrochemical behaviour consistent with one chemically and electrochemically reversible ferrocene redox couple. Cyclic voltammetry of the complexes **19**, **20** and **29** showed both ferrocene and ruthenium redox processes. The electrochemistry of **7** was complex and not intensively investigated.

Reaction of **1** with multi-functional secondary amines was used to produce a number of polymeric materials which were investigated using cyclic voltammetry of DMF solutions, carbon paste electrodes and drop-coated electrodes. Attempts to covalently bind one of these polymers to a glassy carbon electrode were unsuccessful. The most electrochemically stable form of electrode investigated was the carbon paste electrode, although the materials did not appear to show great promise for use in such applications, due to irreversible chemical changes in the polymers and quick decay of the ferrocene redox signal upon subjection to cyclic voltammetry.

Acknowledgements

My undertaking to study towards a doctoral degree would naturally have foundered and come to a sorry end long ago, if I had needed to rely solely on my own very limited abilities and resources. For this reason I wish to acknowledge and thank a number of people who have provided valuable assistance during this period.

Firstly I must thank my dear wife, who allowed me the opportunity, supported me financially, drew the cyclic voltammograms, and has acted in the capacity of a full-time domestic servant for the last several months as I have laboured to put 'pen to paper'. Jo, I considered dedicating this Thesis to you; as you can see, I have not, because you deserve better than that rather dubious honour!

By giving first mention to the efforts of my spouse I in no way want to detract from the credit which should also be given to those who have helped me academically. I would like to thank my supervisor Bill Henderson for his enthusiasm, endless ideas, and direction in my research. Brian Nicholson patiently taught me what little I have grasped concerning X-ray crystallography; Allen Oliver was also helpful in this area, and consented to look over the crystallographic details contained in this work. Special praise must be given to the efforts of Alison Downard of the University of Canterbury, who taught me about electrochemistry, advised me on my ideas, did a considerable amount of work on my behalf, and read through Chapters 5 and 6 of this Thesis. She has in effect served as another very valuable supervisor, for little gain to herself. My co-workers in the lab have provided ideas from time to time, as well as inspiring me with their competence and practicality, which I often envy. The work of Steve Alley, who kindly consented to do the proof-reading, is gratefully acknowledged. Thanks also to Peter Boyd of the University of Auckland for an invitation to use electrochemical equipment, as well as to Cliff Rickard of the University of Auckland, Ward Robinson of the University of Canterbury, and John Fawcett of the University of Leicester, for collection of X-ray crystal data sets.

Financial assistance was provided through scholarships by both the University of Waikato and the William Georgetti Trust, and was greatly appreciated.

Contents

List of Figures

List of Schemes

List of Tables

List of Abbreviations and Symbols

Å	Angstrom	A	electrode surface area
AA	atomic absorption	Ac	acetyl
AE	auxiliary electrode	An	aniline
av.	average	B.P.	boiling point
BE	bulk electrolysis	bipy	bipyridine
BPPFA	*N*,*N*-dimethyl-1-[-2,2'-bis-(diphenylphosphino)ferrocenyl]-ethylamine	br	broad
Bu	butyl	Bz	benzyl
C	Celsius or Coulomb	CCDC	Cambridge Crystallographic Data Centre
CEP	tris(2-cyanoethyl)phosphine	COD	1,5-cyclo-octadiene
Cp	cyclopentadienyl, or substituted cyclopentadienyl	Cp*	pentamethylcyclopentadienyl ligand
CSD	Cambridge Structural Database	CV	cyclic voltammogram
Cy	cyclohexyl	Cym	cymene
δ	chemical shift	d	doublet
dba	*trans*,*trans*-dibenzylidene-acetone	DDQ	2,3-dichloro-5,6-dicyanoquinone
dec.	decomposed	ΔE_P	peak potential difference
Δi	change in current	DIOP	2,3-*O*-isopropylidene-2,3-dihydroxy-1,4-bis-(diphenylphosphino)butane
DMF	N,N'-dimethylformamide	DMSO	dimethylsulfoxide
D_O	diffusion coefficient for O	dpmf	1,1'-bis(diphenyl-phosphinomethyl)ferrocene

dppf	1,1'bis(diphenyl-phosphino)ferrocene	D_R	diffusion coefficient for R
E	applied potential	$E_{(P/2)A}$	anodic half-peak potential
$E_{(P/2)C}$	cathodic half-peak potential	$E_{1/2}$	half-wave potential
E_f	final potential	E_i	initial potential
E_λ	switching potential	E_{PA}	anodic peak potential
E_{PC}	cathodic peak potential	E°'	formal redox potential
fac	facial	FAD	flavin adenine dinucleotide
Fc	ferrocenyl	FMN	flavin mononucleotide
g	gram	GC	glassy carbon
GC-MS	gas chromatography-mass spectrometry	hept.	heptet
HOMO	highest occupied molecular orbital	HPLC	high performance liquid chromatography
hr	hour	Hz	Hertz
i	*ipso* or *iso*	i_{APP}	applied current
IC_{50}	concentration required to kill 50% of population	i_{PA}	anodic peak current
i_{PC}	cathodic peak current	IR	infra-red
J	coupling constant	Josiphos	2-[-1-(diphenylphosphino)-ethyl]-1-(diphenylphosphino)-ferrocene
K	rate constant	k_b	reverse rate constant
k_f	forward rate constant	l or L	litre
m	*meta*	m	metre, medium (IR), or multiplet (NMR)
M	molar	m	moles of analyte in solution
M.P.	melting point	*m/z*	mass to charge ratio
Me_2Hpz	dimethylpyrazole	Mes*	supermesityl
min	minute	mol	mole

M_r	molecular weight	*n*	straight chain
NADP	nicotinamide adenine dinucleotide phosphate	NADPH	reduced NADP
NMR	nuclear magnetic resonance	*o*	*ortho*
OTf	$CF_3SO_3^-$	*p*	*para*
Ph	phenyl	phosferrox	phosphinoferrocenyl-oxazoline
PPFA	*N*,*N*-dimethyl-1-[-2-(diphenylphosphino)-ferrocenyl]ethylamine	ppm	parts per million
Pr	propyl	PTFA	cyclopentadienyl(7-dimethyl-amino-1-diphenyl-phosphino-4,5,6,7-tetrahydroindenyl) iron
Q	total charge passed	*R*	*rectus*
rac	racemic (c.f. *meso*)	Rc	ruthenocene
RDS	rate-determining step	RE	reference electrode
R_f	retention factor	s	singlet (NMR) or strong (IR)
S	*sinister*	sat.	saturated
SCE	saturated calomel electrode	*sec*	secondary
soln.	solution	solv	coordinated solvent
t	tertiary	t	triplet (NMR) or time (electrochemistry)
THF	tetrahydrofuran	tlc	thin-layer chromatography
Tol	tolyl	TPA	1,3,5-triaza-7-phosphaadamantane
TRAP	2,2"-bis[1-(diGRPphosphino)-ethyl]-1,1"-biferrocene, GRP = alkyl/aryl	unres.	unresolved
UV	ultraviolet	UV-vis	ultraviolet-visible

v	scan rate	V	Volt
w	weak	w/w	weight/weight
WE	working electrode	x	fraction of species reacted by bulk electrolysis

Chapter 1: Ferrocenylphosphines; A Literature Review

The work described in this thesis is principally concerned with research into novel ferrocenylphosphine compounds. This review has therefore been structured so as to provide an overview of the main areas of interest with respect to research into these compounds. Two principal reasons probably account for the majority of work carried out with ferrocenylphosphine compounds to date: one is the utility of 1,1'-bis(diphenylphosphino)ferrocene (dppf) as a bidentate phosphine ligand; the other is the role both dppf and planar chiral ferrocenylphosphines have played in the development of transition metal-catalysed reactions. As well as giving consideration to both these areas, the present Chapter describes the miscellany of other ferrocenylphosphines which have been reported.

1.1 Chemistry of 1,1'-Bis(diphenylphosphino)-ferrocene (dppf)

First synthesised in 1965[1], the chemistry of dppf has since been extensively developed. Much information can be found in a recent comprehensive review, which discusses preparative techniques, coordination chemistry, spectroscopic characterisation and catalysis, among other things[2]. The information presented here therefore draws principally on the literature from 1995 onwards for examples, though it should be noted that the general ideas which drive research into this ligand were formulated earlier.

1.1.1 Coordination Modes of Dppf

One aspect of dppf chemistry making it a useful ligand is its coordinative flexibility. Most usually dppf will form chelating complexes, and it is able to stabilise a variety of coordination numbers at the metal centre. For instance, a complex of low coordination number is obtained by addition of dppf, followed by PPh_3, to a solution of $AgClO_4$[3]. This leads to formation of the trigonal planar compound $[Ag(PPh_3)(dppf)]ClO_4$ **1**[¥]. Synthesis of complexes of even lower coordination number, where dppf is the only ligand for a two-coordinate metal centre, appear to be impracticable since the geometry of the ligand precludes such linear *trans*-coordination without bringing the metal atom within bonding distance of the ferrocenyl iron atom. Of course, two-coordinate complexes are possible where dppf acts as a bridging ligand, but such situations will be discussed later.

Four-coordinate square-planar complexes of dppf are well-known, and are important in catalysis. Recently reported examples include the anthracenyl-containing $PdBr(C_{14}H_9)(dppf)$ **2**[4] (the 10-chloroanthracene derivative was also isolated), pentafluorophenyl derivatives $Pt(C_6F_5)_2(dppf)$ **3**, $Pd(C_6F_5)_2(dppf)$, $Pt(C_6F_5)Cl(dppf)$ and $Pd(C_6F_5)Br(dppf)$[5], $Pt(C_6H_5)_2(dppf)$ and $PtI_2(dppf)$[6], Pd(dba)(dppf) (dba = *trans,trans*-dibenzylidene-acetone)[7] and $M(dppf)_2$ (M = Pt, Pd)[8]. The compound $Pt(C_{18}H_8)(dppf)$ **4** was prepared in order to investigate the chemistry of the trialkyne 'pocket'[9]. A more complex permutation of these Group 10 square-planar complexes is $Ag_2Pd_2Cl_2(dppf)_2(\mu^3\text{-}S)_2$ **5**, a tetranuclear complex with bridging sulfur atoms[10]. A very similar compound, $[Pt_2Tl(dppf)_2(\mu^3\text{-}S)_2]NO_3$, can be prepared by reaction of $Pt_2(dppf)_2(\mu^3\text{-}S)_2$[11] with $TlNO_3$, and metathesised to give the PF_6 salt **6**[12]. The compound $Pt_2(\mu^2\text{-}H)(\mu^2\text{-}CHCH_2Ar)(dppf)_2$ **7** (Ar = *p*-methoxyphenyl) also displays bridging of two group 10 metals, and was prepared by a variety of routes, one of which involved formation of $[Pt(H)(dppf)]_2$ as a transient species[13]. Such square-planar dppf

[¥] Numbers are used to denote those compounds graphically represented in this introductory Chapter, but compound numbers used throughout the rest of this thesis start anew in Chapter 2, and are unrelated to those given here.

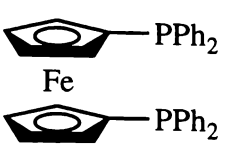

dppf

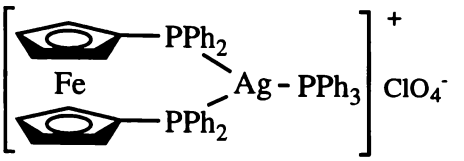

1

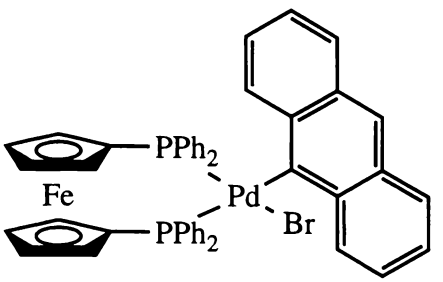

2

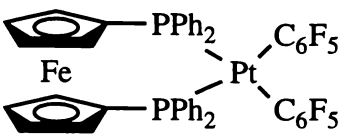

3

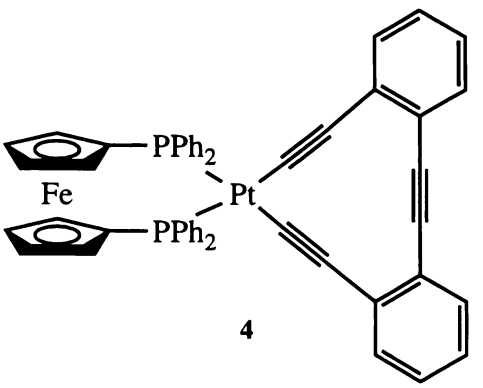

4

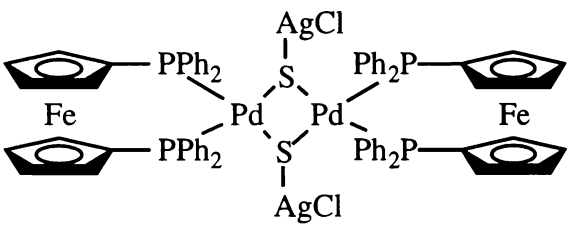

5

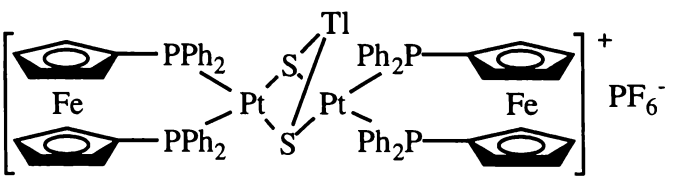

6

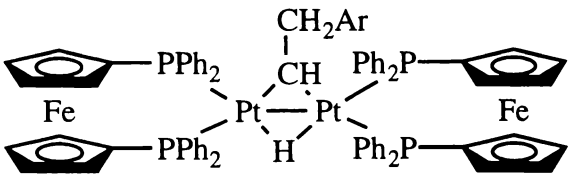

7

complexes have been put to use in molecular architecture, with the building of the square metallomacrocycles **8** and **9** by combination of the reactive aqua complexes $[M(H_2O)_2(dppf)][OTf]_2$ (M = Pd, Pt, OTf = $CF_3SO_3^-$) with 2,7-diazapyrene[14]. The same report describes the synthesis of similar molecular squares by reaction of the aqua complexes with the dog-leg molecule bis-[4-(4'-pyridyl)phenyl]iodonium triflate. The ability of dppf to stabilise four-coordinate complexes extends to tetrahedral complexes, such as $HgCl_2(dppf)$, for which the crystal structure was recently reported[15], though the compound has long been known[16]. The dimeric compounds $[Cu(\mu\text{-}X)(dppf)]_2$ (X = NO_3, O_2CH, I **10**), in which the copper occupies a tetrahedral environment, are also known[17]. Several Ru(II) piano-stool complexes of the general formula $[RuXCp^*(dppf)]^{n+}$ (where X may be anionic or neutral, n = 0 or 1, Cp* = pentamethylcyclopentadienyl ligand) have been reported[18], including Ru(H)Cp*(dppf) **11**[19]. Compound **11** was initially synthesised as a model for biological systems in which H_2 is used to perform one-electron reductions, and it was found to be a unique catalyst for one-electron reductions of ferrocene and methylviologen with H_2, and to be a catalyst for other reactions also. More will be said about the catalytic abilities of **11** later.

The same workers also reported the formation of the Ru(IV) pentavalent complexes $[Ru(H)XCp^*(dppf)]PF_6$ (X = Cl, Br, I[19a]; H[19b]), derived from **11**. Although no crystal structures were reported, these are presumably trigonal bipyramidal structures[20], as is the case with another group 8 compound, $Fe(CO)_3(dppf)$ **12**[21].

Octahedral complexes of dppf are common, and a number of recent examples have been reported. Many of these involve Ru(II): the compounds $RuCl(H)(CO)(dppf)PPh_3$, $[Ru(H)(CO)(dppf)(L)PPh_3]PF_6$ (L = pyridine or acetonitrile), $RuCl(CH{=}CHR)(CO)(dppf)PPh_3$ (R = CMe_3 **13**, *p*-MeC_6H_4), $RuCl(CH{=}CHR)(CO)(dppf)Me_2Hpz$ (R = CMe_3, *p*-MeC_6H_4, Me_2Hpz = dimethylpyrazole), $RuCl(C{\equiv}CR)(CO)(dppf)PPh_3$ (R = CMe_3, *p*-MeC_6H_4) and $RuCl[C{\equiv}C\text{-}p\text{-}MeC_6H_4)](CO)(dppf)Me_2Hpz$ have only one octahedral centre; two linked octahedra are seen in the compounds $Ru_2(CH{=}CH\text{-}p\text{-}C_6H_4CH{=}CH)Cl_2(CO)_2(dppf)_2(PPh_3)_2$ **14** and $Ru_2(C{\equiv}C\text{-}$

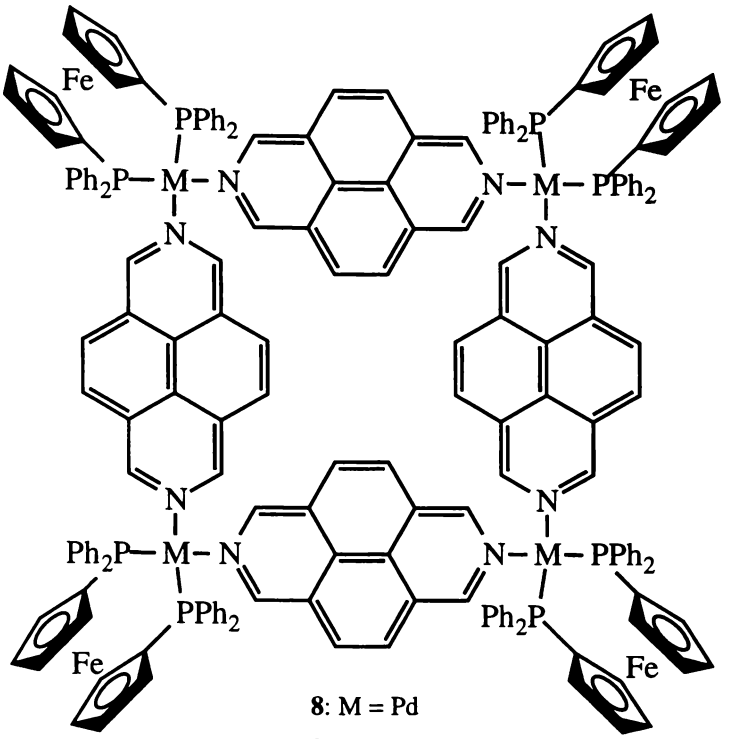

8: M = Pd
9: M = Pt

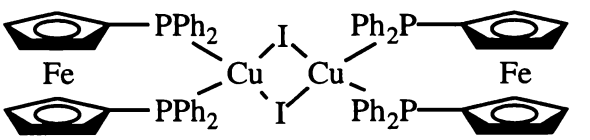

10

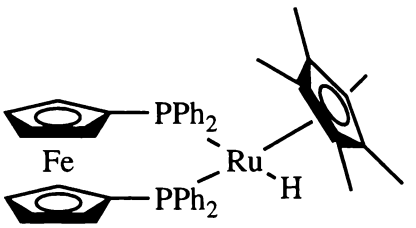

11

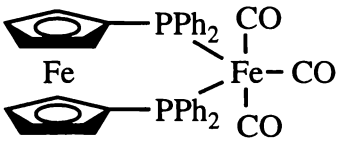

12

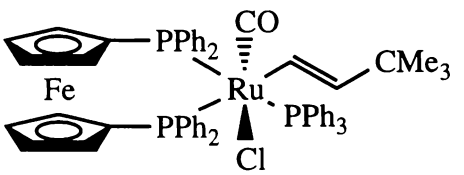

13

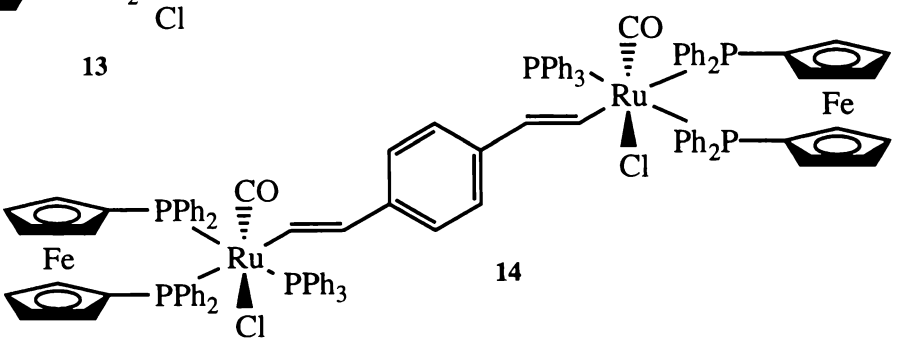

14

p-$C_6H_4C{\equiv}C)Cl_2(CO)_2(dppf)_2(PPh_3)_2$ **15**[22]. These last two compounds were prepared as 1:1 diastereoisomeric mixtures, where the chloride and carbonyl ligands can be in either the *meso* (as shown) or *dl* configuration. Other reported Ru(II) six-coordinate compounds are $[Ru(bipy)_2(dppf)][PF_6]_2$ (bipy = 2,2'-bipyridine), along with related compounds in which the bipyridyl ligands were derivatised[23], and the dihydride complex $Ru(H)_2(dppf)_2$[24]. The carbonyl compounds *fac*-$W(CO)_3(dppf)(L)$ (L = $NCCH_3$ **16**, PMe_3, PPh_2H, PPh_2OH) also display octahedral geometry[25], as do *fac*-$MnX(CO)_3(dppf)$ (X = Cl, H)[26]. Even higher coordination numbers are occasionally seen with dppf, as is the case with the seven-coordinate compound $WI_2(CO)_3(dppf)$, recently shown to result from the oxidation of **16** with I_2[25], although its synthesis had been reported previously[27].

The unique ability of dppf to act as a chelating ligand in the great variety of different coordination spheres demonstrated above stems from a capacity to modify its steric bite through twisting and tilting of cyclopentadienyl (Cp) rings relative to each other, along with some bending of phosphorus atoms away from the planes of the Cp rings[28].

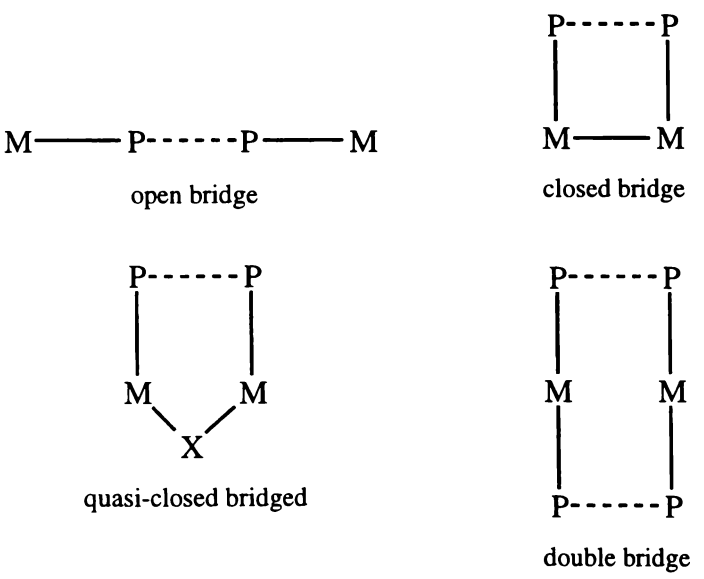

Scheme 1.1: Bridging modes of dppf (P------P = dppf, M = metal centre).

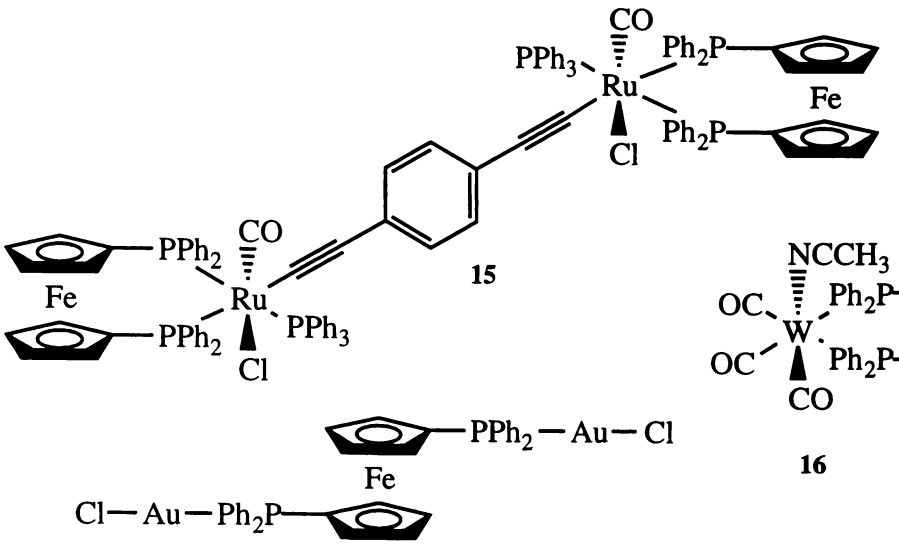

15

16

17

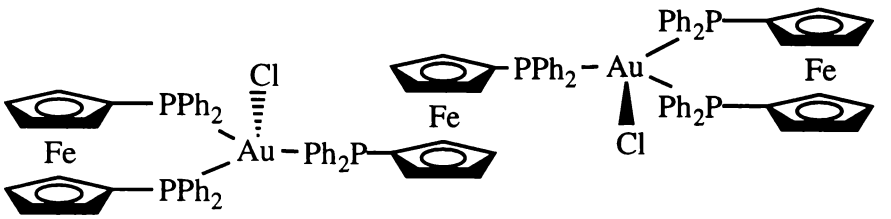

18

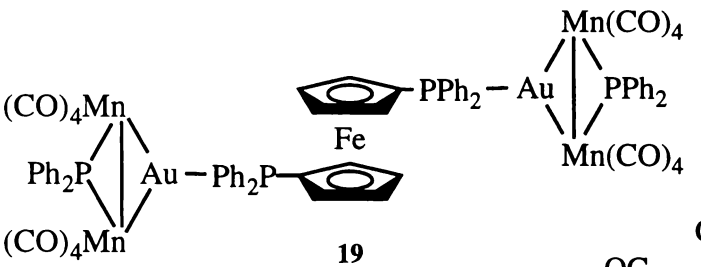

19

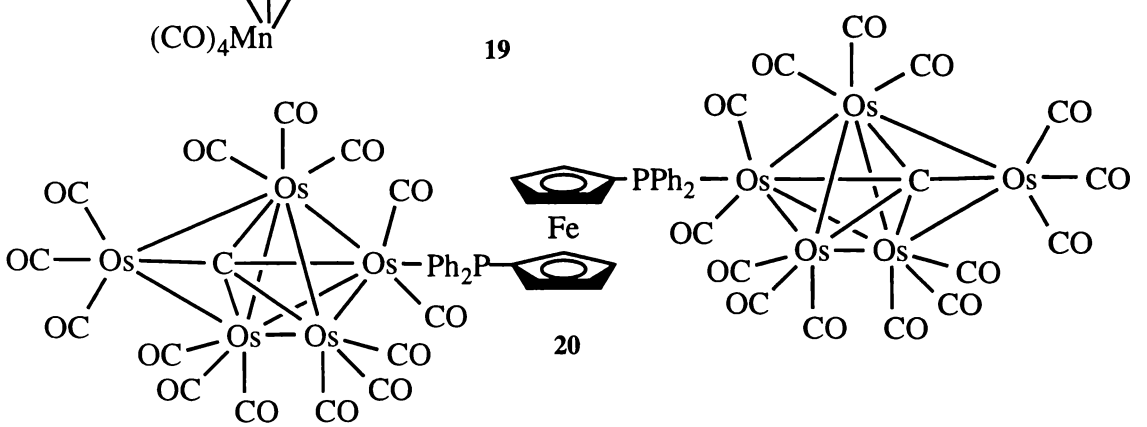

20

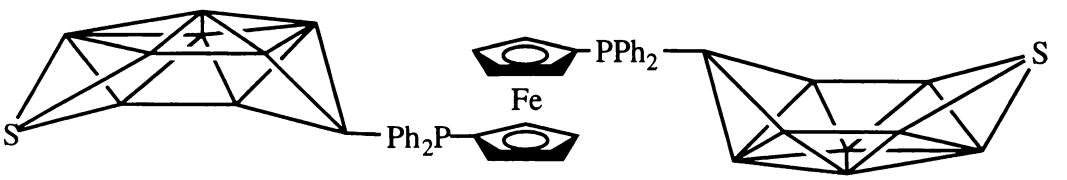

21 (vertex = BH)

Dppf does not always act as a chelating ligand, but is also commonly observed to act as a bridging ligand, a phenomenon which in recent times has been especially thoroughly investigated for the case of gold complexes. Varieties of bridging modes observed with dppf are illustrated systematically in Scheme 1.1. Recent examples of open bridge systems include numerous variations of Au_2X_2(μ-dppf) (X = Me, C_6H_5, $C_{10}H_7$, $C_{14}H_9$, $C_{16}H_9$, C≡CPh, C≡CBu^t [29]; Cl **17**, C_6F_5[30]; Br, I, pyridinethiolate, diethyldithiocarbamate[31]; CF_3CO_2[32], $Co(CO)_4$[33]), and two compounds containing both bridging and chelating dppf, Au_2X_2(μ-dppf)(dppf-*P*,*P'*)$_2$ (X = Cl **18**[34], NO_3[35]). Metal clusters have also been linked using dppf, giving the compounds $[Fe_3(CO)_9(\mu\text{-}CO)_2]_2$(μ-dppf)[36], $[Fe_3(\mu^3\text{-}S)_2(CO)_8]_2$(μ-dppf)[8], $[AuMn_2(\mu\text{-}PPh_2)(CO)_8]_2$(μ-dppf) **19**[37] and $[Os_5C(CO)_{14}]_2$(μ-dppf) **20**[38]. Similarly, dppf has served as an open bridge ligand in reactions with Lewis acidic boranes, thiaboranes and carboranes, giving products such as arachno-9-(arachno-9'-dppf-6'SB_9H_{11})-6-SB_9H_{11} **21**[39]. The ultimate expression of this open-bridged motif is the production of the polymeric material $[AuCl(dppf)]_n$ **22**; the regular nature of the polymer was confirmed by X-ray crystallography[35].

A closed bridge is seen where dppf bridges a metal-metal bond. A number of examples of this have been reported in the field of cluster chemistry[40], including: $Os_4(\mu\text{-}H)(CO)_{10}$(μ-dppf), where dppf lies along one edge of an osmium tetrahedron[41]; $Fe_3(\mu^3\text{-}S)_2(CO)_7$(μ-dppf)[8]; $Fe_3(CO)_8(\mu\text{-}CO)_2$(μ-dppf), in which the three bridging ligands all span the same metal-metal bond[36]; $RhRu_3H_3B(CO)_7$(Cp*)(μ-dppf) **23** and $AuRhRu_3H_2B(CO)_8$(Cp*)(μ-dppf) **24**[42]. To these examples can be added the dinuclear compound $Co_2[\mu^2\text{-}(MeO_2C)_2C_2](CO)_4$(μ-dppf) **25**[43].

A quasi-closed bridge refers to any compound where a dppf bridge is supported by another bridging group, but there is no metal-metal bond. An example of this is the compound $Au_2(\mu\text{-}SCH_2CH_2CH_2S)$(μ-dppf)[44], with the gold atoms linearly coordinated. An interesting compound which falls somewhere between displaying closed and quasi-closed bonding behaviour is $Au_2(\mu\text{-}S)$(μ-dppf)[45]. While it is formally quasi-closed, the linearly coordinated golds form a sharp angle of 77.6° at the bridging sulfur, giving a short gold-gold distance

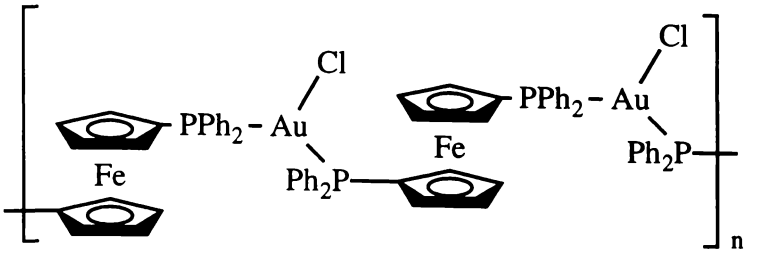

22

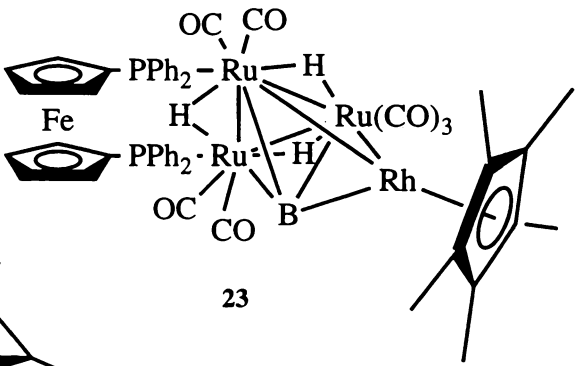

23

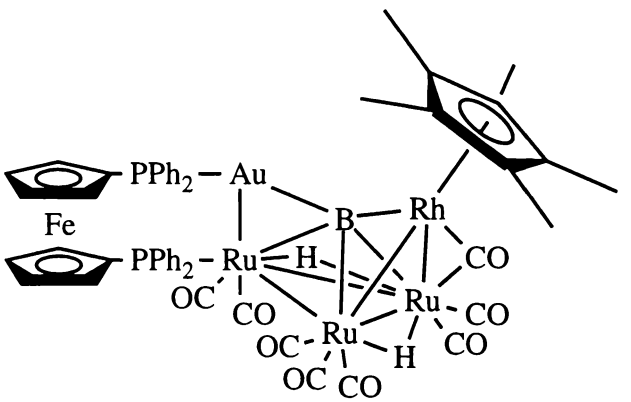

24

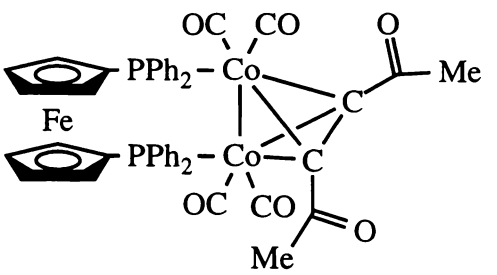

25

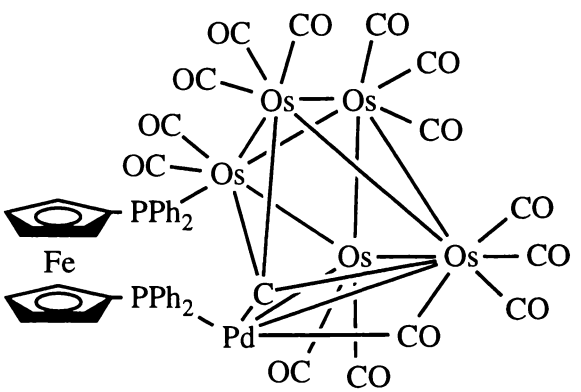

26

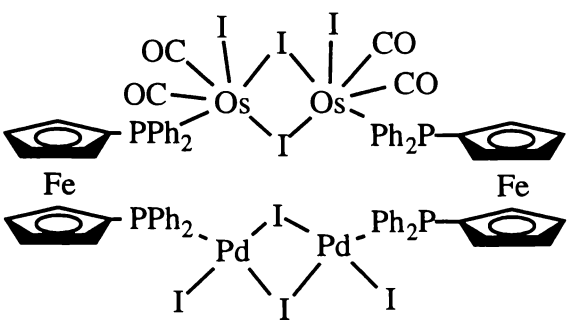

27

of 2.88 Å, within the range of aurophilic interaction. A number of other compounds showing similar behaviour were reported by the same group. Cluster chemistry also provides examples of quasi-closed bridges, for example, $Os_5PdC(CO)_{13}(\mu\text{-}CO)(\mu\text{-}dppf)$ **26**[37]. An example of a doubly-bridged structure is provided by $[OsPd(\mu\text{-}I)_2I_2(CO)_2(\mu\text{-}dppf)]_2$ **27**[37].

As well as displaying chelating and bridging modes, dppf sometimes acts as a monodentate ligand, but this is rather uncommon. Examples include the compounds $Fe(CO)_4$(dppf-*P*)[46], $Co_2[\mu^2\text{-}(MeO_2C)_2C_2](CO)_5$(dppf-*P*) (a monodentate relative of **25**)[43] and $RhRu_3B(Cp^*)(\mu\text{-}H)_3(CO)_8$(dppf-*P*) **28**[42].

1.1.2 Use of Dppf in Catalysis

In the late 1970's Hayashi *et al.* demonstrated the superiority of $PdCl_2$(dppf) as a catalyst for the cross-coupling of Grignard reagents and electrophilic organics over the classical $PdCl_2(PPh_3)_2$ and other possibilities[47]. Since that time the homogeneous catalytic chemistry of dppf has been widely explored, particularly with respect to cross-coupling reactions of various kinds, and especially Grignard cross-coupling. A general mechanism for the catalytic cycle of PdX_2(dppf) in Grignard cross-coupling is given in Scheme 1.2. Some representative examples of reactions catalysed by dppf complexes are given in Scheme 1.3.

No doubt the catalytic potential of simple Pd and Pt complexes of dppf accounts for the large amount of research still being carried out into syntheses of these compounds (see Section 1.1.1). The advantage of $PdCl_2$(dppf) as a catalyst of Grignard cross-coupling reactions over other traditional catalysts is ascribed to the large bite angle of dppf (99.1°), which forces other species ligated to the Pd into closer proximity, aiding expulsion of conjoined products in the reductive elimination step. Catalysis with dppf complexes is also observed to suppress the undesirable β-elimination products seen with many other comparable catalytic systems[48].

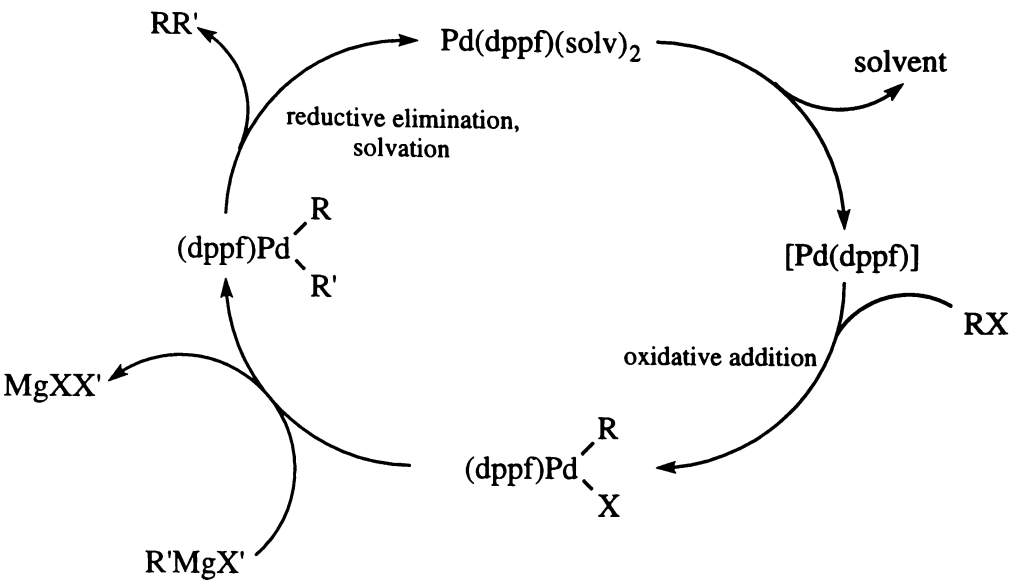

Scheme 1.2: Catalytic cycle observed in Grignard cross-coupling reactions catalysed by $PdCl_2(dppf)$. The active species is thought to be the $Pd(solv)_2(dppf)$ (solv = coordinated solvent) species.

Research is still ongoing into these types of reactions, e.g. in one recent study the rate of oxidative addition of phenyl iodide to Pd(dppf)(dba) was investigated[7]. Two recent papers also describe the use of $PdCl_2(dppf)$ in order to perform desired syntheses by the cross-coupling of an organometallic compound with a halo-organic compound, a route which is by now well-travelled. A representative sample of the reactions reported in these papers is given in Scheme 1.4.

Other papers have reported work with potential ruthenium catalysts. The complex $Ru(H)_2(dppf)_2$ has been prepared with a view to exploring its catalytic activity[24], and that of the potentially more active derivative $[Ru(H)(dppf)_2]^+$. At present, more success has been seen in the work of Hembre *et al.*[19] with compound **11**. They found that by using a catalytic amount of **11**, ferrocenium or methylviologen could be reduced by one electron in the presence of H_2, using base to react with the H^+ produced. Further study of H_2 activation by **11** revealed unprecedented coupling of a carbon-carbon bond-forming reaction to H_2 oxidation, catalysed by **11** at a concentration of 1 mol% (Scheme 1.5).

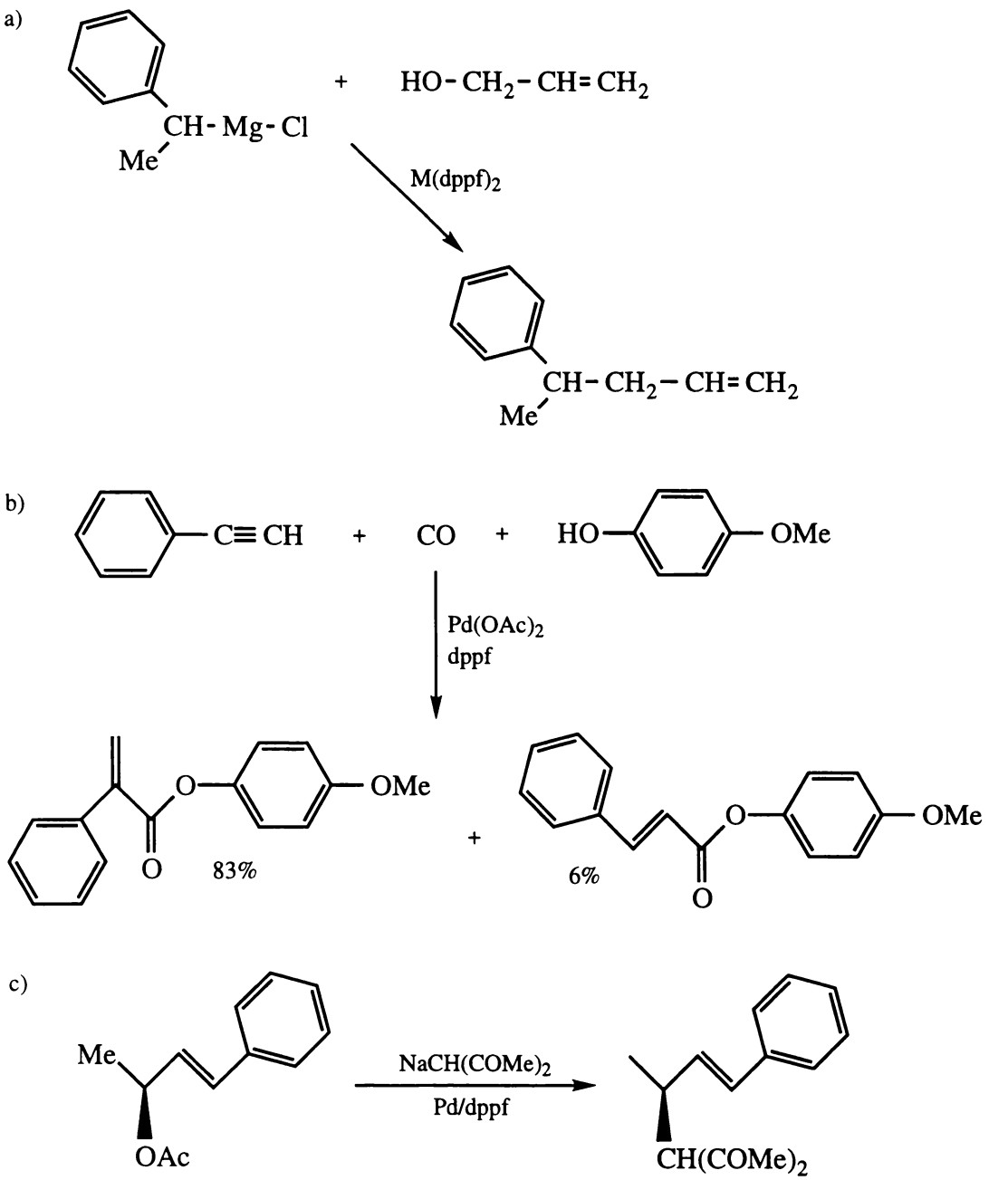

Scheme 1.3: Reactions catalysed by dppf complexes. a) Cross-coupling of a Grignard reagent and an alcohol[47b]. b) Carbonylative coupling of a terminal alkyne with a phenol[49]. c) Nucleophilic substitution, with retention of stereochemistry[50]. It should be noted that for this application $Ph_2PCH_2CH_2PPh_2$ (dppe) proved a superior ligand.

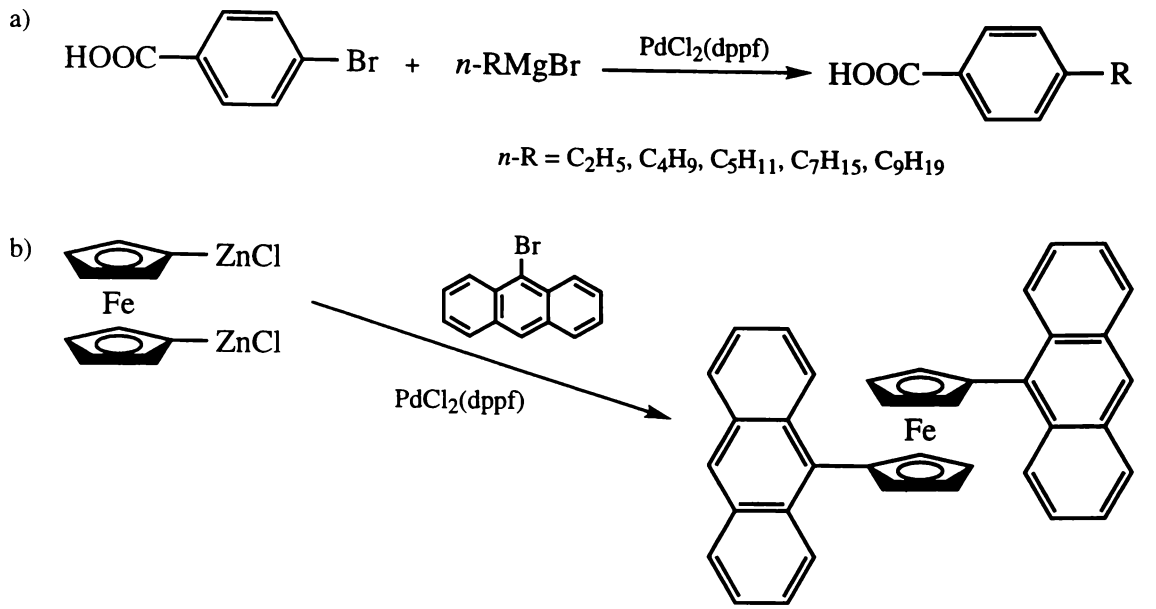

Scheme 1.4: a) Cross-coupling of 4-bromobenzoic acid with a Grignard reagent, catalyst concentration 1 mol%[51]. b) Synthesis of 1,1'-bis(anthracenyl)ferrocene, catalyst concentration 5 mol% w.r.t. ferrocene[4].

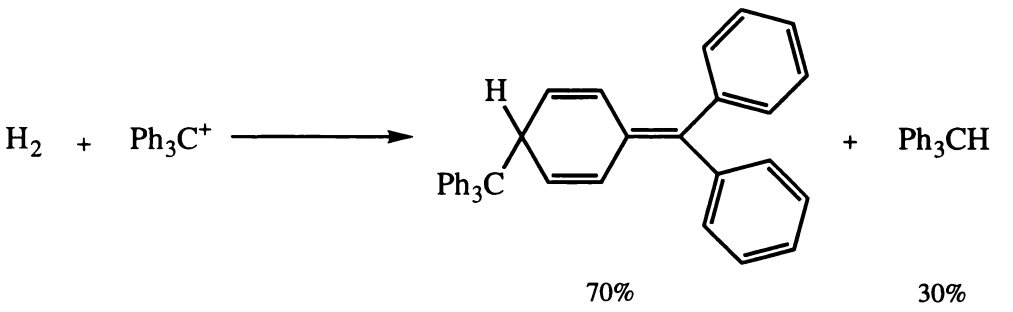

Scheme 1.5: Dimerisation of the trityl cation, coupled with H_2 reduction, catalysed by **11**.

Studies into attempts to prepare heterogenous catalysts by thermal decomposition of $MCl_2(dppf)$ (M = Ni, Pt, Pd)[52] are still in their infancy, but show how these compounds have become established materials of choice in many areas of investigation into catalysis.

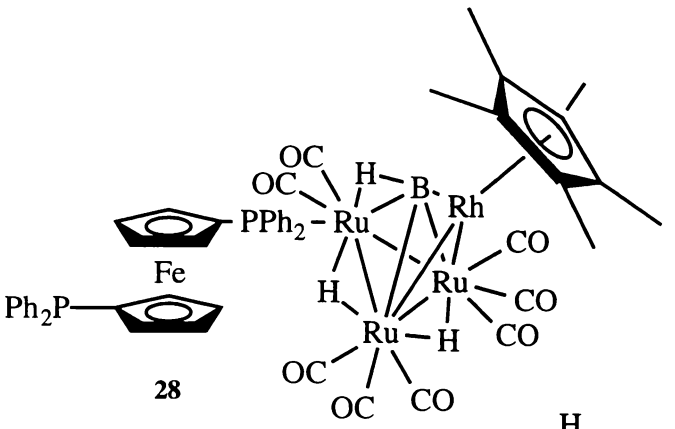

28

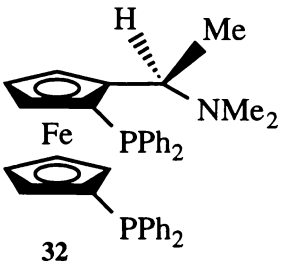

32

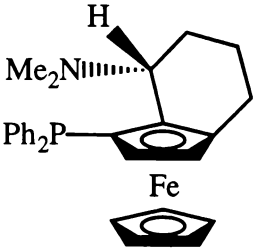

33

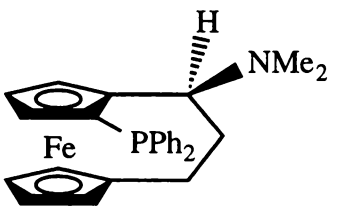

34

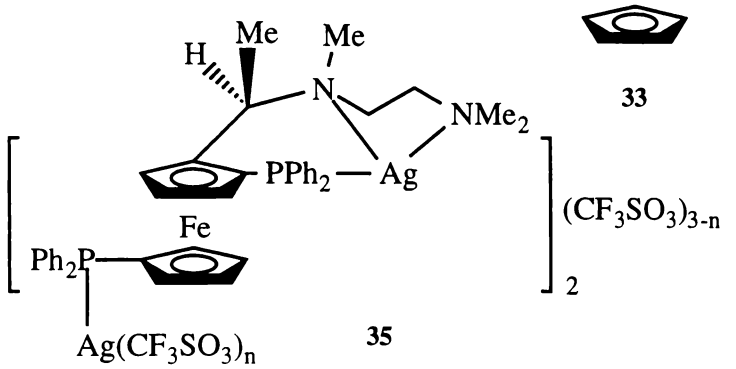

35

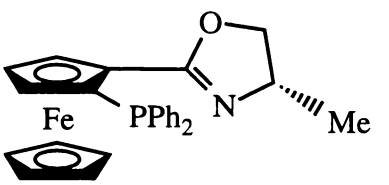

36

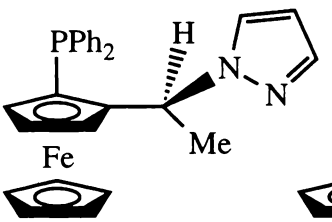

37

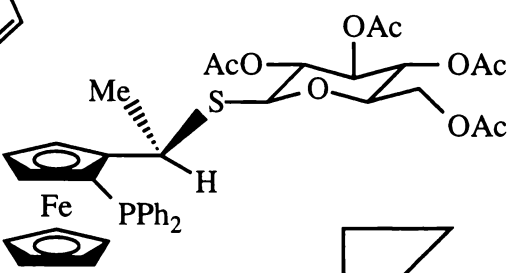

38

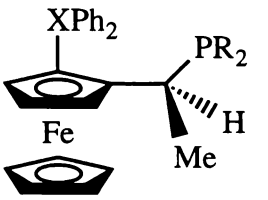

40a: R = Ph
b: R = Cy

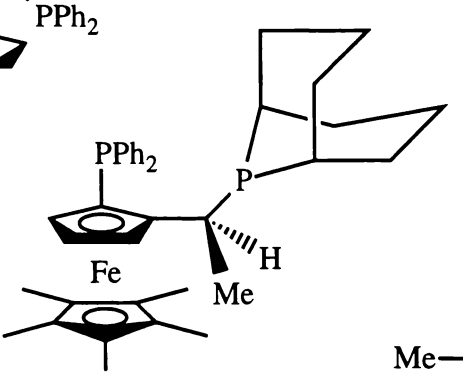

42

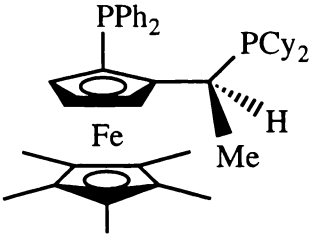

41

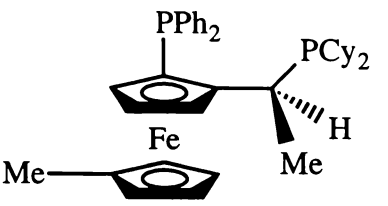

43

1.2 Enantioselective Catalysis With Planar Chiral Ferrocenes

In principle, the most efficient way to obtain a chiral product is through the use of a chiral catalyst, rather than using stoichiometric amounts of a chiral starting material or chiral auxiliary. Given the success of dppf as a ligand in catalytic systems (Section 1.1.2), it therefore seems inevitable in hindsight that similar ferrocenylphosphine ligands exhibiting chirality would be designed and used to prepare transition metal complexes with the potential for use in homogeneous asymmetric catalysis. Within the last few decades a great amount of research has been carried out in this area, and it would be beyond the scope of the present Chapter to cover all relevant literature, so the reader is referred to other reviews[53] for further information. A helpful overview at a more popular level was also recently given in *Chemical & Engineering News*[54].

In designing chiral ferrocenylphosphine ligands, not only is the concept of carbon-centred chirality important, but that of planar chirality is also. Scheme 1.6 shows a generalised picture of a ferrocene molecule bearing two substituents. In this situation it will be seen that if the substituents are different two enantiomers are possible. This is what is referred to as planar chirality. Assignment of a chirality descriptor for a planar chiral ferrocene is done by viewing the molecule from above the substituted ring. Substituents are prioritised according to the usual Cahn-Ingold-Prelog rules. If the shortest path around the ring from the substituent with highest priority to that next in the hierarchy is in the clockwise direction, the

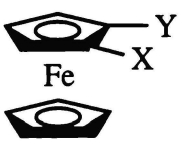

Scheme 1.6: Ferrocene moiety with two substituents. Where X and Y are different, planar chirality will result.

descriptor is (*R*), otherwise it is (*S*). Where an element of central chirality is also present, it is usually written as the first descriptor, with that for planar chirality second. The descriptor for planar chirality is also often distinguished by a subscript p, e.g. (S,R_p)[55].

The original, and now classic, preparation of a planar chiral ferrocenylphosphine was the synthesis of (*R*)-*N*,*N*-dimethyl-1-[(*S*)-2-(diphenylphosphino)ferrocenyl]ethylamine [(R,S_p)-PPFA] **31**. This was prepared by the route shown in Scheme 1.7. Ugi *et al.*[56] demonstrated that the enantiomeric amine **29** could be used as a highly effective directing group in *ortho*-lithiation, giving predominantly the (S_p) planar chiral enantiomer **30**. This route was later used by Hayashi *et al.*[57] to prepare the phosphine (R,S_p)-PPFA **31**. The same group later extended this methodology to prepare the dimethylphosphine derivative of **31** and other related compounds, as well as the opposite enantiomer[58]. Nickel or palladium complexes of (R,S_p)-PPFA **31** and closely related compounds were then shown to enantioselectively catalyse the Grignard cross-coupling reaction between 1-phenylethylmagnesium chloride and vinyl bromide, giving optically active 3-methyl-3-phenyl-propene[59]. In the case of (R,S_p)-PPFA) a 68% *ee* (*R*) was obtained for this reaction. Other reaction substrates were also investigated.

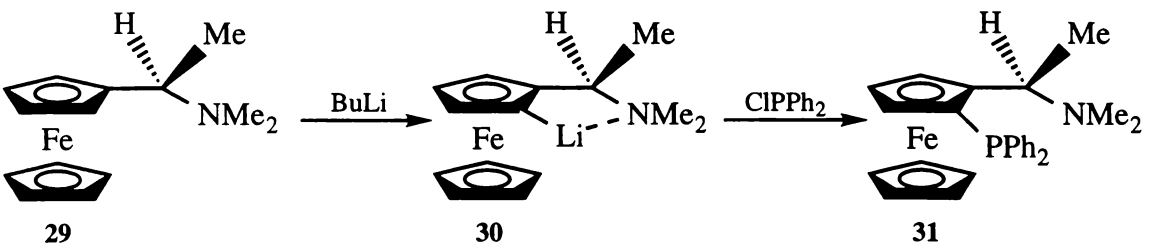

Scheme 1.7: Synthetic route used to produce (R,S_p)-PPFA **31**.

In more recent years research into PPFA and related ligands such as (R,S_p)-BPPFA **32**[58] has remained a very active field. Publications have included work on alternative synthetic routes to (aminoethylferrocenyl)phosphine compounds of the PPFA type[60], preparation of new ferrocenylphosphines[61] such as (R,R_p)-PTFA **33**[62] and (S,S_p)-1-(diphenylphosphino)-2,1'-[(1-*N*,*N*-dimethylamino)-1,3-propanediyl]ferrocene **34**[63], preparation and study of new

complexes[64] such as $PdCl_2(PTFA)$[65] and $[Ag_3(L)_2][CF_3SO_3]_3$ [L = (R,S_p)-2-{CH(Me)N(Me)$CH_2CH_2NMe_2$}-1,1'-diphenylphosphinoferrocene] **35**[66], and investigations of catalytic activity[67], including patent applications[68]. Representative examples of asymmetric catalysis by complexes of ferrocenylphosphines substituted at the 2- position by aminoethyl groups are given in Scheme 1.8.

The preparation of planar chiral ferrocenylphosphines has from the time of the original work on PPFA **31**[57,58] until the present largely followed the same principles. Initially ferrocene is derivatised with a side chain having central chirality. This side chain is then used to direct *ortho*-lithiation of the ferrocene in an enantioselective manner, and the lithium species reacted to give a phosphine. The original side chain may then be replaced or modified. So far consideration has only been given to the preparation of compounds where the final product contains an -$CH(NR_2)CH_3$ side chain. However, a variety of other approaches have been developed.

One alternative set of ferrocenylphosphine compounds recently developed for enantioselective catalysis is the oxazolinylferrocenylphosphines[69], such as "(S,S_p)-Me-phosferrox" **36**[70]. These compounds have some preparative advantages over PPFA-type compounds, and research into their synthesis and efficacy in catalytic systems is ongoing[71]. A concurrent development has been the investigation of pyrazole-containing ferrocenylphosphines of the type epitomised by (S,R_p)-2-(1-pyrazolylethyl)-1-(diphenylphosphino)ferrocene **37**[72], which has also proved a productive line of research[73]. Other coordinating moieties which have been included at the β-position of the directing side chain are the Cp group[74], which was used to make rhodium(I) and ruthenium(II) complexes, sulfur-containing groups[75] such as in (R,S_p)-2-[1-(S-tetra-acetylthioglucose)ethyl]-1-(diphenylphosphino)ferrocene **38**[76], selenium-containing groups[75a], and imine functions[77]. One ligand has been developed where central chirality of the oxazolinylferrocenylphosphine is removed by transformation of the oxazolinyl group into an ester function, giving a molecule with only planar chirality, which was shown nevertheless to be suitable for use in asymmetric catalysis[78].

a)

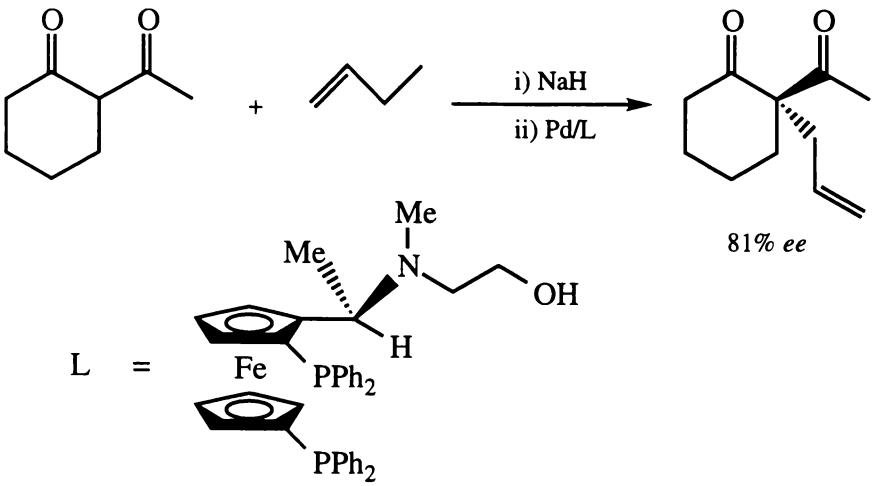

b)

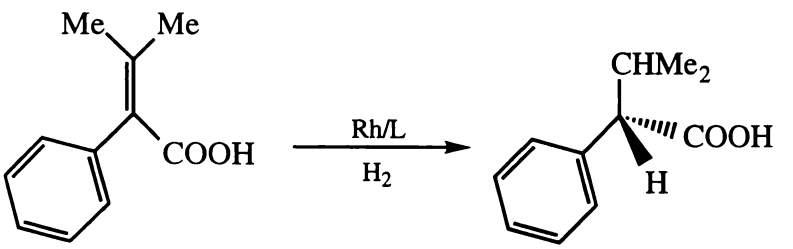

98.4% *ee*

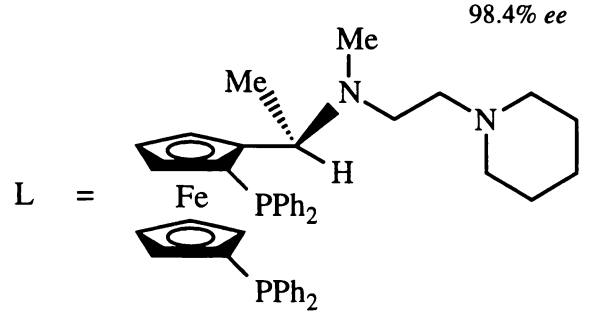

c)

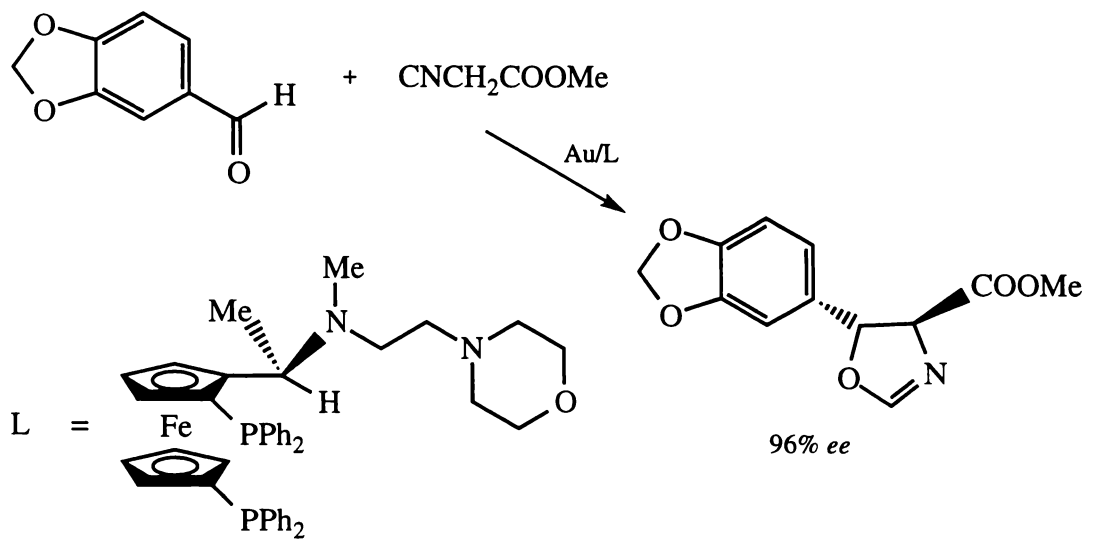

96% *ee*

Scheme 1.8: a) Reaction of an allylic substrate with a nucleophile[79]. b) Rhodium-catalysed olefin hydrogenation[80]. c) Aldol-type reaction of an aldehyde with an α-isocyanocarboxylate[81].

However, arguably the most important group of asymmetric ligands to have been developed from the original PPFA-type ligands thus far are the 1,2-diphosphines. The first compound of this type was included in the first detailed report on asymmetric ferrocenylphosphines[58], which also included PPFA **31**. This was (R,S_p)-2-[-1-(diphenylphosphino)ethyl]-1-(diphenylphosphino)ferrocene **39a**, and it was prepared by reflux of an acetylated derivative of (R,S_p)-PPFA **31** with diphenylphosphine for 7 hours in methanol (see Scheme 1.9). Preparation of the acetyl intermediate required heating of (R,S_p)-PPFA **31** with acetic anhydride at 100° C for two hours in a sealed glass tube.

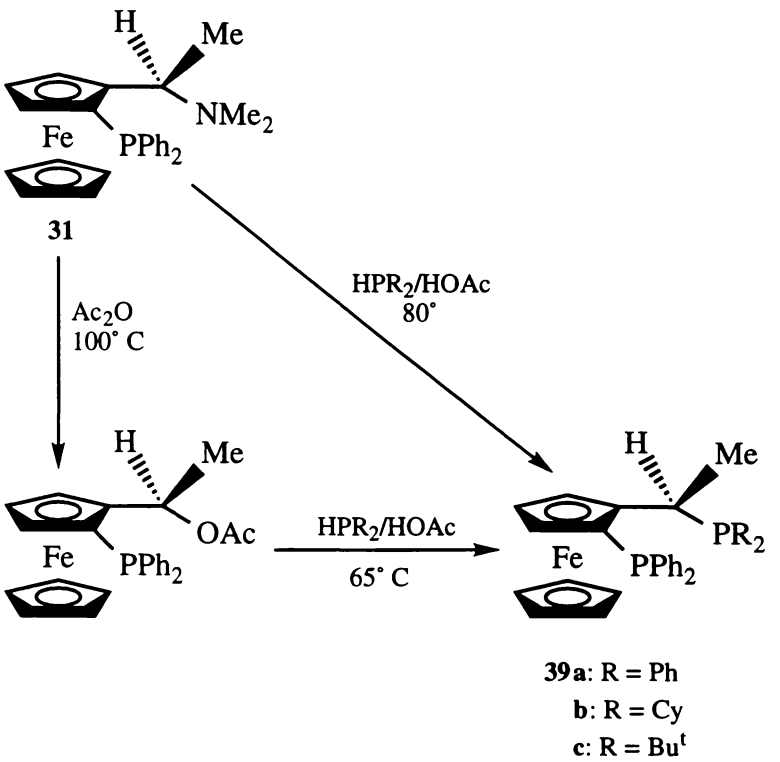

Scheme 1.9: Synthesis of compounds **39a-c**. The older two-step route involving acetylation has been superseded by the more convenient direct formation of the product.

Synthesis of these compounds only became more convenient in more recent times, when Togni *et al.*[82] showed that **39a** could be prepared in greater than 80% yield in a one-step reaction, by heating (R,S_p)-PPFA **31** with diphenylphosphine for 3.5 hours at 80° C in acetic acid, leading to displacement of the amine group with the phosphine. The dicyclohexyl **39b** and *t*-butyl **39c** derivatives were also described, both prepared by the

same method in high yield. These ligands are commonly known as 'Josiphos'-type ligands, having been named after one of the laboratory technicians involved in their preparation.

A number of Josiphos-type ligands have since been prepared. The final step in the preparation of these compounds is always essentially the same procedure described for **39a-c** above; reaction of an amine precursor with the appropriate secondary phosphine in hot acetic acid. It can be seen that a variety of different combinations of planar and central chirality are available, depending on the precursor chosen (e.g., compounds **40a** and **40b**, the enantiomers of **39a** and **39b**[83]). Work on new synthetic routes to the amine precursors has allowed the synthesis of compounds such as **41**, **42** and **43**, where a bulky lower Cp ring is introduced[84]. The general synthetic method has been extended by the use of primary phosphine reagents to produce tridentate chiral ligands of the type **44**, an area of interest since chiral triphosphines have not been intensively studied in asymmetric catalysis[85]. The secondary phosphine **45** has also been made in rather low yield using a primary phosphine as the nucleophile[85a]. Enantiomerically pure P-chiral ligands have also been synthesised, such as **46a** and **46b**[83], and a variety of unusual phosphorus functionalities have been incorporated into Josiphos-type ligands, as seen with **42**, **47**[86] and **48a-f**[87].

Josiphos-type ligands have generated great interest in view of their excellent catalytic properties, especially their versatility over a variety of different reactions, first demonstrated for enantioselective hydrogenation, allylic alkylation and hydroboration reactions[82,88]. Some representative examples of homogeneous asymmetric catalysis using Josiphos-type ligands are given in Scheme 1.10. The success of all the PPFA-type ligands discussed in this Section as asymmetric catalysts can be attributed to a general principle: two heteroatoms in the ligand bind to the metal centre, while a chiral centre undergoes secondary interactions with the substrate, also bound to the metal centre. In Josiphos-type ligands, the two phosphine moieties are again bound to the metal, but in this case they also fulfil the requirements for forming a 'chiral pocket' for the substrate, without the need for another substituent to specifically interact with the substrate[89]. Since the planar-chiral ferrocenyl group constitutes a substituent of both the phosphine moieties, it will have an effect on the

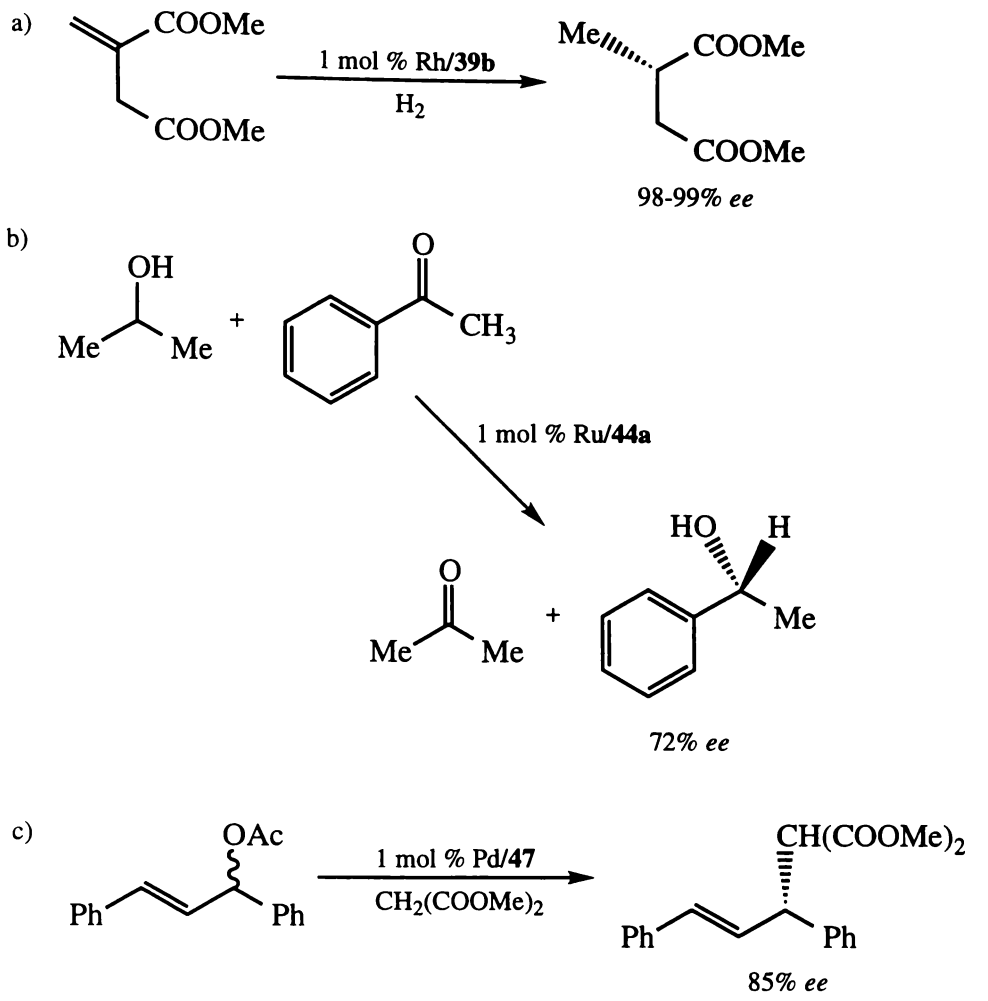

Scheme 1.10: Representative examples of the use of Josiphos-type ligands in asymmetric catalysis. a) Hydrogenation reaction using the original 'Josiphos'[82]. b) Asymmetric hydrogen transfer from an alcohol to a ketone[85a]. c) Allylic alkylation reaction, similar to that in Scheme 1.3c, but in this case inducing chirality in the substrate[86].

shape of this chiral pocket. For this reason at least one study has been carried out on the effect of metallocene bulk on enantiomeric excess in these compounds, by variation of the non-coordinating Cp ring substituents and replacement of iron by ruthenium[90]. NMR studies have also been used extensively to try and elucidate the nature of the solution structures adopted by Josiphos-type ligands[91], and reactivity studies are ongoing[92].

Josiphos-type ligands have become the first asymmetric ferrocenylphosphines to be successfully applied in commercial settings[54]. Scheme 1.11 shows the routes used to

produce an intermediate in the synthesis of (+)-Biotin[93], the herbicide (*S*)-Metolachlor[53c,54], and an intermediate in the production of Dextromethorphan, a cough remedy[94]. Patents have also been secured for similar catalytic systems[95], and the interest in Josiphos-type ligands is such that a variety have quickly been offered commercially by at least one chemical supplier[96].

Another set of ferrocenylphosphine ligands developed for asymmetric catalysis is epitomised by the first of its class, (*R*,*R*)-(S_p,S_p)-2,2"-bis[1-(diphenylphosphino)ethyl]-1,1"-biferrocene [(*R*,*R*)-(S_p,S_p)-PhTRAP] **49a**[97]. Compounds of this kind have come to be known as TRAPs, referring to the *trans*-chelating nature of these phosphine ligands; all other chiral ferrocenylphosphines discussed so far have been designed to produce *cis*-complexes. Note that as with Josiphos-type ligands, these compounds contain a carbon spacer between the phosphorus and the Cp ring. TRAP ligands can be produced with either (*R*,*R*)-(S_p,S_p)- or (*S*,*S*)-(R_p,R_p)- chirality, and with a wide variety of different phosphorus substituents (**49b-j**). The alkylphosphines (*R*,*R*)-(S_p,S_p)-Bu^{n}TRAP **49b**, -Pr^{n}TRAP **49c** and -Pr^{i}TRAP **49d** were prepared in order to investigate the effect of having phosphorus substituents which were less bulky and rigid[98]. The closely related compounds (*R*,*R*)-(S_p,S_p)-EtTRAP **49e** and -Bu^{i}TRAP **49f** were separately reported[99]. Other arylphosphine-containing TRAPs have also been prepared[100], **49g-j**.

The method which has been used for the synthesis of TRAPs involves several steps[97,100], and is pictured in Scheme 1.12. After initial enantioselective *ortho*-halogenation of the starting material, the amine function is quaternised. The ammonium salt thus formed is then reacted with a phosphinate salt formed *in situ* by reaction of *n*-butyl-lithium and diphenylphosphine oxide, giving a ferrocenylphosphine oxide. The initial report on the preparation of **49a** stated that the next step, involving coupling of ferrocenes, was achieved by reaction with a Ni(0) complex in DMF at 120° C for 12 hours[97]. It has more recently been shown that this process can be carried out in the solid state by reaction with activated

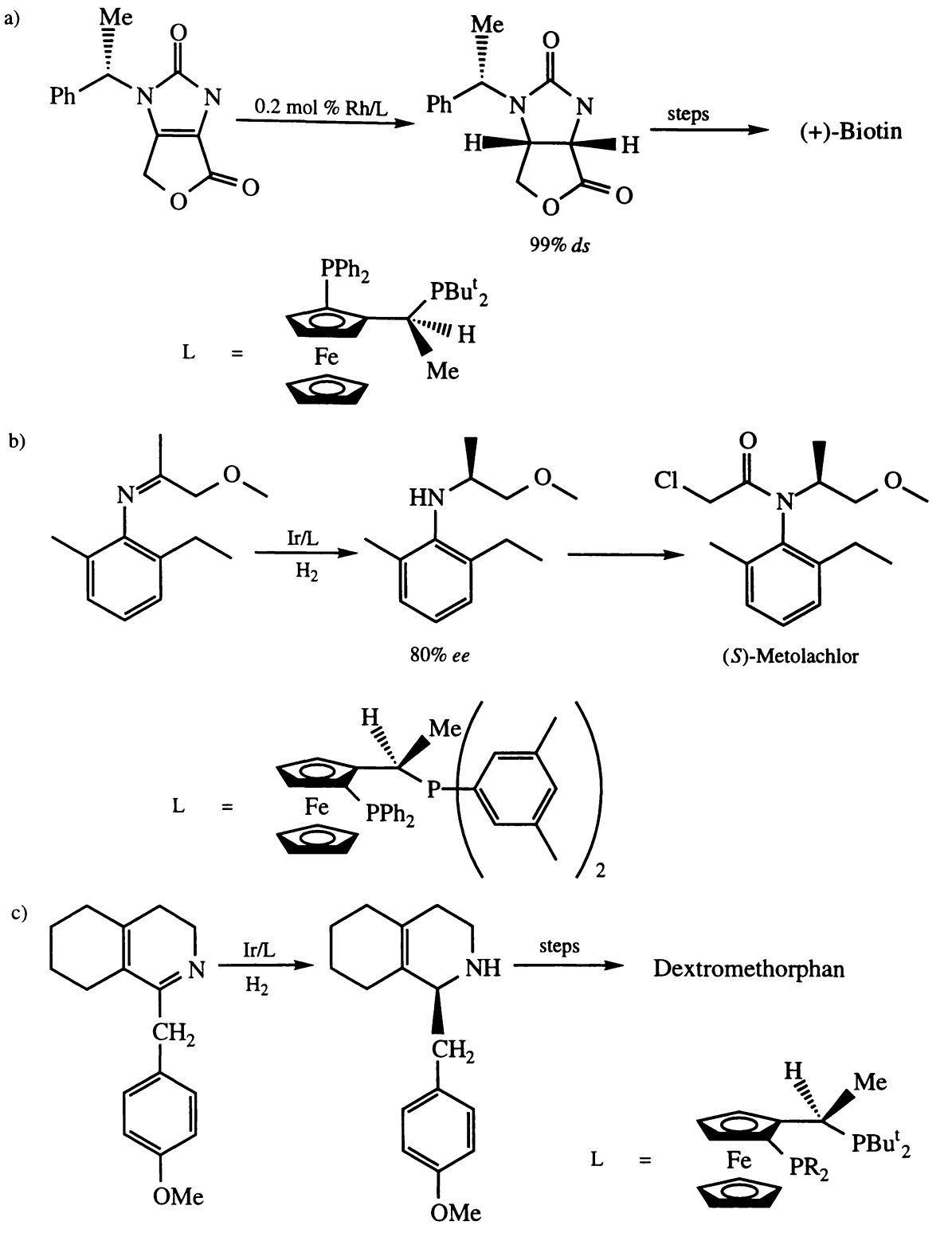

Scheme 1.11: Commercial processes currently in use. a) Synthesis of a (+)-Biotin precursor in high diastereoisomeric and enantiomeric excess. b) Synthesis of (*S*)-Metolachlor. The rather low enantiomeric excess is acceptable for an agri-chemical, and the catalyst shows exceptionally high activity[53c], with an substrate/iridium ratio ≤ 1 000 000. c) Synthesis of a Detromethorphan intermediate.

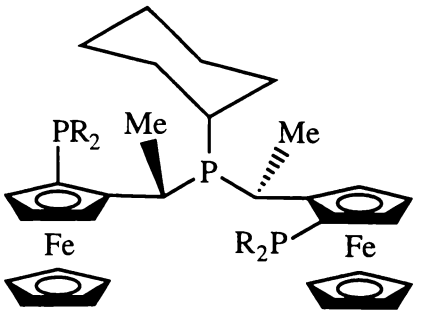

44a: R = Ph
b: R = 3,5-Me-(C_6H_3)
c: R = 3,5-CF_3-(C_6H_3)

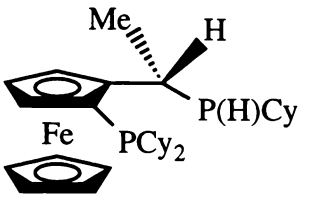

45

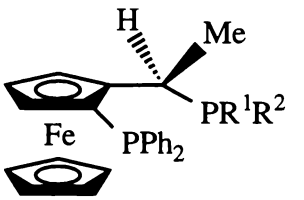

46a: R^1 = Ph, R^2 = Cy
b: R^1 = Ph, R^2 = *o*-An

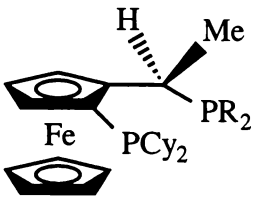

48a: R = 2-MeO-C_6H_4
b: R = 3-MeO-C_6H_4
c: R = 4-MeO-C_6H_4
d: R = 3-Me-C_6H_4
e: R = 4-Me-C_6H_4
f: R = 3,5-$Me_2C_6H_3$

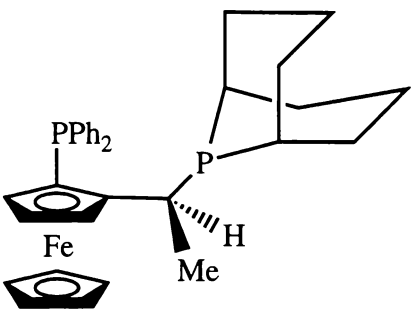

47

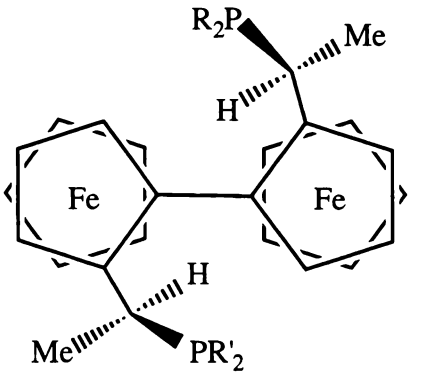

49a: R = R' = Ph
b: R = R' = Bu^n
c: R = R' = Pr^n
d: R = R' = Pr^i
e: R = R' = Et
f: R = R' = Bu^i
g: R = R' = *p*-MeO-Ph
h: R = R' = *p*-Cl-Ph
i: R = R' = 2-furyl
j: R = Ph, R' = *p*-Tol

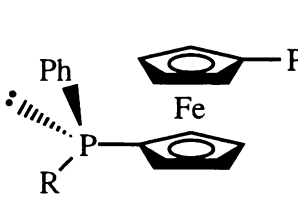

50a: R = 2-OMe-C_6H_4
b: R = 1-naphthyl

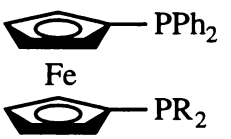

51a: R = Pr^i
b: R = Bu^t

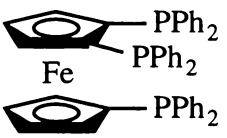

52

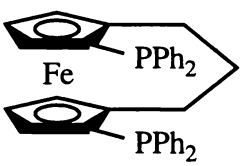

53

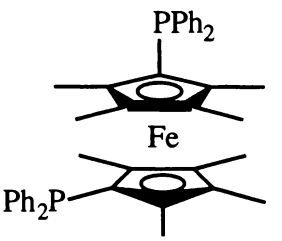

54

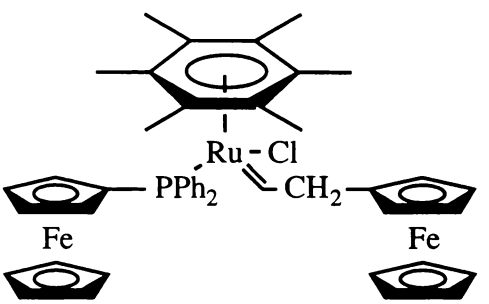

55

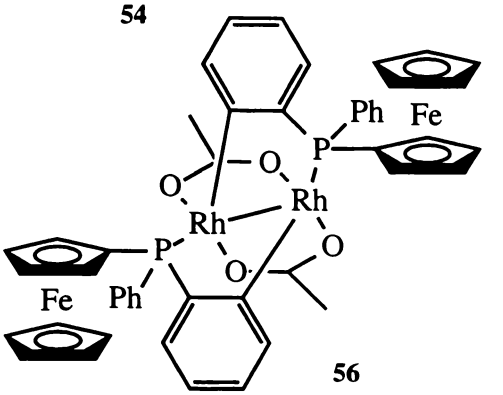

56

copper[100], typically at 130° C for 12 hours. The phosphine oxide functions are reduced by reaction with triethylamine and trichlorosilane in a sealed vacuum tube at 100° C, typically for 10 hours.

TRAP ligands have been used to prepare complexes with Pt(II)[97,100], Pd(II)[97,100], Rh(I)[98,99,100,101] and Ir(I)[100], in each case giving *trans*-chelated square-planar complexes; in the case of the first two metals, ligands were chloride, while for the latter two metals one carbonyl and one chloride were coordinated. Rhodium complexes prepared *in situ* have been shown to be effective catalysts for the enantioselective hydrosilylation of ketones[98,102] and keto-esters[103], Michael addition of vinyl species to α-cyano carboxylates[104], and for hydrogenation of certain olefins[99,101]. A patent has also been lodged for the preparation of optically active succinic acids, by hydrogenation of suitable precursors using rhodium-TRAP catalyst systems[105]. Some representative reactions are presented in Scheme 1.13.

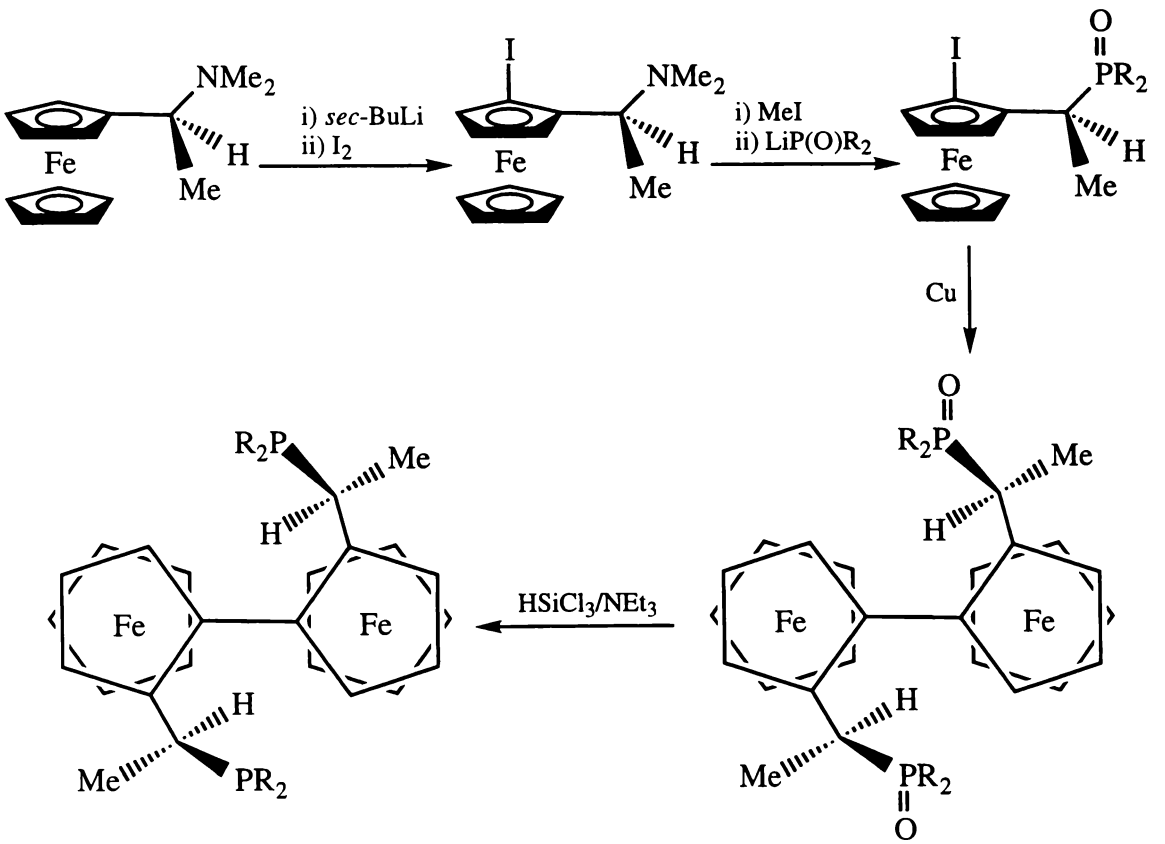

Scheme 1.12: General method for the synthesis of TRAPs.

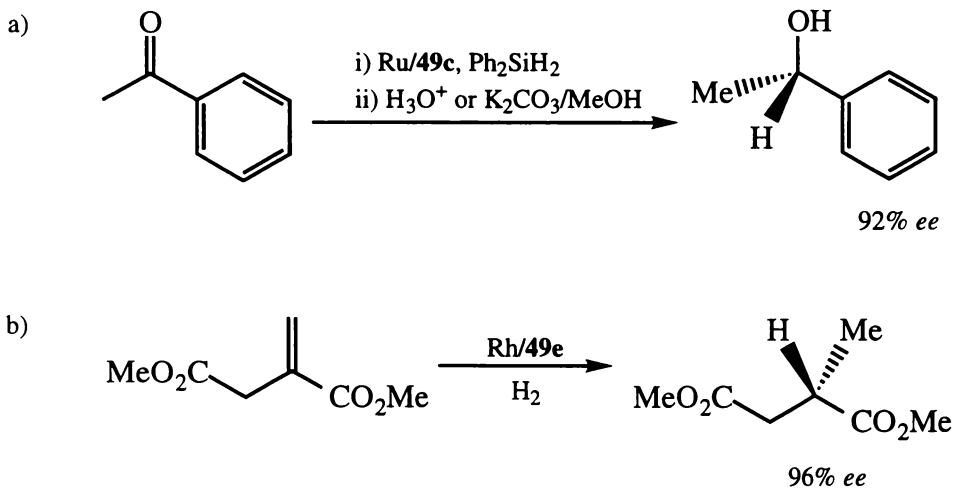

Scheme 1.13: Enantioselective catalysis by complexes containing TRAPs. a) Hydrosilylation[98]. b) Asymmetric hydrogenation to give a succinate[101].

1.3 Other Ferrocenylphosphines

There is a large body of literature to do with ferrocenylphosphine chemistry where the reported results do not concern either dppf chemistry or enantioselective catalysis, although they are usually related to these two topics in some sense. The following three Sections group this research on the basis of distance between the ferrocene function and the phosphine moiety.

1.3.1 Ferrocenylphosphines with a Direct Cp-P Link

By far the greatest amount of research into ferrocenylphosphines has been carried out with compounds containing a direct P-Cp bond; this holds true even for research other than that presented in Sections 1.1 and 1.2 (note that every compound discussed in those Sections has at least one P-Cp bond, with the exception of TRAP ligands).

A number of these compounds are simple derivatives of dppf, where the phenyl groups have been exchanged for other organic moieties. The simplest of these would be 1,1'-diphosphinoferrocene[106], while 1,1'-bis(dimethylphosphino)ferrocene[107], 1,1'-bis(di-*i*-propylphosphino)ferrocene[108] and 1,1'-bis(di-*t*-butylphosphino)ferrocene[109] have also been recently reported. As well as these compounds where all four phosphine substituents are identical, a number of compounds have been reported where the two substituents on the phosphorus are inequivalent, including *rac*-Fe(η^5-$C_5H_4PPhBu^t$)$_2$[109,110], and the *rac*- and *meso*- forms of Fe(η^5-C_5H_4PMePh)$_2$[111]. The most recent reports are of enantioselective syntheses giving (*S*,*S*)-1,1'-bis(methylphenylphosphino)ferrocene[112] and the compounds **50a** and **50b**[113]. In other instances the phosphine fragments on each Cp ring are different, as in the case of compounds **51a**[108a], and **51b**[109]. Other ferrocenylphosphines closely related to dppf are obtained by adding other derivatives to one[114] or both[115] of the Cp rings, including a triphosphine **52**[116], [3]ferrocenophanes such as **53**[61b], and the octa-methyl derivative **54**[117]. The monodentate equivalent of dppf, $FcPPh_2$ (Fc = ferrocenyl)[118], has also been widely used as a ligand in a number of coordination studies[119], giving compounds like the diferrocenyl ruthenium complex **55**[120], the di-rhodium complex **56**, where a phenyl ring from each of the $FcPPh_2$ ligands is coordinated to a metal centre[121], and *fac*-$ReCl(CO)_3(FcPPh_2)_2$ **57**[122]. As is the case with dppf, numerous variations on the theme of $FcPPh_2$ have been reported and investigated, most notably Fc_2PPh[119d,e,123], and to a lesser degree Fc_3P[119d,e,124]. Other compounds which have been reported include $FcPMe_2$[107b,125], $FcPEt_2$[123d] and $FcPPr^i_2$[108c]. Several studies have been made into the preparation of P-chiral ferrocenyl phosphines of this type[123e], such as **58**[126] and **59**[127]. Other variations involve derivatisation of the Cp ring to which the phosphorus is not bonded, as with **60**[128] and **61**[129]. Recent reports by Butler *et al.*[130] include several such derivatives, as well as more complex structures like **62**, which is in one sense a dppf-type compound.

Other ferrocenylphosphine compounds which belong to the class being reviewed in this Section are the ferrocenylphosphines[131] pictured in Figure 5.8, as well as the ferrocenylphosphine polymers discussed in Section 6.1.1.

1.3.2 Ferrocenylphosphines Containing a Cp-C-P Link

With the notable exception of the Josiphos-type ligands and TRAPs discussed in Section 1.2, very little has been published in the literature concerning compounds where the phosphine is separated from the ferrocenyl moiety by a carbon spacer. This is in contrast with the vast amount which has been published with regards to ferrocenylphosphines with a direct P-Cp link, and suggests that there is much work that could be carried out into developing synthetic methods and applications for ferrocenylmethylphosphines and related compounds.

The earliest reported compound of this type was $FcCH_2PPh_2$, originally prepared by the reduction of the ylide $FcCH{=}PPh_3$ with $LiAlH_4$[132]. A later synthesis used the reflux of diphenylphosphine with either $[FcCH_2NMe_3]I$ or $FcCH_2OH$ in aqueous solution for 18 or 24 hours respectively to give the desired product[133]. It was shown that $(FcCH_2)_2PPh$ could also be synthesised by reaction of phenylphosphine and $[FcCH_2NMe_3]I$ under the same reaction conditions. The phosphine oxide and sulfide derivatives of $FcCH_2PPh_2$ have also been prepared[133,134], but no 'true' complexation chemistry has been reported. However, as shown in Scheme 1.14, reaction of an *ortho*-lithiated ferrocenylamine with Me_3SnCl gives a stannyl derivative which can be reacted with diphenylphosphine in order to give an *ortho*-metallated derivative of $FcCH_2PPh_2$[135].

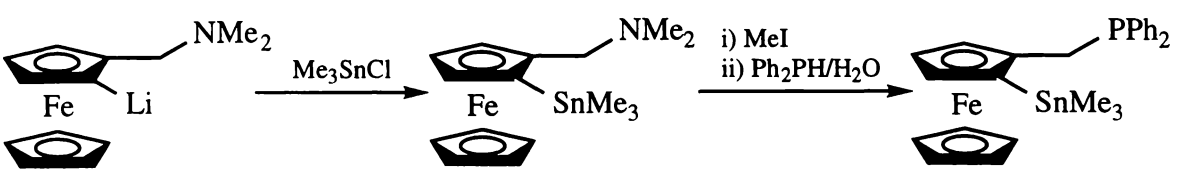

Scheme 1.14: Synthesis of an *ortho*-metallated $FcCH_2PPh_2$ derivative.

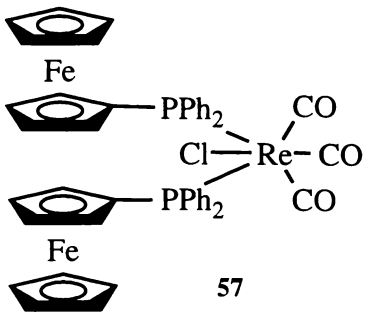

57

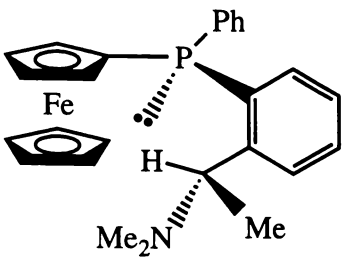

58

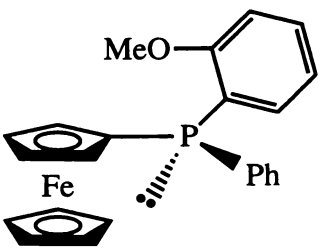

59

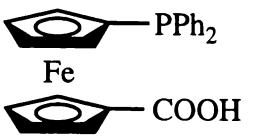

60

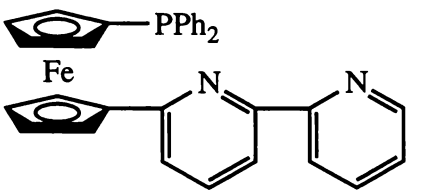

61

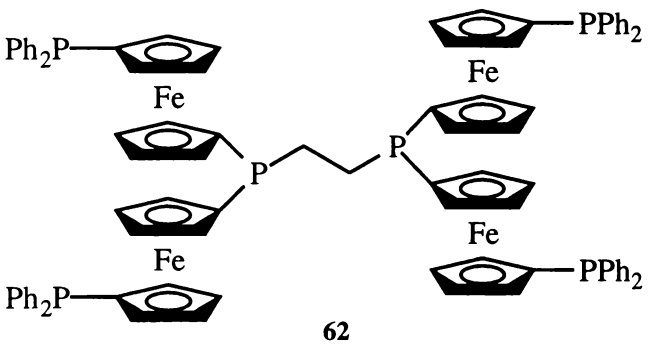

62

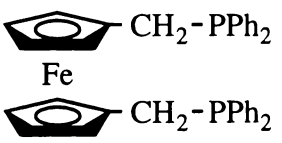

63

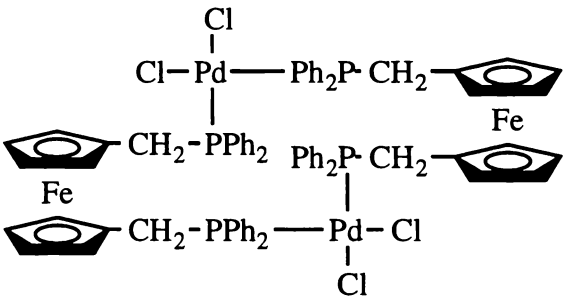

64

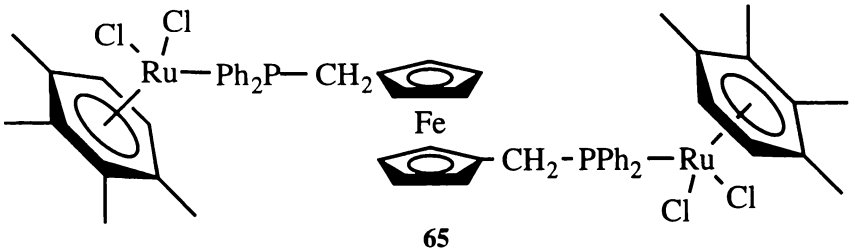

65

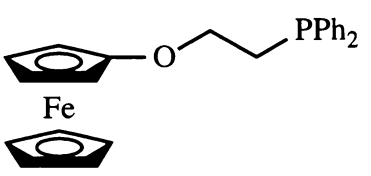

66

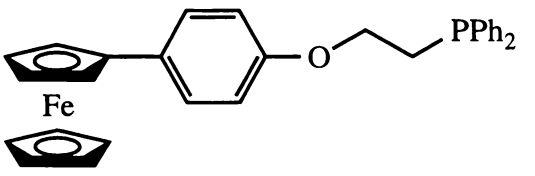

67

Surprisingly, in view of the vast amount of literature concerning dppf, the analogous compound 1,1'-bis(diphenylphosphinomethyl)ferrocene (dpmf) **63** was not synthesised until 1994, along with a doubly-bridged palladium complex **64**[136]. It was prepared by reaction of $Fe(\eta^5\text{-}C_5H_4CH_2Cl)_2$ with lithium diphenylphosphide. More recently the bimetallic bridged complex **65** has been reported, along with others of similar structure, where the arene group is C_6Me_6, *p*-cymene, 1,2,3,5-$Me_4C_6H_2$, 1,3,5-$Me_3C_6H_3$ or 1,2,3-$Me_3C_6H_3$[137]. The similar compound $Rh_2Cl_4Cp^*_2(dpmf)$[138] is also known. So then, only a very limited number of dpmf **63** complexes have been prepared, in spite of the fact that dpmf **63** appears to be a flexible ligand suitable for further coordination studies.

1.3.3 Other Ferrocenylphosphines

A limited number of compounds have been reported where the phosphine moiety is separated from the ferrocenyl group by an ethylene function or something greater. Two similar ferrocenylphosphine ethers are the compounds **66**[139] and **67**[140]. Another compound which has been used to generate several different complexes is the keto-ferrocenylphosphine **68**[141]. Compound **69** is prepared by the novel method of electrochemical oxidation of a cobalt complex to which is coordinated two FcC≡CH ligands and triphenylphosphine. Following oxidation, intramolecular insertion of the phosphine leads to formation of **69** in 38% yield. Another unusual ferrocenylphosphine is the [5]phosphaferrocenophane **70**[142].

1.4 Redox Behaviour of Ferrocenylphosphines

Discussion so far has centred largely about structural features of ferrocenylphosphines, but study of these compounds is also attractive to researchers because of the straightforward redox behaviour of ferrocene, which is well known for its ability to be reversibly converted

to the stable ferrocenium cation by electrochemical or chemical means. The electrochemical behaviour of ferrocenylphosphines is discussed at length in Section 5.1.2. One potential use for the redox properties of ferrocene is dealt with in Chapter 6. Discussion at this point will be limited to giving some illustrative examples showing how the redox behaviour of a ferrocenylphosphine ligand can be put to use in a complex.

Where ligands in a complex contain a ferrocene unit, there is the potential to tune the spectroscopic or reactivity properties of the metal centre in the complex by changing the oxidation state of the ferrocene. This is similar to changes which might be induced in a complex by replacing one ligand, such as Cp, with another, such as Cp*. However, changing the oxidation state of a ferrocenyl ligand would allow easily reversible control of reactivity. Studies into compound **57** and the related complex $ReCl(CO)_3(dppf)$ have been driven by this kind of thinking[122]. Study of the ligands **66** and **67** has produced interesting results; both were designed to perform differently depending on the ferrocene redox state. In the case of **66**, the ligand was designed to contain a function which would bind strongly to Rh (phosphine), and another that would bind weakly (ether)[139]. The binding affinities of the ether function can be modified by changing the redox state of the ferrocene function. Thus the fascinating result of oxidising the complex $[Rh(\mathbf{66})_2]BF_4$ is to induce a reaction involving both dimerisation and replacement of the ether functions by ligand phenyl groups, as shown in Scheme 1.15. The entire process, involving a two-electron oxidation of the starting material, is entirely reversible under cyclic voltammetric conditions (for information on cyclic voltammetry see Section 5.1.1.1).

Interesting results are also obtained with studies of the complex **71**, which contains ligand **67**. Oxidation of the ferrocene groups leads to greater lability of the arene functions[140], leading to faster intramolecular arene-arene exchange reactions as well as faster rates of catalysis for olefin isomerisation[143].

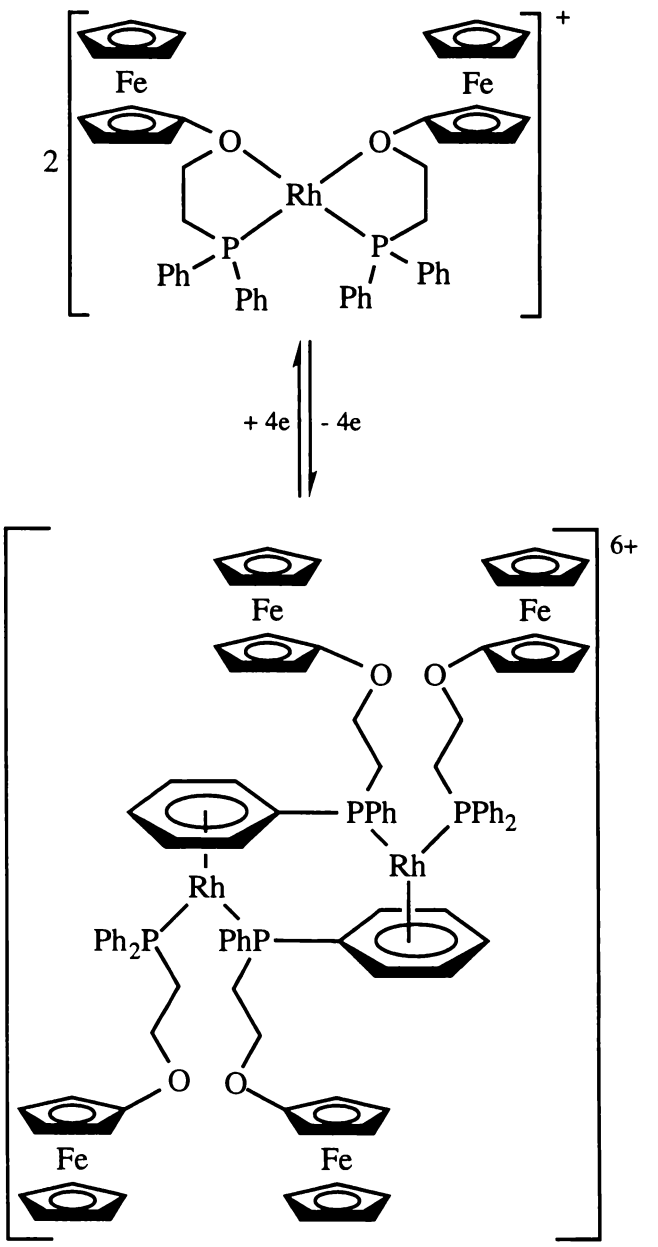

Scheme 1.15: Oxidation of ferrocene groups in a Rh complex leads to a complex dimerisation reaction, resulting from increased lability of the ether functions neighbouring the ferrocene groups.

1.5 Related Topics

Research into ferrocenylphosphine compounds is of course only a part of the very large field of study into metallocenes which has from the beginning been an integral part of organometallic chemistry. Much of this material is related to ferrocenylphosphine chemistry,

but is beyond the scope of this review. For information on ferrocenylphosphine chalcogenides[5,144], ferrocenylphosphites[145], phosphonites[146] and phosphonates[147], ferrocenylphosphonium salts[148], metallocenylphosphines[149], ferrocenylarsines[83,107c], ferrocenyl compounds with phosphorus-phosphorus bonds[150], and other unusual ferrocenylphosphorus compounds[151], refer to the references indicated. Section 6.1.1 contains information on [1]phosphaferrocenophanes.

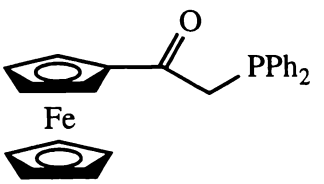

68

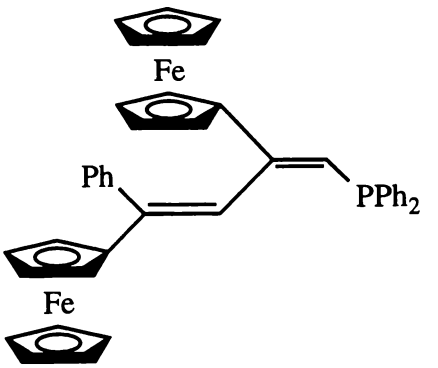

69

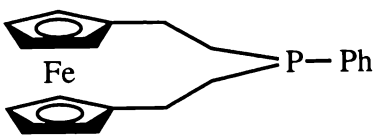

70

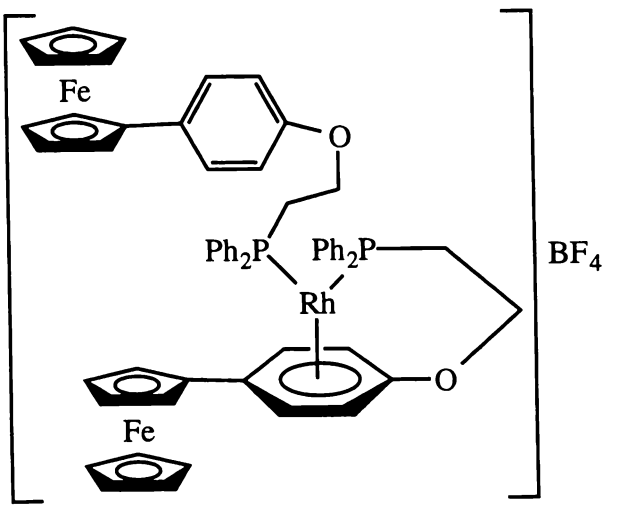

71

1.6 References

1 G. P. Sollott, J. L. Snead, S. Portnoy, W. R. Peterson Jr., H. E. Mertwoy, *Chem. Abstr.*, 1965, **63**, 18147b.

2 K.-S. Gan, T. S. A. Hor, *1,1'-Bis(diphenylphosphino)ferrocene - Coordination Chemistry, Organic Syntheses, and Catalysis*, in *Ferrocenes*, A. Togni, T. Hayashi (Ed.), 1995, VCH Verlagsgesellschaft mbH, Weinheim, p. 3.

3 M. C. Gimeno, P. G. Jones, A. Laguna, C. Sarroca, *J. Chem. Soc., Dalton Trans.*, 1995, 1473.

4 I. R. Butler, L. J. Hobson, S. J. Coles, M. B. Hursthouse, K. M. A. Malik, *J. Organomet. Chem.*, 1997, **540**, 27.

5 S. Coco, P. Espinet, *J. Organomet. Chem.*, 1994, **484**, 113.

6 T. J. Colacot, R. A. Teichman, R. Cea-Olivares, J.-G. Alvarado-Rodrigues, R. A. Toscano, W. J. Boyko, *J. Organomet. Chem.*, 1998, **557**, 169.

7 C. Amatore, G. Broeker, A. Jutand, F. Khalil, *J. Am. Chem. Soc.*, 1997, **119**, 5176.

8 Z.-G. Fang, P. M. N. Low, S.-C. Ng, T. S. A. Hor, *J. Organomet. Chem.*, 1994, **483**, 17.

9 J. D. Bradshaw, L. Guo, C. A. Tessier, W. J. Youngs, *Organometallics*, 1996, **15**, 2582.

10 G. Li, S. Li, A. L. Tan, W.-H. Yip, T. C. W. Mak, T. S. A. Hor, *J. Chem. Soc., Dalton Trans.*, 1996, 4315.

11 M. Zhou, C.-F. Lam, K. F. Mok, P.-H. Leung, T. S. A. Hor, *J. Organomet. Chem.*, 1994, **476**, C32.

12 M. Zhou, Y. Xu, A.-M. Tan, P.-H. Leung, K. F. Mok, L.-L. Koh, T. S. A. Hor, *Inorg. Chem.*, 1995, **34**, 6425.

13 M. A. Zhuravel, D. S. Glueck, L. M. Liable-Sands, A. L. Rheingold, *Organometallics*, 1998, **17**, 574.

14 P. J. Stang, B. Olenyuk, J. Fan, A. M. Arif, *Organometallics*, 1996, **15**, 904.

15 J. McGinley, V. McKee, C. J. McKenzie, *Acta Cryst.*, 1998, **C54**, 345.

16 B. Corain, B. Longato, G. Favero, D. Ajo, G. Pilloni, U. Russo, F. R. Kreissl, *Inorg. Chim. Acta*, 1989, **157**, 259. K. R. Mann, W. H. Morrison Jr., D. N. Hendrickson, *Inorg. Chem.*, 1974, **13**, 1180.

17 S. P. Neo, Z.-Y. Zhou, T. C. W. Mak, T. S. A. Hor, *J. Chem. Soc., Dalton Trans.*, 1994, 3451.

18 M. Sato, M. Asai, *J. Organomet. Chem.*, 1996, **508**, 121.

19 a) R. T. Hembre, J. S. McQueen, *Angew. Chem. Int. Ed. Engl.*, 1997, **36**, 65. b) R. T. Hembre, J. S. McQueen, V. W. Day, *J. Am. Chem. Soc.*, 1996, **118**, 798.

20 F. A. Cotton, G. Wilkinson, *Advanced Inorganic Chemistry*, 1988, 5th Ed., John Wiley & Sons, New York, 879.

21 T.-J. Kim, K.-H. Kwon, S.-C. Kwon, J.-O. Baeg, S.-C. Shim, D.-H. Lee, *J. Organomet. Chem.*, 1990, **389**, 205.

22 A. Santos, J. Lopez, J. Montoya, P. Noheda, A. Romero, A. M. Echavarren, *Organometallics*, 1994, **13**, 3605.

23 V. W.-W. Yam, V. W.-M. Lee, K.-K. Cheung, *J. Chem. Soc., Dalton Trans.*, 1997, 2335.

24 S. P. Nolan, T. R. Belderrain, R. H. Grubbs, *Organometallics*, 1997, **16**, 5569.

25 S. C. N. Hsu, W.-Y. Yeh, M. Y. Chiang, *J. Organomet. Chem.*, 1995, 121.

26 S. Onaka, M.-A. Haga, S. Takagi, M. Otsuka, K. Mizuno, *Bull. Chem. Soc. Jpn.*, 1994, **67**, 2440.

27 P. K. Baker, S. G. Fraser, P. Harding, *Inorg. Chim. Acta*, 1986, **116**, L5.

28 K.-S. Gan, T. S. A. Hor, *1,1'-Bis(diphenylphosphino)ferrocene - Coordination Chemistry, Organic Syntheses, and Catalysis*, in *Ferrocenes*, A. Togni, T. Hayashi (Ed.), 1995, VCH Verlagsgesellschaft mbH, Weinheim, p. 18-27, and references therein.

29 V. W.-W. Yam, S. W.-K. Choi, K.-K. Cheung, *J. Chem. Soc., Dalton Trans.*, 1996, 3411.

30 M. C. Gimeno, A. Laguna, C. Sarroca, *Inorg. Chem.*, 1993, **32**, 5926.

31 F. Canales, M. C. Gimeno, P. G. Jones, A. Laguna, C. Sarroca, *Inorg. Chem.*, 1997, **36**, 5206.

32 P. M. N. Low, Z.-Y. Zhang, T. C. W. Mak, T. S. A. Hor, *J. Organomet. Chem.*, 1997, **539**, 45.

33 S. Onaka, Y. Katsukawa, M. Yamashita, *J. Organomet. Chem.*, 1998, **564**, 249.

34 A. Houlton, D. M. P. Mingos, D. M. Murphy, D. J. Williams, *Acta Cryst.*, 1995, C**51**, 30.

35 L.-T. Phang, T. S. A. Hor, Z.-Y. Zhou, T. C. W. Mak, *J. Organomet. Chem.*, 1994, **469**, 253.

36 E. Stein, F. Y. Fujiwara, *J. Organomet. Chem.*, 1996, **525**, 31.

37 J. W.-S. Hui, W.-T. Wong, *J. Chem. Soc., Dalton Trans.*, 1997, 2445.

38 P. M. N. Low, A. L. Tan, T. S. A. Hor, *Organometallics*, 1996, **15**, 2595.

39 K. J. Donaghy, P. J. Carroll, L. G. Sneddon, *Inorg. Chem.*, 1997, **36**, 547.

40 D. S. Shepard, B. F. G. Johnson, A. Harrison, S. Parsons, S. P. Smidt, L. J. Yellowlees, D. Reed, *J. Organomet. Chem.*, 1998, **563**, 113. M. I. Bruce, P. A. Humphrey, O. bin Shawkataly, M. R. Snow, E. R. T. Tiekink, W. R. Cullen, *Organometallics*, 1990, **9**, 2910.

41 Y.-Y. Choi, W.-T. Wong, *J. Organomet. Chem.*, 1997, 121.

42 J. R. Galsworthy, C. E. Housecroft, A. L. Rheingold, *J. Chem. Soc., Dalton Trans.*, 1996, 2917.

43 C. J. McAdam, N. W. Duffy, B. H. Robinson, J. Simpson, *J. Organomet. Chem.*, 1997, **527**, 179.

44 M. Viotte, B. Gautheron, I. Nifant'ev, L. G. Kuz'mina, *Chem. Abstr.*, 1997, **126**, 75013.

45 F. Canales, M. C. Gimeno, A. Laguna, P. G. Jones, *J. Am. Chem. Soc.*, 1996, **118**, 4839. F. Canales, M. C. Gimeno, A. Laguna, P. G. Jones, *Organometallics*, 1996, **15**, 3412.

46 T. S. A. Hor, L.-T. Phang, *Chem. Abstr.*, 1997, **126**, 277574e. T. S. A. Hor, L.-T. Phang, *J. Organomet. Chem.*, 1990, **381**, 121. T.-J. Kim, S.-C. Kwon, Y.-H. Kim, N. H. Heo, M. M. Teeter, A. Yamano, *J. Organomet. Chem.*, 1991, **426**, 71.

47 a) T. Hayashi, M. Konishi, M. Kumada, *Tetrahedron Lett.*, 1979, 1871. b) T. Hayashi, M. Konishi, M. Kumada, *J. Organomet. Chem.*, 1980, **186**, C1.

48 D. E. Bergstrom, M. K. Ogawa, *J. Am. Chem. Soc.*, 1978, **100**, 8106. R. H. Grubbs, A. Miyashita, M. Liu, P. Burk, *J. Am. Chem. Soc.*, 1978, **100**, 2418. D. L. Reger, E. C. Culbertson, *J. Am. Chem. Soc.*, 1976, **98**, 2789.

49 K. Itoh, M. Miura, M. Nomura, *Tetrahedron Lett.*, 1992, **33**, 5369.

50 T. Hayashi, A. Yamamoto, T. Hagihara, *J. Org. Chem.*, 1986, **51**, 723.

51 N. A. Bumagin, E. V. Luzikova, *J. Organomet. Chem.*, 1997, **532**, 271.

52 O. L. Casagrande Jr., A. E. Gerbase, F. C. Stedile, F. O. V. Cunha, L. Amaral, I. J. R. Baumvol, *Polyhedron*, 1997, **16**, 171.

53 a) T. Hayashi, *Asymmetric Catalysis with Chiral Ferrocenylphosphine Ligands*, in *Ferrocenes*, A Togni, T. Hayashi (Ed.), 1995, VCH Verlagsgesellschaft mbH, Weinheim, p. 105. b) H. B. Kagan, P. Diter, A. Gref, D. Guillaneux, A. Masson-Szymczak, F. Rebiere, O. Riant, O. Samuel, S. Taudien, *Pure & Appl. Chem.*, 1996, **68**, 29. c) A. Togni, *Angew. Chem. Int. Ed. Engl.*, 1996, **35**, 1475. d) B. M. Trost, *Acc. Chem. Res.*, 1996, **29**, 355. e) M. Kumada, *J. Organomet. Chem.*, 1995, **500**, 195. f) M. Sawamura, Y. Ito, *Chem. Rev.*, 1992, **92**, 857. g) C. J. Richards, A. J. Locke, *Tetrahedron: Asymmetry*, 1998, **9**, 2377. More general review on asymmetric catalysis, including ferrocenylphosphines: E. J. Corey, A. Guzman-Perez, *Angew. Chem. Int. Ed. Engl.*, 1998, **37**, 388.

54 S. Borman, *Chemical & Engineering News*, July 22 1996, 38.

55 G. Wagner, R. Herrmann, *Chiral Ferrocene Derivatives. An Introduction*, in *Ferrocenes*, A Togni, T. Hayashi (Ed.), 1995, VCH Verlagsgesellschaft mbH, Weinheim, p. 173-174.

56 D. Marquarding, H. Klusacek, G. Gokel, P. Hoffmann, I. Ugi, *J. Am. Chem. Soc.*, 1970, **92**, 5389.

57 T. Hayashi, K. Yamamoto, M. Kumada, *Tetrahedron Lett.*, 1974, 4405.

58 T. Hayashi, T. Mise, M. Fukushima, M. Kagotani, N. Nagashima, Y. Hamada, A. Matsumoto, S. Kawakami, M. Konishi, K. Yamamoto, M. Kumada, *Bull. Chem. Soc. Jpn.*, 1980, **53**, 1138.

59 T. Hayashi, M. Tajika, K. Tamao, M. Kumada, *J. Am. Chem. Soc.*, 1976, **98**, 3718. T. Hayashi, M. Konishi, M. Fukushima, T. Mise, M. Kagotani, M. Tajika, M. Kumada, *J. Am. Chem. Soc.*, 1982, **104**, 180.

60 J. A. S. Howell, K. Humphries, P. McArdle, D. Cunningham, G. Nicolosi, A. Patti, M. A. Walsh, *Tetrahedron: Asymmetry*, 1997, **8**, 1027. L. Schwink, P. Knochel, *Tetrahedron Lett.*, 1996, **37**, 25. W. Brieden, *Chem. Abstr.*, 1996, **125**, 143018x. C. Ganter, T. Wagner, *Chem. Ber.*, 1995, **128**, 1157.

61 a) B. F. M. Kimmich, C. R. Landis, D. R. Powell, *Organometallics*, 1996, **15**, 4141. b) G. Kutschera, C. Kratky, W. Weissensteiner, M. Widhalm, *J. Organomet. Chem.*, 1996, **508**, 195. c) A. Ohno, M. Yamane, T. Hayashi, N. Oguni, M. Hayashi, *Tetrahedron: Asymmetry*, 1995, **6**, 2495. d) A. Yamazaki, T. Morimoto, K. Achiwa, *Tetrahedron: Asymmetry*, 1993, **4**, 2287. e) M. Sawamura, H. Nagata, H. Sakamoto, Y. Ito, *J. Am. Chem. Soc.*, 1992, **114**, 2586.

62 B. Jedlicka, C. Kratky, W. Weissensteiner, M. Widhalm, *J. Chem. Soc., Chem. Commun.*, 1993, 1329.

63 A. Mernyi, C. Kratky, W. Weissensteiner, M. Widhalm, *J. Organomet. Chem.*, 1996, **508**, 209.

64 R. Fernandez-Galan, F. A. Jalon, B. R. Manzano, J. Rodriguez-de la Fuente, M. Vrahami, B. Jedlicka, W. Weissensteiner, G. Jogl, *Organometallics*, 1997, **16**, 3758. M. Viotte, B. Gautheron, R. G. Parish, R. G. Pritchard, *Acta Cryst.*, 1996, C**52**, 1891. R. E. Blumer, F. Lianza, P. S. Pregosin, H. Rüegger, A. Togni, *Inorg. Chem.*, 1993, **32**, 2663.

65 B. Jedlicka, R. E. Ruelke, W. Weissensteiner, R. Fernandez-Galan, F. A. Jalon, B. R. Manzano, J. Rodriguez-de la Fuente, N. Veldman, H. Kooijman, A. L. Spek, *J. Organomet. Chem.*, 1996, **516**, 97.

66 F. Lianza, A. Macchioni, P. Pregosin, H. Rüegger, *Inorg. Chem.*, 1994, **33**, 4999.

67 S. Kaneko, T. Yoshino, T. Katoh, S. Terashima, *Tetrahedron: Asymmetry*, 1997, **8**, 829. J.-F. Marcoux, S. Wagaw, S. L. Buchwald, *J. Org. Chem.*, 1997, **62**, 1568. Y. Nishibayashi, J. D. Singh, Y. Arikawa, S. Uemura, M. Hidai, *J. Organomet. Chem.*, 1997, **531**, 13. A. Togni, S. D. Pastor, G. Rihs, *J. Organomet. Chem.*,

1990, **381**, C21. K. Yamamoto, J. Wakatsuki, R. Sugimoto, *Bull. Chem. Soc. Jpn.*, 1980, **53**, 1132.

68 T. Hayashi, *Chem. Abstr.*, 1997, **126**, 31651n. N. Kawamura, *Chem. Abstr.*, 1996, **125**, 57975a.

69 Y. Nishibayashi, K. Segawa, K. Ohe, S. Uemura, *Organometallics*, 1995, **14**, 5486. T. Sammakia, H. A. Latham, D. R. Schaad, *J. Org. Chem.*, 1995, **60**, 10.

70 C. J. Richards, A. W. Mulvaney, *Tetrahedron: Asymmetry*, 1996, **7**, 1419.

71 Y. Nishibayashi, I. Takei, S. Uemura, M. Hidai, *Organometallics*, 1998, **17**, 3420. Y. Nishibayashi, K. Segawa, Y. Arikawa, K. Ohe, M. Hidai, S. Uemura, *J. Organomet. Chem.*, 1997, **545-546**, 381. K. H. Ahn, C.-W. Cho, J. Park, S. Lee, *Tetrahedron: Asymmetry*, 1997, **8**, 1179. A. Chesney, M. R. Bryce, R. W. J. Chubb, A. S. Batsanov, J. A. K. Howard, *Tetrahedron: Asymmetry*, 1997, **8**, 2337. Y. Nishibayashi, K. Segawa, H. Takada, K. Ohe, S. Uemura, *Chem. Commun.*, 1996, 847. T. Sammakia, H. A. Latham, *J. Org. Chem.*, 1995, **60**, 6002.

72 U. Burckhardt, L. Hintermann, A. Schnyder, A. Togni, *Organometallics*, 1995, **14**, 5415. A. Schnyder, L. Hintermann, A. Togni, *Angew. Chem. Int. Ed. Engl.*, 1995, **34**, 931.

73 A. Schnyder, A. Togni, U. Wiesli, *Organometallics*, 1997, **16**, 255. U. Burckhardt, M. Baumann, A. Togni, *Tetrahedron: Asymmetry*, 1997, **8**, 155. U. Burckhardt, M. Baumann, G. Trabesinger, V. Gramlich, A. Togni, *Organometallics*, 1997, **16**, 5252. U. Burckhardt, V. Gramlich, P. Hofmann, R. Nesper, P. S. Pregosin, R. Salzmann, A. Togni, *Organometallics*, 1996, **15**, 3496.

74 Y. Nishibayashi, I. Takei, M. Hidai, *Organometallics*, 1997, **16**, 3091.

75 a) Y. Nishibayashi, K. Segawa, J. D. Singh, S. Fukuzawa, K. Ohe, S. Uemura, *Organometallics*, 1996, **15**, 370. b) J. Spencer, V. Gramlich, R. Häusel, A. Togni, *Tetrahedron: Asymmetry*, 1996, **7**, 41.

76 A. Albinati, P. S. Pregosin, K. Wick, *Organometallics*, 1996, **15**, 2419.

77 T. Hayashi, C. Hayashi, Y. Uozumi, *Tetrahedron: Asymmetry*, 1995, **6**, 2503.

78 W. Zhang, T. Kida, Y. Nakatsuji, I. Ikeda, *Tetrahedron Lett.*, 1996, **37**, 7995.

79 T. Hayashi, K. Kanehira, T. Hagihara, M. Kumada, *J. Org. Chem.*, 1988, **53**, 113.

80 T. Hayashi, N. Kawamura, Y. Ito, *J. Am. Chem. Soc.*, 1987, **109**, 7876. T. Hayashi, N. Kawamura, T. Ito, *Tetrahedron Lett.*, 1988, **29**, 5969.

81 Y. Ito, M. Sawamura, T. Hayashi, *Tetrahedron Lett.*, 1987, **28**, 6215. T. Hayashi, M. Sawamura, Y. Ito, *Tetrahedron*, 1992, **48**, 1999.

82 A. Togni, C. Breutel, A. Schnyder, F. Spindler, H. Landert, A. Tijani, *J. Am. Chem. Soc.*, 1994, **116**, 4062.

83 N. C. Zanetti, F. Spindler, J. Spencer, A. Togni, G. Rihs, *Organometallics*, 1996, **15**, 860.

84 H. C. L. Abbenhuis, U. Burckhardt, V. Gramlich, A. Togni, A. Albinati, B. Müller, *Organometallics*, 1994, **13**, 4481.

85 a) P. Barbaro, C. Bianchini, A. Togni, *Organometallics*, 1997, **16**, 3004. b) P. Barbaro, A. Togni, *Organometallics*, 1995, **14**, 3570.

86 H. C. L. Abbenhuis, U. Burckhardt, V. Gramlich, C. Kollner, P. S. Pregosin, R. Salzmann, A. Togni, *Organometallics*, 1995, **14**, 759.

87 F. Spindler, B. Pugin, H.-P. Jallet, H.-P. Buster, U. Pittelkow, H.-U. Blaser, *Chem. Abstr.*, 1997, **126**, 19005x.

88 C. Breutel, P. S. Pregosin, R. Salzmann, A. Togni, *J. Am. Chem. Soc.*, 1994, **116**, 4067.

89 P. Barbaro, P. S. Pregosin, R. Salzmann, A. Albinati, R. W. Kunz, *Organometallics*, 1995, **14**, 5160. P. S. Pregosin, R. Salzmann, A. Togni, *Organometallics*, 1995, **14**, 842.

90 H. C. L. Abbenhuis, U. Burckhardt, V. Gramlich, A. Martelletti, J. Spencer, I. Steiner, A. Togni, *Organometallics*, 1996, **15**, 1614.

91 P. S. Pregosin, G. Trabesinger, *J. Chem. Soc., Dalton Trans.*, 1998, 727.

92 R. Dorta, A. Togni, *Organometallics*, 1998, **17**, 3423.

93 J. McGarrity, F. Spindler, R. Fuchs, M. Eyer, *Chem. Abstr.*, 1995, **122**, 81369q.

94 S. C. Stinson, *Chemical & Engineering News*, Jan 19 1998, 49.

95 B. Pugin, *Chem. Abstr.*, 1997, **126**, 185879e. B. Pugin, *Chem. Abstr.*, 1997, **126**, 8302r. B. Pugin, *Chem. Abstr.*, 1996, **125**, 276188z. F. Spindler, A. Wirth-Tijani, H. Landeret, *Chem. Abstr.*, 1994, **121**, 301077q.

96 *Fluka catalogue*, 1997/1998, p. 511 numbers 36677, 36678, 36679, and p. 609 numbers 43164, 43166.

97 M. Sawamura, H. Hamashima, Y. Ito, *Tetrahedron: Asymmetry*, 1991, **2**, 593.

98 M. Sawamura, R. Kuwano, Y. Ito, *Angew. Chem. Int. Ed. Engl.*, 1994, **33**, 111.

99 M. Sawamura, R. Kuwano, Y. Ito, *J. Am. Chem. Soc.*, 1995, **117**, 9602.

100 M. Sawamura, H. Hamashima, M. Sugawara, R. Kuwano, Y. Ito, *Organometallics*, 1995, **14**, 4549.

101 R. Kuwano, M. Sawamura, Y. Ito, *Tetrahedron: Asymmetry*, 1995, **6**, 2521.

102 R. Kuwano, M. Sawamura, J. Shirai, M. Takahashi, Y. Ito, *Tetrahedron Lett.*, 1995, **36**, 5239.

103 M. Sawamura, R. Kuwano, J. Shirai, Y. Ito, *Synlett*, 1995, 347.

104 M. Sawamura, H. Hamashima, Y. Ito, *Tetrahedron*, 1994, **50**, 4439. M. Sawamura, H. Hamashima, Y. Ito, *J. Am. Chem. Soc.*, 1992, **114**, 8295.

105 Y. Ito, *Chem. Abstr.*, 1996, **124**, 8239j.

106 M. J. Burk, M. F. Gross, *Tetrahedron Lett.*, 1994, **35**, 9363.

107 a) M. Adachi, M. Kita, K. Kashiwabara, J. Fujita, N. Ititaka, S. Kurachi, S. Ohba, D.-M. Jin, *Bull. Chem. Soc. Jpn.*, 1992, **65**, 2037. b) Y. Kiso, M. Kumada, K. Tamao, M. Umeno, *J. Organomet. Chem.*, 1973, **50**, 297. c) J. J. Bishop, A. Davison, M. L. Katcher, D. W. Lichtenberg, R. E. Merill, J. C. Smart, *J. Organomet. Chem.*, 1971, **27**, 241.

108 a) A. G. Avent, R. B. Bedford, P. A. Chaloner, S. Z. Dewa, P. B. Hitchcock, *J. Chem. Soc., Dalton Trans.*, 1996, 4633. b) M. J. Burk, T. G. P. Harper, J. R. Lee, C. Kalberg, *Tetrahedron Lett.*, 1994, **35**, 4963. c) W. R. Cullen, S. J. Rettig, T.-C. Zheng, *Organometallics*, 1992, **11**, 853.

109 W. R. Cullen, T.-J. Kim, F. W. B. Einstein, T. Jones, *Organometallics*, 1985, **4**, 346.

110 I. R. Butler, W. R. Cullen, T.-J. Kim, F. W. B. Einstein, T. Jones, *J. Chem. Soc., Chem. Commun.*, 1984, 719.

111 G. E. Herberich, S. Moss, *Chem. Ber.*, 1995, **128**, 689. G. E. Herberich, S. Moss, A. Schultz, *Acta Cryst.*, 1996, C**52**, 1080.

112 E. B. Kaloun, R. Merdes, J.-P. Genet, J. Uziel, S. Juge, *J. Organomet. Chem.*, 1997, **529**, 455.

113 U. Nettekoven, M. Widhalm, P. C. J. Kamer, P. W. N. M. Van Leeuwen, *Tetrahedron: Asymmetry*, 1997, **8**, 3185.

114 P. Zanello, G. Opromolla, G. Giorgi, G. Sasso, A. Togni, *J. Organomet. Chem.*, 1996, **506**, 61. N. W. Duffy, C. J. McAdam, B. H. Robinson, J. Simpson, *Inorg. Chem.*, 1994, **33**, 5343.

115 R. A. Brown, A. Houlton, R. M. G. Roberts, J. Silver, *Polyhedron*, 1992, **11**, 2611.

116 I. R. Butler, L. J. Hobson, S. M. E. Macan, D. J. Williams, *Polyhedron*, 1993, **12**, 1901.

117 M. Viotte, B. Gautheron, M. M. Kubicki, Y. Mugnier, R. V. Parish, *Inorg. Chem.*, 1995, **34**, 3465.

118 G. P. Sollott, W. R. Peterson Jr., *J. Organomet. Chem.*, 1969, **19**, 143. G. P. Sollott, H. E. Mertwoy, S. Portnoy, J. L. Snead, *J. Org. Chem.*, 1963, **28**, 1090.

119 a) S. Otto, A. Roodt, *Acta Cryst.*, 1997, C**53**, 1414. b) F. Estevan, J. Latorre, E. Peris, *Polyhedron*, 1993, **12**, 2153. c) W. R. Cullen, S. T. Chacon, M. I. Bruce, F. W. B. Einstein, R. H. Jones, *Organometallics*, 1988, **7**, 2273. d) J. C. Kotz, C. L. Nivert, J. M. Lieber, R. C. Reed, *J. Organomet. Chem.*, 1975, **91**, 87. e) J. C. Kotz, C. L. Nivert, *J. Organomet. Chem.*, 1973, **52**, 387.

120 P. Stepnicka, R. Gyepes, O. Lavastre, P. H. Dixneuf, *Organometallics*, 1997, **16**, 5089.

121 F. Estevan, P. Lahuerta, J. Latorre, E. Peris, S. Garcia-Granda, F. Gomez-Beltran, A. Aguirre, M. A. Salvado, *J. Chem. Soc., Dalton Trans.*, 1993, 1681.

122 T. M. Miller, K. J. Ahmed, M. S. Wrighton, *Inorg. Chem.*, 1989, **28**, 2347.

123 a) T. E. Muller, J. C. Green, D. M. P. Mingos, C. M. McPartlin, C. Whittingham, D. J. Williams, T. M. Woodroffe, *J. Organomet. Chem.*, 1998, **551**, 313. b) J. Granifo, A. Vega, M. T. Garland, *Polyhedron*, 1998, **17**, 1729. c) R. D. Pergola, C. Bandini, F. Demartin, E. Diana, L. Garlaschelli, P. L. Stanghellini, P. Zanello, *J. Chem. Soc., Dalton Trans.*, 1996, 747. d) T. C. Zheng, W. R. Cullen, S. J. Rettig, *Organometallics*, 1994, **13**, 3594. e) V. S. Tolkunova, A. S. Peregudov, Y. Y. Gorelikova, A. I. Krylova, E. N. Tavetkov, V. D. Vil'chevskaya, D. N. Kravtsov, *Chem. Abstr.*, 1991, **115**, 29561n. f) A. Houlton, R. M. G. Roberts, J. Silver, M. G. B. Drew, *J. Chem. Soc., Dalton Trans.*, 1990, 1543.

124 C. U. Pittman Jr., G. O. Evans, *J. Organomet. Chem.*, 1972, **43**, 361.

125 G. R. Knox, P. L. Pauson, D. Willison, *Organometallics*, 1992, **11**, 2930.

126 I. R. Butler, W. R. Cullen, S. J. Rettig, A. S. C. White, *J. Organomet. Chem.*, 1995, **492**, 157.

127 J. M. Brown, J. C. P. Laing, *J. Organomet. Chem.*, 1997, **529**, 435.

128 P. Stepnicka, J. Podlaha, R. Gyepes, M. Polasek, *J. Organomet. Chem.*, 1998, **552**, 293. J. Podlaha, P. Stepnicka, J. Ludvik, I. Cisarova, *Organometallics*, 1996, **15**, 543.

129 I. R. Butler, M. Kalaji, L. Nehrlich, M. Hursthouse, A. I. Karaulov, K. M. A. Malik, *J. Chem. Soc., Chem. Commun.*, 1995, 459. I. R. Butler, *Polyhedron*, 1992, **11**, 3117.

130 I. R. Butler, S. C. Quayle, *J. Organomet. Chem.*, 1998, **552**, 63. I. R. Butler, R. L. Davies, *Synthesis*, 1996, 1350.

131 A. Masson-Szymczak, O. Riant, A. Gref, H. B. Kagan, *J. Organomet. Chem.*, 1996, **511**, 193.

132 P. L. Pauson, W. E. Watts, *J. Chem. Soc.*, 1963, 2990.

133 G. Marr, T. M. White, *J. Chem. Soc., Perkin Trans. I*, 1973, 1955.

134 C. Charrier, F. Mathey, *Tetrahedron Lett.*, 1978, 2407. G. Marr, B. J. Wakefield, T. M. White, *J. Organomet. Chem.*, 1975, **88**, 357.

135 S. Hoppe, H. Weichmann, K. Jurkschat, C. Schneider-Koglin, M. Drager, *J. Organomet. Chem.*, 1995, **505**, 63.

136 Y. Yamamoto, T. Tanase, I. Mori, Y. Nakamura, *J. Chem. Soc., Dalton Trans.*, 1994, 3191.

137 J.-F. Mai, Y. Yamamoto, *J. Organomet. Chem.*, 1998, **560**, 223.

138 J.-F. Ma, Y. Yamamoto, *J. Organomet. Chem.*, 1997, **545**, 577.

139 E. T. Singewald, C. A. Mirkin, C. L. Stern, *Angew. Chem. Int. Ed. Engl.*, 1995, **34**, 1624.

140 C. A. Sassano, C. A. Mirkin, *J. Am. Chem. Soc.*, 1995, **117**, 11379. A. M. Allgeier, C. A. Mirkin, *Organometallics*, 1997, **16**, 3071.

141 A. Louati, M. Huhn, *Inorg. Chem.*, 1993, **32**, 3601. D. Matt, M. Huhn, J. Fischer, A. De Cian, W. Klaui, I. Tkatchenko, M. C. Bonnet, *J. Chem. Soc., Dalton Trans.*, 1993, 1173. A. Louati, M. Gross, L. Douce, D. Matt, *J. Organomet. Chem.*, 1992, **438**, 167. P. Braunstein, L. Douce, F. Balegroune, D. Grandjean, D. Bayeul, Y. Dusausoy, P. Zanello, *New J. Chem.*, 1992, **16**, 925.

142 O. J. Curnow, G. Huttner, S. J. Smail, M. M. Turnbull, *J. Organomet. Chem.*, 1996, **524**, 267.

143 C. S. Slone, C. A. Mirkin, G. P. A. Yap, I. A. Guzei, A. L. Rheingold, *J. Am. Chem. Soc.*, 1997, **119**, 10743.

144 M. C. Gimeno, P. G. Jones, A. Laguna, C. Sarroca, *J. Chem. Soc., Dalton Trans.*, 1998, 1277. G. Pilloni, B. Longato, G. Bandoli, B. Corain, *J. Chem. Soc., Dalton Trans.*, 1997, 819. M. Bolte, F. Naumann, A. S. K. Hashmi, *Acta Cryst.*, 1997, C**53**, 1785. B. M. Yamin, O. bin Shawkataly, H.-K. Fun, K. Sivakumar, *Acta Cryst.*, 1996, C**52**, 1966. G. Pilloni, G. Valle, C. Corvaja, B. Longato, B. Corain, *Inorg. Chem.*, 1995, **34**, 5910. M. C. Gimeno, P. G. Jones, A. Laguna, C. Sarroca, *J. Chem. Soc., Dalton Trans.*, 1995, 3563. Z.-G. Fang, T. S. A. Hor, Y.-S. Wen, L.-K. Liu, T. C. W. Mak, *Polyhedron*, 1995, **14**, 2403. G. Pilloni, B. Corain, M. Degano, B. Longato, G. Zanotti, *J. Chem. Soc., Dalton Trans.*, 1993, 1777. V. S. Tolkunova, E. N. Tsvetkov, A. S. Peregudov, A. I. Krylova, Yu. Yu. Gorelikova, V. D. Vil'chevskaya, D. N. Kravtsov, *Chem. Abstr.*, 1990, **112**, 158519s.

145 M. Herberhold, H.-D. Brendel, A. Hofmann, B. Hofmann, W. Milius, *J. Organomet. Chem.*, 1998, **556**, 173.

146 I. E. Nifant'ev, L. F. Manzhukova, M. Yu. Antipin, Yu. T. Struchkov, E. E. Nifant'ev, *Chem. Abstr.*, 1996, **124**, 29967k.

147 W. Henderson, A. G. Oliver, A. J. Downard, *Polyhedron*, 1996, **15**, 1165.

148 V. I. Boev, L. V. Snegur, V. N. Babin, Yu. S. Nekrasov, *Russ. Chem. Rev.*, 1997, **66**, 613. S. Z. Ahmed, C. Glidewell, G. Ferguson, *Acta Cryst.*, 1996, C**52**, 1634. C. Imrie, T. A. Modro, P. H. Van Rooyen, *Polyhedron*, 1994, **13**, 1677. C. Glidewell, C. M. Zakaria, *Acta Cryst.*, 1994, C**50**, 233.

149 T. Gutmann, E. Dombrowski, N. Burzlaff, W. A. Schenk, *J. Organomet. Chem.*, 1998, **552**, 91. W. A. Schenk, T. Gutmann, *J. Organomet. Chem.*, 1998, **552**, 83. S. Li, B. Wei, P. M. N. Low, H. K. Lee, T. S. A. Hor, F. Xue, T. C. W. Mak, *J. Chem. Soc., Dalton Trans.*, 1997, 1289. I. Ara, E. Delgado, J. Fornies, E. Hernandez, E. Lalinde, N. Mansilla, M. T. Moreno, *J. Chem. Soc., Dalton Trans.*, 1996, 3201. S. Rigny, V. I. Bakhmutov, B. Nuber, J.-C. Leblanc, C. Moise, *Inorg. Chem.*, 1996, **35**, 3202. D. L. DuBois, C. W. Eigenbrot Jr., A. Miedaner, J. C. Smart, *Organometallics*, 1986, **5**, 1405.

150 R. Pietschnig, E. Niecke, M. Nieger, K. Airola, *J. Organomet. Chem.*, 1997, **529**, 127. R. Pietschnig, E. Niecke, *Organometallics*, 1996, **15**, 891. S. G. Baxter, R. L. Collins, A. H. Cowley, S. F. Sena, *Inorg. Chem.*, 1983, **22**, 3475.

151 E. Herdtweck, F. Jakle, M. Wagner, *Organometallics*, 1997, **16**, 4737. M. R. St J. Foreman, A. M. Z. Slawin, J. D. Woollins, *Chem. Commun.*, 1997, 1269. M. R. St J. Foreman, A. M. Z. Slawin, J. D. Woollins, *J. Chem. Soc., Dalton Trans.*, 1996, 3653. T. Hayase, Y. Inoue, T. Shibata, K. Soai, *Tetrahedron: Asymmetry*, 1996, **7**, 2509. F. Jakle, M. Mattner, T. Priermeier, M. Wagner, *J. Organomet. Chem.*, 1995, **502**, 123. B. Delavaux-Nicot, Y. Guari, B. Douziech, R. Mathieu, *J. Chem. Soc., Chem. Commun.*, 1995, 585. A. Meetsma, P. L. Buwalda, J. C. Van de Grampel, *Acta Cryst.*, 1988, C**44**, 58.

Chapter 2: Synthesis and Characterisation of Ferrocenyl-Phosphorus Compounds

2.1 Introduction

2.1.1 Hydroxymethylphosphines

One class of phosphines which has been the subject of investigation for several decades now is the hydroxymethylphosphines, the archetypal example of which is $P(CH_2OH)_3$, first isolated in 1958[1]. A variety of hydroxymethylphosphines have since been published in the literature[2], and some examples are given in Scheme 2.1. The initial focus for research into hydroxymethylphosphines sprang from the role of $P(CH_2OH)_3$ as the active ingredient in treatment processes being investigated by the textile industry from the early 1950's onward[3]. These processes, using $[P(CH_2OH)_4]Cl$ (or "tetrakis" as it is known in industry) as the starting material, are used to produce fabrics with flame-retardant properties. The chemistry of the most significant industrial method used is as follows[4]:

1. The $[P(CH_2OH)_4]Cl$ phosphonium salt is reacted with base in order to produce $P(CH_2OH)_3$ along with some other products[5].

2. The resulting solution is then applied to the fabric and exposed to ammonia vapours. Hydroxymethylphosphine groups can undergo condensation reactions with N-H bonds, and so the reaction of $P(CH_2OH)_3$ with ammonia leads to formation of a cross-linked polymer containing numerous linkages of the type $P\text{-}CH_2\text{-}N\text{-}CH_2\text{-}P$.

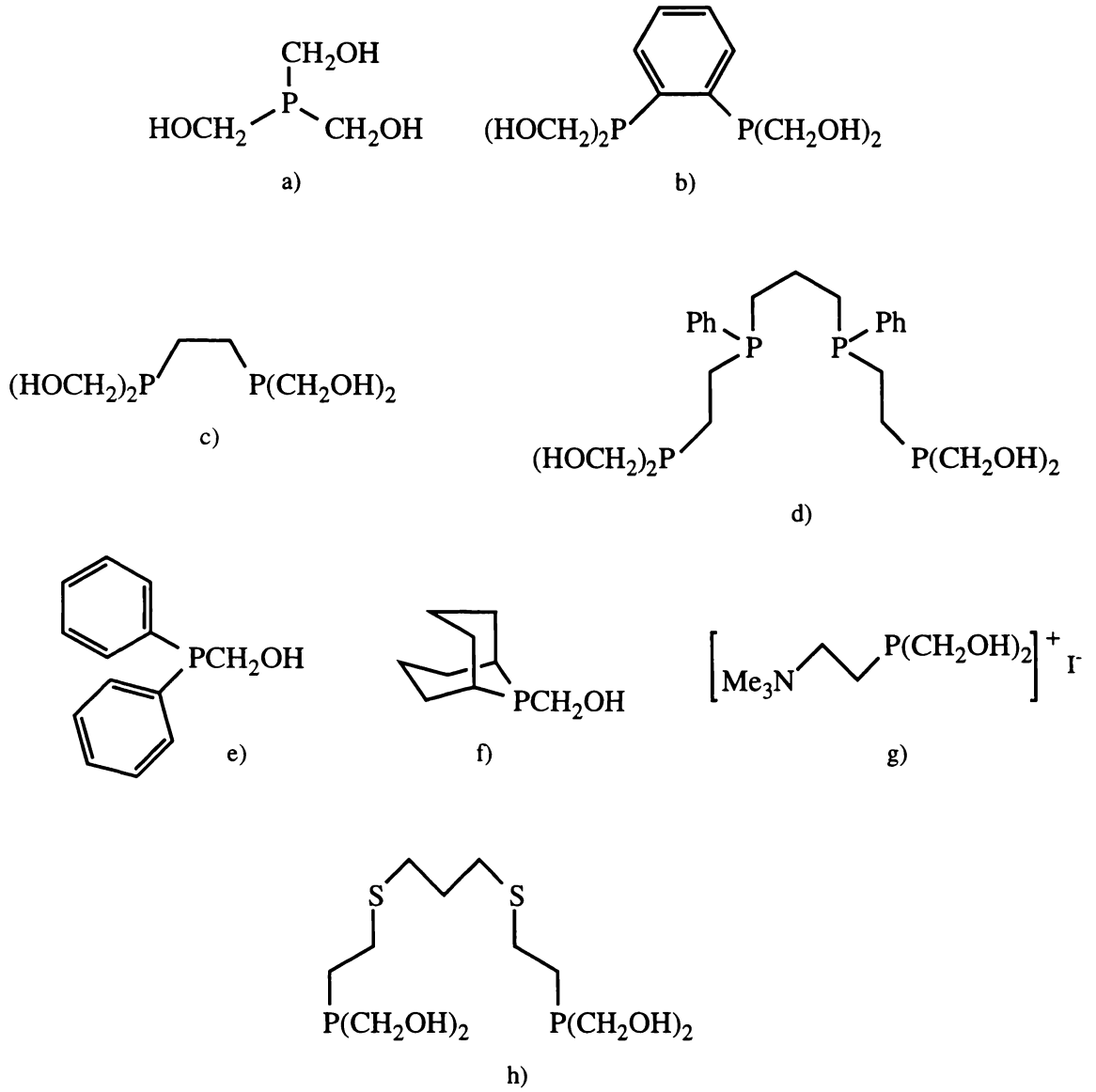

Scheme 2.1: Examples of hydroxymethylphosphines. Literature references: a), e)[2a]; b), c)[2d]; d)[2b]; f)[2f] (not isolated except as phosphonium salt); g)[2g]; h)[2c].

3. The fabric is then exposed either to air or to dilute hydrogen peroxide or perborate in order to oxidise the phosphine moieties to phosphine oxides, thus stabilising the system.

The resultant finish is said to be colourless, odourless and washable[4]. While these industrial systems are not directly relevant to the present study, the brief overview given demonstrates one of the characteristics of hydroxymethylphosphines and related systems such as hydroxymethylphosphonium salts which makes them worthy of investigation - their reactivity[6]. In some situations hydroxymethylphosphine fragments can react as disguised

P-H bonds, as in Step 1 of the above process, where one CH_2OH group is removed using base; one might similarly react a phosphonium salt of the type R_3PH^+ with a base in order to obtain the phosphine[7]. In other situations hydroxymethylphosphine fragments can react as active alcohols[8], for instance in reaction with amines containing N-H bonds, as in Step 2 above. These reactions and some others which hydroxymethylphosphines have been demonstrated to undergo are presented below. Some reactions specific to $P(CH_2OH)_3$ are shown in Scheme 2.2.

Reaction of the phosphonium salt with base to give a phosphine[2a]:

$$[R_3PCH_2OH]^+ + NR_3 \rightarrow R_3P + CH_2O + [R_3NH]^+$$

Reaction with N-H bonds[2f,6,9]:

$$R_2PCH_2OH + HNR_2 \rightarrow R_2PCH_2NR_2$$

Reaction with activated alkenes[8]:

$$R_2PCH_2OH + CH_2{=}CHCN \rightarrow R_2PCH_2CH_2CN$$

$$R_2PCH_2OH + CH_2{=}CHCOOH \rightarrow R_2PCH_2CH_2COOH$$

$$R_2PCH_2OH + CH_2{=}CHCONH_2 \rightarrow R_2PCH_2CH_2CONH_2$$

Reaction with silyl chlorides to give silyl ethers[6]:

$$R_2PCH_2OH + R_3SiCl \rightarrow PCH_2OSiR_3$$

Reaction with isocyanates to give carbamate esters[6]:

$$R_2PCH_2OH + O{=}C{=}NR \rightarrow R_2PCH_2OC(O)NHR$$

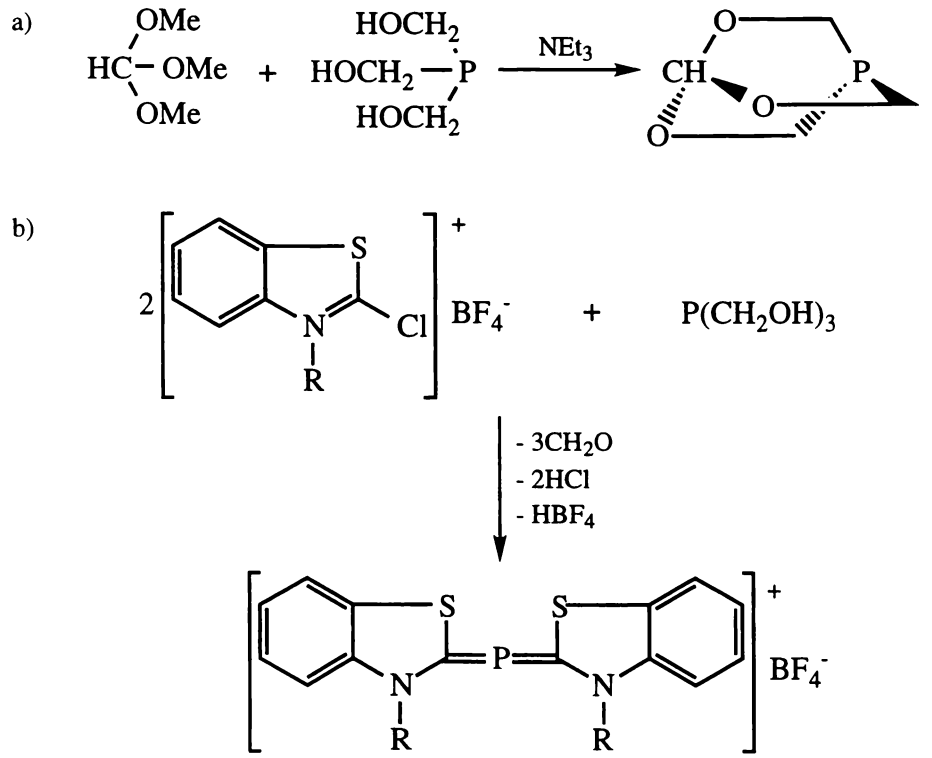

Scheme 2.2: Reactions of $P(CH_2OH)_3$; a) Production of 3,5,8-trioxa-1-phosphabicyclo[2.2.2]octane[10]. b) A phosphacyanin[11].

While the reactive nature of hydroxymethylphosphines means they have considerable potential for use in the preparation of a wide range of phosphine ligands, the reactivity of this class of phosphines has received relatively little attention from the academic research community, with most of the research into possible derivatives carried out by the textile industry. Two important examples of the possibilities offered to coordination chemists by derivatives of hydroxymethylphosphines are presented below:

1. $P(CH_2CH_2CN)_3$ (CEP) can be prepared by the reaction of acrylonitrile with $P(CH_2OH)_3$[8], although it was originaly synthesised by reaction of acrylonitrile with PH_3[12]. CEP is of interest because of the variety of potential bonding modes[13], and coordination chemistry studies have included syntheses of mononuclear complexes of Ni(II)[14], Pt(II)[15], Pd(II)[13], Hg(II)[16,13], Cr(0)[17], Mo(0)[17], Ru(II)[18], Ag(I)[19], Au(I)[20,15], Cu(I)[13], Ir(I)[21], a dinuclear complex with a Mo_2(IV) core[22], and a cluster with a Ni_4(0) core[23].

2. Reaction of formaldehyde with $P(CH_2OH)_3$ and hexamethylenetetramine yields 1,3,5-triaza-7-phosphaadamantane (TPA, Scheme 2.3)[24], of interest because of its air-stability, water-solubility and small cone angle at the phosphorus. These characteristics have made it a useful ligand for structure[25], catalysis[26], and reactivity[27] studies.

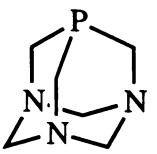

Scheme 2.3: The ligand 1,3,5-triaza-7-phosphaadamantane (TPA).

2.1.2 Water-Soluble Metal Complexes

Aside from the reactive nature of hydroxymethylphosphines, the other prominent attribute of this class of compounds which is of interest to chemists is their water-solubility. Phosphines which are soluble in aqueous media are of great interest as ligands for metal complexes, forming water-soluble species which have potential for use in industrial catalysis[28]. Because of its industrial relevance, the use of hydroxymethylphosphines to produce water-soluble metal complexes is a potentially important development.

A number of complexes of $P(CH_2OH)_3$ itself have been synthesised, including: $M[P(CH_2OH)_3]_4$ (M = Pt, Pd, Ni)[29]; $MCl_2[P(CH_2OH)_3]_2$ (M = Pt, Pd), $RhCl(CO)[P(CH_2OH)_3]_2$ and $RhCl_3[P(CH_2OH)_3]_3$[2e]; $MX_2[P(CH_2OH)_3]_2$ (M = Pt, Pd, X = Br, I), $PtMe_2[P(CH_2OH)_3]_2$ and $PtMeX[P(CH_2OH)_3]_2$ (X = Cl, Br, I)[30]; $[Au\{P(CH_2OH)_3\}_4]Cl$[31]; and $RuCl_2[P(CH_2OH)_3]_2[P(CH_2OH)_2H]_2$[32]. All these complexes are reported as water-soluble. Figure 2.1 shows the X-ray crystal structure for $Pd[P(CH_2OH)_3]_4$[30], one of only two $P(CH_2OH)_3$ complexes for which such a structure determination has been made, so far as the author is aware (the other structure being for

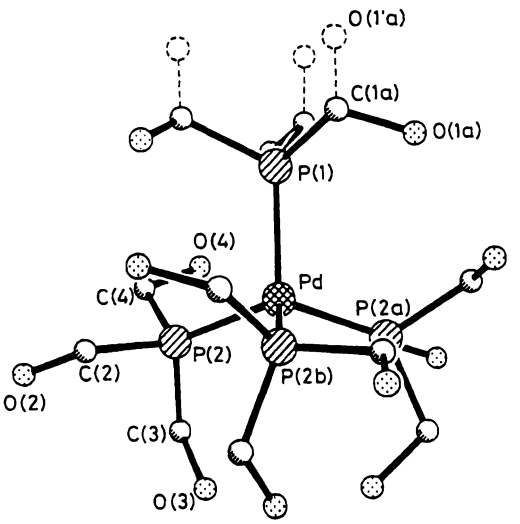

Figure 2.1: The X-ray crystal structure of $Pd[P(CH_2OH)_3]_4$[29].

$[Au\{P(CH_2OH)_3\}_4]Cl$[31]). The hydrophilic OH groups of the ligands surround the complex and shield the metal centre, showing why the complex is readily hydrated and water-soluble.

Some of these $P(CH_2OH)_3$ complexes have shown interesting chemistry[33]. The compound $Pt[P(CH_2OH)_3]_4$ appears to exist in solution in equilibrium with $\{HPt[P(CH_2OH)_3]_4\}OH$[30], as illustrated in Scheme 2.4, by intramolecular oxidative addition of water to the complex. This is a unique situation, as complexes of the type $[HPt(PR_3)_4]^+$ were previously only known for R = Et at -137° C, in equilibrium with $[HPt(PR_3)_3]^+$[29]. The investigators of this behaviour rationalise the unusual stability of the five-co-ordinate species, as well as the generally good stability of $P(CH_2OH)_3$ complexes, by treating the $[P(CH_2OH)_3]_4$ ligand shell as a pseudo-tetradentate ligand, where the four phosphine centres are linked by hydrogen-bonding of the OH moieties[30]. The $[HPt\{P(CH_2OH)_3\}_4]^+$ species is thus seen as being equivalent to $[HPtP(CH_2CH_2PPh_2)_3]^+$, a species with high stability due to the chelating nature of the phosphine ligand.

Another interesting point concerning chemical behaviour of $P(CH_2OH)_3$ complexes is that the complexes $M[P(CH_2OH)_3]_4$ (M = Pt, Pd or Ni) act as effective catalysts for the formation of $P(CH_2OH)_3$ from phosphine and formaldehyde[29]. The proposed mechanism[34] for this

behaviour is shown in Scheme 2.5. The investigators attribute the ability of other salts such as $K_2[PtCl_4]$ to catalyse the same reaction between phosphine and formaldehyde to the formation of $P(CH_2OH)_3$-containing metal species in solution[34].

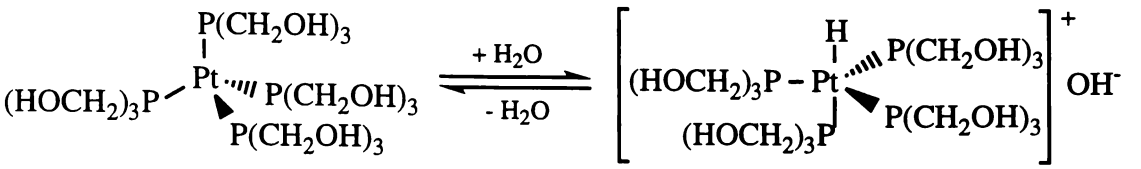

Scheme 2.4: Equilibrium sustained by $Pt[P(CH_2OH)_3]_4$ in water.

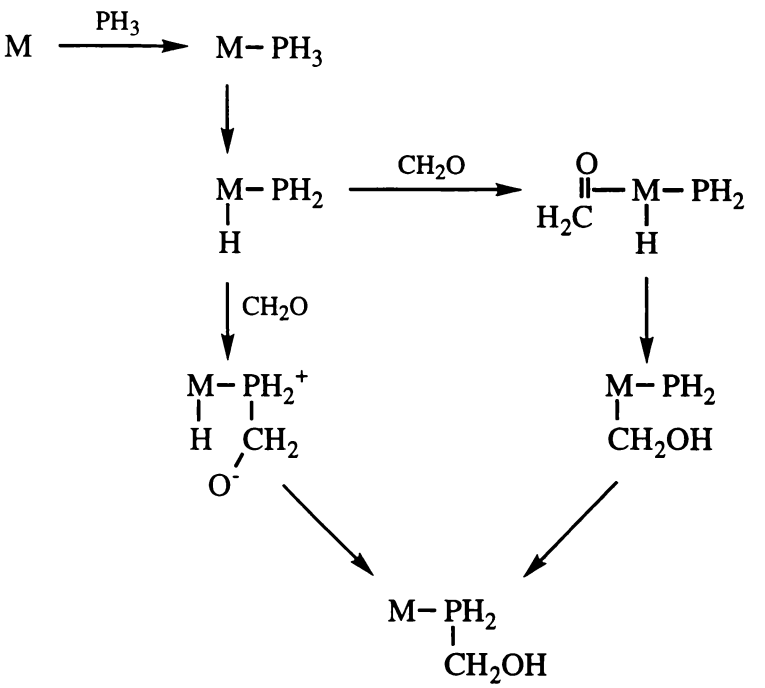

Scheme 2.5: Proposed mechanism for the formation of $P(CH_2OH)_3$ from phosphine. The formaldehyde addition steps are repeated twice over in order to produce the final product.

A large number of complexes have been reported for other hydroxymethylphosphine ligands[2b-e,i,35,36]. Some of these are shown in Scheme 2.6, along with some related hydroxyalkylphosphine complexes designed to be water-soluble[37].

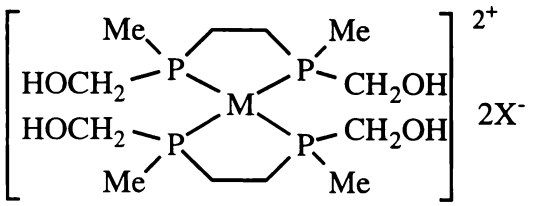

a) M = Ni, X = Br
b) M = Pd, X = Cl

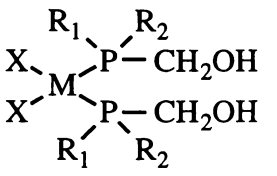

c) $R_1 = R_2 = Ph$, M = Pt, X = Cl
d) $R_1 = Me$, $R_2 = CH_2OH$, M = Pt, X = Cl

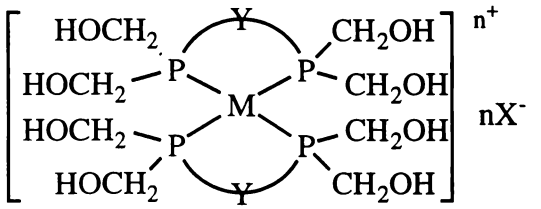

e) $Y = C_2H_4$, M = Au, n = 1, X = Cl
f) $Y = C_6H_4$, M = Au, n = 1, X = Cl
g) $Y = C_6H_4$, $M = Re(O)_2$, n = 1, X = I
h) $Y = C_2H_4$, $M = Re(O)_2$, n = 1, X = Cl
i) $Y = C_6H_4$, M = Pt, n = 2, X = Cl
j) $Y = C_6H_4$, M = Pd, n = 2, X = Cl
k) $Y = C_2H_4$, M = Pt, n = 2, X = Cl
l) $Y = C_2H_4$, M = Ni, n = 2, X = Cl

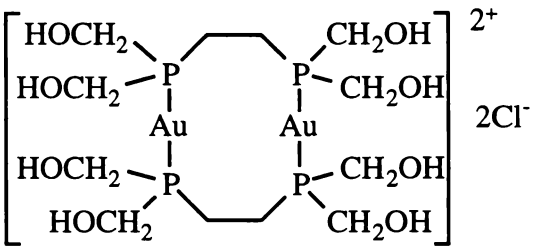

m)

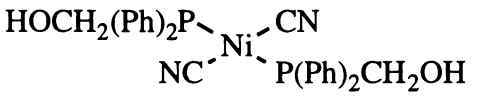

n)

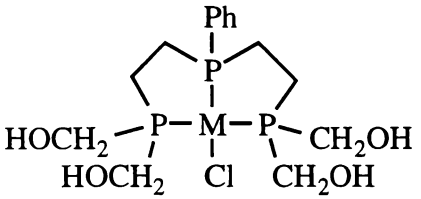

o) M = Rh
p) M = Pt

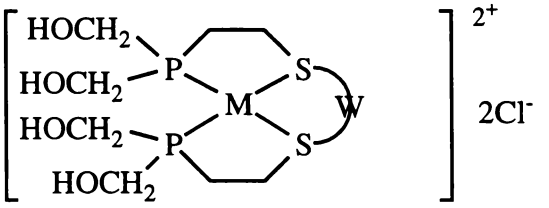

q) $W = C_3H_6$, M = Pt
r) $W = C_6H_4$, M = Pt
s) $W = C_3H_6$, M = Pd
t) $W = C_6H_4$, M = Pd

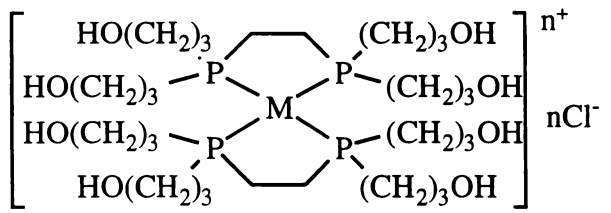

u) M = Ni, n = 2
v) M = Rh, n = 1

w) $[Mo(II)(CpCH_2CH_2NH_3^+)(CO)_2\{(HOCH_2)_2PC_2H_4P(CH_2OH)_2\}]^{2+}$

Scheme 2.6: Examples of hydroxymethylphosphine (and two hydroxypropylphosphine) complexes. d) is sparingly water-soluble. For l) and n), water-solubility was not reported. All other complexes are water-soluble. References: a), b)[35]; c), d)[2e]; e), f), m)[36a]; g), h)[36b]; i), j), k)[2d]; l), w)[36d]; n)[36f]; o), p)[2i,36c]; q), r), s), t)[2c]; u), v)[37].

While the primary reason for development of such hydroxymethylphosphine complexes has been to produce water-soluble complexes suitable for use in industrial catalysis, the present situation is that literature identifying specific practical uses for such complexes is scant. In 1973 a mixture of $[RhCl(cyclohexene)_2]_2$ with two molar equivalents of $P(CH_2OH)_3$ in ethanol[2e] was found to rapidly catalyse hydrogenation and isomerisation of oct-1-ene, although it was thought that colloidal Rh metal may in fact have been the active species. More recently $P(CH_2OH)_3$ was grafted to silica and used as an immobilised ligand for binding to Rh and Rh-Co Clusters[38]. These clusters showed high catalytic activity in the gas phase hydroformylation of ethene and propene to give aldehydes under mild conditions, but these results are not directly relevant to a discussion of homogeneous catalysis. Aside from the production of $P(CH_2OH)_3$ from phosphine, mentioned earlier, the only study of which the author is aware in which hydroxymethylphosphine complexes have been successfully applied to solution catalysis, is one involving the complexes $[Ir(COD)\{P(CH_2OH)_3\}_3]Cl$ and $[RhH_2\{P(CH_2OH)_3\}_4]Cl$[39]. The former complex catalysed the selective C=C hydrogenation of cinnamaldehyde in a biphasic mixture of water and benzene at 100° C, while the latter catalysed the hydroformylation of 1-pentene to hexanal and 2-methylpentanal under similar conditions. While the actual use of hydroxymethylphosphine complexes in catalysis has been limited, there appear to be potential advantages in using hydroxymethylphosphines in industrial applications, when compared to systems already in place. The most prominent class of water-soluble phosphines presently in use for industrial catalysis is sulfonated phosphines, such as trisulfonated triphenylphosphine (TPPTS)[28] (Scheme 2.7). Chemical modifications of such sulfonated arylphosphines are difficult, making it impracticable to tune ligand properties such as lipophilicity[2b]. Hydroxymethylphosphines would provide an improvement in this respect.

The gold and rhenium complexes e)-g) and m) (Scheme 2.6) were investigated not for their potential in catalysis but because Au-199 and Re-188 are both radioactive isotopes which can be used in radiotherapy. By modifying compounds e)-g), m) by inclusion of some group such as a peptide designed to specifically target the desired area, complexes could be produced which are water-soluble, stable, chemically inert *in vivo*, and which would

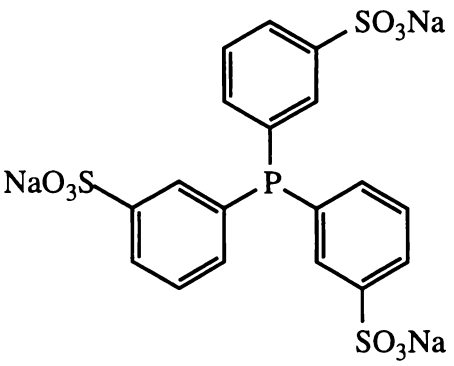

Scheme 2.7: The water-soluble ligand TPPTS.

carry radiation to the desired location[2b]. Tc-99 was recently shown to form a very stable and soluble, though uncharacterised, *in vivo* complex with $P(CH_2OH)_3$, suggesting a future use for Tc-99 labelled biomolecules with hydroxymethylphosphine functions[40] in the development of radiopharmaceuticals[36a,b].

2.2 Results and Discussion

2.2.1 Syntheses of Ferrocenylphosphines and Related Compounds

From the literature discussions which have been presented in Chapter 1 and Section 2.1, it may be surmised that the combination of hydroxymethylphosphine functionalities with ferrocene could provide a very fruitful area of research. It would allow the synthetic potential and water-solubility of hydroxymethylphosphine moieties to be brought together with the proven catalytic abilities of ferrocenylphosphines. In other applications the redox-active nature of ferrocene could be useful. The results presented in this Section represent the first steps toward the realisation of these ideas, discussing syntheses of a variety of ferrocenylphosphines and related compounds. Later Sections report on characterisation of these compounds and the preparation and characterisation of complexes.

The compound $FcCH_2P(CH_2OH)_2$ **1** can be synthesised (Scheme 2.8) by the overnight reflux of a methanolic solution of $[FcCH_2NMe_3]I$ and $P(CH_2OH)_3$. The known compound $[FcCH_2NMe_3]I$ was synthesised by literature methods, and the $P(CH_2OH)_3$ was generated *in situ* from reaction of $[P(CH_2OH)_4]Cl$ with KOH[2a]. The first step in this reaction is presumably a *trans*-quaternisation[41], producing $[FcCH_2P(CH_2OH)_3]I$ and NMe_3. The NMe_3 could conceivably deprotonate the intermediate product $[FcCH_2P(CH_2OH)_3]I$, leading to production of **1**, but due to its gaseous nature the NMe_3 might also be lost from solution. For this reason a large excess of NEt_3 is added at this stage to ensure removal of a hydroxymethyl group, giving the product **1** [^{31}P-NMR ($CDCl_3$): δ -19.3], which is easily purified by removal of solvent, extraction into ether, and recrystallisation, with a yield of 70%. Production of **1** by direct reaction of ferrocene with $P(CH_2OH)_3$ in refluxing methanol was attempted but no reaction was observed.

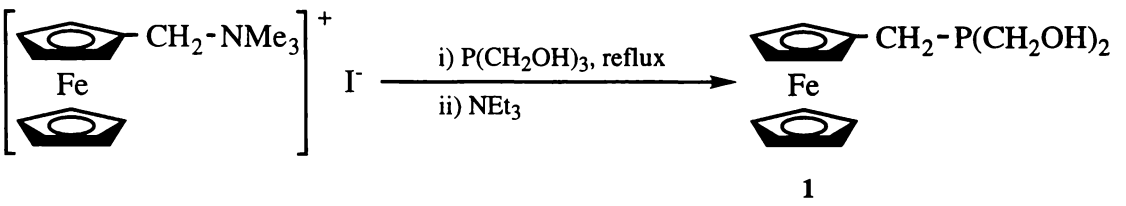

Scheme 2.8: Synthetic method for the preparation of **1**.

As was described in Section 1.2, ferrocenylphosphines where a carbon spacer is required between the phosphorus atom and the Cp ring are often prepared by the reaction of a secondary phosphine[42] (and in at least one case a primary phosphine[43]) with an aminomethylene moiety on the Cp ring. The preparation of compound **1** by reaction of $P(CH_2OH)_3$ with $[FcCH_2NMe_3]I$ involves a similar reaction. In some situations the use of a hydroxymethylphosphine rather than a secondary phosphine for such reactions could prove advantageous, since hydroxymethylphosphines (which are only mildly air-sensitive) should prove easier to handle than the equivalent secondary phosphines. The common reagent Ph_2PH, for instance, is air-sensitive and is in fact liable to spontaneously ignite[44]. In addition, it is a trivial matter to prepare a hydroxymethylphosphine *in situ* from its crystalline and air-stable hydroxymethylphosphonium precursor, as with the preparation of $P(CH_2OH)_3$

used in the synthesis of **1** from $[P(CH_2OH)_4]Cl$. Secondary phosphines with the general formula R_2PH can be reacted to give $[R_2P(CH_2OH)_2]Cl$ species suitable for storage and later reaction in this way.

To see whether the synthetic method used for preparation of **1** could be extended to the preparation of other $FcCH_2PR_2$ species, a synthesis of the known compound $FcCH_2PPh_2$[45] **2** was attempted. Curiously, although this compound was first prepared in 1963[45a], its complexation chemistry as a ligand has never been investigated (Section 1.3.2). The preparation was achieved by the overnight reaction under reflux of a methanolic solution of $[FcCH_2NMe_3]I$ and Ph_2PCH_2OH (Scheme 2.9). The Ph_2PCH_2OH was generated *in situ* by the reaction of $[Ph_2P(CH_2OH)_2]Cl$ (prepared by literature methods[2a,f]) with KOH. After overnight reflux excess NEt_3 was added, and an organic extraction followed by purification of the product *via* chromatography gave the product **2** in moderate yield.

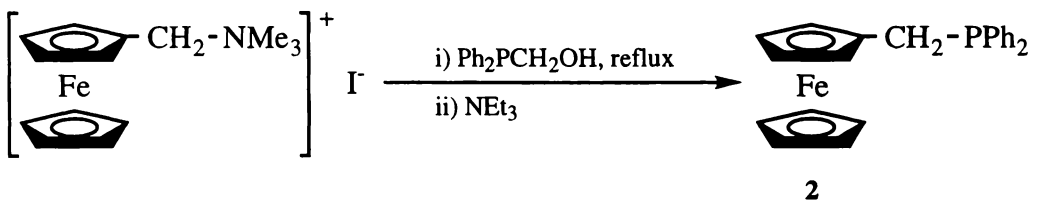

2

Scheme 2.9: Synthetic method for the preparation of **2**.

A number of other products were prepared using **1** as a starting material. These synthetic routes are described below and summarised in Scheme 2.10.

The phosphine oxide $FcCH_2P(O)(CH_2OH)_2$ **3** [^{31}P-NMR ($CDCl_3$): δ 45.8] was prepared in good yield by stirring a methanolic solution of **1** with hydrogen peroxide . Workup of this product had to be carried out without elevating the temperature of the reaction solution above room temperature, or extensive oxidation of the ferrocene moiety was observed. Elemental analysis of **3** proved to be non-reproducible and inaccurate, although the product appeared pure by NMR. This difficulty with elemental analysis has been attributed to the inclusion of water into the crystal lattice of the product through strong hydrogen-bonding. Although

drying under vacuum did not remove this water, water was evolved during melting point determination. Thermogravimetric analysis showed a large endothermic peak at 99.3° C, confirming the presence of water in the lattice.

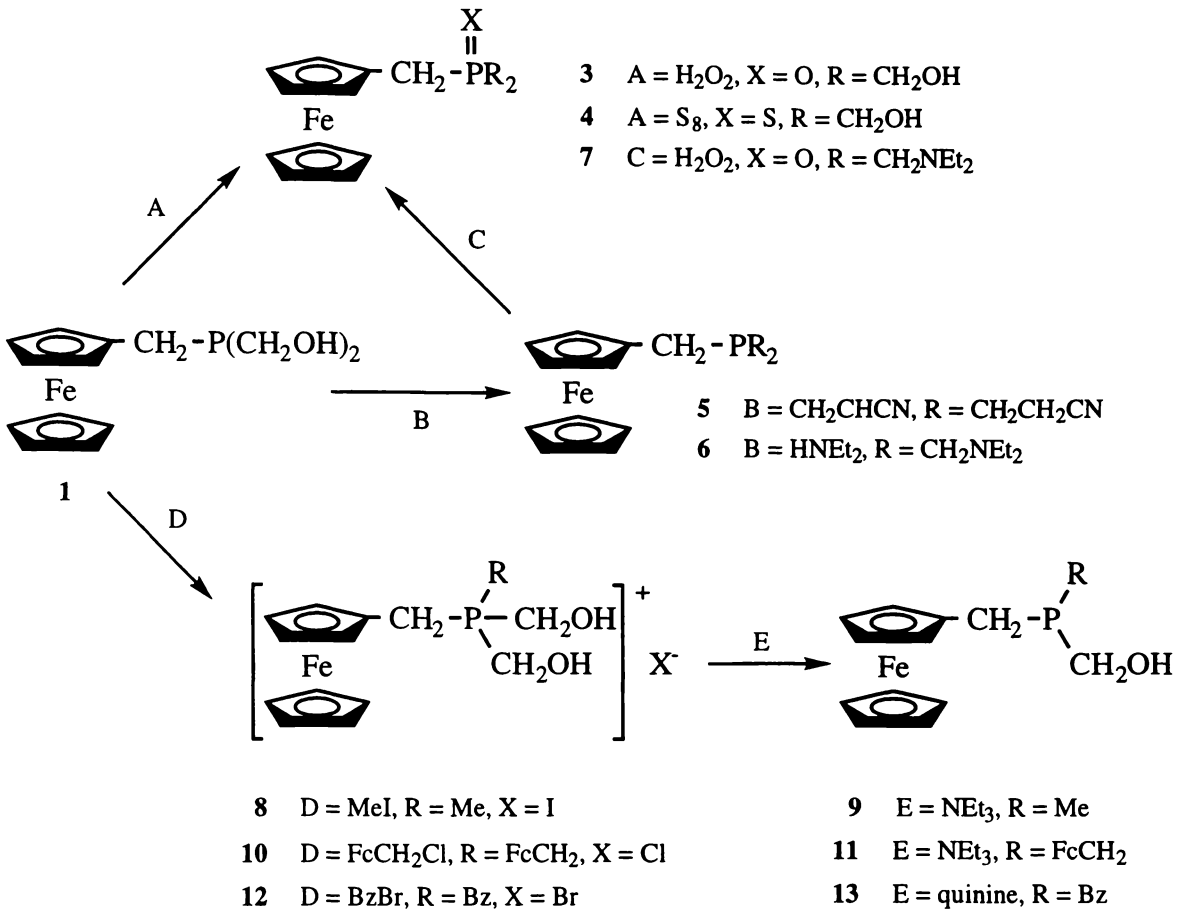

Scheme 2.10: Syntheses described in this Section using **1** as the starting material. Note however that **12** and **13** were not fully characterised or isolated as pure materials.

The sulfide $FcCH_2P(S)(CH_2OH)_2$ **4** [^{31}P-NMR ($CDCl_3$): δ 44.0] was prepared in good yield by reaction of **1** with elemental sulfur in refluxing toluene. The production of both the oxide **3**[46] and sulfide **4**[47] are standard reactions for tertiary phosphines and are in no way unique to hydroxymethylphosphines.

The cyanoethylphosphine $FcCH_2P(CH_2CH_2CN)_2$ **5** [^{31}P-NMR ($CDCl_3$): δ -22.1] was prepared by reaction of **1** with acrylonitrile, showing that **1** can undergo Michael additions

with activated alkenes, as is the case for other hydroxymethylphosphines (Section 2.1.1). Like the related compound $P(CH_2CH_2CN)_3$ described in Section 2.1.1, compound **5** has the potential to be a multidentate ligand and to show interesting bonding modes.

The Mannich-type condensation reaction of primary or secondary amines with hydroxymethylphosphine groups (Section 2.1.1) was shown to apply to compound **1** by the reaction of **1** with diethylamine. Stirring of a dichloromethane solution of the starting materials under nitrogen led to production of the mildly air-sensitive compound $FcCH_2P(CH_2NEt_2)_2$ **6** [^{31}P-NMR ($CDCl_3$): δ -48.3]. Like compound **5**, this is a compound with potential for a variety of bonding modes, containing two "hard" nitrogen donors as well as a "soft" phosphorus donor, similar to other P,N mixed-donor ligands[48]. Reaction of **6** with $PtCl_2$(COD) (COD = 1,5-cyclo-octadiene) was attempted in order to see what was produced; NMR evidence suggested the formation of up to six different products, and the behaviour of this compound as a ligand has not been investigated further.

Complete characterisation of **6** was not carried out, but it was instead characterised as the phosphine oxide $FcCH_2P(O)(CH_2NEt_2)_2$ **7** [^{31}P-NMR ($CDCl_3$): δ 45.0]. This was synthesised by the controlled oxidation of **6** with hydrogen peroxide. Preparation of this compound was a useful demonstration of the ability of **1** to covalently bond to amine-containing materials; **7** was in fact synthesised as a model compound for the preparation of polymers by reaction of **1** with multifunctional primary amines. Studies of the preparation and electrochemistry of such polymers are described in Chapter 6.

The racemic compound $FcCH_2P(Me)(CH_2OH)$ **9** [^{31}P-NMR ($CDCl_3$): δ -33.1] was prepared in two steps, by first alkylating **1** with methyl iodide to give the phosphonium salt $[FcCH_2P(Me)(CH_2OH)_2]I$ **8** [^{31}P-NMR ($CDCl_3$): δ 26.2], then removing a hydroxymethyl group by treatment with NEt_3. This general route for the derivatisation of hydroxymethylphosphines, where the phosphine is reacted with RX (X = Cl, Br, I) and then a hydroxymethyl group is removed with base, was previously known[2a,8,49], and can conceivably be used in the production of a great variety of different ferrocenylphosphines

using **1** as the starting material. One outcome of this reaction is the production of racemates; this may have contributed to the fact that unlike most other compounds described in this Section, compound **9** proved difficult to crystallise. This makes it difficult to purify, since it was found that chromatography on silica gel is also of little use. It is the author's experience that all hydroxymethylphosphines tend to lose a hydroxymethyl group to some extent when eluted on chromatographic plates, giving a secondary phosphine or similar products. While this makes exposure to silica a potential synthetic route to the production of secondary phosphines, it rules out silica chromatography as a purification method in most cases.

An example of the use of the synthetic route outlined in the previous paragraph, for which the production of racemates is not a problem, is the preparation of the phosphonium salt $[(FcCH_2)_2P(CH_2OH)_2]Cl$ **10** [^{31}P-NMR ($CDCl_3$): δ 22.3]. This was achieved by stirring of **1** with $FcCH_2Cl$ in dichloromethane under nitrogen. The $FcCH_2Cl$ was prepared by a literature method[50] and used immediately, but appeared to be rather unstable, perhaps accounting for the rather low yields for this reaction in contrast to others described in this section. Compound **10** was then reacted with NEt_3 to give the bis(ferrocenylmethyl)phosphine $(FcCH_2)_2PCH_2OH$ **11** [^{31}P-NMR ($CDCl_3$): δ -17.1].

The use of chiral ferrocenylphosphines in asymmetric catalysis and synthesis is now an important area of work, as was discussed in Section 1.2. In addition to this, the production of phosphines chiral at the phosphorus atom (P-chiral) is an area of research of great general interest to many different areas of chemistry[51], including not only asymmetric catalysis[52] and synthesis, but also chemotherapy, agriculture and bioinorganic chemistry[53,54]. P-chiral ligands have found use in inorganic chemistry[55], and in fact some work has been done on developing P-chiral ferrocenylphosphines not just as racemates[56] but in enantiomerically pure form[57]; these ferrocenylphosphines have been described in Chapter 1. A novel enantioselective route to P-chiral ferrocenylphosphines might be to use the synthetic method described above for the synthesis of compounds **9** and **11**. A compound could be prepared

with three different substituents on the phosphorus, with enantioselectivity provided by use a chiral amine for the transformation of the phosphonium salt $[FcCH_2P(R)(CH_2OH)_2]^+$ to the final phosphine $FcCH_2P(R)CH_2OH$. The amine would thus serve as a chiral auxiliary. To test this notion, a crude preparation of $[FcCH_2(Bz)(CH_2OH)_2]Br$ **12** [^{31}P-NMR ($CDCl_3$): δ 26.0] was synthesised by reaction of benzyl bromide with **1**. It was decided this would be more appropriate for examining these ideas than compound **8** since the benzyl group of **12** would provide more steric contrast to the neighbouring hydroxymethyl groups than the methyl group of **8**. ^{31}P-NMR was then used to monitor reaction of **12** with the chiral amine quinine, chosen for its ready availability, showing that as expected this appeared to form the phosphine $FcCH_2(Bz)CH_2OH$ **13** [^{31}P-NMR ($CDCl_3$): δ -15.0].

A sample of the product **13** was then prepared for NMR analysis and a small amount of the chiral secondary amine (*R*)-(+)-N-benzyl-α-methyl-benzylamine added to the mixture (Scheme 2.11). As compound **13** underwent Mannich-type reaction with the amine, ^{31}P-NMR showed the disappearance of the signal for compound **13** and the appearance of two signals upfield at a chemical shift consistent with formation of the expected adduct. The two signals presumably correspond to the two diastereoisomers (*R*,*R*)-$FcCH_2P^*(Bz)CH_2N(Bz)(C^*HMePh)$ and (*S*,*R*)-$FcCH_2P^*(Bz)CH_2N(Bz)(C^*HMePh)$, and the equal intensities of the two signals showed that in fact no enantioselectivity was evident (Figure 2.2). If this route is to prove effective it will obviously require adjustments such as a more effective basic reagent or reaction at low temperature. Such possibilities have not yet been investigated further.

Two products were prepared specifically for electrochemical investigations (see Chapter 5). The first of these is $[FcCH_2P(H)Ph_2]BF_4$ **14** [^{31}P-NMR ($CDCl_3$): δ 6.3, d, ^{1}J(P-H) = 511 Hz] prepared by the controlled addition of a dilute solution of HBF_4 in slight excess to compound **2** under nitrogen. This compound decomposes on storage. The second is $FcCH_2P(O)Ph_2$ **15** [^{31}P-NMR ($CDCl_3$): δ 29.0] prepared by oxidation of **2** with hydrogen peroxide in a similar fashion to compounds **3** and **7**.

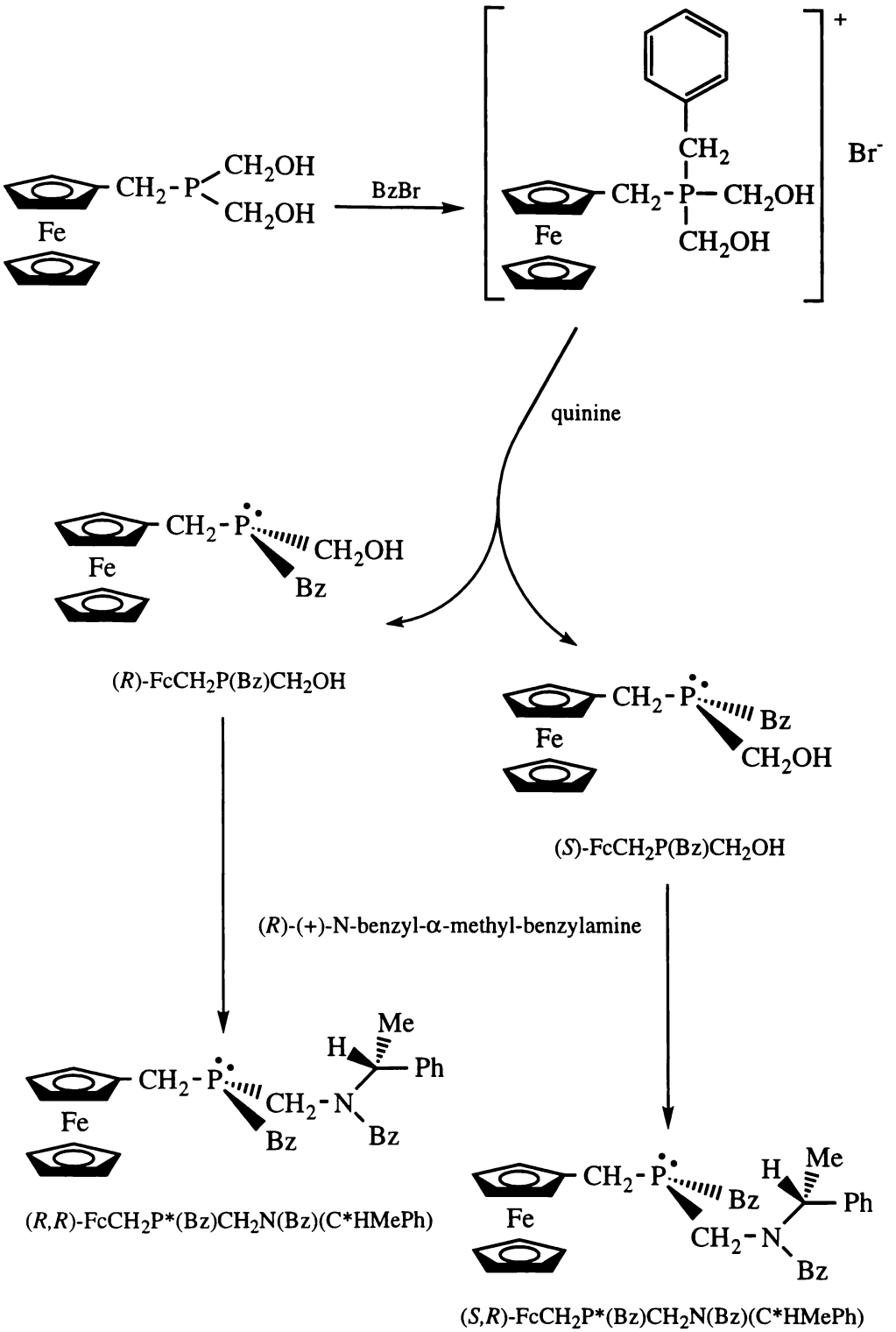

Scheme 2.11: Total reaction path used to test the notion that enantioselective preparation of phosphines chiral at phosphorus may be possible by use of an enantiomerically pure amine as a chiral auxiliary; the transformation of the phosphonium salt **12** to the phosphine **13**, and further reaction with a secondary amine.

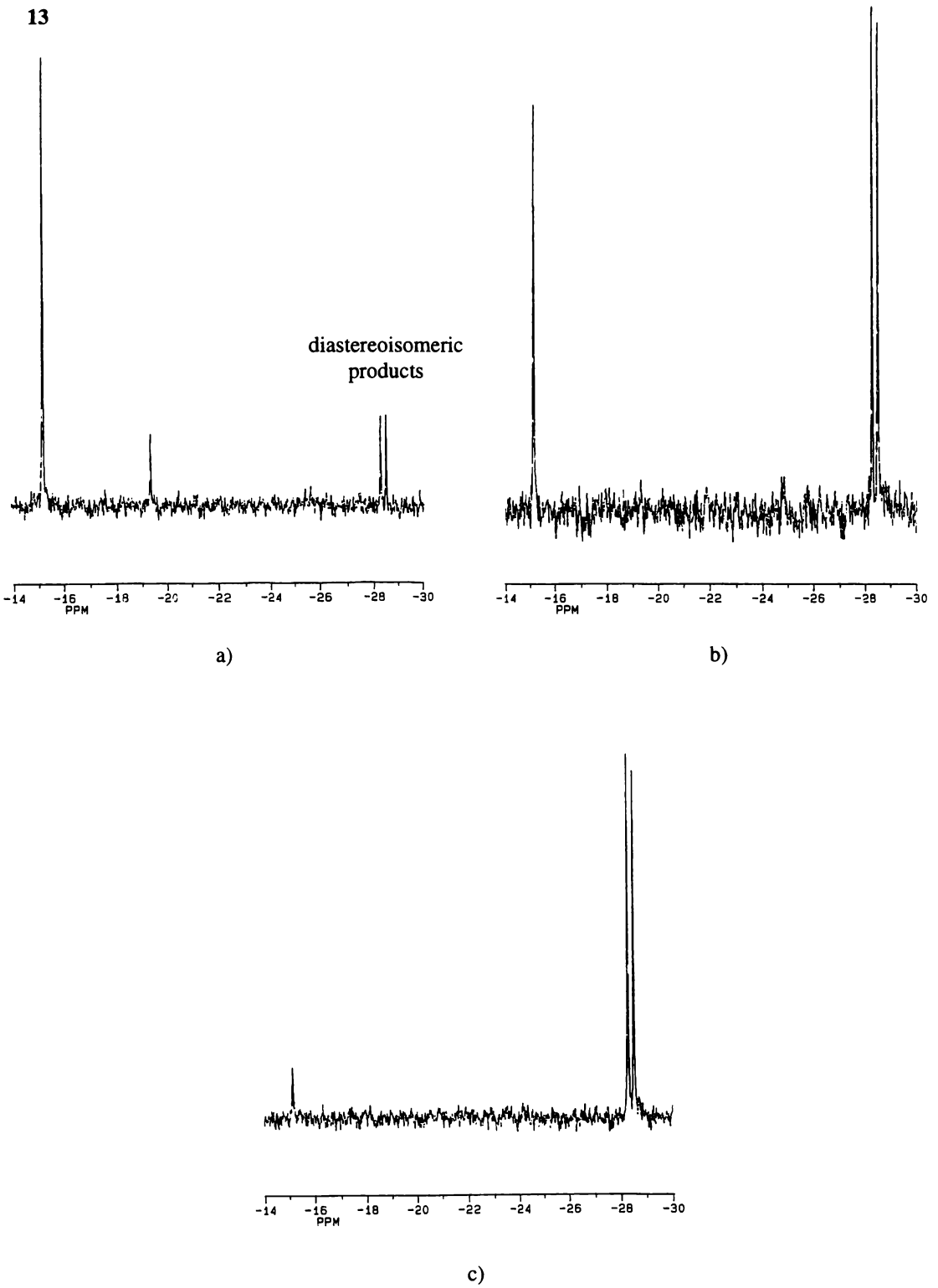

Figure 2.2: ^{31}P-NMR spectra of **13** in $CDCl_3$; a) directly after addition of (*R*)-(+)-N-benzyl-α-methyl-benzylamine, b) after *ca.* 10 minutes, c) after *ca.* 20 minutes, appearing to show the two diastereoisomers forming in essentially equal amounts.

2.2.2 Electrospray Mass Spectrometric (ESMS) Analysis of Ferrocenyl-Phosphorus Compounds

It is only recently that use has been made of ESMS in order to investigate ferrocene derivatives. While the first investigation[58] of this kind demonstrated that ferrocene and its derivatives are oxidised by ESMS to the ferrocenium cation, rather than undergoing protonation, further experience has shown that certain ferrocene-containing compounds can exhibit protonation during ESMS[59]. Relative levels of the $[M]^+$ and $[M + H]^+$ signals observed can fluctuate from sample to sample, and the oxidisability and basicity of the particular compound being investigated influence which of the two signals is dominant. This makes the recording of high-resolution spectra important in studies of this kind. In the present study the neutral ferrocene derivatives **1**, **2**, **3**, **4**, **5** and **9** were characterised by ESMS and in each of these cases the $[M]^+$ ion dominated over $[M + H]^+$ formation. However, for the compounds **6** and **7** the $[M + H]^+$ species was observed in preference to $[M]^+$. This is presumably because of the presence of basic amine functionalities in these two compounds, allowing the protonated species to be more easily formed than is the case with the other neutral ferrocene derivatives investigated. In the case of compound **7** the phosphine oxide group may also act as a good H^+ acceptor. The dominant species observed for compound **11** was the $[M + O]^+$ species; this suggests that the phosphine is being electrochemically oxidised to the phosphine oxide at the cone tip (further oxidation of the ferrocene moiety accounts for the positive charge). Surprisingly, the $[M]^+$ ion was not observed even at very low cone voltages.

Greater sensitivity in the ESMS detection of the uncoordinated phosphines **1**, **5**, and **6** was achieved using a previously published method[60] whereby $AgNO_3$ is added to samples. In spectra of samples treated in this way the $[M]^+$ or $[M + H]^+$ ion is still visible but is typically dominated by strong $[M + Ag]^+$ and $[2M + Ag]^+$ ion signals. Curiously, this method did not appear to be so effective in the case of compound **9**. It was thought that addition of Na^+ to samples of the phosphine oxide **3** and sulfide **4** in the form of NaCl might act in a similar fashion to the Ag^+ by forming charged complexes *in situ* and thus increasing sensitivity of

detection for these compounds. This method has previously been successfully employed for the ESMS detection of a ferrocenylether[61]. However, while the $[M + Na]^+$ signals were visible in the ESMS spectra, the $[M]^+$ signals were easily the most significant.

Because of their ionic nature, compounds **7**, **10** and **12** gave easily detectable $[M - X]^+$ (X = Cl, Br, I) signals. Compound **10** also gave a prominent peak corresponding to $[M - Fc - Cl + H]^+$, showing an interesting but unexplained lability of one of the ferrocenyl groups.

The results reported here are essentially in agreement with a previous study of the behaviour of ferrocenylphosphines under ESMS conditions[62].

2.2.3 X-Ray Crystal Structure Determinations for Compounds $FcCH_2P(CH_2OH)_2$ **1**, $FcCH_2PPh_2$ **2**, $FcCH_2P(S)(CH_2OH)_2$ **4** and $[FcCH_2P(Me)(CH_2OH)_2]I$ **8**

Structure elucidation by X-ray diffraction was performed for compounds **1**, **2**, **4** and **8**. Selected bond lengths and angles and structure diagrams are given in Figures 2.3, 2.4, 2.5 and 2.6 and Tables 2.1, 2.2, 2.3, and 2.4 respectively. In each case the Cp rings adopted an eclipsed conformation, with the phosphorus atom directed away from the ferrocene unit. Intramolecular bond distances and angles for all four compounds are within normal ranges.

Structures of hydroxymethylphosphines and related species should be of interest for their hydrogen-bonding, and indeed structures of the three compounds **1**, **4** and **8** show a variety of hydrogen-bonded structural motifs.

In **1**, hydrogen-bonding leads to an elegant array of ten-membered rings of the type O(2)-C(2)-P-C(3)-O(3)-H···O(2)-H···O(3)-H between three neighbouring molecules (Figure 2.7).

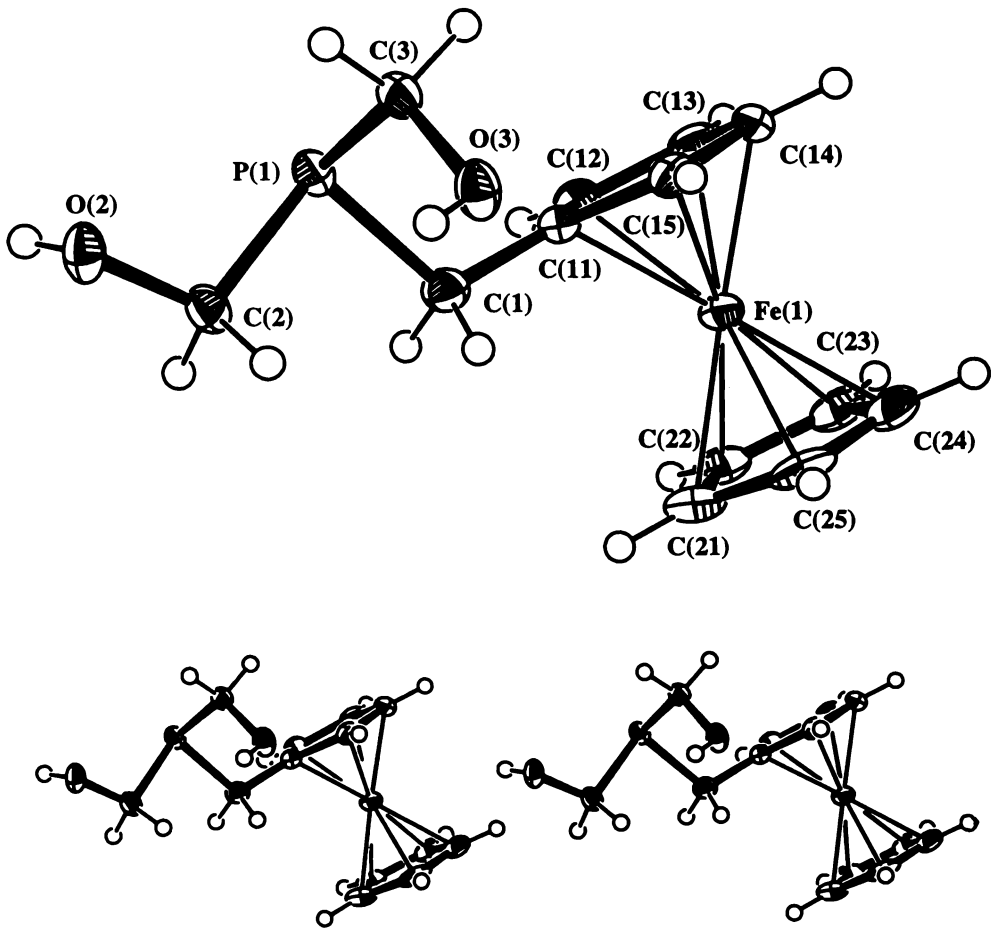

Figure 2.3: ORTEP diagram of the X-ray crystal structure of **1**, with stereo view.

This hydrogen-bonding system propagates up the 2_1 screw axis parallel to the *a* axis. The distance between hydrogen-bonded oxygens is 2.675 Å for O(2)-H···O(3) interactions, and 2.662 Å for O(3)-H···O(2). The H···O distances are 1.962 Å and 1.942 Å respectively, while hydrogen bond angles are respectively 167.0° and 164.9°. This was the first structure reported for a free hydroxymethylphosphine, probably because hydroxymethylphosphines are generally either slightly air-sensitive or non-crystalline at room temperature. Another crystal structure has subsequently been published, for $(HOCH_2)_2PCH_2CH_2P(CH_2OH)_2$[36d]; this structure displayed extensive hydrogen-bonding interactions in the plane of the *b* and *c* axes. Related structures are discussed in Section 2.2.6 (hydroxymethylphosphine complexes) and Chapter 3 (hydroxymethylphosphine chalcogenides).

Table 2.1: *Selected bond lengths (Å) and angles (°) for compound 1.*

Cp Fe-C av.	2.040(4)	P(1)-C(1)	1.858(4)
range	2.034(4) - 2.047(5)	P(1)-C(2)	1.862(4)
Cp C-C av.	1.414(6)	O(3)-C(3)	1.423(5)
range	1.399(7) - 1.424(6)	O(2)-C(2)	1.429(5)
C(1)-C(11)	1.489(6)	O(2)-H(2)	0.74(5)
P(1)-C(3)	1.851(4)	O(3)-H(3)	0.73(5)
C(11) - C(15)		C(11)-C(1)-P(1)	114.6(3)
range	107.2(4) - 108.6(4)	O(2)-C(2)-P(1)	111.9(3)
C(21) - C(25)		O(3)-C(3)-P(1)	116.2(3)
range	107.6(5) - 108.7(4)	C(15)C(11)-C(1)	125.0(4)
C(3)-P(1)-C(1)	101.3(2)	C(12)-C(11)-C(1)	127.7(4)
C(3)-P(1)-C(2)	99.5(2)	H(2)-O(2)-C(2)	113(4)
C(1)-P(1)-C(2)	95.0(2)	H(3)-O(3)-C(3)	110(4)

Table 2.2: *Selected bond lengths (Å) and angles (°) for compound 2.*

P(1)-C(1)	1.860(3)	C-C for Cp rings av.	1.413(5)
P(1)-C(31)	1.840(3)	range	1.382(6)-1.437(6)
P(1)-C(41)	1.837(3)	C-C for Ph rings av.	1.388(4)
C(1)-C(11)	1.500(4)	range	1.378(5)-1.399(4)
C(1)-P(1)-C(31)	100.34(13)	C(31)-P(1)-C(41)	103.02(12)
C(1)-P(1)-C(41)	100.99(14)	P(1)-C(1)-C(11)	111.6(2)
distance of Fe(1) out of substituted Cp ring			1.6475(15)
distance of Fe(1) out of unsubstituted Cp ring			1.6486(17)
angle between planes of Ph rings			56.90(10)

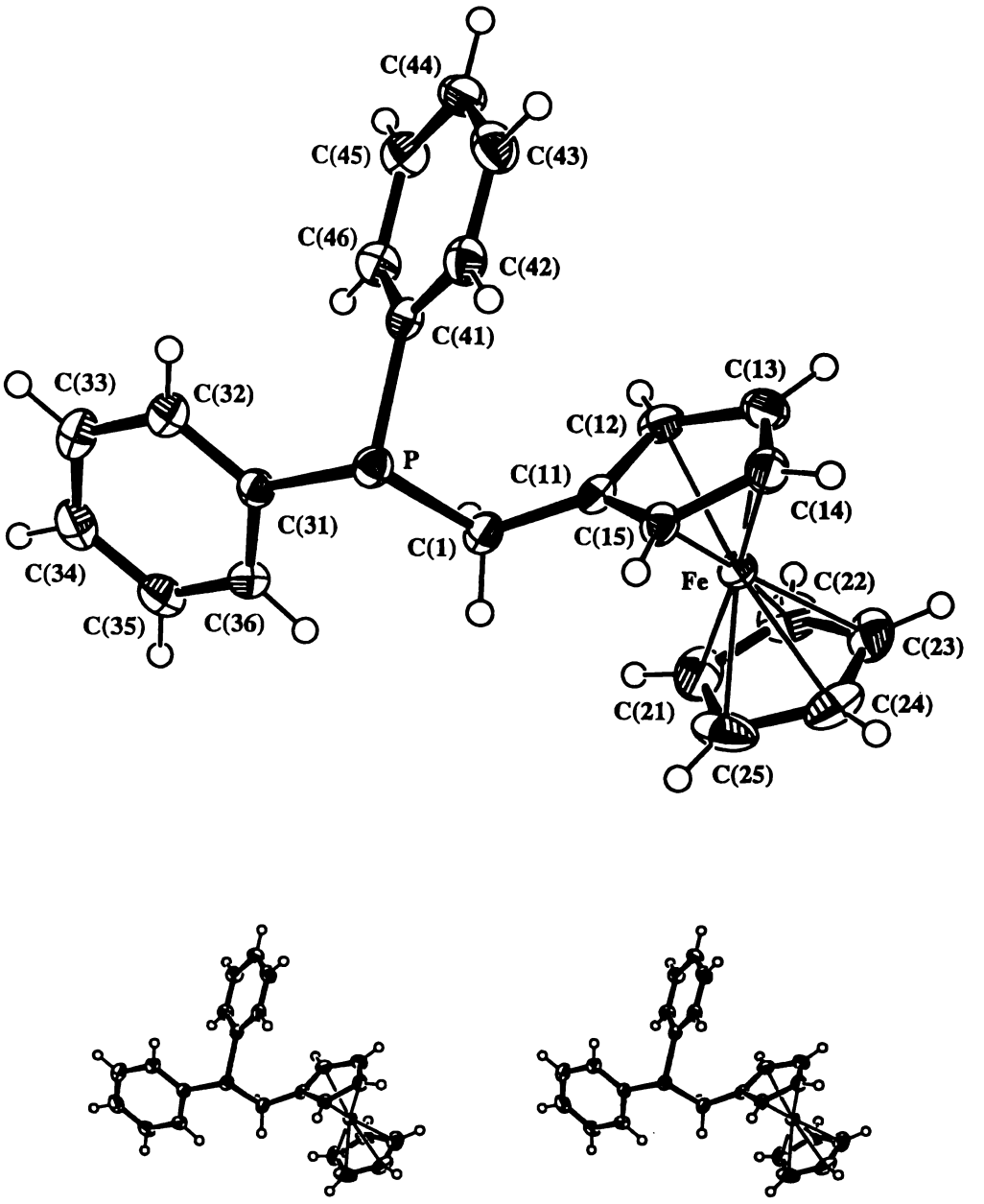

Figure 2.4: ORTEP diagram of the X-ray crystal structure of **2**, with stereo view.

Compound **4** crystallises with two independent molecules in the unit cell, and with a hydrogen-bonding array that consists of short discrete networks of O-H···O bonds which terminate at sulfur with an O-H···S hydrogen bond. The hydrogen-bonding array is presented in Figure 2.8, and relevant distances and angles are given in Table 2.5.

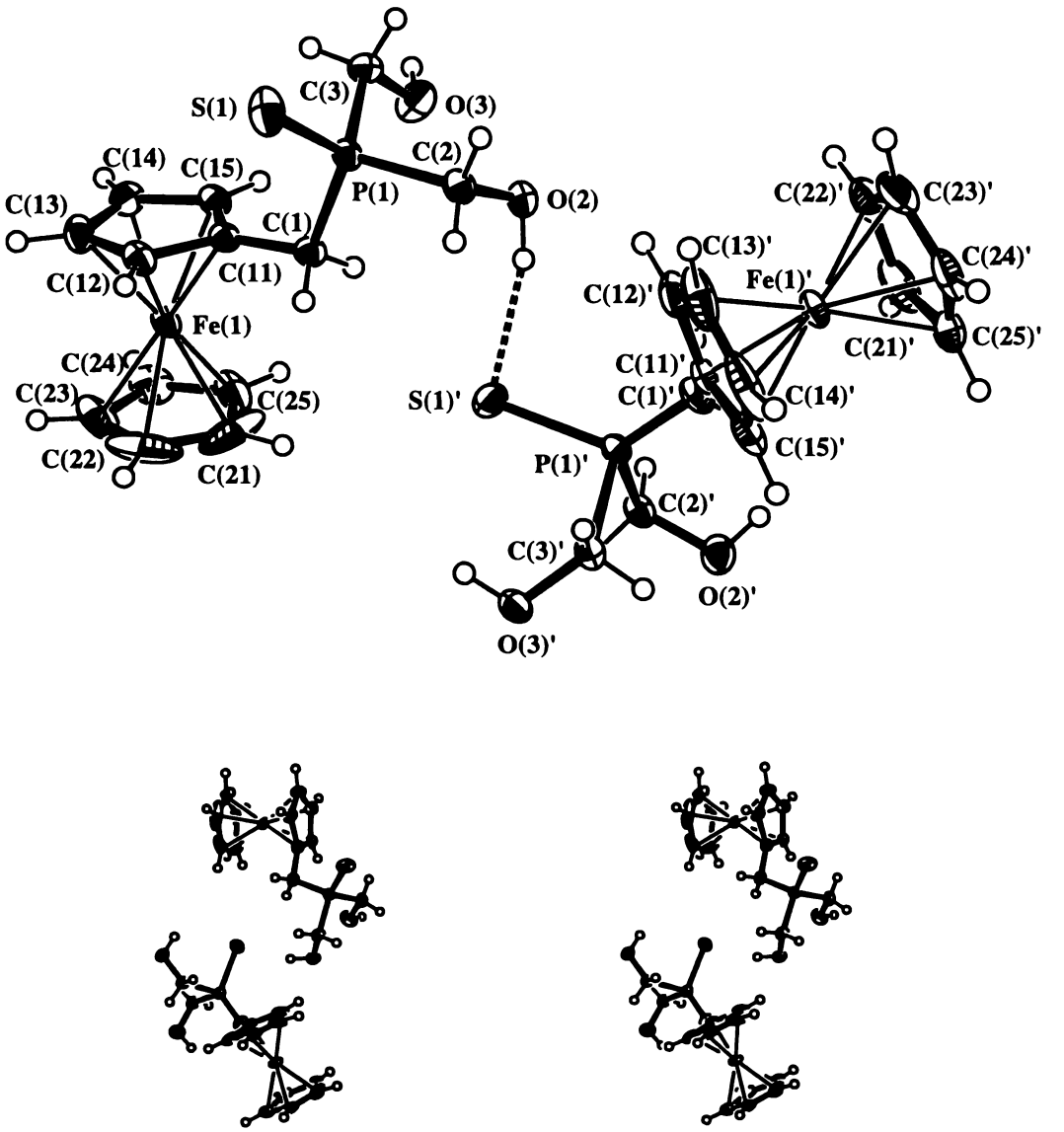

Figure 2.5: ORTEP diagram of the X-ray crystal structure of **4**, with stereo view.

Phosphine oxides are good hydrogen bond acceptors and many crystal structures have been reported which show strong intra- and inter-molecular hydrogen-bonding of the phosphine oxide functionality[63]. In contrast, relatively few crystal structures have been reported where there is potential to study hydrogen-bonding behaviour of phosphine sulfides[63]. Although it would be expected that the phosphine sulfide functionality is a weaker hydrogen bond acceptor than the oxide, the observed O···S distances of 3.1 and 3.3 Å in the structure of **4** suggest a reasonably intense hydrogen-

Table 2.3: *Selected bond lengths (Å) and angles (°) for molecules 1 and 2 of compound* ***4****. Elsewhere molecule 2 is denoted by apostrophes.*

		molecule 1	molecule 2
Fe-C	av.	2.035(2)	2.031(2)
	range	2.018(3) - 2.045(2)	2.019(2) - 2.042(3)
Cp C-C	av.	1.404(4)	1.408(4)
	range	1.347(5) - 1.427(6)	1.390(4) - 1.424(3)
P(1)-C(1)		1.817(2)	1.823(2)
P(1)-C(3)		1.821(2)	1.825(2)
P(1)-C(2)		1.836(2)	1.829(2)
P(1)-S(1)		1.9556(8)	1.9614(8)
C(1)-C(11)		1.496(3)	1.501(3)
C(2)-O(2)		1.413(3)	1.407(3)
C(3)-O(3)		1.415(3)	1.423(3)
C(11) - C(15) range		107.4(2)-108.5(2)	107.2(2)-108.9(2)
C(21) - C(25) range		105.8(3)-109.6(3)	107.7(2)-108.2(2)
C(1)-P(1)-C(3)		106.0(1)	106.1(1)
C(1)-P(1)-C(2)		105.2(1)	104.6(1)
C(3)-P(1)-C(2)		106.4(1)	105.8(1)
C(1)-P(1)-S(1)		116.43(8)	117.74(8)
C(3)-P(1)-S(1)		111.66(8)	109.99(8)
C(2)-P(1)-S(1)		110.48(8)	111.78(8)
C(11)-C(1)-P(1)		113.4(2)	116.1(2)
O(2)-C(2)-P(1)		114.3(2)	111.45(14)
O(3)-C(3)-P(1)		111.1(2)	110.79(14)
C(12)-C(11)-C(1)		126.6(2)	126.4(2)
C(15)-C(11)-C(1)		126.0(2)	125.8(2)

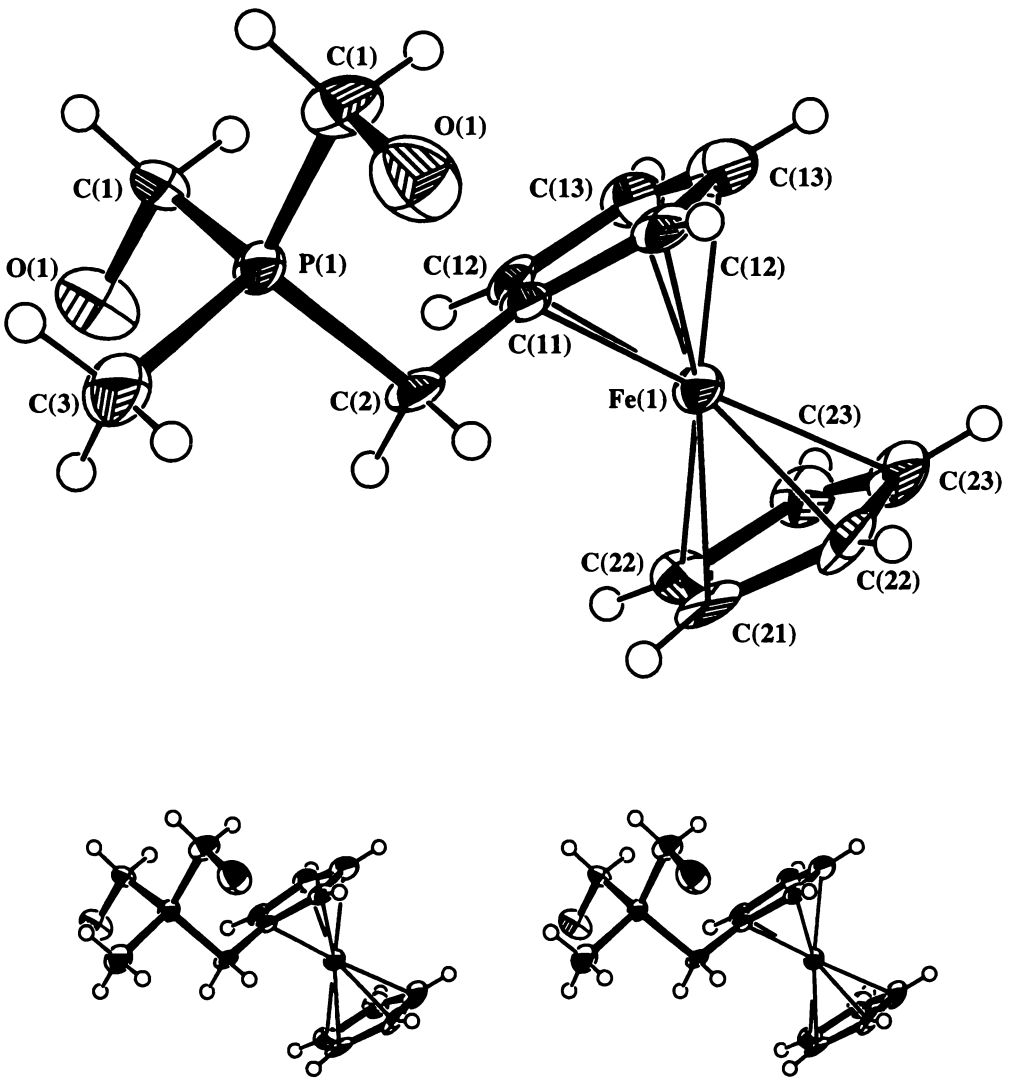

Figure 2.6: ORTEP diagram of the X-ray crystal structure of the cation of **8**, with stereo view.

bonding interaction. One point of interest in this hydrogen-bonding network is the presence of a nearly 'perfect' example of the bifurcated hydrogen bond, from O(2)'-H to both O(2) and O(3), with bond distances and angles almost equivalent for both halves of the bond (see Table 2.5). The greater length of the H···O contacts in the 3-centre bifurcated bond in comparison to the two-centre 'linear' hydrogen bond O(3)-H···O(3)' is normal for such systems[64], and presumably arises from steric repulsion between the two acceptors. This provides a clear example of the way in which hydrogen bond distances can be influenced by crystal-packing effects[65]. Another example of such crystal-packing effects is seen in this structure, in the difference of about 0.2 Å in the distances of the two O-H···S hydrogen bonds, when the species involved in both cases are chemically identical.

Table 2.4: *Selected bond lengths (Å) and angles (°) for compound 8.*

Fe-C av.	2.034(15)	P(1)-C(2)	1.79(2)
range	1.99(2) - 2.06(1)	P(1)-C(3)	1.81(2)
C(11) - C(13) av.	1.42(2)	P(1)-C(1)	1.82(2)
range	1.36(3) - 1.43(2)	C(1)-O(1)	1.38(2)
C(21) - C(23) av.	1.42(2)	C(2)-C(11)	1.51(3)
range	1.38(3) - 1.44(2)		
C(11) - C(13)		C(3)-P(1)-C(1)	109.1(6)
range	107(2) - 109(1)	C(1)-P(1)-C(1)'	110.5(9)
C(21) - C(23)		O(1)-C(1)-P(1)	107.0(9)
range	103(2) - 113(2)	C(11)-C(2)-P(1)	113(1)
C(2)-P(1)-C(3)	109.0(9)	C(12)-C(11)-C(2)	126.4(8)
C(2)-P(1)-C(1)	109.6(6)		

Table 2.5: *Hydrogen bond lengths and angles for the hydrogen-bonding array in compound 4. The bifurcated nature of the hydrogen-bonding between O(2)'-H and O(2) and O(3) means these bonds are longer than is the case for the O(3)-H···O(3)' hydrogen bond.*

	H-acceptor distance (Å)	O-acceptor distance (Å)	O-H-acceptor angle (°)
O(2)'-H···O(2)	2.29	3.06	143
O(2)'-H···O(3)	2.28	2.99	136
O(3)-H···O(3)'	1.84	2.74	159
O(2)-H···S'	2.23	3.14	163
O(3)'-H···S	2.56	3.33	143

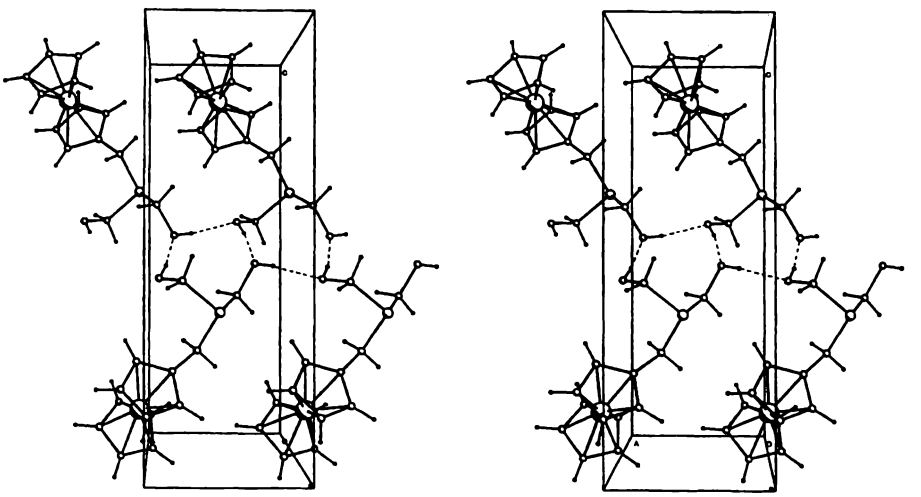

Figure 2.7: Stereo PLUTO diagram depicting the hydrogen-bonding array observed for **1**.

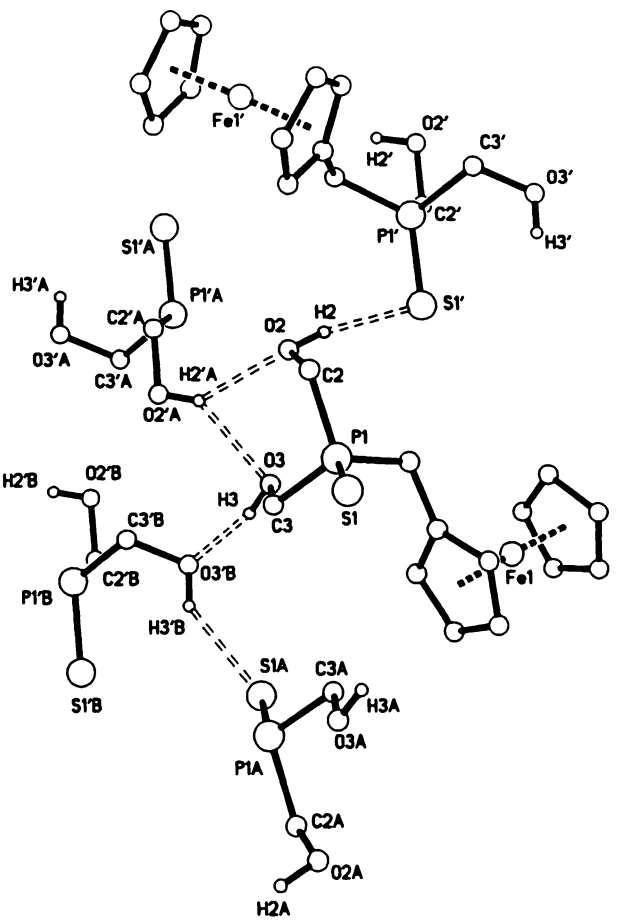

Figure 2.8: A SHELXTL PC-PX diagram depicting the hydrogen-bonding array observed for **4**.

The quality of crystallographic data obtained for compound **8** is appreciably lower than for the structure determinations of **1** and **4**, and the hydroxyl hydrogens could not be reliably located. However, the probable hydrogen-bonding pattern in this system can be deduced. The shortest oxygen-oxygen distances in the crystal are 4.267 Å, which precludes any appreciable hydrogen-bonding interactions between oxygens, in contrast with the situation for the other two structures. Instead the crystal packing is characterised by a pattern of I···H-O(1)-C(1)-P-C(1)'-O(1)'-H···I···H-O(1) hydrogen-bonding interactions between the cations and anions, propagating in the direction of the *b* axis (Figure 2.9). The O···I distance is 3.386 Å, and the C(1)-O(1)···I angle is 105.5 °. Hydroxymethyl-anion hydrogen-bonding interactions are also probable in the X-ray crystal structure of compound **18** discussed in Section 2.2.6.

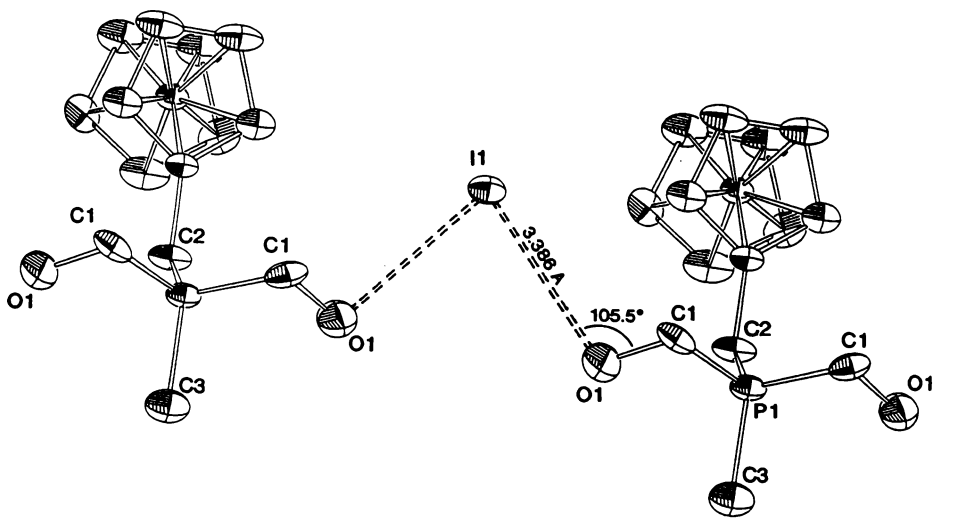

Figure 2.9: ZORTEP diagram depicting hydrogen-bonding for **8**.

Compound **2** offers no opportunities for hydrogen bonding, so this is of course not a feature of the crystal packing for this compound, in contrast to the other three compounds discussed in this Section.

2.2.4 Synthesis and Analysis of Ferrocenylphosphine-Metal Complexes

Several complexes were made using **1** as a phosphine ligand: The platinum(II) *cis*-$PtCl_2[FcCH_2P(CH_2OH)_2]_2$ **16** [^{31}P-NMR (d^6-DMSO): δ 7.8, s, ^1J(Pt-P) = 3428], palladium(II) $PdCl_2[FcCH_2P(CH_2OH)_2]_2$ **17** [^{31}P-NMR (d^6-DMSO): δ 32.4], gold(I) $[Au\{FcCH_2P(CH_2OH)_2\}_2]Cl$ **18** [^{31}P-NMR (d^6-DMSO): δ 36.2] and η^6-*p*-cymene ruthenium(II) $RuCl_2(\eta^6\text{-}C_{10}H_{14})[FcCH_2P(CH_2OH)_2]$ **19** [^{31}P-NMR ($CDCl_3$): δ 25.9] complexes. In addition, the complex $RuCl_2(\eta^6\text{-}C_{10}H_{14})[FcCH_2PPh_2]$ **20** [^{31}P-NMR ($CDCl_3$): δ 28.8] was prepared using **2** as the phosphine ligand. All complexes were synthesised by procedures standard for these kinds of metal-phosphine-halide complexes. Compounds **16** and **17** were prepared by displacement of the labile COD ligand from MCl_2(COD) (M = Pt **16** or Pd **17**). The products were largely insoluble in the dichloromethane in which the reaction was performed and so precipitated out and could be collected by filtration, then washed with dichloromethane to remove any remaining COD and **1**. Compound **18** was prepared by the reaction of AuCl(CNBu^t) with two equivalents of **1** and collected by precipitation of the product with petroleum spirits and filtration. It was initially thought that this reaction yielded the monophosphine complex $[Au\{FcCH_2P(CH_2OH)_2\}]Cl$ (and was reported as such in an initial communication[66]), and the product was only subsequently characterised as the bisphosphine complex. Even if the reaction is carried out with a 1:1 mole ratio of the reagents **18** will form in preference to the monophosphine complex. The monophosphine complex can be prepared as an unstable product by reaction of **1** with Au(tetrahydrothiophene)Cl. Degradation of this product gives a green coloured residue, even under nitrogen, suggesting it is unstable with respect to unknown redox processes, with oxidation of the ferrocene centre to the green-coloured ferrocenium equivalent. Compounds **19** and **20** were prepared by the bridge-splitting reaction of the appropriate ligand with $[RuCl_2(\eta^6\text{-}C_{10}H_{14})]_2$ under nitrogen [the ligand being either **1**, giving **19**, or **2**, giving **20**]. The crude products thus obtained can be easily purified by recrystallisation. Satisfactory elemental microanalytical data were obtained for all complexes, and compounds **18** and **20** were characterised by X-ray crystallography as

described in Section 2.2.6.

NMR data for the complexes **16** and **17** suggest that they are both square-planar with a *cis* configuration. In the case of **16** evidence for this is seen in the large ^{1}J(Pt-P) splitting of the ^{31}P-NMR signal of **16** at δ 7.8 (3428 Hz), which has been recognised as characteristic of *cis*-phosphine Pt complexes[67]. In addition, the CH_2 groups present in **16** exhibit a five-line multiplet pattern in ^{13}C-NMR which has been established as being characteristic of *cis* configuration for compounds of this sort, where there is an $A[X]_2$ spin system with virtual coupling[68]. ^{31}P-NMR of **17** indicates this Pd complex exists as only one isomer in solution, unlike some other similar Pd complexes. The CH_2 groups of **17** do not exhibit such a well-defined multiplet pattern for ^{13}C-NMR as do those of **16**, but consist of broad doublets, which have also been identified as indicative of *cis* conformation in this type of compound[68].

2.2.5 ESMS Analysis of Ferrocenylphosphine-Metal Complexes

While compounds **16** and **17** could not be induced to give interpretable ESMS spectra, compounds **18**, **19** and **20** were able to be characterised in this way. The gold complex **18** showed strong peaks for the parent cation $(L)_2Au^+$ (*m/z* 781) as well as the mono-phosphine species $(L)Au^+$ (*m/z* 489) (L = **1**) (Figure 2.10). Gold(I) phosphine complexes have been the subject of a detailed ESMS study, and ions of the type observed in this work were reported[69]. The stable carbocation $FcCH_2^+$ was observed at *m/z* 199; this ion is also observed as a fragment ion for the parent phosphine **1** (see Section 2.2.2), together with other $FcCH_2X$ type compounds[59]. Under the conditions employed for analysis of **19** and **20** one peak was observed, arising from the exchange of a chloride ligand for an acetonitrile solvent molecule (Figure 2.11).

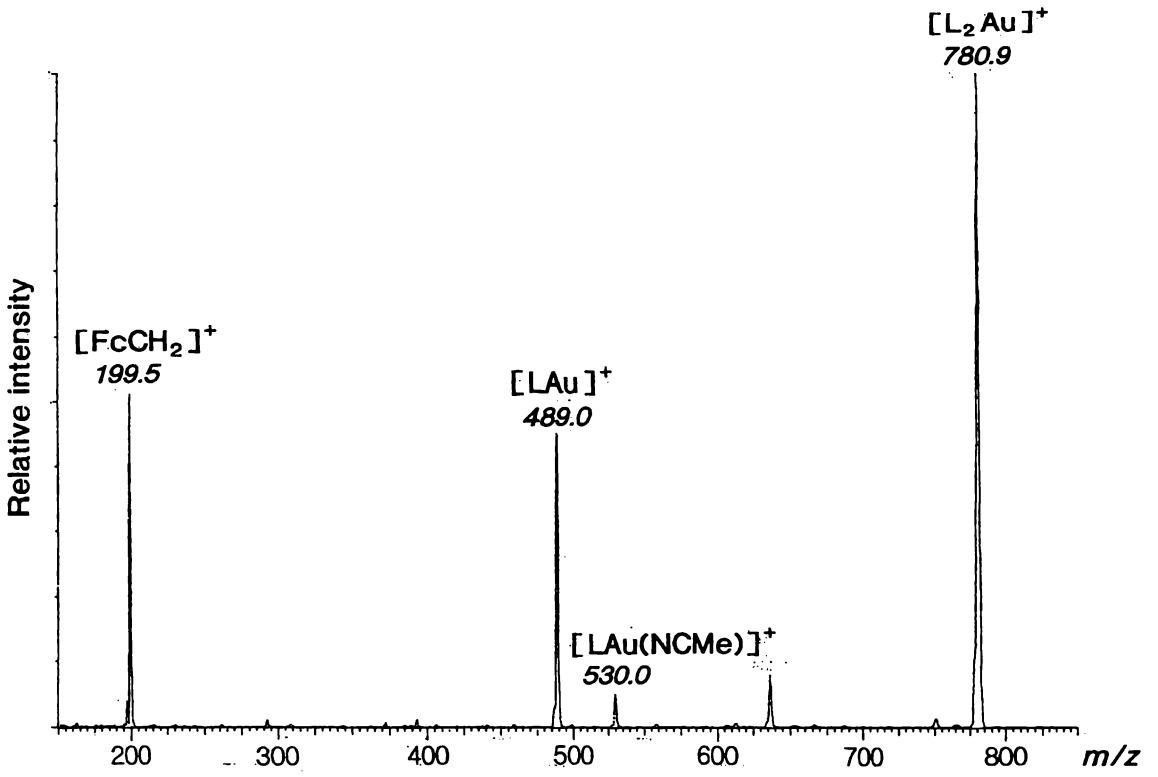

Figure 2.10: ESMS spectrum of **18**, run in water/acetonitrile at a cone voltage of 100 V (L = **1**).

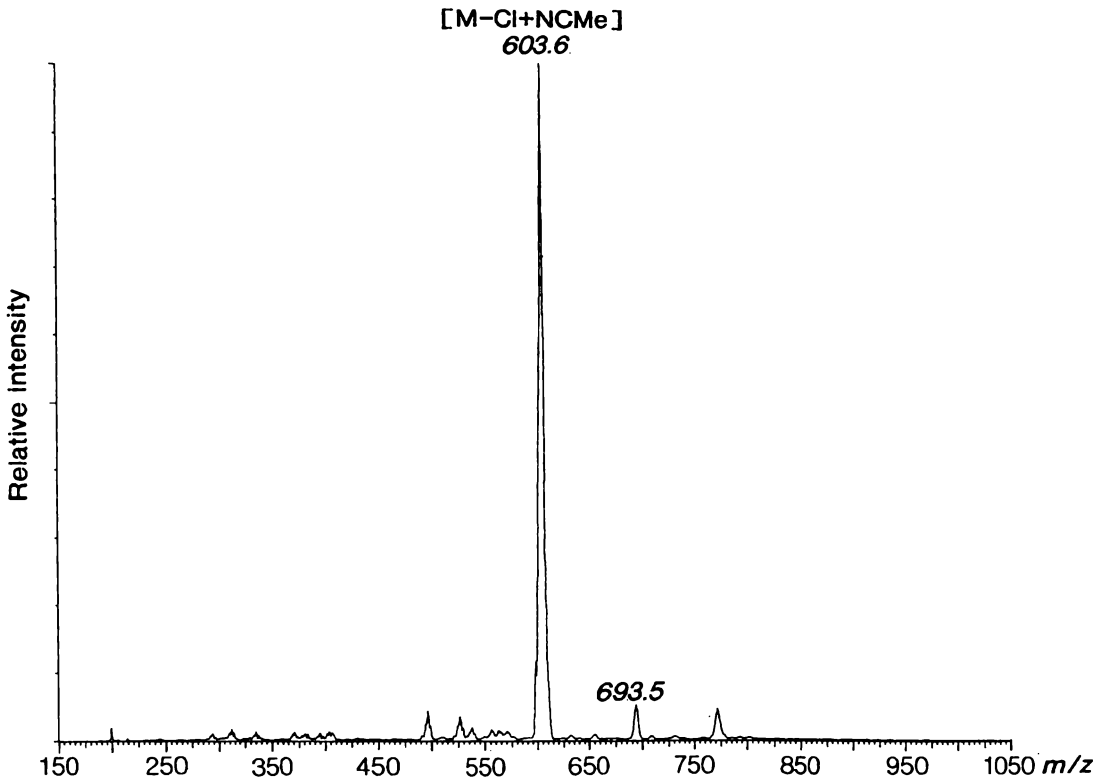

Figure 2.11: ESMS spectrum of compound **19**, run in water/acetonitrile at a cone voltage of 60 V (M = **19**).

2.2.6 X-Ray Crystal Structure Determinations for Compounds $[Au\{FcCH_2P(CH_2OH)_2\}_2]Cl$ **18** and $RuCl_2(\eta^6\text{-}C_{10}H_{14})(FcCH_2PPh_2)$ **20**

Crystals of **18** suitable for study by X-ray crystallography were obtained by recrystallisation from methanol/diethyl ether as outlined in Section 2.3.1.15. The structure obtained shows that the lattice contains the cation $[Au\{FcCH_2P(CH_2OH)_2\}_2]^+$, consisting of the gold(I) centre linearly-coordinated by two phosphine ligands **1**. Although not crystallographically necessitated, the cation has approximately two-fold rotational symmetry about the gold atom, as can easily be seen from inspection of Figure 2.12, where the structure is shown. Table 2.6 gives selected bond lengths and angles.

As well as the cation, the lattice also contains a water molecule of crystallisation and the chloride counter-ion. The chloride ion occupies two positions, one on an inversion centre, Cl(1), and another which is disordered with only 50% occupancy, Cl(2). Another source of disorder is the oxygen O(2), which shows about 70% occupancy of the dominant position, with an alternative position O(2a) (not shown in Figure 2.12) having about 30% occupancy.

The shortest Au···Cl distance in the lattice, Au(1)···Cl(1), is 3.436(2) Å, a distance a little greater than the sum of the van der Waals' radii (3.41 Å); any bonding interaction between the gold and chlorine atoms in the crystal must therefore be very weak. Additionally, the shortest gold-gold distance in the lattice is 5.8588 Å, which excludes the possibility of any bonding interactions between gold atoms. No hydroxyl hydrogen atoms could be located in the final difference map, but consideration of interatomic distances in the structure suggest hydrogen-bonding consists of a two-dimensional network in the plane of the *a* and *b* axes. In the direction of the *a* axis, hydrogen-bonding is probable between O(4), O(6) (that is, the water of crystallisation) and O(2) [or O(2a)] of the adjacent molecule [O(4)···O(6) = 2.707 Å, O(6)···O(2a) = 2.748 Å, O(6)···O(2) = 3.135 Å, C(4)-O(4)···O(6) = 109.9°,

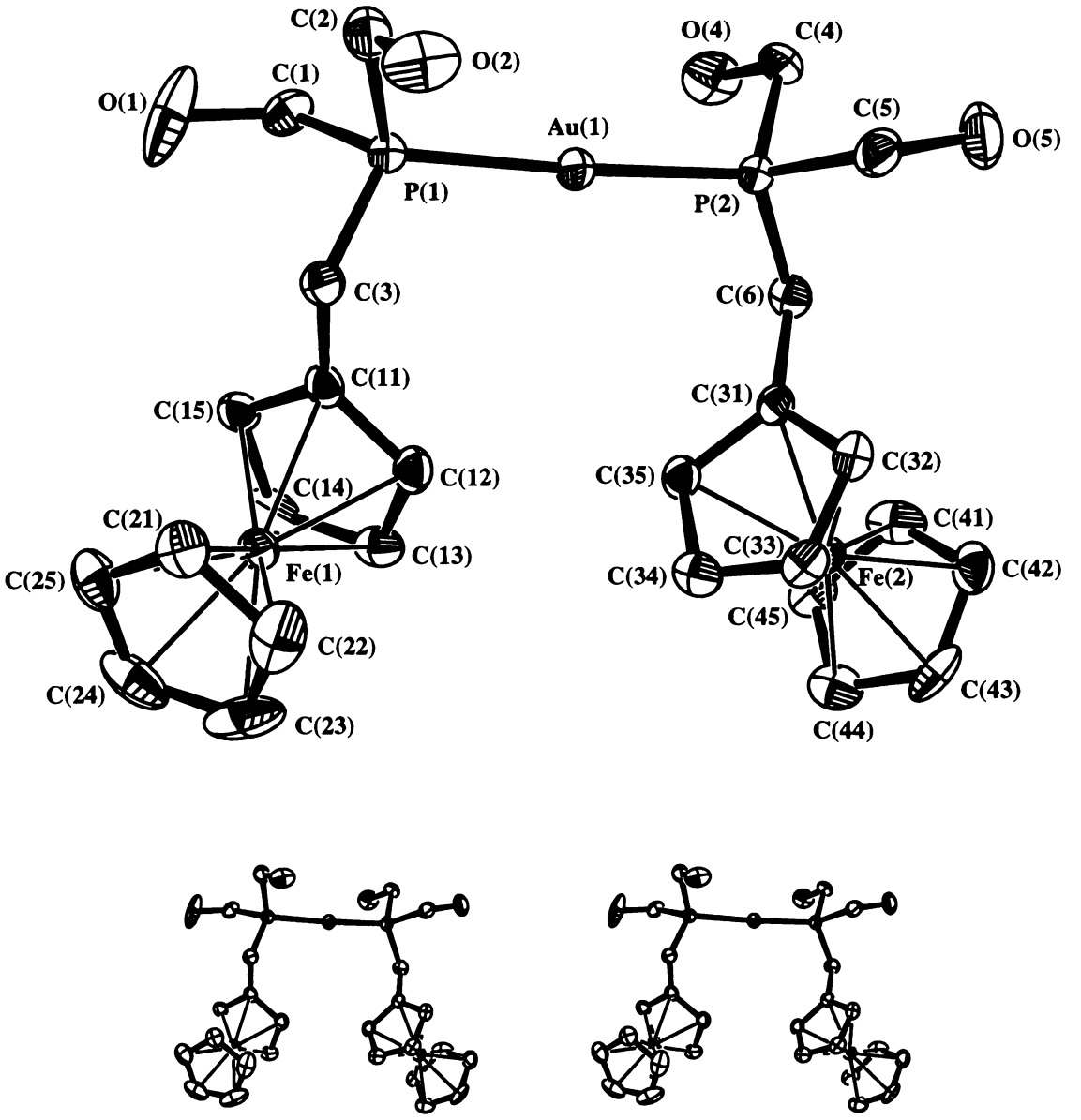

Figure 2.12: ORTEP diagram of **18**, with stereo view. The water molecule O(6), the anions, and O(2a) have been omitted for clarity.

C(2)-O(2)···O(6) = 100.0°, C(2)-O(2a)···O(6) = 122.2°]. In the direction of the *b* axis, a hydrogen bond is probable between O(4) and O(5) of adjacent molecules [O(4)···O(5) = 2.636 Å, C(4)-O(4)···O(5) = 109.9°]. Interatomic distances also suggest some hydrogen-bonding from O-H functions to both Cl(1) and Cl(2) is possible, with a number of O···Cl

Table 2.6: *Selected bond lengths (Å) and angles (°) for 18.*

Au(1)-P(2)	2.310(2)	Au(1)-P(1)	2.311(2)
P(1)-C(3)	1.821(6)	P(1)-C(1)	1.830(7)
P(1)-C(2)	1.839(7)	P(2)-C(6)	1.822(6)
P(2)-C(5)	1.831(7)	P(2)-C(4)	1.835(7)
O(1)-C(1)	1.428(9)	O(2)-C(2)	1.391(10)
O(4)-C(4)	1.432(9)	O(5)-C(5)	1.419(9)
C(3)-C(11)	1.505(9)	C(6)-C(31)	1.508(8)
P(2)-Au(1)-P(1)	176.51(6)	C(3)-P(1)-C(1)	105.0(3)
C(3)-P(1)-C(2)	103.2(3)	C(1)-P(1)-C(2)	103.9(3)
C(3)-P(1)-Au(1)	117.0(2)	C(1)-P(1)-Au(1)	114.0(2)
C(2)-P(1)-Au(1)	112.4(2)	C(6)-P(2)-C(5)	105.6(3)
C(6)-P(2)-C(4)	102.4(3)	C(5)-P(2)-C(4)	101.0(3)
C(6)-P(2)-Au(1)	117.3(2)	C(5)-P(2)-Au(1)	114.2(2)
C(4)-P(2)-Au(1)	114.4(2)	O(2)-C(2)-P(1)	112.4(5)
O(1)-C(1)-P(1)	113.1(5)	C(11)-C(3)-P(1)	112.7(4)
O(4)-C(4)-P(2)	110.9(4)	O(5)-C(5)-P(2)	112.2(5)
C(31)-C(6)-P(2)	112.7(4)	C(12)-C(11)-C(3)	126.2(6)
C(15)-C(11)-C(3)	126.5(6)	C(3)-C(11)-Fe(1)	125.2(4)
C(32)-C(31)-C(6)	126.8(6)	C(35)-C(31)-C(6)	126.1(6)
C(6)-C(31)-Fe(2)	126.4(4)		
Fe-C average		2.046(7) Å	
Fe-C range		2.026(7) - 2.060(7)	
C-C bonds of Cp average		1.417(10)	
range		1.386(11) - 1.430(9)	

distances of around 3 Å [O(2)···Cl(1) = 3.018 Å, O(2a)···Cl(2) = 2.476 Å, O(1)···Cl(2) = 3.193 Å, O(5)···Cl(2) = 2.925 Å, C(2)-O(2)···Cl(1) = 107.6°, C(2)-O(2a)···Cl(2) = 152.5°, C(1)-O(1)···Cl(2) = 129.6°, C(5)-O(5)···Cl(2) = 100.5°].

Several X-ray structures for hydroxymethylphosphine-gold(I) complexes have been reported, all very recently; the tetrahedral $[Au\{P(CH_2OH)_3\}_4]Cl$ and trigonal planar $[Au(Ph_2PCH_2OH)_3]Cl$ complexes[31], along with $[Au\{(HOH_2C)_2PC_6H_4P(CH_2OH)_2\}_2]Cl$ and $[Au_2\{(HOH_2C)_2PCH_2CH_2P(CH_2OH)_2\}_2]Cl_2$[36a], both of which contain chelating phosphine ligands. Of these, the latter compound is the one most structurally similar to **18**, containing two linearly-coordinated gold centres. However, unlike compound **18** this complex displays strong aurophilic interactions between the two gold atoms of the same molecule. Hydrogen-bonding interactions between hydroxymethyl groups are not noted in either of the two papers reporting these hydroxymethylphosphine-gold complexes, although such interactions must surely be present.

Crystals of **20** suitable for X-ray analysis were obtained by diffusion recrystallisation from dichloromethane/30-40° C petroleum spirits as described in Section 2.3.1.17. The structure obtained contained three independent molecules in the asymmetric unit along with three dichloromethane molecules. The three independent molecules of **20** are shown individually in Figures 2.13, 2.14 and 2.15. Selected bond lengths and angles are listed in Table 2.7. A number of structures have been reported for compounds analogous to compound **20**[70].

All three independent molecules share some common characteristics with respect to conformation. Geometry about the Ru(1) displays a piano stool conformation; that is, coordination is octahedral with the cymene group occupying one facial site. This geometry is somewhat distorted, so that the bond angles between the chloride and phosphine substituents of the ruthenium centre are between 84° and 89°, slightly lower than the idealised value of 90°. In addition, the Ru(1) and ferrocene group adopt an *anti* configuration about the P(1)-C(1) bond, and there is a staggered arrangement of substituents about the Ru(1)-P(1) bond.

Molecules 1 and 2 are clearly almost identical in all respects, the greatest difference being a *ca.* 10° disparity in rotation of the isopropyl group about the C(54)-C(3) bond. This is in contrast to molecule 3, which is significantly different to the other two in several respects.

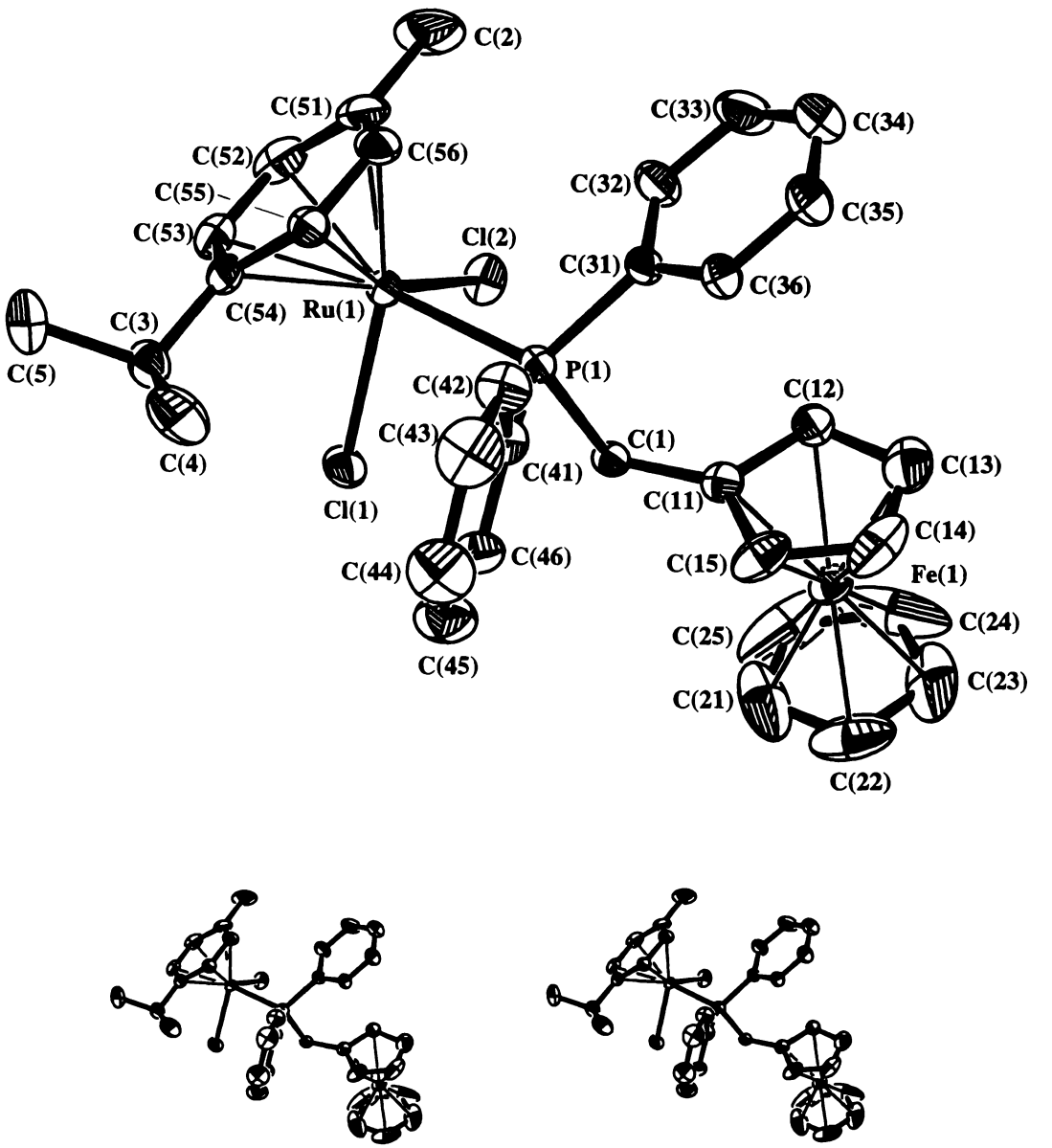

Figure 2.13: ORTEP diagram of molecule one of **20**, with stereo view.

Firstly, the orientation of the cymene ligand is inverted with respect to the rest of the molecule. In addition, the planes in which the phenyl rings lie are different, a difference which could be approximately described by saying a mirror plane through C(41), P(1) and

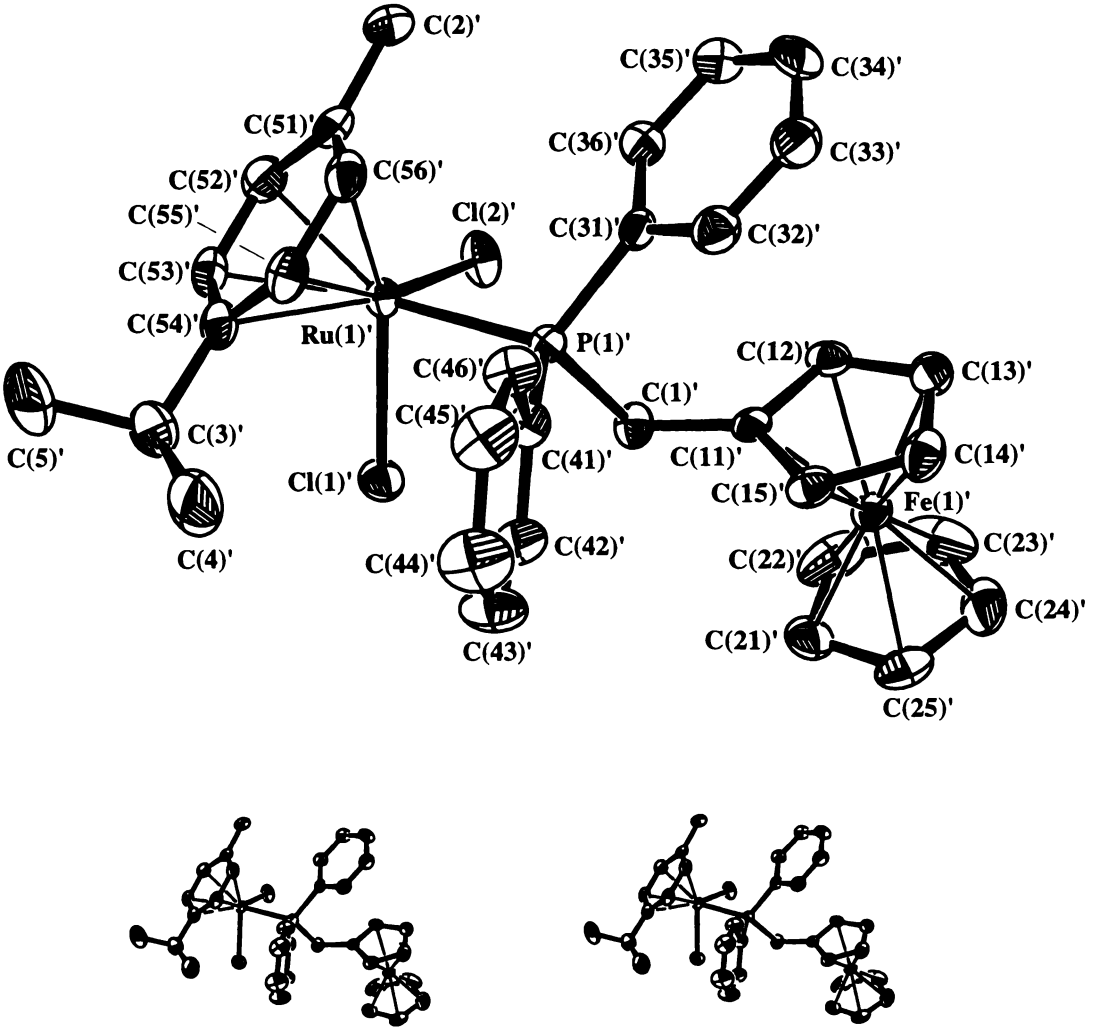

Figure 2.14: ORTEP diagram of molecule two of **20**, with stereo view.

C(31) would transform the phenyl rings of molecule 1 or 2 into those of molecule 3 Finally, the position of the isopropyl group about the C(54)-C(3) bond is rotated about 70° and 80° from those of molecules 1 and 2 respectively.

No notable sources of disorder were observed in the structure - only in the unsubstituted Cp ring of molecule one were the ellipsoids 'stretched out'. However, the refinement values such as R_1 and GOF are poor in the refined structure. This is probably accounted for by the exceptionally long unit cell *b* axis, which is about 61 Å in length. During data collection, spots along this axis would as a result be very closely spaced, leading to overlap and poorly

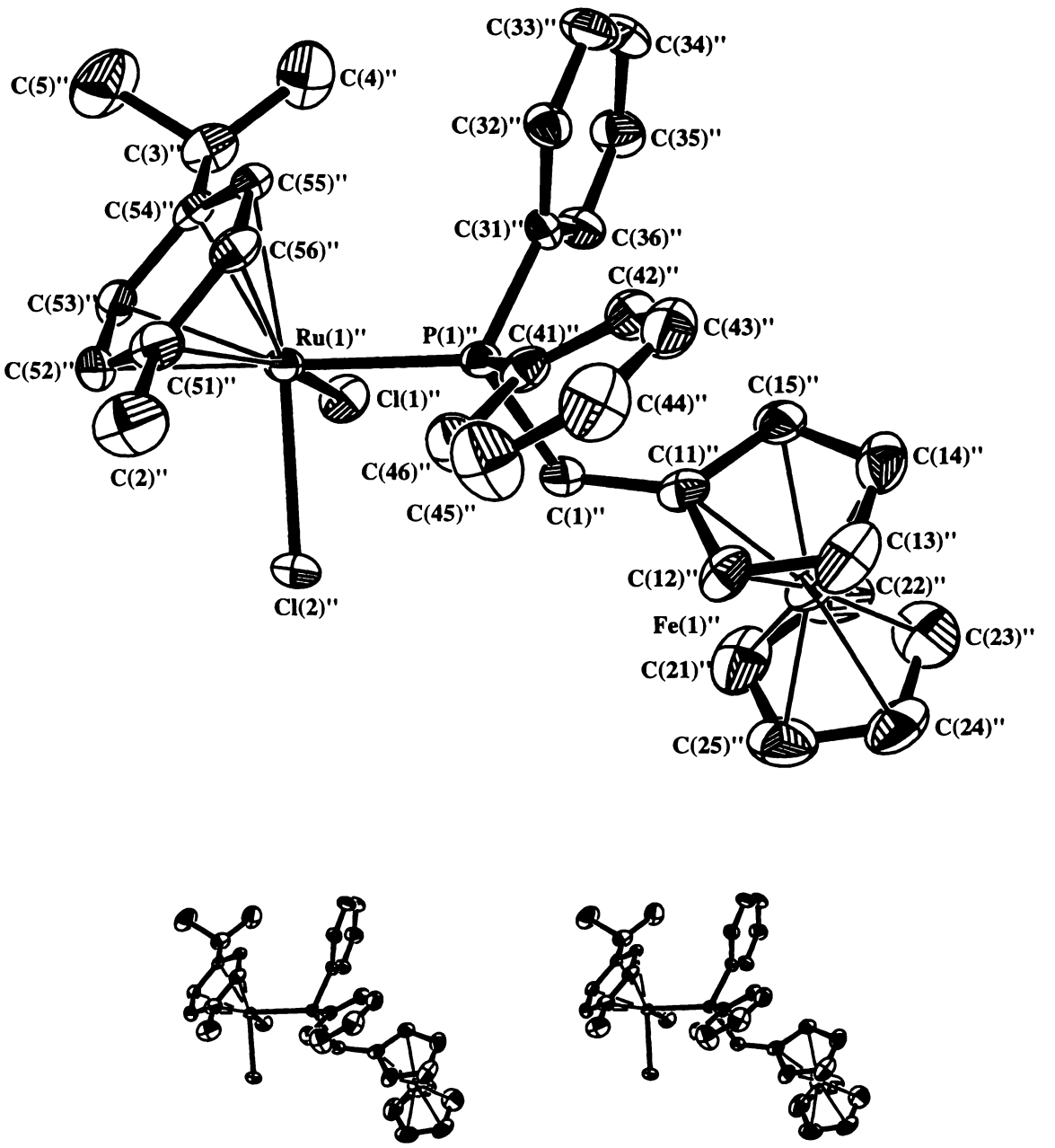

Figure 2.15: ORTEP diagram of molecule three of **20**, with stereo view.

resolved data. In fact, before solving in the correct space group, the initial choice of space group for this structure proved to be incorrect, a result of systematic absences in the k direction being undetected due to overlap of neighbouring spots.

Table 2.7: *Selected bond lengths (Å) and angles (°) for* ***20****. Elsewhere molecule 2 is denoted by apostrophes and molecule 3 by double apostrophes.*

		molecule 1	molecule 2	molecule 3
Ru(1)-Cl(1)		2.4031(18)	2.4109(18)	2.4113(17)
Ru(1)-Cl(2)		2.4182(17)	2.4137(17)	2.4112(18)
Ru(1)-P(1)		2.3507(18)	2.3483(18)	2.3494(18)
P(1)-C(1)		1.854(6)	1.843(7)	1.850(7)
P(1)-C(31)		1.820(7)	1.824(7)	1.827(7)
P(1)-C(41)		1.820(7)	1.823(7)	1.821(7)
C(1)-C(11)		1.492(9)	1.493(9)	1.493(10)
C(51)-C(2)		1.494(11)	1.510(11)	1.504(11)
C(54)-C(3)		1.512(10)	1.515(11)	1.518(10)
C(3)-C(4)		1.506(12)	1.502(13)	1.502(13)
C(3)-C(5)		1.525(11)	1.526(12)	1.545(12)
C-C for Cp rings	range	1.325(18)-1.441(10)	1.384(13)-1.423(9)	1.381(14)-1.434(12)
	average	1.386(15)	1.405(12)	1.405(13)
C-C for Ph rings	range	1.369(12)-1.404(9)	1.372(10)-1.404(9)	1.371(13)-1.405(10)
	average	1.385(11)	1.386(11)	1.387(11)
C-C for Cym ring	range	1.378(11)-1.436(12)	1.389(11)-1.436(10)	1.384(11)-1.436(10)
	average	1.412(11)	1.415(11)	1.412(11)
distance of Ru(1) out of plane of Cym ring		1.7020(40)	1.7022(40)	1.6942(40)
distance of Fe(1) out of planes of Cp rings (averaged for both)		1.6464(52)	1.6577(44)	1.6484(48)
P(1)-Ru(1)-Cl(1)		84.99(6)	84.67(6)	86.81(6)
P(1)-Ru(1)-Cl(2)		86.97(6)	86.95(6)	85.35(6)
Cl(1)-Ru(1)-Cl(2)		87.78(7)	88.56(7)	88.60(7)
Ru(1)-P(1)-C(1)		115.8(2)	115.2(2)	114.5(2)
Ru(1)-P(1)-C(31)		114.6(2)	116.3(2)	115.6(2)
Ru(1)-P(1)-C(41)		112.1(2)	110.6(2)	112.0(2)
P(1)-C(1)-C(11)		113.2(5)	113.6(5)	113.6(5)
C(54)-C(3)-C(4)		114.8(7)	113.8(8)	114.0(7)

Table 2.7 continued

C(54)-C(3)-C(5)	109.7(7)	108.5(8)	109.2(7)
C(4)-C(3)-C(5)	110.6(7)	111.4(8)	110.2(8)
Torsion angles:			
Ru(1)-P(1)-C(1)-C(11)	164.68(39)	161.36(41)	-164.75(43)
P(1)-Ru(1)-C(51)-C(2)	62.39(97)	58.05(93)	-61.74(89)
P(1)-C(1)-C(11)-C(12)	-94.18(69)	-97.70(68)	-79.44(80)
C(11)-C(1)-P(1)-C(41)	-71.08(53)	-76.19(56)	71.68(57)
C(11)-C(1)-P(1)-C(31)	39.88(54)	34.58(58)	-38.72(59)
C(4)-C(3)-C(54)-C(55)	-9.00(102)	-20.82(117)	-167.49(71)
C(5)-C(3)-C(54)-C(55)	116.28(81)	103.80(94)	68.77(92)
angle between planes of Ph rings	51.03	54.51	52.01

2.2.7 Anti-Tumour Activity of Ferrocenylphosphine Complexes

The platinum, palladium and gold hydroxymethylphosphine complexes **3-5** each contain a metal with known anticancer activity[71], as well as phosphine[72] and ferrocene units[73], which can both also show anti-tumour properties (in the case of ferrocene as the ferrocenium ion). Consideration was given to the possibility that in these complexes the combined effect of the sub-units might make them useful anti-tumour agents. This approach, whereby several functionalities which are individually active against tumours are combined into one compound, has been attempted by other researchers, resulting in compounds such as $(AuCl)_2(dppf)$[74] (combination of gold, phosphine and ferrocene) and *trans*-$PtCl_2(DMSO)[NC_5H_4\text{-}2\text{-}OTi(C_5H_5)_2Cl]$[75] (DMSO = dimethylsulfoxide; combination of Pt and titanocene). However, both **16** and **17** are too insoluble in methanol or water to be tested, while **18** was tested for cytotoxicity and found to be inactive, with an IC_{50} of 250,051 $\mu g.ml^{-1}$ using the P388 antitumour assay.

2.3 Experimental

2.3.1 Syntheses

Reactions were carried out in solvents of LR grade or better, in air unless otherwise stated. Petroleum spirits was of B.P. 60-80° C except where otherwise stated. The starting materials $[FcCH_2NMe_3]I$[76], $PtCl_2(COD)$[77], $PdCl_2(COD)$[78], $AuCl(CNBu^t)$[79], AuCl(tetrahydrothiophene)[80] and $[RuCl_2(\eta^6\text{-}C_{10}H_{14})]_2$[81] were prepared by literature methods; $[P(CH_2OH)_4]Cl$ was obtained as Retardol C from Albright & Wilson Ltd., Oldbury, UK, as an 80% w/w aqueous solution and used as supplied. Elemental analyses were performed by the Microanalytical Laboratory, Chemistry Department, University of Otago, Dunedin, New Zealand. The Fourier-transform IR spectra were obtained using a Bio-Rad FTS40 spectrometer, and run as KBr disks except for those cases where the product was an oil, in which case spectra of the neat product were obtained. Melting points were determined using a Reichert Thermopan melting-point microscope and are uncorrected.

Electrospray mass spectra were obtained in positive-ion mode with a VG Platform II mass spectrometer using a 1:1 v/v acetonitrile - water mobile phase. The compounds were dissolved in the mobile phase to give a solution typically of approximate concentration 0.1 mM. The diluted solution was injected into the spectrometer via a Rheodyne injector fitted with a 10 μL sample loop. A Thermo Separation Products SpectraSystem P1000 LC pump delivered the solution to the mass spectrometer source (60° C) at a flow rate of 0.01 ml min^{-1}, and nitrogen was employed both as a drying and nebulising gas. Cone voltages were typically varied from 10 to 100 V, in order to maximise spectrum quality. Excellent agreement between observed and calculated isotope distribution patterns was observed for all major peaks. Theoretical isotope patterns were calculated using the *Isotope* program[82]. Small quantities of $AgNO_3$ or NaCl were added as appropriate to aid ion formation.

The NMR spectra were obtained using a Bruker AC300 spectrometer, with spectra referenced to residual solvent lines. Solvents were assigned the following chemical shift values with respect to $SiMe_4$: $CDCl_3$, 7.26 (^1H), 77.06 (^{13}C); d^6-DMSO, 2.6 (^1H), 39.5 (^{13}C); D_2O, 3.5 (MeOH, ^1H), 49.3 (MeOH, ^{13}C). In the case of ^{31}P-NMR, chemical shift assignment was with respect to a simple external reference of 85% orthophosphoric acid. The spectrometer was operated at 75.47 MHz for ^{13}C, 300.13 MHz for ^1H, and 121.51 MHz for ^{31}P. Two-dimensional NMR experiments were used to unambiguously assign signals for compounds **1** and **5**. Comparison of these results with other spectra aided in the full assignment of the rest of the compounds. Scheme 2.12 depicts the labelling scheme used in assignment of ferrocenyl NMR signals.

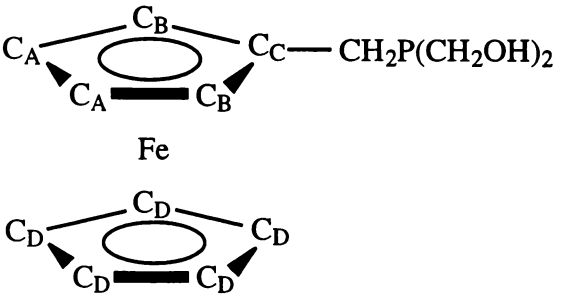

Scheme 2.12: Atom labelling used in NMR assignments of the ferrocenyl rings, shown for compound **1**.

Thermogravimetric analysis of **3** was carried out using a Perkin-Elmer DSC6 calorimeter, with the sample heated from 50° to 160° C at 15° C min^{-1}. Anti-tumour testing of compound **18** was carried out at the Chemistry Dept. of the University of Canterbury, Christchurch, New Zealand.

2.3.1.1 Synthesis of $FcCH_2P(CH_2OH)_2$ 1

A solution of $[P(CH_2OH)_4]Cl$ (38.54 g of 80% w/w aq. soln., 0.162 mol) in methanol (40 ml) was deoxygenated and placed under a nitrogen atmosphere, and KOH (8.52 g, 0.152 mol) added. The mixture was stirred for 1 hr before being added dropwise to a

deoxygenated solution of $[FcCH_2NMe_3]I$ (19.98 g, 52.2 mmol) in methanol (40 ml) under nitrogen with stirring. The reaction mixture was refluxed under nitrogen for 20 hr, and the solvent was then removed under vacuum until large amounts of precipitate were observed. Water (30 ml), diethyl ether (85 ml) and NEt_3 (35 ml) were added and the solution stirred for 1 hr. The aqueous layer was removed and re-extracted with diethyl ether (30 ml), and both ether extracts were combined and washed with water (3 × 20 ml), then filtered. Removal of the ether under reduced pressure yielded the crude product as a microcrystalline orange solid (14.33 g, 49.06 mmol, 94% yield). Recrystallisation by addition of petroleum spirits to warm dichloromethane/methanol solution followed by cooling to *ca.* -30° C gave yellow/orange crystals of **1** suitable for X-ray crystal structure analysis (10.69 g, 36.60 mmol, 70% yield), M.P. 104-106° C. Found: C, 53.5; H, 6.2; N, 0.0%. $C_{13}H_{17}FeO_2P$ requires: C, 53.5; H, 5.9; N, 0.0%. IR (cm^{-1}): 3371 (s), 3289 (s), 1463 (w), 1269 (w), 1232 (w), 1185 (w), 1434 (m), 1412 (m), 1104 (m), 1038 (w), 1003 (s), 922 (w), 885 (w), 854 (m), 827 (m), 807 (m), 754 (w), 657 (w), 572 (w), 500 (m), 483 (m). ESMS (with added $AgNO_3$){cone voltage = 60 V}: *m/z* 690.8 $[2M + Ag]^+$, 398.9 $[M + Ag]^+$, 292.1 $[M]^+$, 199.0 $[FcCH_2]^+$. $^{31}P-\{^1H\}$ NMR ($CDCl_3$): δ -19.3. ^1H NMR ($CDCl_3$): δ 2.59 (O<u>H</u>, broad s), 2.96 (FcC<u>H</u>$_2$P, s, 2H), 4.04-4.10 and 4.25-4.33 (PC<u>H</u>$_2$O, m, 4H), 4.09 (C_A-<u>H</u>, t, J = 2 Hz, 2H), 4.14 (C_D-<u>H</u>, s, 5H), 4.18 (C_B-<u>H</u>, t, J = 2 Hz, 2H). $^{13}C-\{^1H\}$ NMR ($CDCl_3$): δ 18.66 (Fc<u>C</u>H$_2$P, d, J = 11 Hz), 61.72 (P<u>C</u>H$_2$O, d, J = 23 Hz), 67.73 (C_A, s), 68.80 [C_B, s], 68.89 [C_D, s], 84.22 [C_C, s].

2.3.1.2 Synthesis of $FcCH_2PPh_2$ 2

A solution of $[Ph_2P(CH_2OH)_2]Cl$ (2.006 g, 7.09 mmol) in methanol (30 ml) was purged and placed under nitrogen, then KOH added (0.359 g, 6.39 mmol). The solution was stirred under nitrogen for two hr. $[FcCH_2NMe_3]I$ (2.002 g, 5.23 mmol) was dissolved in methanol (40 ml) in another flask and purged and placed under nitrogen. The first solution was then added dropwise to the second, and the resulting solution refluxed under nitrogen for 18 hr. Most solvent was removed under vacuum and a mixture of water (40 ml), diethyl ether (40 ml) and NEt_3 (30 ml) was added. This mixture was stirred for 4 hr, and the organic layer

isolated and filtered before washing with water (3 × 20ml). Removal of solvent under vacuum gave an orange oil. This material was purified by tlc, with dichloromethane used to charge the plate, and 10% diethyl ether in petroleum spirits used as the eluting solvent. The desired product ran with R_f = 0.73, and after removal from the plate and drying under vacuum, **2** was yielded as an orange oil which slowly crystallised (0.505 g, 1.31 mmol, 25%), M.P. 80-84° C. Crystals suitable for X-ray crystal structure analysis were obtained serendipitously by recrystallisation from a mixture of water, diethyl ether, and petroleum spirits. Found: C, 72.1; H, 5.4%. $C_{23}H_{21}FeP$ requires: C, 71.9; H, 5.5%. IR (cm^{-1}): 1583 (w), 1480 (w), 1469 (w), 1432 (m), 1305 (w), 1182 (w), 1102 (m), 1023 (m), 999 (m), 924 (w), 840 (w), 816 (s), 741 (s), 695 (s), 479 (s). ESMS {cone voltage = 20 V}: *m/z* 384.2 $[M]^+$. $^{31}P-\{^1H\}$ NMR ($CDCl_3$): δ -11.8. ^1H NMR ($CDCl_3$): δ 3.16 ($FcC\underline{H}_2P$, s, 2H), 3.92 (C_B-H, unres. t, 2H), 3.98 (C_A-H, t, J = 2 Hz, 2H), 4.10 (C_D-H, s, 5H), 7.31-7.42 (Ph-H, m, 10H). $^{13}C-\{^1H\}$ NMR ($CDCl_3$): δ 30.29 ($FcCH_2P$, d, J = 14 Hz), 67.42 (C_A, s), 68.84 (C_D, s), 69.23 (C_B, d, J = 4 Hz), 84.33 (C_C, d, J = 17 Hz), 128.35 (*p*-C, s), 128.54 (*m*-C, d, J = 17 Hz), 132.93 (*o*-C, d, J = 19 Hz), 138.85 (*i*-C, d, J = 15 Hz).

2.3.1.3 *Synthesis of $FcCH_2P(O)(CH_2OH)_2$ 3*

Aqueous hydrogen peroxide (10 ml, 0.234% w/v, 0.688 mmol) was added to a solution of **1** (0.200 g, 0.685 mmol) in MeOH (20 ml). The resulting solution was stirred in air for 7 min before partly removing the solvent under vacuum (temperature was maintained at *ca.* 15° C), causing the product **2** to precipitate. This was filtered off under vacuum and washed with water, then dried under vacuum yielding the crude product as a yellow powder (0.157 g, 0.511 mmol, 75%). Yellow crystals of **3** were obtained by recrystallisation using the same method as for **1** (0.120 g, 0.389 mmol, 55%), M.P. 126-135° C. Found: C, 48.6; H, 5.9%. $C_{13}H_{17}FeO_3P.0.67H_2O$ requires: C, 48.8; H, 5.8%. IR (cm^{-1}): 3310 (s), 3272 (s), 3137 (s), 2897 (m), 1690 (br, w), 1464 (w), 1426 (m), 1409 (m), 1241 (w), 1206 (m), 1144 (s), 1128 (s), 1104 (m), 1090 (m), 1038 (s), 1022 (m), 999 (m), 923 (w), 891 (w), 859 (m), 833 (m), 812 (m), 791 (m), 731 (m), 701 (m), 661 (w), 501 (m), 486 (m), 456 (m). ESMS (with added NaCl) {cone voltage = 40 V}: *m/z* 638.9 $[2M + Na]^+$, 331.1 [M +

Na]$^+$, 308.1 [M]$^+$. ^{31}P-{^{1}H} NMR ($CDCl_3$): δ 45.8. ^{1}H NMR (d^6-DMSO): δ 2.95 (FcC$\underline{H}_2$P, d, J = 12 Hz, 2H), 3.72 (PC$\underline{H}_2$O, d, J = 3 Hz, 4H), 4.18 (C_A-$\underline{H}$, t, J = 2 Hz, 2H), 4.23 (C_D-$\underline{H}$, s, 5H), 4.29 (C_B-$\underline{H}$, s, 2H). ^{13}C-{^{1}H} NMR ($CDCl_3$): δ 25.81 (Fc$\underline{C}H_2$P, d, J = 56 Hz), 55.30 (P$\underline{C}H_2$O, d, J = 80 Hz), 68.49 (C_A, s), 69.06 (C_D, s), 69.26 (C_B, s), C_C not observed.

2.3.1.4 Synthesis of $FcCH_2P(S)(CH_2OH)_2$ 4

Elemental sulfur (0.043 g, 1.35 mmol) and **1** (0.202 g, 0.693 mmol) were dissolved in toluene (20 ml) with a small amount of methanol present to effect full solubilisation. The solution was refluxed in air for 3 hr and most of the solvent removed under vacuum. The solution was cooled to *ca.* -30° C and crystals formed. These were collected by vacuum filtration and washed with toluene before drying under vacuum to yield the crude product as a yellow powder (0.188 g, 0.579 mmol, 84%). Dark orange crystals of **4**, suitable for X-ray crystal structure analysis, were obtained by recrystallisation using the same method as for **1** (0.162 g, 0.500 mmol, 72%), M.P. 115-118° C. Found: C, 48.0; H, 5.3%. $C_{13}H_{17}FeO_2PS$ requires: C, 48.2; H, 5.3%. IR (cm^{-1}): 3407 (s), 3326 (s), 3264 (s), 1389 (w), 1361 (w), 1164 (w), 1105 (m), 1041 (s), 1027 (s), 999 (w), 881 (w), 850 (w), 826 (m), 802 (m), 753 (w), 690 (w), 627 (m), 610 (w), 573 (w), 555 (w), 500 (m), 483 (m), 436 (w). ESMS (with added NaCl) {cone voltage = 40 V}: *m/z* 670.9 [2M + Na]$^+$, 347.1 [M + Na]$^+$, 324.0 [M]$^+$. ^{31}P-{^{1}H} NMR ($CDCl_3$): δ 44.0. ^{1}H NMR ($CDCl_3$): δ 3.23 (FcC$\underline{H}_2$P, d, J = 13 Hz, 2H), 3.87-3.91 (PC$\underline{H}_2$O, m, 4H), 4.15 (C_D-$\underline{H}$, s, 5H), 4.18 (C_A-$\underline{H}$, t, J = 2 Hz, 2H), 4.24 (C_B-$\underline{H}$, s, 2H). ^{13}C-{^{1}H} NMR ($CDCl_3$): δ 30.11 (Fc$\underline{C}H_2$P, d, J = 42 Hz), 58.62 (P$\underline{C}H_2$O, d, J = 54 Hz), 68.87 (C_A, s), 69.10 (C_B, s), 69.18 (C_D, s), C_C not observed.

2.3.1.5 Synthesis of $FcCH_2P(CH_2CH_2CN)_2$ 5

Compound **1** (0.400 g, 1.37 mmol) was dissolved in methanol (20 ml) and acrylonitrile (0.20 ml, 3.04 mmol) added. The solution was stoppered and stirred in air for 90 min, after which time the solvent was removed under vacuum. Crystallisation from chloroform/diethyl ether was used to precipitate an impurity, with the supernatant decanted off and the solvent removed to yield the product **5** as an orange oil, which hardens to a semi-crystalline solid when cooled to 0° C overnight (0.428 g, 1.27 mmol, 92%). A sample for elemental analysis was obtained by twice washing a portion of the solid with diethyl ether prior to analysis. The product proved too amorphous to be suitable for melting point determination. Found: C, 59.6; H, 5.7; N, 8.2%. $C_{17}H_{19}FeN_2P$ requires: C, 60.4; H, 5.7; N, 8.3%. IR (cm^{-1}): 3334 (s), 2248 (w), 1651 (s), 1560 (s), 1481 (s), 1423 (s), 1393 (w), 1347 (w), 1327 (s), 1276 (w), 1104 (m), 1038 (m), 1023 (m), 1001 (m), 924 (w), 819 (s), 679 (m), 589 (s), 498 (s), 484 (s). ESMS (with added $AgNO_3$) {cone voltage = 60 V}: *m/z* 783.2 $[2M + Ag]^+$, 445.0 $[M + Ag]^+$, 338.0 $[M]^+$, 198.9 $[FcCH_2]^+$. $^{31}P-\{^1H\}$ NMR ($CDCl_3$): δ -22.1. ^1H NMR ($CDCl_3$): δ 1.57-1.78 ($C\underline{H}_2CN$, m, 4H), 2.31 ($PC\underline{H}_2CH_2$, t of d, J = 10 Hz, J = 8 Hz, 4H), 2.69 ($FcC\underline{H}_2P$, d, J = 4 Hz), 4.05 (C_B-$\underline{H}$, t, J = 2 Hz, 2H), 4.11 (C_A-$\underline{H}$, t, J = 1 Hz, 2H), 4.12 (C_D-$\underline{H}$, s, 5H). $^{13}C-\{^1H\}$ NMR ($CDCl_3$): δ 14.48 ($P\underline{C}H_2CH_2$, d, J = 23 Hz), 22.29 ($\underline{C}H_2CN$, d, J = 17 Hz), 27.72 ($Fc\underline{C}H_2P$, d, J = 17 Hz), 68.09 (C_A, s), 68.58 (C_B, s), 68.96 (C_D, s), 81.87 (C_C, d, J = 6 Hz), 119.30 ($\underline{C}N$, d, J = 12 Hz).

2.3.1.6 Synthesis of $FcCH_2P(CH_2NEt_2)_2$ 6 and $FcCH_2P(O)(CH_2NEt_2)_2$ 7

Compound **1** (0.200 g, 0.683 mmol) was dissolved in dichloromethane (10 ml) and placed under nitrogen. $HNEt_2$ (1.00 ml, 9.71 mmol) was added and the solution stirred for 2 hr, after which time the solvent was removed under vacuum, giving **6** as a yellow oil. ESMS (with added $AgNO_3$) {cone voltage = 60 V}: *m/z* 911.7 $[2M + Ag]^+$, 856.5 $[2M + Ag - NEt_2 + OH]^+$, 801.4 $[2M + Ag - 2NEt_2 + 2OH]^+$, 403.2 $[M + H]^+$, 198.9 $[FcCH_2]^+$. $^{31}P-\{^1H\}$ NMR ($CDCl_3$): δ -48.3. ^1H NMR ($CDCl_3$): δ 0.99 ($CH_2C\underline{H}_3$, t, J = 7 Hz, 12H), 2.53-2.69

($C\underline{H}_2CH_3$ and $FcC\underline{H}_2P$ and $PC\underline{H}_2N$, m, 14H), 4.03 (C_A-$\underline{H}$, t, J = 2 Hz, 2H), 4.08-4.09 (C_B-$\underline{H}$ and C_D-$\underline{H}$, m, 7H). ^{13}C-{^1H} NMR ($CDCl_3$): δ 11.75 ($CH_2\underline{C}H_3$, s), 27.00 ($Fc\underline{C}H_2$, d, J = 16 Hz), 48.14 ($\underline{C}H_2CH_3$, d, J = 9 Hz), 53.66 ($P\underline{C}H_2N$, d, J = 7 Hz), 67.36 (C_A, s), 68.77 (C_D, s), 68.97 (C_B, s), 84.56 (C_C, d, J = 8 Hz). The product was redissolved in methanol (30 ml) and aqueous hydrogen peroxide solution added (5 ml, 0.469%, 0.690 mmol). The mixture was stirred for 15 min, then most of the solvent was removed under vacuum with the temperature of the mixture maintained at *ca.* 15° C. The residue was extracted with ether (20 ml), and the organic layer washed with water (3 × 10 ml) and dried under vacuum to give the crude product as a pale orange solid (0.249 g, 0.595 mmol, 87%). Recrystallisation from acetone/pentane cooled to *ca.* -30° C gave **7** as an orange powder (0.154 g, 0.368 mmol, 54%). More product, though less pure, can be obtained by recrystallisation of the evaporated supernatant. M.P. 102-107° C. Found: C, 60.2; H, 8.6; N, 6.5%. $C_{21}H_{35}FeN_2OP$ requires: C, 60.3; H, 8.4; N, 6.7%. IR (cm^{-1}): 3095 (m), 2964 (s), 2931 (s), 2872 (m), 2810 (s), 1466 (m), 1457 (m), 1422 (w), 1386 (m), 1371 (m), 1336 (w), 1297 (w), 1252 (m), 1243 (s), 1199 (m), 1170 (s), 1141 (s), 1104 (s), 1064 (m), 1039 (w), 1019 (w), 998 (m), 976 (w), 926 (w), 860 (m), 816 (s), 784 (m), 597 (w), 490 (s), 434 (m). ESMS {cone voltage = 20 V}: *m/z* 837.3 $[2M + H]^+$, 419.1 $[M + H]^+$. ^{31}P-{^1H} NMR ($CDCl_3$): δ 45.0. ^1H NMR ($CDCl_3$): δ 0.98 ($CH_2C\underline{H}_3$, t, J = 7 Hz, 12H), 2.60-2.77 ($C\underline{H}_2CH_3$ and $PC\underline{H}_2N$, m, 12H), 3.02 ($FcC\underline{H}_2P$, d, J = 14 Hz, 2H), 4.09 (C_A-$\underline{H}$, t, J = 2 Hz, 2H), 4.11 (C_D-$\underline{H}$, s, 5H), 4.22 (C_B-$\underline{H}$, t, J = 2 Hz, 2H). ^{13}C-{^1H} NMR ($CDCl_3$): δ 11.25 ($CH_2\underline{C}H_3$, s), 28.93 ($Fc\underline{C}H_2P$, d, J = 60 Hz), 48.28 ($\underline{C}H_2CH_3$, d, J = 7 Hz), 50.35 ($P\underline{C}H_2N$, d, J = 82 Hz), 67.99 (C_A, s), 68.99 (C_D, s), 69.44 (C_B, s), 79.26 (C_C, s).

2.3.1.7 Synthesis of [$FcCH_2P(Me)(CH_2OH)_2$]I **8**

Compound **1** (0.302 g, 1.03 mmol) was dissolved in methanol (10 ml), and methyl iodide (1.0 ml, 16 mmol) was slowly added with swirling. The solution was heated to 50° C for 15 min, then diethyl ether (120 ml) added to precipitate the product as a yellow powder (0.411 g, 0.946 mmol, 92%). Recrystallisation from hot methanol gave orange crystals of **8**

suitable for X-ray crystal structure analysis (0.306 g, 0.705 mmol, 68%), M.P. *ca.* 170° C (dec.). Found: C, 38.8; H, 4.5%. $C_{14}H_{20}FeIO_2P$ requires: C, 38.7; H, 4.6%. IR (cm^{-1}): 3253 (s), 1427 (m), 1404 (w), 1388 (w), 1306 (w), 1285 (w), 1200 (w), 1103 (w), 1035 (s), 996 (m), 960 (m), 921 (m), 882 (m), 865 (w), 839 (m), 814 (m), 499 (s), 479 (s). ESMS {cone voltage = 20 V}: *m/z* 307.2 $[M - I]^+$, 291.2 $[M - I - CH_4]^+$. $^{31}P-\{^1H\}$ NMR (d^6-DMSO): δ 26.2. ^1H NMR (d^6-DMSO): δ 1.67 ($C\underline{H}_3$, d, J = 14 Hz, 3H), 3.57 ($FcC\underline{H}_2P$, d, J = 14 Hz, 2H), 4.29-4.43 (Cp-H and $PC\underline{H}_2O$, m, 11H). $^{13}C-\{^1H\}$ NMR (d^6-DMSO): δ 3.15 ($\underline{C}H_3$, d, J = 48 Hz), 22.18 ($Fc\underline{C}H_2P$, d, J = 41 Hz), 55.54 ($P\underline{C}H_2O$, d, J = 56 Hz), 72.53 (C_A, s), 72.94 (C_D, s), 73.24 (C_B, s), 78.84 (C_C, s).

2.3.1.8 Synthesis of $FcCH_2P(Me)CH_2OH$ ***9***

Compound **8** (0.167 g, 0.384 mmol) was dissolved in diethyl ether (40 ml) and water (25 ml) and NEt_3 (1.0 ml, 14 mmol) added. The mixture was stirred for 2 hr. The organic layer was then extracted and washed with water (2 × 20 ml) before drying under vacuum. The product **9** was obtained as a yellow oil (0.099 g, 0.360 mmol, 94%). Attempts to purify this product further by chromatography were unsuccessful. IR (cm^{-1}): 3361 (s), 3092 (s), 2966 (s), 2897 (s), 2814 (s), 1636 (w), 1466 (s), 1421 (s), 1351 (m), 1287 (m), 1233 (m), 1195 (w), 1152 (w), 1104 (s), 1021 (s), 1002 (s), 925 (s), 897 (s), 818 (s), 716 (w), 593 (w). ESMS {cone voltage = 10 V}: *m/z* 291.4 $[M + CH_3]^+$, 277.3 $[M + H]^+$. $^{31}P-\{^1H\}$ NMR ($CDCl_3$): δ -33.1. ^1H NMR ($CDCl_3$): δ 0.98 ($C\underline{H}_3$, d, J = 3 Hz, 3H), 2.60-2.64 ($FcC\underline{H}_2P$, m, 2H), 3.81 ($PC\underline{H}_2O$, d, J = 8 Hz, 2H), 4.07-4.11 (Cp-H, m, 9H). $^{13}C-\{^1H\}$ NMR ($CDCl_3$): δ 7.12 ($\underline{C}H_3$, d, J = 15 Hz), 26.64 ($Fc\underline{C}H_2P$, d, J = 14 Hz), 62.27 ($P\underline{C}H_2O$, d, J = 15 Hz), 67.59 (C_A, s), 68.70 (C_B, s), 68.79 (C_D, s), 84.08 (C_C, d, J = 8 Hz).

2.3.1.9 Synthesis of $[(FcCH_2)_2P(CH_2OH)_2]Cl$ ***10***

$FcCH_2OH$ (0.503 g, 2.33 mmol) was dissolved in dichloromethane (20 ml, dry and oxygen-free), purged and placed under nitrogen. Oxalyl chloride (0.4 ml, 5 mmol) was added and the reaction stirred under nitrogen for 90 min. This mixture was dried under vacuum, then

redissolved in dichloromethane (20 ml, dry and oxygen-free). Compound **1** (0.681 g, 2.33 mmol) was added and the reaction stirred overnight. The product thus formed was dried under vacuum and methanol (7 ml) and the residue heated to *ca.* 50° C before filtering off the supernatant. Diethyl ether (40 ml) was used to precipitate the product. After cooling to *ca.* -30° C, the product **10** was filtered off as a yellow microcrystalline solid (0.354 g, 0.672 mmol, 28.9%). M. P. *ca.* 220° C (dec.). Found: C, 54.4; H, 5.4%. $C_{24}H_{28}ClFe_2O_2P$ requires: C, 54.7; H, 5.3%. IR (cm^{-1}): 3250 (s), 2980 (w), 2956 (w), 2918 (w), 2892 (w), 1427 (s), 1404 (m), 1386 (m), 1307 (w), 1285 (w), 1214 (w), 1200 (w), 1102 (m), 1035 (s), 996 (m), 960 (s), 920 (s), 882 (m), 865 (w), 839 (m), 814 (s), 498 (s), 479 (s). ESMS {cone voltage = 40 V}: *m/z* 490.9 $[M]^+$, 476.9 $[M - CH_2]^+$, 460.8 $[M - CH_2O]^+$, 307.4 $[M - C_5H_5FeC_5H_4 + H]^+$, 291.2 $[M - C_5H_5FeC_5H_4 - OH + H]^+$, 199.5 $[FcCH_2]^+$. $^{31}P-\{^1H\}$ NMR (d^6-DMSO): δ 22.3. ^1H NMR (d^6-DMSO): δ 3.40 (O<u>H</u>, s, 2H), 3.52 (FcC<u>H</u>$_2$P, d, J = 13 Hz, 4H), 4.20 (PC<u>H</u>$_2$O, d, J = 6 Hz, 4H), 4.26 (C_D-<u>H</u>, s, 10H), 4.27 (C_A-<u>H</u>, unres. t, 4H), 4.39 (C_B-<u>H</u>, unres. t, 4H). $^{13}C-\{^1H\}$ NMR (d^6-DMSO): δ 21.37 (Fc<u>C</u>H$_2$P, d, J = 37 Hz), 54.49 (P<u>C</u>H$_2$O, d, J = 53 Hz), 72.41 (C_A, s), 72.95 (C_D, s), 73.46 (C_B, s), 78.68 (C_C, s).

2.3.1.10 Synthesis of $(FcCH_2)_2PCH_2OH$ 11

Water (10 ml) and diethyl ether (10 ml) were added to compound **10** (0.300 g, 0.570 mmol). After addition of NEt_3 (3 ml) the mixture was stirred for 10 min, and the organic layer removed and washed with water (10 ml × 3). This was filtered and dried under reduced pressure. Diffusion recrystallisation from dichloromethane/30°-40° C petroleum spirits yielded the product **11** as an orange powder (0.125 g, 0.272 mmol, 48%), M.P. 129-135° C. Found: C, 60.0; H, 5.3%. $C_{23}H_{25}Fe_2OP$ requires: C, 60.0; H, 5.5%. IR (cm^{-1}): 3389 (s, br), 3089 (s), 2943 (w), 2905 (m), 2840 (w), 1632 (m, br), 1467 (m), 1440 (m), 1413 (m), 1354 (w), 1236 (w), 1196 (m), 1103 (s), 1038 (s), 1014 (s), 998 (s), 925 (m), 839 (s), 810 (s), 713 (w), 667 (w), 602 (w), 483 (s), 425 (m). ESMS {cone voltage = 20 V}: *m/z* 476.3 $[M + O]^+$, 355.2 $[M + O - C_5H_5Fe]^+$, 231.0 $[Fc\text{-}CH{=}PH_2]^+$, 214.1 $[Fc\text{-}CHO]^+$. $^{31}P-\{^1H\}$ NMR ($CDCl_3$): δ -17.1. ^1H NMR ($CDCl_3$): δ 2.55-2.67 (FcC<u>H</u>$_2$P, m,

4H), 3.79 ($PC\underline{H}_2O$, d × d, J = 6 × 8 Hz, 2H), 4.09 (C_A-H, t, J = 2 Hz, 4H), 4.11-4.12 (C_B-H and C_D-H, m, 14H). ^{13}C-{^1H} NMR ($CDCl_3$): δ 24.65 ($Fc\underline{C}H_2P$, d, J = 16 Hz), 60.41 ($P\underline{C}H_2O$, d, J = 20 Hz), 67.70 (C_A, d, J = 7 Hz), 68.66 (C_B, d, J = 3 Hz), 68.88 (C_D, s), 84.30 (C_C, d, J = 10 Hz).

2.3.1.11 *Synthesis of* $[FcCH_2P(H)Ph_2]BF_4$ **14**

Compound **2** (0.100 g, 0.259 mmol) was dissolved in diethyl ether (5 ml), purged and placed under nitrogen. A solution of HBF_4 in acetonitrile (5.6 ml, 48 mmol L^{-1}, 0.269 mmol) was purged and placed under nitrogen before being added dropwise over 20 min to the ether solution. Solution was stirred for a further 5 min, then petroleum spirits (20 ml) and a small amount of diethyl ether were added, causing the product to separate out as an oil. The supernatant was removed and the oil washed with petroleum spirits (3 × 5 ml), then dried under vacuum for two days, giving the product as a yellow oil (0.113 g, 0.239 mmol, 92%). IR (cm^{-1}): 3440 (m, br), 3092 (w), 3062 (w), 2963 (w), 2922 (w), 1637 (w), 1589 (w), 1485 (w), 1439 (s), 1407 (m), 1385 (m), 1121 (s), 1083 (s), 1063 (s), 1040 (s), 999 (s), 923 (m), 900 (m), 832 (m), 742 (s), 691 (s), 521 (m), 490 (s), 463 (m). ESMS {cone voltage = 40 V}: *m/z* 384.4 $[M - H - BF_4]^+$, 198.6 $[FcCH_2]^+$. ^{31}P-{^1H} NMR ($CDCl_3$): δ 6.31 [d, ^1J(P-H) = 511 Hz]. ^1H NMR ($CDCl_3$): δ 4.57-4.70 ($Fc\underline{C}H_2P$ and Cp-H, m, 11H), 7.99-8.27 (Ph-H, m, 10H). ^{13}C-{^1H} NMR ($CDCl_3$): δ 23.82 ($Fc\underline{C}H_2P$, d, J = 43 Hz), 69.55 (C_A, s), 69.89 (C_D, s), 70.03 (C_B, s), 78.15 (C_C, d, J = 611 Hz), 115.43 (*i*-C, d, J = 82 Hz), 130.20 (*o*-C, d, J = 13 Hz), 133.67 (*m*-C, d, J = 10 Hz), 135.14 (*p*-C, s).

2.3.1.12 *Synthesis of* $FcCH_2P(O)Ph_2$ **15**

Compound **2** (0.100 g, 0.260 mmol) was placed in a flask with hydrogen peroxide (0.190 g, 6% soln., 0.335 mmol), water (5 ml), methanol (35 ml) and dichloromethane (10 ml). The solution was stirred for 1 hr before most of the solvent was removed under vacuum without heating. Once the product had largely precipitated out of solution diethyl ether was added, and this organic layer was then washed with water (3 × 10 ml). As methanol was

removed by washing from the organic layer, some product precipitated, necessitating the addition of some dichloromethane to help solubilisation. Solvent was removed giving the crude product in quantitative yield as a yellow powder. Recrystallisation by vapour diffusion from dichloromethane/petroleum spirits at 4° C gave the product **15** as a brown powder (0.086 g, 0.215 mmol, 83%). M.P. 203-205° C (dec.). Found: C, 68.4; H, 5.1%. $C_{23}H_{21}FeOP$ requires: C, 69.0; H, 5.3%. IR (cm^{-1}): 1437 (m), 1385 (w), 1208 (w), 1183 (s), 1121 (m), 1101 (m), 1071 (w), 1001 (w), 928 (w), 821 (m), 744 (s), 726 (s), 696 (s), 604 (w), 537 (s), 508 (m), 490 (s). ESMS {cone voltage = 100 V}: *m/z* 801.4 $[2M + H]^+$, 401.2 $[M + H]^+$, 335.0 $[M - Cp]^+$, 198.6 $[FcCH_2]^+$. $^{31}P-\{^1H\}$ NMR ($CDCl_3$): δ 29.0 (s). ^1H NMR ($CDCl_3$): δ 3.42 ($FcC\underline{H}_2P$, d, J = 13 Hz, 2H), 4.01 (C_A-$\underline{H}$ and C_B-$\underline{H}$, s, 4H), 4.08 (C_D-$\underline{H}$, s, 5H), 7.39-7.70 (Ph-$\underline{H}$, m, 10H). $^{13}C-\{^1H\}$ ($CDCl_3$): δ 33.38 ($Fc\underline{C}H_2P$, d, J = 67 Hz), 68.02 (C_A, s), 68.90 (C_D, s), 69.85 (C_B, s), 77.77 (C_c, d, J = 3 Hz), 128.43 (*o*-C, d, J = 11 Hz), 131.27 (*m*-C, d, J = 9 Hz), 131.76 (*p*-C, s), 133.06 (*i*-C, s).

2.3.1.13 Synthesis of cis-$PtCl_2[FcCH_2P(CH_2OH)_2]_2$ **16**

Phosphine **1** (0.100 g, 0.343 mmol) and $PtCl_2(COD)$ (0.064 g, 0.172 mmol) were dissolved in dichloromethane (10 ml, LR grade) and stirred for 30 min. The resulting precipitate was removed by vacuum filtration, and dried under vacuum, giving **16** as a yellow powder (0.128 g, 0.151 mmol, 88 %), M.P. *ca.* 210° C (dec.). Found: C, 37.1; H, 4.5%. $C_{26}H_{34}Cl_2Fe_2O_4P_2Pt$ requires: C, 36.7; H, 4.0%. IR (cm^{-1}): 3410 (s), 3093 (w), 2919 (w), 2853 (w), 1462 (w), 1427 (m), 1405 (m), 1386 (m), 1237 (w), 1173 (w), 1105 (m), 1038 (s), 1028 (s), 1002 (m), 924 (w), 878 (m), 832 (m), 747 (w), 501 (m), 484 (m), and 452 (m). $^{31}P-\{^1H\}$ NMR (d^6-DMSO): δ 7.8 [s, ^1J(Pt-P) = 3428 Hz]. ^1H NMR (d^6-DMSO): δ 3.25 ($FcC\underline{H}_2P$, J = 5 Hz, 2H), 4.04-4.19 (C_A-$\underline{H}$, C_D-$\underline{H}$, and $PC\underline{H}_2O$, m, 15H), and 4.34 (C_B-$\underline{H}$, unresolved t, 2H). $^{13}C-\{^1H\}$ NMR (d^6-DMSO): δ 25.51 ($Fc\underline{C}H_2P$, m), 58.62 ($P\underline{C}H_2O$, m), 71.49 (C_A, s), 72.57 (C_D, s), 73.70 (C_B, s), and 83.65 (C_C, s).

2.3.1.14 Synthesis of $PdCl_2[FcCH_2P(CH_2OH)_2]_2$ 17

Phosphine **1** (0.1248 g, 0.427 mmol) and $PdCl_2$(COD) (0.051 g, 0.214 mmol) were dissolved in dichloromethane (5 ml) and stirred for 15 min. The solution was cooled to 4° C before the precipitate was removed by vacuum filtration, washed with dichloromethane, and dried under vacuum. Product **17** was obtained as an orange/brown powder insoluble in most common organic solvents, (0.145 g, 0.191 mmol, 89 %), M.P. *ca.* 185° C (dec.). Found: C, 41.7; H, 4.4%. $C_{26}H_{34}Cl_2Fe_2O_4PdP_2$ requires: C, 41.0; H, 4.5%. IR (cm^{-1}): 3389 (s), 3094 (m), 2918 (w), 2852 (w), 1462 (w), 1427 (m), 1405 (m), 1386 (m), 1299 (w), 1237 (w), 1175 (w), 1105 (m), 1139 (s), 1126 (s), 1103 (m), 923 (w), 879 (m), 858 (m), 829 (m), 594 (w), 500 (m), 484 (m), and 444 (m). ^{31}P-{^1H} NMR (d^6-DMSO): δ 32.4 (s). ^1H NMR (d^6-DMSO): δ 3.24 (FcC$\underline{H}_2$P, d, J = 7 Hz, 2H), and 4.04-4.44 (Cp-$\underline{H}$, and PC$\underline{H}_2$O, m, 13H). ^{13}C-{^1H} NMR (d^6-DMSO): δ 24.26 (Fc$\underline{C}H_2$P, m), 57.67 (P$\underline{C}H_2$O, m), 69.49 (C_A, s), 70.48 (C_D, s), 71.33 (C_B, s), and 81.64 (C_C, s).

2.3.1.15 Synthesis of $[Au\{FcCH_2P(CH_2OH)_2\}_2]Cl$ 18

Phosphine **1** (0.093 g, 0.314 mmol) and AuCl(CNBu^t) (0.050 g, 0.159 mmol) were dissolved in dichloromethane (5 ml) and the solution stirred for 15 min. Petroleum spirits (B.P. 40-60° C, 10 ml) was added and the resulting precipitate removed by vacuum filtration. This was then dried under vacuum to give the product **18** as a yellow powder (0.105 g, 0.129 mmol, 80.6%). Recrystallisation from hot methanol/diethyl ether yielded golden needles suitable for X-ray crystal structure analysis (0.069 g, 0.084 mmol, 53%). M.P. 127-134° C. Found: C, 37.1; H, 3.9%. $C_{26}H_{34}AuClO_4P_2Fe_2.H_2O$ requires: C, 37.4; H, 4.3%. IR (cm^{-1}): 3259 (s, br), 1408 (m), 1386 (m), 1298 (w), 1242 (w), 1185 (w), 1106 (m), 1038 (s), 1027 (s), 1002 (m), 926 (w), 887 (m), 804 (m), 595 (w), 504 (m), 483 (m), and 445 (w). ESMS {cone voltage = 100 V}: *m/z* 780.9 $[AuL_2]^+$, 489.0 $[AuL]^+$, 199.5 $[FcCH_2]^+$, (L = **1**). ^{31}P-{^1H} NMR (d^6-DMSO): δ 36.2 (s). ^1H NMR (d^6-DMSO): δ 3.14

(FcC$\underline{H}_2$P, s, 2H), 4.05-4.08 (PC$\underline{H}_2$O, m, 4H), 4.20 (C_A-$\underline{H}$, t, J = 2 Hz, 2H), 4.24 (C_D-$\underline{H}$, s, 5H), and 4.26 (C_B-$\underline{H}$, t, J = 2, 2H). ^{13}C-{^{1}H} NMR ($CDCl_3$): δ 24.90 (Fc$\underline{C}H_2$P, m), 59.53 (P$\underline{C}H_2$O, m), 71.73 (C_A, s), 72.69 (C_D, s), 73.15 (C_B, s), and 84.48 (C_C, s).

2.3.1.16 Synthesis of $RuCl_2(\eta^6\text{-}C_{10}H_{14})[FcCH_2P(CH_2OH)_2]$ ***19***

$[RuCl_2(\eta^6\text{-}C_{10}H_{14})]_2$ (0.070 g, 0.114 mmol) was dissolved in dichloromethane (10 ml) which was purged and placed under nitrogen before addition of **1** (0.066 g, 0.227 mmol). The mixture was refluxed for 20 min and the solvent removed under vacuum to give the crude product as a dark oil in quantitative yield. Vapour diffusion recrystallisation from dichloromethane/ethanol with pentane yielded the product as a brown powder (0.093 g, 0.155 mmol, 68%). M.P. 181-188° C. Found: C, 46.2; H, 5.5%. $C_{23}H_{31}Cl_2FeO_2PRu$ requires: C, 46.2; H, 5.2%. IR (cm^{-1}): 3398 (s), 3174 (m), 3082 (m), 3043 (s), 2964 (m), 2873 (m), 1498 (w), 1467 (m), 1441 (m), 1384 (m), 1105 (m), 1036 (s), 1023 (s), 1002 (m), 924 (m), 890 (m), 864 (m), 823 (m), 811 (m), 777 (w), 508 (s), 479 (s), 460 (m), 444 (s), 426 (m). ESMS {cone voltage = 60 V}: *m/z* 603.6 $[M - Cl + CH_3CN]^+$. ^{31}P-{^{1}H} NMR ($CDCl_3$): δ 25.9 (s). ^{1}H NMR ($CDCl_3$): δ 1.23 [CH(C$\underline{H}_3$)$_2$, d, J = 7 Hz, 6H], 2.05 (C$\underline{H}_3$, s, 3H), 2.78 [C$\underline{H}$(CH$_3$)$_2$, hept., J = 7 Hz, 1H], 3.24 (FcC$\underline{H}_2$P, d, J = 8 Hz, 2H), 4.16 (C_D-$\underline{H}$, s, 5H), 4.18-4.19 (PC$\underline{H}_2$O and C_A-$\underline{H}$, m, 6H), 4.29 (C_B-$\underline{H}$, s, 2H), 5.44 [CH$_3$C(C$\underline{H}$)$_2$, d, J = 6 Hz, 2H], 5.50 [(CH$_3$)$_2$CHC(C$\underline{H}$)$_2$, d, J = 6 Hz, 2H]. ^{13}C-{^{1}H} NMR ($CDCl_3$): δ 18.36 (C$\underline{H}_3$, s), 22.21 [CH(C$\underline{H}_3$)$_2$, s], 24.88 (Fc$\underline{C}H_2$P, d, J = 19 Hz), 30.75 [C$\underline{H}$(CH$_3$)$_2$, s], 58.34 (P$\underline{C}H_2$O, d, J = 31 Hz), 68.46 (C_A, s), 69.23 (C_D, s), 69.69 (C_B, s), 80.66 (C_C, s), 85.51 [CH$_3$C(C$\underline{H}$)$_2$, d, J = 4 Hz], 87.98 [(CH$_3$)$_2$CHC(C$\underline{H}$)$_2$, d, J = 4 Hz], 96.41 [CH$_3$C$\underline{C}$(CH)$_2$, s], 107.11 [(CH$_3$)$_2$CH$\underline{C}$(CH)$_2$, s].

2.3.1.17 Synthesis of $RuCl_2(\eta^6\text{-}C_{10}H_{14})(FcCH_2PPh_2)$ ***20***

$[RuCl_2(\eta^6\text{-}C_{10}H_{14})]_2$ (0.037 g, 0.0609 mmol) was dissolved in dichloromethane (10 ml) which was purged and placed under nitrogen before addition of **2** (0.047 g, 0.122 mmol).

The mixture was refluxed for 15 min and the solvent removed under vacuum to give the crude product as a dark oil in quantitative yield. Vapour diffusion recrystallisation from dichloromethane with 30-40° petroleum spirits at 4° C yielded the product as large dark purple crystals suitable for X-ray crystallography (0.070 g, 0.102 mmol, 84%). M.P. *ca.* 200° C (dec.). Found: C, 52.6; H, 4.7%. $C_{33}H_{35}Cl_2FePRu.CH_2Cl_2$ requires: C, 52.6, H, 4.8%. IR (cm^{-1}): 3053 (m), 2963 (m), 1409 (m), 1469 (m), 1433 (s), 1481 (m), 1386 (m), 1319 (w), 1276 (w), 1237 (w), 1196 (m), 1160 (w), 1103 (s), 1057 (m), 1026 (m), 1000 (m), 926 (m), 821 (s), 750 (s), 728 (s), 696 (s), 663 (m), 597 (m), 483 (w). ESMS {cone voltage = 60 V}: *m/z* 695.5 $[M - Cl + CH_3CN]^+$, 384.5 $[\mathbf{2}]^+$. $^{31}P-\{^1H\}$ NMR ($CDCl_3$): δ 28.8. ^1H NMR ($CDCl_3$): δ 0.86 [$CH(C\underline{H}_3)_2$, d, J = 7 Hz, 6H], 1.82 ($C\underline{H}_3$, s, 3H), 2.50 [$C\underline{H}(CH_3)_2$, hept., J = 7 Hz, 1H], 3.32 ($FcC\underline{H}_2P$, s, 2H), 3.63 (C_A-$\underline{H}$, d, J = 7 Hz, 2H), 3.70 (C_B-$\underline{H}$, d, J = 2 Hz, 2H), 3.99 (C_D-$\underline{H}$, s, 5H), 5.08 [$CH_3C(C\underline{H})_2$, d, J = 6 Hz, 2H], 5.22 [$(CH_3)_2CHC(C\underline{H})_2$, d, J = 6 Hz, 2H], 7.32-7.71 [Ph-$\underline{H}$, m, 10H]. $^{13}C-\{^1H\}$ NMR ($CDCl_3$): δ 17.30 ($\underline{C}H_3$, s), 21.48 [$CH(\underline{C}H_3)_2$, s], 25.36 ($Fc\underline{C}H_2P$, d, J = 22 Hz), 30.00 [$\underline{C}H(CH_3)_2$, s], 67.04 (C_A, s), 68.75 (C_D, s), 70.05 (C_B, s), 80.72 (C_C, d, J = 9 Hz), 85.61 [$CH_3C(\underline{C}H)_2$, d, J = 5 Hz], 90.08 [$(CH_3)_2CHC(\underline{C}H)_2$, d, J = 4 Hz], 94.09 [$CH_3\underline{C}(CH)_2$, s], 108.40 [$(CH_3)_2CH\underline{C}(CH)_2$, s], 127.79 (*m*-C, d, J = 9 Hz), 130.47 (*p*-C, s), 132.20 [*i*-C, d, J = 42 Hz], 133.95 (*o*-C, d, J = 9 Hz).

2.3.1.18 *Production of Chiral $FcCH_2P(Bz)CH_2OH$ 13, and Reaction with a Secondary Amine.*

Compound **1** (0.099 g, 0.338 mmol) was dissolved in methanol (10 ml) and heated to 45° C. Benzyl bromide (0.20 ml, 1.7 mmol) was then added dropwise and the mixture stirred for 15 min. Solvent was removed under reduced pressure to give a yellow oil which was then crystallised from methanol/diethyl ether by cooling a solution to *ca.* -30° C, giving the crude phosphonium salt **12** as a yellow powder (0.075 g, 0.165 mmol, 49%). ESMS {cone voltage = 10 V}: *m/z* 503.1 $[M - Br - 2CH_2OH + 2Bz]^+$ (34%), 443.1 $[M - Br - CH_2OH + Bz]^+$ (62%), 412.4 $[M - Br - 2CH_2OH + Bz + H]^+$ (22%), 383.1 $[M - Br]^+$ (100%), 352.5 $[M - Br - CH_2O]^+$ (72%). $^{31}P-\{^1H\}$ NMR (d^6-DMSO): δ 26.0 (s). $^{13}C-\{^1H\}$ NMR (d^6-

DMSO): δ 19.41 ($P\underline{C}H_2Bz$, d, J = 38 Hz), 23.93 ($Fc\underline{C}H_2P$, d, J = 38 Hz), 52.37 ($P\underline{C}H_2O$, d, J = 55 Hz), 70.32 (C_A, s), 70.81 (C_D, s), 71.23 (C_B, s), 76.31 (C_C, s), 129.75 (*p*-C, s), 130.07 (*i*-C, d, J = 8 Hz), 130.87 (*m*-C, s), 131.91 (*o*-C, d, J = 5 Hz). Compound **12** (0.049 g, 0.106 mmol), was dissolved with quinine (0.081 g, 0.213 mmol) in a two-phase system of water (10 ml) and diethyl ether (10 ml). These were stirred for 1 hr, and the organic layer removed and solvent removed to give crude **13** in quantitative yield. $^{31}P-\{^1H\}$ NMR ($CDCl_3$): δ -15.0 (s). To the $CDCl_3$ solution of **13** in the NMR tube was then added a few drops of (*R*)-(+)-N-benzyl-α-methyl-benzylamine. ^{31}P-NMR spectra were run periodically over a 20 min period in order to monitor the formation of the two diastereoisomers of the product. $^{31}P-\{^1H\}$ NMR ($CDCl_3$): δ -28.5, -28.3 [(*R*,*R*) and (*R*,*S*) adducts, 2 × s].

2.3.2 X-ray Crystal Structure Determinations for Compounds $FcCH_2P(CH_2OH)_2$ **1**, $FcCH_2PPh_2$ **2**, $FcCH_2P(S)(CH_2OH)_2$ **4** and $[FcCH_2P(Me)(CH_2OH)_2]I$ **8**

Crystallographic data for compounds **1**, **2**, **4** and **8** are given in Table 2.8. Crystals were obtained by procedures detailed in Section 2.3.1. Raw data were corrected for absorption based on a series of ψ scans.

In all four structures the solutions were found by direct methods and developed routinely. Full-matrix least-squares refinement was based on F^2, with all non-hydrogen atoms anisotropic. Hydrogen atoms were included in calculated positions with isotropic temperature factors 1.2 times that of the U_{iso} of the atom to which they are bonded, with the following exceptions: in **1** atoms H(2) and H(3) (bonded to atoms O(2) and O(3) respectively) were located in a penultimate electron density map and refined with fixed isotropic temperature factors; in **4** atoms H(2) and H(3) and H(2)' and H(3)' (bonded to atoms O(2), O(3), O(2)' and O(3)' respectively) were located in a penultimate electron

density map and refined in a riding model; in **8** the hydroxyl hydrogen could not be located and was therefore not included. Calculated positions for the C(3) methyl group of **8** were established such that the C(3)-P bond configuration was staggered.

Drawing programmes XPMA[83] and PLUTO assisted in the investigation of hydrogen-bonding, and structures have been illustrated with ORTEP[84], ZORTEP[85], PLUTO and SHELXTL/PC-XP[86].

Appendix A gives complete lists of atomic coordinates, bond parameters and tables of thermal parameters and hydrogen atom coordinates for the structure determinations of **1**, **2**, **4** and **8**. In the case of **1**, **4** and **8** this data has also been deposited at the Cambridge Crystallographic Data Centre (CCDC)[87]. The CCDC reference number is 186/706.

2.3.3 X-Ray Crystal Structure Determinations for Compounds $[Au\{FcCH_2P(CH_2OH)_2\}_2]Cl$ **18** and $RuCl_2(\eta^6\text{-}C_{10}H_{14})[FcCH_2PPh_2]$ **20**

Crystals of **18** and **20** were obtained by the methods outlined in Section 2.3.1. Full crystallographic data for both compounds is given in Table 2.9. The data collection for both structures nominally covered over a hemisphere of reciprocal space, by a combination of three sets of exposures; each set had a different ϕ angle for the crystal and each exposure covered 0.3° in ω. The crystal to detector distance was 5.0 cm. In hindsight it appears that in the case of **20** a longer crystal to detector distance would have been desirable in order to avoid the problems of low resolution of spots in the k direction due to the exceptionally long *b* axis of the unit cell. The data sets were corrected empirically for absorption using SADABS[88]. The structures were solved by Patterson methods and developed routinely. Full-matrix least squares refinement was based on F^2.

Table 2.8: *Crystallographic data for compounds 1, 2, 4 and 8.*

	1	2	4	8
Empirical formula	$C_{13}H_{17}FeO_2P$	$C_{23}H_{21}FeP$	$C_{13}H_{17}FeO_2PS$	$C_{14}H_{20}FeIO_2P$
M_r	292.10	384.22	324.15	434.02
space group	$P2_12_12_1$	$P_{2(1)}$	$P_{\bar{1}}$	Pnma
crystal system	orthorhombic	monoclinic	triclinic	orthorhombic
a (Å)	6.299(2)	10.3723(7)	10.765(1)	14.875(7)
b (Å)	11.561(2)	8.2245(10)	11.024(2)	9.727(8)
c (Å)	17.519(2)	10.9666(8)	12.791(1)	10.868(6)
α (°)	90	90	67.93(1)	90
β (°)	90	104.755(5)	80.69(1)	90
γ (°)	90	90	77.95(1)	90
V (Å^3)	1275.8(4)	904.68(14)	1369.9(3)	1572(2)
density (g.cm^{-3})	1.521	1.410	1.572	1.833
Z	4	2	4	4
F(000)	608	400	672	856
μ(Mo-K_α) (mm^{-1})	1.29	0.92	1.360	3.019
temperature (°C)	-115	-115(2)	-83(2)	-115(2)
crystal size (mm)	0.70 × 0.45 × 0.25	0.8 × 0.4 × 0.2	0.32 × 0.24 × 0.19	0.50 × 0.20 × 0.15
θ range	2.11° < θ <25°	2.03° < θ < 30.00°	2.54° < θ < 25°	2.32° < θ < 22.49°
total reflections	1421	2963	5560	1275
unique reflections	1401	2822	4736	1095

R_{int}	0.0140	0.0254	0.0106	0.0367
T_{min}	- [ϑ]	0.298	0.675	0.3643
T_{max}	- [ϑ]	0.377	0.953	0.6467
$R_1 (I > 2\sigma(I))$	0.0297	0.0342	0.0269	0.0704
wR_2 (all data)	0.0667[⊗]	0.0792[℘]	0.0648[⊕]	0.2025[∅]
GOF	0.957	1.092	1.048	0.979
e⁻ density max (e.Å^{-3})	0.385	0.407	0.315	1.678
e⁻ density min (e.Å^{-3})	-0.294	-0.226	-0.389	-1.208
Flack x-parameter	0.04(3)	-0.02(2)	-	-
diffractometer	Nicolet R3	Nicolet R3	Siemens P4	Nicolet R3
solution and refinement programmes	SHELXS-86[89] SHELXL-93[90]	SHELXS-86, SHELXL-93	SHELXTL-PC[91], SHELXL-93	SHELXS-86, SHELXL-93

[ϑ] Absorption correction was performed but transmission factors were not recorded.

[⊗] $w = [\sigma^2(F_o^2) + (0.0593P)^2]^{-1}$ where $P = (F_o^2 + 2F_c^2)/3$

[℘] $w = [\sigma^2(F_o^2) + (0.0425P)^2 + 0.10P]^{-1}$ where $P = (\max(F_o^2,0) + 2F_c^2)/3$

[⊕] $w = [\sigma^2(F_o^2) + (0.0288P)^2 + 1.09P]^{-1}$ where $P = [\max(F_o^2,0) + 2F_c^2]/3$

[∅] $w = [\sigma^2(F_o^2) + (0.1327P)^2]^{-1}$ where $P = [\max(F_o^2, 0) + 2F_c^2]/3$

Table 2.9: *Crystallographic data for compounds 18 and 20.*

	18	**20**
Empirical formula	$C_{26}H_{36}AuClFe_2O_5P_2$	$C_{34}H_{37}Cl_4FePRu$
M_r	834.60	775.33
space group	P2/c	$P2_1/n$
crystal system	monoclinic	monoclinic
a (Å)	12.3838(2)	10.6555(6)
b (Å)	6.3295(1)	60.958(3)
c (Å)	36.8279(2)	15.5291(8)
α (°)	90	90
β (°)	92.360(1)	94.5170(10)
γ (°)	90	90
V (Å^3)	2884.24(7)	10055.4(9)
density (g.cm^{-3})	1.922	1.536
Z	4	12
F(000)	1640	4728
μ(Mo-K_α) (mm^{-1})	1.29	1.11
temperature (°C)	-70	-70
crystal size (mm)	0.54 × 0.20 × 0.02	0.39 × 0.28 × 0.22
θ range	1.11° < θ < 26.40°	2.34° < θ < 26.41°
total reflections	16938	49849
unique reflections	6338	19138
R_{int}	0.0409	0.0378
T_{min}	0.6960	0.665114
T_{max}	0.91027	0.834692
R_1 ($I > 2\sigma(I)$)	0.0419	0.0790
wR_2 (all data)	0.0912[⊗]	0.1543[•]
GOF	1.149	1.259
e$^-$ density max (e.Å^{-3})	1.172[⊕]	1.495
e$^-$ density min (e.Å^{-3})	-1.391[⊕]	-1.566
diffractometer	Siemens SMART CCD	Siemens SMART CCD
solution and refinement programmes	SHELXS-97, SHELXL-97	SHELXS-97, SHELXL-97

[⊗] $w = [\sigma^2(F_O^2) + (0.0295P)^2 + 8.96P]^{-1}$ where $P = (\max(F_O^2,0) + 2F_C^2)/3$ [⊕] Close to the gold atom.

[•] $w = [\sigma^2(F_O^2) + (0.0000P)^2 + 80.12P]^{-1}$ where $P = (\max(F_O^2,0) + 2F_C^2)/3$

In **18** the oxygen O(2) was disordered over two positions and was refined as O(2) and O(2a), with occupancies refined to 70.8% and 29.2% respectively while temperature factors for the two atoms were restrained to 0.05. Temperature factors were subsequently allowed to refine without constraint, while occupancy was fixed. Only half the Cl(2) sites were occupied, and so refinement was carried out with occupancy set to 50%. Since Cl(1) occupied an inversion centre between two gold cations, the combined effect of the two chlorine atom positions was to provide one negative charge for each Au(I) atom. Refinement was carried out with all non-hydrogen atoms except O(2a) anisotropic and with hydrogen atoms included in calculated positions with isotropic temperature factors 1.2 times that of the U_{iso} of the atom to which they are bonded. Hydrogen atoms of the hydroxyl groups and the water molecule could not be found in the difference map and so were not included in the refinement.

For **20** all non-hydrogen atoms were refined anisotropically, and hydrogen atoms were included in calculated positions with isotropic temperature factors 1.2 times that of the U_{iso} of the atom to which they are bonded. Hydrogen atoms positions for the methyl functionalities C(2), C(4) and C(5) of the three independent molecules were calculated by positioning of the methyl group such that the conformation obtained gave the best fit to the electron density distribution observed. Many of the large residual peaks in the electron density map are located near the solvent of crystallisation molecules and may be the result of slight solvent disorder, though of a scale which does not merit modelling. As discussed above the refinement is of poor quality, probably because of problems arising from data collection for a unit cell with an exceptionally long *b* axis.

Drawing programmes XPMA[83] and PLUTO assisted in the investigation of hydrogen bonding, and structures have been illustrated with ORTEP[84].

Complete lists of atomic coordinates, bond parameters and tables of thermal parameters and hydrogen atom coordinates for both structures can be found in Appendix A.

2.4 References

1 M. Reuter, L. Orthner, *Chem. Abstr.*, 1960, **54**, 14125a.

2 a) M. Grayson, *J. Am. Chem. Soc.*, 1963, **85**, 79. b) K. V. Katti, *Current Science*, 1996, **70**, 219. c) C. J. Smith, V. S. Reddy, S. R. Karra, K. V. Katti, L. J. Barbour, *Inorg. Chem.*, 1997, **36**, 1786. d) V. S. Reddy, K. V. Katti, C. L. Barnes, *J. Chem. Soc., Dalton Trans.*, 1996, 1301. e) J. Chatt, G. J. Leigh, R. M. Slade, *J. Chem. Soc., Dalton Trans.*, 1973, 2021. f) J. Fawcett, P. A. T. Hoye, R. D. W. Kemmitt, D. J. Law, D. R. Russell, *J. Chem. Soc., Dalton Trans.*, 1993, 2563. g) F. Bitterer, S. Kucken, O. Stelzer, *Chem. Ber.*, 1995, **128**, 275. h) D. G. Gilheany, C. M. Mitchell, *Preparation of Phosphines*, in *The Chemistry of Organophosphorus Compounds*, F. R. Hartley (Ed.), 1990, John Wiley & Sons Ltd., New York, Vol. **1**, p. 175. i) C. J. Smith, V. S. Reddy, K. V. Katti, *J. Chem. Soc., Dalton Trans.*, 1998, 1365.

3 A. W. Frank, D. J. Daigle, S. L. Vail, *Textile Res. J.*, 1982, **52**, 678.

4 E. D. Weil, *Flame Retardants*, in *Handbook of Organophosphorus Chemistry*, R. Engel (Ed.), 1992, Marcel Dekker, Inc., New York, p. 707. D. J. Daigle, A. W. Frank, *Textile Res. J.*, 1982, **52**, 751.

5 W. Vullo, *J. Org. Chem.*, 1968, **33**, 3665.

6 A. W. Frank, D. J. Daigle, S. L. Vail, *Textile Res. J.*, 1982, **52**, 738.

7 D. G. Gilheany, C. M. Mitchell, *Preparation of Phosphines*, in *The Chemistry of Organophosphorus Compounds*, F. R. Hartley (Ed.), 1990, John Wiley & Sons Ltd., New York, Vol. **1**, p. 174, 175.

8 W. J. Vullo, *I & EC Product Research and Development*, 1966, **5**, 346.

9 M. T. Reetz, S. R. Waldvogel, *Angew. Chem. Int. Ed. Engl.*, 1997, **36**, 865. S. J. McLain, *J. Am. Chem. Soc.*, 1983, **105**, 6355. S. J. McLain, *Inorg. Chem.*, 1986, **25**, 3124.

10 E. J. Boros, K. J. Coskran, R. W. King, J. G. Verkade, *J. Am. Chem. Soc.*, 1966, **88**, 1140.

11 D. E. C. Corbridge, *Phosphorus, An Outline of its Chemistry, Biochemistry and Technology*, 2nd Ed., 1980, Elsevier, Amsterdam, p. 187.

12 M. M. Rauhut, I. Hechenbleikner, H. A. Currier, F. C. Schaefer, V. P. Wystrach, *J. Am. Chem. Soc.*, 1959, **81**, 1103.

13 A. J. Blake, G. P. McQuillan, *J. Chem. Soc., Dalton Trans.*, 1984, 1849.

14 a) B. M. Foxman, H. Mazurek, *Inorg. Chem.*, 1979, **18**, 113. b) B. M. Foxman, P. L. Goldberg, H. Mazurek, *Inorg. Chem.*, 1981, **20**, 4368. c) B. M. Foxman, J. Jaufmann, B. Sullivan, *Inorg. Synth.*, 1983, **22**, 113.

15 Md. N. I. Khan, C. King, J. P. Fackler Jr., R. E. P. Winpenny, *Inorg. Chem.*, 1993, **32**, 2502.

16 N. A. Bell, L. A. March, I. W. Nowell, *Inorg. Chim. Acta*, 1989, **156**, 195.

17 F. A. Cotton, D. J. Darensbourg, W. H. Ilsley, *Inorg. Chem.*, 1981, **20**, 578.

18 W. Caetano, J. J. F. Alves, B. S. L. Neto, D. W. Franco, *Polyhedron*, 1995, **14**, 1295.

19 C. W. Liu, H. Pan, J. P. Fackler Jr., G. Wu, R. E. Wasylishen, M. Shang, *J. Chem. Soc., Dalton Trans.*, 1995, 3691.

20 A. R. Al-Arfaj, M. S. Hussain, A. A. Isab, M. N. Akhtar, *Acta Cryst.*, 1996, C**52**, 550. J. P. Fackler Jr., R. J. Staples, M. N. I. Khan, R. E. P. Winpenny, *Acta Cryst.*, 1994, C**50**, 1020. Z. Assefa, R. J. Staples, J. P. Fackler Jr., *Inorg. Chem.*, 1994, **33**, 2790.

21 A. G. Orpen, P. G. Pringle, M. B. Smith, K. Worboys, *J. Organomet. Chem.*, 1998, **550**, 255.

22 F. A. Cotton, L. M. Daniels, S. C. Haefner, E. N. Walke, *Inorg. Chim. Acta*, 1996, **247**, 105.

23 M. J. Bennett, F. A. Cotton, B. H. C. Winguist, *J. Am. Chem. Soc.*, 1967, **89**, 5366.

24 D. J. Daigle, T. J. Decuir, J. B. Robertson, D. J. Darensbourg, *Inorg. Synth.*, 1998, **32**, 40. D. J. Daigle, A. B. Peppermann Jr., S. L. Vail, *J. Heterocycl. Chem.*, 1974, **17**, 407.

25 J. M. Forward, D. Bohmann, J. P. Fackler Jr., R. J. Staples, *Inorg. Chem.*, 1995, **34**, 6330. Z. Assefa, B. G. McBurnett, R. J. Staples, J. P. Fackler Jr., B. Assmann, K. Angermaier, H. Schmidbaur, *Inorg. Chem.*, 1995, **34**, 75. Z. Assefa, B. G. McBurnett, R. J. Staples, J. P. Fackler Jr., *Inorg. Chem.*, 1995, **34**, 4965. Z. Assefa, B. G. McBurnett, R. J. Staples, J. P. Fackler Jr., *Acta Cryst.*, 1995, C**51**, 1742. J. M. Forward, Z. Assefa, R. J. Staples, J. P. Fackler Jr., *Inorg. Chem.*, 1996, **35**, 16. J. M. Forward, J. P. Fackler Jr., R. J. Staples, *Organometallics*, 1995, **14**, 4194.

26 D. J. Darensbourg, F. Joo, M. Kannisto, A. Katho, J. H. Reibenspies, D. J. Daigle, *Inorg. Chem.*, 1994, **33**, 200. D. J. Darensbourg, N. W. Stafford, F. Joo, J. H. Reibenspies, *J. Organomet. Chem.*, 1995, **488**, 99.

27 B. Assmann, K. Angermaier, H. Schmidbaur, *J. Chem. Soc., Chem. Commun.*, 1994, 941. B. Assmann, K. Angermaier, M. Paul, J. Riede, H. Schmidbaur, *Chem. Ber.*, 1995, **128**, 891. E. C. Alyea, G. Ferguson, S. Kannan, *Chem. Commun.*, 1998, 345.

28 W. A. Herrmann, C. W. Kohlpaintner, *Angew. Chem. Int. Ed. Engl.*, 1993, **32**, 1524.

29 K. N. Harrison, P. A. T. Hoye, A. G. Orpen, P. G. Pringle, M. B. Smith, *J. Chem. Soc., Chem. Commun.*, 1989, 1096.

30 J. W. Ellis, K. N. Harrison, P. A. T. Hoye, A. G. Orpen, P. G. Pringle, M. B. Smith, *Inorg. Chem.*, 1992, **31**, 3026.

31 D. E. Berning, K. V. Katti, C. L. Barnes, W. A. Volkert, *Chem. Ber./Recueil*, 1997, **130**, 907.

32 L. Higham, A. K. Powell, M. K. Whittlesey, S. Wocadlo, P. T. Wood, *Chem. Commun.*, 1998, 1107.

33 P. G. Pringle, M. B. Smith, *Platinum Metals Rev.*, 1990, **34**, 74.

34 P. A. T. Hoye, P. G. Pringle, M. B. Smith, K. Worboys, *J. Chem. Soc., Dalton Trans.*, 1993, 269.

35 R. Bartsch, S. Hietcamp, S. Morton, H. Peters, O. Stelzer, *Inorg. Chem.*, 1983, **22**, 3624.

36 a) D. E. Berning, K. V. Katti, C. L. Barnes, W. A. Volkert, A. R. Ketring, *Inorg. Chem.*, 1997, **36**, 2765. b) V. S. Reddy, D. E. Berning, K. V. Katti, C. L. Barnes, W. A. Volkert, A. R. Ketring, *Inorg. Chem.*, 1996, **35**, 1753. c) C. J. Smith, V. S. Reddy, K. V. Katti, *J. Chem. Soc., Chem. Commun.*, 1996, 2557. d) G. F. Nieckarz, T. J. R. Weakley, W. K. Miller, B. E. Miller, D. K. Lyon, D. R. Tyler, *Inorg. Chem.*, 1996, **35**, 1721. e) D. L. Davies, J. Neild, L. J. S. Prouse, D. R. Russell, *Polyhedron*, 1993, **12**, 2121. f) H. Hope, M. M. Olmstead, P. P. Power, M. Viggiano, *Inorg. Chem.*, 1984, **23**, 326.

37 G. T. Baxley, W. K. Miller, D. K. Lyon, B. E. Miller, G. F. Nieckarz, T. J. R. Weakley, D. R. Tyler, *Inorg. Chem.*, 1996, **35**, 6688.

38 T. Shido, T. Okazaki, M. A. Ulla, T. Fujimoto, M. Ichikawa, *Catalysis Letters*, 1993, **17**, 97.

39 A. Fukuoka, W. Kogusi, M. Hirano, L. McCaffrey, W. Henderson, S. Koyima, unpublished results.

40 D. E. Berning, K. V. Katti, P. R. Singh, C. Higgenbothan, V. S. Reddy, W. A. Volkert, *Nucl. Med. Biol.*, 1996, **23**, 617.

41 D. E. C. Corbridge, *Phosphorus, an outline of its Chemistry, Biochemistry and Technology*, 2nd Ed., 1980, Elsevier, Amsterdam, p. 178.

42 H. C. L. Abbenhuis, U. Burckhardt, V. Gramlich, A. Togni, A. Albinati, B. Muller, *Organometallics*, 1994, **13**, 4481. S. Hoppe, H. Weichmann, K. Jurkschat, C. Schneider-Koglin, M. Drager, *J. Organomet. Chem.*, 1995, **505**, 63. H. C. L. Abbenhuis, U. Burckhardt, V. Gramlich, A. Martelletti, J. Spencer, I. Steiner, A. Togni, *Organometallics*, 1996, **15**, 1614. A. Schnyder, L. Hintermann, A. Togni, *Angew. Chem. Int. Ed. Engl.*, 1995, **34**, 931. H. C. L. Abbenhuis, U. Burckhardt, V. Gramlich, C. Kollner, P. S. Pregosin, R. Salzmann, A. Togni, *Organometallics*, 1995, **14**, 759. A. Togni, C. Breutel, A. Schnyder, F. Spindler, H. Landert, A. Tijani, *J. Am. Chem. Soc.*, 1994, **116**, 4062. C. Breutel, P. S. Pregosin, R. Salzmann, A. Togni, *J. Am. Chem. Soc.*, 1994, **116**, 4067.

43 P. Barbaro, C. Bianchini, A. Togni, *Organometallics*, 1997, **16**, 3004. P. Barbaro, A. Togni, *Organometallics*, 1995, **14**, 3570.

44 R. S. Edmundson, *Dictionary of Organophosphorus Compounds*, 1988, Chapman and Hall Ltd., London, D-01037, p. 357.

45 a) P. L. Pauson, W. E. Watts, *J. Chem. Soc.*, 1963, 2990. b) G. Marr, T. M. White, *J. Chem. Soc., Perkin I*, 1973, 1955. c) G. Marr, B. J. Wakefield, T. M. White, *J. Organomet. Chem.*, 1975, **88**, 357. d) C. Charrier, F. Mathey, *Tetrahedron Lett.*, 1978, 2407.

46 H. R. Hays, D. J. Peterson, *Tertiary Phosphine Oxides*, in *Organic Phosphorus Compounds*, G. M. Kosolapoff, L. Maier (Ed.), 1972, Wiley-Interscience, New York, Vol. **3**, p. 343.

47 D. E. C. Corbridge, *Phosphorus, an outline of its Chemistry, Biochemistry and Technology*, 2nd Ed., 1980, Elsevier, Amsterdam, p. 163.

48 Selected references: M. Bardaji, M. Kustos, A.-M. Caminade, J.-P. Majoral, B. Chaudret, *Organometallics*, 1997, **16**, 403. A. L. Balch, M. M. Olmstead, S. P. Rowley, *Inorg. Chim. Acta*, 1990, **168**, 255. G. R. Newkome, D. W. Evans, F. R. Fronczek, *Inorg. Chem.*, 1987, **26**, 3500.

49 H. Hellman, O. Schumacher, *Angew. Chem.*, 1960, **72**, 211.

50 S. B. Wilkes, I. R. Butler, A. E. Underhill, M. B. Hursthouse, D. E. Hibbs, K. M. A. Malik, *J. Chem. Soc., Dalton Trans.*, 1995, 897.

51 O. I. Kolodiazhnyi, *Tetrahedron: Asymmetry*, 1998, **9**, 1279.

52 H. B. Kagan, M. Sasaki, *Optically Active Phosphines: Preparation, Uses and Chiroptical Properties*, in *The Chemistry of Organophosphorus Compounds*, F. R. Hartley (Ed.), 1990, John Wiley & Sons Ltd., New York, Vol. **1**, p. 51.

53 T. Imamoto, *Optically Active Phosphorus Compounds*, in *Handbook of Organophosphorus Compounds*, R. Engel (Ed.), 1992, Marcel Dekker Inc., New York, p. 1.

54 K. M. Pietrusiewicz, M. Zablocka, *Chem. Rev.*, 1994, **94**, 1375.

55 Selected examples: A. Bader, T. Nullmeyers, M. Pabel, G. Salem, A. C. Willis, S. B. Wild, *Inorg. Chem.*, 1995, **34**, 384. K. Angermaier, A. Sladek, H. Schmidbaur, *Z. Naturforsch.*, 1996, **51b**, 1671. J. Albert, J. Granell, J. Minguez, G. Muller, D. Sainz, P. Valerga, *Organometallics*, 1997, **16**, 3561.

56 G. E. Herberich, S. Moss, *Chem. Ber.*, 1995, **128**, 689. I. R. Butler, W. R. Cullen, T.-J. Kim, F. W. B. Einstein, T. Jones, *J. Chem. Soc., Chem. Commun.*, 1984, 719. W. R. Cullen, T.-J. Kim, F. W. B. Einstein, T. Jones, *Organometallics*, 1985, **4**, 346.

57 E. B. Kaloun, R. Merdes, J.-P. Genet, J. Uziel, S. Juge, *J. Organomet. Chem.*, 1997, **529**, 455. J. M. Brown, J. C. P. Laing, *J. Organomet. Chem.*, 1997, **529**, 435. I. R. Butler, W. R. Cullen, S. J. Rettig, A. S. C. White, *J. Organomet. Chem.*, 1995, **492**, 157.

58 X. Xu, S. P. Nolan, R. B. Cole, *Anal. Chem.*, 1994, **66**, 119. See also: G. J. Van Berkel, F. Zhou, *Anal. Chem.*, 1995, **67**, 3958.

59 W. Henderson, A. G. Oliver, A. J. Downard, *Polyhedron*, 1996, **15**, 1165.

60 W. Henderson, G. M. Olsen, *Polyhedron*, 1996, **15**, 2105.

61 K. Wang, X. Han, R. W. Gross, G. W. Gokel, *J. Am. Chem. Soc.*, 1995, **117**, 7680.

62 W. Henderson, G. M. Olsen, *Polyhedron*, 1998, **17**, 577.

63 For relevant references and more extended discussion of this area, refer to Chapter 3.

64 R. Taylor, O. Kennard, W. Versichel, *J. Am. Chem. Soc.*, 1984, **106**, 244.

65 R. Taylor, O. Kennard, *Acc. Chem. Res.*, 1984, **17**, 320.

66 N. J. Goodwin, W. Henderson, J. K. Sarfo, *Chem. Commun.*, 1996, 1551.

67 T. G. Appleton, H. C. Clark, L. E. Manzer, *Coord. Chem. Rev.*, 1973, **10**, 335.

68 D. A. Redfield, J. H. Nelson, *Inorg. Nucl. Chem. Letters*, 1974, **10**, 727. D. A. Redfield, L. W. Cary, J. H. Nelson, *Inorg. Chem.*, 1975, **14**, 50.

69 R. Colton, K. L. Harrison, Y. A. Mah, J. C. Traeger, *Inorg. Chim. Acta*, 1995, **231**, 65.

70 A. Hafner, A. Muhlebach, P. A. van der Schaaf, *Angew. Chem. Int. Ed. Engl.*, 1997, **36**, 2121. M. R. J. Elsegood, D. A. Tocher, *Polyhedron*, 1995, **14**, 3147. W. Keim, P. Kraneburg, G. Dahmen, G. Deckers, U. Englert, K. Linn, T. P. Spaniol, G. Raabe, C. Kruger, *Organometallics*, 1994, **13**, 3085. P. Pertici, E. Pitzalis, F. Marchetti, C. Rosini, P. Salvadori, M. A. Bennett, *J. Organomet. Chem.*, 1994, **466**, 221. J. Browning, G. W. Bushnell, K. R. Dixon, R. W. Hilts, *J.*

Organomet. Chem., 1993, **452**, 205. P. Salvadori, P. Pertici, F. Marchetti, R. Lazzaroni, G. Vitulli, M. A. Bennett, *J. Organomet. Chem.*, 1989, **370**, 155. R. D. Brost, G. C. Bruce, S. R. Stobard, *J. Chem. Soc., Chem. Comm.*, 1986, 1580. M. A. Bennett, G. B. Robertson, A. K. Smith, *J. Organomet. Chem.*, 1972, **43**, C41.

71 *Metal Compounds in Cancer Therapy*, S. P. Fricker (Ed.), 1994, Chapman & Hall, London. P. J. Sadler, *Adv. Inorg. Chem.*, 1991, **36**, 1. J. Reedijk, *Chem. Commun.*, 1996, 801.

72 S. J. Berners-Price, P. J. Sadler, *Structure and Bonding*, 1988, **70**, 27. S. J. Berners-Price, P. J. Sadler, *Chem. Br.*, June 1987, 541.

73 I. Haiduc, C. Silvestru, *Coord. Chem. Rev.*, 1990, **99**, 253.

74 D. T. Hill, G. R. Girard, F. L. McCabe, R. K. Johnson, P. D. Stupik, J. H. Zhang, W. M. Reiff, D. S. Eggleston, *Inorg. Chem.*, 1989, **28**, 3529.

75 M. Bernardini, T. J. Emge, J. G. Brennan, *Inorg. Chem.*, 1993, **32**, 2724.

76 D. Lednicer, C. R. Hauser, *Org. Synth. Coll.*, 1973, **5**, 434.

77 J. X. McDermott, J. F. White, G. M. Whitesides, *J. Am. Chem. Soc.*, 1976, **98**, 6521.

78 D. Drew, J. R. Doyle, *Inorg. Synth.*, 1972, **13**, 52.

79 W. Schneider, K. Angermaier, A. Sladek, H. Schmidbaur, *Z. Naturforsch.*, 1996, **51b**, 790.

80 R. Uson, A. Laguna, M. Laguna, *Inorg. Synth.*, 1989, **26**, 85.

81 M. A. Bennett, T.-N. Huang, T. W. Matheson, A. K. Smith, *Inorg. Synth.*, 1982, **21**, 74.

82 L. J. Arnold, *J. Chem. Educ.*, 1992, **69**, 811.

83 L. Zsolnai, H. Pritzkow, 1994, University of Heidelberg.

84 C. K. Johnson, M. N. Burnett, *ORTEP-III Version 1.0.2*. Windows 32-bit Version 1.0.β compiled by L. J. Farrugia, Dept. of Chemistry, University of Glasgow.

85 L. Zsolnai, H. Pritzkow, 1994, University of Heidelberg.

86 G. M. Sheldrick, *SHELXTL/PC-XP*, Release 4.2, Seimens Analytical X-Ray Instruments, Madison, WI, 1991.

87 N. J. Goodwin, W. Henderson, B. K. Nicholson, J. K. Sarfo, J. Fawcett, D. R. Russell, *J. Chem. Soc., Dalton Trans.*, 1997, 4377.

88 R. H. Blessing, *Acta Cryst.*, 1995, **A51**, 33.

89 G. M. Sheldrick, *SHELXS-86, Program for Solving Crystal Structures*, University of Göttingen, 1986.

90 G. M. Sheldrick, *SHELXL-93, Program for Refining Crystal Structures*, University of Göttingen, 1993.

91 G. M. Sheldrick, *SHELXTL PC*, Release 4.2, Seimens Analytical X-Ray Instruments, Madison, WI, 1991.

Chapter 3: Hydrogen-Bonding in Hydroxymethylphosphine Chalcogenides

3.1 Introduction

The P=O functional group is well recognised as a good hydrogen bond acceptor[1], and a large number of crystal structures have been investigated involving hydrogen bonds to the P=O functional group. These include a number of structures involving O-H groups as hydrogen bond donors, forming intramolecular[2] or intermolecular hydrogen bonds[3]. Of particular relevance to the present study are several examples of ferrocenylphosphine oxide structures exhibiting hydrogen-bonding from OH groups[4]. That phosphine oxides are good acceptors for hydrogen bonds is demonstrated by the deliberate use of triphenylphosphine oxide as a co-crystallising agent for alcohols[5] and other donors[1], as well as the successful competition of phosphine oxides with other hydrogen bond acceptors for hydrogen bond donors. An example demonstrating both these phenomena comes from X-ray crystal structures involving both carboxylic acid groups and triphenylphosphine oxide. C=O groups are good hydrogen bond acceptors, and the propensity of carboxylic acids to form hydrogen-bonded dimers in the solid state has been well documented[6]. However, in the presence of triphenylphosphine oxide, carboxylic acids tend to form hydrogen bonds from O-H to the phosphine oxide rather than the C=O group[7]. An intramolecular example is also known; the X-ray crystal structure shows a carboxylic acid group preferentially hydrogen-bonding to a phosphine oxide moiety in the molecule rather than hydrogen-bonding to another carboxylic acid group[8]. Figure 3.1 displays several X-ray crystal structures of hydrogen-bonded phosphine oxides relevant to the preceding discussion.

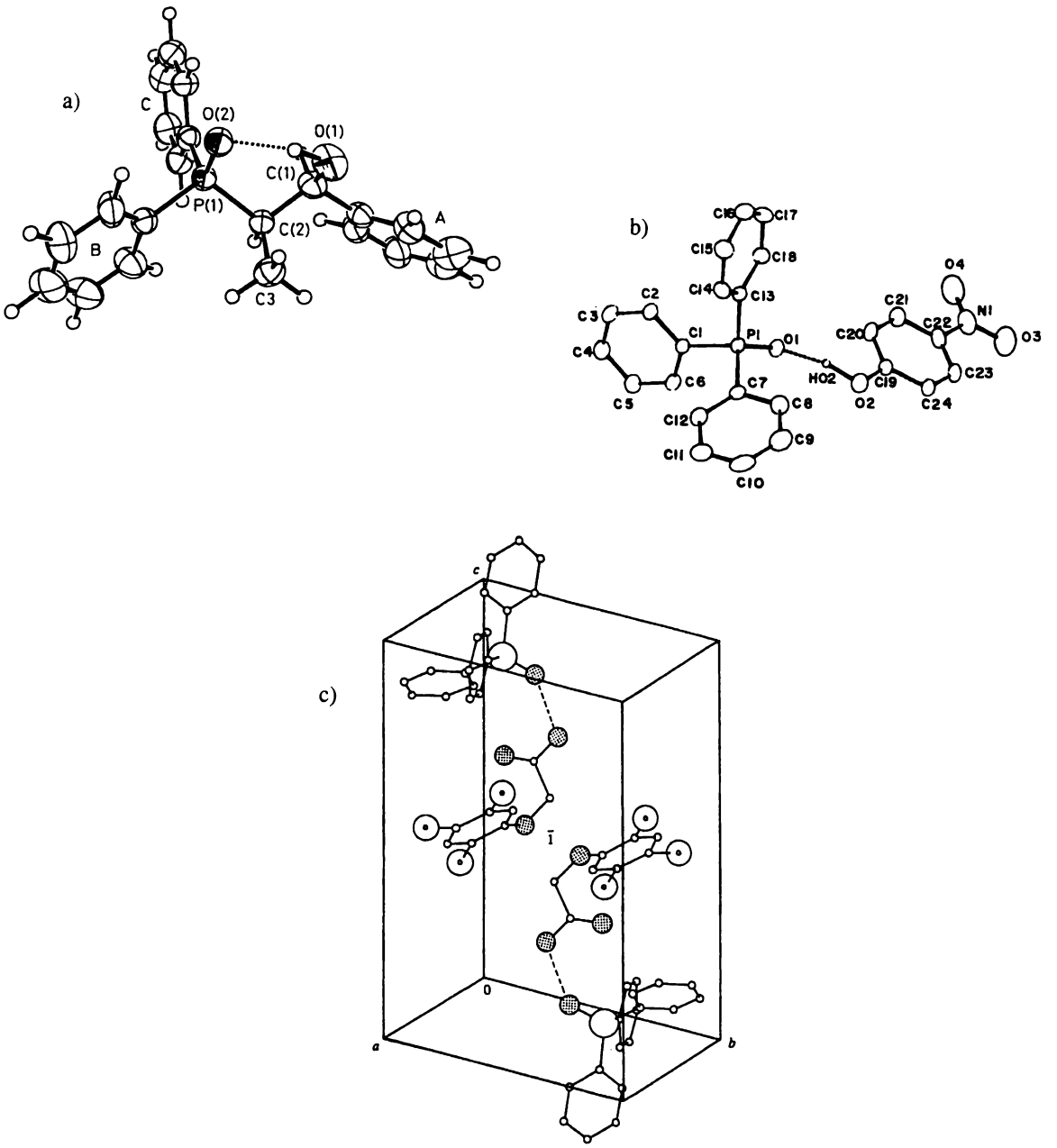

Figure 3.1: a) An intramolecular hydrogen bond observed for the hydroxyalkylphosphine oxide 2-(1*RS*,2*RS*)diphenylphosphinoyl-1-phenylpropan-1-ol[2b]. b) The co-crystallisation of *p*-nitrophenol with triphenylphosphine oxide[5a]. c) The co-crystallisation of (2,4,5-trichlorophenoxy)acetic acid with triphenylphosphine oxide[7e].

An especially interesting demonstration of the power of phosphine oxides as hydrogen bond acceptors is provided by 1,5-methyl-6-phenyl-1,2,3-oxathiazin-4(3*H*)-one 2,2-dioxide (see Scheme 3.1)[9]. In chloroform solution, and in crystals grown from chloroform, it exists as the amide with NH···O=C intermolecular hydrogen bonds. However, in the presence of

triphenylphosphine oxide it is tautomerised to the enol form, which is then stabilised by an O-H···O=P hydrogen bond. This hydrogen bond forms even though the acyl sulfonamide group provides a number of other potential hydrogen bond acceptors. Inducing intramolecular rearrangement of a species through formation of an intermolecular hydrogen bond in this way is unusual to say the least.

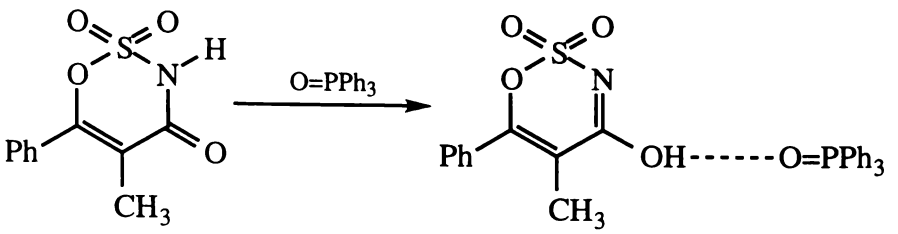

Scheme 3.1: Tautomerisation of an enol function in the presence of triphenylphosphine oxide in solution.

In view of the many known examples of structurally characterised hydrogen-bonded phosphine oxides, there is a surprising lack of X-ray crystal structures known for other hydrogen-bonded phosphine chalcogenides. A search of the Cambridge Structural Database (CSD)[10] and literature reveals a number of structures containing hydroxyl fragments hydrogen-bonded to phosphine sulfides. Interestingly, six of these are 1-hydroxyalkylphosphine sulfides, and are thus related to the structure of $FcCH_2P(S)(CH_2OH)_2$ **4** described in Section 2.2.1 of this thesis. These six structures consist of the series $Me_2P(S)C(OH)Me_2$, $Me_2P(S)C(OH)(CH_2)_5$, $Me_2P(S)C(OH)(Me)C(O)Me$, $Me_2P(S)C(OH)(Ph)C(O)Ph$, and $Me_2P(S)CH(OH)COOH$[11], along with the secondary phosphine sulfide $(Ph)(H)P(S)C(OH)Me_2$[12]. Some other structures are also known[13]. A search of the CSD reveals only two examples of structures containing tertiary phosphine selenides hydrogen-bonded by OH donors: in one instance a water molecule serves as the donor[14], while in the other it is ethanol in the crystal matrix[15], but the acceptor molecule is the same in both cases, tris(2,6-dimethoxyphenyl)phosphine selenide. The structure of the related compound $Ph_2P(Se)(OH)$ is known[16], and displays intermolecular hydrogen bonds with P=Se groups as the acceptors.

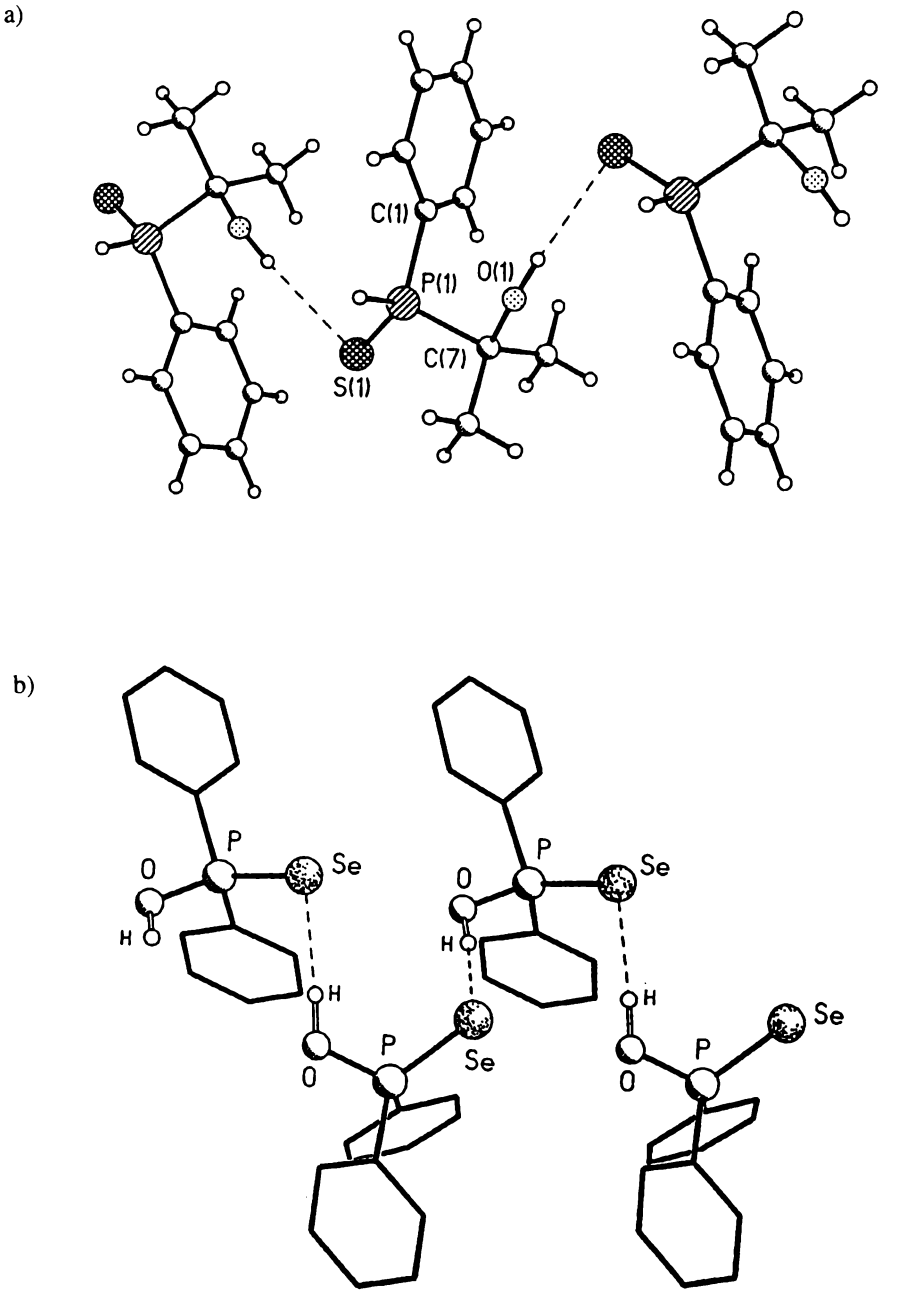

Figure 3.2: Structures of a) (Ph)P(S)(H)C(OH)Me_2[12] and b) $Ph_2P(Se)(OH)$[16] showing the hydrogen-bonding networks.

Structures of a representative hydrogen-bonded phosphine sulfide and the compound $Ph_2P(Se)(OH)$ are shown in Figure 3.2. A search of the CSD revealed no structures for tertiary phosphine tellurides.

In view of the paucity of hydrogen-bonded structures involving heavier chalcogenides as hydrogen bond acceptors, it is not surprising that the author knows of no homologous series of hydrogen-bonded phosphine oxide, sulfide and selenide molecules. The study of such a series has obvious benefits because effects, such as different steric constraints, on crystal packing and the hydrogen-bonding system adopted is minimised. It was therefore with the aim of comparing the hydrogen-bonding characteristics of phosphine oxides, sulfides and selenides that the study described in this chapter was undertaken.

3.2 Results and Discussion

3.2.1 X-Ray Crystal Structure Determinations

An X-ray crystallographic investigation of the homologous series of compounds $Ph_2P(O)CH_2OH$ **21**, $Ph_2P(S)CH_2OH$ **22** and $Ph_2P(Se)CH_2OH$ **23** was carried out in order to allow direct comparison of hydrogen-bonding from the hydroxymethyl group to the different phosphine chalcogenide acceptors. These three compounds were prepared by literature methods[17], and crystals of **22** and **23** were obtained as described in the same publication. Crystals of **21** suitable for X-ray crystallographic analysis were grown by diffusion crystallisation from dichloromethane with 30-40° C petroleum spirits. Crystal morphology in each case was large clear prisms.

The structures obtained for **21**, **22** and **23** are shown in Figures 3.3, 3.4 and 3.5 respectively, and selected bond lengths and angles are presented in Table 3.1. In each case the hydroxyl hydrogen could be clearly located in the difference map.

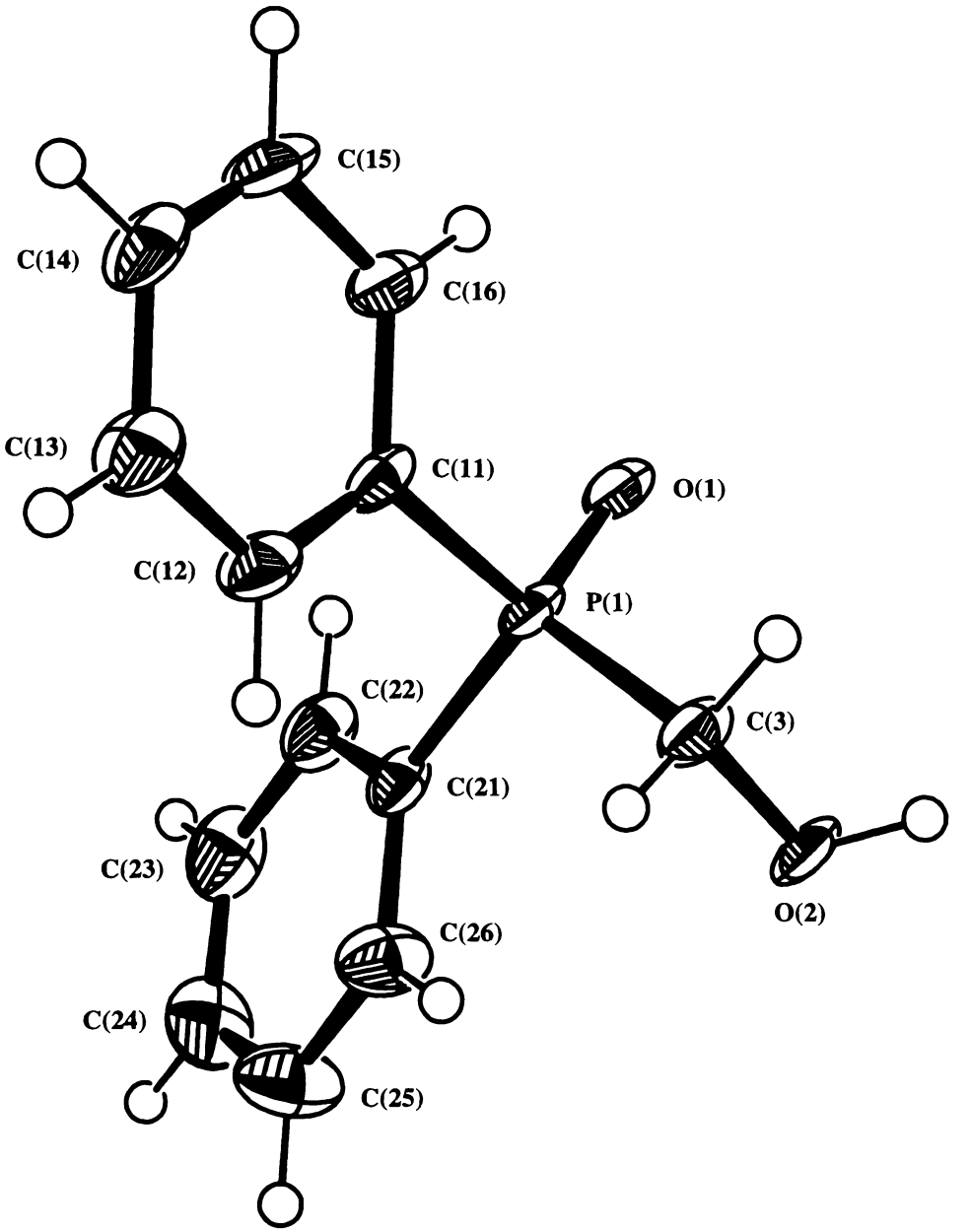

Figure 3.3: ORTEP diagram of **21**.

It is clear that the oxide **21** adopts a different arrangement in the solid state compared with the sulfide **22** and selenide **23**, which are isomorphous and so have almost identical crystal structures. In all three cases intermolecular hydrogen-bonding was evident.

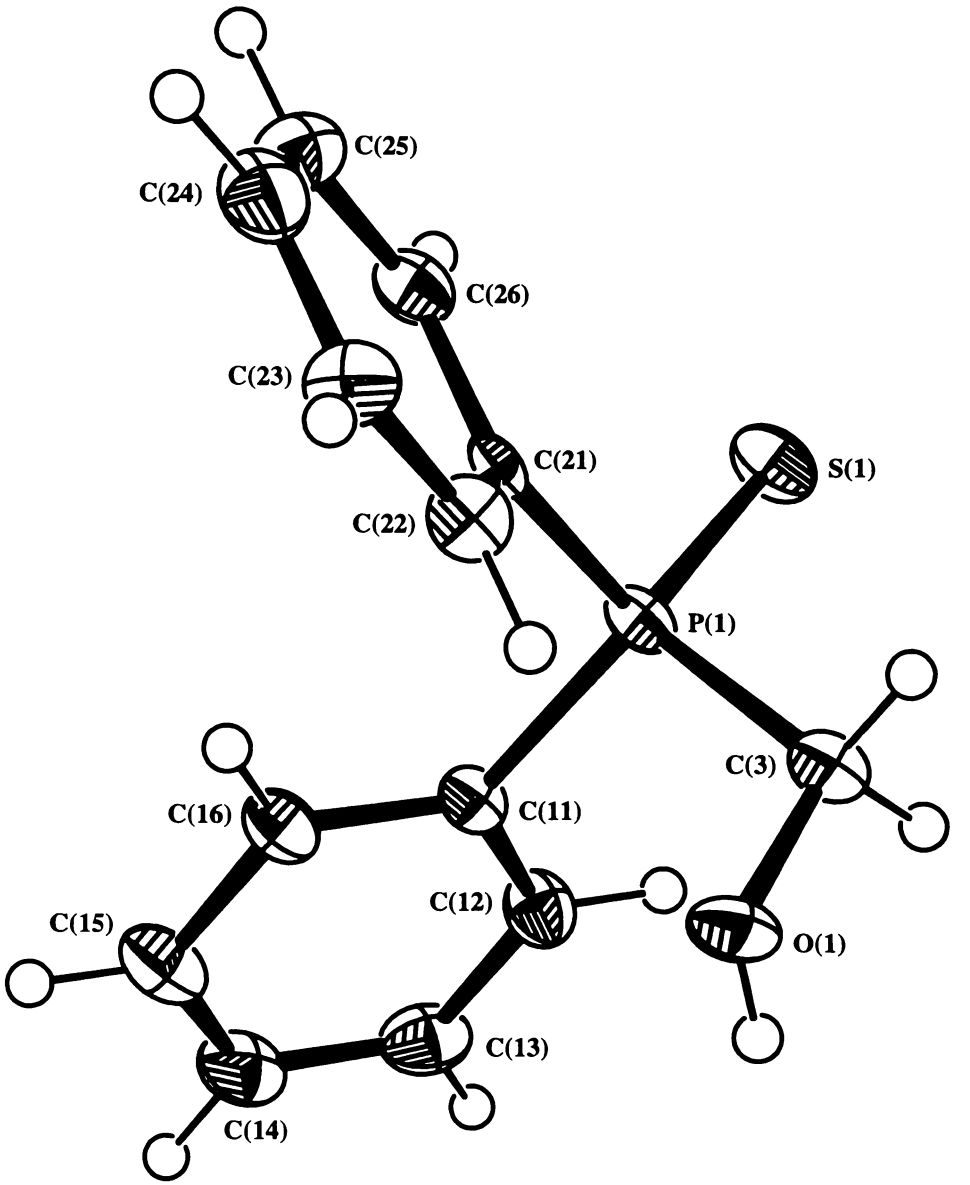

Figure 3.4: ORTEP diagram of **22**.

Compound **21** crystallises in the triclinic space group $P_{\bar{1}}$, and adopts a dimer motif with the inversion centre of the unit cell located between the two hydrogen-bonded molecules. A stereo view of this hydrogen-bonding system is presented in Figure 3.6. The appearance of the dimer is highly reminiscent of the characteristic pattern seen for carboxylic and organophosphorus acids, with the OH group of each molecule in **21** pointing to the P=O

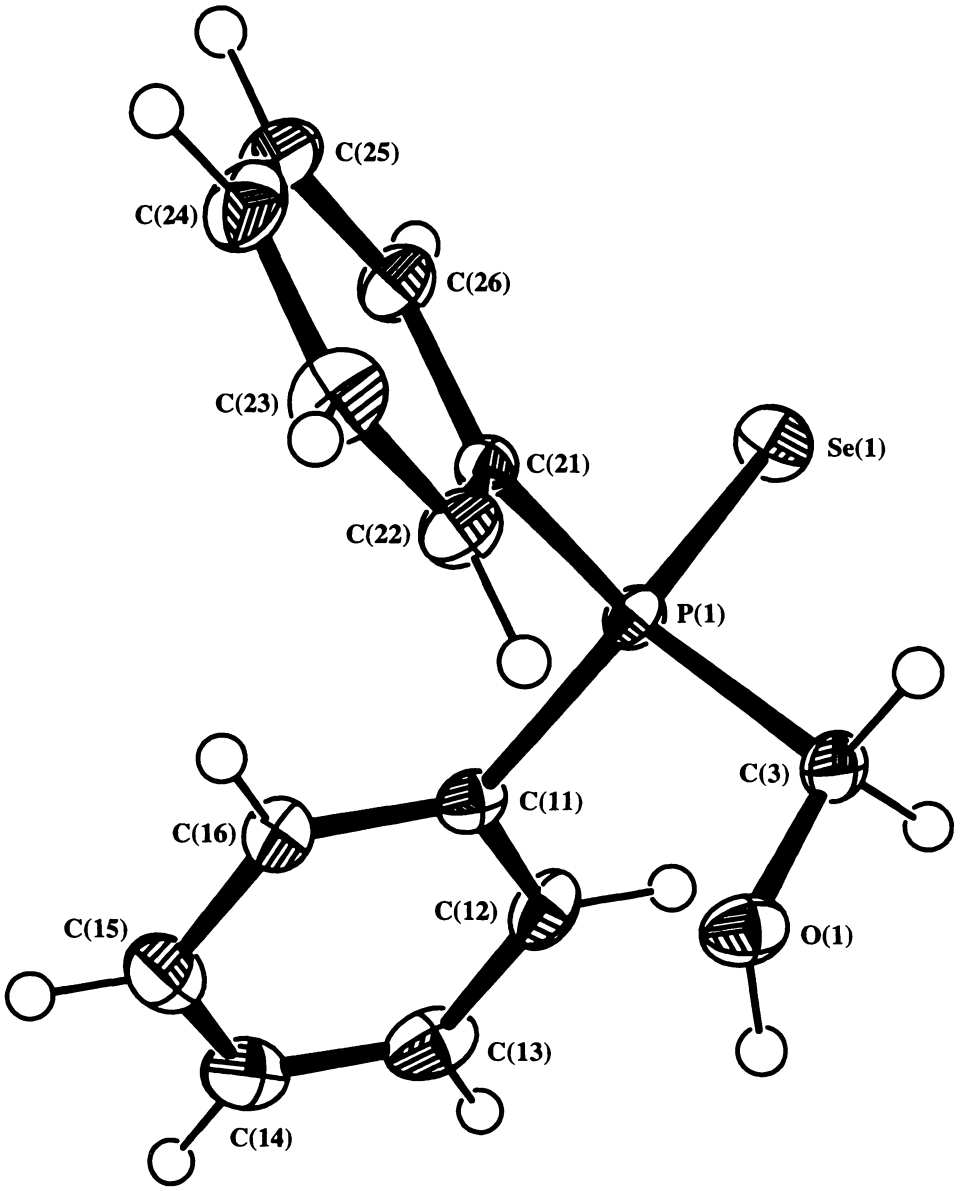

Figure 3.5: ORTEP diagram of **23**.

group of the other. Hydrogen bond parameters are unexceptional and are as follows: O(2)···O(1) = 2.7076 Å, H(2)···O(1) = 1.8186 Å, O(2)-H(2)···O(1) = 176.77°, H(2)···O(1)-P(1) = 116.06°.

A number of chemical characteristics, such as the possession of *d* orbitals and softness, are shared by S and Se, but not by O. Therefore it is not surprising that the solid state behaviour

Table 3.1: *Selected bond lengths (Å) and angles (°) for the compounds* ***21***, ***22*** *and* ***23***. *In the case of compound* ***21*** *the hydroxyl atoms are in actual fact O(2) and H(2), but are designated O(1) and H(1) in this table to maintain consistency with the other two structures. X(1) refers to the chalcogenide atom.*

	21 (X = O)	**22** (X = S)	**23** (X = Se)
P(1)-X(1)	1.497(3)	1.9738(13)	2.1194(8)
P(1)-C(3)	1.816(4)	1.829(5)	1.847(3)
P(1)-C(11)	1.813(4)	1.821(4)	1.803(3)
P(1)-C(21)	1.803(4)	1.799(4)	1.797(3)
C(3)-O(1)	1.421(5)	1.424(4)	1.410(4)
O(1)-H(1)	0.8900	0.8359	0.9262
ring C-C range:	1.366(6)-1.397(6)	1.375(7)-1.396(5)	1.366(5)-1.394(5)
average:	1.384(6)	1.384(6)	1.381(5)
C(11)-P(1)-X(1)	111.32(16)	112.75(13)	112.92(11)
C(21)-P(1)-X(1)	111.56(16)	113.00(13)	113.20(10)
C(3)-P(1)-X(1)	114.33(16)	110.36(13)	109.82(11)
C(11)-P(1)-C(21)	108.02(17)	107.27(18)	107.81(14)
C(11)-P(1)-C(3)	104.19(18)	105.3(2)	104.89(14)
C(21)-P(1)-C(3)	106.97(18)	107.72(19)	107.75(16)
P(1)-C(3)-O(1)	109.2(3)	112.1(3)	111.3(2)
C(3)-O(1)-H(1)	107.48	106.29	106.80
angle between planes of rings	74.73(13)	84.63(13)	83.51(10)
X(1)-P(1)-C(3)-O(1) torsion angle	-64.0(3)	-166.31(23)	-167.19(19)

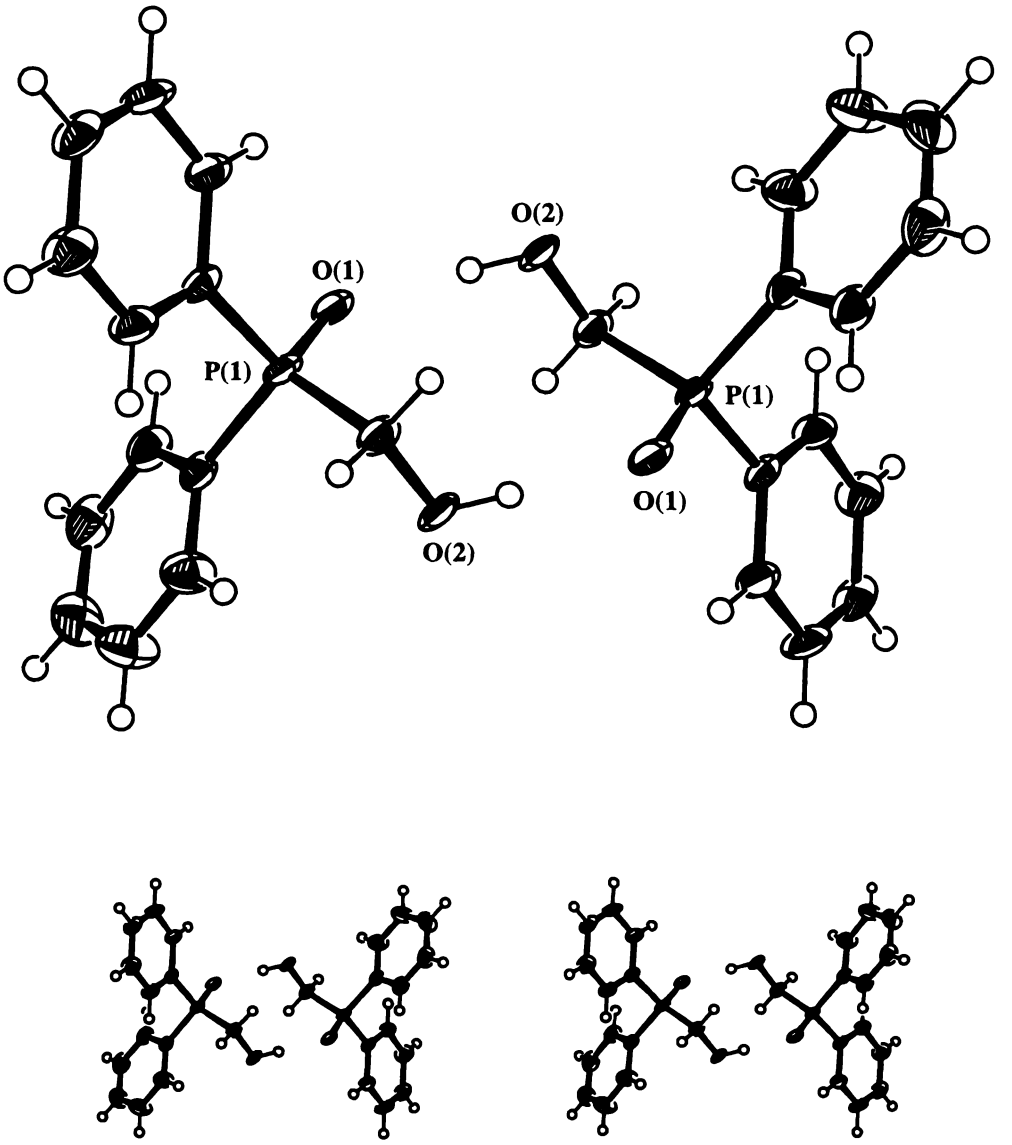

Figure 3.6: ORTEP diagram of hydrogen-bonding in **21**, with stereo view.

of **22** and **23** is almost identical, while being in contrast to the behaviour of **21**. In both **22** and **23** the hydrogen-bonding network consists of infinite intermolecular chains propagating along the glide plane in the direction of the *c* axis (Figures 3.7 and 3.8). Hydrogen-bonding parameters for **22** are: S(1)···O(1) = 3.2225 Å, H(1)···S(1) = 2.3870 Å, O(1)-H(1)···S(1) = 178.11°, H(1)···S(1)-P(1) = 87.21°. Values for hydrogen bond parameters in the literature[11,12,13] suggest this is an unexceptional example, although O-H···S angles are usually considerably more acute than is the case for **22**. Hydrogen bond parameters for **23** are:

Se(1)···O(1) = 3.3136 Å, H(1)···Se(1) = 2.4022 Å, O(1)-H(1)···Se(1) = 171.45°, H(1)···Se(1)-P(1) = 84.20°. Previously reported[14,15] O···Se distances in the two examples known of phosphine selenides hydrogen-bonded by O-H groups are 3.338 Å and 3.461 Å, suggesting the hydrogen-bonding interaction in **23** is relatively strong. It is interesting to note that **23** does not adopt the alternative motif of infinite O-H···O-H chains, common in alcohols, since this suggests Se is quite a good hydrogen bond acceptor, contrary to what might be expected.

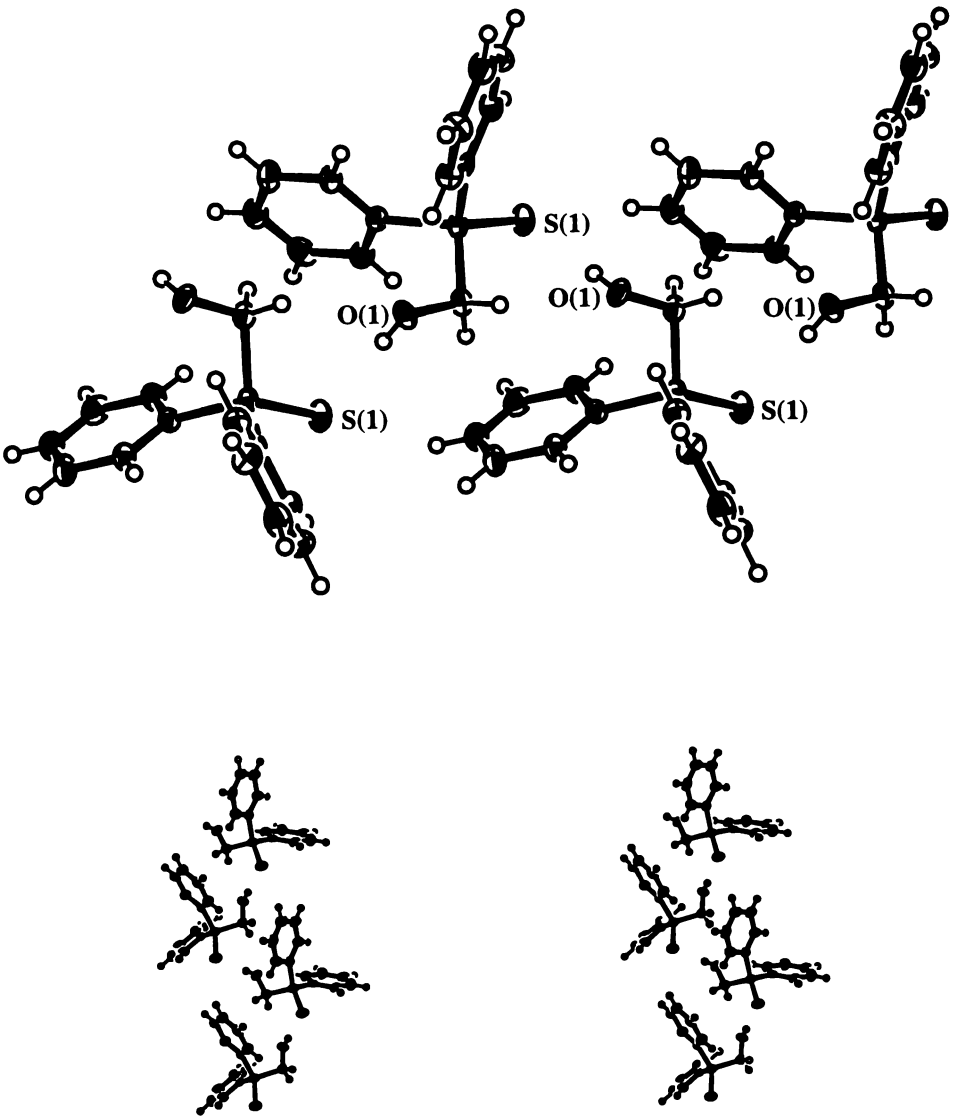

Figure 3.7: ORTEP diagram of hydrogen-bonding in **22**, with stereo view.

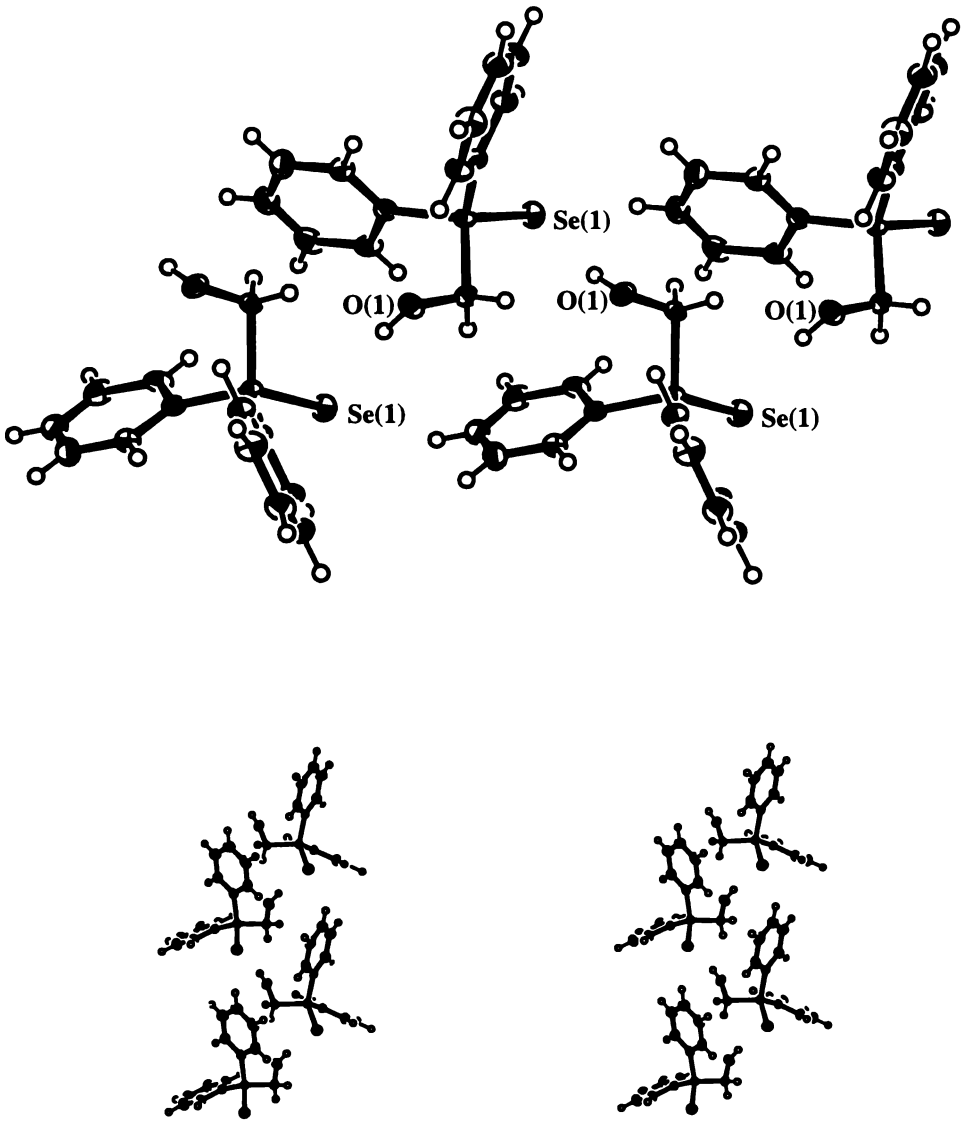

Figure 3.8: ORTEP diagram of hydrogen-bonding in **23**, with stereo view.

The adoption by **21** of a different hydrogen-bonding motif than that seen for **22** and **23** is reflected in the X-P-C-O torsion angle, which is around 65° for **21** (Table 3.1), in accord with the *gauche* conformation about the P(1)-C(3) bond which is required for dimerisation. In contrast this torsion angle is about 100° wider for **22** and **23** (Table 3.1), with these molecules adopting an *anti* conformation about the P(1)-C(3) bond.

3.2.2 Theoretical Considerations

The results presented here beg the question: when the steric characteristics of the three compounds examined in this chapter are very similar, what factor(s) influence **22** and **23** to adopt a different solid state conformation to **21**? Without further experimentation only the most tentative of answers can be presented here, but clearly if steric characteristics are not responsible for the difference, electronic factors must be. In this Section it will be argued that the difference may stem from a tendency for the hydrogen bond geometry to be influenced by the location of regions of electron density on the acceptor atom.

One of the most controversial questions raised by research into hydrogen bond geometry concerns whether or not hydrogen bonds tend to form along the lone-pair directions of the acceptor atom[18,19]. Since hydrogen bonds are essentially electrostatic interactions it seems intuitively sensible to suggest the hydrogen atoms of donor groups should point to lobes of electron density on the acceptor atom. However, in view of the many other crystal packing forces which help determine hydrogen bond geometry it has been difficult to emphatically prove or disprove this proposition. A statistical analysis of hydrogen bonds of the type O-H···O< in X-ray crystal structures of polyalcohols, saccharides and related ROH compounds found no preference for hydrogen-bonding along the lone-pair directions[20], although a marked tendency to lie in the lone-pair *plane* was observed[19]. A study of neutron diffraction data confirmed this result[21]. However, a similar study of hydrogen-bonding to ketone and ester acceptor groups, using the CSD, concluded that hydrogen bonds did in fact point toward lone-pairs[22]. Another study of 1357 intermolecular N-H···O=C hydrogen bonds concluded that there was a statistically significant tendency for hydrogen bonds to occur within 10° of the idealised lone-pair directions[23]. Other findings concerning doubly hydrogen-bonded amide systems are in accord with this[24]. A spectroscopic study of F-H···O< hydrogen bonds in the gas phase showed the bonds to lie in approximately the oxygen lone-pair directions[25].

The author is not aware of any studies concerning lone-pair directionality involving phosphine chalcogenides as hydrogen bond acceptors - and since the pattern of electron density of a hydrogen bond acceptor is very obviously dependent on the functional group involved, findings concerning hydrogen bond directionality for phosphine chalcogenides may be quite different to the results presented above. One reason this area may have not been investigated by crystallographers (in spite of the utility of phosphine oxides as hydrogen bond acceptors) in the same way hydrogen-bonding to carbonyl groups has been investigated, is the ongoing uncertainty about the true nature of the phosphine chalcogenide bond. Traditionally the structure and chemistry of phosphine chalcogenides has been interpreted in terms of the Lewis structure **a** in Scheme 3.2, with the multiple bond described as arising from the interaction of a *d* orbital on the phosphorus centre with a *p* orbital on the chalcogenide centre[26]. However, for theoretical and empirical reasons it is better to consider this as being in resonance with the other Lewis structures **b** and **c** shown in Scheme 3.2[27]. Debate centres around what emphasis should be placed on the various resonance modes, and

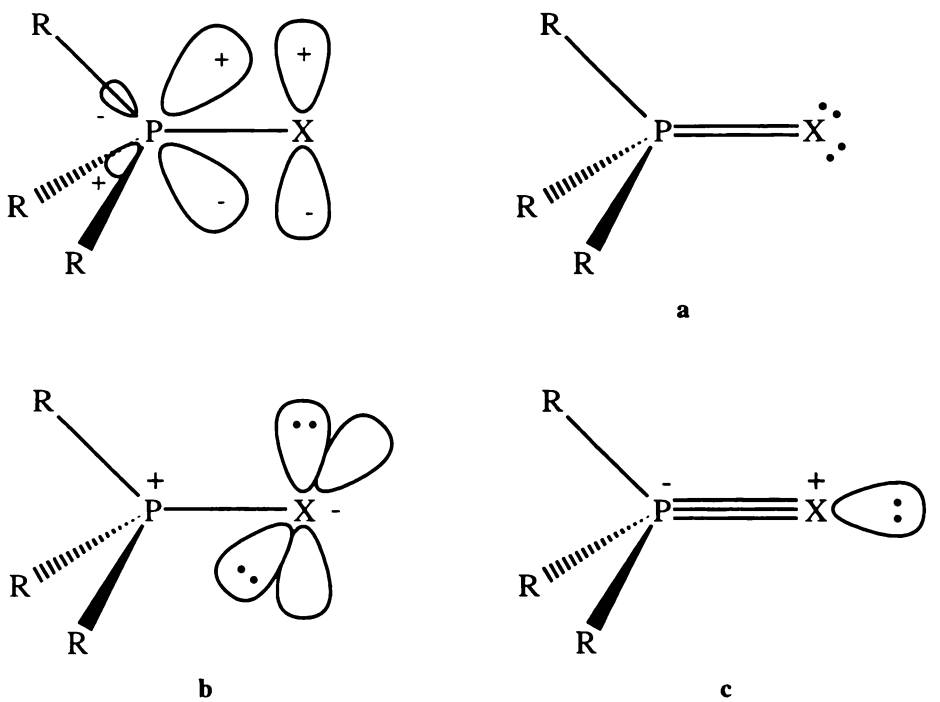

Scheme 3.2: Structure **a** is the usual way of depicting a phosphine-chalcogenide bond, and it is pictured as arising from the interaction shown at top left. Resonance structures **b** and **c** should be preferred for theoretical reasons.

how this varies as the chalcogenide is changed. The influence each of these resonance forms has on the group's coordinative activity is as follows: if **a** is dominant, donation from X (X = O, S, Se) to a Lewis acid such as a metal will give a P-X-M angle of around 120°; if **b** is dominant, the angle is about 90°; while if **c** is dominant, linear coordination should be seen. In actual fact it has been experimentally observed that metal complexes of phosphine oxides[28] give P-O-M angles of 140-180°. Analogous complexes of sulfides and selenides[29] give P-X-M angles of 115-98°. This behaviour has been rationalised by presuming that oxygen is a better π back-donor toward the phosphorus than sulfur or selenium[27]. The greater multiply-bonded nature of the P=O bond (Lewis structure **c**) therefore lends itself to linear σ-coordination to an acceptor. Likewise, the more singly-bonded nature of the P=S or P=Se bond (Lewis structure **b**) leads to a much more acute angle of coordination.

Whatever the merits may be of the proposed theoretical models, the central finding is that the electron density distribution around X is believed to vary in such a way as to account for the lowering of the P-X-M bond angle as X goes from O to S to Se. Changes in the spread of electron density around X could similarly help account for the different solid state orientations of **21**, **22** and **23**. As noted above the H···X-P hydrogen bond angles for **21**, **22** and **23** are 116.06°, 87.21° and 84.20° respectively, a trend with similarities to that seen with P-X-M species. While the hydrogen bond to the phosphine oxide is nowhere near linear, a dimer might be favoured here since this gives greater flexibility in close packing of other parts of the molecule[30]. However, the greater van der Waals' radii of S and Se would mean that the H···X-P angle imposed by dimerisation of **22** or **23** would be greater than is the case for **21**. Combined with a more 'side-on' distribution of electron density in **22** and **23** this may be enough to cause **22** and **23** to favour the zig-zag chain motif where the hydrogen bond angle can be more acute and so be more in line with areas of electron density on the chalcogenide atom.

As stated before, this hypothesis is necessarily highly speculative - only when large numbers of hydrogen-bonded phosphine chalcogenides have been characterised will it be possible to say whether there is any statistically significant tendency for hydrogen bonds to form along

lines of electron density for these functional groups. Conversely, the results of such a study could also provide supporting evidence for the actual position of electron density lobes in phosphine chalcogenides.

The fact that hydrogen bond directionality is influenced by many factors other than those discussed above is seen with compound **4**, the X-ray crystal structure of which was discussed in Section 2.2.3. The two hydrogen bond H···S=P angles observed in the structure were quite different, with H(2)···S(1)'-P(1)' = 102.76° and H(3)'···S(1)-P(1) = 128.81°.

3.3 Experimental

Crystallographic data for the compounds **21**, **22** and **23** are presented in Table 3.2. The data collection for all structures nominally covered over a hemisphere of reciprocal space, by a combination of two sets of exposures. In the first each exposure covered 0.3° for a total of 52° in ω. The second run covered 360° in ϕ (the mounting axis) also using 0.3° increments between frames. The crystal to detector distance was 4.0 cm. All frames were processed using program SAINT to give the raw data sets, which were corrected empirically for absorption using SADABS[31]. In the case of **21** data collection and absorption corrections were carried out improperly, with a detrimental effect on the quality of the final model, though overall atomic arrangements and connectivity are reliable. The structures were solved by Patterson methods and developed routinely. Full-matrix least squares refinement was based on F^2. Refinement was carried out with all non-hydrogen atoms anisotropic and with hydrogen atoms included in calculated positions with isotropic temperature factors 1.2 times that of the U_{iso} of the atom to which they are bonded. Hydrogen atoms of the hydroxyl groups were found in the penultimate difference maps and refined isotropically.

Table 3.2: Crystallographic data for compounds 21, 22 and 23.

	21	22	23
Empirical formula	$C_{13}H_{13}O_2P$	$C_{13}H_{13}OPS$	$C_{13}H_{13}OPSe$
M_r	232.20	248.26	295.16
space group	$P\bar{1}$	Pccn	Pccn
crystal system	triclinic	orthorhombic	orthorhombic
a (Å)	6.0135(6)	13.8007(9)	13.8650(4)
b (Å)	8.6415(9)	19.8777(15)	19.8190(6)
c (Å)	12.3855(14)	9.0603(6)	9.1740(2)
α (°)	105.701(2)	90	90
β (°)	90.177(3)	90	90
γ (°)	104.789(4)	90	90
V (Å^3)	597.28(11)	2485.5(3)	2521.00(20)
density (g.cm^{-3})	1.291	1.327	1.555
Z	2	8	8
F(000)	244	1040	1104
μ(Mo-K$_\alpha$) (mm^{-1})	0.21	0.36	-#
temperature (°C)	- 132	- 132	- 132
crystal size (mm)	0.58 × 0.56 × 0.20	0.80 × 0.70 × 0.15	0.80 × 0.40 × 0.16
θ-range	2.54° < θ < 23.27°	2.85° < θ < 23.14°	2.85° < θ < 23.43°
total reflections	2522	4663	6864
unique reflections	1680	1568	2014
R_{int}	0.1116	0.0523	0.0399
T_{min}	-0.001782$^{\varnothing}$	0.193269	0.721418
T_{max}	1.000000$^{\varnothing}$	1.000000	1.000000
R_1 ($I > 2\sigma(I)$)	0.0701	0.0658	0.0354
wR_2 (all data)	0.2116*	0.1942^	0.0867•
GOF	1.101	1.163	1.079
e$^-$ density max (e.Å^{-3})	0.417	0.539	0.489
e$^-$ density min (e.Å^{-3})	-0.763	-0.485	-1.204
diffractometer	Siemens SMART CCD	Siemens SMART CCD	Siemens SMART CCD
solution and refinement programmes	SHELXS-97[32], SHELXL-97[33]	SHELXS-97, SHELXL-97	SHELXS-97, SHELXL-97

$^{\varnothing}$ Due to an error in data processing these transmission factors are nonsensical. # Not reported. * $w = [\sigma^2(F_o^2) + (0.1451P)^2 + 0.00P]^{-1}$ where $P = [Max(F_o^2, 0) + 2F_c^2]/3$. ^ $w = [\sigma^2(F_o^2) + (0.1301P)^2 + 1.40P]^{-1}$ where $P = [Max(F_o^2, 0) + 2F_c^2]/3$. • $w = [\sigma^2(F_o^2) + (0.0411P)^2 + 1.78P]^{-1}$ where $P = [Max(F_o^2, 0) + F_c^2]/3$.

Drawing programmes XPMA[34] and PLUTO assisted in the investigation of hydrogen-bonding, and structures have been illustrated with ORTEP 3[35].

Complete lists of atomic coordinates, bond parameters and tables of thermal parameters and hydrogen atom coordinates for the three structures can be found in Appendix A.

3.4 References

1 M. C. Etter, P. W. Baures, *J. Am. Chem. Soc.*, 1988, **110**, 639.

2 a) P. J. Steel, M. A. Battiste, C. R. Cambell, *Acta Cryst.*, 1992, C**48**, 690. b) A. D. Buss, W. B. Cruse, O. Kennard, S. Warren, *J. Chem. Soc., Perkin Trans. I*, 1984, 243.

3 a) M. Gray, B. J. Chapell, N. J. Taylor, V. Snieckus, *Angew. Chem. Int. Ed. Engl.*, 1996, **35**, 1558. b) M. A. Brown, P. J. Cox, R. A. Howie, O. A. Melvin, O. J. Taylor, J. L. Wardell, *J. Organomet. Chem.*, 1995, **498**, 275. c) J. B. Rampal, K. D. Berlin, N. S. Pantaleo, A. McGuffy, D. van der Helm, *J. Am. Chem. Soc.*, 1981, **103**, 2032. d) F. Allen, O. Kennard, L. Nassimbeni, R. Sheperd, S. Warren, *J. Chem. Soc., Perkin Trans. II*, 1974, 1530.

4 J. Podlaha, P. Stepnicka, J. Ludvik, I. Cisarova, *Organometallics*, 1996, **15**, 543. M. Bolte, F. Naumann, A. S. K. Hashmi, *Acta Cryst.*, 1997, C**53**, 1785. G. Pilloni, B. Corain, M. Degano, B. Longato, G. Zanotti, *J. Chem. Soc., Dalton Trans.*, 1993, 1777.

5 a) R. M. Fuquen, J. R. Lechat, *Acta Cryst.*, 1992, C**48**, 1690. b) C. Lariucci, R. H. de Almeida Santos, J. R. Lechat, *Acta Cryst.*, 1986, C**42**, 1825.

6 J. Bernstein, M. C. Etter, L. Leiserowitz, *The Role of Hydrogen Bonding in Molecular Assemblies*, in *Structure Correlations*, H.-B. Burgi, J. D. Dunitz (Ed.), 1994, VCH Verlagsgesellschaft mbH, Weinheim, V. **2**, p. 458.

7 a) D. E. Lynch, G. Smith, K. A. Byriel, C. H. L. Kennard, A. K. Whittaker, J. V. Hanna, *Aust. J. Chem.*, 1994, **47**, 1401. b) D. E. Lynch, G. Smith, N. J. Calos, C.

H. L. Kennard, A. K. Whittaker, K. S. Jack, A. C. Willis, *Aust. J. Chem.*, 1993, **46**, 1535. c) D. E. Lynch, G. Smith, K. A. Byriel, C. H. L. Kennard, *Acta Cryst.*, 1993, C**49**, 718. d) D. E. Lynch, G. Smith, K. A. Byriel, C. H. L. Kennard, *Acta Cryst.*, 1993, C**49**, 285. e) D. E. Lynch, G. Smith, K. A. Byriel, C. H. L. Kennard, *Aust. J. Chem.*, 1992, **45**, 835.

8 A. Avey, D. M. Schut, T. J. R. Weakley, D. R. Tyler, *Inorg. Chem.*, 1993, **32**, 233.

9 M. C. Etter, R. D. Gillard, W. B. Gleason, J. K. Rasmussen, R. W. Duerst, R. B. Johnson, *J. Org. Chem.*, 1986, **51**, 5405.

10 April 1997 release, F. H. Allen, J. E. Davies, J. J. Galloy, O. Johnson, O. Kennard, C. F. Macrea, E. M. Mitchell, J. M. Smith, D. G. Watson, *J. Chem. Inf. Comput. Sci.*, 1991, **32**, 187.

11 G. Grossmann, K. Kruger, G. Ohms, A. Fischer, P. G. Jones, J. Goerlich, R. Schmutzler, *Inorg. Chem.*, 1997, **36**, 770.

12 F. Uhlig, E. Herrmann, D. Schädler, G. Ohms, G. Grossmann, S. Besser, R. Herbst-Irmer, *Z. anorg. allg. Chem.*, 1993, **619**, 1962.

13 S. Hayase, T. Erabi, M. Wada, *Acta Cryst.*, 1994, C**50**, 1276. S. Manhart, A. Schier, M. Paul, J. Riede, H. Schmidbaur, *Chem. Ber.*, 1995, **128**, 365. L. D. Quin, A. T. McPhail, S. O. Lee, K. D. Onan, *Tetrahedron Lett.*, 1974, 3473.

14 M. Wada, S. Hayase, M. Fujiwara, T. Kawaguchi, T. Iwasaki, A. Uo, T. Erabi, *Bull. Chem. Soc. Jpn.*, 1996, **69**, 655.

15 D. W. Allen, N. A. Bell, L. A. March, I. W. Nowell, *Polyhedron*, 1990, **9**, 681.

16 M. J. Pilkington, A. M. Z. Slawin, D. J. Williams, J. D. Woollins, *Main Group Chemistry*, 1995, **1**, 145.

17 W. Henderson, G. M. Olsen, *Polyhedron*, 1996, **15**, 2105.

18 J. Bernstein, M. C. Etter, L. Leiserowitz, *The Role of Hydrogen Bonding in Molecular Assemblies*, in *Structure Correlation*, H.-B. Burgi, J. D. Dunitz (Ed.), 1994, VCH Verlagsgesellschaft mbH, Weinheim, V. **2**, p. 463.

19 R. Taylor, O. Kennard, *Acc. Chem. Res.*, 1984, **17**, 320.

20 J. Kroon, J. A. Kanters, J. G. C. M. Van Duijneveldt-Van de Rijdt, F. B. Van Duinjneveldt, J. A. Vliegenthart, *J. Mol Struct.*, 1975, **24**, 109, cited in J. Bernstein, M. C. Etter, L. Leiserowitz, *The Role of Hydrogen Bonding in Molecular Assemblies*, in *Structure Correlation*, H.-B. Burgi, J. D. Dunitz (Ed.), 1994, VCH Verlagsgesellschaft mbH, Weinheim, V. **2**, p. 457.

21 C. Ceccarelli, G. A. Jeffrey, R. Taylor, *J. Mol. Struct.*, 1981, **70**, 255, cited in R. Taylor, O. Kennard, *Acc. Chem. Res.*, 1984, **17**, 320.

22 J. P. Glusker, P. Murray-Rust, *J. Am. Chem. Soc.*, 1984, **106**, 1018.

23 R. Taylor, O. Kennard, W. Versichel, *J. Am. Chem. Soc.*, 1983, **105**, 5761.

24 J. Bernstein, M. C. Etter, L. Leiserowitz, *The Role of Hydrogen Bonding in Molecular Assemblies*, in *Structure Correlation*, H.-B. Burgi, J. D. Dunitz (Ed.), 1994, VCH Verlagsgesellschaft mbH, Weinheim, V. **2**, p. 472.

25 D. J. Millen, *Croat. Chem. Acta*, 1982, **55**, 133.

26 K. M. Mackay, R. A. Mackay, *Introduction to Modern Inorganic Chemistry*, 4th Ed., 1989, Blackie & Son Ltd., Glasgow, p. 64.

27 N. Burford, *Coord. Chem. Rev.*, 1992, **112**, 1.

28 For example: N. Burford, B. W. Royan, R. E. v. H. Spence, T. S. Cameron, A. Linden, R. D. Rogers, *J. Chem. Soc., Dalton Trans.*, 1990, 1521.

29 For example: N. Burford, B. W. Royan, R. E. v. H. Spence, R. D. Rogers, *J. Chem. Soc., Dalton Trans.*, 1990, 2111.

30 J. Bernstein, M. C. Etter, L. Leiserowitz, *The Role of Hydrogen Bonding in Molecular Assemblies*, in *Structure Correlation*, H.-B. Burgi, J. D. Dunitz (Ed.), 1994, VCH Verlagsgesellschaft mbH, Weinheim, V. **2**, p. 460.

31 R. H. Blessing, *Acta Cryst.*, 1995, A**51**, 33.

32 G. M. Sheldrick, *SHELXS-97, Program for Solving Crystal Structures*, University of Göttingen, 1997.

33 G. M. Sheldrick, *SHELXS-97, Program for Solving Crystal Structures*, University of Göttingen, 1997.

34 L. Zsolnai and H. Pritzkow, 1994, University of Heidelberg.

35 C. K. Johnson, M. N. Burnett, *ORTEP-III Version 1.0.2*. Windows 32-bit Version 1.0.β compiled by L. J. Farrugia, Dept. of Chemistry, University of Glasgow.

Chapter 4: Synthesis and Characterisation of Primary and Secondary Ferrocenylphosphines and Related Compounds

4.1 Introduction

4.1.1 Primary and Secondary Phosphines

Primary and secondary phosphines (RPH_2 and R_2PH respectively) are generally reactive species, with a great deal of chemistry accessible through manipulation of the P-H bond. Examples of the many such reactions include reaction of P-H species with unsaturated compounds, acid halides, halogens, alkali metals and Lewis acids such as borane, as well as hydrolysis of the C-P bond in some instances[1]. Scheme 4.1 gives some examples of chemistry undertaken with primary and secondary phosphines.

One very notable aspect of primary and secondary phosphine chemistry is their predisposition towards breakage of the weak P-H bond and formation of complexed phosphide or phosphinidine fragments upon reaction with metal centres[2]. These formally anionic ligands can coordinate to a single metal centre, or form bridging or capping ligands in multinuclear species. The chemistry of phosphide and phosphinidine ligands formed from secondary or primary phosphines is discussed in Section 4.2.3 with respect to metal carbonyl clusters.

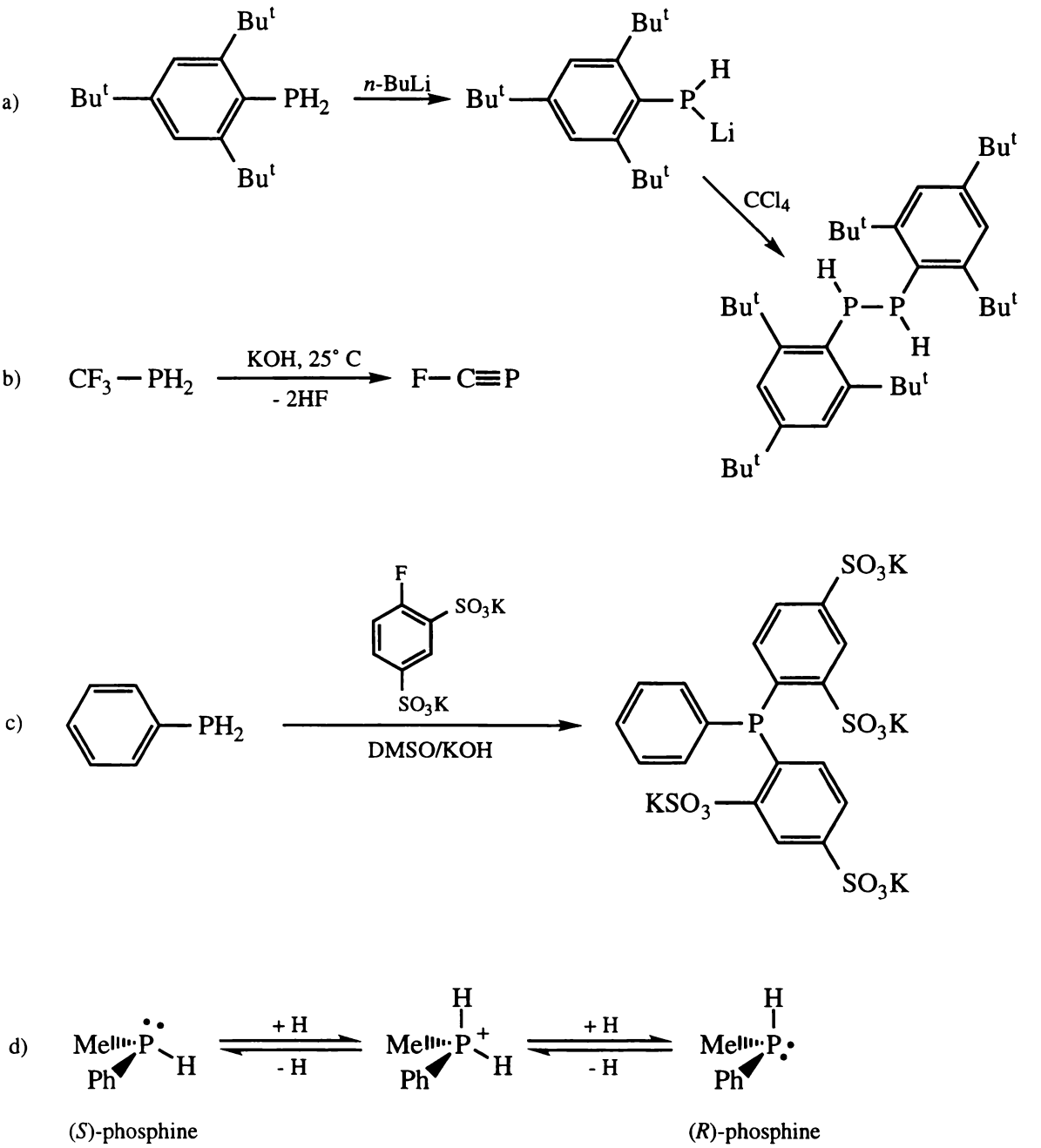

Scheme 4.1: Some reported reactions involving primary and secondary phosphines. d) Relative to tertiary phosphines, chiral secondary phosphines are very difficult to isolate in enantiomerically pure form, since racemisation occurs rapidly by both acid (shown here) and basic mechanisms. References: a)[3]; b)[4]; c)[5]; d)[6].

Primary and secondary phosphines are generally sensitive toward air-oxidation, this constituting an important practical consideration where they are to be used. Generally primary phosphines, and to a lesser extent secondary phosphines, will oxidise very readily in the presence of oxygen; a number of these phosphines are in fact pyrophoric[7]. Tertiary phosphines will generally oxidise, whether by exposure to air or through deliberate synthesis, to give the corresponding phosphine oxide, as typified by the synthesis of compounds **3**, **7** and **15** described in Chapter 1. Uncontrolled oxidation of primary phosphines, on the other hand, generally leads to a mixture of the phosphonous [RP(H)(O)OH] and phosphonic (RPO_3H_2) acids, while secondary phosphine oxidation will lead to the phosphinic acid [$R_2P(O)OH$][1]. In both cases this results from insertion of the first attached oxygen into the P-H bond, leaving the phosphorus atom again open to oxidative attack[8]. Scheme 4.2 shows this process for a primary phosphine.

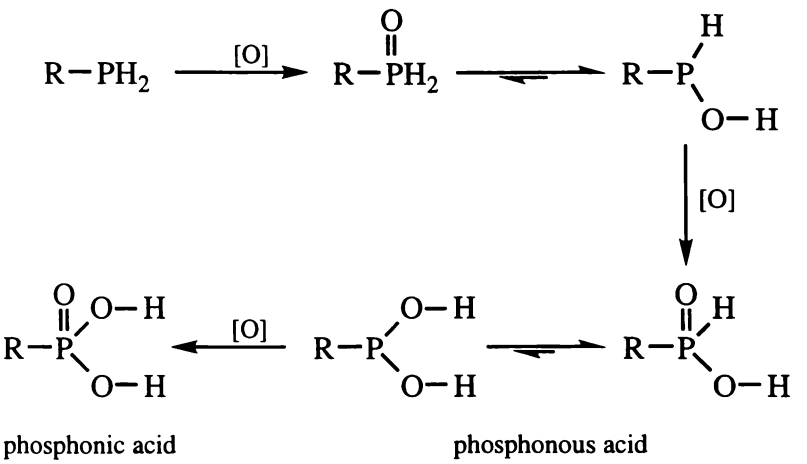

Scheme 4.2: Usual route of oxidation for a primary phosphine.

Isolation of primary or secondary phosphine oxides has only been possible under strictly controlled conditions[9], or with the use of bulky organic groups[10]. The susceptibility of primary and secondary phosphines to oxidation has led to the widespread use of borane adducts as protecting groups for these phosphines during various syntheses or purifications[11].

Because of the reactive character of primary and secondary phosphines, preparation of such phosphines with ferrocenyl group(s) incorporated into the molecule would provide a useful means for the further formation of other ferrocene-containing compounds, through reaction of the phosphine with a suitable functional group on a target molecule. In fact the secondary phosphine $(Fc)_2PH$ has been prepared[12], and has been used to produce a ferrocene-derivatised analogue of the well-known chiral ligand 2,3-*O*-isopropylidene-2,3-dihydroxy-1,4-bis(diphenylphosphino)butane (DIOP)[13] (Scheme 4.3). The only other ferrocene-derived primary and secondary phosphines known to the author are 1,1'-diphosphinoferrocene[14], and the chiral ferrocenylphosphine previously depicted as compound **46** in Chapter 1[15].

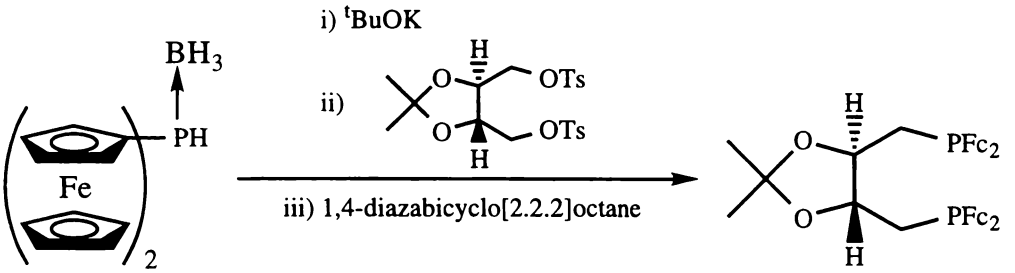

Scheme 4.3: Reaction of borane-protected $(Fc)_2PH$ to give a ferrocene-derivatised DIOP ligand.

4.1.2 The Relation of Primary Phosphines to Hydroxymethylphosphines

Hydroxymethylphosphines have already been discussed in Chapter 2, and the fact that in certain instances hydroxymethylphosphine moieties react as disguised P-H bonds was discussed in Section 2.1.1. In fact, formaldehyde can be inserted into a P-H bond to form a hydroxymethylphosphine fragment, as is demonstrated by the fact that $[P(CH_2OH)_4]Cl$ is made industrially by the reaction of PH_3 with formaldehyde and hydrochloric acid[16,17]. Without the presence of the acid, $P(CH_2OH)_3$ is formed by this reaction[18] (Scheme 4.4a). In alkaline media formaldehyde can add further to $P(CH_2OH)_3$, not to form the

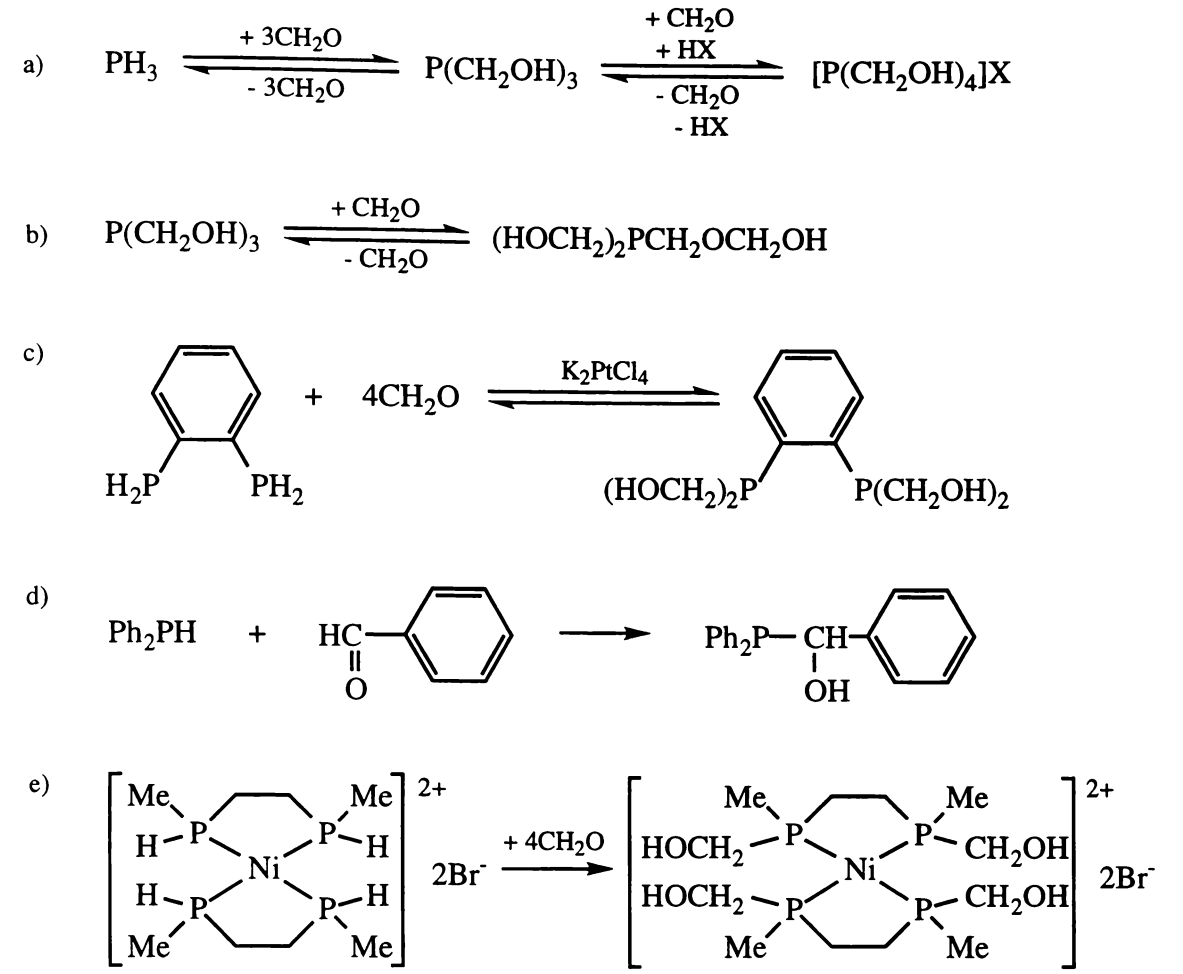

Scheme 4.4: a) The interaction between PH_3 and formaldehyde[18]. b) The reaction of $P(CH_2OH)_3$ with formaldehyde under alkaline conditions to give a monohemiformal. Formaldehyde can add further, several times for every hydroxymethyl group, to give a variety of products[20]. c) Synthesis of the hydroxymethylphosphine $(HOCH_2)_2C_6H_4(CH_2OH)_2$[19]. d) Insertion of an aldehyde into a P-H bond; synthesis of α-hydroxybenzyldiphenylphosphine[22a]. e) Insertion of formaldehyde into the P-H bond of a complexed secondary phosphine. Formaldehyde was supplied to this reaction as paraformaldehyde[23].

hydroxymethylphosphonium salt but to give hemiformals[20] (Scheme 4.4b). In fact, insertion of formaldehyde into a P-H bond is the most usual route for the synthesis of any hydroxymethylphosphine[21], either directly (Scheme 4.4c), or through formation of the hydroxymethylphosphonium salt which is then treated with base. Aldehydes can also be inserted into P-H bonds in a similar way to give derivatised hydroxymethylphosphines of

the type $R_2PCHROH$[10b,22] (Scheme 4.4d). Interestingly, insertion of formaldehyde into the P-H bond of a complexed secondary phosphine to give the corresponding hydroxymethylphosphine complex has also been reported[23] (Scheme 4.4e), a process similar to the catalysis of $P(CH_2OH)_3$ formation from PH_3 by metal complexes discussed in Section 2.1.2.

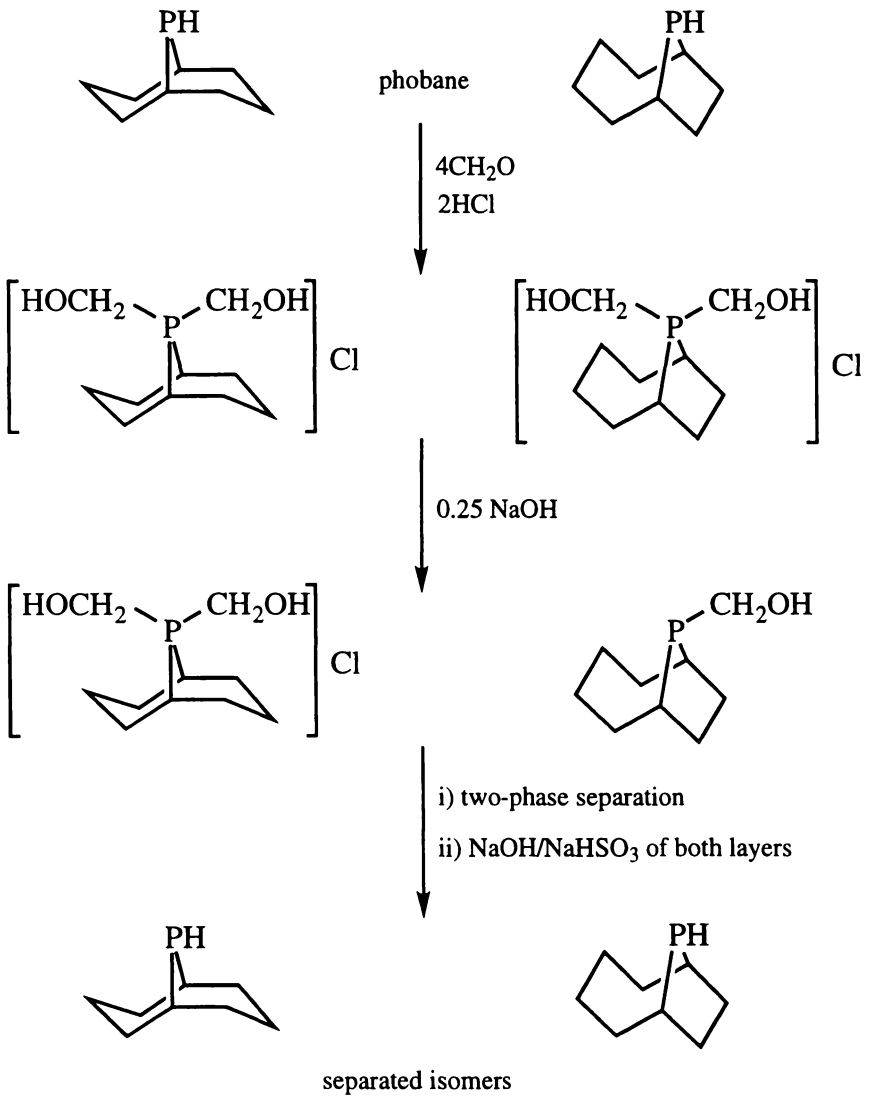

Scheme 4.5: Separation of phobane isomers by reversible addition of formaldehyde to the P-H bond.

One important aspect of these reaction systems is that addition of formaldehyde to P-H bonds is a reversible process, as is apparent from the fact that distillation of $P(CH_2OH)_3$ yields phosphine[24]. However, the removal of formaldehyde from a hydroxymethylphosphine to form a secondary or primary phosphine has not often been

utilised synthetically. The reversible nature of this reaction was reported very recently as being used for the separation of two isomers of the secondary phosphine 'phobane'[25] (Scheme 4.5). The secondary phosphine was first reacted with formaldehyde and acid in order to form the two isomeric phosphonium salts. Addition of NaOH in the correct amount then allowed removal of a hydroxymethyl moiety from one isomer without any reaction with the other isomer, due to differing reactivities. The two isomers could then be separated by extraction of the aqueous solution with pentane, leaving the salt in the aqueous layer. Both isomers were transformed back to the secondary phosphine by treatment with base and sodium bisulfite, the latter acting as a formaldehyde abstractor. Phobane is an important starting material in the production of certain ferrocenylphosphines[26] discussed in Section 1.2. The only other example, of which the author is aware, of primary or secondary phosphine synthesis from a hydroxymethylphosphine is the recently described formation of $RuCl_2[P(CH_2OH)_3]_2[P(CH_2OH)_2H]_2$[27] from reaction of $P(CH_2OH)_3$ with either $RuCl_3.H_2O$ or $RuCl_2(PPh_3)_3$.

4.2 Results and Discussion

4.2.1 Synthesis and Characterisation of Ferrocenylphosphines and a Ferrocenylphosphinic Acid

The research described in this Chapter was prompted by two serendipitous observations. Firstly, it was noted that if compound **1** was refluxed in ethanol or isobutyl alcohol, rather than methanol, unidentified side products of the reaction were observed with downfield shifts in the ^{31}P-NMR (δ = - 130, -54 ppm); these showed large splittings (*ca.* 200 Hz) into a triplet and doublet respectively when the spectrum was non-decoupled. Secondly, silica gel chromatography of a mixture containing compound **11** produced a band which also gave a ^{31}P-NMR signal of δ -54 ppm, which split into a doublet, J = 197 Hz, in the non-

decoupled spectrum. These NMR signals clearly indicated that formation of stable primary and secondary phosphines was taking place under these conditions, and so it was decided to attempt deliberate syntheses.

The primary phosphine $FcCH_2PH_2$ **24** [^{31}P-NMR ($CDCl_3$): δ -129.1, t, ^{1}J(P-H) = 194 Hz] was prepared by the refluxing of compound **1** with one equivalent of sodium metabisulfite (a formaldehyde abstracting agent) in a two-phase system of water and petroleum spirits (B.P. 60-80° C), giving a crystalline solid which could be purified by sublimation (Scheme 4.6). It was soon realised that this primary phosphine was remarkably air-stable. In this connection it is noteworthy that the yield obtained from carrying out the reaction in air was not significantly lower than that obtained from carrying out the reaction under nitrogen. Obviously an air-stable primary phosphine provides great advantages over an air-sensitive or pyrophoric primary phosphine in preparative applications. The stability of **24** was tested by elemental analysis on a sample stored in an unsealed vial at room temperature after one and two months, with exemplary results. This was supported by gas chromatography-mass spectrometry (GC-MS) analysis of **24** 79 days after sublimation (Figure 4.1), showing the product to be pure. After 48 days in air no oxidation products could be detected by ^{31}P-NMR. The experience of the author has been that the earliest preparations of **24** have remained stable under these normal storage conditions for about two years with no sign of degradation. While no rigorous examination has been carried out of air-stability in solution this also appears to be good.

Very few other reports have been made concerning air-stable primary phosphines. Of these phosphines the most frequently used is 2,4,6-tri-*t*-butylphenylphosphine ('supermesitylphosphine', or Mes*PH_2), first reported in 1982[28] and later described as 'quite stable in air'[29]. In the solid state it will oxidise in a matter of months, but is air-stable to the extent that it can be recrystallised in air from hot isopropanol[30]. No doubt the relative air-stability of supermesitylphosphine has encouraged its use in general chemical applications in preference to other primary phosphines, and studies utilising this compound and closely related derivatives are not uncommon[2b,3,4,10c,31]. Although not so air-stable,

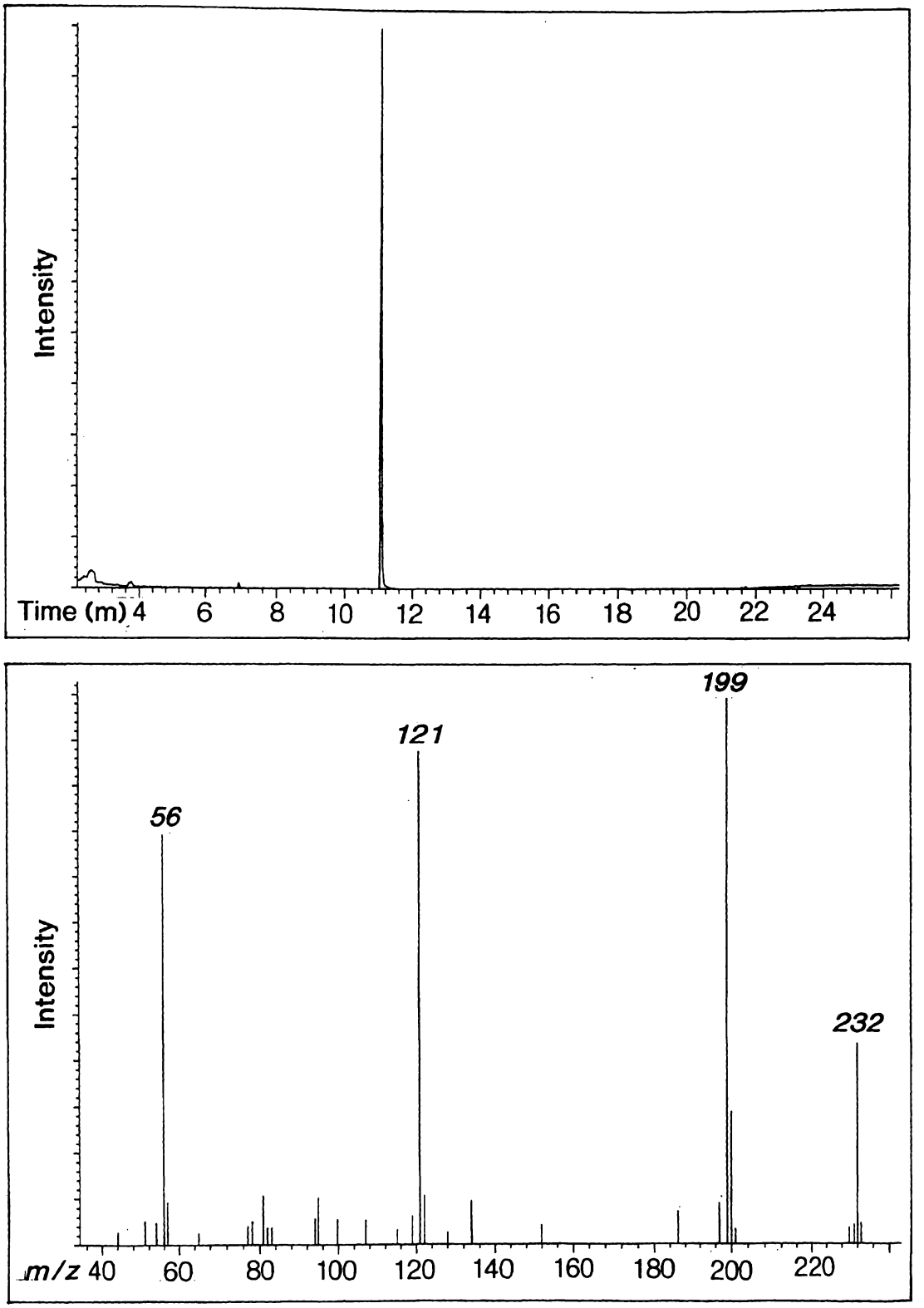

Figure 4.1: GC-MS trace of **24** after 79 days of air-storage, showing only one chromatographic peak due to the product (top). The lower spectrum shows the MS of the GC peak, with the *m/z* assignment being as follows: 232 $[M]^+$, 199 $[FcCH_2]^+$, 121 $[FeCp]^+$, 56 $[Fe]^+$.

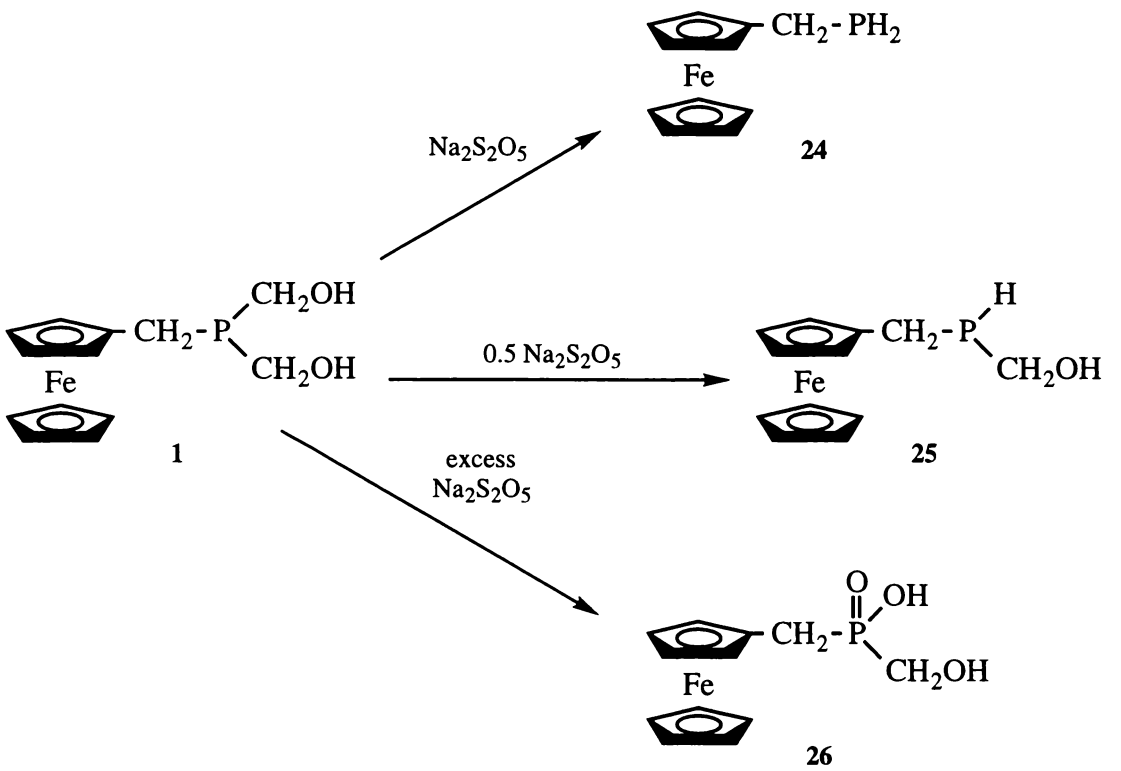

Scheme 4.6: Syntheses based on the reaction of **1** with sodium metabisulfite, giving the products **24**, **25** and **26**.

mesitylphosphine is also a frequently used phosphine[32,33]. So far as the author is aware the only other known example of air-stable primary phosphines is a series of eleven cationic compounds with the formula $[R'_2R''N(CH_2)_mPH_2]I$, as shown in Table 4.1[34]. No details were reported other than that the compounds were air-stable in the solid state, and that compound 1 of Table 4.1 oxidised very slowly in aqueous solution exposed to air. So then, compound **24** is most unusual and in fact may set the benchmark for primary phosphine air-stability.

Proposing a mechanism for air-stability in supermesitylphosphine is straightforward; steric congestion would seem the obvious cause. Again, it might be postulated that the positively charged nature of compounds of the type $[R'R''_2N(CH_2)_mPH_2]I$ mitigates against attack by electrophilic oxygen. However, no mechanism is here proposed to account for the air-stable

Table 4.1: *The 11 air-stable compounds in the series having the general formula* $[R'_2R''N(CH_2)_mPH_2]I$[34].

	R'	R"	m
1	Me	Me	2
2	Me	Me	3
3	C_5H_{10}	Me	2
4	C_4H_8O	Me	2
5	Me	C_6H_{13}	2
6	Me	C_7H_{15}	2
7	Me	C_8H_{17}	2
8	Me	$C_{12}H_{25}$	2
9	Me	$C_{16}H_{33}$	2
10	Me	$C_{18}H_{37}$	2
11	$R'_2R''N(CH_2)_m$ = 2-(1-methyl-2-pyrrolidinyl)ethyl		

nature of **24**. It is certainly not due to steric factors, as the ferrocenylmethyl fragment is not sterically bulky. In addition the X-ray crystal structure determination of **24** (see Section 4.2.2) shows the phosphine function points away from the ferrocenyl group, ruling out the possibility of any type of bonding interaction with the iron. The synthesis and comparative study of related structures such as $FcPH_2$, $FcCH_2CH_2PH_2$ and $RcCH_2PH_2$ [Rc = $(\eta^5$-$C_5H_5)Ru(\eta^5$-$C_5H_4)$] may be helpful in providing information about what structural elements are important to air-stability.

The secondary phosphine $FcCH_2P(H)CH_2OH$ **25** [^{31}P-NMR ($CDCl_3$): δ -51.4, d, ^1J(P-H) = 204 Hz] has also been prepared by a method analogous to that used to make **24**; compound **1** is reacted with a little over a half-equivalent of sodium metabisulfite in a two-phase system in air (Scheme 4.6). However, diethyl ether is used for the organic layer, since **25** is not soluble in petroleum spirits. This compound appears to be stable with respect to air oxidation, but is unstable with respect to disproportionation. In the solid state, a two week period is enough for **25** to be almost completely transformed into a 1:1 mixture of **1** and **24**.

Table 4.2: *Disproportionation of 25. A fresh sample of 25 was made up in $CDCl_3$, and its disproportionation to 1 and 24 monitored by integration of signals for the three compounds in the non-decoupled ^{31}P-NMR spectrum, over several days. The proportion of peak area for each product is expressed as a percentage of the total.*

	25	**1**	**24**
four hours	88.3	6.4	6.2
one day	83.2	9.4	7.3
two days	76.3	12.6	11.2
three days	66.0	18.5	15.5

Table 4.2 shows the disproportionation taking place in a $CDCl_3$ solution at room temperature over several days, as monitored by ^{31}P-NMR. The reasons why **1** and **24** should be energetically favoured over **25** are unclear. However, it is not difficult to draw a feasible concerted mechanism by which disproportionation might take place (Scheme 4.7). A concerted mechanism seems preferable to one involving the release of free formaldehyde as this would presumably fail to lead to a 1:1 ratio of products, with a greater level of **24** being seen instead.

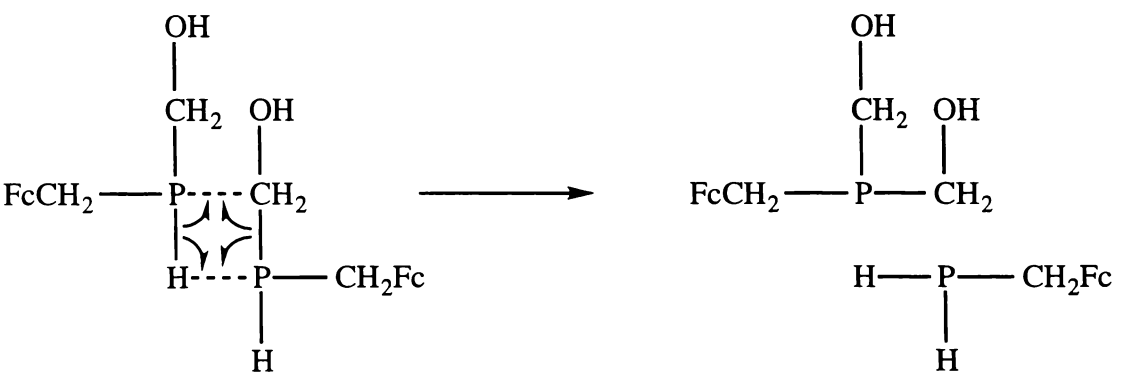

Scheme 4.7: A concerted mechanism for the disproportionation of **25** to **1** and **24**.

It was found that reacting **1** with a large excess of sodium metabisulfite in a two-phase system of water and petroleum spirits (B.P. 60-80° C) did not lead to synthesis of the primary phosphine **24** as might be expected. Instead the phosphinic acid $FcCH_2P(O)(OH)CH_2OH$ **26** [^{31}P-NMR (D_2O): δ 37.4]was produced as the major product (Scheme 4.6), with most of the colour in the reaction two-phase system present in the aqueous layer. This product proved difficult to isolate, for several reasons: The aqueous layer from which **26** was isolated contained various sodium salts used in the reaction; compound **26** could be present in the reaction mixture as the conjugate base $Na^+[FcCH_2P(O)(O^-)CH_2OH]$; the solubility properties of the acid and its conjugate base in various solvents were not as distinct as might be hoped; the free acid was rather soluble in both water and organic solvents. Nevertheless, Section 4.3.1.3 describes methods for the synthesis of **26** as a crude preparation in moderate yield, or as a pure compound in very low yield. It of interest to observe that **26** is produced from this reaction, since metabisulfite is usually considered a reducing rather than oxidising agent, and in this regard it is noteworthy that **26** is still formed when the reaction is carried out in the absence of oxygen.

An attempt was made to produce $(FcCH_2)_2PH$ from **11** using the same method outlined for **24** and **25** above. However, it was found that the formaldehyde in **11** was much more difficult to remove than was the case for **1**; refluxing a diethyl ether/water two-phase system containing **11**, in the presence of one equivalent of sodium metabisulfite, for ten days yielded only incomplete reaction. The solvents were therefore removed and replaced with the higher boiling isopropyl alcohol, and reflux carried out for 16 hours. No substantial increase in product level was obtained by this. Addition of another half-equivalent of metabisulfite and reflux for a further eight hours led to the production of significant levels of oxidation products with no substantial increase in the level of desired product.

However, there are other possible means for achieving this reaction, or indeed any synthesis of a primary or secondary phosphine from the hydroxymethylphosphine equivalent, which may prove more effective. As was noted in Section 2.2.1, the author has observed that silica gel chromatography of hydroxymethylphosphines on tlc plates generally leads to at

least some loss of a hydroxymethyl group, yielding a secondary phosphine. In fact a sample of $(FcCH_2)_2PH$ has been serendipitously obtained in this way and partially characterised (see first paragraph of this Section). Stirring of hydroxymethylphosphines with silica gel could thus provide a means of preparative synthesis. Solid-state pyrolysis reactions also have some potential for producing primary and secondary phosphines from hydroxymethylphosphines; a sample of **1** was heated under vacuum to 120° C, leading to the sublimation of a mixture of products. The major product was in fact unreacted **1**, but **24** and **25** were also present as the next most dominant species. Pyrolysis in the presence of a reagent such as metabisulfite may be more effective. As was alluded to at the start of this Section, heating of **1** to temperatures greater than *ca.* 80° C in solution also leads to formaldehyde loss from the molecule with consequent formation of **24** and **25**.

4.2.2 Synthesis of Complexes of $FcCH_2PH_2$ **24**

Several complexes of the primary phosphine **24** have been prepared, in order to show that despite its air-stability, **24** still displays normal phosphine coordinative behaviour. The compounds prepared are represented in Scheme 4.8.

The Mo(0) complex $Mo(CO)_5(FcCH_2PH_2)$ **27** [^{31}P-NMR ($CDCl_3$): δ -63.2, t, ^1J(P-H) = 315 Hz] was prepared by the standard technique of irradiating a tetrahydrofuran (THF) solution of $Mo(CO)_6$ under nitrogen in the presence of **24**. Irradiation with the high energy UV light leads to replacement of a carbonyl with a labile THF molecule, which is in turn displaced by the phosphine ligand. When the reaction is carried out using equimolar amounts of the two reagents, considerable amounts of the di- and tri-substituted complexes are also produced as side-products. The use of $Mo(CO)_6$ in large excess minimises the levels of these impurities. Unlike the two starting materials, **27** does not appear to be volatile. If stored in the solid state at -30° C, **27** is moderately stable, but in solution, or in the solid state at room temperature, it is susceptible to degradation on exposure to air.

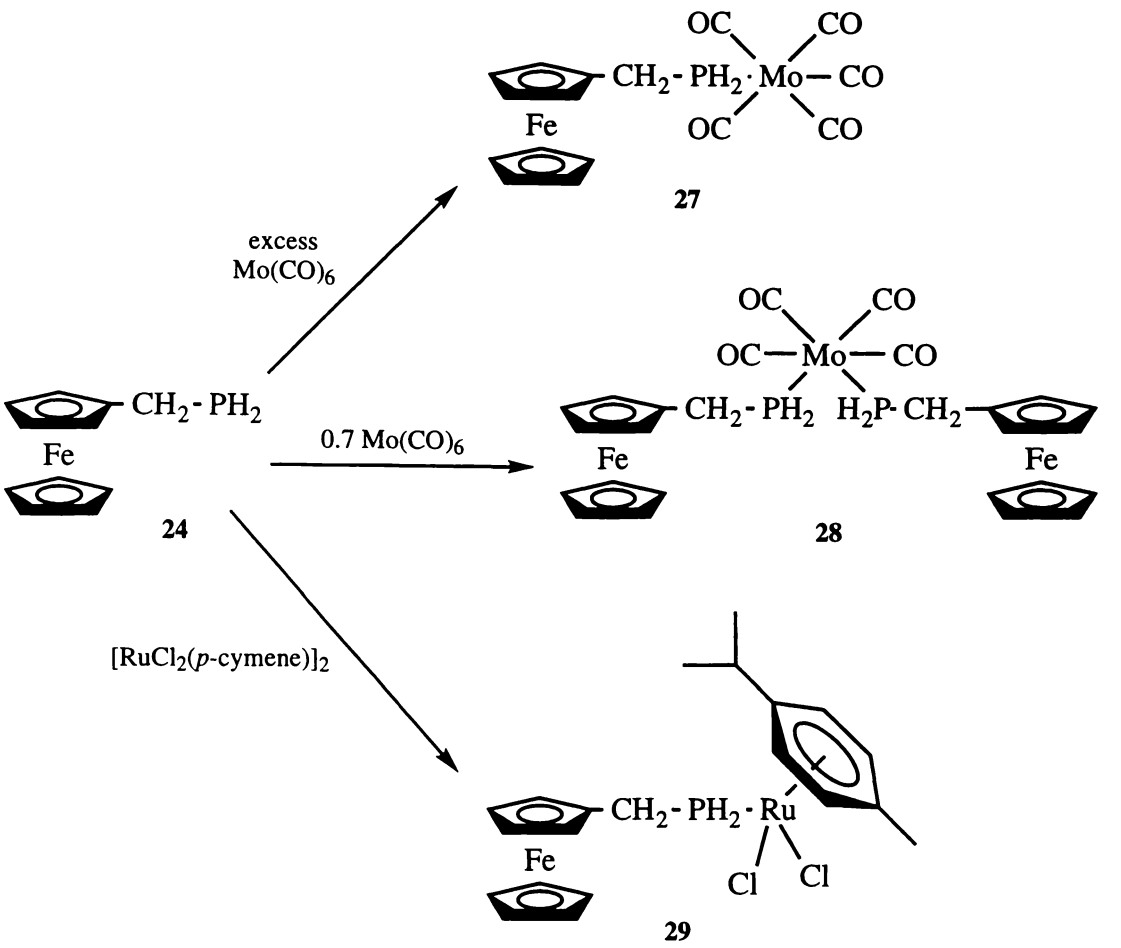

Scheme 4.8: Complexes prepared using **24** as a ligand.

The di-substituted product $Mo(CO)_4(FcCH_2PH_2)_2$ **28** [^{31}P-NMR ($CDCl_3$): δ -55.9, t, ^{1}J(P-H) = 308 Hz] was produced in low yield by heating a decalin solution of $Mo(CO)_6$ and **24** to 100° C for 15 hours. The product crystallised out of the cooled and evaporating solution as spherical crystals. Compound **28** appeared to be more air-stable than **27**, although over a period of weeks the crystals did darken.

Examples of such mono- and di-substituted Mo(0) carbonyl phosphine complexes are not uncommon[35], and indeed these compounds are also not the first mononuclear Mo carbonyl phosphinoferrocene compounds synthesised, with $Mo(CO)_5PFc_3$ being one early example of a previously reported compound of this type[36].

The Ru(II) cymene complex $[RuCl_2(\eta^6\text{-}C_{10}H_{14})(FcCH_2PH_2)]$ **29** [^{31}P-NMR ($CDCl_3$): δ -27.7, t, ^1J(P-H) = 359 Hz] was also synthesised, by a method similar to that used in preparing the compounds **19** and **20** discussed in Section 2.2.4, through the bridge-splitting reaction of $[RuCl_2(\eta^6\text{-}C_{10}H_{14})]_2$. This gave a complex which was air-stable, in accord with normal coordinative behaviour for a primary phosphine[37].

4.2.3 Reaction of $FcCH_2PH_2$ **24** with Triruthenium Dodecacarbonyl

Numerous papers have been published in which ferrocene groups are linked to metal carbonyl cluster compounds, the rationale behind such work often consisting of interest in the potential of ferrocene-containing materials for various technological applications. A number of these compounds are simply complexes of various ferrocenylphosphines (discussed in Chapter 1)[38]. Other groups by which ferrocenes have been coordinated to metal carbonyl clusters include unsaturated C-C bonds[39], a bridging amido ligand[40], and a pyridyl group[41]. By pyrolysis of Ru clusters containing tertiary ferrocenylphosphines Cullen *et al.* have isolated a variety of clusters containing bridging or capping phosphide- or phosphinidine-ferrocene units[42]. The production of a cobalt cluster with both a bridging PFc_2 and a capping PFc moiety has also been accomplished through the reaction of $FcPCl_2$ with $NaCo(CO)_4$ at room temperature[43]. A few of these structures containing bridging or capping phosphorus are shown in Scheme 4.9.

In view of the predisposition of primary phosphines toward formation of phosphide or phosphinidine fragments when reacting with metal centres (Section 4.1.1), the reaction of a primary ferrocenylphosphine such as **24** with metal carbonyl clusters should prove an effective way of producing clusters with capping or bridging phosphinidine- or phosphide-ferrocene moieties. The reactions of primary (and secondary[44]) phosphines with metal carbonyl clusters have in fact been rather extensively investigated and many products characterised[35b,45], including those shown in Scheme 4.10.

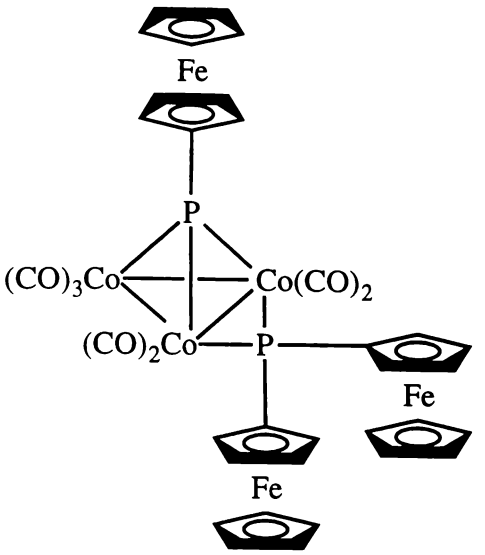

a)

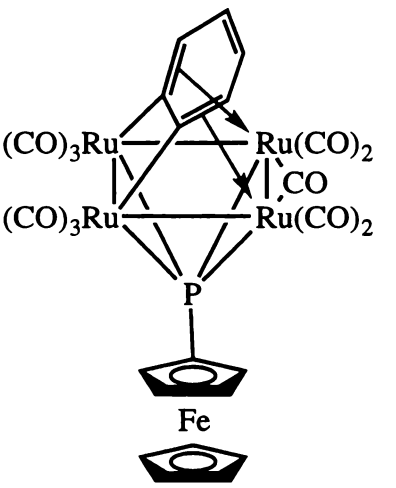

b)

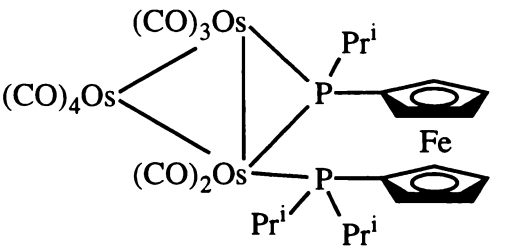

c)

Scheme 4.9: Some metal carbonyl clusters containing bridging or capping phosphide- or phosphinidine-ferrocene moieties. References: a)[43]; b)[42a]; c)[42b].

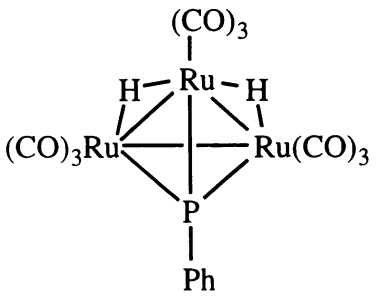

a)

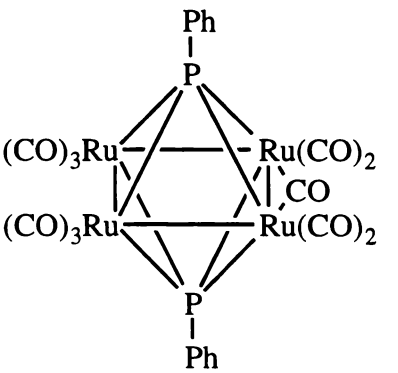

b)

Scheme 4.10: Two products obtained from the reaction of $PhPH_2$ with $Ru_3(CO)_{12}$. a) A monacapped tri-ruthenium cluster[46]. b) A bicapped tetra-ruthenium cluster[47].

The reaction of **24** with $Ru_3(CO)_{12}$ was carried out in refluxing cyclohexane and led to the formation of at least seven products, judging by the number of bands which could be succesfully separated by preparative tlc on silica gel. Only two major products were isolated however, and these were unambiguously characterised as $Ru_3(CO)_9(\mu^2\text{-H})_2(\mu^3\text{-PCH}_2\text{Fc})$ **30** [^{31}P-NMR ($CDCl_3$): δ 76.9] and $Ru_4(CO)_{11}(\mu^4\text{-PCH}_2\text{Fc})_2$ **31** [^{31}P-NMR ($CDCl_3$): δ 193.0]; a comparison of carbonyl region IR data for **30** and **31** with data for related compounds is given in Table 4.3, showing the close relationship between the observed bands of related compounds. Microanalytical data were satisfactory, and the ESMS data, which also support this assignment, are discussed in detail in the following Section 4.2.4. Both compounds appeared pure by ^{31}P-NMR. The structures of compounds **30** and **31** are shown in Scheme 4.11, and are of course analogous to the compounds $Ru_3(CO)_9(\mu^2\text{-H})_2(\mu^3\text{-PPh})$ and $Ru_4(CO)_{11}(\mu^4\text{-PPh})_2$ shown in Scheme 4.10. The synthesis of **30** and **31** was achieved by following a literature preparation[46] for $Ru_3(CO)_9(\mu^2\text{-H})_2(\mu^3\text{-PPh})$, and this again highlights the normal behaviour of **24** in an application requiring a primary phosphine.

Table 4.3: *Comparison of IR data for compounds 30 and 31 with analogous compounds previously reported in the literature.*

Compound	ν(CO) (cm^{-1})
30	2105 (m), 2072 (s), 2046 (s), 2028 (m), 2014 (s), 1998 (s), 1984 (m)
$Ru_3H_2(CO)_9(PPh)$[35b,46]	2104 (m), 2073 (s), 2047 (s), 2045 (s, sh), 2028 (m), 2016 (s), 1997 (s), 1984 (m)
$Ru_3H_2(CO)_9(PC_6H_4OCH_3)$[45c]	2106 (s), 2073 (s), 2045 (s), 2024 (w), 2014 (s), 1996 (s), 1981 (s)
31	2077 (w), 2037 (s), 2015 (s), 1979 (m), 1829 (w)
$Ru_4(CO)_{11}(PPh)_2$[47]	2075 (m), 2035 (s), 2018 (m), 1980 (m), 1838 (w)
$Fe_4(CO)_{11}(PPh)_2$[47]	2070 (w), 2025 (s), 2010 (m), 1986 (m), 1832 (w)

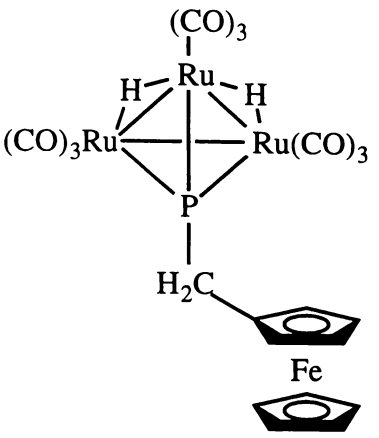

30

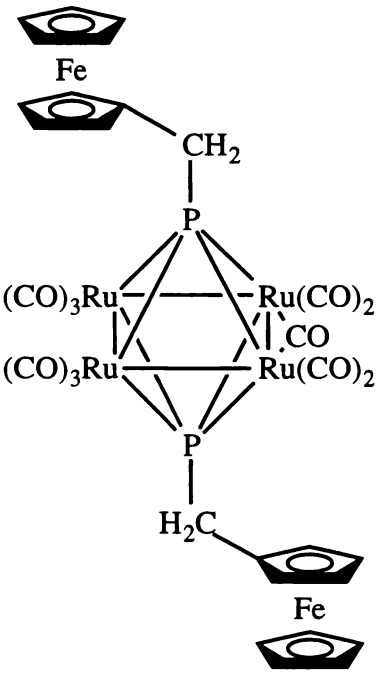

31

Scheme 4.11: Structures of compounds **30** and **31**.

In spite of good evidence pointing to the integrity of the samples, some doubt must still be expressed over the purity of **31** obtained by the method described in Section 4.3.1, on the basis of small unassignable redox processes observed in electrochemical investigation of this compound. This question remains to be answered by further investigation. During electrochemical studies no such difficulties were encountered for **30**.

4.2.4 ESMS Analysis of Compounds $FcCH_2PH_2$ **24**, $FcCH_2P(H)CH_2OH$ **25**, $FcCH_2P(O)(OH)CH_2OH$ **26**, $Mo(CO)_5(FcCH_2PH_2)$ **27**, $Mo(CO)_4(FcCH_2PH_2)_2$ **28**, $RuCl_2(\eta^6\text{-}C_{10}H_{14})(FcCH_2PH_2)$ **29**, $Ru_3(CO)_9(\mu^2\text{-}H)_2(\mu^3\text{-}PCH_2Fc)$ **30** and $Ru_4(CO)_{11}(\mu^3\text{-}PCH_2Fc)_2$ **31**

For a brief discussion of previous research into the ESMS of ferrocenylphosphines, see Section 2.2.2. Both compounds **24** and **25** gave $[M]^+$ peaks, arising from oxidation of the ferrocenyl moiety in the electrospray mechanism, rather than $[M + H]^+$ peaks. Compound **26** was detected in negative ion mode and gave a peak corresponding to $[M - H]^-$, as would be expected from an acid. Compound **29** gave an unusual spectrum in which the major peak of *m/z* 618.6 corresponds to a species with the formula $[Ru(P(H)CH_2Cp)(\eta^6\text{-}C_{10}H_{14})(CH_3CN)(\mathbf{24})]^+$, i.e. the chlorines have been lost and the ruthenium is coordinated to acetonitrile, *p*-cymene, **24** and a phosphide derived from **24** where the iron and a Cp ring have been lost. Another peak occurs with *m/z* 654.6; presumably this species is $[RuCl(\eta^6\text{-}C_{10}H_{14})(PH_2CH_2Cp)(CH_3CN)(\mathbf{24})]^+$, and eliminates HCl to give the dominant peak with *m/z* 618.6.

Compounds **27**, **28**, **30** and **31** together constitute an interesting test of the generality of a method for the detection of neutral metal carbonyl compounds developed by Nicholson *et al.*[48]. The method involves addition of a small amount of sodium methoxide to the ESMS sample immediately before injection. In most situations the methoxide will attack a CO ligand, since these are susceptible to nucleophilic attack, in order to give a negatively-charged species $[M + MeO]^-$ directly detectable by ESMS. However, if hydride groups are present, the methoxide may react to give methanol and a detectable parent ion $[M - H]^-$. Both these situations are encountered with the compounds **27**, **28**, **30** and **31**.

On treatment with methoxide, **27** is detectable as a peak corresponding to $[M - H]^-$, with the abstracted proton probably being one of the relatively labile P-H protons. At a cone voltage of 20 V a small peak is also seen corresponding to $[M - H - CO]^-$; loss of carbonyl groups is a normal phenomenon seen with this technique and the degree to which carbonyls are lost can be tuned by varying the cone voltage. A peak corresponding to $[M - H]^-$ is also seen for **28**. Interestingly, a large peak is also seen corresponding to $[Mo(PH_2CH_2Cp)(CO)(\mathbf{24})]^-$. This peak is probably not formed as a result of methoxide treatment, but is due to simple fragmentation of the parent molecule (the negative charge perhaps being carried on the cyclopentadienyl ring). Such a fragmentation process is not surprising in view of the fact that the material which must thus be lost from the parent compound **28** could form the stable species $[Fe(Cp)(CO)_3]^+$.

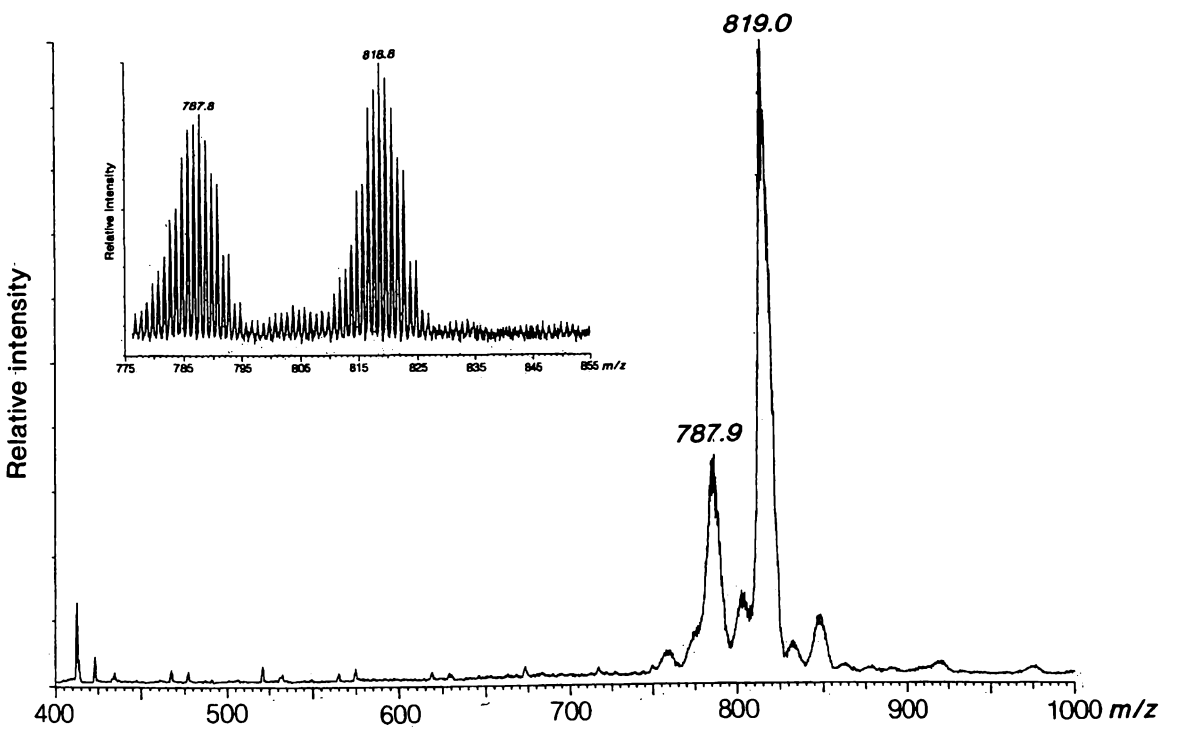

Figure 4.2: ESMS spectrum for **30**, with the inset showing a high resolution mass spectrum of the same compound. In cluster compounds of this sort where isotope patterns become complex, comparison of high resolution and calculated spectra is important in exact assignment of peaks. Assignment for this compound is: *m/z* 819.0 $[M + MeO]^-$, 787.9 $[M - H]^-$.

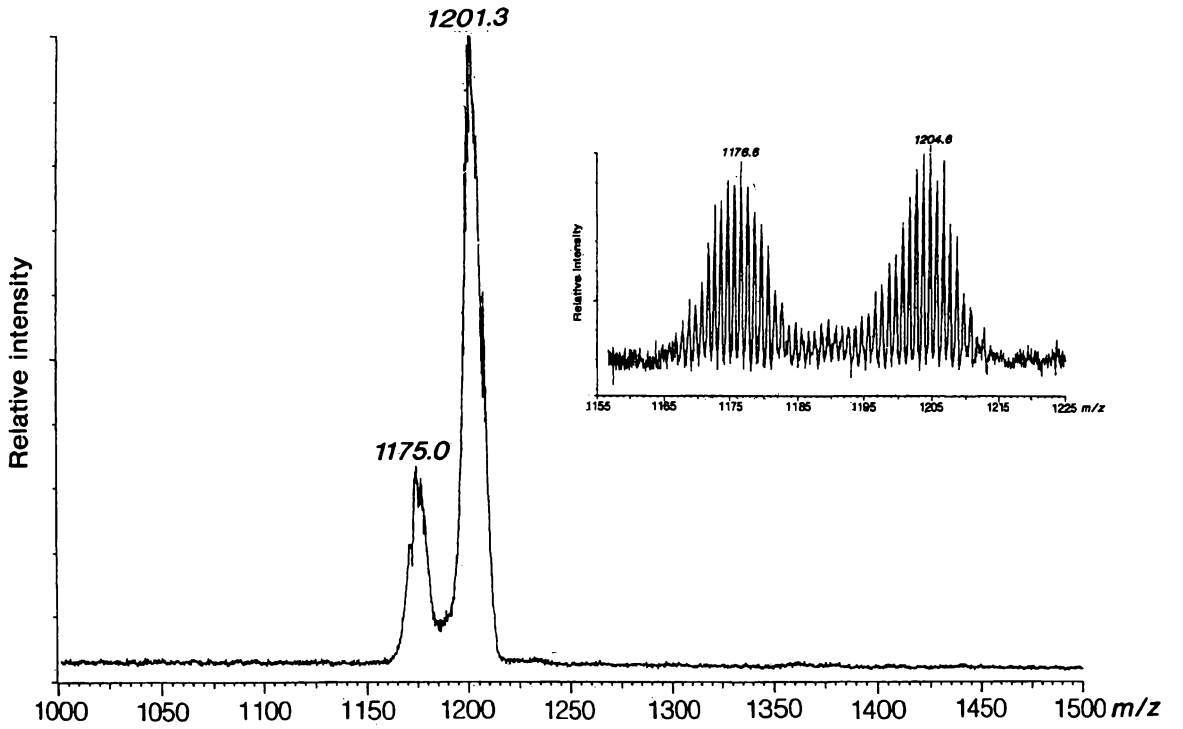

Figure 4.3: ESMS spectrum for **31**, with the inset showing a high resolution mass spectrum of the same compound. Assignment for this compound is: *m/z* 1203.3 $[M + MeO]^-$, 1175.0 $[M + MeO - CO]^-$.

Compound **30** shows two peaks, the larger one corresponding to $[M + MeO]^-$, and the smaller one to $[M - H]^-$ (Figure 4.2). The first peak is presumably produced by the expected methoxide addition, while the second results from removal of one of the bridging hydrides in the molecule. Compound **31** also shows two peaks under the conditions used, the first corresponding to the methoxide addition adduct, and the second corresponding to the subsequent loss of a carbonyl group (Figure 4.3).

4.2.5 X-Ray Crystal Structure Determinations for Compounds $FcCH_2PH_2$ **24**, $Mo(CO)_5(FcCH_2PH_2)$ **27**, $Mo(CO)_4(FcCH_2PH_2)_2$ **28**

Crystallographic confirmation of the structure of **24** was considered important in establishing beyond all doubt that this air-stable compound was indeed a primary phosphine. Similarly the structures of compounds **27** and **28** were desirable in order to help confirm normal coordinating behaviour of the ligand.

The structure of **24** is shown in Figure 4.4 along with selected bond lengths and angles. The gross morphology is typical of other structures discussed in Chapter 2, with the phosphorus atom pointing away from the ferrocene fragment and the Cp rings in an eclipsed formation. No notable intermolecular interactions were observed. It should be noted that the P-H hydrogen atoms were located as peaks in the difference map, but are not in ideal positions for tetrahedral geometry about the phosphorus atom. They have been included for clarity, but probably do not represent the true hydrogen atom positions, which may well be highly disordered. However, the P-C bond length of 1.850(3) Å can be compared with data from other sources. This bond length is identical within experimental error to bond lengths both calculated (1.8574 Å)[49] and measured by electron diffraction (1.858 ± 0.003 Å)[50] for $MePH_2$. A search of the CSD[51] revealed only two other crystal structures reported for uncoordinated primary phosphines, these being for mesitylphosphine[33] and a (9-anthracenyl)phosphine dimer[52] (Scheme 4.12). The crystal structure of the previously mentioned compound $[Me_3N(CH_2)_2PH_2]I$ has also been determined[34]. The C-P bond lengths for these three compounds are 1.807(5) Å, 1.864(5) Å, and 1.89(3) Å respectively, so the same parameter for **24** lies within the values for these previously reported structures, as well as being very similar to P-C bond lengths for other compounds characterised in this thesis.

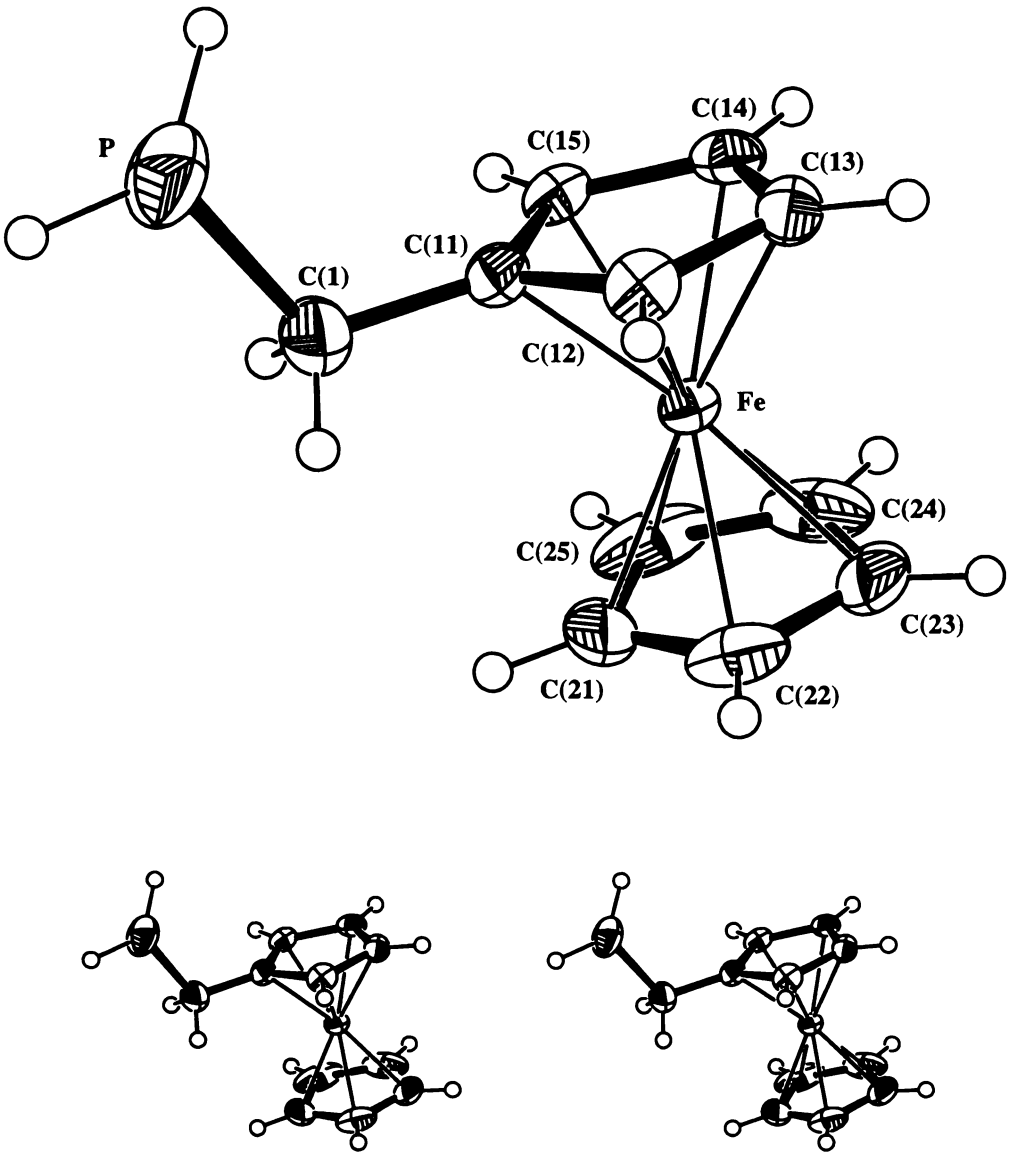

Figure 4.4: ORTEP X-ray crystal structure diagram of **24**, with stereo view. Selected bond lengths and angles: C(11)-C(1) =1.492(4) Å, C(1)-P = 1.850(3) Å, Fe-C range = 2.022(3)-2.042(2) Å, average = 2.035 Å; C(11)-C(1)-P = 113.7(2)°.

The structures for compound **27** and **28** are of course closely related. A search of the CSD revealed only one other structure reported with the general formula $Mo(CO)_{n-m}(RPH_2)_m$ (this structure being *fac*-$[Mo(CO)_3\{H_2PC(Me)=CH_2\}_3]$[53]): another structure has been reported very recently, this structure being *cis*-$Mo(CO)_4[Bu^nN\{(CH_2)_2\text{-}PH_2\}_2]$[54]. The paucity of known structures is surprising in view of the large number of molybdenum carbonyl

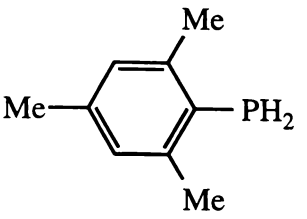

a)

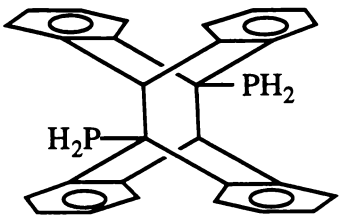

b)

Scheme 4.12: Two uncoordinated primary phosphines for which structures have previously been elucidated; a) mesitylphosphine, b) (9-anthracenyl)phosphine dimer.

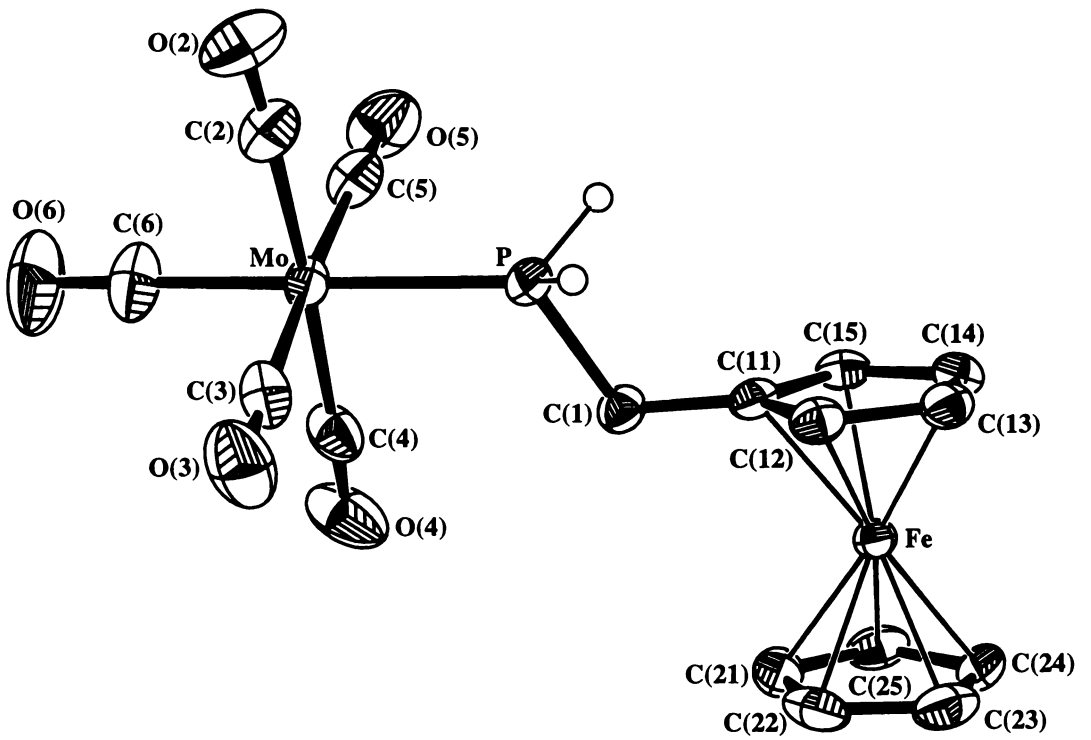

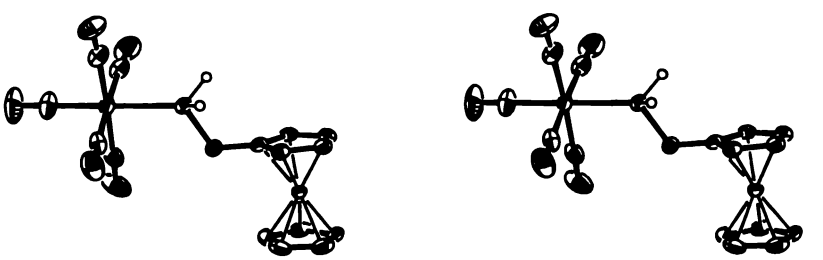

Figure 4.5: ORTEP X-ray crystal structure diagram of **27**, with stereo view.

phosphine derivatives which are known, including complexes containing primary phosphines with other ligands. It will be noted that the former compound is a tri-substituted compound, unlike **27** or **28**. No mono-substituted compound analogous to **27** has been reported. The structures of **27** and **28** are shown in Figures 4.5 and 4.6 respectively, and selected bond lengths and angles are given in Tables 4.4 and 4.5.

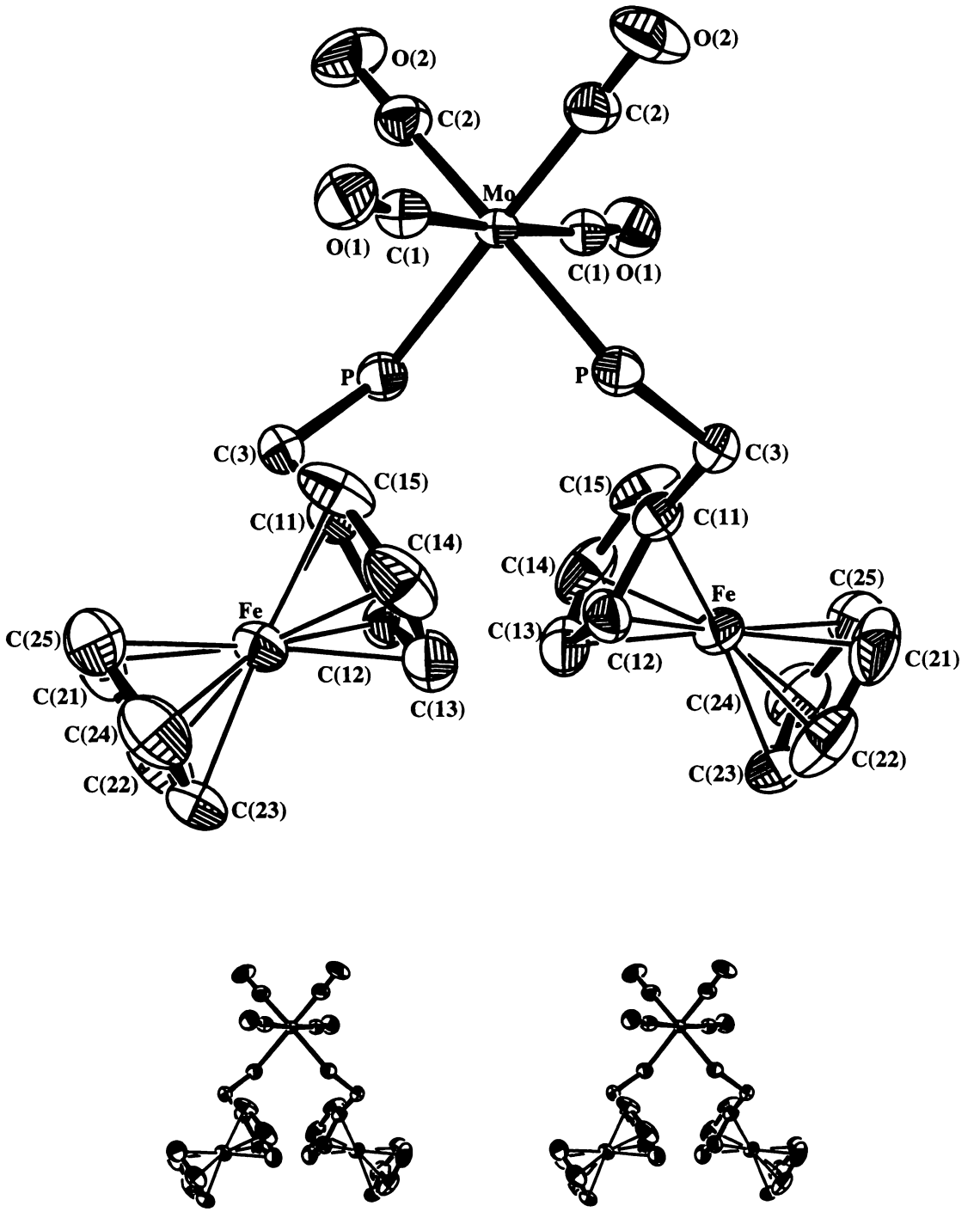

Figure 4.6: ORTEP X-ray crystal structure diagram of **28**, with stereo view.

Table 4.4: *Selected bond lengths (Å) and angles (°) for 27.*

P-Mo	2.5056(10)	P-H(2A)	1.250
C(1)-P	1.836(3)	P-H(2B)	1.257
C(11)-C(1)	1.494(4)	C(2)-O(2)	1.148(5)
Mo-C(2)	2.048(4)	C(3)-O(3)	1.143(5)
Mo-C(3)	2.019(4)	C(4)-O(4)	1.137(5)
Mo-C(4)	2.043(4)	C(5)-O(5)	1.140(6)
Mo-C(5)	2.063(4)	C(6)-O(6)	1.148(5)
Mo-C(6)	2.007(4)		
Cp rings range:	1.403(6)-1.432(5)	average:	1.417(5)
Mo-P-C(1)	118.84(11)	P-Mo-C(2)	91.39(12)
C(11)-C(1)-P	114.3(2)	P-Mo-C(3)	90.44(12)
C(1)-P-H(2A)	94.53	P-Mo-C(4)	90.09(13)
C(1)-P-H(2B)	98.05	P-Mo-C(5)	86.36(12)
Mo-P-H(2A)	123.69	P-Mo-C(6)	178.0(2)
Mo-P-H(2B)	123.51	C(6)-Mo-C(2)	89.3(2)
C(3)-Mo-C(5)	176.8(2)	C(6)-Mo-C(3)	91.5(2)
C(2)-Mo-C(4)	176.2(3)	C(6)-Mo-C(4)	89.4(2)
		C(6)-Mo-C(5)	91.7(2)

Compound **27** adopts the expected arrangement whereby steric interactions in the molecule are minimised by *anti* conformation of the ferrocenyl and $Mo(CO)_5$ groups about the C(1)-P bond [torsion angle C(11)-C(1)-P-Mo = 179.49(20)]. The C(1)-P-Mo-C(2) torsion angle is also around 180°. Together these factors mean there is an approximate mirror plane through the molecule in the plane C(11)-P-Mo. The replacement of a carbonyl group with the ligand **24**, which is not such a good back-bonding acceptor, is observed in a marginal lengthening of the C(6)-O(6) bond, since electron density is thus greater in the C-O anti-bonding orbitals *trans* to the phosphine. Geometry about the molybdenum is almost perfectly octahedral. No noteworthy intermolecular interactions were observed. Parameters for the phosphine hydrogens given in Table 4.5 show that these hydrogens form very acute angles with C(1), and wide angles with Mo, giving a ligand with a very small cone angle.

Table 4.5: *Selected bond lengths (Å) and angles (°) for* **28**.

P(1)-Mo(1)	2.518(2)	Mo(1)-C(1)	2.047(8)
P(1)-C(3)	1.843(7)	Mo(1)-C(2)	1.984(8)
C(3)-C(11)	1.508(10)	C(1)-O(1)	1.138(9)
		C(2)-O(2)	1.156(9)
Cp rings range:	1.36(2)-1.433(11)	average:	1.401(13)
C(11)-C(3)-P(1)	111.3(5)	P(1)-Mo(1)-C(1)	91.8(2)
C(3)-P(1)-Mo(1)	122.0(3)	P(1)-Mo(1)-C(2)	179.1(2)
Mo(1)-C(1)-O(1)	175.0(7)	P(1)-Mo(1)-P(1)*	89.37(9)
Mo(1)-C(2)-O(2)	177.9(7)	P(1)-Mo(1)-C(1)*	90.6(2)
C(1)-Mo(1)-C(1)*	176.6(4)	P(1)-Mo(1)-C(2)*	90.4(2)
C(2)-Mo(1)-C(2)*	89.8(5)		

* Denotes atom related by symmetry operation.

It can be seen from the crystal structure that the phosphine ligands in **28** lie in a *cis* configuration. The ferrocene units are not oriented away from each other, but instead lie quite close together. Unlike **27**, the orientation about the C-P bond is not *anti*, but is instead reasonably acute [torsion angle Mo(1)-P(1)-C(3)-C(11) = -65.17(59)°]. While the geometry around the molybdenum is octahedral, it is clear that the carbonyls C(1)-O(1) are bent away from the ferrocene groups. As with **27**, the bond length of the carbonyl *trans* to the phosphine [C(2)-O(2) = 1.156(9) Å] is slightly longer is the case for the *cis* carbonyl [C(1)-O(1) = 1.138(9) Å]. The P-H hydrogens could not be located in the difference map, and were instead included in calculated positions. The molecule lies on a crystallographic two-fold rotational axis.

P-Mo bond lengths for **27** and **28** are similar, and are essentially the same as the average P-Mo distance for the compounds *fac*-$[Mo(CO)_3\{H_2PC(Me)CH_2\}_3]$ and *cis*-$Mo(CO)_4[Bu^nN\{(CH_2)_2\text{-}PH_2\}_2]$ described earlier (P-Mo = 2.501(1) Å and 2.510, 2.515 Å

respectively). These distances lie within the normal range for Mo(0) phosphine complexes[55], which are usually somewhat shorter than distances in Mo(IV)[56] or Mo(V)[31a] species.

4.2.6 X-Ray Crystal Structure Determination for $Ru_3(CO)_9(\mu^2\text{-}H)_2(\mu^3\text{-}PCH_2Fc)$ **30**

The X-ray crystal structure obtained for compound **30** is depicted in Figures 4.7 and 4.8, and selected bond lengths and angles are listed in Table 4.6. The compound crystallised in the $P_{\bar{1}}$ space group with two independent molecules in the asymmetric unit. The major difference between the two molecules concerns the position of the two bridging hydrogens, which of course can also be viewed as a difference in orientation of the ferrocenyl group about the capping phosphorus-carbon bond; other atoms also show minor shifts in relative position. In many respects details of the structure are similar to those for the structure of $Ru_3(CO)_9(\mu^2\text{-}H)_2(PPh)$, in which the three crystallographically independent molecules reported differed only in orientation of the phenyl ring above the triangle of ruthenium atoms[46]. Bond lengths for compound **30** are very similar to those reported for $Ru_3(CO)_9(\mu^2\text{-}H)_2(PPh)$ and another previously reported analogous structure, $Ru_3(CO)_9(\mu^2\text{-}H)_2(PC_6H_4OCH_3)$[45d]. The unbridged Ru-Ru bond [Ru(1)-Ru(2) = 2.838 Å, Ru(2')-Ru(3') = 2.839 Å] is shorter than those Ru-Ru bonds supported by a bridging hydrogen [Ru(1)-Ru(3) = 2.931 Å, Ru(2)-Ru(3) = 2.927 Å, Ru(1')-Ru(2') = 2.946 Å, Ru(1')-Ru(3') = 2.938 Å]. This confirms the position of the bridging hydrogens which were in any case located as the four highest residual electron density peaks after inclusion of all other atoms. The distance from P to the Ru at the apex of the two bridging hydrogens [P(1)-Ru(3) = 2.315 Å, P(1')-Ru(1') = 2.317 Å] is greater than the other P-Ru distances [P(1)-Ru(2) = 2.293 Å, P(1)-Ru(1) = 2.283 Å, P(1')-Ru(2') = 2.284 Å, P(1')-Ru(3') = 2.278 Å]. The average Ru-H distance is 1.764 Å, and the average Ru-H-Ru bond angle 112.6°. In both independent molecules the ferrocene unit is situated such that it lies above an Ru-Ru bond bridged by hydrogen. Steric interactions with carbonyl groups may be the

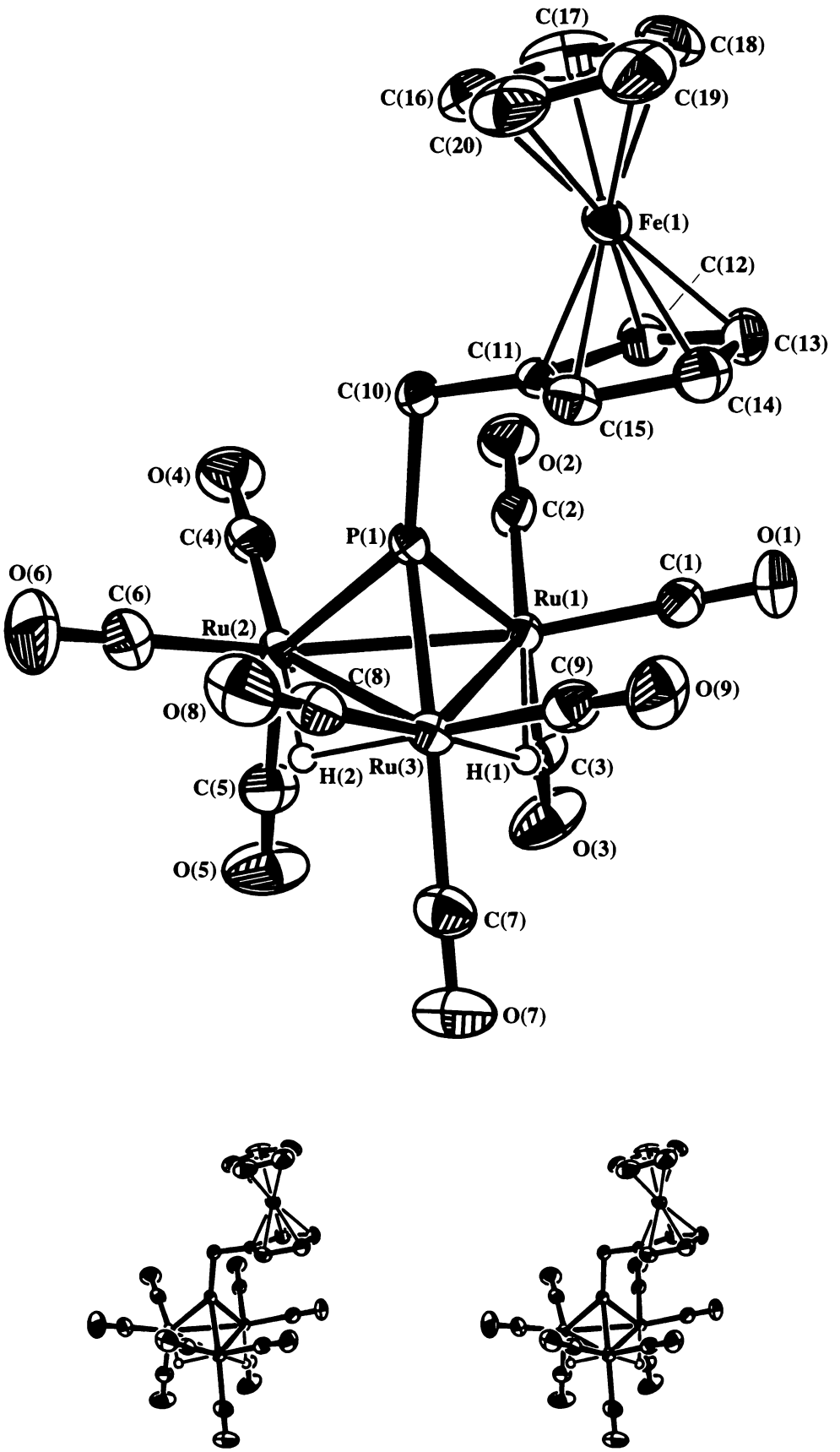

Figure 4.7: ORTEP X-ray crystal structure diagram of the first molecule of **30**, with stereo view.

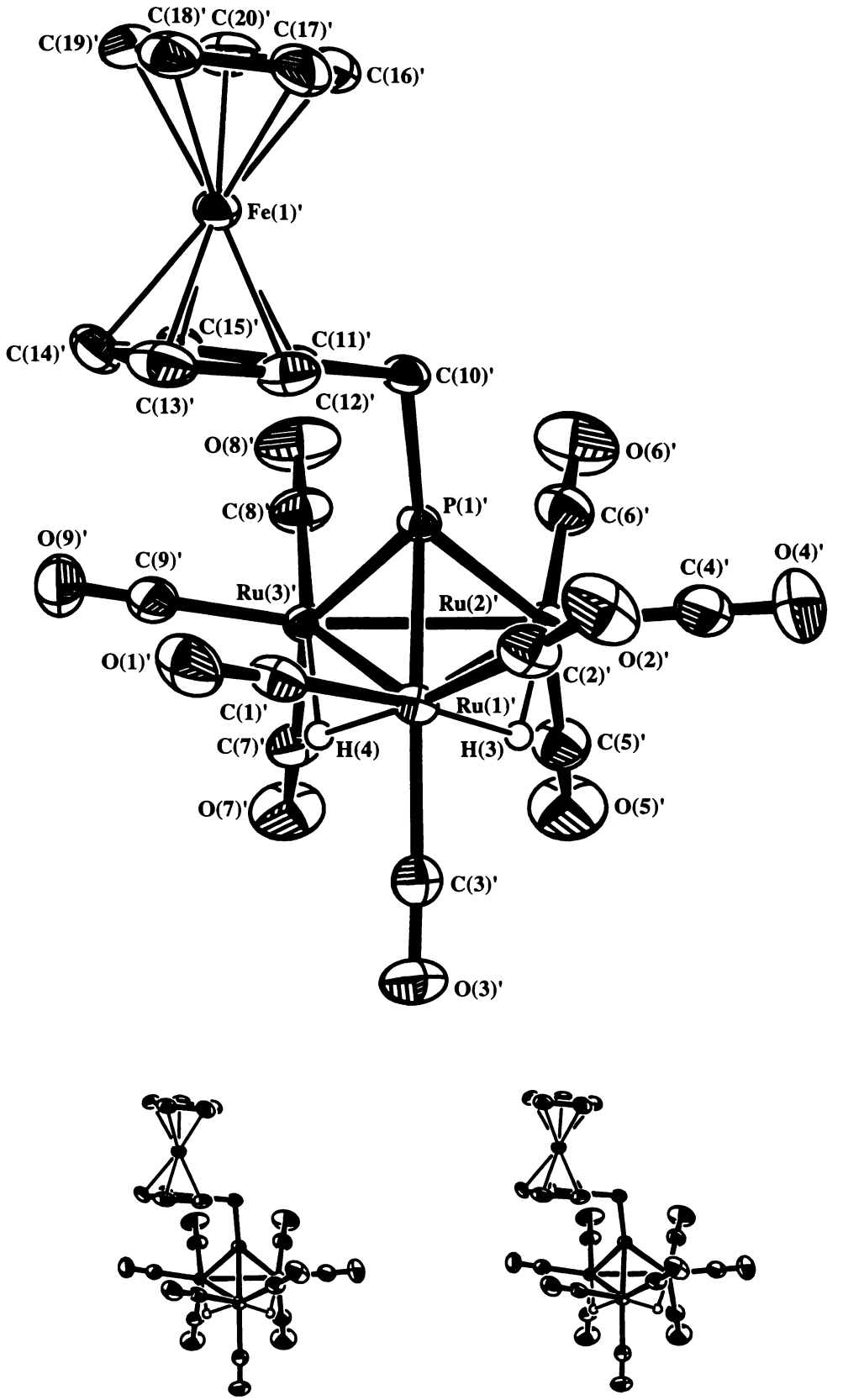

Figure 4.8: ORTEP X-ray crystal structure diagram of the second molecule of **30**, with stereo view.

Table 4.6: *Selected bond lengths (Å) and angles (°) for the X-ray crystal structure of* ***30****.*

Ru(1)-Ru(2)	2.8379(5)	Ru(1)'-Ru(2)'	2.9463(6)
Ru(1)-Ru(3)	2.9311(5)	Ru(1)'-Ru(3)'	2.9377(5)
Ru(2)-Ru(3)	2.9267(5)	Ru(2)'-Ru(3)'	2.8386(5)
Ru(1)-P(1)	2.2828(9)	Ru(1)'-P(1)'	2.3168(8)
Ru(2)-P(1)	2.2930(8)	Ru(2)'-P(1)'	2.2840(8)
Ru(3)-P(1)	2.3153(9)	Ru(3)'-P(1)'	2.2778(8)
Ru(1)-H(1)	1.838	Ru(1)'-H(3)	1.766
Ru(3)-H(1)	1.755	Ru(2)'-H(3)	1.734
Ru(2)-H(2)	1.711	Ru(1)'-H(4)	1.795
Ru(3)-H(2)	1.785	Ru(3)'-H(4)	1.727
av. Fe-C for substituted Cp ring	2.038(3)	av. Fe'-C' for substituted Cp ring	2.045(3)
av. Fe-C for unsubstituted Cp ring	2.031(4)	av. Fe'-C' for unsubstituted Cp ring	2.038(3)
Ru(1)-Ru(2)-Ru(3)	61.100(11)	Ru(1)'-Ru(2)'-Ru(3)'	61.004(9)
Ru(2)-Ru(1)-Ru(3)	60.944(9)	Ru(2)'-Ru(1)'-Ru(3)'	57.688
Ru(1)-Ru(3)-Ru(2)	57.957(11)	Ru(1)'-Ru(3)'-Ru(2)'	61.380
Ru(1)-P(1)-Ru(3)	79.20(3)	Ru(1)'-P(1)'-Ru(3)'	79.48(3)
Ru(1)-P(1)-Ru(2)	76.66(3)	Ru(1)'-P(1)'-Ru(2)'	79.64(3)
Ru(2)-P(1)-Ru(3)	78.85(3)	Ru(2)'-P(1)'-Ru(3)'	76.96(3)
Ru(1)-Ru(3)-P(1)	49.91(2)	Ru(1)'-Ru(3)'-P(1)'	50.84(2)
Ru(1)-Ru(2)-P(1)	51.51(2)	Ru(1)'-Ru(2)'-P(1)'	50.67(2)
Ru(2)-Ru(1)-P(1)	51.83(2)	Ru(2)'-Ru(1)'-P(1)'	49.69(2)
Ru(2)-Ru(3)-P(1)	50.24(2)	Ru(2)'-Ru(3)'-P(1)'	51.62(2)
Ru(3)-Ru(1)-P(1)	50.89(2)	Ru(3)'-Ru(1)'-P(1)'	49.67(2)
Ru(3)-Ru(2)-P(1)	50.91(2)	Ru(3)'-Ru(2)'-P(1)'	51.42(2)
Ru(1)-P(1)-C(10)	132.06(11)	Ru(1)'-P(1)'-C(10)'	127.30(11)
Ru(2)-P(1)-C(10)	138.82(10)	Ru(2)'-P(1)'-C(10)'	138.32(11)
Ru(3)-P(1)-C(10)	128.64(11)	Ru(3)'-P(1)'-C(10)'	132.97(11)
P(1)-C(10)-C(11)	109.5(2)	P(1)'-C(10)'-C(11)'	110.8(2)
Ru(1)-H(1)-Ru(3)	109.3	Ru(1)'-H(3)-Ru(2)'	114.6
Ru(2)-H(2)-Ru(3)	113.6	Ru(1)'-H(4)-Ru(3)'	113.0
Ru(1)-Ru(2)-C(4)	94.74(11)	Ru(1)'-Ru(2)'-C(4)'	103.28(12)
Ru(1)-Ru(3)-C(9)	97.91(10)	Ru(1)'-Ru(3)'-C(9)'	99.53(12)

Table 4.6 continued

Ru(2)-Ru(1)-C(2)	95.05(10)	Ru(2)'-Ru(1)'-C(2)'	95.06(11)
Ru(2)-Ru(3)-C(8)	97.01(11)	Ru(2)'-Ru(3)'-C(8)'	95.20(12)
Ru(3)-Ru(1)-C(1)	100.18(10)	Ru(3)'-Ru(1)'-C(1)'	95.69(11)
Ru(3)-Ru(2)-C(6)	103.96(12)	Ru(3)'-Ru(2)'-C(6)'	96.12(12)

factor that makes this a preferable conformation to one where the ferrocenyl group lies over the unbridged Ru-Ru bond, since the equatorial carbonyl groups flanking a H-bridged Ru-Ru bond are splayed wider than is the case for unsupported Ru-Ru bonds (e.g., bond angles: Ru(3)-Ru(2)-C(6) = 104.0°, Ru(1)-Ru(2)-C(4) = 94.7°). In both molecules the ferrocene cyclopentadienyl rings adopt an eclipsed conformation.

4.3 Experimental

4.3.1 Syntheses

For a description of general experimental and analytical practices, see Section 2.3.1. However, the following differences and additional information should be noted.

1. IR of carbonyl compounds were run only over the carbonyl stretch region, and usually as a solution, solvent used being noted in specific preparations.

2. In the case of carbonyl compounds electrospray mass spectra were run in negative ion mode, with the addition of small amounts of NaOMe to aid ion formation.

3. Where integration of ^{31}P-NMR spectra was required, acquisition delay was increased from 2 s to 3 s, and spectra were run in non-decoupled mode. Two-dimensional NMR experiments helped in the unambiguous assignment of spectra for compound **24**.

4. GC-MS was run using a HP 5890 Series 1 Gas Chromatograph coupled to a HP 3970 Series Mass Selective Detector. The column was a HP1 column containing cross-linked methylsilicone gum 24 m × 0.2 mm × 0.33 μm film thickness. The operating system was a Pascal Chemstation. A HP 7673A Autosampler was used to inject 1 μL of a dichloromethane solution of **24**, and temperature was increased from 80° to 280° C at a rate of 8° C min^{-1}, with 1.5 min hold time.

*4.3.1.1 Synthesis of $FcCH_2PH_2$ **24***

Compound **1** (4.003 g, 13.70 mmol) and sodium metabisulfite (2.605 g, 13.70 mmol) were added to a two-phase solvent system consisting of distilled H_2O (60 ml) and petroleum spirits (boiling range 60-80° C, 60 ml). The mixture was stirred and refluxed in air for three hr. After the mixture had cooled the aqueous layer was removed and the organic layer washed with distilled water (3 × 20 ml). The solvent was removed under vacuum to yield the crude product as an orange crystalline solid (1.913 g, 8.245 mmol, 60%). The crude product was slowly sublimed over one week (30° C, dynamic vacuum of 0.01 mm Hg) onto a water-cooled coldfinger, yielding the pure product as orange crystals (1.662 g, 7.161 mmol, 52%) which can be stored in air at ambient temperature. M.P. 44-46° C. Thirty-three days after preparation found: C, 56.87; H, 5.75%. Sixty-one days after preparation found: C, 57.07; H, 5.52%. Calculated for $C_{11}H_{13}FeP$: C, 56.94; H, 5.65%. IR (cm^{-1}): 3091 (w), 2903 (w), 2285 (P-H) (s), 1769 (w), 1640 (w), 1463 (m), 1409 (m), 1391 (m), 1232 (m), 1194 (w), 1103 (s), 1076 (m), 1037 (m), 1023 (s), 998 (m), 924 (m), 862 (m), 817 (s), 500 (s), 481 (s). ESMS {cone voltage = 20}: *m/z* 232.4 $[M]^+$. GC-MS: *m/z*: 232 $[M]^+$, 199 $[FcCH_2]^+$, 121 $[FeCp]^+$, 56 $[Fe]^+$. ^{31}P-{^{1}H} NMR ($CDCl_3$): δ -129.1 [t, ^{1}J(P-H) = 194 Hz]. ^{1}H NMR ($CDCl_3$): δ 2.62 ($FcC\underline{H}_2P$, s, 2H), 2.94 [$P\underline{H}_2$, d of t, ^{1}J(P-H) =

192 Hz, $^{3}J(H-H)$ = 8 Hz, 2H], 4.08 (C_A-H, t, J = 2 Hz, 2H), 4.12 (C_B-H, t, J = 2 Hz), 4.14 (C_D-H, s, 5H). $^{13}C-\{^{1}H\}$ NMR ($CDCl_3$): δ 14.58 (FcCH$_2$P, d, J = 9 Hz), 67.47 (C_A, s), 67.97 (C_B, s), 68.80 (C_D, s), 89.15 (C_C, d, J = 3 Hz).

4.3.1.2 Synthesis of $FcCH_2P(H)CH_2OH$ 25

Compound **1** (0.100 g, 0.342 mmol) and sodium metabisulfite (0.037 g, 0.195 mmol) were dissolved in a two-phase system consisting of water (10 ml) and diethyl ether (10 ml). The mixture was refluxed with stirring for three hr, at which point the organic phase was removed and washed with water (3 × 10 ml). Removal of the solvent under reduced pressure gave the product **25** as a yellow oil (0.070 g, 0.268 mmol, 78%). Found: C, 55.25; H, 5.97%. Calc., $C_{12}H_{15}FeOP$: C, 55.00; H, 5.77%. IR (cm^{-1}): 3927 (w), 3509 (m), 3331 (s, br), 3093 (s), 2906 (s), 2849 (m), 2284 (P-H) (s), 1763 (w), 1724 (w), 1642 (w), 1466 (s), 1412 (s), 1287 (w), 1234 (m), 1192 (m), 1105 (s), 1037 (s), 1021 (s), 1003 (s), 947 (m), 925 (s), 820 (s), 709 (w), 639 (w), 594 (w), 496 (s), 483 (s), 421 (m). ESMS {cone voltage = 20 V}: *m/z* 262.4 $[M]^+$. $^{31}P-\{^{1}H\}$ NMR: δ -51.4 [d, $^{1}J(P-H)$ = 204 Hz]. ^{1}H NMR ($CDCl_3$): δ 2.78-2.82 (FcCH$_2$P, m, 2H), 3.06-3.82 [PH, m, $^{1}J(P-H)$ = 204 Hz, 1H], 4.06-4.15 (Cp-H and PCH$_2$O, m, 11H). $^{13}C-\{^{1}H\}$ NMR ($CDCl_3$): δ 18.48 (FcCH$_2$P, d, J = 11 Hz), 57.92 (PCH$_2$O, d, J = 15 Hz), 67.71 (C_A, d, J = 7 Hz), 68.31-68.46 (C_B, m), 68.89 (C_D, s), 86.13 (C_c, d, J = 7 Hz).

4.3.1.3 Synthesis of $FcCH_2P(O)(OH)CH_2OH$ 26

Method A: Compound **1** (0.100 g, 0.344 mmol) and sodium metabisulfite (0.300 g, 1.58 mmol) were dissolved in a two-phase system of water (10 ml) and diethyl ether (10 ml). This mixture was refluxed overnight. After cooling, a small amount of NaOH was added to the reaction to ensure alkalinity, which was confirmed with litmus paper. The aqueous layer was then removed and acidified with *ca.* 2 mol L^{-1} HCl, and extracted with chloroform (2 × 20 ml). Removal of solvent under reduced pressure yields the crude product **26** as a yellow oil (0.024 g, 0.0813 mmol, 24%), which proved difficult to purify by crystallisation.

Method B: Compound **1** (0.200 g, 0.683 mmol) and sodium metabisulfite (0.601 g, 3.16 mmol) were dissolved in a two-phase system of water (10 ml) and diethyl ether (10 ml). This mixture was refluxed overnight. The aqueous layer was removed and dried under reduced pressure with heating to no more than *ca.* 35° C. The residue was purified by tlc, with neat MeOH as the eluting solvent. The product band was yellow and ran with an R_f of 0.35. Recrystallisation of this product was carried out from warm MeOH/diethyl ether cooled to *ca.* -30° C. The material thus obtained was then dissolved in water (10 ml) and a small amount of *ca.* 2 mol L^{-1} HCl added. This acid solution was then extracted with ethyl acetate (1 × 10 ml). Removal of solvent from the organic layer under reduced pressure gave **26** as a yellow crystalline solid in poor yield, but in purity suitable for elemental analysis (0.005 g, 0.0017 mmol, 2%). M. P. *ca.* 170° C (dec.). Found: C, 48.6; H, 4.7%. $C_{12}H_{15}FeO_3P$ requires: C, 49.0; H, 4.5%. IR (cm^{-1}): 3380 (m), 1637 (m), 1465 (w), 1403 (w), 1208 (w), 1151 (w), 1105 (m), 1069 (s), 1040 (s), 977 (s), 921 (w), 881 (w), 817 (m), 784 (w), 466 (w), 419 (w). ESMS {cone voltage = 20 V, negative ion mode}: *m/z* 293.3 $[M - H]^-$. $^{31}P-\{^1H\}$ NMR (D_2O): δ 37.4. ^1H NMR (D_2O): δ 3.00 ($FcC\underline{H}_2P$, d, J = 15 Hz, 2H), 3.72 ($PC\underline{H}_2O$, d, J = 6 Hz, 2H), 4.40 (C_A-H, unres. t, 2H), 4.45 (C_D-H, s, 5H), 4.50 (C_B-H, unres. t, 2H). $^{13}C-\{^1H\}$ NMR (D_2O): δ 29.94 ($Fc\underline{C}H_2P$, d, J = 86 Hz), 58.88 ($P\underline{C}H_2O$, d, J = 108 Hz), 68.04 (C_A, s), 69.39 (C_D, s), 69.76 (C_B, s), 81.17 (C_C, s).

4.3.1.4 Synthesis of $Mo(CO)_5(FcCH_2PH_2)$ 27

Compound **24** (0.100 g, 0.430 mmol) and $Mo(CO)_6$ (1.546 g, 5.857 mmol) were dissolved in dry, oxygen-free THF and placed under nitrogen. The solution was exposed to UV light and stirred for three hours. Solvent was then removed and the residue heated to 30° C for several days under dynamic vacuum until all excess $Mo(CO)_6$ had sublimed onto a coldfinger. The product was then dissolved in dry, oxygen-free dichloromethane and filtered to remove Mo degradation products. Removal of the solvent under reduced pressure gave the product **27** as a yellow powder (0.191 g, 0.407 mmol, 95%). Crystals suitable for an X-ray crystal structure analysis were obtained by cooling of a hot methanolic solution to *ca.* -30° C, although most of the compound in solution decomposed due to exposure to

oxygen. M.P. 123-127° C. Found: C, 41.7; H, 2.7%. $C_{16}H_{13}FeMoO_5P$ requires: C, 41.1; H, 2.8%. IR (cm^{-1}) (petroleum spirits): 2077 (w), 1989 (m), 1955 (s), 1917 (w). ESMS {cone voltage = 20 V}: *m/z* 468.6 $[M - H]^-$, 440.5 $[M - H - CO]^-$. $^{31}P-\{^1H\}$ NMR ($CDCl_3$): δ -63.2 [d, $^1J(P-H)$ = 315 Hz]. ^1H NMR ($CDCl_3$): δ 2.92 ($FcC\underline{H}_2P$, d × t, J = 7 Hz, J = 4 Hz, 2H), 4.12-4.15 (Cp-H, m, 9H), 4.36 [$P\underline{H}_2$, d × t, $^1J(P-H)$ = 320 Hz, $^3J(H-H)$ = 7 Hz, 2H]. $^{13}C-\{^1H\}$ NMR ($CDCl_3$): δ 23.04 ($Fc\underline{C}H_2P$, d, J = 23 Hz), 68.12 (C_B, d, J = 2 Hz), 68.31 (C_A, s), 68.99 (C_D, s), 85.02 (C_C, s), 203.94, 204.76 and 204.88 (CO, 3 × s).

4.3.1.5 Synthesis of $Mo(CO)_4(FcCH_2PH_2)_2$ 28

Compound **24** (0.146 g, 0.627 mmol), and $Mo(CO)_6$ (0.118 g, 0.446 mmol) were dissolved in decalin (10 ml) and a small quantity of petroleum spirits (0.5 ml). The solution was purged and placed under nitrogen, before heating at 100° C for 15 hr. As the solution cooled orange crystals of **28** were formed, which were removed by filtration. Partial evaporation of the supernatant under nitrogen over several days allowed collection of more crystals, giving the overall final yield of **28** (0.0305 g, 0.0454 mmol, 20.3%). The crystals proved suitable for X-ray crystal structure elucidation and other forms of analysis, but the presence of decomposition products which were difficult to separate from the desirable crystals made a sound elemental analysis unobtainable. M.P. 141-145° C. Found: C, 48.0; H, 4.1%. $C_{26}H_{26}Fe_2MoO_4P_2$ requires: C, 46.5; H, 3.9%. IR (cm^{-1}): 2074 (w), 2020 (s), 1995 (w), 1945 (s), 1913 (s), 1873 (s). ESMS {cone voltage = 20 V}: *m/z* 672.2 $[M - H]^-$, 467.1 $[M - 3CO - FeCp]^-$. $^{31}P-\{^1H\}$ NMR ($CDCl_3$): δ -55.9 [t, $^1J(P-H)$ = 308 Hz]. ^1H NMR ($CDCl_3$): δ 2.79-2.85 [$FcC\underline{H}_2P$, d × t, $^2J(P-H)$ = 3 Hz, $^3J(H-H)$ = 7 Hz, 2H], 4.12-4.15 (Cp-H, m, 9H), 4.16 [$P\underline{H}_2$, d × t, $^1J(P-H)$ = 318 Hz, $^3J(H-H)$ = 7 Hz, 2H]. $^{13}C-\{^1H\}$ NMR ($CDCl_3$): δ 23.14 ($Fc\underline{C}H_2P$, s), 68.05 (C_A, s), 68.31 (C_B, s), 68.95 (C_D, s), 107.79 (C_C, s), 199.67 and 200.42 (CO, 2 × s).

4.3.1.6 Synthesis of $RuCl_2(\eta^6\text{-}C_{10}H_{14})(FcCH_2PH_2)$ 29

Compound **24** (0.060 g, 0.259 mmol) and $[RuCl_2(\eta^6\text{-}C_{10}H_{14})]_2$ (0.079 g, 0.130 mmol) were dissolved in dichloromethane and the solution purged and placed under nitrogen. The solution was refluxed for 20 min, before solvent was removed under reduced pressure to give the crude product in quantitative yield. Vapour diffusion recrystallisation from dichloromethane with pentane gave **29** as a brown powder (0.120 g, 0.222 mmol, 86%). M.P. 187-190° C (dec.). Found: C, 46.6; H, 5.1%. $C_{21}H_{27}Cl_2FePRu$ requires: C, 46.9; H, 5.1%. IR (cm^{-1}): 3445 (s), 3089 (w), 3037 (m), 2961 (s), 2921 (m), 2872 (w), 2361 (s), 2338 (m), 1652 (m), 1468 (m), 1459 (m), 1386 (m), 1240 (w), 1200 (w), 1122 (w), 1104 (m), 1071(m), 1059 (m), 1037 (m), 1022 (m), 1000 (m), 924 (m), 887 (s), 848 (w), 820 (s), 800 (m), 736 (w), 668 (w), 498 (s), 482 (s), 448 (m), 422 (m). ESMS {cone voltage = 60 V}: *m/z* 654.6 $[M + \mathbf{24} + CH_3CN - Cl - FeCp]^+$, 618.6 $[M + \mathbf{24} + CH_3CN - 2Cl - H - FeCp]^+$. $^{31}P\text{-}\{^1H\}$ NMR ($CDCl_3$): δ -27.7 [t, $^1J(P\text{-}H)$ = 359 Hz]. ^1H NMR ($CDCl_3$): δ 1.21 [$CH(C\underline{H}_3)_2$, d, J = 7 Hz, 6H], 2.16 ($ArC\underline{H}_3$, s, 3H), 2.72 [$C\underline{H}(CH_3)_2$, h, J = 7 Hz, 1H], 3.13 ($FcC\underline{H}_2P$, d × t, J = 9 Hz, J = 6 Hz, 2H), 4.14 ($C_D\text{-}\underline{H}$, s, 5H), 4.17 ($C_A\text{-}\underline{H}$, d, J = 2 Hz), 4.19 ($C_B\text{-}\underline{H}$, d, J = 2 Hz), 4.81 [$P\underline{H}_2$, d × t, $^1J(P\text{-}H)$ = 358 Hz, $^3J(H\text{-}H)$ = 6 Hz, 2H], 5.20 [$CH_3C(C\underline{H})_2$, d, J = 6 Hz, 2H], 5.33 [$Pr^iC(C\underline{H})_2$, d, J = 6 Hz, 2H]. $^{13}C\text{-}\{^1H\}$ NMR ($CDCl_3$): δ 18.55 ($Ar\underline{C}H_3$, s), 18.61 ($Fc\underline{C}H_2P$, d, J = 28 Hz), 22.31 [$CH(\underline{C}H_3)_2$, s], 30.91 [$\underline{C}H(CH_3)_2$, s], 68.24 (C_A, s), 68.54 (C_B, s), 69.14 (C_D, s), 83.91 (C_C, s), 85.74 [$CH_3C(\underline{C}H)_2$, d, J = 5 Hz], 85.99 [$Pr^iC(\underline{C}H)_2$, d, J = 3 Hz], 102.69 [$CH_3\underline{C}(CH)_2$, s], 105.90 [$(CH_3)_2CH\underline{C}(CH)_2$, s].

4.3.1.7 Reaction of 24 with $Ru_3(CO)_{12}$

Compound **24** (0.0500 g, 0.216 mmol) and $Ru_3(CO)_{12}$ (0.138 g, 0.216 mmol) were dissolved in cyclohexane (20 ml), purged, and refluxed under nitrogen for 75 min. After the solution had cooled solvent was removed under vacuum. The product mixture was applied to a tlc plate as a dichloromethane solution and eluted with 15% dichloromethane in 60°-80°

C petroleum spirits. The second yellow band at R_f 0.508 and a series of dark closely overlapping bands between the baseline and R_f 0.157 were both removed using MeOH and dried under vacuum to give crude yields of $Ru_3(CO)_9(\mu^2\text{-}H)_2(\mu^3\text{-}PCH_2Fc)$ **30** (0.0263 g, 0.0334 mmol, 15.5%) and $Ru_4(CO)_{11}(\mu^3\text{-}PCH_2Fc)_2$ **31** (0.0338 g, 0.0288 mmol, 13.4%). Orange block crystals of **30** suitable for elemental analysis and X-ray crystal structure analysis were obtained by slow evaporation of a B.P. 60°-80° C petroleum spirits solution at -30° C. Black feather-like crystals of **31** suitable for elemental analysis were obtained by recrystallisation from warm pentane/dichloromethane/ether.

Compound **30**: Found: C, 30.8; H, 1.9%. $C_{20}H_{13}FeO_9PRu_3$ requires: C, 30.5; H, 1.7%. For IR data see Table 4.3. ESMS see Figure 4.2. $^{31}P\text{-}\{^1H\}$ NMR ($CDCl_3$): δ 76.9 (s).

Compound **31**: Found: C, 34.3; H, 1.5%. $C_{33}H_{22}Fe_2O_{11}P_2Ru_4$ requires: C, 33.8; H, 1.9%. For IR data see Table 4.3. ESMS see Figure 4.3. $^{31}P\text{-}\{^1H\}$ NMR ($CDCl_3$): δ 193.0 (s).

4.3.2 X-Ray Crystal Structure Determinations for Compounds $FcCH_2PH_2$ **24**, $Mo(CO)_5(FcCH_2PH_2)$ **27** and $Mo(CO)_4(FcCH_2PH_2)_2$ **28**

Crystals for structural determinations were obtained according to the methods outlined in Section 4.3.1. Crystal data for the three structures are given in Table 4.7. In the case of compounds **24** and **28** raw data were corrected for absorption based on a series of ψ scans.

For **27** data collection nominally covered over a hemisphere of reciprocal space, by a combination of three sets of exposures; each set had a different ϕ angle for the crystal and each exposure covered 0.3° in ω. The crystal to detector distance was 5.0 cm. This data set was corrected empirically for absorption using SADABS[57].

Table 4.7: *Crystallographic data for compounds 24, 27 and 28.*

	24	**27**	**28**
Empirical formula	$C_{11}H_{13}FeP$	$C_{16}H_{13}FeMoO_5P$	$C_{26}H_{26}Fe_2MoO_4P_2$
M_r	232.04	468.02	672.05
space group	$P2_1/c$	$P2_1$	C2/c
crystal system	monoclinic	monoclinic	monoclinic
a (Å)	13.7111(9)	7.48160(10)	20.626(3)
b (Å)	7.5225(5)	10.44120(10)	10.426(2)
c (Å)	10.5662	11.53050(10)	12.3240(10)
α (°)	90	90	90
β (°)	107.448(5)	96.7800(10)	90.950(10)
γ (°)	90	90	90
V (Å^3)	1039.7(1)	894.43(2)	2649.9(7)
density (g.cm^{-3})	1.482	1.738	1.685
Z	4	2	4
F(000)	480	464	1352
μ(Mo-K_α) (mm^{-1})	1.29	1.62	1.70
temperature (°C)	-105	-70	-105
crystal size (mm)	0.52 × 0.44 × 0.24	0.28 × 0.20 × 0.08	0.38 × 0.30 × .014
θ range	3.11° < θ < 30.00°	1.78° < θ < 28.27°	2.19° < θ < 26.99°
total reflections	3406	5604	3147
unique reflections	3032	2093	2899
R_{int}	0.0279	0.0265	0.0265
T_{min}	0.408	0.755	0.525
T_{max}	0.560	0.908	0.612
R_1 ($I > 2\sigma(I)$)	0.0411	0.0213	0.0621
wR_2 (all data)	0.1235[⊗]	0.0476[⊕]	0.1495[⌀]
GOF	1.032	1.037	1.067
e$^-$ density max (e.Å^{-3})	0.639	0.293	1.025
e$^-$ density min (e.Å^{-3})	-0.454	-0.403	-0.476
diffractometer	Nicolet R3	Siemens SMART CCD	Siemens P4
solution and refinement programmes	SHELXS-86[58], SHELXL-93[59]	SHELXS-86, SHELXL-93	SHELXS-86, SHELXL-93

[⊗] $w = [\sigma^2(F_o^2) + (0.0525P)^2 + 0.81P]^{-1}$ where $P = [\max(F_o^2, 0) + 2F_c^2]/3$. [⊕] $w = [\sigma^2(F_o^2) + (0.0229P)^2 + 0.00P]^{-1}$ where $P + [\text{Max}(F_o^2) + 2F_c^2]/3$. [⌀] $w = [\sigma^2(F_o^2) + (0.0570P)^2 + 1.31P]^{-1}$ where $P = [\text{Max}(F_o^2, 0) + 2F_c^2]/3$.

Structures were solved by direct methods and developed routinely. Full-matrix least-squares refinement was based on F^2, with all non-hydrogen atoms anisotropic and with hydrogen atoms (except for P-H hydrogens) included in calculated positions with isotropic temperature factors 1.2 times that of the U_{iso} of the atom to which they are bonded. For both **24** and **27** a penultimate electron density map showed two peaks which could be assigned to the H-atoms on the P, although the validity of this assignment was dubious in the case of **24**. These were included in fixed positions in the final refinement cycles. These hydrogen atoms could not be located in the case of **28**, and so were included in calculated positions. Diagrams were drawn using ORTEP 3[60].

4.3.3 X-Ray Crystal Structure Determination for $Ru_3(CO)_9(\mu^2\text{-}H)_2(\mu^3\text{-}PCH_2Fc)$ **30**

Crystallographic data for **30**: Crystals were obtained by the method outlined in Section 4.3.1.7, and data collected using a Siemens P4 Diffractometer. $C_{20}H_{13}FeO_9PRu_3$, M_r = 787.33; triclinic, space group $P\bar{1}$, a = 9.961(1) Å, b = 15.506(3) Å, c = 16.496(2) Å, α = 83.96(1)°, β = 88.72(1)°, γ = 80.79(1)°, V = 2501.0(6) Å^3, density = 2.091 g.cm^{-3} for Z = 4, F(000) = 1512, λ = 0.71073 Å, T = -73° C, crystal size = 0.70 × 0.62 × 0.56 mm. A total of 9576 reflections were collected using ω scans with 2.52° < θ < 25.00°. Of these 8809 were unique (R_{int} = 0.0072 after absorption correction applied, based on ψ-scans, $T_{max,min}$ 0.728, 0.842). Structures were solved by direct methods and developed routinely. Full-matrix least-squares refinement was based on F^2, with all non-hydrogen atoms anisotropic. Hydrogen atoms were included in calculated positions with isotropic temperature factors 1.2 times that of the U_{iso} of the atom to which they are bonded, except for hydride hydrogens, which were located in the difference map and refined in a riding model. The refinement converged at R_1 = 0.0220 [for 8012 reflections with (I) > 2σ(I)] and wR_2 = 0.0493 (all data) {w = [$\sigma^2(F_o^2)$ + (0.0195P)^2 + 3.5167P]$^{-1}$ where P = (F_o^2 + 2F_c^2)/3}; final GOF 1.079. The final difference map showed no peak greater than

0.480 e.Å^{-3} and no hole greater than -0.375 e.Å^{-3}. Programmes used for solution and refinement were SHELXTL-PC[61] and SHELXL-93[59]. Structure illustrations were drawn using ORTEP 3[60].

4.4 References

1 L. Maier, *Prog. Inorg. Chem.*, 1963, **5**, 27. L. Maier, *Primary, Secondary, and Tertiary Phosphines*, in *Organic Phosphorus Compounds*, G. M. Kosolapoff, L. Maier (Ed.), 1972, Wiley-Interscience, New York, V. **1**, p. 11, 26.

2 W. Levason, *Phosphine Complexes of Transition Metals*, in *The Chemistry of Organophosphorus Compounds*, F. R. Hartley (Ed.), 1990, John Wiley & Sons Ltd., New York, V. **1**, p. 577. See also for example: a) I. V. Kourkine, M. D. Sargent, D. S. Glueck, *Organometallics*, 1998, **17**, 125. b) D. K. Wicht, I. V. Kourkine, B. M. Lew, J. M. Nthenge, D. S. Glueck, *J. Am. Chem. Soc.*, 1997, **119**, 5039. c) H.-C. Böttcher, M. Graf, K. Merzweiler, C. Bruhn, *Polyhedron*, 1997, **16**, 3253. d) R. L. Wells, H. Rahbarnoohi, P. B. Glaser, *Organometallics*, 1996, **15**, 3204.

3 A. H. Cowley, J. E. Kilduff, T. H. Newman, M. Pakulski, *J. Am. Chem. Soc.*, 1982, **104**, 5820.

4 E. P. O. Fuchs, M. Hermesdorf, W. Schnurr, W. Rösch, H. Heydt, M. Regitz, P. Binger, *J. Organomet. Chem.*, 1988, **338**, 329. H. Eshtiagh-Hosseini, H. W. Kroto, J. F. Nixon, S. Brownstein, J. R. Morton, K. F. Preston, *J. Chem. Soc., Chem. Comm.*, 1979, 653. H. W. Kroto, J. F. Nixon, N. P. C. Simmons, N. P. C. Westwood, *J. Am. Chem. Soc.*, 1978, **100**, 446.

5 F. Bitterer, O. Herd, A. Hessler, M. Kuhnel, K. Rettig, O. Stelzer, W. S. Sheldrick, S. Nagel, N. Rösch, *Inorg. Chem.*, 1996, **35**, 4103.

6 A. Bader, T. Nullmeyers, M. Pabel, G. Salem, A. C. Willis, S. B. Wild, *Inorg. Chem.*, 1995, **34**, 384.

7 R. S. Edmundson, *Dictionary of Organophosphorus Compounds*, 1988, Chapman and Hall Ltd., London; e.g., $MePH_2$ (M-00277, p. 570), $EtPH_2$ (E-00123, p. 418).

8 H. R. Hays, D. J. Peterson, *Tertiary Phosphine Oxides*, in *Organic Phosphorus Compounds*, G. M. Kosolapoff, L. Maier (Ed.), 1972, Wiley-Interscience, New York, p. 345.

9 S. A. Buckler, M. Epstein, *J. Am. Chem. Soc.*, 1960, **82**, 2076. M. M. Rauhut, H. A. Currier, *J. Org. Chem.*, 1961, **26**, 4626. M. M. Rauhut, I. Hechenbleikner, H. A. Currier, V. P. Wystrach, *J. Am. Chem. Soc.*, 1958, **80**, 6690.

10 a) W. McFarlane, C. T. Regius, *Polyhedron*, 1997, **16**, 1855. b) J. R. Goerlich, R. Schmutzler, *Z. anorg. allg. Chem.*, 1994, **620**, 898. c) N. Yoshifuji, K. Shibayama, K. Toyota, N. Inamoto, *Tetrahedron Lett.*, 1983, **24**, 4227.

11 For example: K. Bourumeau, A.-C. Gaumont, J.-M. Denis, *Tetrahedron Lett.*, 1997, **38**, 1923. D. C. Bradley, I. S. Harding, A. D. Keefe, M. Motevalli, D. H. Zheng, *J. Chem. Soc., Dalton Trans.*, 1996, 3931. A. Bader, M. Pabel, A. C. Willis, S. B. Wild, *Inorg. Chem.*, 1996, **35**, 3874.

12 H. B. Kagan, P. Diter, A. Gref, D. Guillaneux, A. Masson-Szymczak, F. Rebiere, O. Riant, O. Samuel, S. Taudien, *Pure & Appl. Chem.*, 1996, **68**, 29.

13 Synthesis of original DIOP ligand: T. P. Dang, H. B. Kagan, *J. Am. Chem. Soc.*, 1972, **94**, 6429.

14 M. J. Burk, M. F. Gross, *Tetrahedron Lett.*, 1994, **35**, 9363.

15 P. Barbaro, C. Bianchini, A. Togni, *Organometallics*, 1997, **16**, 3004.

16 A. W. Frank, D. J. Daigle, S. L. Vail, *Textile Res. J.*, 1982, **52**, 678.

17 A. Hoffman, *J. Am. Chem. Res.*, 1921, **53**, 1684.

18 D. E. C. Corbridge, *Phosphorus, An Outline of its Chemistry, Biochemistry and Technology*, 1980, 2nd Ed., Elsevier, Amsterdam, p.179.

19 V. S. Reddy, K. V. Katti, C. L. Barnes, *J. Chem. Soc., Dalton Trans.*, 1996, 1301.

20 W. Vullo, *J. Org. Chem.*, 1968, **33**, 3665.

21 See Section 2.1 for references to hydroxymethylphosphines, e.g. those cited in Scheme 2.1 - these contain syntheses.

22 a) G. Muller, D. Sainz, *J. Organomet. Chem.*, 1995, **495**, 103. b) H. Hellmann, J. Bader, H. Birkner, O. Schumacher, *Ann.*, 1962, **659**, 49. c) P. A. T. Hoye, private communication.

23 R. Bartsch, S. Hietkamp, S. Morton, H. Peters, O. Stelzer, *Inorg. Chem.*, 1983, **22**, 3624.

24 J. W. Ellis, K. N. Harrison, P. A. T. Hoye, A. G. Orpen, P. G. Pringle, M. B. Smith, *Inorg. Chem.*, 1992, **31**, 3026.

25 J. H. Downing, V. Gee, P. G. Pringle, *Chem. Commun.*, 1997, 1527.

26 H. C. L. Abbenhuis, U. Burckhardt, V. Gramlich, C. Kollner, P. S. Pregosin, R. Salzmann, A. Togni, *Organometallics*, 1995, **14**, 759.

27 L. Higham, A. K. Powell, M. K. Whittlesey, S. Wocadlo, P. T. Wood, *Chem. Commun.*, 1998, 1107.

28 V. K. Issleib, H. Schmidt, C. Wirkner, *Z. anorg. allg. Chem.*, 1982, **488**, 75.

29 M. Yoshifuji, K. Shibayama, M. Inamoto, *J. Am. Chem. Soc.*, 1983, **105**, 2495.

30 D. S. Glueck, private communication.

31 a) R. Felsberg, S. Blaurock, S. Jelonek, T. Gelbrich, R. Kirmse, A. Voigt, E. Hey-Hawkins, *Chem. Ber./Recueil*, 1997, **130**, 807. b) G. W. Rabe, I. A. Guzei, A. L. Rheingold, *Inorg. Chem.*, 1997, **36**, 4914. c) M.-A. David, D. K. Wicht, D. S. Glueck, G. P. A. Yap, L. M. Liable-Sands, A. L. Rheingold, *Organometallics*, 1997, **16**, 4768. d) D. J. Brauer, F. Bitterer, F. Dörrenbach, G. Hessler, O. Stelzer, C. Krüger, F. Lutz, *Z. Naturforsch.*, 1996, **51b**, 1183. e) H. Schmidbaur, G. Weidenhiller, O. Steigelmann, G. Müller, *Chem. Ber.*, 1990, **123**, 285. Supermesityl-containing secondary phosphines: D. K. Wicht, S. N. Paisner, B. M. Lew, D. S. Glueck, G. P. A. Yap, L. M. Liable-Sands, A. L. Rheingold, C. M. Haar, S. P. Nolan, *Organometallics*, 1998, **17**, 652. I. V. Kourkine, M. D. Sargent, D. S. Glueck, *Organometallics*, 1998, **17**, 125.

32 I. V. Kourkine, D. S. Glueck, *Inorg. Chem.*, 1997, **36**, 5160. S. V. Maslennikov, D. S. Glueck, G. P. A. Yap, A. L. Rheingold, *Organometallics*, 1996, **15**, 2483. I. V. Kourkine, S. V. Maslennikov, R. Ditchfield, D. S. Glueck, G. P. A. Yap, L. M. Liable-Sands, A. L. Rheingold, *Inorg. Chem.*, 1996, **35**, 6708.

33 R. A. Bartlett, M. M. Olmstead, P. P. Power, G. A. Sigel, *Inorg. Chem.*, 1987, **26**, 1941.

34 D. J. Brauer, J. Fischer, S. Kucken, K. P. Langhans, O. Stelzer, N. Weferling, *Z. Naturforsch.*, 1994, **49b**, 1511.

35 See for example: a) W. Levason, *Phosphine Complexes of Transition Metals*, in *The Chemistry of Organophosphorus Compounds*, F. R. Hartley (Ed.), 1990, John Wiley & Sons Ltd, New York, Vol. **1**, p. 578. b) A. J. Deeming, S. Doherty, N. I. Powell, *Inorg. Chim. Acta*, 1992, **198-200**, 469. c) O. bin Shawkataly, T. Saminathan, K. Muniswaran, H.-K. Fun, K. Sivakumar, *Acta Cryst.*, 1996, C**52**, 1352. d) J. Kalbitz, E. Leissring, H. Schmidt, *Z. anorg. allg. Chem.*, 1995, **621**, 1605. e) M. A. Beckett, *Identification of Stereochemical (Geometrical) Isomers of $[Mo(CO)_4(L)_2]$ by Infra-Red Spectroscopy*, in *Inorganic Experiments*, J. D. Woollins (Ed.), 1994, VCH, New York, p. 110. f) J. R. Goerlich, A. Fischer, P. G. Jones, R. Schmutzler, *Polyhedron*, 1993, **12**, 2279. g) B. R. Kimpton, W. McFarlane, A. S. Muir, P. G. Patel, J. L. Bookham, *Polyhedron*, 1993, **12**, 2525. h) J. A. Connor, E. M. Jones, G. K. McEwen, *J. Organomet. Chem.*, 1972, **43**, 357.

36 C. U. Pittman Jr., G. O. Evans, *J. Organomet. Chem.*, 1972, **43**, 361.

37 J. F. Van der Maelen Uria, S. Garcia-Granda, J. A. Cabeza, I. del Rio, *Acta Cryst.*, 1994, C**50**, 1064.

38 Y.-Y. Choi, W.-T. Wong, *J. Organomet. Chem.*, 1997, **542**, 121. C. J. McAdam, N. W. Duffy, B. H. Robinson, J. Simpson, *J. Organomet. Chem.*, 1997, **527**, 179. R. D. Pergola, C. Bandini, F. Demartin, E. Diana, L. Garlaschelli, P. L. Stanghellini, P. Zanello, *J. Chem. Soc., Dalton Trans.*, 1996, 747. E. Stein, F. Y. Fujiwara, *J. Organomet. Chem.*, 1996, **525**, 31. J. R. Galsworthy, C. E. Housecroft, A. L. Rheingold, *J. Chem. Soc., Dalton Trans.*, 1996, 2917. Z.-G. Fang, P. M. N. Low, S.-C. Ng, T. S. A. Hor, *J. Organomet. Chem.*, 1994, **483**, 17. T.-J. Kim, S.-C. Kwon, Y.-H. Kim, N. H. Heo, M. M. Teeter, A. Yamano, *J. Organomet. Chem.*, 1991, **426**, 71.

39 A. A. Koridze, V. I. Zdanovich, A. M. Sheloumov, V. Y. Lagunova, P. V. Petravskii, A. S. Peregudov, F. M. Dolgushin, A. I. Yanovsky, *Organometallics*, 1997, **16**, 2285. S. L. Ingham, B. F. G. Johnson, P. R. Raithby, K. J. Taylor, L. J. Yellowlees, *J. Chem. Soc., Dalton Trans.*, 1996, 3521. C. J. McAdam, N. W.

Duffy, B. H. Robinson, J. Simpson, *Organometallics*, 1996, **15**, 3935. L. P. Clarke, J. E. Davies, P. R. Raithby, G. P. Shields, *J. Chem. Soc., Dalton Trans.*, 1996, 4147.

40 W. Imhof, *J. Organomet. Chem.*, 1997, **541**, 109.

41 W.-Y. Wong, W.-T. Wong, *J. Chem. Soc., Dalton Trans.*, 1996, 3209.

42 a) T. C. Zheng, W. R. Cullen, S. J. Rettig, *Organometallics*, 1994, **13**, 3594. b) W. R. Cullen, S. J. Rettig, T. C. Zheng, *Organometallics*, 1992, **11**, 853. c) M. I. Bruce, P. A. Humphrey, O. bin Shawkataly, M. R. Snow, E. R. T. Tiekink, W. R. Cullen, *Organometallics*, 1990, **9**, 2910. d) W. R. Cullen, S. T. Chacon, M. I. Bruce, F. W. B. Einstein, R. H. Jones, *Organometallics*, 1988, **7**, 2273.

43 S. Onaka, H. Muto, Y. Katsukawa, S. Takagi, *J. Organomet. Chem.*, 1997, **543**, 241.

44 J. A. Cabeza, I. del Rio, V. Riera, S. Garcia-Granda, S. B. Sanni, *Organometallics*, 1997, **16**, 3914. H.-C. Böttcher, H. Thönnessen, P. G. Jones, R. Schmutzler, *J. Organomet. Chem.*, 1996, **520**, 15.

45 a) S.-L. Li, Z.-Z. Zhang, J. C. C. Chan, S. C. F. Au-Yeung, T. C. W. Mak, *J. Organomet. Chem.*, 1996, **522**, 155. b) G. Hessler, K. P. Langhans, O. Stelzer, W. S. Sheldrick, *J. Organomet. Chem.*, 1993, **452**, 55. c) K. Natarajan, O. Scheidsteger, G. Huttner, *J. Organomet. Chem.*, 1981, **221**, 301. d) K. Natarajan, L. Zsolnai, G. Huttner, *J. Organomet. Chem.*, 1981, **220**, 365.

46 F. Iwasaki, M. J. Mays, P. R. Raithby, P. L. Taylor, P. J. Wheatley, *J. Organomet. Chem.*, 1981, **213**, 185.

47 J. T. Jaeger, H. Vahrenkamp, *Organometallics*, 1988, **7**, 1746.

48 W. Henderson, J. S. McIndoe, B. K. Nicholson, P. J. Dyson, *Chem. Commun.*, 1996, 1183. W. Henderson, J. S. McIndoe, B. K. Nicholson, P. J. Dyson, *J. Chem. Soc., Dalton Trans.*, 1998, 519.

49 P. C. Fox, J. P. Bowen, N. L. Allinger, *J. Am. Chem. Soc.*, 1992, **114**, 8536.

50 L. S. Bartell, *J. Chem. Phys.*, 1960, **32**, 832.

51 April 1996 release, F. H. Allen, J. E. Davies, J. J. Galloy, O. Johnson, O. Kennard, C. F. Macrae, E. M. Mitchell, G. F. Mitchell, J. M. Smith, D. G. Watson, *J. Chem. Inf. Comput. Sci.*, 1991, **32**, 187.

52 J. Wesemann, P. G. Jones, D. Schomburg, L. Heuer, R. Schmutzler, *Chem. Ber.*, 1992, **125**, 2187.

53 P. G. Edwards, J. S. Fleming, S. S. Liyanage, S. J. Coles, M. B. Hursthouse, *J. Chem. Soc., Dalton Trans.*, 1996, 1801.

54 A. Hessler, S. Kucken, O. Stelzer, W. S. Sheldrick, *J. Organomet. Chem.*, 1998, **553**, 39.

55 For example: D. L. DuBois, C. W. Eigenbrot Jr., A. Miedaner, J. C. Smart, *Organometallics*, 1986, **5**, 1405.

56 K. Starker, M. D. Curtis, *Inorg. Chem.*, 1985, **24**, 3006.

57 R. H. Blessing, *Acta Cryst.*, 1995, A**51**, 33.

58 G. M. Sheldrick, SHELXS-86, Program for solving crystal structures, University of Göttingen, 1986.

59 G. M. Sheldrick, SHELXL-93, Program for Refining Crystal Structures. University of Göttingen, 1993.

60 C. K. Johnson, M. N. Burnett, *ORTEP-III Version 1.0.2*. Windows 32-bit Version 1.0.β compiled by L. J. Farrugia, Dept. of Chemistry, University of Glasgow.

61 G. M. Sheldrick, SHELXTL-PC, Release 4.2, Seimens Analytical X-Ray Instruments, Madison, WI, 1991.

Chapter 5: Electrochemistry

5.1 Introduction

In Chapter 6 an investigation into the preparation of electroactive polymers based on compound **1** is presented. The work discussed in the present Chapter concerns the electrochemistry of many of the ferrocenyl-phosphorus compounds described in Chapters 2 and 4. An examination of the electrochemistry of these compounds was deemed important if an understanding of the electrochemical behaviour of the polymers described in the next Chapter was to be attainable.

5.1.1 Electrochemical Techniques and Theory

In this Section the various electrochemical techniques used in this investigation will be introduced, and electrochemical theory discussed where appropriate.

5.1.1.1 Cyclic Voltammetry

The technique of most importance to the present study is cyclic voltammetry, with the following discussion drawing on a number of introductory descriptions in the literature[1,2]. An understanding of the benefits of cyclic voltammetry as an electroanalytical technique can be seen by comparison with the more classical technique of polarography. Polarography is a technique which allows the measurement of thermodynamic parameters, such as the redox potential, for an electron transfer process taking place at an electrode. It has also long been used for quantitative detection of small amounts of electroactive substances, and is still a

widely used technique among analytical chemists. Cyclic voltammetry is also a technique which allows the determination of both thermodynamic parameters and quantitative analysis, though less reliably than polarography. However, cyclic voltammetry can also provide qualitative information concerning what is happening at the electrode surface - the kinetics and mechanisms of electron transfer. This is important, since electron transfer processes, whether heterogeneous or homogeneous, occur at a finite rate, and are often preceded and followed by chemical reactions.

Figure 5.1 depicts a typical solution cell for a cyclic voltammetric experiment. The essential elements of the equipment are: the working electrode (WE), reference electrode (RE) and auxiliary electrode (AE); the solution of analyte; a means by which to vary the potential between the WE and RE; a device for plotting current against potential at the WE. The function of these parts is outlined in the following discussion.

The WE can be made of any of a variety of conductive materials, although platinum and carbon are the most common. The hanging drop mercury electrode is sometimes used, since it has the advantage of a renewable electrode surface. However, mercury has a limited potential range. In addition, in most cases an electrode with a planar surface is preferred since this simplifies the theory on which various useful equations used in cyclic voltammetry are built. This WE is held stationary in a still solution of the analyte. Starting from some initial potential a linear potential ramp is applied to the WE, i.e., the potential at the electrode is varied linearly with time. Once a predetermined switching potential (E_λ) has been reached the potential ramp is immediately reversed and the experiment is typically completed once the initial potential has again been reached (Figure 5.2). Since the potential range being examined is usually never greater than *ca.* 4 V, and since the scan rate for the potential ramp is typically 20 to 1000 mV s^{-1}, the cyclic voltammetric experiment will usually take in the order of a few seconds to a few minutes to perform.

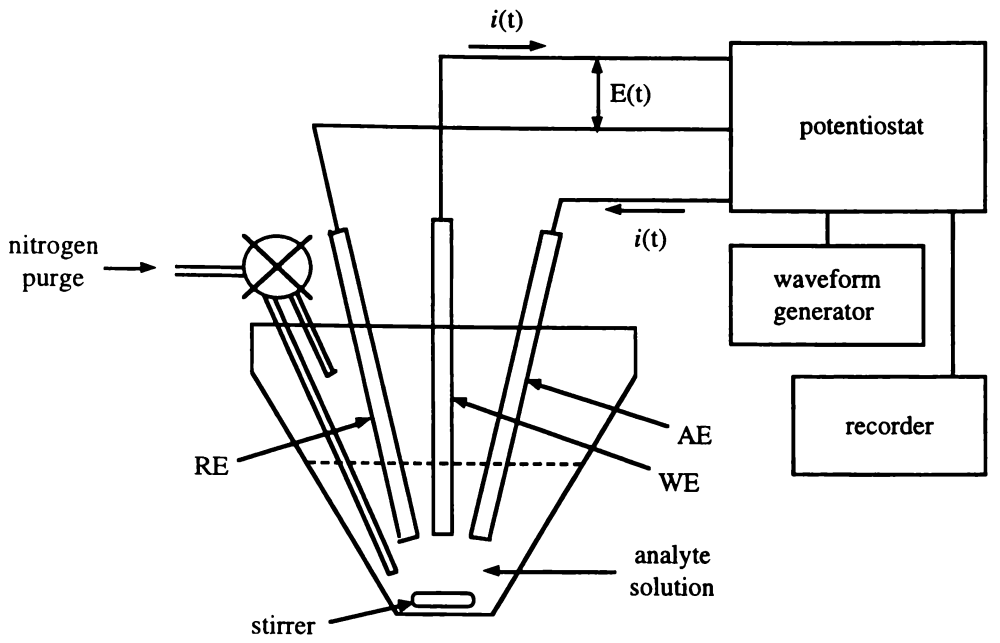

Figure 5.1: Diagram of a solution cell and associated equipment for use in cyclic voltammetry. AE = auxiliary electrode; RE = reference electrode; WE = working electrode; E(t) = applied potential at time t; i(t) = current at time t. Solution can be stirred while solubilising analyte or while purging, but is kept still during the experiment. The waveform generator is used to program the initial, switching and final potentials, along with scan rate, and the potentiostat generates the applied potential.

It is of course impossible to monitor absolute single electrode potentials and so the potential at the WE is measured with respect to an electrode such as the well-known saturated calomel electrode (SCE), this constituting the RE. The RE must provide a stable and reproducible basis for measurement of the potential at the WE. Because of high impedance little current flows through the RE; a third electrode is therefore needed to allow current to flow through the cell and the WE. This third electrode is usually just a simple piece of platinum or silver wire; the AE.

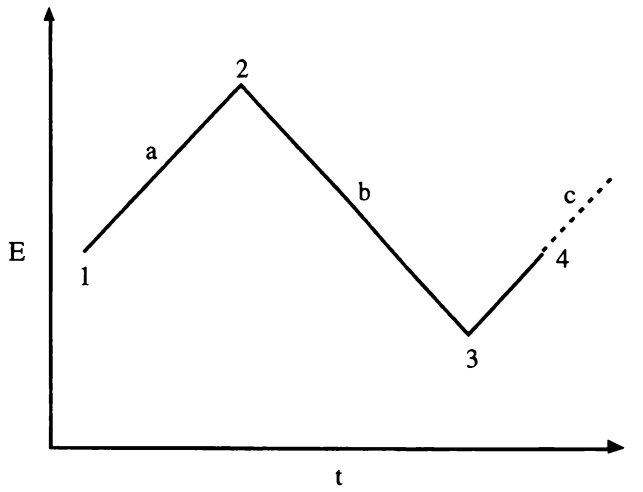

Figure 5.2: A graph of potential applied to the working electrode versus time during a cyclic voltammetric experiment. 1 = initial potential (E_i); 2 = first switching potential ($E_{\lambda 1}$); 3 = second switching potential ($E_{\lambda 2}$); 4 = final potential (E_f), which in this case is the same as E_i. The experiment could be continued for further cycles if desired (dashed line). a = first forward sweep, b = reverse sweep, c = second forward sweep.

The solution being tested can be made up in a variety of solvents, the limiting factor being that the solvent must be electrochemically stable and have sufficient conductivity under cyclic voltammetric conditions. Water, acetonitrile and dichloromethane are common choices. In an aprotic solvent such as acetonitrile it is usually desirable to have the solvent very dry in order to avoid the complication of reactive electrochemically-generated species reacting further with water. In all solvents cyclic voltammetry is usually carried out in the absence of oxygen, which can of course likewise be involved in the redox processes being studied if it is not excluded. The analyte being studied is typically present in concentrations of the order of 1-10 mmol L^{-1}. A supporting electrolyte is also always added to the solution, typically with a concentration of 0.1 mol L^{-1}. This is to ensure conductivity of the solution, and also to avoid mass transport of the analyte species to the working electrode because of electrostatic interactions. It is important to note that one of the central ideas underpinning the

theory behind cyclic voltammetry is that mass transport of analyte to and from the WE must be diffusion controlled. Therefore bulk flow of the solution and migration currents must both be avoided.

So what happens when the cyclic voltammetric experiment is carried out? Figure 5.3 shows the voltammogram obtained from a typical oxidation process, for instance that of ferrocene to ferrocenium. Starting at a potential well below the oxidation potential of the analyte, the

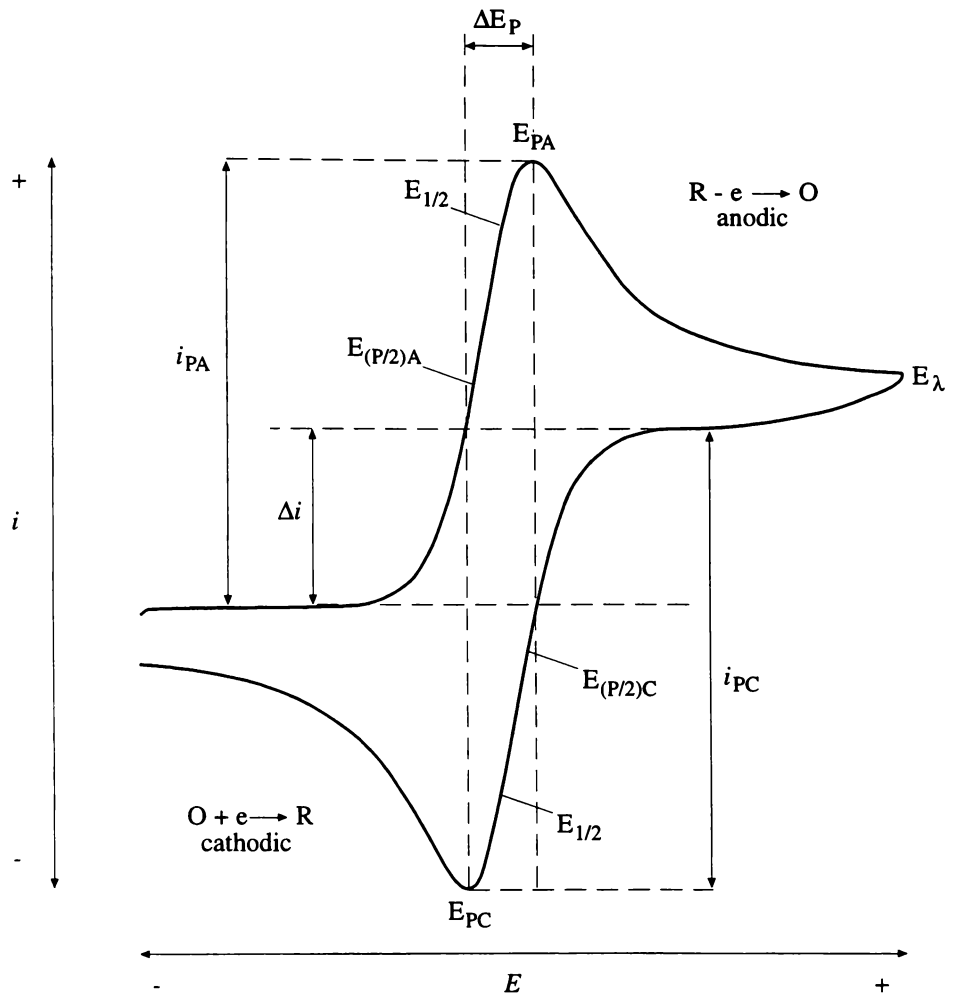

Figure 5.3: A cyclic voltammogram (CV) recorded for a typical redox process. $E_{1/2}$ = half-wave potential, $E_{(P/2)A}$ = anodic half-peak potential, $E_{(P/2)C}$ = cathodic half-peak potential, E_{PA} = anodic peak potential, E_{PC} = cathodic peak potential, $\Delta E_P = E_{PA} - E_{PC}$, E_λ = switching potential, i_{PA} = anodic peak current, i_{PC} = cathodic peak current, Δi = change in current.

potential at the working electrode is increased. At this point only nonfaradaic current can flow (i.e. there is no charge transfer across the electrode/solution interface). As the oxidation potential is approached, any analyte within close proximity of the WE is rapidly oxidised, leading to a surge of current. Current then tails off to a constant value which is controlled by the rate of diffusion of analyte to the WE. If the potential sweep is then reversed the analogous reduction process is similarly observed.

The positions and heights of the current peaks observed in a cyclic voltammogram (CV) can yield information about reversibility of the redox process, its formal potential, and the number of electrons transferred.

An electrode-based redox process is considered to be electrochemically (that is, thermodynamically) reversible if the rates of electron transfer for both reduction and oxidation are fast enough for thermodynamic equilibrium to be maintained at the electrode surface throughout the cyclic voltammetric experiment. Consider the electrochemically reversible reduction:

$$O + ne \rightleftharpoons R \qquad [1]$$

If the usually reasonable approximation is made that diffusion coefficients of O to the electrode and R away from the electrode are the same, then it can be shown that:

$$E_{1/2} = E_{(P/2)C} - 1.09(RT/nF)$$

$$= E_{(P/2)C} - 28.0/n \qquad \text{mV at } 25^\circ \text{ C} \qquad (1)$$

$$E_{1/2} = E_{PC} + 1.109(RT/nF)$$

$$= E_{PC} + 28.48/n \qquad \text{mV at } 25^\circ \text{ C} \qquad (2)$$

Where: $E_{1/2}$ = half-wave potential

$E_{(P/2)C}$ = half-peak potential (cathodic)

E_{PC} = peak potential (cathodic)

If the reverse reaction to mechanism [1] is considered, i.e. a reversible oxidation process, it can similarly be shown that:

$$E_{1/2} = E_{(P/2)A} + 28.0/n \qquad \text{mV at } 25^\circ \text{ C} \qquad (3)$$

$$E_{1/2} = E_{PA} - 28.48/n \qquad \text{mV at } 25^\circ \text{ C} \qquad (4)$$

Where: $E_{(P/2)A}$ = half-peak potential (anodic)

E_{PA} = peak potential (anodic)

The peak potential is simply the potential at which the highest current is recorded for the process (cathodic or anodic) under inspection. This maximum in current is called the peak current (i_P). The half-peak potential is the point at which current is half i_P. The half-wave potential falls about half-way between $E_{P/2}$ and E_P. Researchers are split in their preference for deriving the $E_{1/2}$ from either the $E_{P/2}$ or the E_P. $E_{1/2}$ is called the half-wave potential for reasons pertaining to measurement of the same parameter by polarographic techniques. Although not easy to measure directly on a CV, the $E_{1/2}$ value is important, since:

$$E_{1/2} = E^{\circ\prime} + (RT/nF)\ln[(D_R)^{1/2}/(D_O)^{1/2}] \qquad (5)$$

Where: $E^{\circ\prime}$ = formal redox potential

D_R = diffusion coefficient for R

D_O = diffusion coefficient for O

So that where the approximation is made that $D_R = D_O$:

$$E^{\circ\prime} = E_{1/2} \qquad \text{mV at } 25^\circ \text{ C} \qquad (6)$$

Thus CV data can be used in order to estimate the formal potential of the redox process. From a consideration of equations (2) and (4) it might be presumed that the cyclic

voltammetric peak potentials for the anodic and cathodic processes of a reversible process will lie 28.48/n mV either side of $E_{1/2}$. While the $E_{1/2}$ can indeed be read from the CV as the mid-point between the E_{PA} and E_{PC}, the difference between E_{PA} and E_{PC} (ΔE_P) is in actual fact not invariant but slightly dependant on E_λ, although it is generally close to 59/n mV. These ideas are expressed in equation (7). Note that a reversible electrode process can be conveniently recognised by its adherence to the rule stated in equation (7). Conversely, equation (7) can be used to assess the number of electrons being transferred in a reversible process.

$$\Delta E_P = E_{PA} - E_{PC} = 59/n \qquad \text{mV at } 25^\circ \text{ C} \qquad (7)$$

If the rate of electron transfer across the electrode surface is not fast enough to maintain reversibility as the potential is changed, it is apparent that movement of current will 'lag behind' the potential change in both directions of the cyclic voltammetric experiment. The result is that E_{PA} and E_{PC} will be spread further apart, i.e. ΔE_P becomes greater. Where no part of the cathodic and anodic CV peaks overlap on the potential axis, the redox process is termed electrochemically irreversible. If ΔE_P increases with increasing scan rate, the process is termed quasi-reversible. Theoretically, if scan rates could be made fast enough all apparently reversible electrode processes would of course become progressively quasi-reversible and then irreversible. The greater ΔE_P becomes, the less reliable becomes the mid-point between them as an estimate of E°' [since equation (5) only holds in the case of reversible behaviour].

Another characteristic of reversible cyclic voltammetric processes is that the value of i_P is diffusion-controlled and is characterised by the relationship:

$$i_P \propto v^{1/2} \qquad (8)$$

Where: v = scan rate

Finally, it should be noted that electrochemically reversible systems are characterised by equation (9). This means that i_P is related to the number of electrons involved in the redox process, and peak heights can be used to assess how many electrons are involved in the process by comparison to a known standard with a similar diffusion coefficient. Conversely, if the number of electrons involved in the process is known, the diffusion coefficient for the species can be calculated.

$$i_P = (2.69 \times 10^5)n^{3/2}AD_O^{1/2}v^{1/2}C_O \qquad \text{Amperes at } 25^\circ \text{ C} \qquad (9)$$

Where: A = surface area of the electrode (cm^2)

D_O ($cm^2\ s^{-1}$)

v ($V\ s^{-1}$)

C_O = concentration of O in bulk solution ($mol\ cm^{-3}$)

In electrochemical systems not only must electrochemical reversibility be considered, but also the degree of chemical reversibility. Consider the previously mentioned redox system [1] (page 190). If R is stable in solution, i_{PA} and i_{PC} will be equal. Such a system is regarded as chemically reversible under cyclic voltammetric conditions. Contrast this with reaction [2], where once formed, R reacts with a rate constant K to give X:

$$O + ne \rightleftharpoons R \xrightarrow{K} X \qquad [2]$$

If K is significant and a considerable amount of R is converted to X over the time scale of the cyclic voltammetric experiment, then i_P for the reverse sweep will be smaller than for the forward sweep. If K is large and conversion of R to X is essentially complete over the time scale of the cyclic voltammetric experiment, then the reverse peak will not be observed at all. Clearly a great variety of different ways can be imagined whereby CV results are influenced by chemical reactions coupled to electron transfer steps at the electrode surface. It is generally possible to mathematically model these various systems in such a way as to allow estimation of chemical rate constants from the cyclic voltammetric data.

5.1.1.2 Bulk Electrolysis

Whereas cyclic voltammetry acts only on the analyte present within a short distance of the electrode surface, bulk electrolysis[3] (BE) is a technique whereby all analyte in solution is electrochemically oxidised or reduced. The experimental equipment and conditions are similar to those employed in cyclic voltammetry, with the following differences:

1. The area of the WE is as large as possible, usually a wire gauze, in order to provide greater contact with the solution.

2. The AE is not in contact with the analyte solution, but is present in another compartment, separated by something such as a glass fritt, which ideally does not allow mixing of the analyte and the product of reaction at the AE, yet has a minimal influence on cell resistance. The reason for this is to prevent reaction of cathodic products at the anode and vice-versa, which would defeat the purpose of the BE.

3. The solution is stirred, in order to transport analyte to the WE for reaction.

There are two basic ways in which the desired oxidation or reduction can be carried out. These are known as controlled-potential, and controlled-current, methods.

BE using controlled-potential involves setting the potential in the cell at a level which should ensure electron transfer at the electrode surface takes place until the desired redox process has been completed, after which time current flow slows considerably. Monitoring of the current being produced in the system is thus used as a means of determining when BE is completed. To illustrate this, consider an analyte which can undergo two one-electron oxidations, with E°' for the first oxidation being 0.5 V and the second 1.0 V. Potential could be set at 0.75 V in order to complete the first oxidation step but avoid the second. Current would initially flow freely in the cell, but once analyte was exhausted only

nonfaradaic currents could flow, and the experimenter would know that the experiment was complete. Where both O and R are fully soluble, the proportion of O which will react for a given applied potential is given by the equation (10).

$$x = [1 + 10^{\{(E - E^{\circ\prime})n/0.059\}}]^{-1} \qquad \text{at } 25^{\circ}\text{ C} \qquad (10)$$

Where: x = fraction of O reacted

E = applied potential

It can thus be shown that under standard conditions 99% reduction of O to R requires a potential 118/n mV more negative than E°', oxidation of O to R a potential 118/n more positive than E°'.

In controlled-current BE, the current flowing in the cell is instead set at a desired level and the potential produced in the cell is monitored. Consider the situation envisaged in the previous paragraph. If this analyte were to be electrolysed using controlled-current, potential in the cell would be expected to remain at about 0.5 V until the first oxidation was complete, and which point potential would rise rapidly to about 1.0 V. After the second oxidation was completed potential would again begin to rise rapidly, because of the high impedance now present in the cell in the absence of easily oxidisable species. Monitoring of the potential could thus be used to stop BE at the desired stage.

In practice it may prove easier to simply pass the desired number of electrons into or out of solution in accordance with the amount of analyte in solution. This is a variation of the controlled-current method, but the amount of current which should be allowed to pass is calculated beforehand, rather than inferred from monitored potentials. The advantage of this method is that it overcomes the problem of sources of impedance in the cell circuit, such as the AE glass fritt, which can mean the measured potential is quite different to the potential at

the WE surface. The number of coulombs of charge which has been passed is easily obtained from equation (11), and the amount of charge desired for complete reaction can be calculated from (12).

$$Q = i_{APP}t \qquad (11)$$

$$Q = nmF \qquad (12)$$

Where: Q = total charge passed

i_{APP} = the applied current

t = time

m = moles of analyte in solution

BE can be used to produce electrochemical products in quantities sufficient to allow their study by other means.

5.1.1.3 Microelectrode Steady-State Voltammetry

In microelectrode steady-state voltammetry a WE with a very small working surface area is used[4], and the CV is run at a slow scan rate. Under these conditions starting material is quickly used up near the electrode surface and therefore electron transfer very rapidly becomes diffusion-limited. For this reason no peaks are seen in the redox wave of a microelectrode CV, but simply a sinusoidal curve linking the baseline level of current before the E°' of the redox process to a different current level after the redox process. The change in current (Δi) for the redox process provides a measure of the number of electrons involved and can be compared to data obtained from another microelectrode CV or to resolve overlapping CV peaks into components of measurable relative size. In addition, the steady-state voltammetric technique provides information concerning the oxidation state of species

in the bulk solution, that is, the extent to which species are present in their oxidised or reduced form. The concepts behind use of microelectrodes are similar to those governing the use of rotating disk electrodes[5], which are used for similar purposes.

5.1.1.4 Spectroelectrochemistry

BE can be carried out in small electrolytic cells while the solution is monitored by UV-vis spectroscopy[4a]. If suitable diagnostic wavelengths are available this technique can be used to observe the way levels of various species change in solution as the BE progresses.

5.1.2 Electrochemistry of Ferrocenylphosphines

Ferrocene can be oxidised to give the ferrocenium cation at moderate potentials, and in a process which is electrochemically and chemically reversible under cyclic voltammetric conditions[6]. These factors have made the electrochemical study of ferrocene-containing compounds an attractive field in which a lot of work has been done by those interested in redox-active compounds. One application for the redox characteristics of ferrocene is discussed in Chapter 6.

A large number of studies have been published concerning the redox properties of complexes containing ferrocenylphosphines as ligands[6,7]. Some of these studies contain a superficial examination of the free phosphines, but studies of any depth are rather rarer. It is these studies of free ferrocenylphosphines which will be the primary focus in this Section.

The earliest extensive study of the electrochemistry of ferrocenylphosphines was carried out by Kotz *et al.*[8] on $FcPPh_2$, Fc_2PPh and PFc_3. Redox processes were reported to be fully electrochemically and chemically reversible in acetonitrile, and were attributed to oxidation at the ferrocene functions. Separate oxidation processes were observed for each ferrocene group in the second and third of these compounds, a phenomenon which implies that

intramolecular electronic interaction exists between the ferrocene groups. However, the finding of full chemical reversibility is at odds with research carried out during the last decade which has found that the electrochemistry of ferrocene phosphines is rather complex. Indeed, full reversibility appears questionable in view of earlier publication of the CV of $FcPPh_2$ by Kotz himself[9]. This earlier publication noted that the CV appeared reversible if potential was not taken higher than 0.8 V [vs. saturated calomel electrode (SCE)], but chemical complications were evident when the potential range was greater. Several peaks which were seen when the potential was scanned to 1.5 V (vs. SCE) were unassigned except by assuming redox processes at the phosphorus atom (Figure 5.4). Unfortunately no mention was made concerning the range of scan rates investigated. It should be noted that electrochemistry of $FcPPh_2$ has been briefly investigated more recently and nothing but an apparently reversible $E_{1/2}$ value was reported[71]. However, very recent research[10] shows that there are clearly important chemical complications in the electrochemistry of $FcPPh_2$ (again in acetonitrile), if the positive switching potential exceeds the ferrocene redox wave by more than about 0.2-0.3 V. In passing it might be noted that the same publication reported that the redox waves seen for Fc_3P (earlier investigated by Kotz *et al.*[8]) were irreversible. Against this rather confused research background it seems to have become accepted in the literature that there are no chemical complications involved in the redox behaviour of $FcPPh_2$[11,12]. A more realistic view might be to say that oxidation of this species does result in chemical complications, but that if the switching potential is set close enough to the redox wave, the time for reaction is too small for any noticeable effect to be seen.

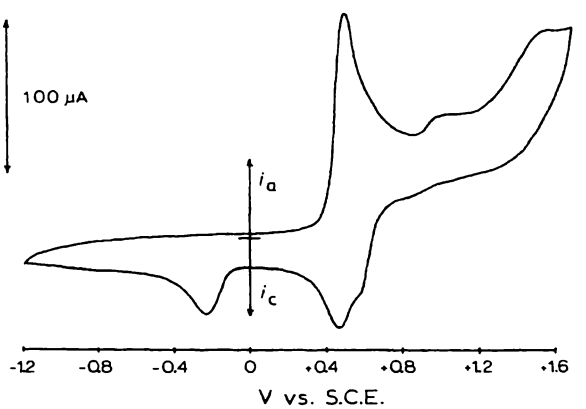

Figure 5.4: CV of $FcPPh_2$ in acetonitrile, with the first forward sweep being in the anodic direction[9].

The most intensive investigation of ferrocenylphosphine electrochemistry has naturally focussed on the widely-used dppf. An $E_{1/2}$ value for this compound, determined by DC polarography, was first published in 1974[7o]. Likewise, other investigations since then have reported the $E_{1/2}$ for the ferrocene-based redox couple of dppf without any further discussion[7b,c,h,j,l]. Pilloni *et al.* were the first to report more extensive details of the electrochemistry of this ligand in 1989[13] prior to publication of the results of an intensive electrochemical investigation in 1991[14]. A representative CV is shown in Figure 5.5. It was found that dppf underwent a one-electron electrochemically reversible oxidation followed by an irreversible chemical reaction.

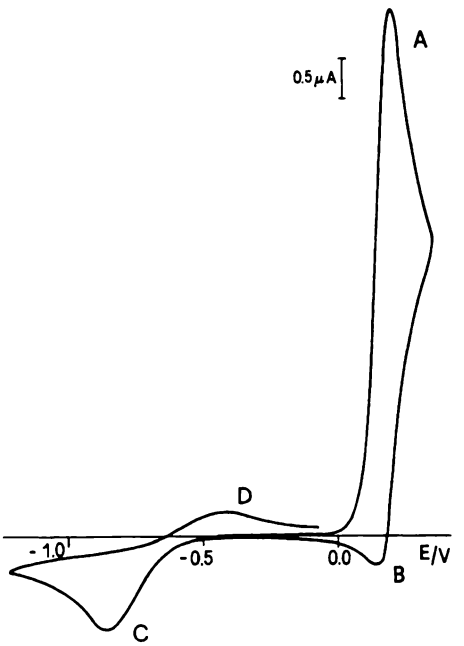

Figure 5.5: CV of 10 mM dppf in 1,2-dichloroethane with a scan rate of 200 mV s^{-1}. The first forward scan is in the anodic direction. Potentials are referenced to FcH\FcH$^+$.

Peak A is assigned to the oxidation of dppf to dppf$^+$. Peak B is the coupled reduction peak. Peak C is a reduction dependent on the further chemical reaction of the oxidation product dppf$^+$, and peak D is an oxidation associated with the reduction peak C. By comparison with authentic samples, peak C has been assigned to the reduction of the phosphonium species

$dppfH^+$, and peak D to the oxidation of molecular hydrogen in the presence of dppf, according to the following reaction:

$$dppfH^+ \underset{-\,e}{\overset{+\,e}{\rightleftharpoons}} dppf + 1/2H_2$$

Under conditions of BE it was found that removal of 0.66 electrons per molecule of dppf led to formation of $dppfH^+$ and dppfO (i.e. the phosphine oxide) in a ratio of *ca.* 2:1 (as evidenced by cyclic voltammetric currents and ^{31}P-NMR). This can be accounted for by the reaction:

$$3dppf + H_2O \longrightarrow 2dppfH^+ + dppfO + 2e$$

Removal of 1.33 electrons per dppf by BE leads to a similar 2:1 ratio of $dppfH_2^{2+}$ to $dppfO_2$. These products are presumably formed sequentially by progression from the reaction above to those given below:

$$2dppfH^+ \rightleftharpoons dppf + dppfH_2^{2+}$$

$$dppfO + H_2O + dppf \xrightarrow{-\,2e} dppfO_2 + dppfH_2^{2+}$$

It was concluded that the primary oxidation product $dppf^+$ was behaving in the usual fashion for a phosphinium radical cation. The localisation of charge onto the phosphorus atom was convincingly demonstrated by the reaction with 3,3-dimethyl-2-*t*-butylbut-1-ene, a reagent known to trap phosphinium radical cations. Under conditions of low temperature and fast scan rate, where dppf oxidation appears reversible, presence of this alkene leads to concomitant loss of the cathodic peak, and mass spectrometry reveals the presence of the expected adduct. The proposed mechanism for the entire reaction (Scheme 5.1) is more tenuous (though it has a precedent in the literature on phosphine oxidation[15]) and is based on what can be determined about the kinetics.

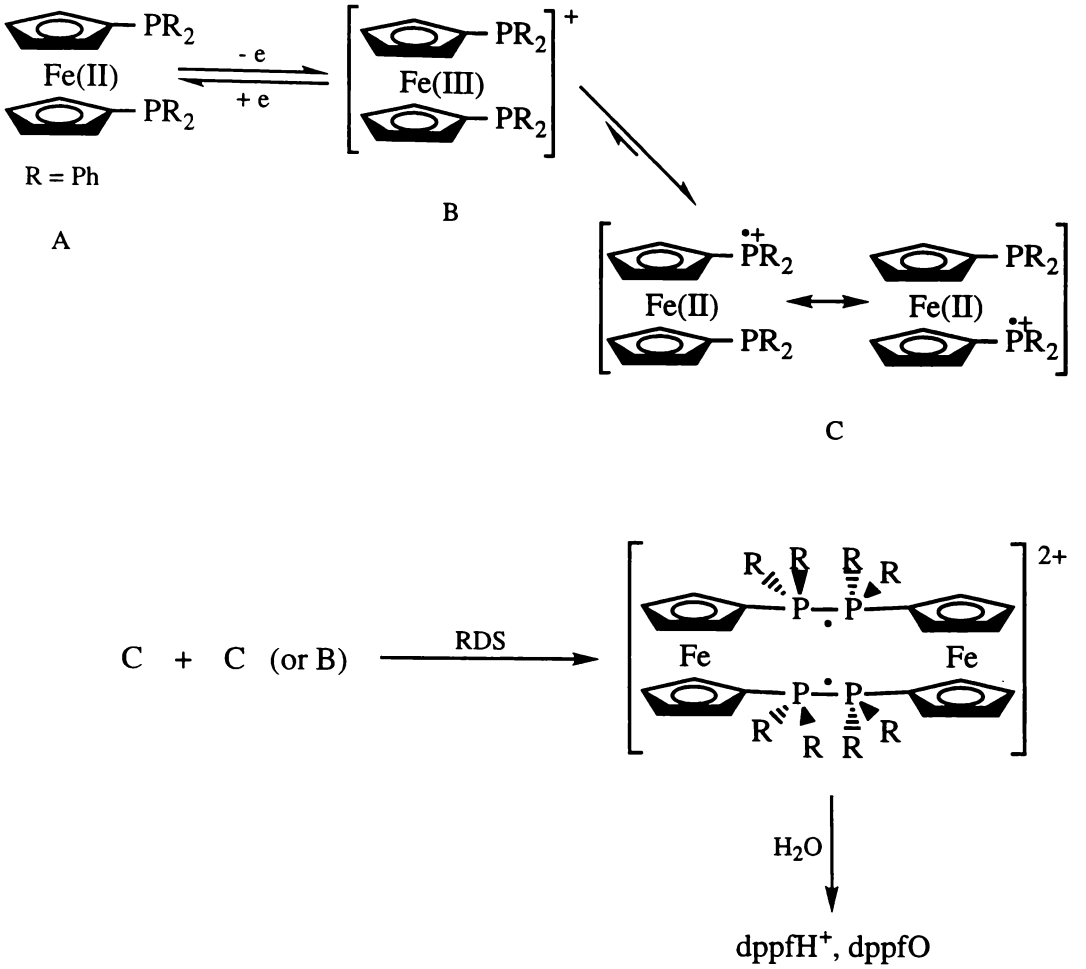

Scheme 5.1: Proposed mechanism for the reaction of dppf^{+} to give the observed oxidation products. The dimerisation step is thought to be rate-determining.

Zanello *et al.*[12] confirmed the chemical irreversibility of the dppf oxidation, and accepted the above mechanism, suggesting that in dppf the HOMO is no longer the iron-based a_1' orbital but is an anti-bonding phosphino-based orbital. They also investigated a number of derivatives of dppf, substituted at the 2-position with $-CH(CH_3)OH$, $-CH(CH_3)SH$, $-CH{=}CH_2$, and $-CH(CH_3)N(CH_3)_2$. The behaviour of these compounds was found to be similar to that of dppf, with the substituents imparting a greater or lesser degree of chemical reversibility upon the oxidation process. For the first three of these compounds, a one-electron BE followed by mass spectrometric analysis of the products was carried out, and

showed the presence of phosphine oxide products. The behaviour of compounds with the substituents $-CH(CH_3)SCH(Ph)CH(CH_3)N(CH_3)_2$ and $CH(CH_3)N(CH_3)(CH_2)_2N(CH_3)_2$ was also investigated and found to be rather more complicated.

Kotz *et al.*[16] investigated the electrochemical behaviour of 1-(dimethylaminomethyl)-2-(diphenylphosphino)ferrocene, and found it to be very complicated; the CV (Figure 5.6) was left essentially unassigned.

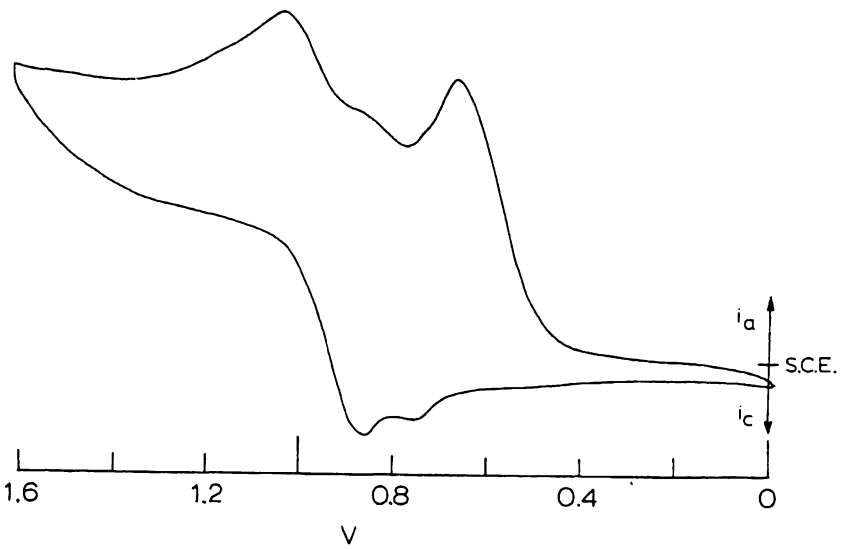

Figure 5.6: CV for 2 mM 1-(dimethylaminomethyl)-2-(diphenylphosphino)ferrocene in dichloromethane, forward sweep in the anodic direction[16]. Scan rate was not reported.

Podlaha *et al.*[17] have investigated the electrochemistry of 1-(diphenylphosphino)-1'-(carboxy)-ferrocene and found this also to be complex (Figure 5.7). The peak A_1 is considered to be due to oxidation of the iron(II) to iron(III). Quick intramolecular electron transfer occurs to regenerate iron (II) and the resulting positively charged phosphorus atom then quickly forms the phosphine oxide. This phosphine oxide is postulated to be the species responsible for the oxidation peak A_2 at higher potential. However, this assignment was made only on the basis that the redox potential of the synthesised phosphine oxide corresponds to that of peak A_2, and so in the present author's opinion it must be considered tentative. Peaks B and C were assigned to processes at the carboxylic acid group.

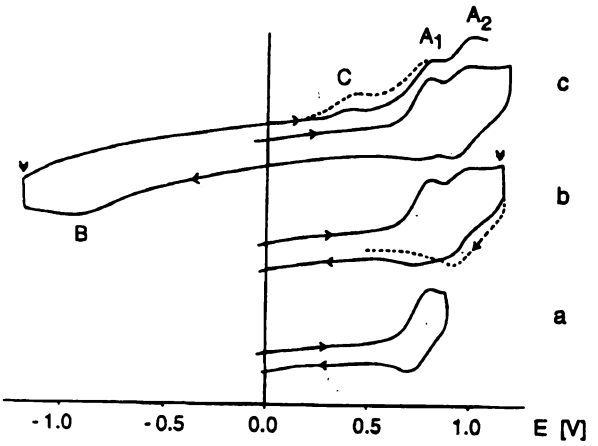

Figure 5.7: CVs of *ca.* 1 mM 1-(diphenylphosphino)-1'-(carboxy)-ferrocene in acetonitrile, with different switching potentials. Dotted lines represent effect caused by BE at the potentials indicated by arrows. Scan rate 250 mV min^{-1}.

Figure 5.8 shows the chemical structure and CVs of two ferrocenylphosphines which have been recently investigated[18]. In the case of compound a), a chemically irreversible oxidation is seen, followed by a quasi-reversible wave. The first oxidation is thought to result from oxidation of the iron(II) to iron(III) with rapid transfer of the positive charge to the phosphorus, leaving the iron(II) free to exhibit another oxidation wave, this one chemically reversible. Essentially the same process is seen for compound b), but the ferrocene centres can communicate electronically and so separate oxidation processes are seen corresponding to the two ferrocene centres.

A similar pattern is seen in the CV of 1-[6-(2,2'-bipyridyl]-1'-(butylphenylphosphino)ferrocene - a chemically irreversible oxidation followed by a reversible wave[19]. However, the first oxidation is here attributed to phosphorus oxidation with no mediation by ferrocene. This is in contrast to the thinking of all other recent investigations of similar compounds, as described above. The reason for assuming the first oxidation takes place at the ferrocene centre in all of the ferrocenylphosphines discussed above is that electrochemical oxidation of phosphine centres in compounds such as

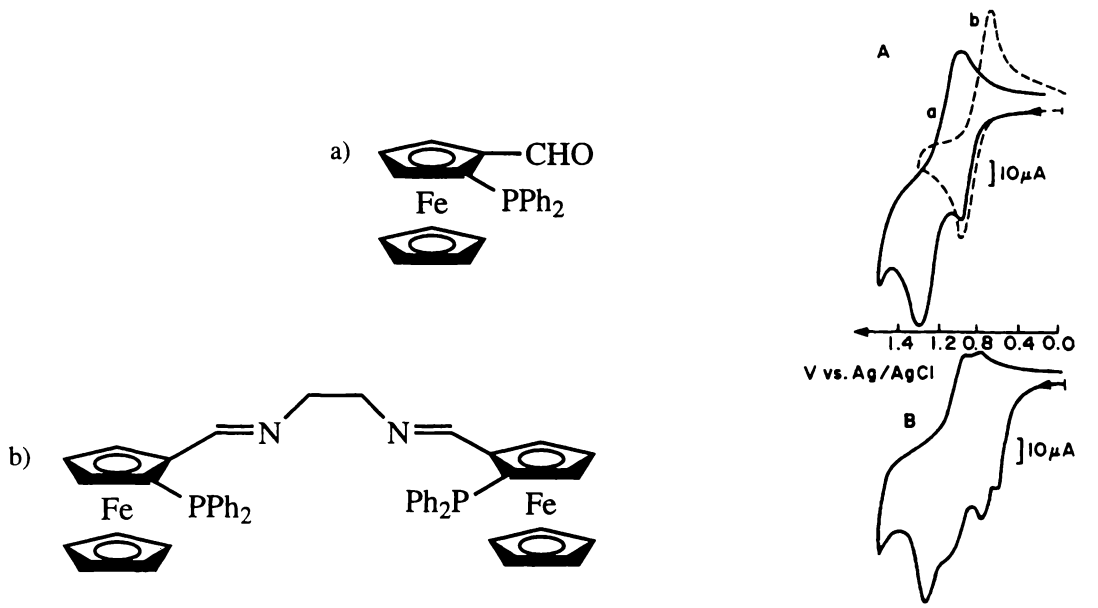

Figure 5.8: Chemical structure and CVs in dichloromethane for two ferrocenylphosphines recently investigated. Scan rate 100 mV s^{-1}. The dashed line is the CV for ferrocenylaldehyde.

triphenylphosphine[20] takes place at considerably higher potentials than is the case for these ferrocene derivatives, which usually show redox potentials removed from that of ferrocene by a few hundred mV at most.

All electrochemical studies discussed so far have involved a phosphine centre directly bonded to the Cp ring[21], so that all imply the same pattern of charge being transferred from the iron to the phosphine centre by an intramolecular mechanism. Some studies have also been carried out where this is not the case. A study of $Fc(C_6H_4)O(CH_2)_2PPh_2$ states only a redox potential for the compound[22], but studies of $FcC(O)CH_2PPh_2$ are more comprehensive[7d,23]. The electrochemistry of this compound exhibits only one broad anodic and chemically irreversible wave over the potential range investigated, corresponding to loss of one electron. However, exhaustive BE leads to loss of two electrons from the molecule. A one-electron BE leads to a product mix giving several ^{31}P-NMR peaks in the range 9-30 ppm (c.f. -19.1 ppm for the starting material). Also, in this product mix no ferrocenium species could be detected spectroscopically. This led to the conclusion that this compound reacts in a similar way to dppf, with charge first centred on the iron atom but quickly

transferred to the phosphorus, which then undergoes further reactions, allowing the ferrocenyl group to be re-oxidised in exhaustive BE. This transfer from iron to phosphorus was assumed to be an intramolecular reaction, but no evidence for this interpretation was offered. In view of the fact that no conjugation network exists for transferral of charge from iron to phosphorus, c.f. the case for dppf, the intramolecular nature of this electron transfer is perhaps disputable (although there might be through-space Fe-P interaction).

It is worth noting that so far as the author is aware, no electrochemical studies have been carried out on ferrocenylphosphines where the phosphorus is separated from the Cp ring by a carbon spacer. The studies described in the remainder of this Chapter concern ferrocenylphosphines and related compounds of this type and might therefore be expected to behave differently to those examples which have been reviewed in this Section.

5.2 Results and Discussion

5.2.1 Survey of the Electrochemistry of Ferrocenylphosphines and Their Derivatives

Cyclic voltammetric investigations were carried out with a number of the compounds described in Chapters 2 and 4. This Section provides an overview of the behaviour of these compounds, in addition to two others. The compound $FcCH(Me)P(CH_2OH)_2$ **32** was obtained in crude yield, but the synthetic method and characterisation were considered too poor to merit description in Chapter 2. Details can be found in Appendix B. $FcCH_2P(S)Ph_2$ **33** was gifted to the author by Dr. William Henderson and was prepared by ultrasonication of a dichloromethane solution of **2** in the presence of elemental sulfur.

Except where stated otherwise, cyclic voltammetric experiments were carried out in anhydrous acetonitrile with 0.1 M $Bu^n_4NPF_6$ as the depolariser, with a Pt disk WE, Pt wire

AE, and Ag/Ag^+ (10 mM $AgNO_3$ and 0.1 M $Bu^n_4NPF_6$ in acetonitrile) RE. Voltammetric response of compounds was generally examined over a range of scan rates from 20 to 500 mV s^{-1}, using solutions of *ca.* 1 mM.

*5.2.1.1 Ferrocenylphosphines $FcCH_2P(CH_2OH)_2$ **1**, $FcCH_2PPh_2$ **2**, $FcCH_2P(CH_2CH_2CN)_2$ **5**, $(FcCH_2)_2PCH_2OH$ **11**, $FcCH_2PH_2$ **24**, $FcCH_2P(H)CH_2OH$ **25** and $FcCH(Me)P(CH_2OH)_2$ **32***

It would be fair to say that the electrochemistry of the ferrocenylphosphines investigated in this Section proved rather complex. The electrochemistries of **1**, **2**, **5** and **11** received more intensive investigation in order to attempt to elucidate the mechanisms involved, and the results of this work are outlined in later Sections. In this present Section only the cyclic voltammetric behaviour of these compounds is dealt with. Certain electrochemical parameters for all the title compounds are listed in Table 5.1.

A typical CV utilising an anodic forward potential sweep for compound **1** is shown in Figure 5.9. Two distinct redox processes are observed. As will be shown, this is a general feature of the compounds described in this Section. Both redox processes appear to be essentially electrochemically reversible; from 50 to 500 mV s^{-1}, ΔE_P for both remains constant at 70 mV, close to the idealised value for ΔE_P of *ca.* 60 mV where $n = 1$ [equation (7)]. In addition, the relationship between the first anodic peak current, $i_{PA(1)}$, and $v^{1/2}$ is linear, implying reversibility [equation (8)]. Bearing this in mind, the value of ΔE_P would suggest that both redox processes involve one electron. Comparison of peak currents with equimolar solutions of ferrocene or compound **3** (see below) supports this conclusion. Cyclic voltammetry of **1** in dichloromethane gave similar results, although the cathodic peak for the second anodic redox process gave large and sharp peak currents due to electrode adsorption processes.

Table 5.1: *Electrochemical data at oxidative potentials for some ferrocenylphosphines (ferrocene included as a reference). Subscript 1 refers to the first redox process observed, subscript 2 refers to the second. Potentials are listed in mV vs. Ag/Ag$^+$ (10 mM). Accuracies are ± 5 mV. Ferrocene samples were run one week apart, before starting and then after finishing all other cyclic voltammetric experiments (average given here). Scan rate is 100 mV s^{-1} except where noted otherwise.*

	$E_{PA(1)}$	$E_{PC(1)}$	$E_{1/2(1)}$	$E_{PA(2)}$	$E_{PC(2)}$	$E_{1/2(2)}$
FcH	118	48	83	-	-	-
1	50	-20	15	260	195	238
2*	82	15	49	-	*ca.* 230	-
5^	100	32	66	325	260	293
11	-15	-	-	280	145	213
24	80	10	45	180	118	149
25*	70	-5	32	220	160	190
32*	130	65	98	275	*ca.* 240	245#

* Scan rate 50 mV s^{-1}. ^ Scan rate 20 mV s^{-1}.

Since the apparent gap between the two peak potentials is very small, and the position of the cathodic peak is difficult to estimate, $E_{1/2(2)}$ has been taken to be $E_{PA(2)}$ - 30 mV.

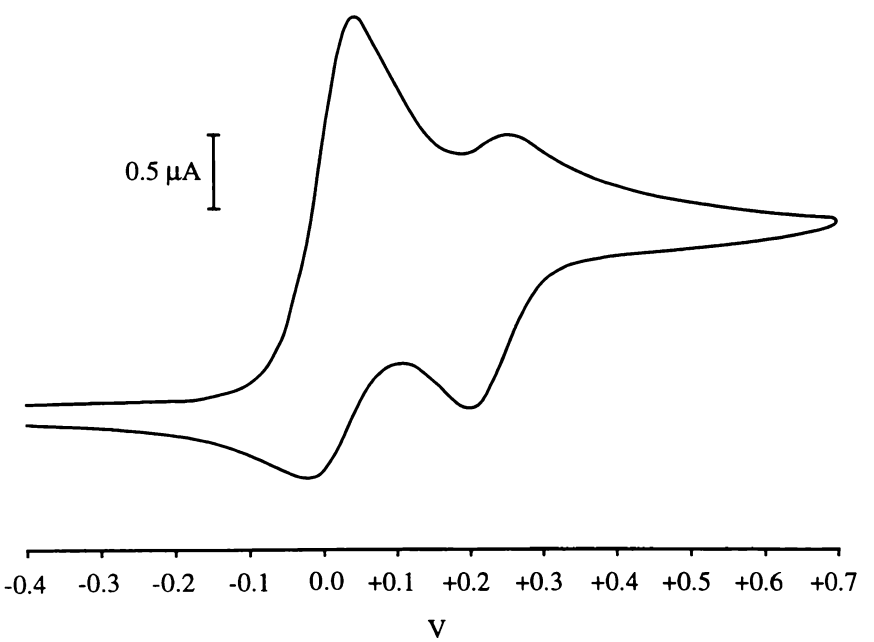

Figure 5.9: CV of 1.4 mM **1**, scan rate 100 mV s^{-1}.

While electrochemically reversible, it is clear that this is not a chemically reversible system. The ratio of $i_{PC(1)}/i_{PA(1)}$ grows closer to one as the scan rate is increased from 20 mV s^{-1} to 500 or 1000 mV s^{-1}. Conversely, the ratio of $i_{PC(2)}/i_{PC(1)}$ falls as scan rate is increased. These observations are consistent with the following mechanism:

$$\mathbf{1} \underset{+e}{\overset{-e}{\rightleftharpoons}} \mathbf{1}^{+} \longrightarrow B^{+} \underset{+e}{\overset{-e}{\rightleftharpoons}} B^{2+} \qquad [3]$$

The first redox wave is due to **1**, which is then transformed into B at a rate comparable to the time scale of the voltammetric experiment; in turn B accounts for the second redox wave. (Note that it should not be inferred from the way [3] is written that the chemical step is necessarily either irreversible or unimolecular.) Also consistent with this mechanism is the observation that at fast scan rates, repeated cycles lead to a decrease in $i_{PA(1)}$ and $i_{PC(1)}$, and an increase in $i_{PA(2)}$ and $i_{PC(2)}$ (Figure 5.10).

The linking of these two processes by a chemical step was confirmed by low temperature cyclic voltammetry of **1**. A series of CVs for **1** as the temperature of the solution was reduced is shown in Figure 5.11. The temperature of the solution was reduced from ambient temperature to -39° C, and the size of the second wave steadily decreased in size until at -30° C this wave had almost completely disappeared. This proves unequivocally that the second wave results from oxidation/reduction of a product produced by further chemical reaction of the initial oxidation product of **1**, in accordance with mechanism [3].

The rate-determining step (RDS) in this reaction is clearly intermolecular, since it is influenced by concentration of the analyte. Figure 5.12 shows CVs of 0.5 mM, 1.0 mM and 5.0 mM solutions of **1** under the same conditions. Testing of various computer models[24] against the real CV data for **1** established that the best fit from the limited number of scenarios tested was where the RDS linking the two anodic redox waves consisted of a

Figure 5.10: CV of 1.4 mM **1** showing seven cycles at a scan rate of 500 mV s^{-1}.

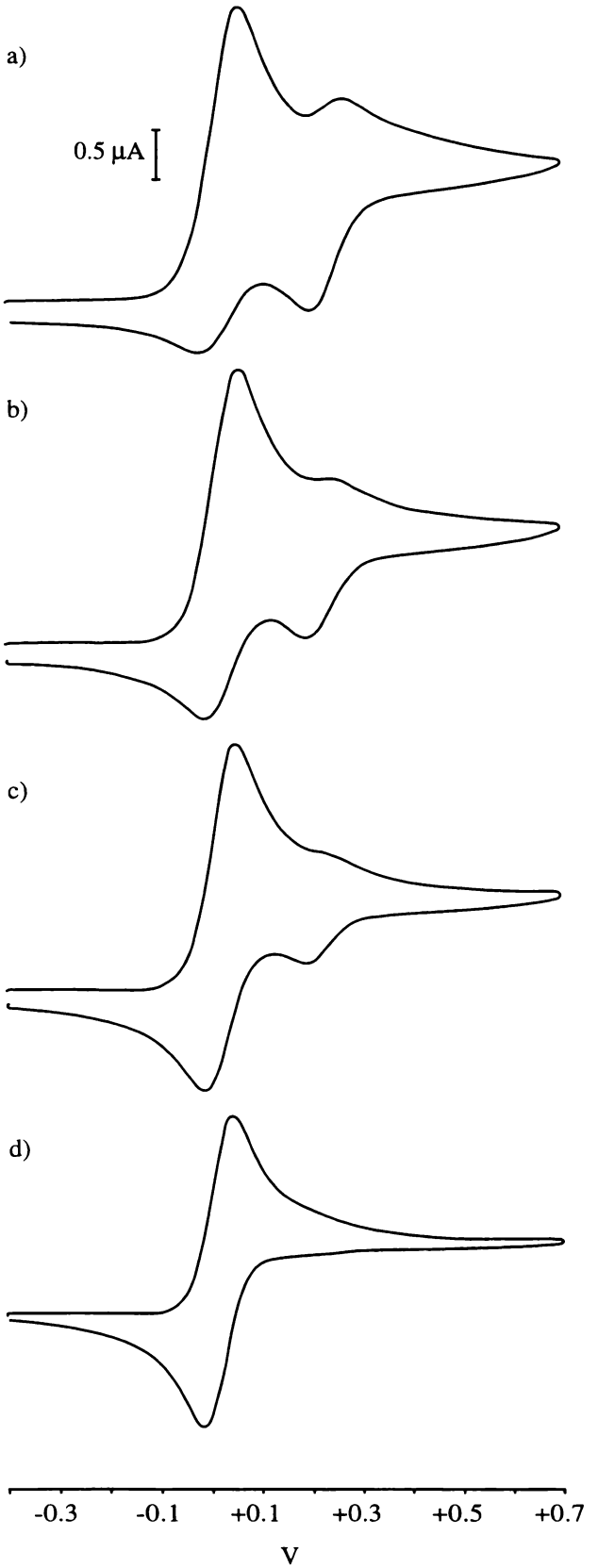

Figure 5.11: CVs of 1.0 mM **1**, scan rate 100 mV s^{-1}, as solution is cooled. a) 17° C; b) 5° C; c) -8° C; d) -30° C.

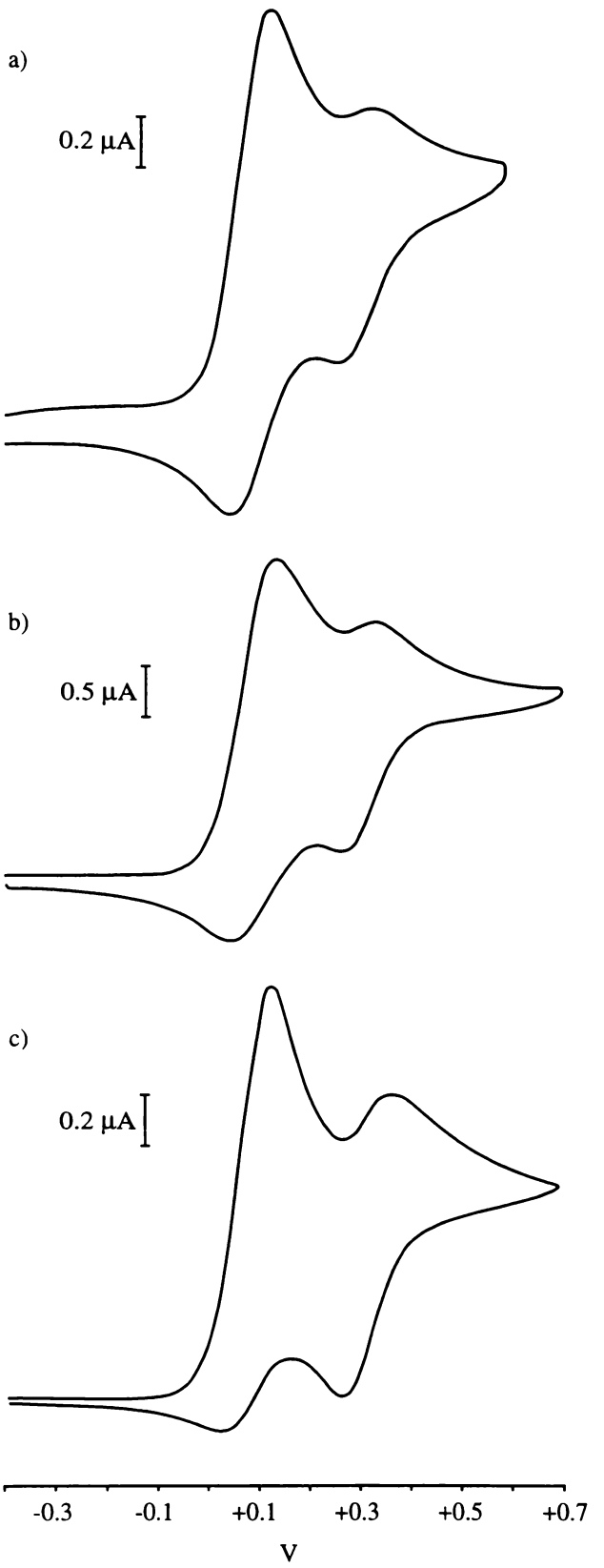

Figure 5.12: CVs of **1**, scan rate 100 mV s^{-1}. a) 0.5 mM, b) 1.0 mM, c) 5.0 mM.

bimolecular reaction between two $\mathbf{1}^+$ ions. In this model all steps were assumed to be reversible, with k_f for the reaction being 10^3 and k_b being 10^{-2}, giving an overall K of 10^5:

$$A \rightleftharpoons B + e \qquad \text{1st redox wave}$$

$$2B \underset{k_b}{\overset{k}{\rightleftharpoons}} C \qquad \text{reaction } (K = 10^5) \qquad [4]$$

$$C \rightleftharpoons D + e \qquad \text{2nd redox wave}$$

A comparison of computer-simulated CVs with experimental results for **1** is given in Figure 5.13.

It will be argued in this Chapter that the initial oxidation process involves oxidation of ferrocene to ferrocenium. This is followed by a reaction which transfers charge to some other part of the molecule, regenerating the ferrocene centre, which can then be reoxidised at a higher potential. In the rest of this Section it will also be shown that this mechanism appears to be general for compounds of the type $FcCH_2PR_2$.

A typical CV for compound **2** is shown in Figure 5.14. This appears to be a fully electrochemically (by the same criteria as **1**) and chemically reversible process, with one-electron transfer. However, if the potential is scanned at 50 mV s^{-1} to a switching potential of *ca.* 1 V a very small cathodic peak is seen at 230 mV on the reverse scan. A similar effect is obtained by scanning at 20 mV s^{-1} with a lower switching potential (Figure 5.15). Note that the value of $i_{PC(2)} - i_{PC(1)}$ is the same for both **2** and **1**. This suggests that **2** undergoes essentially the same processes as **1** but that the chemical step proceeds much more slowly, to the point where the second product {B^+ in mechanism [3] (page 208), C in mechanism [4]} diffuses away from the electrode surface almost as fast as it is formed. As with **1** the RDS for the chemical reaction appears to be intermolecular, as is shown by the CV of a 5.0 mM solution of **2** (Figure 5.16).

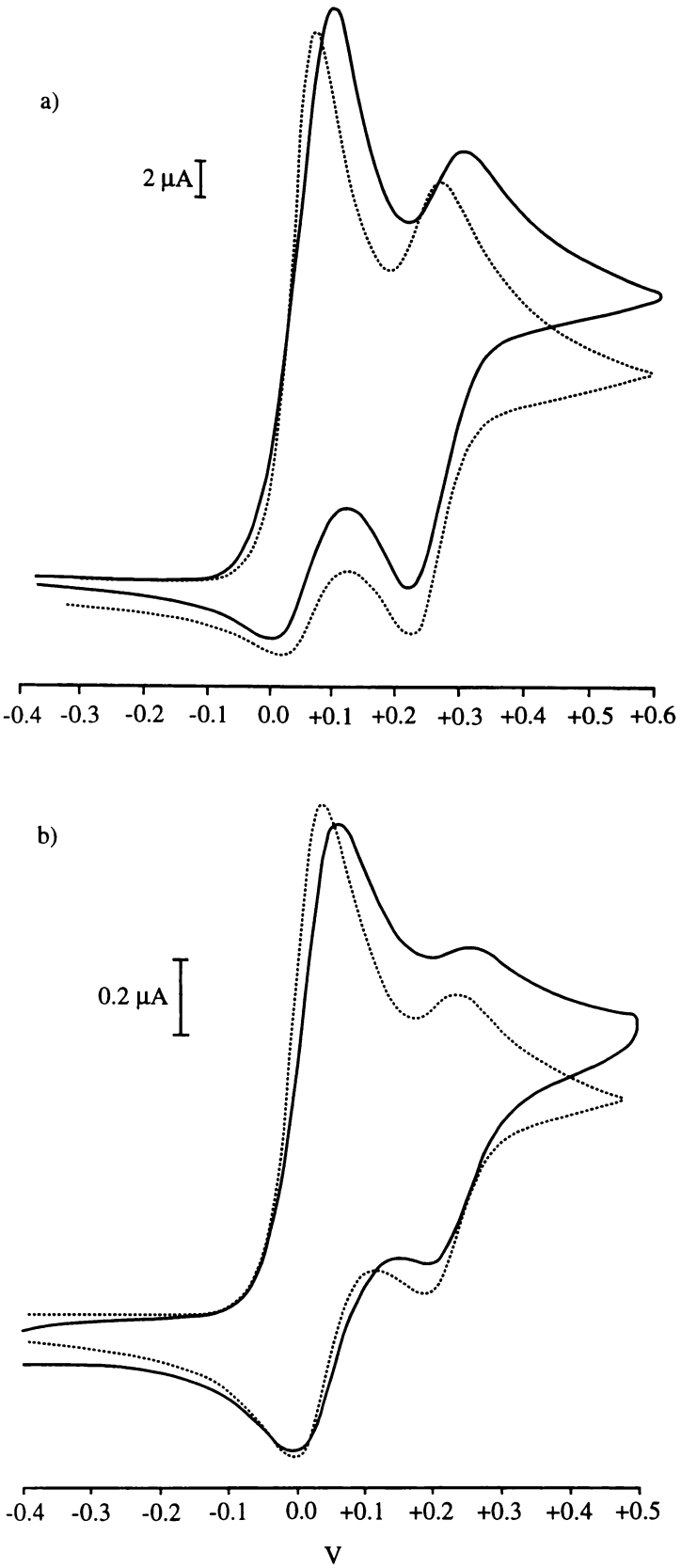

Figure 5.13: A comparison of the results of computer modelling, assuming mechanism [4], with experimental data for **1**, at a) 5 and b) 0.5 mM. Scan rate in each case is 100 mV s^{-1}. A dashed line denotes the computer simulation, the solid line represents empirical data.

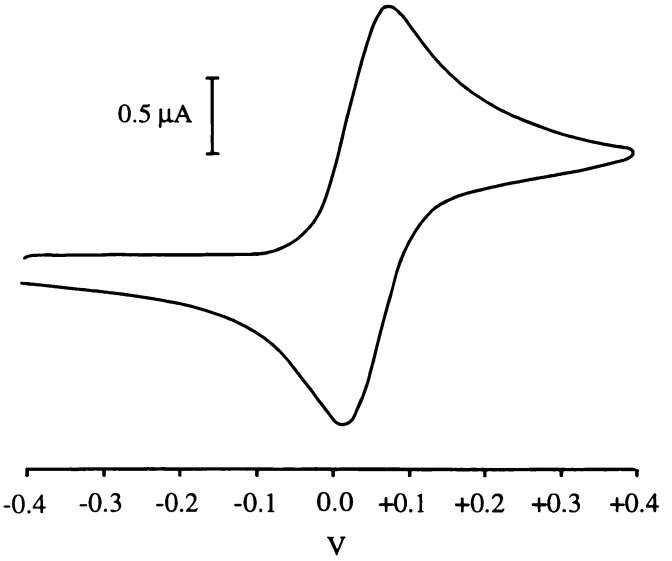

Figure 5.14: CV of 0.9 mM **2**, scan rate 100 mV s^{-1}.

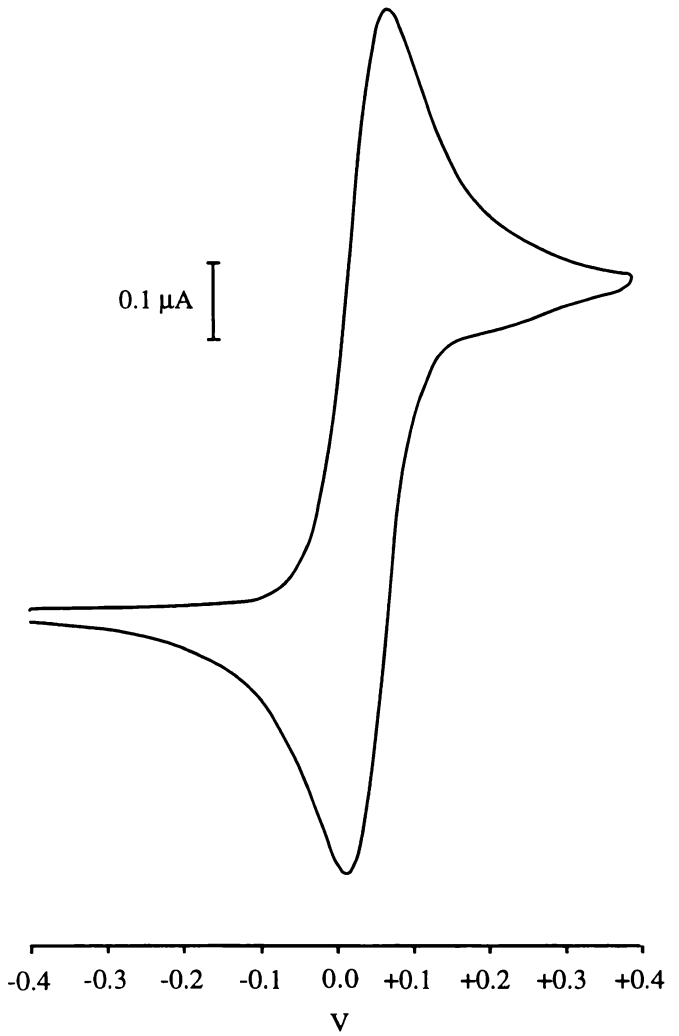

Figure 5.15: CV of 0.9 mM **2**; using a lower scan rate of 20 mV s^{-1}, a small shoulder can be seen at 230 mV in the reverse scan.

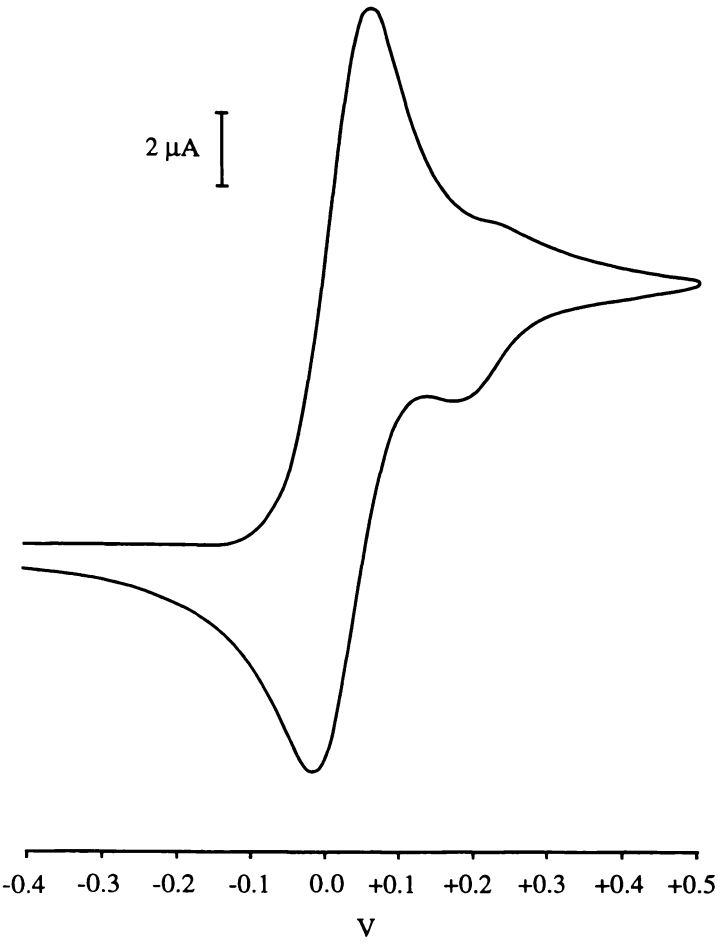

Figure 5.16: CV of 5.0 mM **2**, scan rate 100 mV s^{-1}. At this concentration the second redox wave is quite prominent.

Compound **5** gives similar results to **1** and **2** (Figure 5.17a), although it displayed some quasi-reversible character, with ΔE_P for the first redox process showing an increase from 65 mV to 80 mV with an increase in scan rate from 100 to 500 mV s^{-1}. At a scan rate of 20 mV s^{-1} the second process is pronounced enough to allow an estimation of the position of $E_{PA(2)}$, and so in terms of reactivity **5** appears to be intermediate between **1** and **2**. Unlike **1** and **2**, the rate of the chemical reaction appeared enhanced when a glassy carbon (GC) electrode was used rather than Pt (Figure 5.17b), suggesting that in this case interaction of the cyano- groups with the electrode surface affected the reaction rate. The difference in potential between the first and second redox processes is consistent with what has been seen with compounds **1** and **2**.

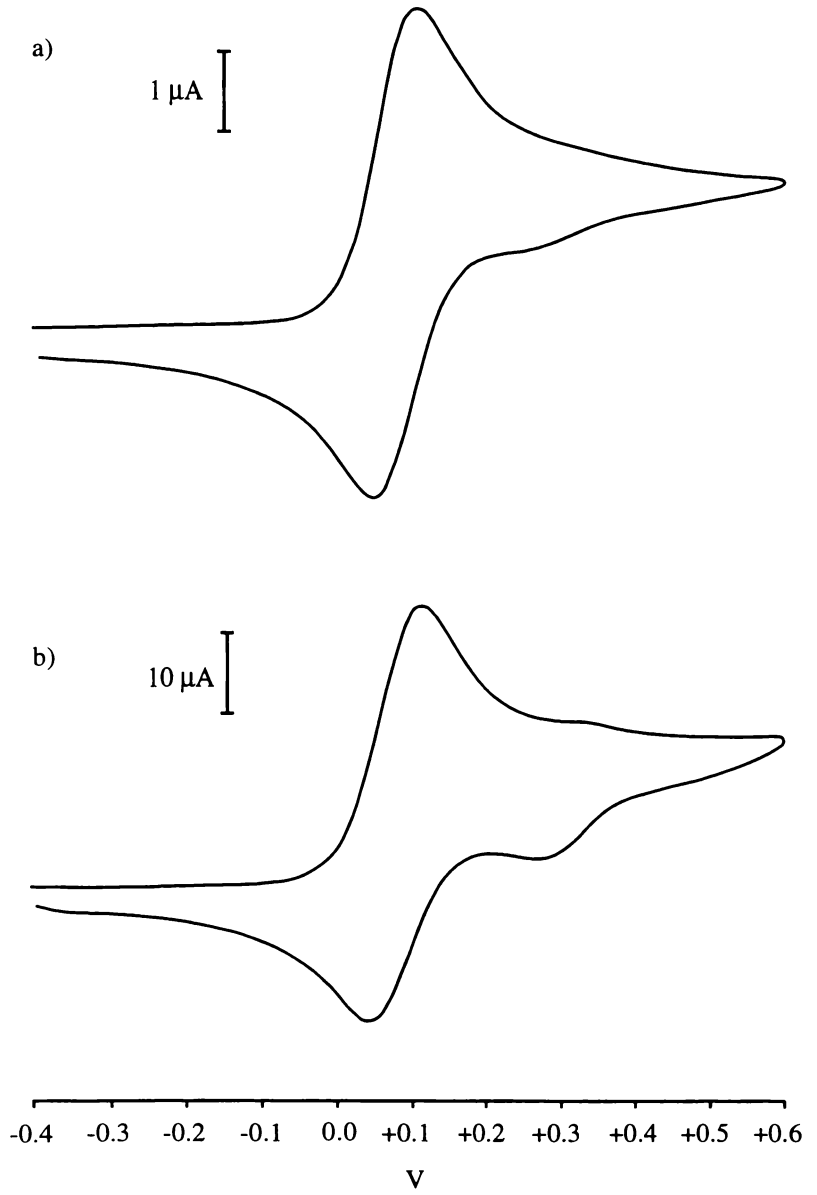

Figure 5.17: a) CV of 3.0 mM **5**, scan rate 100 mV s^{-1}, at Pt. b) At a GC electrode.

Similar behaviour is also observed for compound **32** (Figure 5.18), where the chemical reaction step occurs at an intermediate speed, that is, slower than for the analogous compound **1**. The first anodic peak is broad and has the appearance of two overlapping peaks, but this may be due to the impurities present in this compound. In other respects this compound appears similar to the others described so far, although the two redox processes appear closer together than for **1**, **2**, and **5**. One aspect of the electrochemistry of **32** which might initially appear anomalous is the fact that $E_{1/2(1)}$ is more positive than for any other compound listed in Table 5.1; the replacement of an α-hydrogen (as in compound **1**) with an

α-methyl group (compound **32**), typically considered to be more electron-donating than hydrogen, might be expected to shift the $E_{1/2}$ in the *negative* direction. However, it is possible to consider the substituted Cp ring as a carbanion, and if this is taken into account it will be seen that the α-methyl group could help to distribute the negative charge away from the Cp ring, thus making oxidation of the ferrocenyl group more difficult. The ^{31}P-NMR chemical shift for **32** (Appendix B) is more positive than those of the other ferrocenylphosphines described in this Thesis, suggesting that electron density at the phosphorus is lower in **32** than in those other compounds; again, this is consistent with the idea that the α-methyl group of **32** acts in an electron-withdrawing rather than electron-donating capacity.

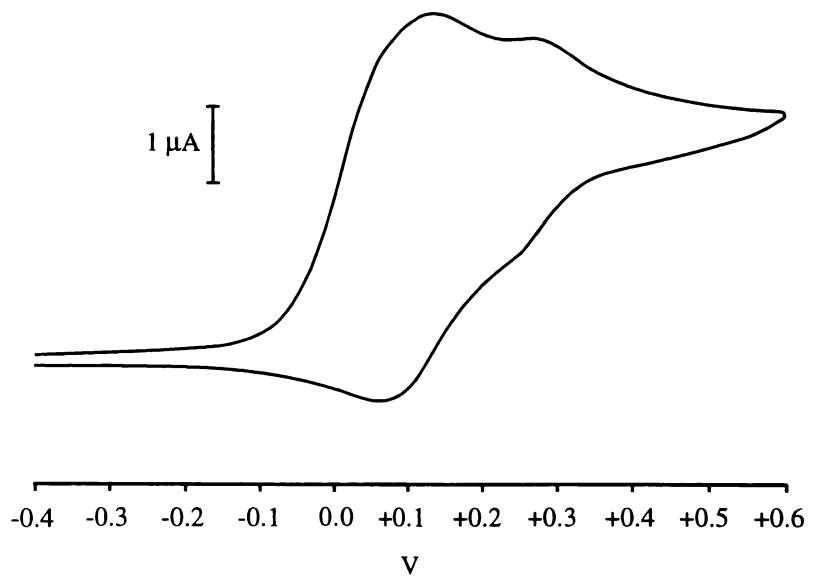

Figure 5.18: CV of *ca.* 1 mM **32**, 20 mV s^{-1} scan rate.

A feature common to the four compounds described so far is the presence of one or two broad cathodic processes of rather low current observed at potentials of *ca.* -1.2 and - 1.8 V. This peak(s) is only observed where the compound concerned has first been subjected to a forward scan to a switching potential which allows for oxidation of the compound.

Compound **24** exhibits a similar pattern to the four compounds discussed so far, but with some important differences. Figure 5.19 shows a typical CV. It can be seen that this is a

relatively reactive system compared to the first four, and that at moderately reductive potentials ($E_{PC(3)}$ = - 0.33 V) a cathodic peak is observed with a peak current ($i_{PC(3)}$) approximating $i_{PC(2)}$. This peak is absent if the potential is not first cycled in the positive direction, and is coupled to a broad oxidative process at *ca.* -0.2 V. Even where the positive switching potential is set between $E_{PA(1)}$ and $E_{PA(2)}$, this irreversible redox couple is observed in the later cycles. As with the other compounds discussed so far, the two redox processes at more positive potentials appear to be chemically coupled, and are both electrochemically reversible. Redox potentials for the two processes were much closer together than for these other compounds, however. Problems were experienced with adsorption of **24** onto both Pt and glassy carbon electrodes, making it difficult to obtain consistent results and values for peak potentials and currents, especially at high scan rates.

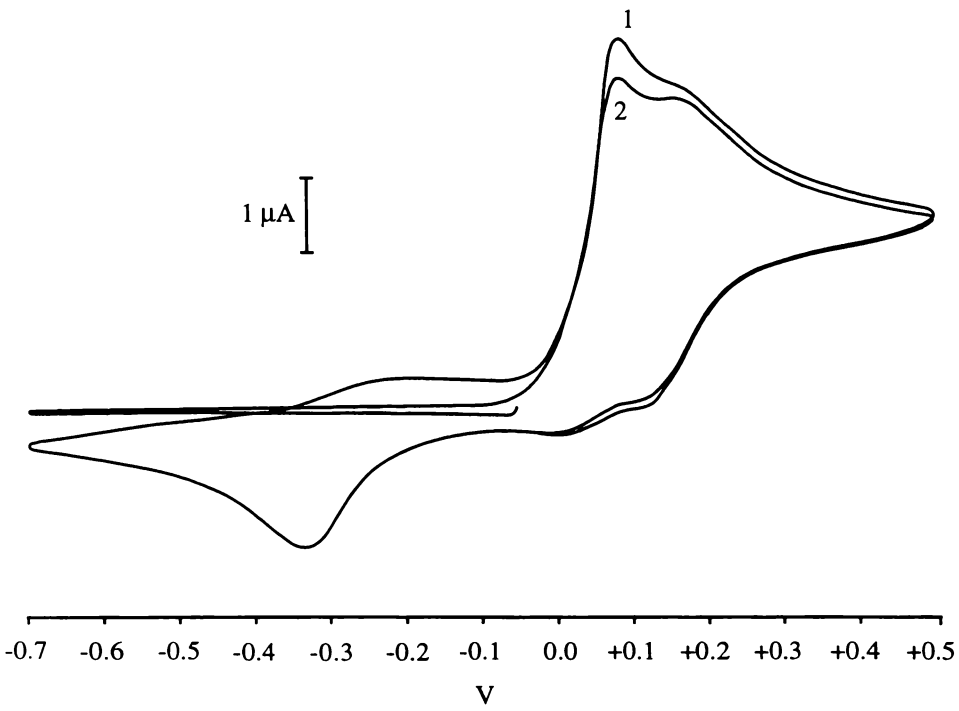

Figure 5.19: CV of 1.0 mM **24**, scan rate 100 mV s^{-1}. Initial scan in the negative direction.

In view of the electrochemical behaviour of **24**, it is surprising to observe that the secondary phosphine **25** behaves in a very similar fashion to **1**, but that the chemical step linking the two oxidative redox processes appears even slower than for **1**. The electrochemical parameters listed in Table 5.1 for **25** are more in keeping with what might be expected, with $E_{1/2(1)}$ and $E_{1/2(2)}$ - $E_{1/2(1)}$ for **25** intermediate between the values for **1** and **24**. A typical CV

is shown in Figure 5.20. As with previous compounds, the redox waves are electrochemically reversible, and small cathodic peaks at low potentials (-1.3, -1.8 V) are seen after sweeping through a positive potential range first.

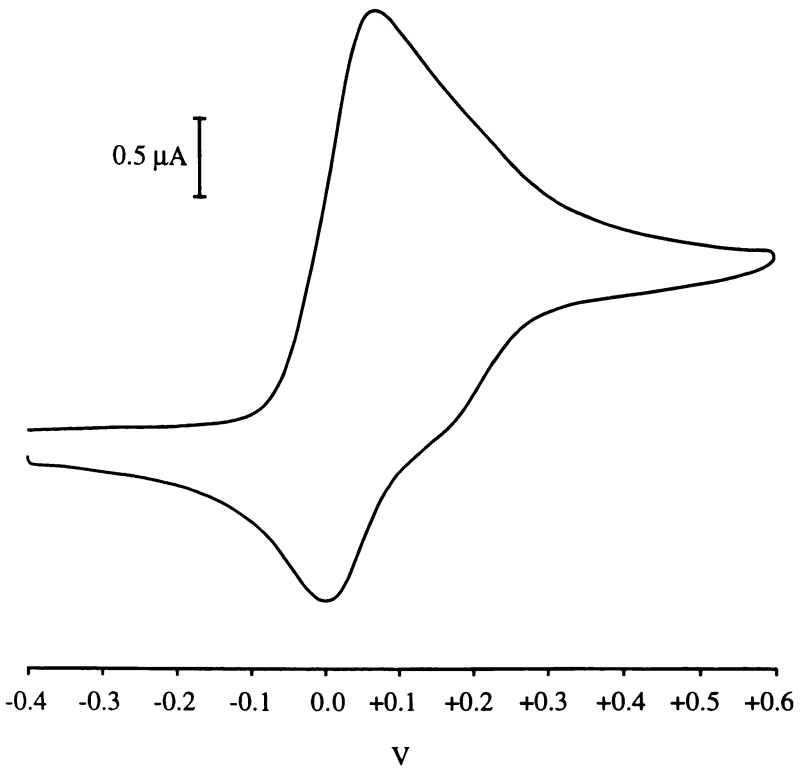

Figure 5.20: CV of 1.1 mM **25**, scan rate 100 mV s^{-1}.

The behaviour of compound **11** is somewhat different to that of all other compounds discussed in this Section, presumably due to the presence of two rather than one ferrocenyl functions. A typical CV is shown in Figure 5.21a. Two processes are seen as in other situations, but in this case the first process is completely chemically irreversible. This is unlike the second wave, which appears fully chemically reversible, and where $i_{PA(2)}/i_{PC(2)} \approx 1$. As with other compounds, a broad reduction wave of low current is seen at *ca.* -1.2 V. The appearance of the wave for the second process is somewhat rounded or broad; this is more easily seen at slower scan rates (Figure 5.21b). This suggests two closely overlapping peaks. It is postulated here that this is a two-electron oxidation process involving the two

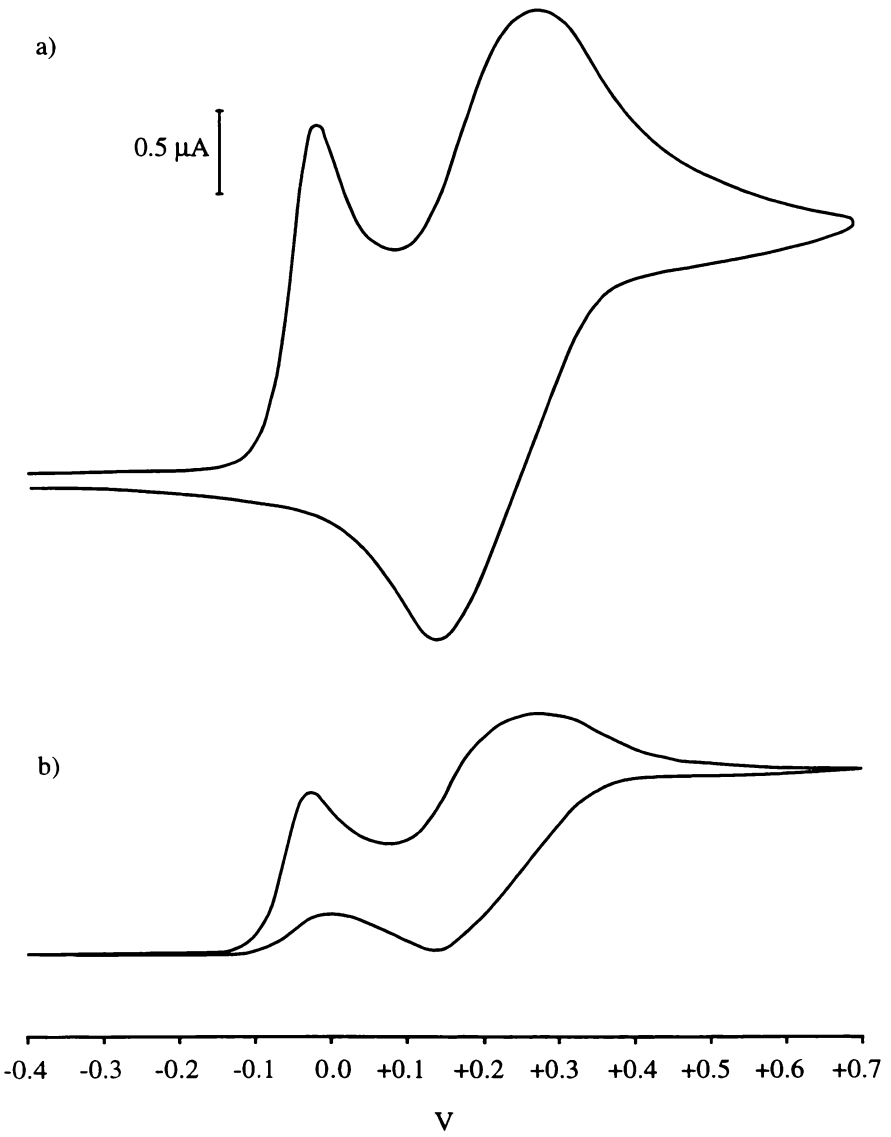

Figure 5.21: CVs of 1.1 mM **11**, a) scan rate 100 mV s^{-1}, b) scan rate 20 mV s^{-1}.

ferrocene centres, and that a small degree of electronic communication between the two centres is responsible for making the wave appear rounded. The ΔE_P for this redox wave is essentially independent of scan rate, and in contrast to all other situations discussed in this Section, is about 135 mV, an observation consistent with two merged redox processes.

Because of the overlapping nature of the waves it is difficult to compare the first and second redox processes in order to ascertain whether the first process should be considered to be one-electron or two-electron. However, comparison of $i_{PA(1)}$ for **11** as shown in Figure 5.21a with the values of $i_{PA(1)}$ for **1** and **2** as seen in Figures 5.9 and 5.14 suggests it may be

a one-electron process. In this situation there is no empirical evidence to suggest that the prominence of the second process is dependent on the reaction following the first process, since there is no variation in the reversibility of the first wave upon which such an observation might be based. However, this might be assumed on the basis of analogy with **1**, **2**, **5**, **24**, **25** and **32**, and a mechanism for oxidation of **11** might therefore be written thus:

$$\mathbf{11} \underset{+\,1e}{\overset{-\,1e}{\rightleftharpoons}} \mathbf{11}^{1+} \longrightarrow O^{1+} \underset{+\,2e}{\overset{-\,2e}{\rightleftharpoons}} O^{3+} \qquad [5]$$

As with compound **1**, it will be argued in this Chapter that the reaction of $\mathbf{11}^{1+}$ to give O^{1+} involves transfer of charge from an oxidised ferrocene centre to another part of the molecule, regenerating the ferrocene fragment. Both ferrocenyl groups are then reoxidised at a higher potential (giving O^{3+}).

Low-temperature cyclic voltammetric work was carried out on compound **11**, in order to attempt to produce a chemically reversible first anodic wave. This was done in dichloromethane in order to allow the temperature to be taken lower than is the case with acetonitrile solutions. However, even at -63° C it was found that the first anodic process was completely irreversible. Of interest, however, was the fact that in dichloromethane solution the two peaks of the second anodic process were more clearly differentiated than in acetonitrile solution, as can be seen in Figure 5.22. The cathodic peak in dichloromethane solution was large, irreproducible, and sharp, due to adsorption onto the electrode surface. Low temperature cyclic voltammetry using an acetonitrile solution was no more successful at inducing any reversibility in the first process than was the dichloromethane solution.

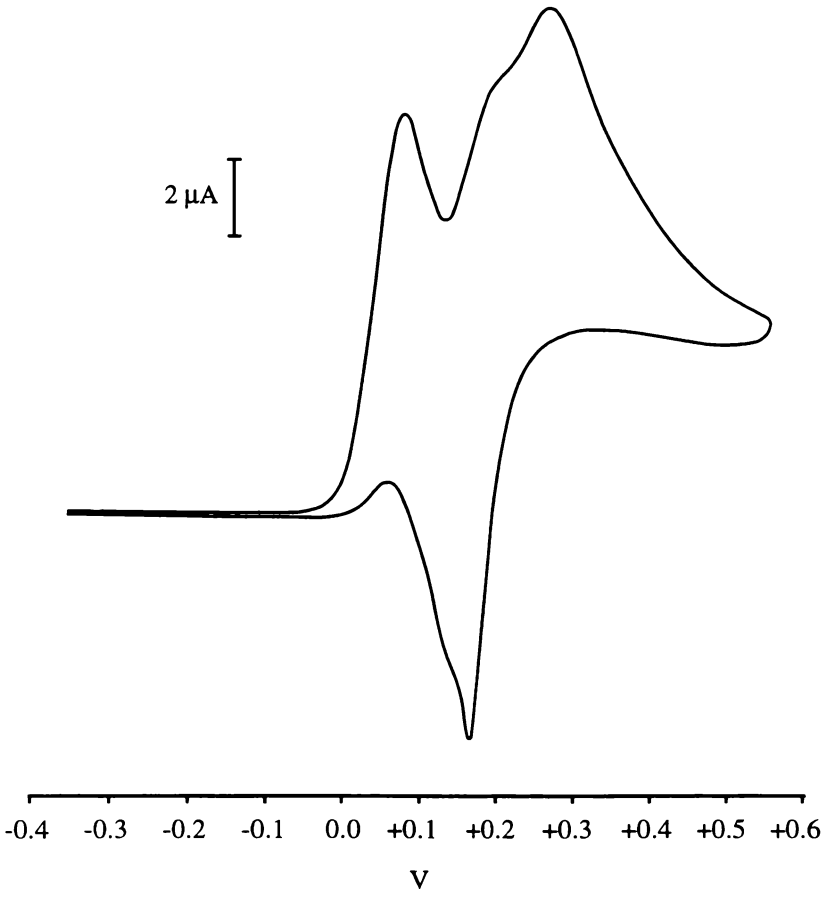

Figure 5.22: CV of 1.0 mM **11**, scan rate 100 mV s^{-1}, in dichloromethane, -63° C. The peaks of the second redox process showed differentiation at ambient temperature also, but the cathodic adsorption processes were much more prominent.

*5.2.1.2 Oxides, Sulfides and Phosphonium Salts $FcCH_2P(O)(CH_2OH)_2$ **3**, $FcCH_2P(O)Ph_2$ **15**, $FcCH_2P(S)(CH_2OH)_2$ **4**, $FcCH_2P(S)Ph_2$ **33**, $[FcCH_2P(Me)(CH_2OH)_2]I$ **8** and $[(FcCH_2)_2P(CH_2OH)_2]Cl$ **10***

The electrochemistry of the title compounds for this Section is much simpler than that observed for the compounds discussed in Section 5.2.1.1. All these compounds exhibit just a single, fully chemically reversible, redox wave assigned to the ferrocene/ferrocenium couple. Electrochemical data for these compounds are given in Table 5.2, and sample CVs are shown in Figure 5.23 and Figure 5.24. Reversibility was determined on the basis of ΔE_P and scan rate dependence of i_P, as with Section 5.2.1.1. The voltammetry of **8** was

Table 5.2: *E_{PA}, E_{PC} and $E_{1/2}$ data for compounds 3, 4, 8, 10, 15 and 33. FcH included as a reference. Potentials are listed in mV vs. Ag/Ag$^+$ (10 mM). Accuracies are ± 5 mV. Scan rate in all cases is 100 mV s^{-1}.*

	E_{PA}	E_{PC}	$E_{1/2}$
FcH	118; 126[$]	48; 63[$]	83; 95[$]
3	128	68	98
4	132	58	90
8	220	160	190
10	250	165	208
15	80	12	46
33[$]	159	70	115

[$] Measurement taken at Auckland University.

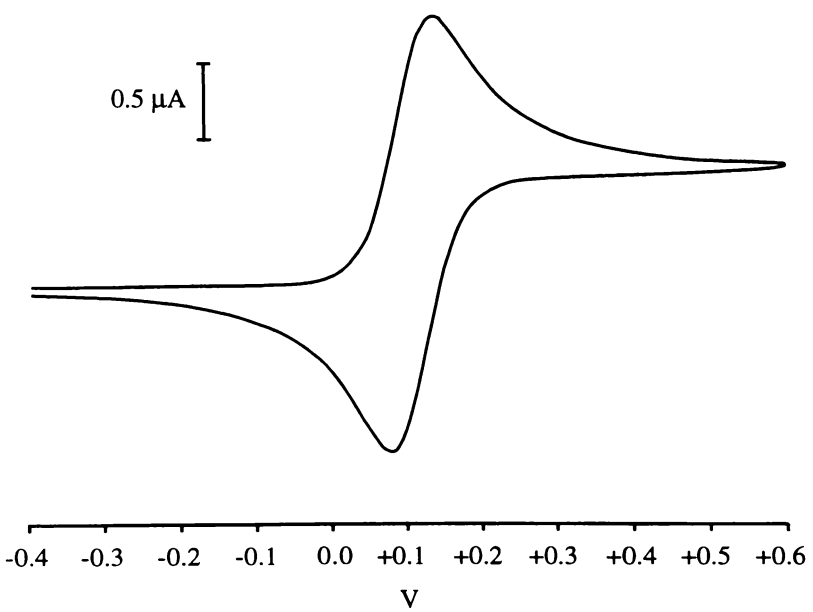

Figure 5.23: CV of 1.0 mM **4**, 50 mV s^{-1} scan rate.

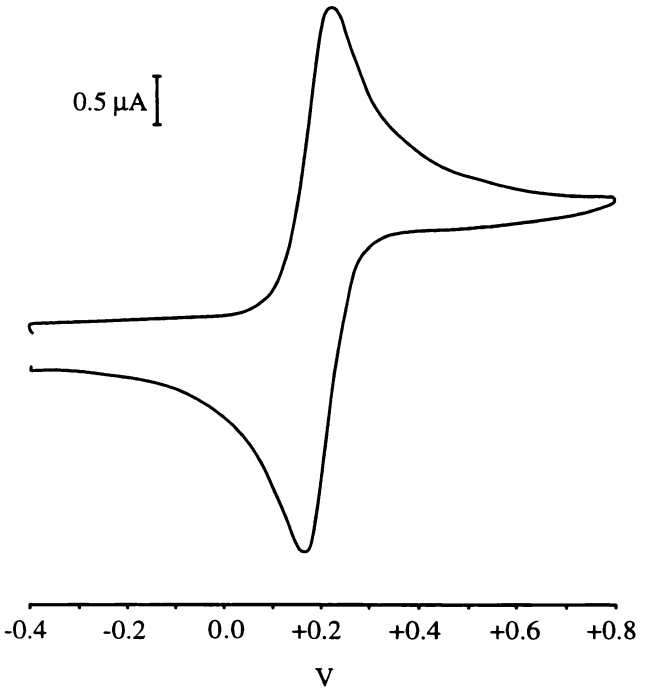

Figure 5.24: CV of 4.7 mM **8** after addition of $TlPF_6$, 50 mV s^{-1} scan rate.

complicated by the presence of the electroactive iodide ion; data for this compound were therefore gathered by first adding an equimolar amount of $TlPF_6$, in order to precipitate out the iodide as TlI.

Some observations can be made based on the data listed in Tables 5.1 and 5.2. Firstly, it is apparent that the presence of a lone pair of electrons on the phosphorus atom is important to the production of the second redox process witnessed for all compounds discussed in Section 5.2.1.1. Use of this lone pair in the production of a chemical bond, through synthesis of a phosphine chalcogenide or phosphonium salt, leads to a stabilisation of these compounds so that redox processes become chemically reversible.

Also, it is apparent that changes in the substituents at phosphorus do not strongly affect the redox potential of the first oxidation wave. The range of $E_{1/2}$ values for all compounds in these two tables, excepting **8** and **10**, extends from 15 to 115 mV, with ferrocene itself listed as 83 mV. The literature states that there is a 85 - 120 mV difference in redox

potentials for the compounds $FcPPh_2$ and $FcP(O)Ph_2$[14,17]. In comparison, the difference in redox potential between **2** and **15** is well within the margin of error. This can be demonstrated by the CV of a mixture of **2** and **15**, in which the main redox process for **2** is indistinguishable from that for **15** (Figure 5.25). This insensitivity of the ferrocene centre to the environment at the phosphorus centre is an important reason why assignment of unknown redox processes by correlation of $E_{1/2}$ or E_P data with data for authentic samples was not strongly pursued in this study.

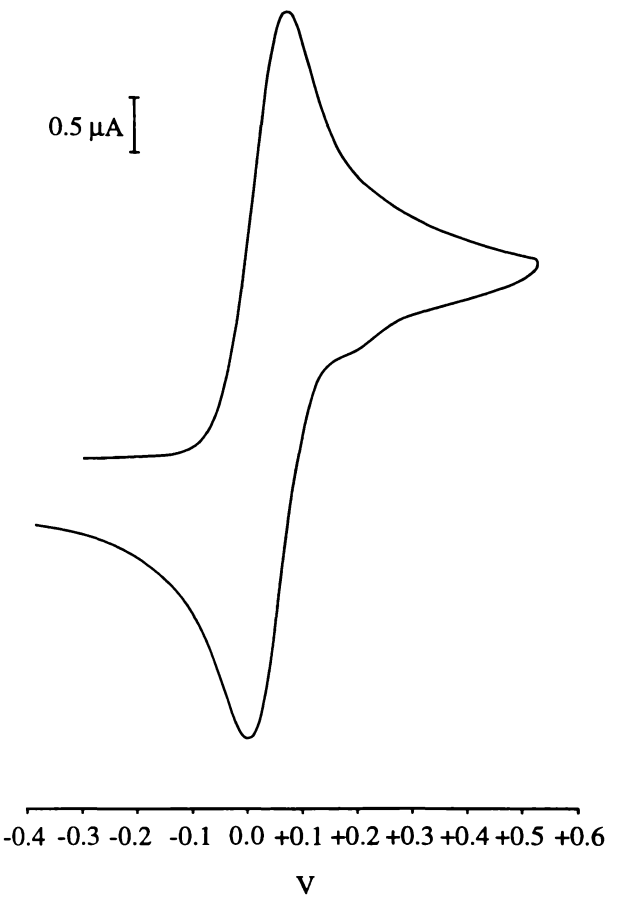

Figure 5.25: CV of a mixture *ca.* 1 mM in both **2** and **15**, scan rate 100 mV s^{-1}. It looks almost identical to a CV for **2** alone.

While the phosphorus environment did not generally strongly influence the ferrocene redox potential, in the phosphonium salts **8** and **10** considerable positive shifts in the redox potential were seen, of 173 and 193 mV respectively with respect to **1**. Clearly there will be

unfavourable electrostatic interactions in the doubly-charged product obtained by oxidation of **8** and **10**, accounting for these positive $E_{1/2}$ values, which are somewhat closer to the $E_{1/2(2)}$ values seen in Table 5.1 than to the $E_{1/2(1)}$ values.

5.2.1.3 $FcCH_2P(O)(CH_2NEt_2)_2$ 7

Compound **7** is of particular importance to the polymer studies described in the next Chapter, since it was designed as a monomeric model for the electrochemical behaviour of polymers formed by the condensation of multifunctional long-chain amines with **1**.

Two typical CVs are shown in Figure 5.26. Three distinct redox processes are apparent at positive potentials, and parameters for these are given in Table 5.3, though the overlapping nature of the peaks makes an accurate assessment difficult. All three waves bear the characteristics of one-electron electrochemically reversible processes. The first process is however chemically irreversible; at a scan rate of 20 mV s^{-1} it appears totally irreversible, but increasing the scan rate gives an increase in the ratio $i_{PC(1)}/i_{PA(1)}$, so that a scan rate of 1 V s^{-1} gives a value for this of *ca.* 1. Even at such a high scan rates the second and third processes are still visible (in the case of the second process only as shoulders on the first wave), but as with compounds discussed in Section 5.2.1.1, the prominence of these following redox processes seems dependent on the degree of reaction of the first oxidation product, implying that they are connected by chemical reaction. It should be noted that even where the switching potential is set at 150 mV, (i.e. prior to $E_{PA(2)}$), the first redox process appears totally irreversible at a scan rate of 20 mV s^{-1}, though it appears fully reversible at very high scan rates. At high scan rates another totally irreversible oxidative process becomes apparent at *ca.* 750 mV. At negative potentials an electrochemically irreversible redox couple is apparent, with E_{PC} = -1.090 V, E_{PA} = -630 mV. The current observed for this process increases in relative importance as scan rate is increased, and as with similar processes observed for the compounds in Section 5.2.1.1, this process at negative potentials is only seen where compound **7** has first been oxidised at positive potentials. The cyclic voltammetric behaviour of **7** was also investigated in DMF and found to be similar to

behaviour exhibited in acetonitrile, although the various peaks were not so well resolved. The complex electrochemical behaviour of **7** is disappointing in view of its implications for the electrochemical stability of polymers described in Chapter 6, which contain similar structures.

Table 5.3: *Electrochemical parameters for the three redox waves of 7, numbered 1, 2 and 3. Potentials are listed in mV vs. Ag/Ag^+ (10 mM). Accuracies are ± 5 mV. Scan rate was 100 mV s^{-1}. Data for an external ferrocene reference given in Table 5.1.*

	1	2	3
E_{PA}	105	195	338
E_{PC}	30	135	275
$E_{1/2}$	68	165	307

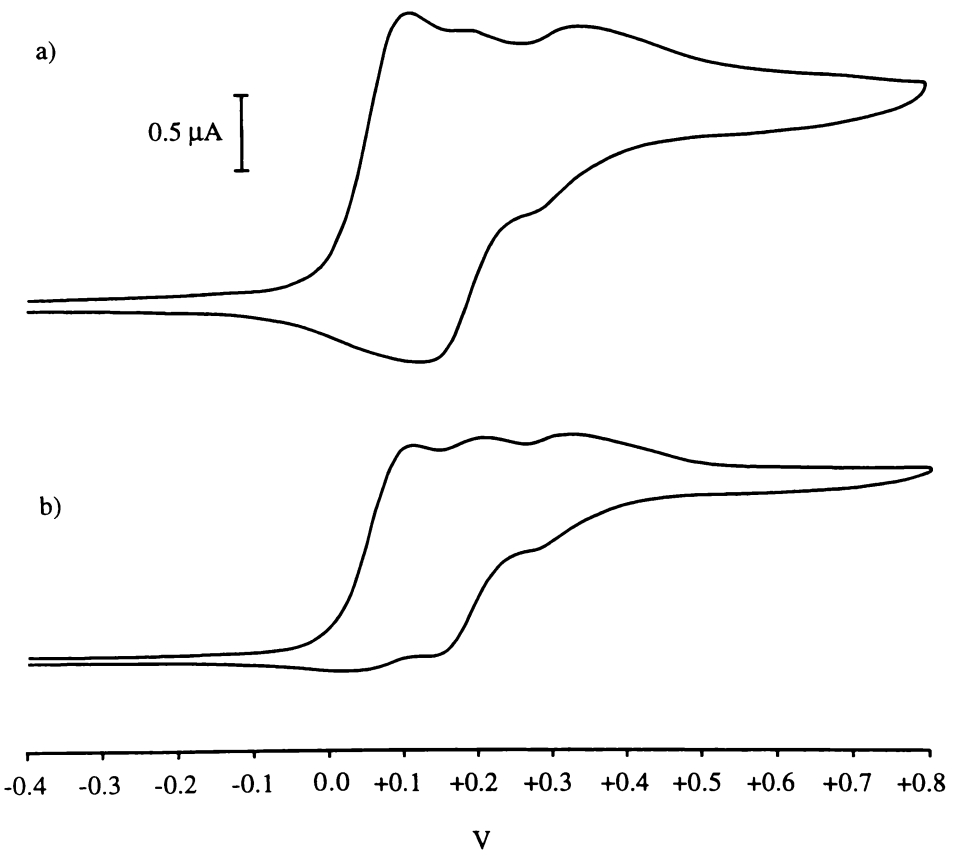

Figure 5.26: CV of 0.9 mM **7**, a) scan rate 100 mV s^{-1}, b) scan rate 50 mV s^{-1}.

5.2.1.4 *Ferrocenylphosphine Complexes* cis- $PtCl_2[FcCH_2P(CH_2OH)_2]_2$ **16**, $PdCl_2[FcCH_2P(CH_2OH)_2]_2$ **17**, $[Au\{FcCH_2P(CH_2OH)_2\}_2]Cl$ **18**, $RuCl_2(\eta^6\text{-}C_{10}H_{14})[FcCH_2P(CH_2OH)_2]$ **19**, $RuCl_2(\eta^6\text{-}C_{10}H_{14})(FcCH_2PPh_2)$ **20** and $RuCl_2(\eta^6\text{-}C_{10}H_{14})(FcCH_2PH_2)$ **29**

The electrochemistry of several complexes of **1** was examined, in addition to the electrochemistry of compounds **20** and **29**, containing the ligands **2** and **24** respectively. In the case of compounds **16**, **17** and **18** it was found that the only dominant feature observed was one electrochemically reversible redox process. Electrochemical data for these compounds are given in Table 5.4. In compounds containing more than one ferrocene unit, separate redox waves for each chemically identical ferrocene unit can result from interaction between ferrocene centres[8,25]. If no such 'communication' is present, all ferrocene centres are oxidised at the same potential. The latter description applies in the case of these compounds, as would be expected, since the length of spacer chain and lack of conjugation between ferrocene groups in **16**, **17** and **18** would make electrochemical interaction unlikely. The ΔE_P in all cases is suggestive of a one-electron rather than a two-electron redox process. This is entirely consistent with the idea of two electrochemically independent

Table 5.4: *Electrochemical data for compounds 16, 17 and 18. Potentials are in mV vs. Ag/Ag$^+$ (10 mM). Accuracies are ± 5 mV. The values for FcH and the first redox wave of 1 are provided for comparison. Scan rate in all cases is 100 mV s^{-1}.*

	E_{PA}	E_{PC}	$E_{1/2}$
FcH	118	48	83
1	50	-20	15
16	150	65	108
17	160	80	120
18	168	90	129

ferrocene centres in each compound undergoing one-electron oxidations. The number of electrons involved in the process could not be estimated from measurement of peak currents, since these compounds displayed limited solubility in acetonitrile, meaning that saturated solutions of unknown concentration were used in order to carry out the measurements.

In addition to the major redox wave, compound **18** also displays some additional behaviour. Where the forward sweep is in the positive direction, the reverse sweep shows a cathodic peak of low current at *ca.* -1.5 V. Associated with this cathodic peak is an anodic peak at *ca.* -0.9 V; on repeat cycles the anodic peak at 168 mV begin to spike in a fashion suggestive of absorption onto the electrode surface, and another anodic peak of low current at *ca.* 1 V appears. When compound **18** is only subjected to moderate voltage extremes, e.g. sweeping from -0.4 to +0.5 V, its behaviour appears simple and entirely analogous to that of **16** and **17**.

Coordination of **1** in these compounds leads to a positive shift in oxidation potential of *ca.* 100 mV. A positive shift in potential for ferrocene-centred oxidations is the usual trend upon coordination of ferrocenylphosphines[7e,f,h,j,l,o,9,13], as would be expected; coordination to the metal centre draws electron density away from the phosphine centre and consequently the ligand, leading to an increase in the ferrocene redox potential.

The compounds **19**, **20** and **29** all showed similar behaviour, and typical CVs are shown in Figures 5.27, 5.28 and 5.29. It will be seen that two main processes are observed, the first being an electrochemically and chemically reversible wave at moderately oxidising potentials. This wave is assigned as a one-electron ferrocene-based oxidation. The second process takes place at more positive potentials and is chemically irreversible, although only in the case of **29** is the corresponding cathodic peak not observed at all. This wave is assigned to the oxidation of Ru(II) to Ru(III), and consequent reaction of the complex. Electrochemical data for the three compounds are given in Table 5.5. Note that ΔE_P for the second process in **19** and **29** is larger than usually observed using the experimental setup employed during

electrochemical studies. This is not quasi-reversible behaviour, since ΔE_p does not change with scan rate. Possibly the shape of the wave is distorted by the small size of the cathodic peak, meaning that the reported measurements of $E_{PC(2)}$ are not accurate.

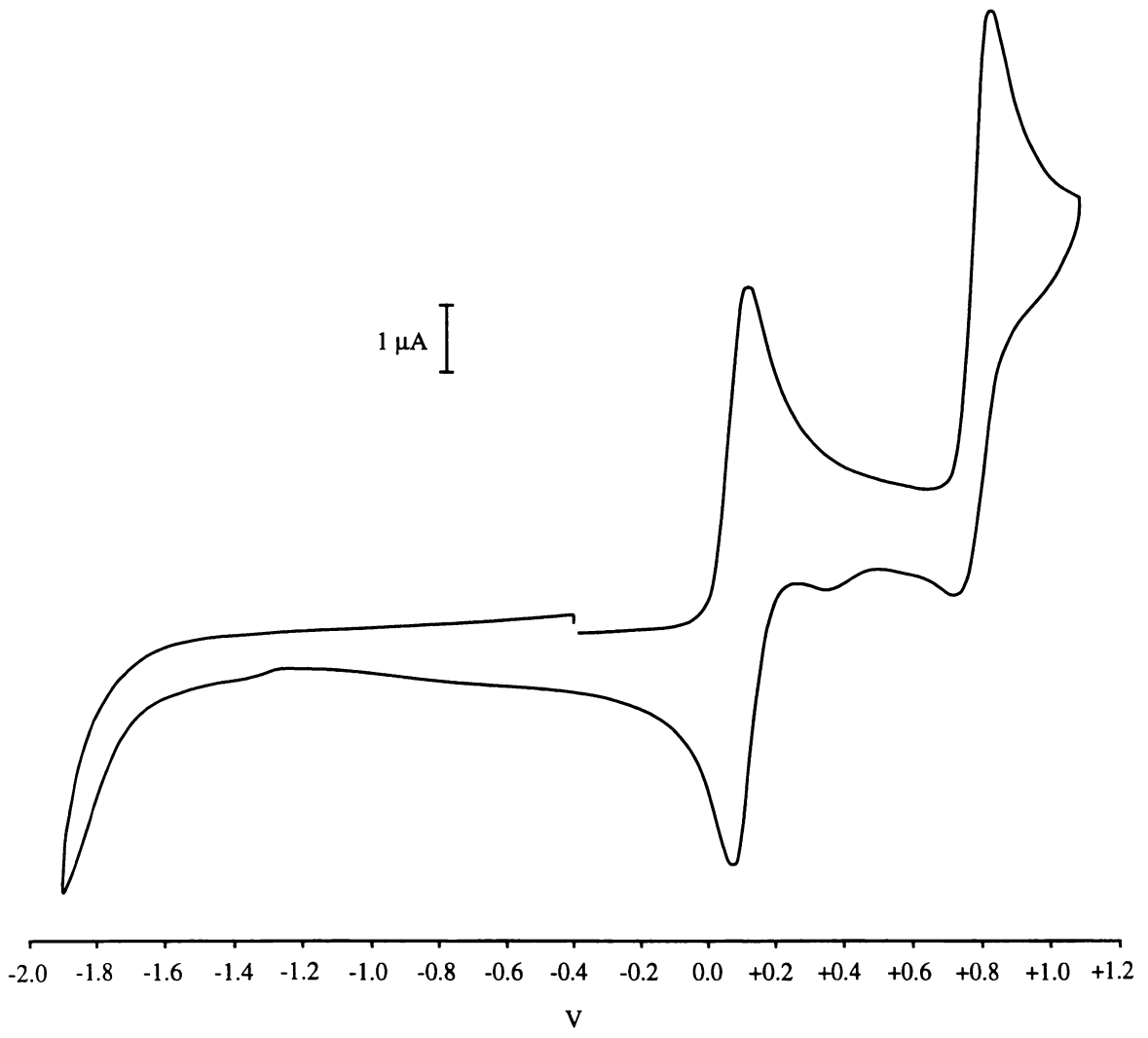

Figure 5.27: CV of 1.1 mM **19**, scan rate 100 mV s^{-1}.

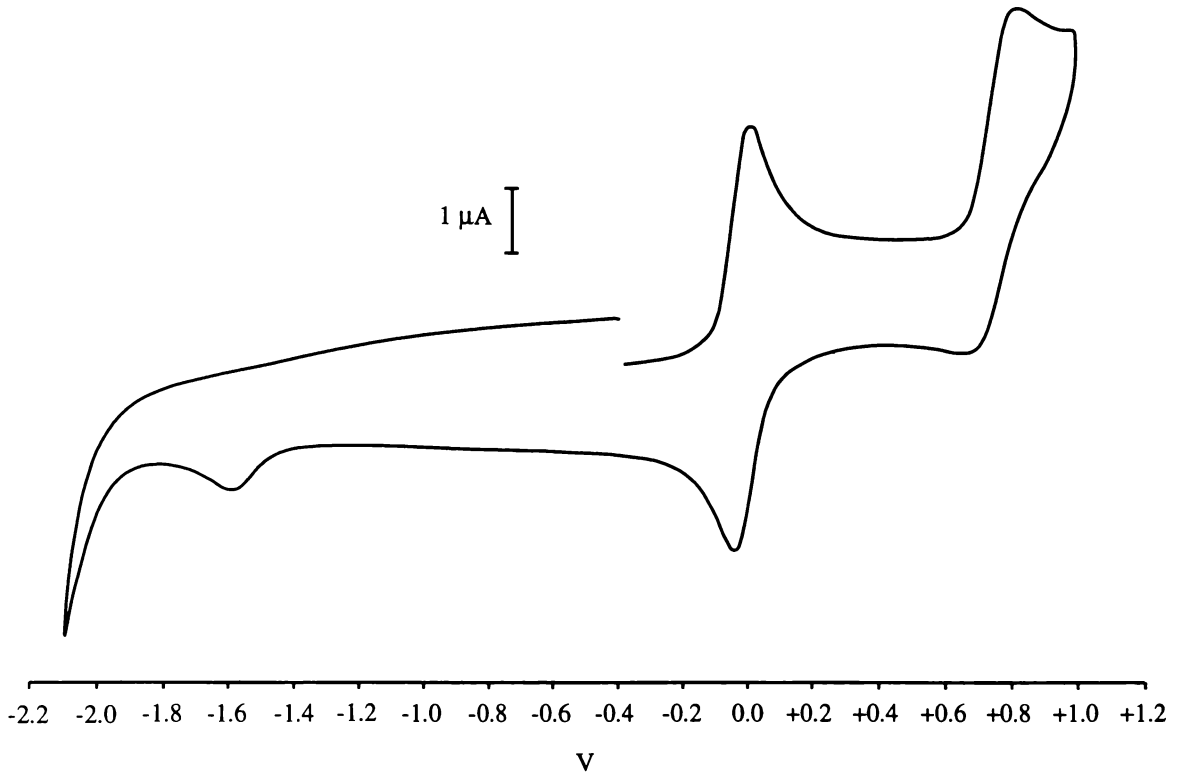

Figure 5.28: CV of 0.9 mM **20**, scan rate 200 mV s^{-1}.

Table 5.5: *Electrochemical data for compounds **19**, **20** and **29**, with data for FcH provided for comparison. Potentials are given in mV vs. Ag/Ag^+ (10 mM). Accuracies are ± 5 mV. Scan rate in all cases is 100 mV s^{-1}.*

	$E_{PA(1)}$	$E_{PC(1)}$	$E_{1/2(1)}$	$E_{PA(2)}$	$E_{PC(2)}$	$E_{1/2(2)}$
FcH	118	48	83	-	-	-
19	122	58	90	845	740	788
20	-5	-68	-37	790	660	725
29	132	72	102	865	-	-

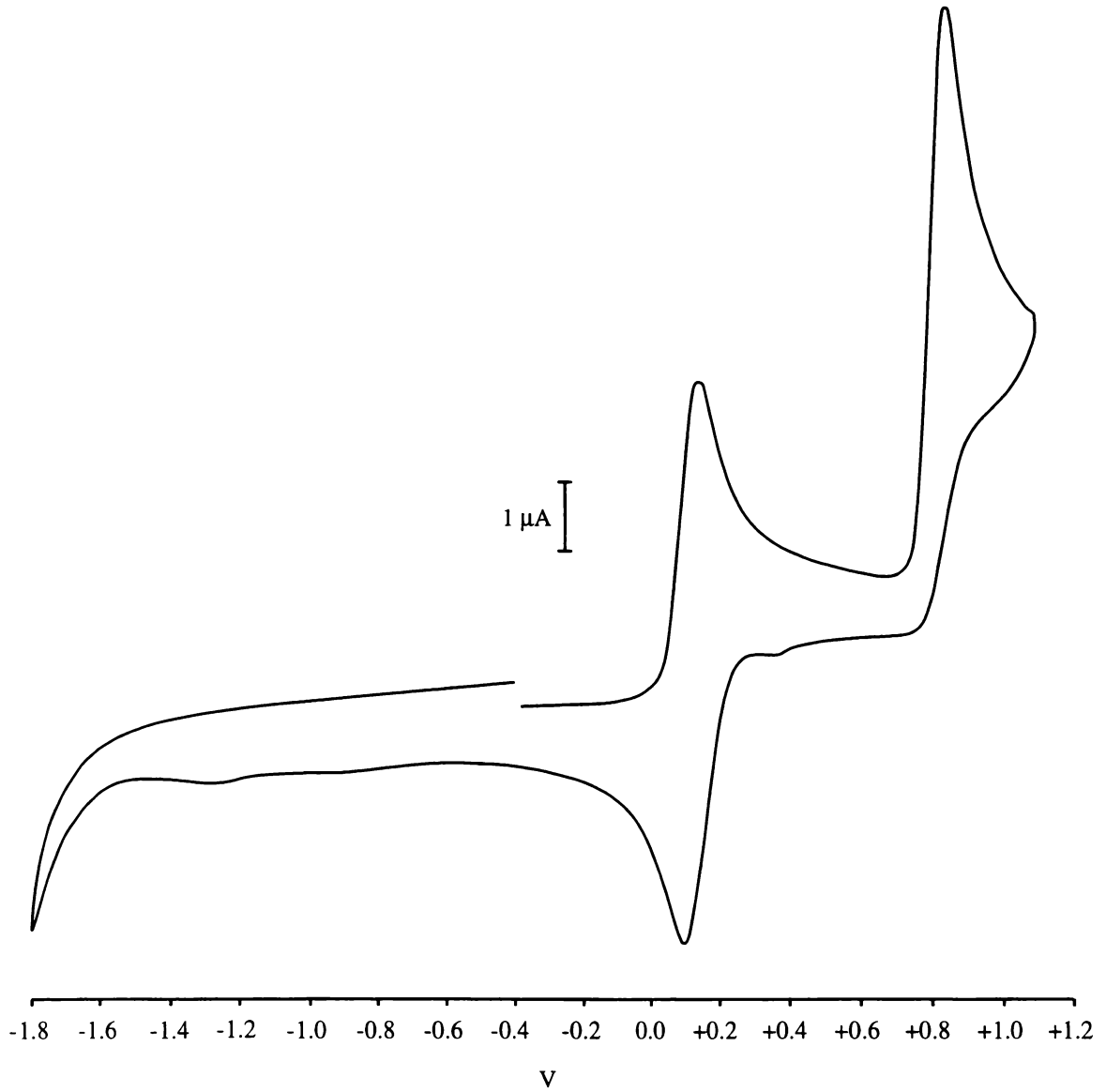

Figure 5.29: CV of 1.1 mM **29**, scan rate 100 mV s^{-1}.

Both **19** and **29** display a minor cathodic peak associated with the ruthenium oxidation, with peak potentials of approximately 340 mV and 350 mV respectively. This gives an appearance to the CVs reminiscent of the behaviour of the free ferrocenylphosphines (Section 5.2.1.1). However, the potentials of the cathodic peaks for **19** and **29**, both major and minor, are too positive to be due to the release of free phosphine during complex reaction. This minor process and another cathodic peak observed for all three complexes at -1.58 V (**19** and **20**) or -1.28 V (**29**), are only seen where the forward sweep first oxidises the Ru(II) centre, and are therefore attributable to reduction of product(s) formed through oxidation of the complex.

One feature of the voltammetry of both **19** and **29** which requires explanation is the fact that in both cases $i_{PA(2)}/i_{PA(1)}$ is considerably greater than 1. In the case of **29** $i_{PA(2)}/i_{PA(1)}$ was in fact closer to 2. This may be due to absorption processes taking place at the electrode surface during the oxidation of the Ru(II) centre. A microelectrode voltammogram of **29** (Figure 5.30) gave a more acceptable ratio of $\Delta i_{(2)}/\Delta i_{(1)}$ of 1.3. The reasons for the remaining discrepancy are uncertain.

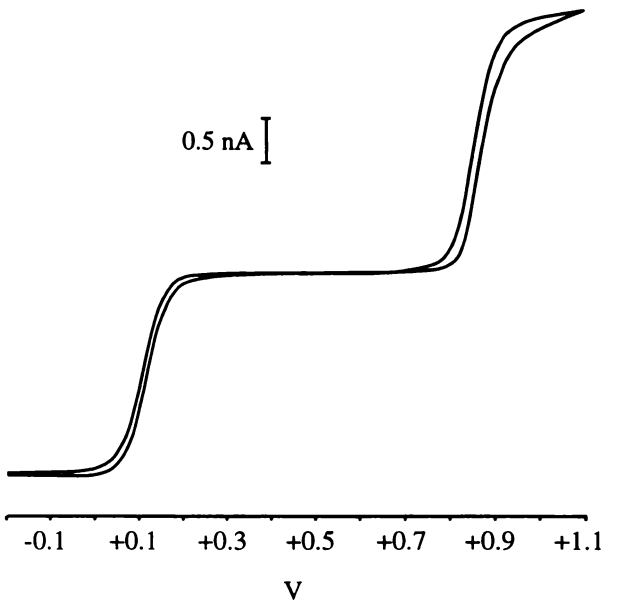

Figure 5.30: A microelectrode voltammogram of 1.1 mM **29**, scan rate 20 mV s^{-1}.

Another unusual feature, in this case involving compound **20**, is the effect of coordination on the redox potential of the ferrocene centre. As was discussed above, coordination to a metal centre would in most cases be expected to shift the redox potential of a ferrocenylphosphine ligand in a positive direction, as electron density is drawn away from the ligand. This general expectation is fulfilled by both **19** and **29**, but in the case of **20** the redox potential of the ligand is actually *lowered* upon coordination, from $E_{1/2}$ of 49 mV to -37 mV. In the very similar Ru(II) complexes $RuCl_2(\eta^6$-hexamethylbenzene$)(FcPPh_2)$ and $RuCl_2(\eta^6$-hexamethylbenzene$)[(\eta^5\text{-}C_5H_4PPh_2)Fe(\eta^5\text{-}C_5H_4COOH)]$, the same situation is encountered; coordination of the ferrocenylphosphine ligand to the ruthenium leads to a drop in the redox potential of the ligand[7a]. This was explained by invoking strong backbonding

from the ruthenium to the phosphine. In the present case however, it is not clear why strong back-bonding should apply to ligand **2**, but not to **1** or **24**. One possibility stems from the fact that arylphosphines are generally known to be better backbonding π-acceptors than alkylphosphines; this is consistent with the lowered redox potentials of **2**, $FcPPh_2$ and $(\eta^5\text{-}C_5H_4PPh_2)Fe(\eta^5\text{-}C_5H_4COOH)$ upon complexation, in contrast to the behaviour of the alkylphosphines **1** and **24**. The electrochemical behaviour of the compounds $RuCl_2(\eta^6\text{-}$hexamethylbenzene$)(FcPPh_2)$ and $RuCl_2(\eta^6\text{-}$hexamethylbenzene$)[(\eta^5\text{-}C_5H_4PPh_2)Fe(\eta^5\text{-}C_5H_4COOH)]$ was also similar to that of compounds **19**, **20** and **29** in other respects. For the former compounds a wave is seen at moderate potentials corresponding to Fc/Fc^+, and another at higher potentials corresponding to Ru(II)/Ru(III). However, the second wave for these compounds was found to be chemically reversible, which was not the case for **19**, **20** and **29**.

5.2.1.5 $Ru_3(CO)_9(\mu^2\text{-}H)_2(\mu^3\text{-}PCH_2Fc)$ **30**

The cyclic voltammetric response of compound **30** has been investigated. It shows a chemically and electrochemically reversible one-electron oxidation with E_{PA} = 150 mV, E_{PC} = 90 mV vs. Ag/Ag^+ (10 mM), clearly attributable to the oxidation/reduction of the ferrocene moiety. The $E_{1/2}$ of 120 mV shows a positive shift of 75 mV with respect to **24** (Table 5.1) under the same conditions, indicating a moderate polarising effect of the cluster upon the ferrocenyl centre similar to that discussed in Section 5.2.1.4. In contrast to what has been reported for related metal carbonyl clusters such as $Ru_3(CO)_{12}$[26,27], $Os_3(CO)_{12}$[26] and $[Os_3(CO)_9\{\mu^3\text{-}\eta^4\text{-}Fe[C_5H_4(C_2SiMe_3)]_2\}]$[28] no two-electron reduction was observed at negative potentials within the solvent limit, nor a one-electron reduction, as observed for many cobalt-containing monocapped trimetal carbonyl clusters[29]. Cluster-based oxidations of **30** were also not observed within the solvent limit.

5.2.2 Further Investigation of the Electrochemical Behaviour of $FcCH_2P(CH_2OH)_2$ **1**, $FcCH_2PPh_2$ **2** and $FcCH_2P(CH_2CH_2CN)_2$ **5**

5.2.2.1 BE Behaviour of $FcCH_2P(CH_2OH)_2$ 1 and $FcCH_2PPh_2$ 2

In order to obtain a better understanding of the electrochemical behaviour of the class of compounds $FcCH_2PR_2$, aspects of which were introduced in Section 5.2.1.1, further studies were carried out using **1** and **2** as representative examples. They were chosen because they represented extremes of electrochemical activity, were available in good quantities, and were stable for long periods of storage.

One-electron oxidative controlled-potential or controlled-current BE of **1** was carried out on several occasions, always yielding a yellow solution with similar electrochemical characteristics. A typical CV obtained from this electrolysed solution is shown in Figure 5.31. Typically the two redox processes observed at positive potentials are of equal size, although this varies somewhat, presumably due to inaccuracies in the level of oxidation

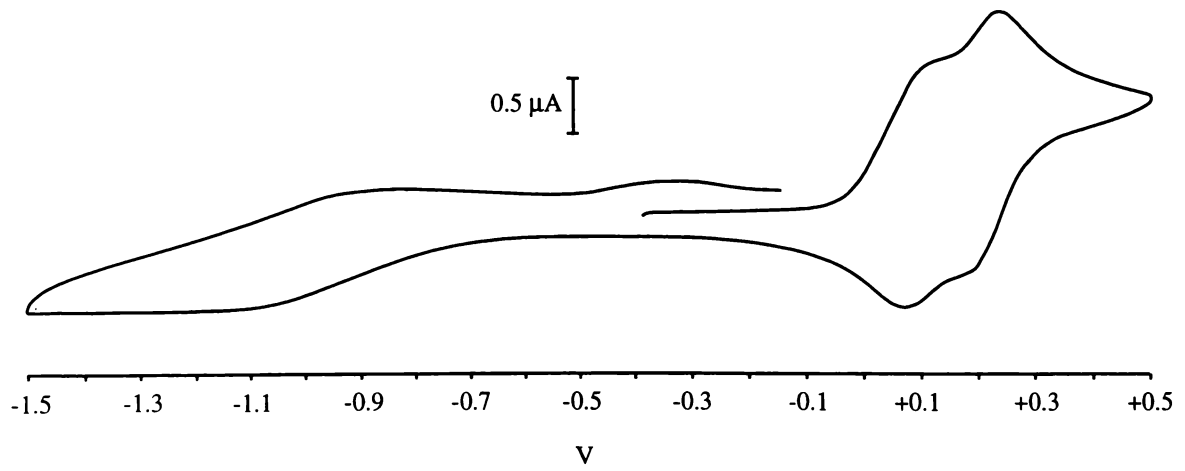

Figure 5.31: CV of a solution of **1** after one-electron controlled-potential oxidation, scan rate 50 mV s^{-1}.

achieved, or perhaps the time for which the solution is left before cyclic voltammetric investigations are carried out. Electrochemical parameters for these processes are provided in Table 5.6, along with those for several other electrolysed solutions discussed in this Section. Both waves appear fully reversible. In addition, prominent waves are observed at cathodic potentials, one reduction (E_{PC} = *ca.* -1.04 V) and two oxidations (E_{PA} = *ca.* -0.89, -0.35 V). These are observed regardless of initial sweep direction. Steady-state voltammetry of the solutions before and after BE implies that a large amount of material becomes electro-inactive during BE, since the level of ferrocene-based anodic current typically drops to one-third of pre-electrolysis levels; over a series of eight BE experiments, the average level of current seen after electrolysis was 35% of the current seen prior to BE, and the range extended from 24% to 54%. The chemical nature of the species produced during BE was investigated by running a ^{31}P-NMR spectrum of the electrolysed solution, which was acquired over a period of 23.5 minutes; a signal at 24 ppm and paired signals at *ca.* 114 and 22 ppm are observed. This spectrum is shown in Figure 5.32.

Table 5.6: *Electrochemical parameters for redox waves observed at positive potentials in solutions of 1 or 2 subjected to one-electron oxidation. Potentials are given in mV, vs. Ag/Ag$^+$ (10 mM). Accuracies are ± 5 mV. Scan rate in all cases is 100 mV s^{-1}.*

	solvent	$E_{PA(1)}$	$E_{PC(1)}$	$E_{1/2(1)}$	$E_{PA(2)}$	$E_{PC(2)}$	$E_{1/2(2)}$
1	CH_3CN	115	60	92.5	235	180	208
1	CH_2Cl_2	-	-	-	355	255	325#
2	CH_3CN	65	-8	29	228	155	192
2	CH_2Cl_2	*ca.* 240	200	230*	342	282	312
2	DMF	65	*ca.* -5^	30	242	155	199

Due to the unusual nature of the cathodic peak, the $E_{1/2}$ for this process has been calculated as E_{PA} -30 mV.

* Due to difficulty in precisely locating the anodic peak, the $E_{1/2}$ for this process has been calculated as E_{PC} +30 mV.

^ This peak is rather broad and could consist of two overlapping peaks.

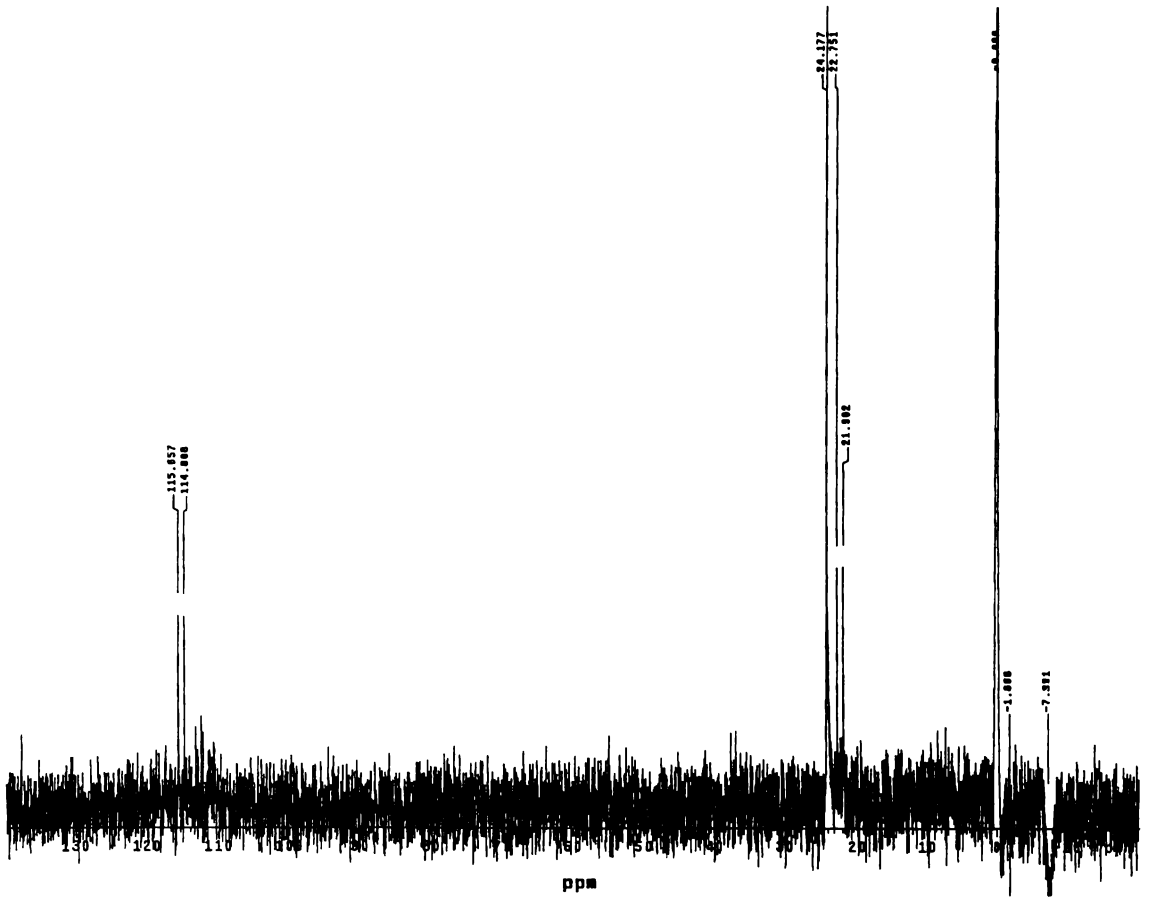

Figure 5.32: ^{31}P-NMR spectrum of an acetonitrile solution of **1** after removal of one electron per molecule by BE. 'Coupling constants' for the 'doublets' at *ca.* 22 and 114 ppm are 102 Hz in both cases.

The one-electron oxidation of **1** proved to be irreversible, regardless of whether the subsequent reductive BE was carried out with a Pt or GC electrode. Attempted reversal of the oxidation with a Pt electrode gave an orange, cloudy solution, with only irreversible anodic processes seen at positive potentials, these giving large currents and sharp irreproducible peaks due to electrode absorption processes. Reversal of oxidation with a GC electrode led to a brown solid crashing out of solution, leaving no colour in solution. Examination of this solid by ^{31}P-NMR in DMF solution suggested that it contained many different compounds (or contained no phosphorus!), since no peaks could be detected.

The electrochemical behaviour of **1** is somewhat different when a one-electron oxidation is carried out in dichloromethane. A typical CV of the electrolysed solution is shown in Figure 5.33. Only one redox process is seen at anodic potentials. The rather large cathodic peak current is suggestive of absorption processes, such as were seen for cyclic voltammetry of the starting material **1**. As with acetonitrile solutions, after the electrolysis the solution was yellow. Use of steady-state voltammetry to assess the level of electro-active ferrocene species in solution was not reliable due to the adsorption processes being seen upon oxidation, which interfered with flow of current.

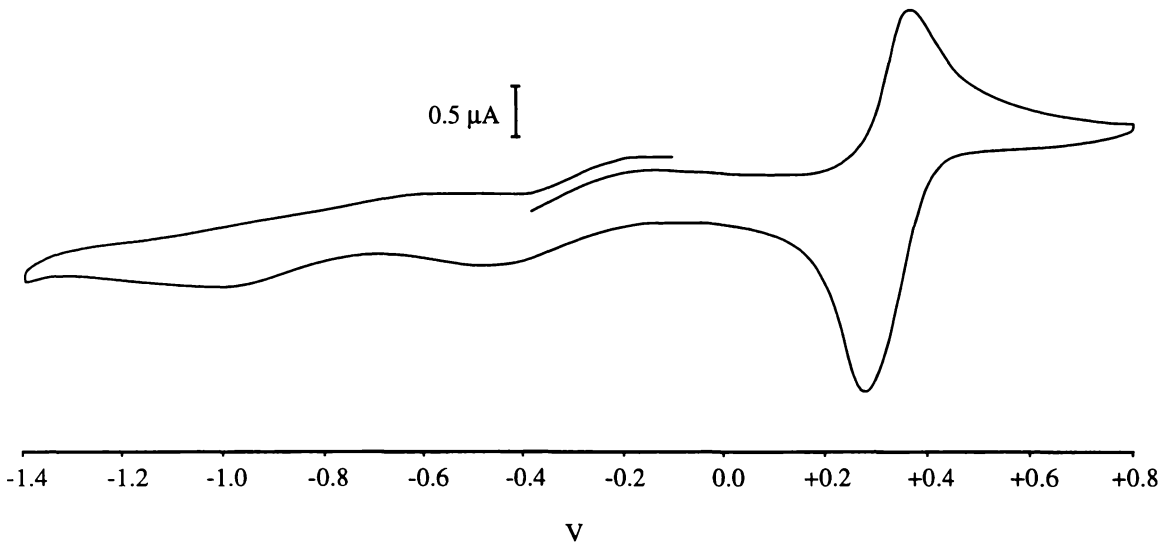

Figure 5.33: CV of a 1.0 mM solution of **1** in dichloromethane after removal of one-electron per molecule by BE, scan rate 100 mV s^{-1}.

The BE behaviour of **2** is in many ways similar to that of **1**. A typical CV for a solution of **2** subjected to a one-electron controlled-potential oxidation is shown in Figure 5.34. As with **1**, two redox processes are seen at positive potentials, which both appear to be fully reversible one-electron processes, and are seen in a ratio of 1:1. The immediately obvious contrast to the behaviour of **1** is the presence of a well-defined and chemically irreversible peak at a potential of -1.27 V, which is observed regardless of direction of the initial forward sweep, and is of comparable size to the two processes at positive potentials. The solution took on a slightly green tinge during BE, but returned to a yellow colour by the time one

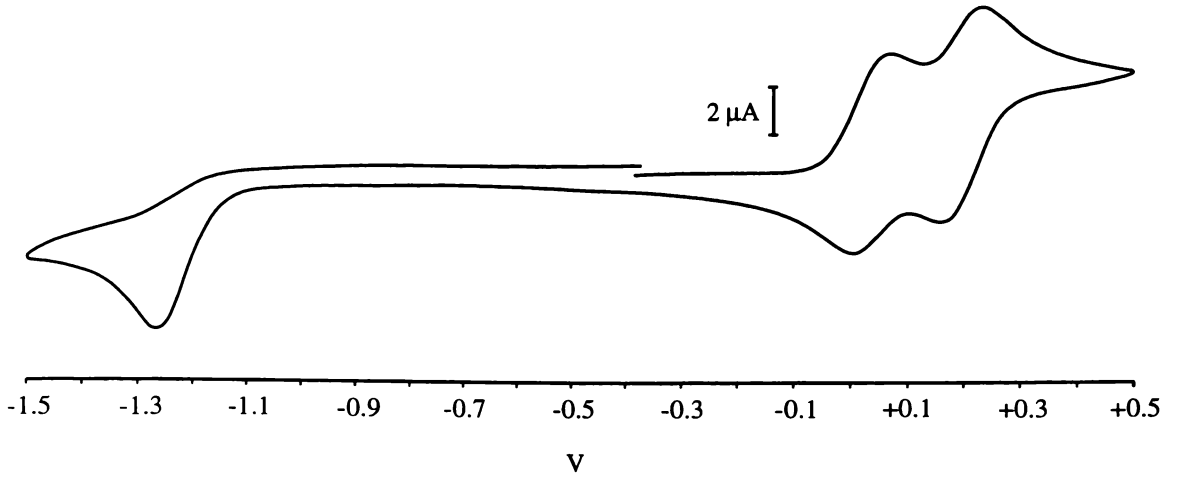

Figure 5.34: CV of 5.0 mM **2** subjected to a one-electron oxidation, scan rate 100 mV s^{-1}.

electron of charge per molecule had been removed. Confirmation of the fact that ferrocenium species were not present in the final solution could be obtained from microelectrode steady-state voltammetry, which showed that although the solution had been oxidised by one electron per molecule, the only reducible species present in the final bulk solution could be reduced only at quite negative potentials, corresponding to the peak at -1.27 V seen by cyclic voltammetry. Steady-state voltammograms illustrating this point are shown in Figure 5.35. A ^{31}P-NMR obtained of a solution of **2** subjected to a one-electron oxidation is shown in Figure 5.36, and comparison with Figure 5.32 shows that both **1** and **2** produce similar chemical species upon BE. The spectrum was obtained over a period of *ca.* 4 minutes. In this case the paired peaks at *ca.* 25 ppm and 110 ppm are present in quite different intensities, but this may stem from the fact that it was generally observed in BE experiments involving both **1** and **2** that over time in solution the peaks at *ca.* 25 ppm would decrease in intensity relative to the peaks at *ca.* 110 ppm. Reconstitution of the NMR sample used for Figure 5.36 to give a solution suitable for cyclic voltammetry showed differences in the cyclic voltammetric behaviour over time, with slight changes in the intensities and potentials of the various peaks apparent (Figure 5.37). A ^{31}P-NMR spectrum obtained from a solution of **2** from which 0.5 electrons per molecule were removed shows large peaks for both the starting material and the oxidation products, as would be expected (Figure 5.38). In contrast to the behaviour of **1**, the BE oxidation of **2** proved to be partially reversible. Controlled-

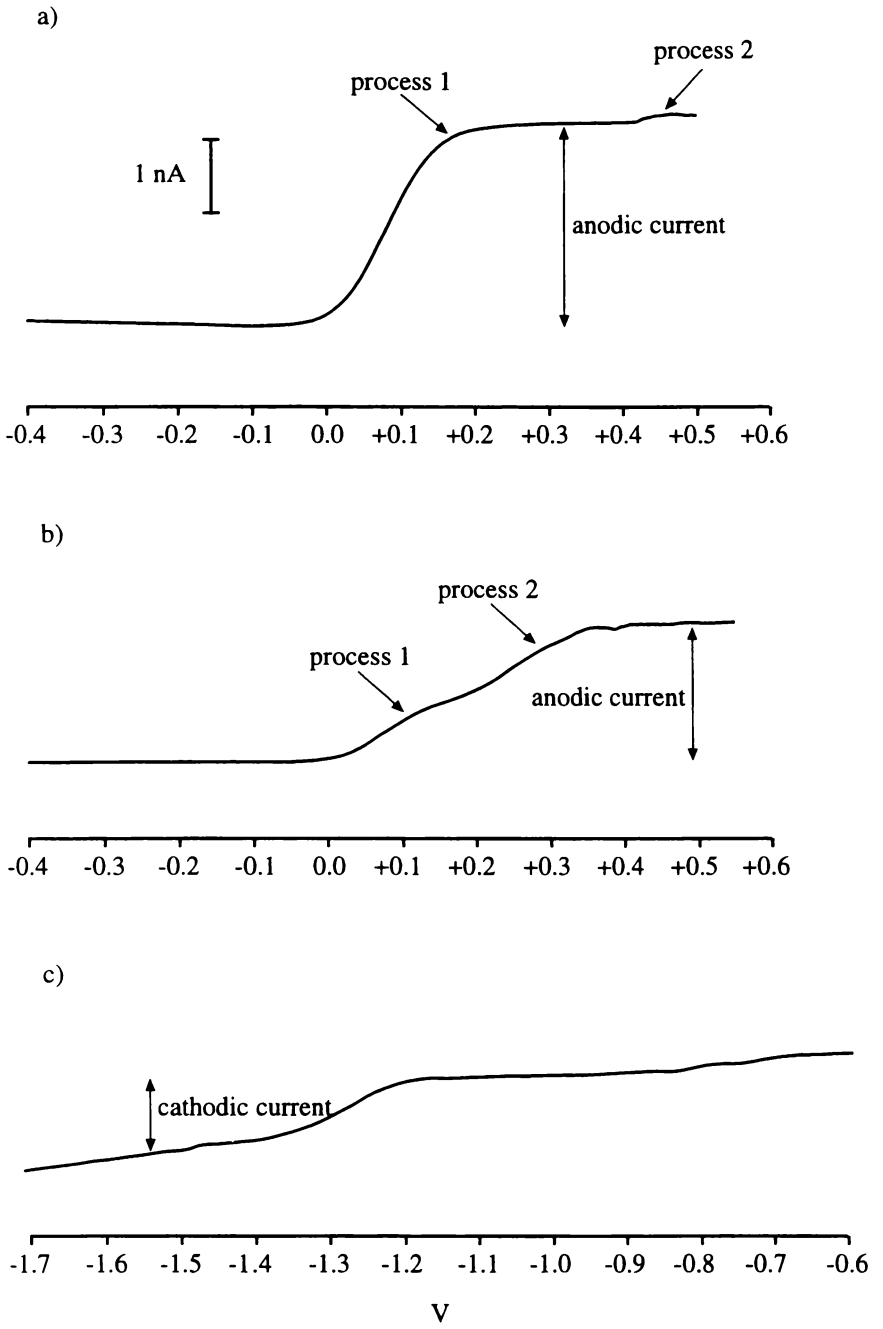

Figure 5.35: Steady-state voltammograms of a 1.0 mM acetonitrile solution of **2**, scan rate 50 mV s^{-1}. a) before BE, a wave is seen corresponding to the major cyclic voltammetric process, with a much smaller shoulder at more positive potentials corresponding to the second cyclic voltammetric process. b) Two redox waves of equal size are seen at positive potentials after BE, with no evidence of ferrocenium species in the bulk solution. c) Only at quite negative potentials is a cathodic current observed.

current one-electron oxidation of a 5.0 mM solution of **2** gave a solution displaying typical cyclic voltammetric behaviour (That is, similar to that shown in Figure 5.34). This was immediately subjected to a controlled-current one-electron reduction. The resulting cyclic voltammetric behaviour is shown in Figure 5.39, and a ^{31}P-NMR for the solution shown in Figure 5.40. Comparison with authentic samples showed that the two largest peaks in the ^{31}P-NMR spectrum were **2** (starting material) and **15** (phosphine oxide) in a ratio of *ca.* 3.7/1 respectively. Two-electron BE of **2** led to a reduction in the size of the first anodic process. The solution also went green, suggesting that this further oxidation was largely assignable to a simple ferrocene/ferrocenium couple. This was confirmed by steady-state voltammetry, which showed 68% of the ferrocene groups in solution to be in the oxidised state.

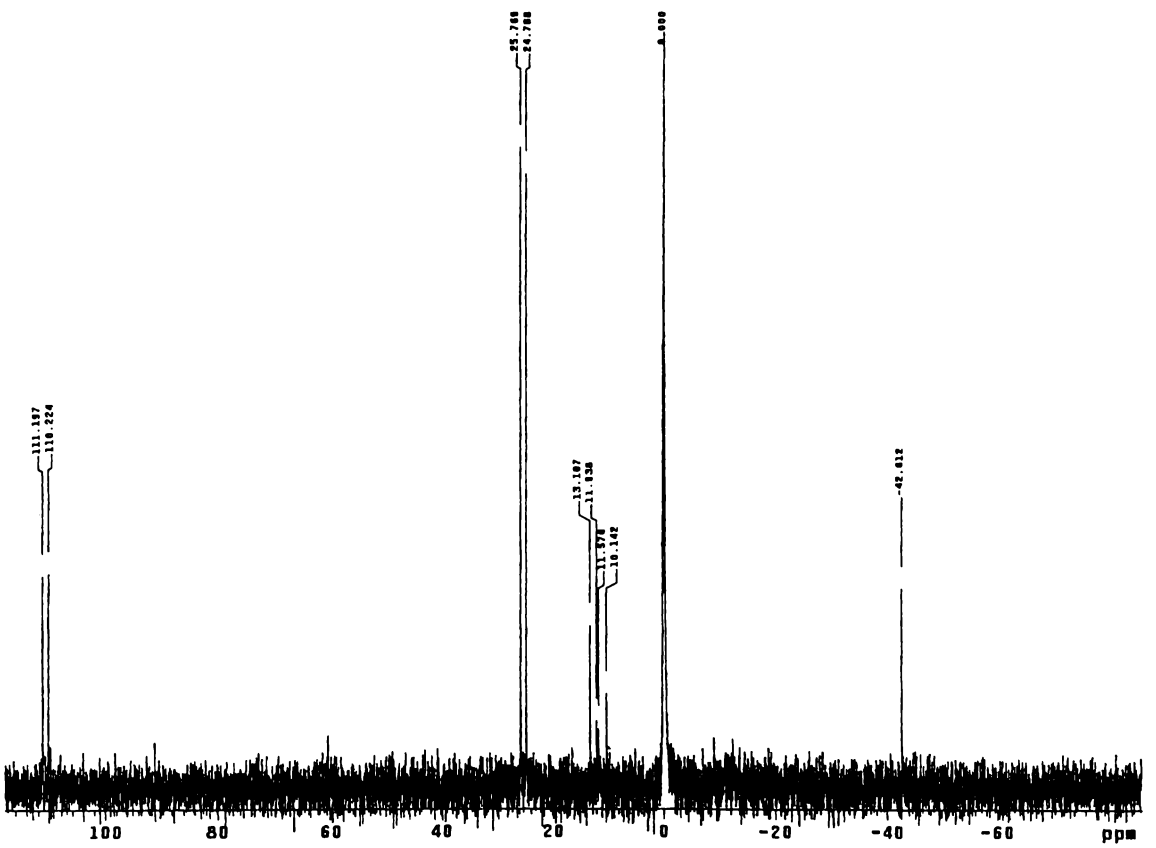

Figure 5.36: ^{31}P-NMR spectrum obtained of the same solution referred to in Figure 5.34. The peak at *ca.* -43 ppm is in fact believed to be an electronic spike. 'Coupling constants' for the two 'doublets' at *ca.* 25 ppm and 110 ppm are 119 and 118 Hz respectively.

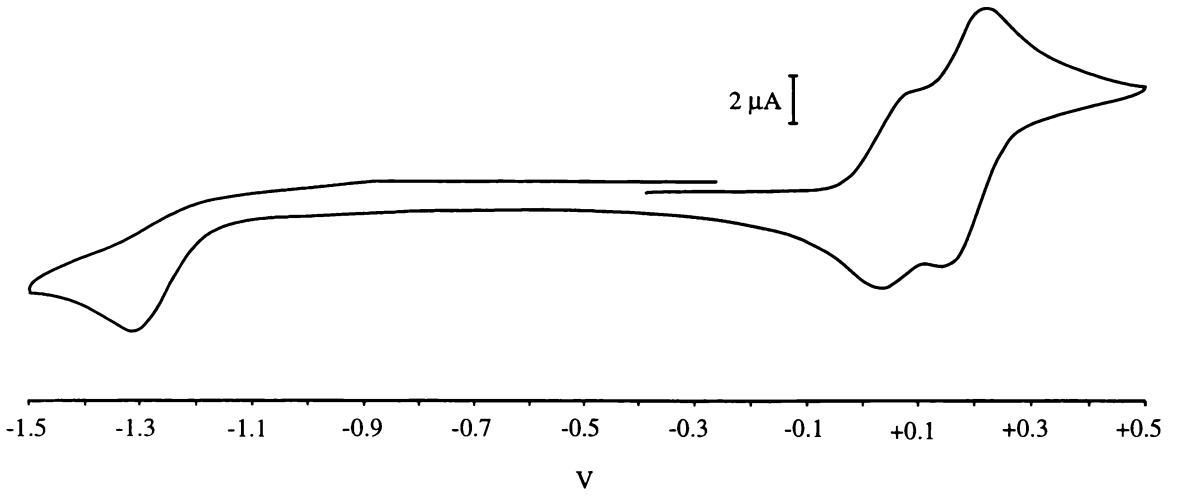

Figure 5.37: CV of a solution made by reconstitution of the NMR solution referred to in Figure 5.36. This is therefore not strictly comparable with the CV of the original solution in Figure 5.34.

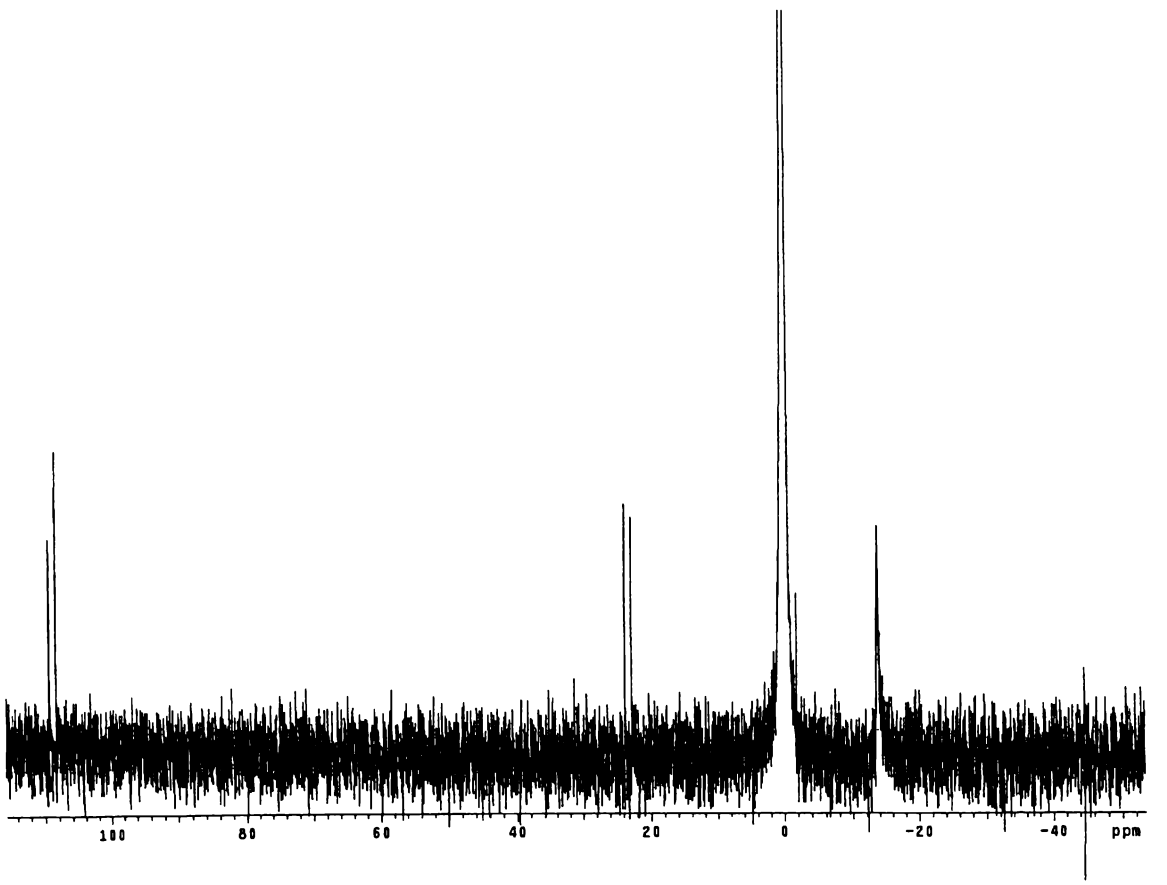

Figure 5.38: ^{31}P-NMR spectrum of an acetonitrile solution of **2** after removal of 0.5 electrons per molecule by BE. A very brief period of reductive BE was required to remove paramagnetic species from solution, allowing the peak for the starting material at -13.7 ppm to be clearly visualised. ^{31}P-{^{1}H} NMR (D_2O): δ 109.3, 108.3, 23.7, 22.8, -13.7.

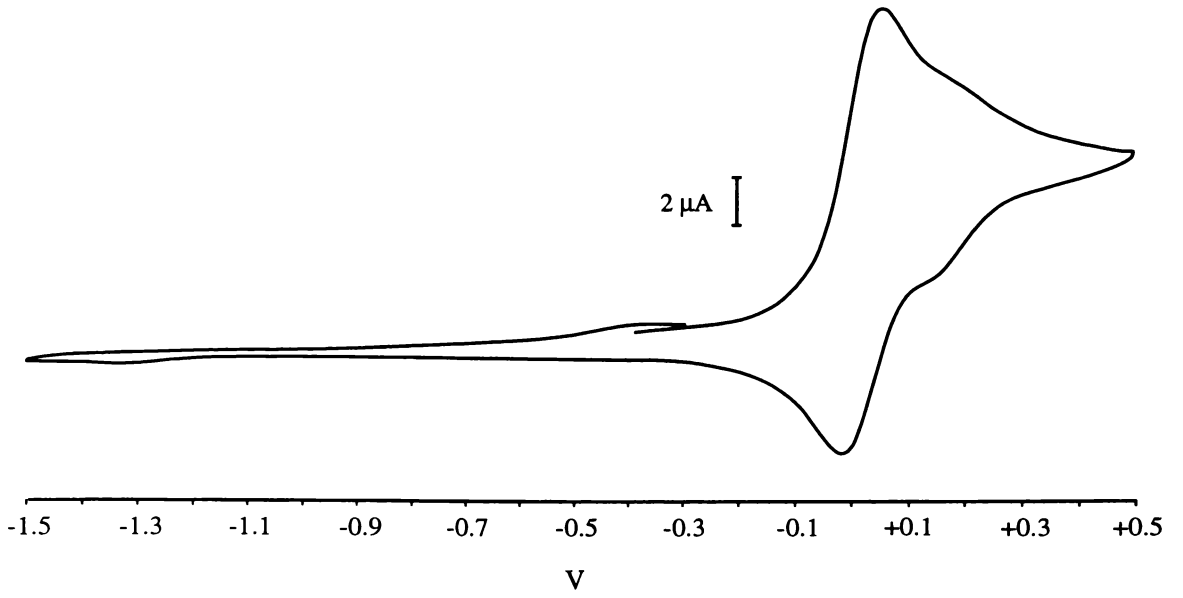

Figure 5.39: CV of a solution obtained by one-electron oxidation and immediate reduction of a 5.0 mM solution of **2**, scan rate 100 mV s^{-1}.

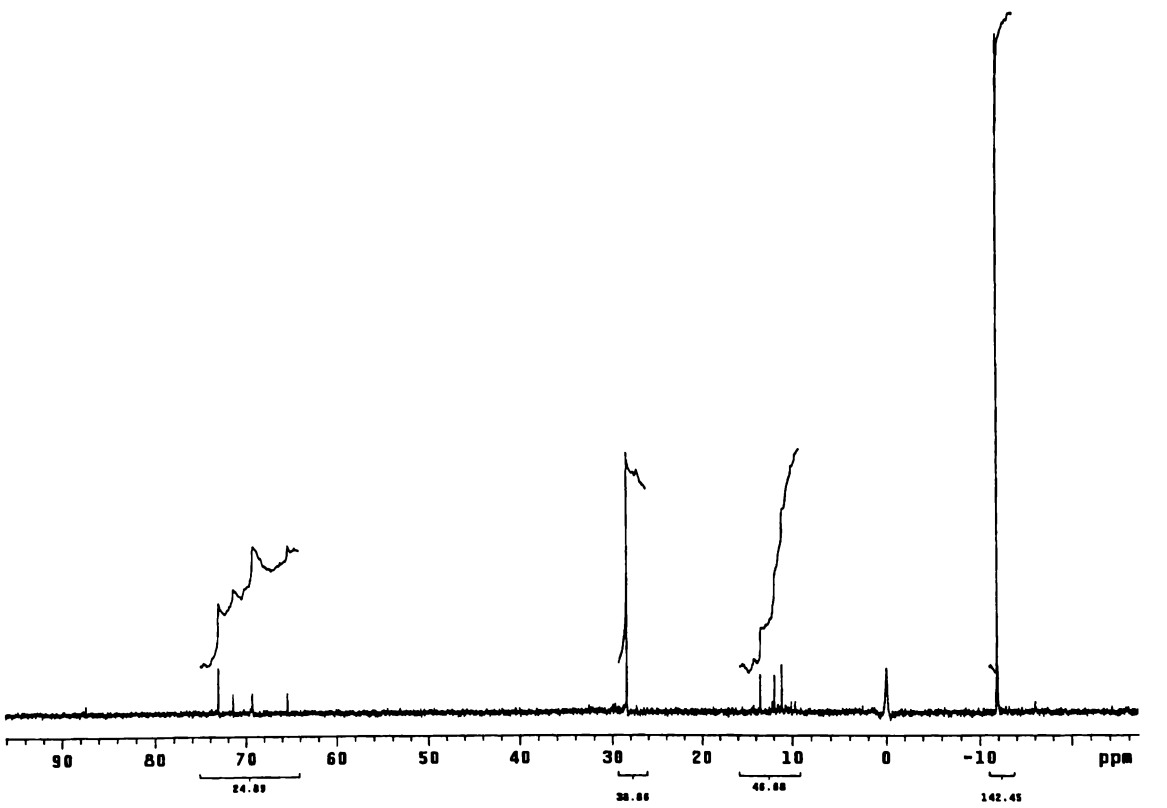

Figure 5.40: ^{31}P-NMR of the solution referred to in Figure 5.39. Comparison with authentic samples showed the peaks at -11.9 ppm and 28.4 ppm to be due to **2** and **15** respectively.

One-electron oxidative BE of **2** was also carried out in both dichloromethane and DMF, in order to study the generality of the behaviour observed in acetonitrile. CVs of the solutions obtained by one-electron controlled-current oxidation of **2** in dichloromethane and DMF are shown in Figure 5.41. In both solutions **2** appears to show essentially the same electrochemical behaviour as in acetonitrile. Electrochemical parameters for the redox processes at positive potentials are listed in Table 5.6. Potential of the reduction peak at negative potentials was -1.125 V and -1.320 V for dichloromethane and DMF solutions respectively. Steady-state voltammetry indicated a drop in total current ascribable to ferrocene species of *ca.* 46% and 47% for dichloromethane and DMF solutions respectively. The production of similar chemical species as in acetonitrile solution was confirmed in the case of DMF solution by acquisition of a ^{31}P-NMR spectrum (Figure 5.42).

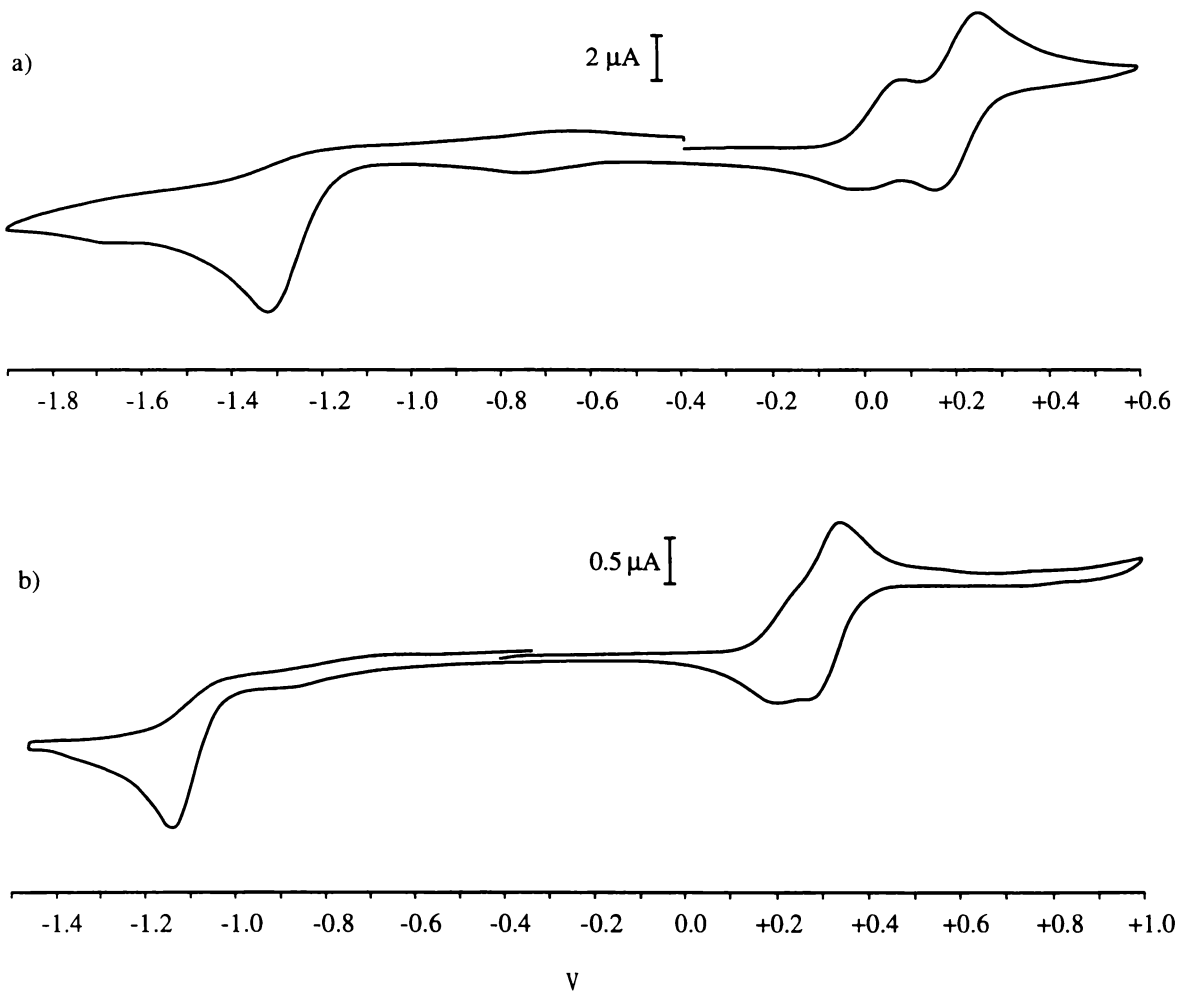

Figure 5.41: CVs of dichloromethane and DMF solutions of **2**, scan rate 100 mV s^{-1}. a) Dichloromethane solution. b) 7.5 mM DMF solution.

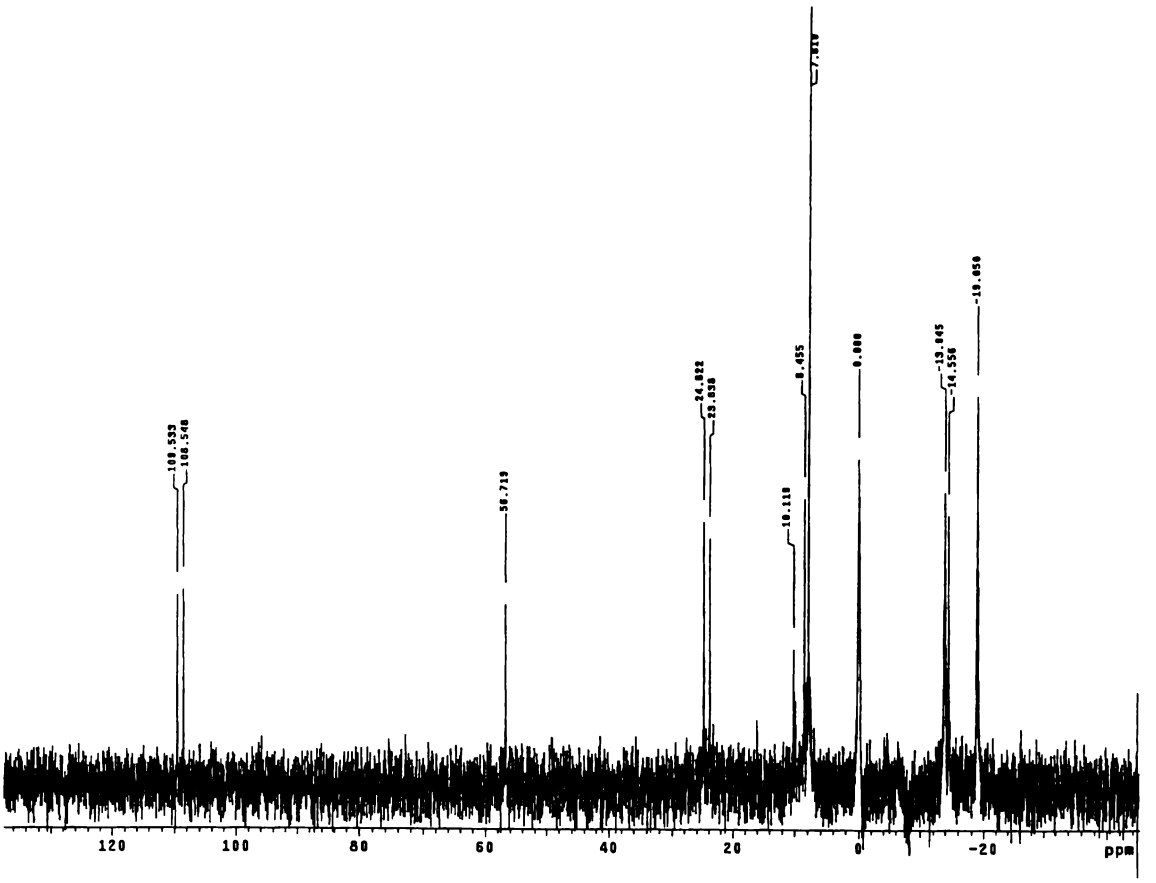

Figure 5.42: ^{31}P-NMR spectrum of a DMF solution of **2** after removal of one electron per molecule by BE. The spectrum was acquired over a period of time, and initially the paired signals at *ca.* 110 and 24 ppm dominated and were roughly equal in intensity. After 119 minutes a variety of other signals can be seen in the spectrum from -19 to + 57 ppm.

The oxidative one-electron BE behaviour of both **1** and **2** might here be summarised by stating that unlike some other ferrocenylphosphines, particularly dppf, reviewed in Section 5.1.2, the initial products formed do not appear to be the expected phosphine oxides or phosphonium salts, but rather products corresponding to two paired NMR signals at *ca.* 25 ppm and 110 ppm. With time these products break down, probably giving a variety of more conventional oxidation products. Further BE leads to production of ferrocenium species.

5.2.2.2 BE of $FcCH_2P(CH_2CH_2CN)_2$ 5

One-electron BE of **5** produced results very similar to those obtained for **1** and **2**, with the CV of the resulting solution shown in Figure 5.43. The solution immediately after BE had a green tinge, and the existence of ferrocenium species was confirmed by steady-state voltammetry, which showed about one half of the ferrocene groups in solution to be in the oxidised state. Over the course of 30 minutes the solution turned yellow, and this was again confirmed by steady-state voltammetry, which showed that as this time passed ferrocene became more and more predominant over ferrocenium until after 30 minutes it was almost all in the former state. The total current resulting from ferrocene groups after electrolysis dropped to 48% of the initially observed current. Electrochemical parameters for the two redox processes at anodic potentials, and the irreversible wave at cathodic potentials, are as follows: $E_{PA(1)}$ = 130 mV, $E_{PC(1)}$ = 70 mV, $E_{1/2(1)}$ = 100 mV, $E_{PA(2)}$ = 310 mV, $E_{PC(2)}$ = 240 mV, $E_{1/2(2)}$ = 275 mV, irreversible wave E_{PC} = - 1.24 V.

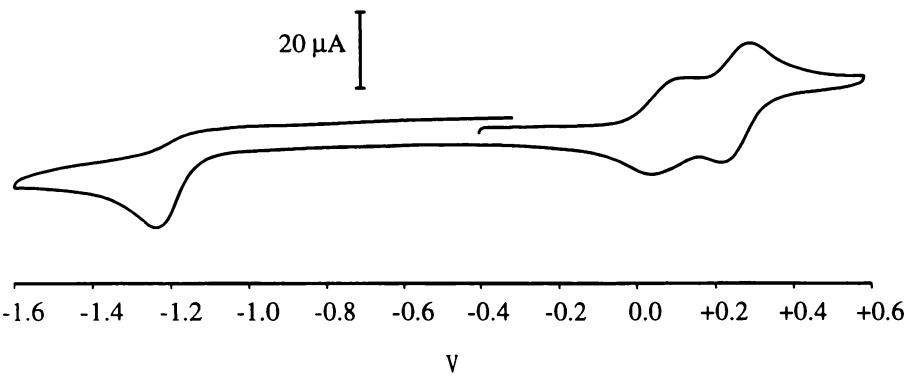

Figure 5.43: CV of 1.0 mM **5** after one-electron oxidative BE, scan rate 100 mV s^{-1}.

5.2.2.3 Spectroelectrochemistry of $FcCH_2PPh_2$ 2

It was asserted in Section 5.2.1.1 that *both* anodic redox waves observed in the cyclic voltammetry of **1**, **2** and other similar compounds result from a Fc/Fc^+ couple. The chemical reaction linking the two waves must therefore consist of the transfer of charge from the

Fe(III) atom produced in the first anodic wave to some other part of the molecule, either intra- or intermolecularly. This allows the regenerated ferrocene moiety to produce another wave, this time at a potential which is higher due to the electrostatic field of the first positive charge still carried in the molecule.

There is justification for the assertion that both waves are ferrocene-based. An inspection of **1** or **2** reveals only two functional groups that would normally be considered to have electrochemical activity under cyclic voltammetric conditions, those being the ferrocenyl group and the phosphine centre. It might therefore be questioned whether the two waves observed in cyclic voltammetry could not result from a ferrocene oxidation and a phosphine oxidation, especially considering that in compounds where the lone pair of the phosphorus has been utilised in bonding, a single redox wave is observed (Section 5.2.1.2). However, neither of the two waves seen for compound **1** and **2** correspond to typical phosphine electrochemical behaviour. Phosphine oxidations are usually seen at higher potentials than is the case here[20], occurring at *ca.* 0.85 - 1.05 V vs. Ag/Ag^+ (10 mM).

In addition, as has already been described, oxidative BE of both **1** and **2** yielded yellow solutions, rather than displaying the blue/green colour characteristic of ferrocenium species. Ferrocenium was however produced in two-electron oxidation of **2**. These results imply that if the two cyclic voltammetric anodic redox waves result from a phosphine and a ferrocene oxidation, the first wave must result from the phosphine oxidation. However, it is hardly tenable to propose that the first wave is a phosphine oxidation, since if this was the case the size of the second, ferrocene-based, oxidation should always be equivalent to a one-electron process. To put this another way, it seems very unlikely that in the case of **2** the one major redox wave observed by cyclic voltammetry should be a phosphine-based oxidation, while the ferrocene centre is either inert under CV conditions, or is only responsible somehow for a low current process such as the cathodic peak seen at *ca.* 230 mV.

So then, a phosphine-based oxidation cannot account for either of the two anodic redox processes, and therefore both must be due to ferrocene oxidation.

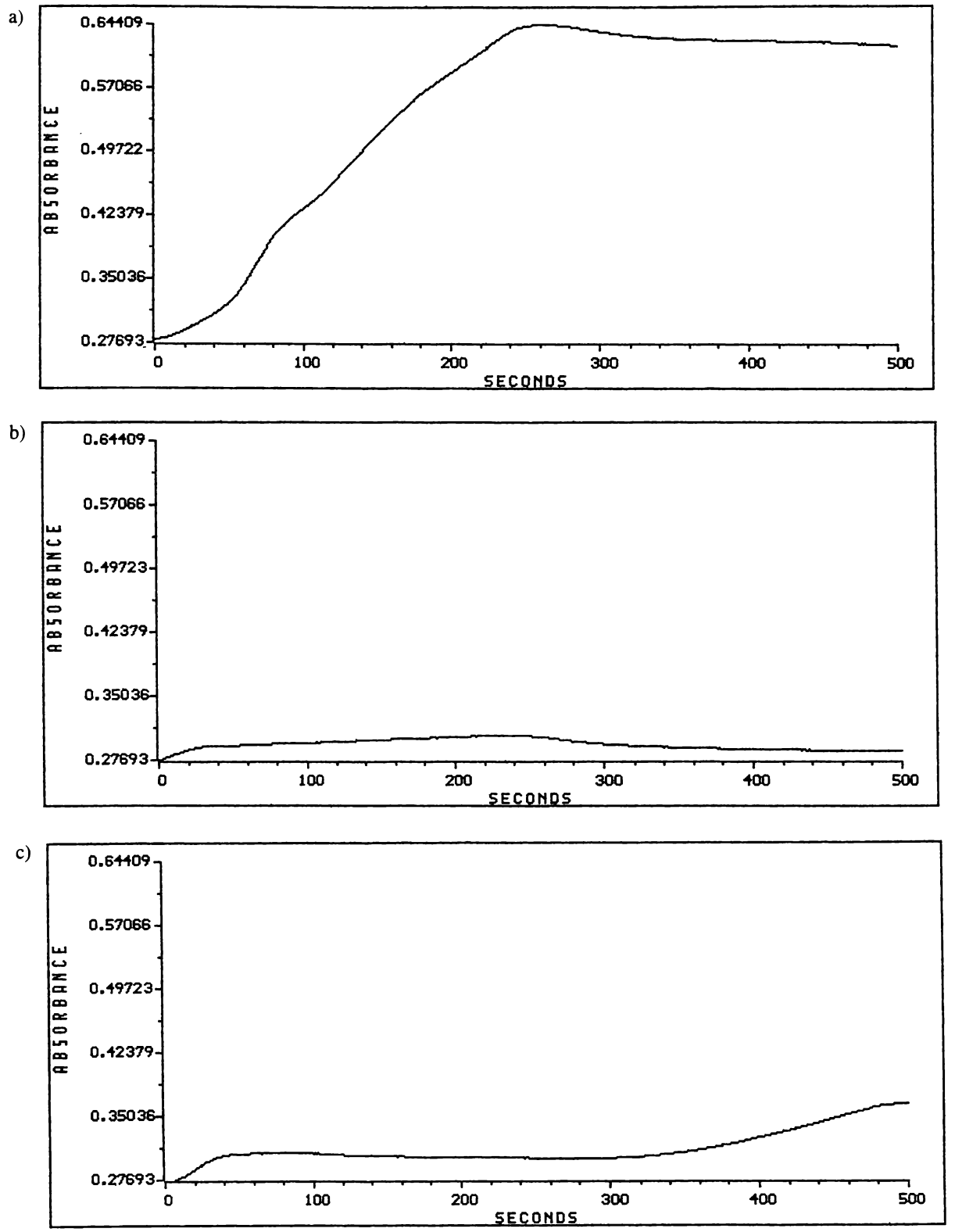

Figure 5.44: The concentration of ferrocenium species in solution during oxidative bulk electrolysis of 1.0 mM solutions, monitored by absorption at 626 nm. Charge was passed at a rate of -1 μC s^{-1} into a cell with a volume of 0.25 cm^3. a) One-electron BE of ferrocene, electrolysis stopped after 240 seconds. b) One-electron BE of **2**, electrolysis stopped after 240 seconds. c) Two-electron oxidation of **2**, electrolysis stopped after 480 seconds.

It was proposed that spectroelectrochemistry could be used to further confirm this idea, by carrying out BE of **2** while monitoring the concentration of ferrocenium using the distinctive 626 nm wavelength. Figure 5.44 shows the relationship of absorbance (equivalent to ferrocenium concentration) to time during various controlled-current oxidative BEs. Figure 5.44a shows the one-electron oxidation of a ferrocene standard, with BE complete after 240 seconds. Behaviour is in line with what would be expected, a steady rise in absorption at the ferrocenium wavelength culminating in a maximum at the end of the oxidation. The unusual shape of the rising section of the absorbance-time plot is the result of an uneven rate of oxidation over the Pt mesh WE and uncontrollable convection in solution. Figure 5.44b shows the one-electron oxidation of **2** using the same absorbance scale. It can be seen that absorbance at this wavelength never becomes very strong. Figure 5.44c shows the two-electron BE of **2**. One electron of charge was passed after 240 seconds, and two electrons after 480 seconds. It can be seen that after an initial rise, the concentration of ferrocenium remained steady, before beginning to rise again during passing of the second electron of charge. These results are consistent with the idea that ferrocenium species are being generated all the way through the bulk electrolysis of **2**, but that during passing of the first electron the ferrocenium species undergoes a chemical reaction in order to regenerate a ferrocene species; after passing of one electron of charge this reaction pathway has been followed to completion, and the concentration of ferrocenium again begins to rise. Problems with reproducibility were encountered with spectroelectrochemistry, due to the lack of bulk flow and consequent uneven oxidation and unpredictable convection streams. This means the results presented here should not be taken as conclusive; nevertheless, they are consistent with what might be expected.

5.2.2.4 *Comparison of BE Products of $FcCH_2P(CH_2OH)_2$ 1 and $FcCH_2PPh_2$ 2 with Phosphine Oxides and Phosphonium Salts*

In the previous Section the reasons for accepting that the two redox waves at anodic potentials seen in cyclic voltammetry of **1** or **2** both involve ferrocene-centred processes were explained. In the literature similar mechanisms have been invoked to explain the

oxidative electrochemistry of a variety of different ferrocenylphosphines, as detailed in Section 5.1.2. In these cases the original Fe(III) charge is invariably presumed to be passed to the phosphine centre to produce a phosphine radical cation as the initial product, through an intramolecular mechanism. This initial product reacts further to give oxidation products such as phosphine oxides, or phosphonium salts through stripping of hydrogen from the solvent.

It was initially thought that a similar mechanism probably applied to compounds **1** and **2** also. After all, when the lone pair of the phosphorus is used in bonding, such as in the phosphine oxides **3** and **15**, only one anodic redox wave is observed in cyclic voltammetry, suggesting that the presence of a phosphine moiety is crucial to further reaction of the initial ferrocenium oxidation product.

However, in the present case BE of **1** and **2** did not appear to produce phosphine oxides or phosphonium salts of the expected type, as has already been briefly mentioned in Section 5.2.2.1. This was confirmed by preparation of both the phosphine oxide **15** and phosphonium salt $[FcCH_2P(H)Ph_2]BF_4$ **14** (Section 2.3.1); these were found to have ^{31}P-NMR signals in $CDCl_3$ of 29.0 ppm (s) and 6.31 ppm (s) respectively. The phosphine oxide **3** was previously synthesised (Section 2.3.1) and gave a signal of 45.8 ppm (s) in $CDCl_3$. Attempts to synthesise the phosphonium salt $[FcCH_2P(H)(CH_2OH)_2]BF_4$ proved unsuccessful.

The cyclic voltammetric behaviour of **3** and **15** has already been described in Section 5.2.1.2. Attempts were also made to perform cyclic voltammetry on **14**. Unfortunately it was found that **14** was too unstable to be made and then transported to Christchurch for testing, therefore the CV of this compound was obtained by addition of a small amount of 40% HBF_4 solution directly to an acetonitrile solution of **2**. Note that this meant a GC electrode was used to obtain CVs, rather than the usual Pt electrode, since GC electrodes are relatively insensitive to the presence of hydrogen and protons in solution. Only one redox process was observed at positive potentials, with E_{PA} = 265 mV, E_{PC} = 178 mV, and $E_{1/2}$ =

222 mV. Comparison of the cyclic voltammetric behaviour of **14** and **15** with cyclic voltammetry of a solution of **2** subjected to one-electron oxidation (Figure 5.34), shows that both **14** and **15** could be interpreted as giving rise to the two anodic redox processes in the electrolysed solution. Since **14** and **15** have already be shown to be absent from the BE solution, this demonstrates the dangers of assigning the identity of redox waves purely on the basis of comparison of their redox potentials with those of authentic samples.

It was mentioned in Section 5.2.1.2 that the cyclic voltammetric redox wave of **15** is practically identical to the first wave of **2**; note also that the redox potential of **3** (Section 5.2.1.2) is intermediate between the first and second waves observed upon cyclic voltammetry of **1** (Section 5.2.1.1). These observations rule out the idea that phosphine oxides are formed on the short cyclic voltammetric timescale, and that they are responsible for the second redox wave at higher potentials, as has been suggested in the literature to describe the behaviour of another ferrocenylphosphine[17].

*5.2.2.5 Chemical Oxidations of $FcCH_2PPh_2$ **2***

In order to try and provide other means for studying the oxidation products observed in BE of **2**, some chemical oxidation systems were trialled. It was found that addition of equimolar $NOBF_4$ to **2** in acetonitrile gave a solution with the CV shown in Figure 5.45, which can be seen to be not truly analogous to solutions produced by electrochemical oxidation. This was confirmed by gradual addition of $NOBF_4$ to **2** in acetonitrile, with monitoring of reactions by ESMS. It was found that the dominant species observed to evolve as oxidation took place was **15**, with a *m/z* of 400.1. Other species seen in lesser amounts were (*m/z*): 800.4 [2M + O], 782.3 [2M - 2H], 414.0 $[M + NO]^+$ and 384.1 $[M]^+$ (cone voltage = 20 V). The presence of the oxygen and nitrogen-containing species in the ESMS spectra shows nitrosonium did not behave as an innocent oxidising agent in this system. It was found that 2,3-dichloro-5,6-dicyano-quinone (DDQ) behaved in a more desirable fashion; a CV obtained by gradual addition of an equimolar amount of DDQ to a solution of **2** in acetonitrile is shown in Figure 5.46, and it can be seen that it provides a better analogy for

electrochemical oxidation than nitrosonium ion. In addition, ^{31}P-NMR of the product solution obtained from the reaction of **2** with DDQ showed paired peaks at *ca.* 110 and 25 ppm to be present, similar to the results seen with electrochemical oxidation.

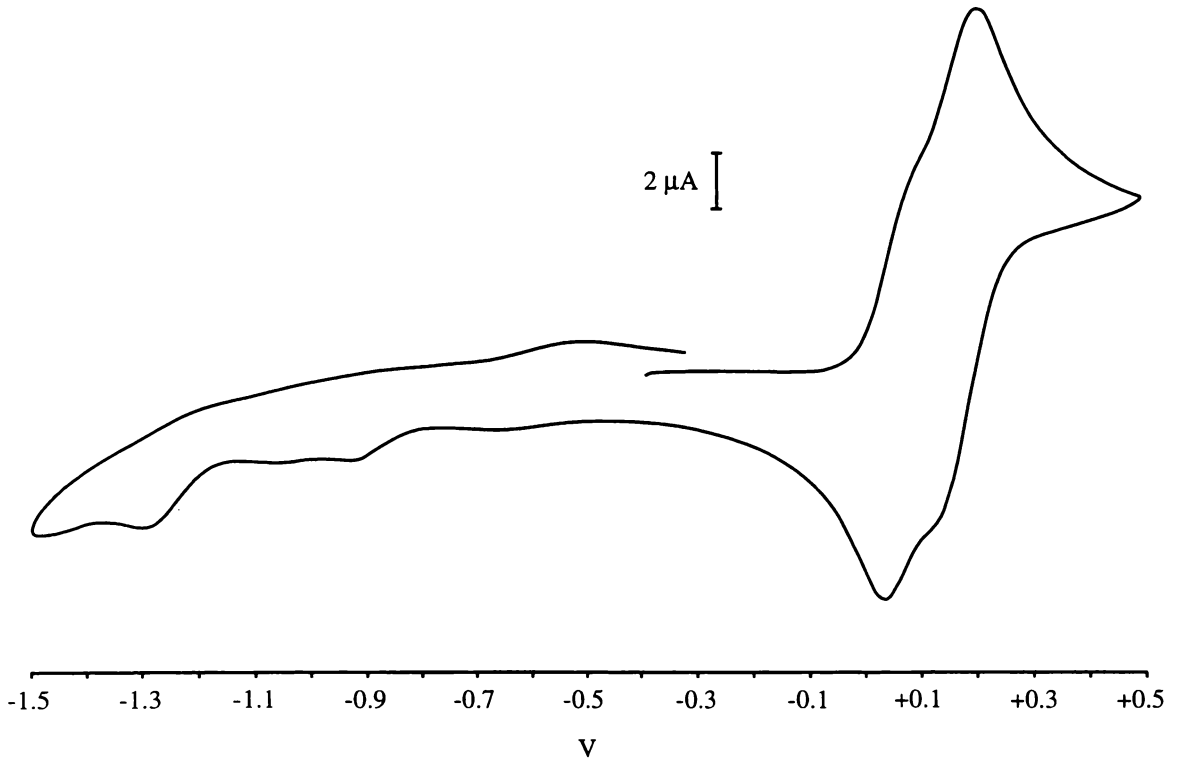

Figure 5.45: CV of the product mixture obtained from reaction of 5.0 mM **2** with $NOBF_4$, scan rate 100 mV s^{-1}.

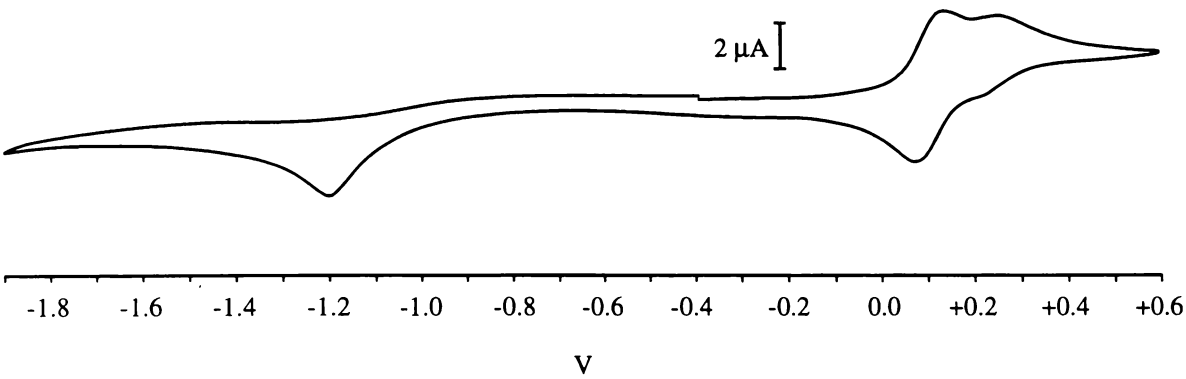

Figure 5.46: CV of the product mixture obtained from reaction of 2.6 mM **2** with an equimolar amount of DDQ, scan rate 100 mV s^{-1}.

Attempts to develop a method for chemical oxidation of **2** were suspended when it was discovered that upon storage in the solid state, the yellow oil **14** was transformed into a brittle red/brown oil over a period of days to weeks. This oil gave interesting electrochemical results, which led to reinvestigation of the material by NMR. A ^{31}P-NMR spectrum is shown in Figure 5.47, and it is clear from this that upon storage **14** reacts to give the same products as those obtained through electrochemical oxidation of **2**. A ^{1}H-NMR spectrum is shown in Figure 5.48. It was found that it was possible to purify this material through silica gel tlc, using a 3:7:10 mixture of ethanol/dichloromethane/petroleum spirits, with a R_f for the desired material of 0.43. Note however, that chromatography led to a decrease in the intensity of the peaks seen at *ca.* 110 ppm by ^{31}P-NMR relative to those at *ca.* 25 ppm, changing the ratio from 1:1 to 1:1.6.

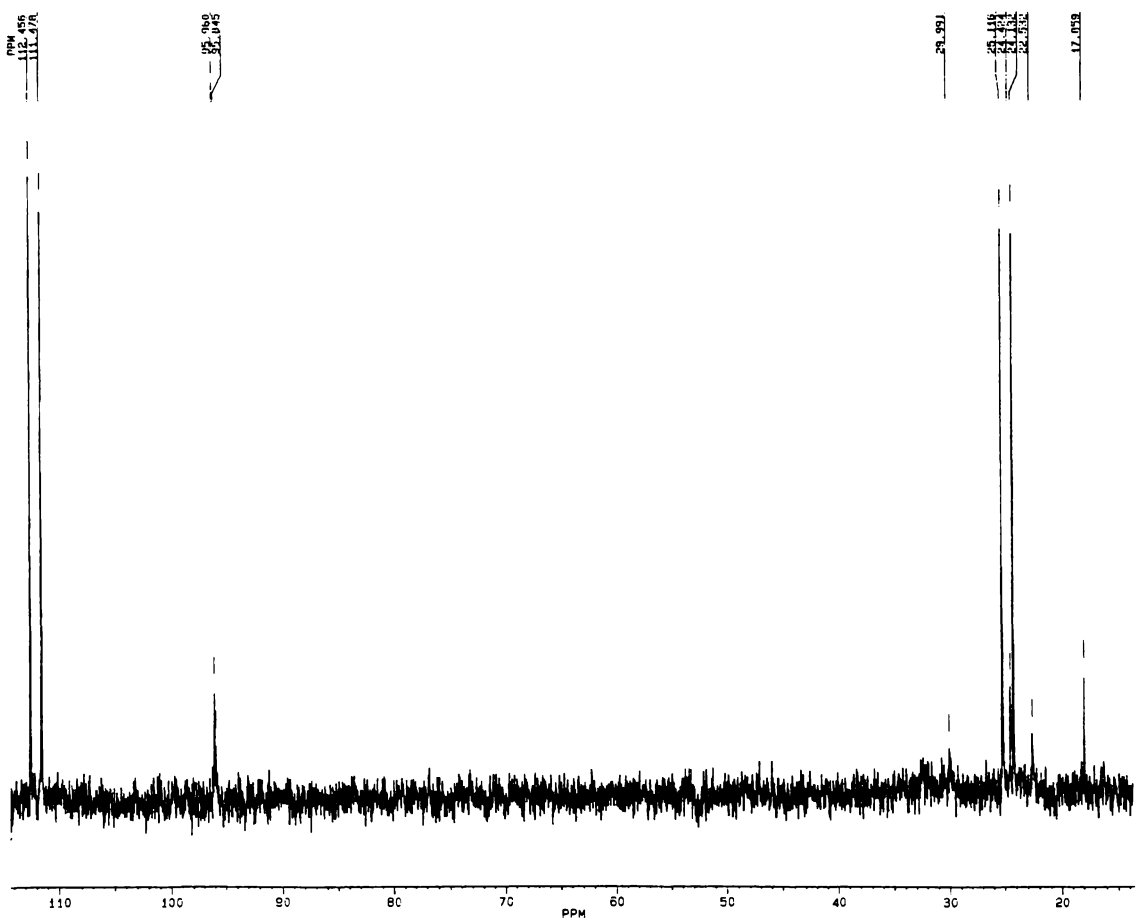

Figure 5.47: ^{31}P-NMR ($CDCl_3$) of a sample of **14** which had been in storage for four months.

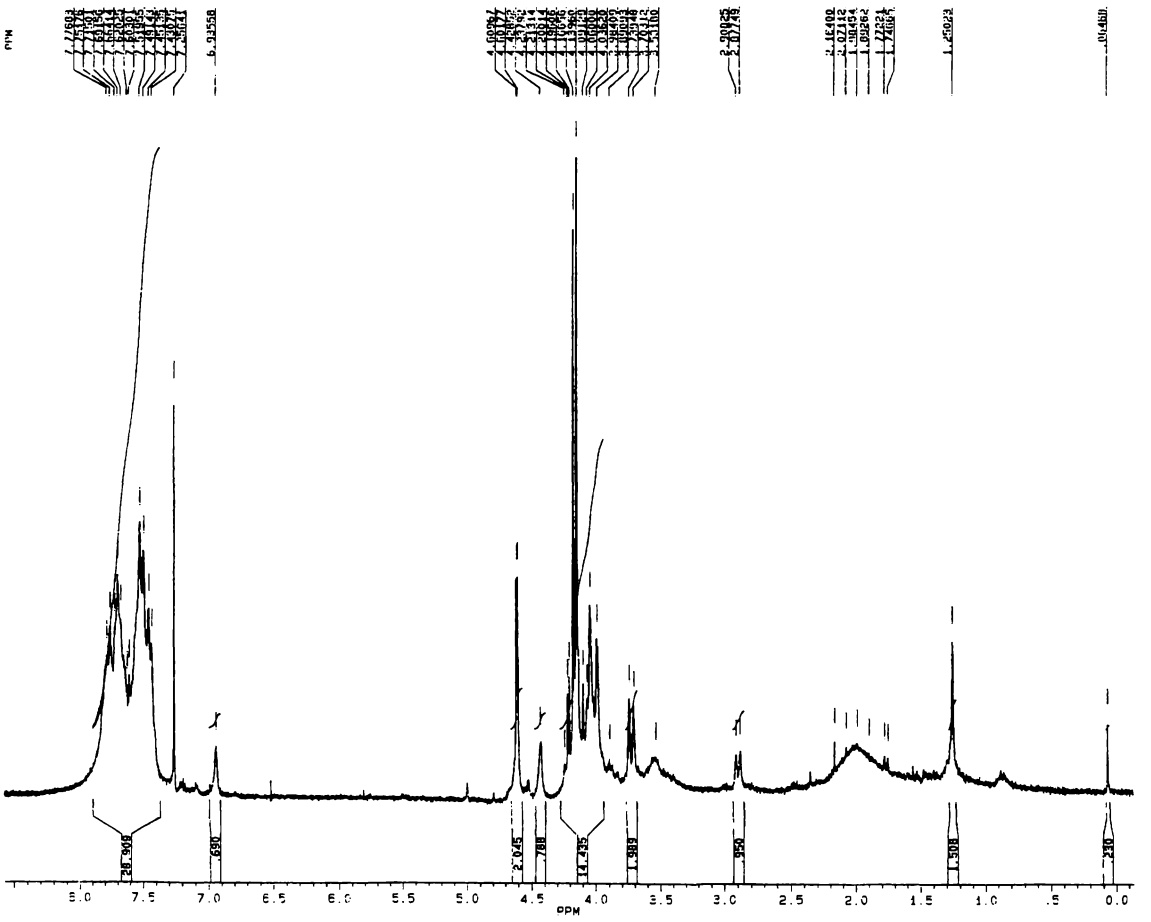

Figure 5.48: ^{1}H-NMR ($CDCl_3$) of the same sample referred to in Figure 5.47.

5.2.2.6 Investigations Into the Identity of Products from BE of $FcCH_2PPh_2$ 2

The isolation of samples of these oxidation products of **2** in reasonable quantities, without the presence of electrolyte, opened the possibility of examination of these products by a range of characterisation techniques.

Attempts at growing a crystal for a X-ray crystal structure determination were unsuccessful, partly due to the lack of stability in solution, even under nitrogen.

More success was achieved using NMR. The acquisition of ^{1}H-NMR and ^{31}P-NMR spectra has already been mentioned (Figures 5.47 and 5.48). A number of elementary observations can be made about the nature of the oxidation products of **2** based on ^{31}P-NMR data. Since the ratio of the pairs of signals was not always maintained at 1:1 it was evident that they

represented different compounds, which will be referred to from now on as compounds **34** (downfield signals) and **35** (upfield signals). The paired or 'doublet' effect could therefore only possibly be the result of P-H coupling, fluorine coupling, or of the formation of diastereoisomers, not of P-P coupling. Proton non-decoupled ^{31}P-NMR spectra revealed that no P-H bonds were involved. The idea that the paired appearance of the ^{31}P-NMR signals for **34** and **35** might be due to fluorine coupling was discounted by examination of the ^{19}F spectrum, which showed a single peak at -151.8 ppm, a chemical shift consistent with literature values[30] for BF_4^-. On the other hand, signal splitting of *ca.* 120 Hz is consistent with the idea of stereoisomer formation (see for instance Figure 2.3). Appearance of the ^{13}C and ^{1}H-NMR spectra showed that these were still dominated by ferrocene and phenyl signals, and that they were present in the expected ratios. A DEPT spectrum failed to show the presence of any CH_2 groups. This apparent lack of CH_2 groups in **34** and **35** is seen as an important finding, since it means that some sort of reaction is occurring at the α-carbon. In spite of extensive investigations involving two-dimensional experiments, little more was learned from NMR. Difficulties with obtaining more information stemmed partly from the unstable nature of the compounds in solution, the existence of a mixture, the presence of impurities in many instances, and the absence of phosphorus coupling in the ^{13}C-NMR, which could have helped pinpoint the crucial signals belonging to the methylene group between the Cp ring and the phosphorus.

ESMS of samples of **34** and **35** also proved helpful. A typical spectrum is shown in Figure 5.49. The principal peaks seen can be assigned as follows: *m/z* 854.8 $[2M + BF_4]^+$, 783.3 $[2M - H + O]^+$, 767.3 $[2M - H]^+$, 647.3 $[M + CpCH_2PPh_2]^+$, 584.6 $[M + PPh_2 + O]$, 569 $[M + PPh_2]$, 415.2 $[M + P]^+$, 401.1 $[M + OH]^+$, 384.1 $[2M]^{2+}$, 199.1 $[FcCH_2]^+$, where M = **2**. The fact that the peak at *m/z* 384.1 was due to a dication was established by examination of the high-resolution spectrum. This pattern of peaks is suggestive of dimer formation, as it seems to represent a progressive loss of fragments from 2M downward.

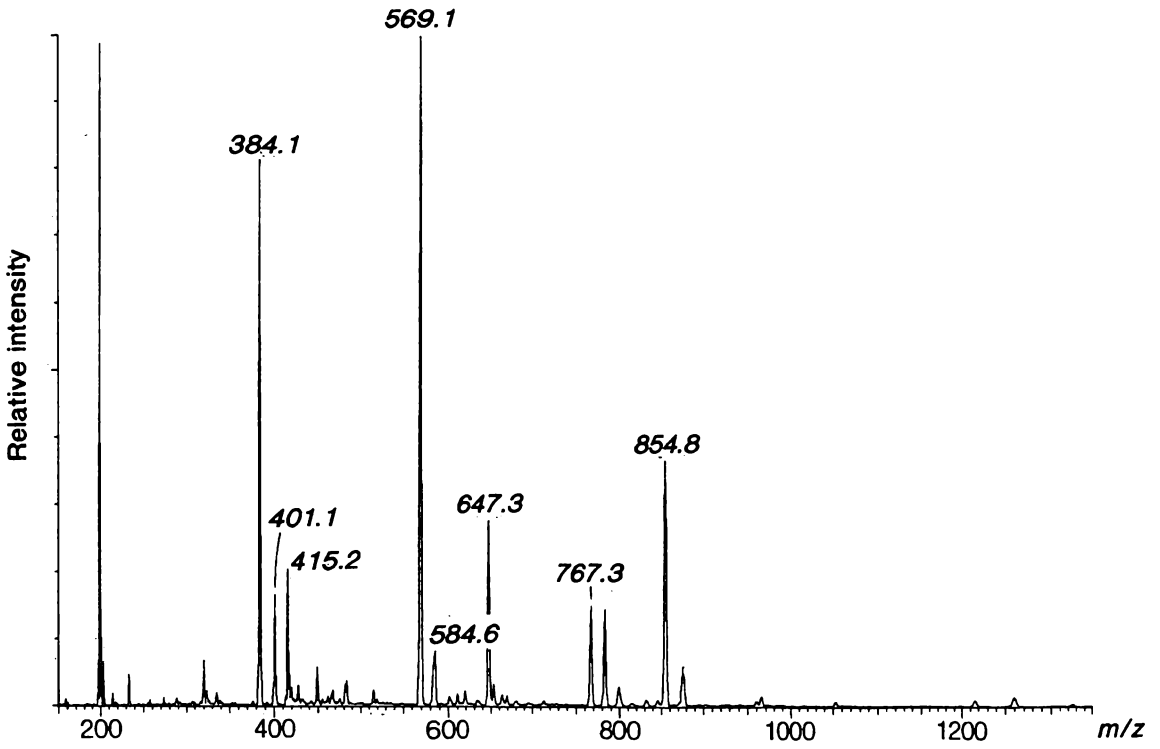

Figure 5.49: ESMS of the sample of **34** and **35** used to obtain the ^{31}P-NMR spectrum in Figure 5.47. At cone voltages of *ca.* 20 V the peak at *m/z* 384.1 predominated, along with the peak at *m/z* 854.8. At intermediate cone voltages the peak at *m/z* 569.1 predominated, while at *ca.* 60 V the peak at *m/z* 647.3 was the most prominent, with the exception of the expected *m/z* 199.1 peak.

5.2.2.7 Postulated Structures for 34 and 35

Devising convincing structures for **34** and **35**, and showing how they could be formed during BE, has proved very difficult. It is the aim of this Section and the next to provide ideas and a working hypothesis concerning the structures of **34** and **35**, and the electrochemical mechanisms involved in their formation. These may be of use in directing future research, but it is not intended that these ideas be viewed as anything more than tentative.

Any postulated structures for **34** and **35** should be able to account for the following points, gleaned from the preceding discussion:

1. Structures must account for initial removal of one electron per molecule of **2**.

2. Oxidation of **2** is largely reversible, mitigating against some possibilities such as loss of phenyl rings. ^{1}H-NMR, ^{13}C-NMR, and ESMS also seem to support the idea that overall integrity of the molecule is retained.

3. When compared to the ferrocenylphosphines listed in Table 5.1, redox potentials seen in BE solutions of **2** are not as positive as might be expected. Of course postulated structures for **34** and **35** should be able to account for the observed CV.

4. The paired nature of the ^{31}P-NMR signals implies stereoisomerism and therefore two chiral centres.

5. The lack of coupling in the ^{31}P-NMR nondecoupled spectrum rules out the possibility of P-H bonds.

6. Chemical shifts of both **34** and **35** imply the phosphine group has been transformed to something else carrying less electron density. The far downfield chemical shifts for **34** also make it unlikely that it is a simple phosphonium salt or oxygenated oxidation product.

7. The CH_2 group present in **2** has been transformed into something else.

8. Dimerisation of some sort is implied by the ESMS spectrum. Any structure postulated should be able to account for the fragmentation pattern observed.

In the author's opinion the most likely way to account for dimerisation, with formation of two stereocentres, positive ^{31}P-NMR chemical shifts, and lack of any CH_2 groups, is to postulate the existence of cyclobutane-type ring structures formed by bonding between the α-carbon and the phosphorus of two molecules of **2**. Two possible structures of this type are presented in Scheme 5.2. It is envisioned that **35** may be a 'head-to-tail' dimer, while **34** is a 'head-to-head' dimer. *Cis-* or *trans-* orientation of the two ferrocene groups about the four-membered ring would in each case account for stereoisomerism, and the close proximity of two positive charges in **34** would account for the downfield nature of the ^{31}P-NMR signal.

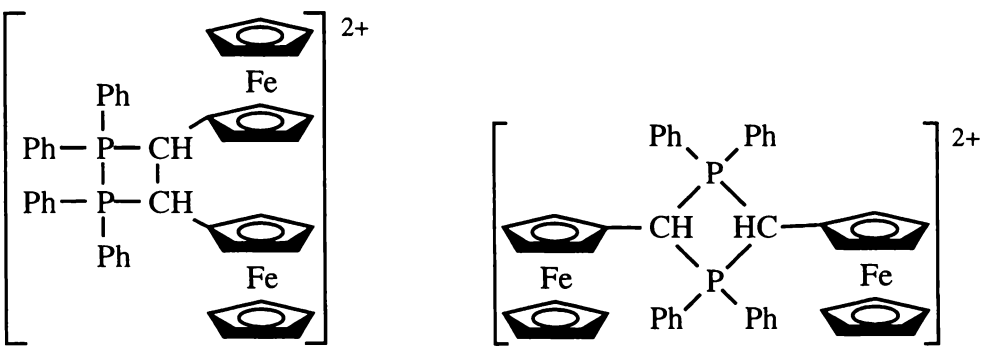

Scheme 5.2: Two possible structures which are postulated for **34** and **35**.

Cyclic voltammetric behaviour could be accounted for by assuming that in both **34** and **35** only one ferrocene group is oxidised within the solvent limit. This idea finds support in the fact that regardless of solvent used, *ca.* one half of the ferrocenyl groups present in solution become electro-inactive upon one-electron BE (Section 5.2.2.1). The oxidation potential for **35** might be expected to be higher than that of **34**, since in **35** there are two positive charges at the β-position, while in **34** one of the positive charges is in the γ-position relative to each ferrocene group. Admittedly, if this is a correct interpretation it might be expected by comparison with other phosphonium salts (Section 5.2.1.2) that the redox potentials of these processes would have been higher. The irreversible wave at cathodic potentials could be accounted for by a phosphorus-based reduction process for compound **34**, giving a bond-centred radical cation. The assignment of this as a phosphorus-based process seems

reasonable since this aspect of the cyclic voltammetric behaviour is different from that of oxidised solutions of **1**, with the difference between **1** and **2** being the phosphorus substituents.

If the postulated structures are correct, assignment of the ESMS spectra presents greater difficulties, since it must be assumed that in the aqueous environment of the mass spectrometer these dimeric species are hydrolysed in a rather unusual fashion. To see if use of an anhydrous solvent made any difference to the fragmentation pattern, ESMS were run in dichloromethane previously distilled over sodium hydride. This gave essentially the same spectrum, making this postulate of hydrolysis seem more unlikely. Nevertheless, if it is assumed that hydrolysis is happening, fragmentation patterns can be devised. Of course it cannot be known which peaks in the ESMS spectrum stem from **34** and which from **35**, and which from both, but a fragmentation route is given in Scheme 5.3 which shows various possibilities for the case of **35**. Importantly, the peak $[2M - H]^+$ is seen, suggesting the loss of CH_2 hydrogen in some way, but the case for the postulated structures would seem stronger if the peaks $[2M - 2H + BF_4]^+$ and $[M - H]^+$ were seen. It is perhaps worth noting here that the $[2M - 2H]^+$ peak was observed as a significant signal in the ESMS of **2** oxidised using nitrosonium, as reported in Section 5.2.2.4.

In summary, it may be said that the structures postulated for **34** and **35** can account for many of the known NMR characteristics of the compounds. However, the cyclic voltammetric and ESMS data do not provide such a convincing fit.

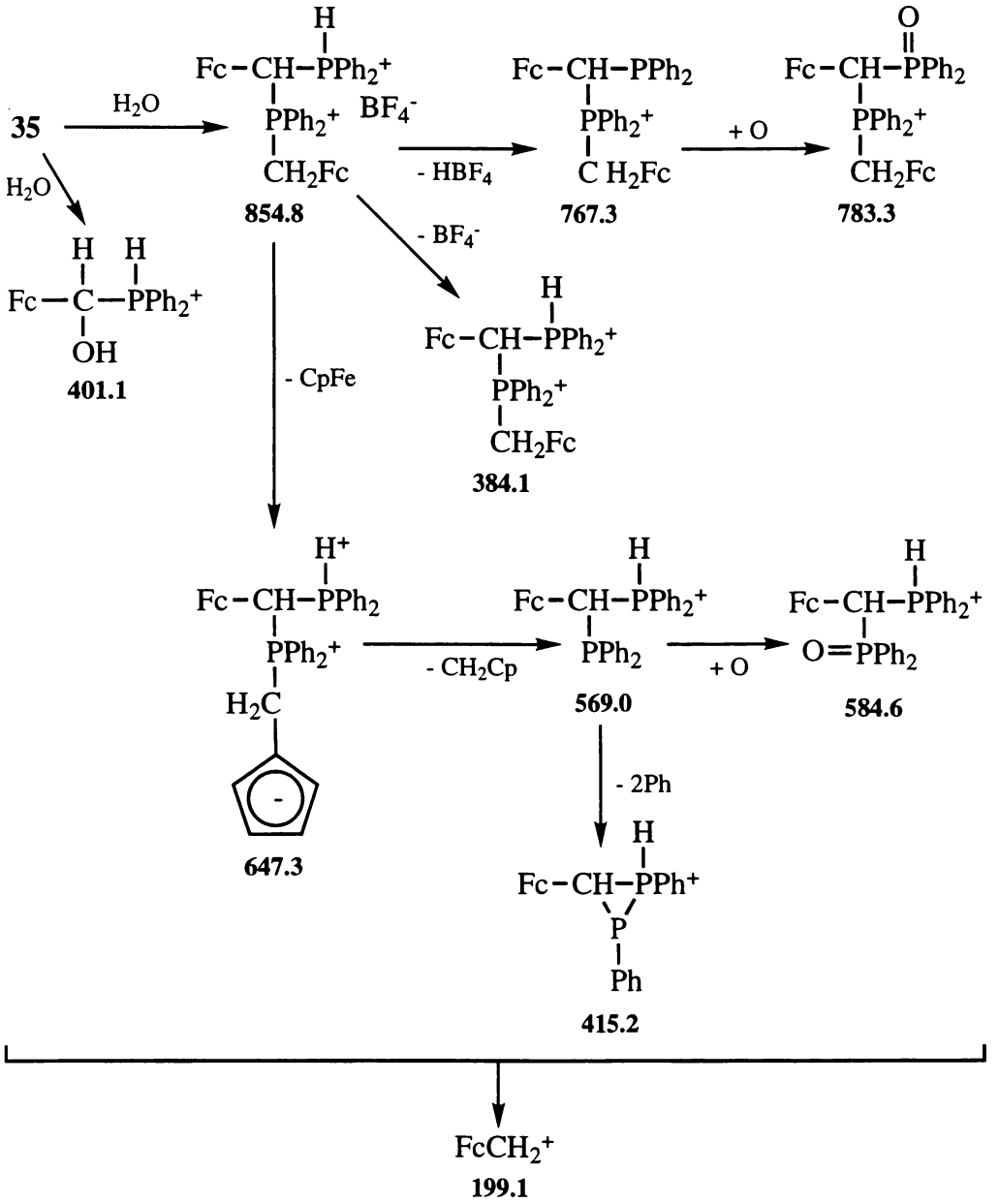

Scheme 5.3: Possible fragmentation route for **35**.

5.2.2.8 Postulated Mechanisms for the Electrochemical Formation of 34 and 35

A satisfactory mechanism explaining the oxidative reactions of **2** should account for both short-term (cyclic voltammetric) and long-term (BE) products. On the cyclic voltammetric time-scale one product displaying a reversible redox process with a potential more positive than that of the starting material appears to be formed. Coupled to this is a small reduction process at negative potentials. The mechanism involves an intermolecular reaction. Computer modelling carried out for **1** suggests that the RDS of the chemical reaction

involves reaction of two charged species to form a product having only half the number of groups available for further oxidation as were originally present (mechanism [4], p. 212). On the BE time scale two products appear to form in roughly equal amounts, producing two redox waves at positive potentials and an irreversible wave at negative potentials. In both cases the ferrocene originally oxidised to ferrocenium is regenerated *via* the ensuing reactions. The proposed mechanism should also be compatible with the formation of **34** and **35** from **14**.

The mechanism proposed here is shown in Scheme 5.4. Initial oxidation of **2** is followed by the release of a hydrogen radical and production of a carbenium ion centred at the α-carbon position. This species is substantially stabilised by donation of electron density from the phosphine as well as the ferrocenyl group. It is envisioned that this step would constitute the

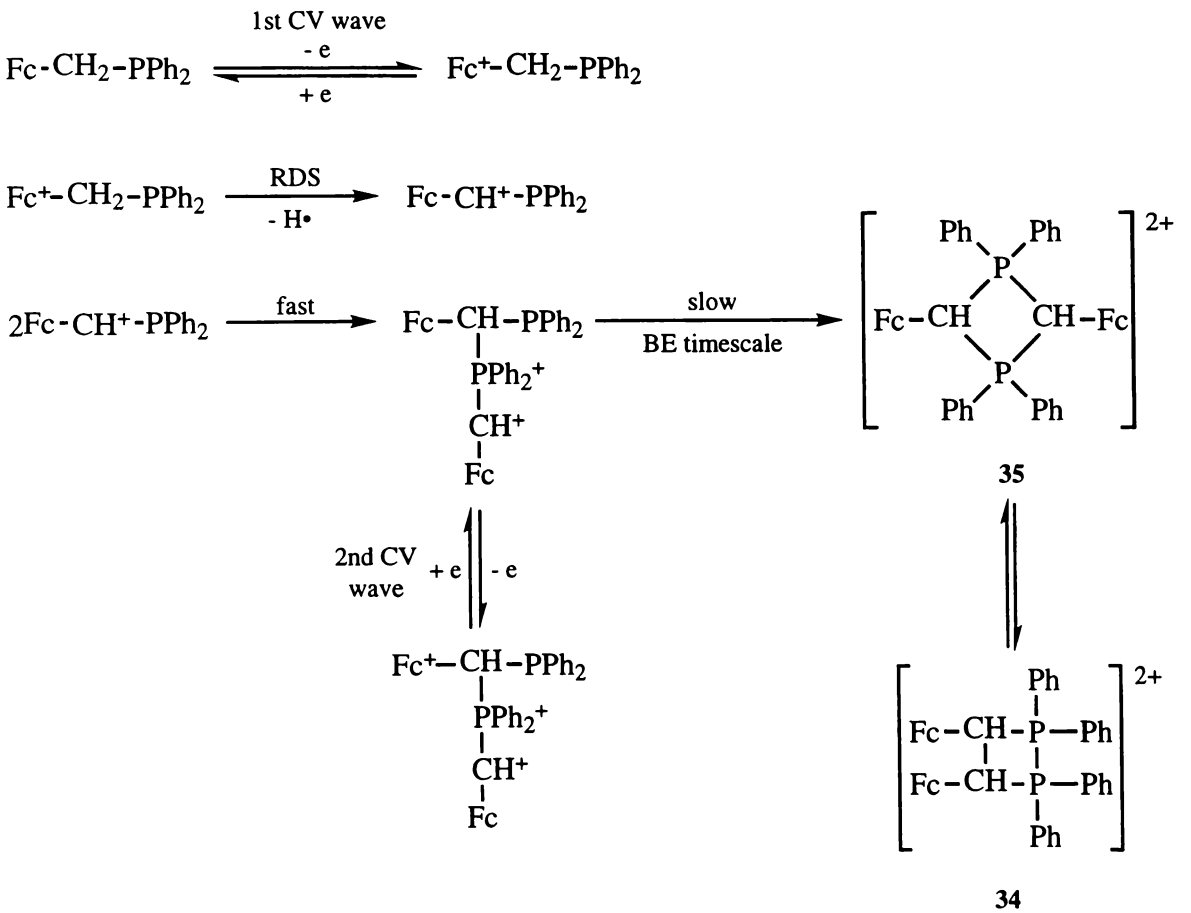

Scheme 5.4: Postulated mechanism for the electrochemical oxidation of **2**, and its relationship to both cyclic voltammetric and BE results.

RDS on the cyclic voltammetric timescale, and that it would be followed by a fast dimerisation reaction between two charged species giving a product in which only one of the ferrocene groups is available for further oxidation within the solvent limit. This dimer would give rise to the second reversible wave seen in cyclic voltammetry. The kinetics for this mechanism would be indistinguishable from the situation postulated in mechanism [4] (p. 212).

Dimerisation takes place by the rapid addition of the phosphine group of one intermediate molecule to the carbenium centre of another. It is postulated that on the BE timescale full cyclisation takes place *via* the complementary reaction to form **35**, but that this step is much slower than the initial dimerisation because of the constraints of ring strain. It is possible that **35** can in turn reversibly rearrange to give **34**.

It has already been established that the first step in oxidation of these compounds is centred on the iron atom; this is not a contentious statement. More unusual is the idea of charge being then shifted from the iron centre to the α-carbon, with consequent loss of hydrogen, a reaction which might be visualised as being either unimolecular, or possibly a bimolecular reaction between two ferrocenium ions giving hydrogen gas as a product. However, there is precedent for this thinking. Ito *et al.*[31] oxidised suitable ferrocene derivatives with DDQ in order to obtain isolable α-carbenium species (Scheme 5.5a). The compound [1.1]ferrocenophane has been studied at length, since when added to concentrated acids it forms the diferrocenium dication with formation of molecular hydrogen, thus providing a potential route to cheap hydrogen evolution[32]. If water is added to this dication, a proton is lost from one of the bridges, with formation of the carbenium species (Scheme 5.5b)[33]. Stable preparations of carbenium compounds of the sort $(Fc)_2CH^+$ are also possible[34]. Similarly the phosphenium-containing salt $[Fc_2P]^+[AlCl_4]^-$ can be prepared by the reaction of Fc_2PCl with $AlCl_3$[35]. One reaction of particular relevance to the present study was reported by Boev[36], whose work is represented in Scheme 5.6. Here chemical oxidation was used to produce an oxidised ferrocenium species, which then underwent homolytic cleavage of a C-H bond to give an α-carbon carbenium ion. The ability of the ferrocene group to stabilise α-

carbenium ions of this type is well-known, and is the basis for the synthesis of many different ferrocene derivatives, including ferrocenylphosphines chiral at the α-carbon[37] (Section 1.2). This stabilisation is due to direct participation of the iron atom in charge delocalisation, meaning that the carbenium centre and its associated Cp ring are generally bent in such a way as to bring the iron and carbenium centres closer together[34,38].

Not all ferrocene compounds containing an α-methylene group give rise to an α-carbenium ion upon electrochemical oxidation; many such compounds have been investigated and shown to have reversible cyclic voltammetric behaviour. However, in the present case the lone pair of the phosphorus can also be involved in charge delocalisation, possibly making this hydrogen-loss reaction more favourable than in most instances. Absence of an available phosphorus lone pair would thus account for the reversible nature of the redox processes described in Sections 5.2.1.2 and compounds **16**, **17** and **18** in Section 5.2.1.4

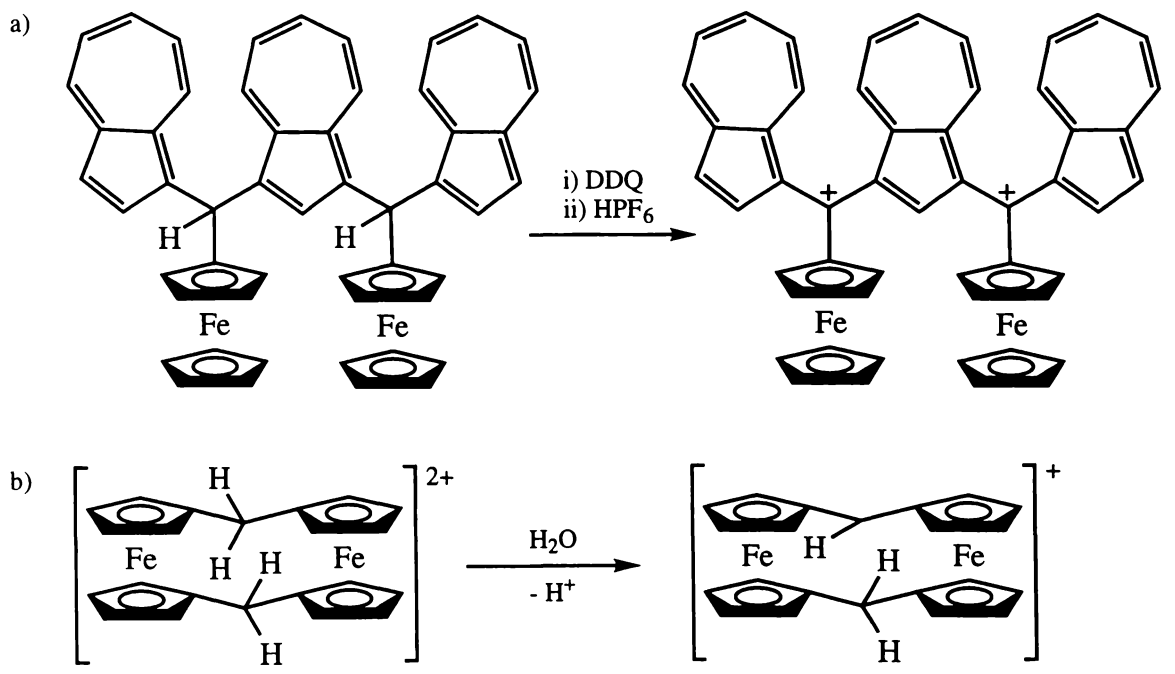

Scheme 5.5: Reactions producing α-carbenium ferrocenyl cations. a) A dicarbenium species stabilised not only by ferrocene but by extensive conjugation. b) In the presence of water the oxidised [1.1]ferrocenophane forms an α-carbenium ion.

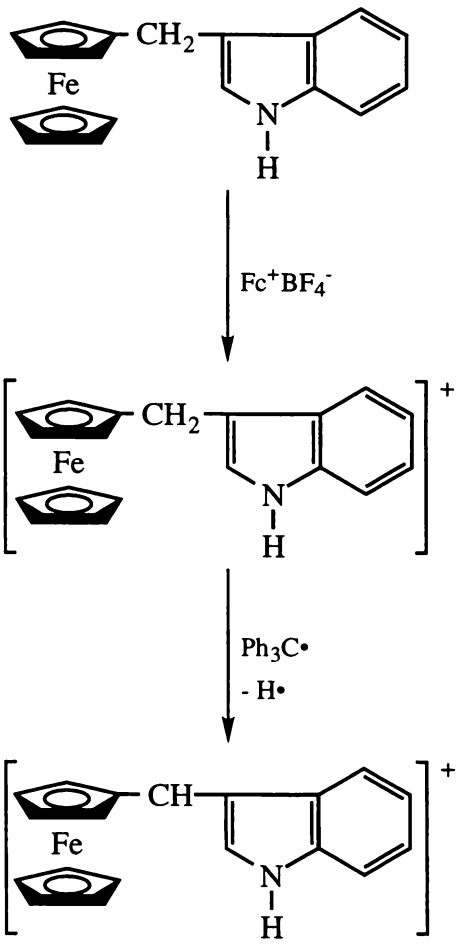

Scheme 5.6: Homolytic cleavage of a C-H bond to give an α-carbenium ion.

The most obvious alternative mechanism which could be proposed is one based on the literature, where perhaps the initial ferrocenium species reacts to give a phosphonium ion, two of which could react together in a RDS in the manner envisaged by Pilloni *et al.*[14] for dppf (see Scheme 5.1). Oxidation of one of the ferrocene centres in the dimer formed would then account for the second oxidation wave seen in cyclic voltammetry. The problem with this mechanism however, is that it requires a fast chemical step involving regeneration of the ferrocene centre *prior* to a cyclic voltammetric RDS consistent with Mechanism [4] (p. 212). If indeed the electrochemical oxidation of **2** involved such a mechanism one would expect to see three waves, due to starting material, the phosphonium species, and the dimer.

The processes of rather low current at cathodic potentials observed in cyclic voltammetry of **2** could result from reduction/oxidation of the carbenium centre of the dimer to a neutral radical.

If indeed **2** forms carbenium ions upon oxidation, in the way elaborated above, then the notion of 'head-to-tail' dimerisation of the sort giving rise to **35** has good support within the literature, since it rests on the idea of phosphine addition to the carbenium species. The synthesis of **1** discussed in Chapter 2 relied on a reaction which might be described as the dissociation of NMe_3 from $[FcCH_2NMe_3]^+$ to give the $FcCH_2^+$ carbenium ion, to which $P(CH_2OH)_3$ then adds, giving $[FcCH_2P(CH_2OH)_3]^+$. This type of reaction is a very common and important route to the synthesis of ferrocene derivatives[37,39]. Again, some reactions reported by Boev are particularly relevant[40]. Reaction of the same ferrocenylmethyl-indole compound shown in Scheme 5.6 in one pot with the hydrogen abstractor $[Ph_3C]BF_4$ and triphenylphosphine gives the phosphonium salt obtained by addition of triphenylphosphine to the carbenium ion initially produced by removal of hydride from the α-carbon. Similarly, reaction of $FcCH_2SO_2C_6H_4CH_3$ with $[Ph_3C]X$ gives the α-carbenium ion, which can then be reacted with triphenylphosphine to give the phosphonium salt with phosphorus bonded to the α-carbon. In view of these findings, it seems very reasonable that two ferrocenylmethylphosphine carbenium ions should react together to give the cyclobutane-type structure **35**.

The case for the formation of **34** by the rearrangement of **35** is less convincing. However, rearrangement of a variety of diphosphacyclo-butane structures by either concerted mechanisms or reversible dissociation/dimerisation has been reported in the literature, including some examples involving ferrocene-phosphorus compounds. A few of these reactions are shown in are shown in Scheme 5.7. In view of the propensity of diphosphacyclo-butane structures of various kinds to undergo these sorts of reactions, the idea of an equilibrium linking structures **34** and **35**, either through dissociation and re-dimerisation in another configuration, or through a concerted mechanism, is perhaps not unreasonable.

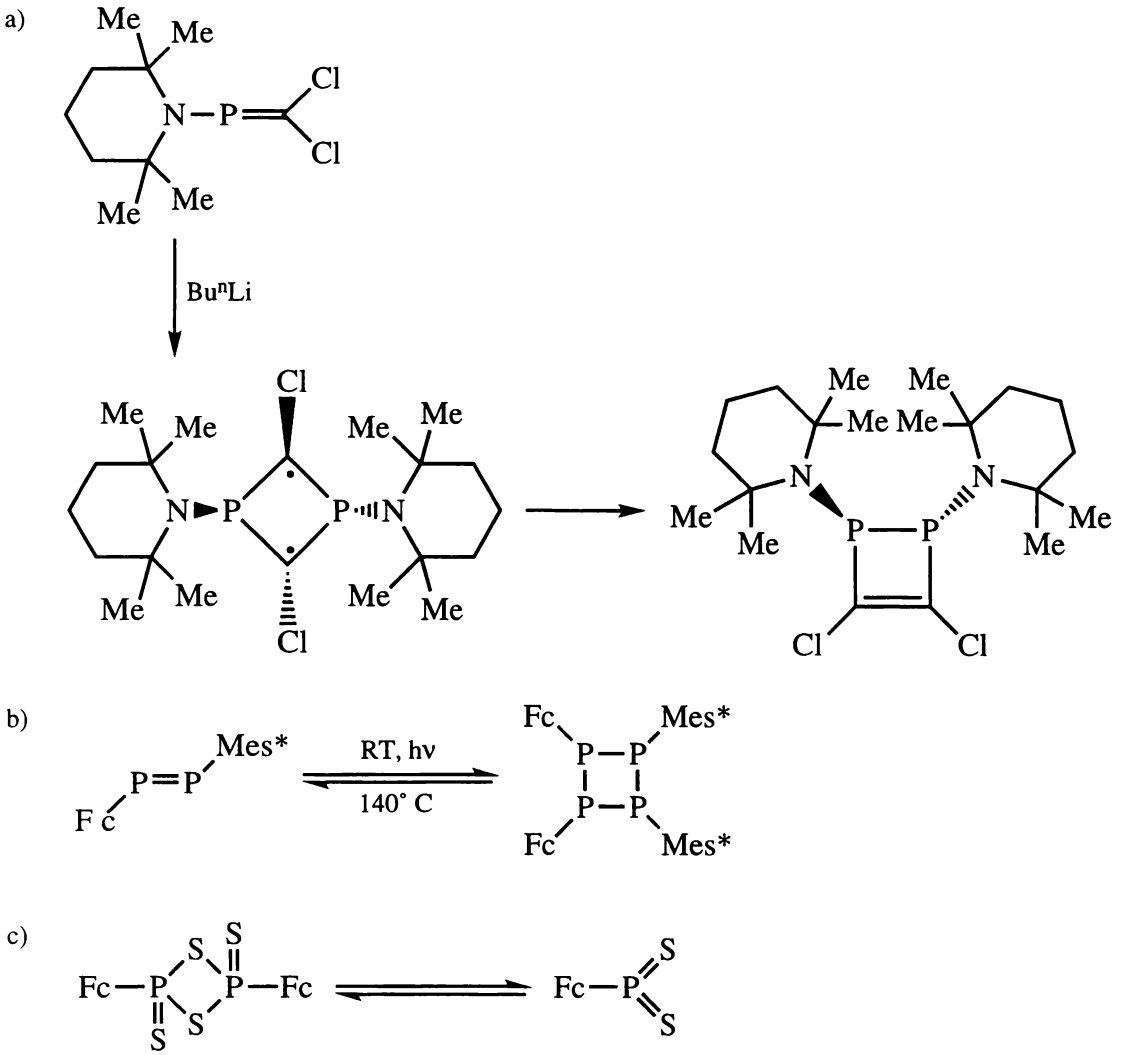

Scheme 5.7: a) Dimerisation of a phosphene produces a diradical which rearranges to give a diphosphabutene product[41]. b) Reversible dimerisation of a ferrocenyl diphosphene[42]. c) This ferrocenyl-phosphorus compound undergoes reversible dissociation in solution to give two dithiophosphine ylides[43].

For instance, if **35** were to dissociate in solution to give $2FcCH^+PPh_2$, the two molecules may recombine to form **34**. It is known that upon storage the $FcCH_2^+$ cation undergoes dimerisation to give [1,2-diferrocenylethane]$^{2+}$. This is thought to occur through the resonance form which can be drawn with the charge resting on the iron, and the α-carbon present as a neutral radical. The two radicals dimerise to give the observed product, and charge is retained at the ferrocene centres[44]. Similarly, in the case of the $FcCH^+PPh_2$

carbenium ion produced by oxidation of **2**, it seems reasonable to suppose that if charge rests to a large degree on the phosphorus, then dimerisation of the 'head-to-head' type which produces **34** might be the end result.

It is not difficult to see how **34** and **35** might form from **14**. Perhaps the ferrocene group is directly oxidised by H^+, and then reacts as suggested above. Alternatively, homolytic cleavage of the P-H bond and a neighbouring C-H bond could release molecular hydrogen and produce the requisite α-carbenium species.

One aspect of the mechanism presented here which is difficult to explain is this: It is proposed that **34** and **35** are formed and linked by a reversible equilibrium. However, the products **34** and **35** were consistently produced in a ratio which is initially roughly 1:1, whether the products are formed as a result of electrochemical oxidation, or degradation of **14**. This seems more like a stoichiometrically imposed ratio than the result of a thermodynamic equilibrium, which would be expected to produce one dominant product. More systematic analysis is required to confirm that the initial ratio of **34** to **35** produced by BE is indeed 1:1, or whether it is variable. Another difficulty with the proposed scheme is that **34** and **35** are not products which would be expected to produce the reversible BE results seen for **2**. However, it is possible that water present in small amounts provides the hydrogen required for the reverse reaction, or even molecular hydrogen still dissolved in the solvent.

5.2.2.9 Applicability of Results to Other Compounds

The results and discussion presented above have centred largely around compound **2**, and to a lesser extent **1**. For the most part results obtained for these two compounds have been in agreement, and with the present state of knowledge it seems reasonable to assume that the behaviour of **1** can be described by the same reaction schemes as those outlined above for **2**. In addition, Section 5.2.1.1 showed that the cyclic voltammetric behaviour of all the compounds of type $FcCH_2PR_2$ shared the same basic characteristics. So then, there is at

present no reason to think that all these compounds do not behave in analogous fashion. Variation in prominence of the second redox wave at anodic potentials could be due to factors such as acidity of the α-carbon, and electron-donating ability of the phosphine. The prominent wave at moderate cathodic potentials seen for compound **24** is presumably due to unique behaviour of the weak P-H bonds; it is conceivable that a reaction of the following sort takes place and accounts for the observed electrochemistry:

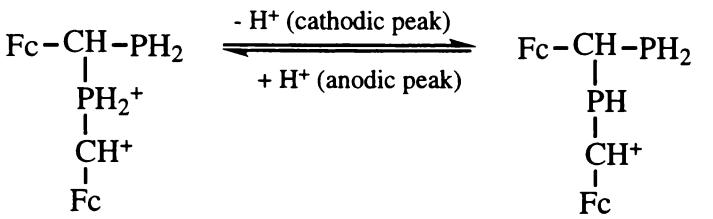

It must be admitted that it is strange that **25** does not exhibit similar behaviour if this is a correct interpretation.

It is presumed that compounds of the types discussed in Sections 5.2.1.2 and 5.2.1.3 show chemically reversible behaviour on the cyclic voltammetric timescale due to the unavailability of the phosphorus lone pair for the stabilisation of a carbenium species.

5.2.3 Further investigations of the Electrochemistry of $(FcCH_2)_2PCH_2OH$ **11**

A limited investigation of into the BE behaviour of **11** was performed. One-electron controlled-potential BE of compound **11** was carried out using an applied potential of 0.05 V and 0.2 V in acetonitrile and dichloromethane solutions respectively; these potentials corresponded to a point after the first irreversible redox process seen in cyclic voltammetry, but before the two merged redox waves of the second process. As with **1** and **2** it was found that the solutions were still yellow at the end of the experiment. Results from both solutions were similar, and confirmed the postulate that the first irreversible redox wave seen

in the CV of **11** is a one-electron oxidation, since the one-electron BE of **11** led to disappearance of this first wave, but gave a CV which was identical in all other respects to that of the original solution. A comparison of the CVs for **11** before and after one-electron oxidation in acetonitrile is shown in Figure 5.50, demonstrating this point. The CV of a dichloromethane solution of **11** after BE is shown in Figure 5.51, and although a comparison with the original CV is not shown, essentially the same thing was seen as with

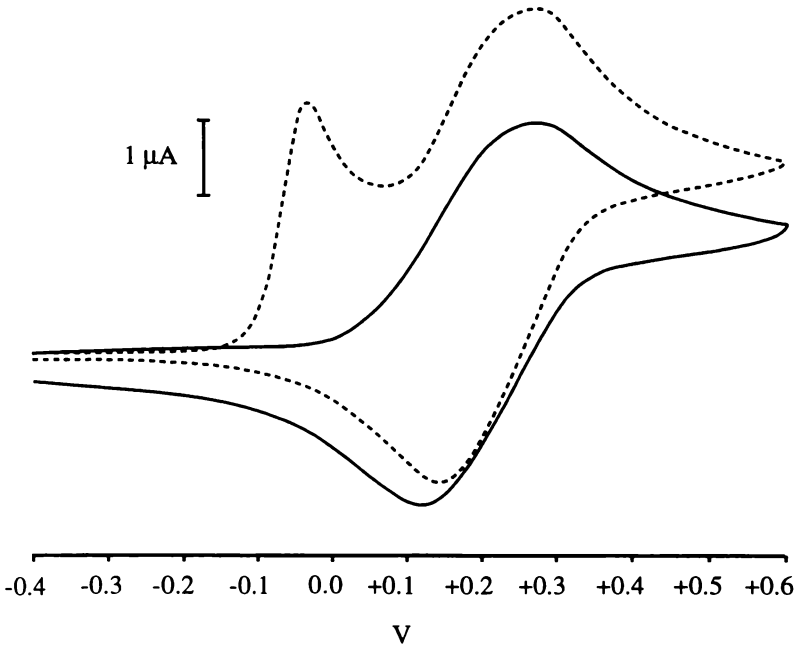

Figure 5.50: CVs of a 1.0 mM acetonitrile solution of **11**, before (dashed line) and after (solid line) one-electron BE, scan rate 100 mV s^{-1}.

the acetonitrile solution; disappearance of the first irreversible redox wave while all other features were maintained. An attempt was made to obtain a sample of the oxidation product(s) for examination using ESMS, by removal of solvent and most of the $Bu^n_4NPF_6$. However, examination of this sample by ESMS showed large peaks corresponding to the electrolyte, and only one other very small and transient peak corresponding to $[M + O]^+$. This should not be taken to mean that the phosphine oxide is a product of electrolysis, however. It has already been reported in Section 2.2.2 that the parent compound **11** is only seen as the $[M + O]^+$ peak under ESMS conditions. On the basis of the cyclic voltammetric (Section 5.2.1.1), BE, and ESMS (Section 2.2.2) behaviour of compound **11**, it can be

surmised that it probably does not behave in the same way as the other ferrocenylphosphine compounds which contain only one ferrocene group. The simplest hypotheses which can be proposed on the basis of all available evidence is that the first CV process corresponds to oxidation of one ferrocene group. This charge is then transferred quickly to the phosphine centre, in the manner postulated for many other ferrocenylphosphines in the literature (Section 5.1.2). At a higher potential both ferrocene groups are reversibly oxidised, but their redox potentials are differentiated due to communication between the two ferrocene centres. The unusual behaviour of **11** whereby only the $[M + O]^+$ peak is seen in ESMS, suggests the possibility that with time the phosphonium species produced by electrochemical oxidation may lead to production of the phosphine oxide as a final product.

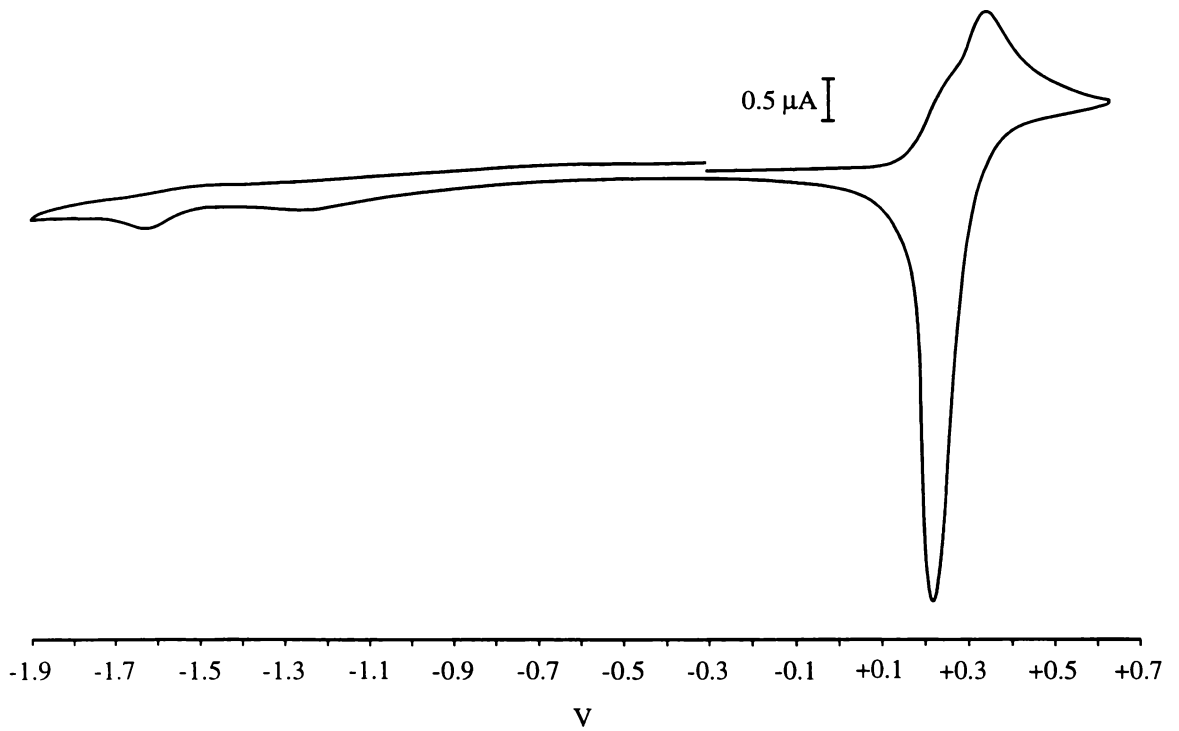

Figure 5.51: CV of a 1.0 mM dichloromethane solution of **11** after one-electron oxidation, scan rate 100 mV s^{-1}.

5.2.4 Further Investigations of the Electrochemistry of $FcCH_2P(O)(CH_2NEt_2)_2$ **7**

A limited amount of work was carried out looking at the BE of **7**. It was found that a yellow solution was retained after removal of one electron per molecule, and a CV of this solution showed a large irreversibly coupled redox wave at negative potentials, along with two waves at positive potentials, the second being considerably smaller than the first. Further oxidation resulted in the formation of ferrocenium species.

Due to the limited nature of the study of **7** described in this Chapter, conclusions concerning the nature of the electrochemical processes and chemical reactions involved are bound to be highly speculative. It will suffice at this stage to state the following: It seems reasonable to assume that as with the ferrocenylphosphines described in this Chapter, the ferrocene group is initially oxidised, but that this charge is passed to another part of the molecule, leading to regeneration of the ferrocene centre and further reactions to produce new species with ferrocene redox potentials higher than those of the starting material **7**. In the absence of an available phosphorus lone pair, the most obvious candidate for acceptance of the ferrocene charge is an amine group.

Amine groups are readily oxidised, at potentials similar to those of phosphines[45], and the ensuing chemical reactions are relatively well understood[46]. Oxidation of aliphatic amines, if water has not been strictly excluded, involves formation of a radical cation, followed by loss of an α-proton, leaving an α-carbon radical which undergoes further reactions[47]. It therefore does not come as a surprise to find that amine-containing ferrocene derivatives often show complex electrochemistry. The complex behaviour of 1-dimethylaminomethyl-2-diphenylphosphinoferrocene has already been discussed in Section 5.1.2[16]. Plenio and Burth studied a variety of different ferrocenylamines, and found that a number of them show up to three electrochemically reversible but chemically irreversible anodic redox processes[48]. The different processes were not assigned. A very recent study of N'-ferrocenylthioureas

showed electrochemical behaviour rather similar to that of **7**, and a complicated reaction scheme involving the oxidised species was proposed[49]. In view of the literature on this subject, it is not surprising to find that **7** also exhibits complex cyclic voltammetric behaviour.

Consideration was given to means by which **7** could be derivatised in order to give an electrochemically stable material. It was thought that this might be achieved by quaternisation of the amine groups. Compound **7** was first reacted with methyl iodide, and then $TlPF_6$ added in order to precipitate out the electroactive iodide, theoretically giving $[FcCH_2P\{CH_2N(Me)Et_2\}_2][PF_6]_2$, although the product mix was not characterised except by cyclic voltammetry. This treatment led to production of much more desirable voltammetric behaviour, with a single electrochemically and chemically reversible wave ascribable to ferrocene oxidation/reduction, and electrochemical parameters E_{PA} = 196 mV, E_{PC} = 135 mV, $E_{1/2}$ = 166 mV. For this reason a similar system was trialled with one polymer in Chapter 6. A large redox process present at *ca.* -0.8 V showed thallium was also present in the product mix.

5.3 Experimental

The work described in this Chapter was largely carried out in two stages totalling three weeks of intensive electrochemical investigations under the supervision of Dr. Alison Downard of the University of Canterbury, Christchurch, New Zealand. Dr. Downard also carried out a number of experiments in the author's absence in order to further investigate these systems. Cyclic voltammetry of compound **33**, and **7** with $TlPF_6$, was investigated at Auckland University, Auckland, New Zealand, by arrangement with Dr. Peter Boyd.

Samples for investigation were obtained according to the methods outlined in Chapters 2 and 4. Ferrocene, $NOBF_4$, DDQ and 40% aqueous HBF_4 solution, were obtained from commercial sources, and were all of LR grade or better.

A glass electrochemical cell with quickfit apertures was used for this work, and it held 5 ml of solution, generally of *ca.* 1 mM in analyte and always 0.1 M in the electrolyte, which was $Bu^n_4NPF_6$. The commercially obtained electrolyte was twice recrystallised from ethanol/water before drying for two days at 100° C. Electrolyte was subsequently stored in a vacuum desiccator in the presence of silica gel. The solvent used was HPLC-grade, and acetonitrile was used except where stated otherwise. Solvent was dried by passing it through a column of neutral alumina (mesh 70-230) directly into the cell. Alumina was initially dried at 400° C and subsequently stored in a vacuum desiccator in the presence of silica gel. The cell and column were both stored at *ca.* 100° C until shortly before experimentation.

5.3.1 Cyclic Voltammetry

Solutions were purged with nitrogen for several minutes before experimentation, and the solution kept under nitrogen for the duration.

A Pt disk electrode embedded in glass with an active surface area 1 mm in diameter was routinely used as the WE, although a GC electrode of 3 mm diameter was often used for comparison, or because of its insensitivity to otherwise active hydrogen-containing species. These electrodes were periodically polished, using either 1 μm diamond paste and oil or Al_2O_3 and water. A Pt wire served as the AE. The RE consisted of an Ag wire in contact with an acetonitrile solution containing 10 mM $AgNO_3$ and 0.1 M $Bu^n_4NPF_6$. This was separated by a glass fritt from a sample of the solution present in the cell, which was separated by another fritt from the bulk solution. The ends of the WE and RE were kept as close together as possible in order to minimise the effect of solution resistance on the measured potentials; solution resistance was not corrected for. Ferrocene was used as an external reference compound.

The potentiostat used was a PAR 174A polarographic analyser, and the waveform generator was a PAR 175 universal programmer. CVs were recorded on a Graphtec WX1200 or an EG & G model RE0092AX-7 recorder.

All samples were investigated at room temperature unless otherwise stated. Variation in scan rates, and judicious selection of scan directions and switching potentials aided in interpretation of the observed processes and their interrelationships.

Cyclic voltammetry of **33** and **7** with $TlPF_6$ was carried out in a perspex cell with a volume of 5 ml. Solvent used was AR-grade acetonitrile distilled over CaH_2 and stored in dry glassware under nitrogen. A Pt disk electrode was used as the WE, a Pt wire served as the AE, and the reference electrode consisted of an Ag wire in contact with a 0.1 M AgCl solution in acetone, separated by a glass fritt from the analyte solution. Potentiostat was a BAS 100A electrochemical analyser, waveform generation and recording of CVs was achieved using the BAS 100W program for Windows '95.

5.3.2 Bulk Electrolysis

For several minutes before the start of experimentation, and then throughout the experiment, purging with nitrogen and stirring of the solution were carried out.

The same RE was used as that described in Section 5.3.1, but the WE was a Pt wire mesh electrode, and the AE was a GC rod in contact with a solution containing 0.1 M electrolyte, separated from the analyte solution by a glass fritt of large surface area. When required the fritt was cleaned with ethanolic KOH in order to minimise impedance.

A PAR 273A potentiostat was used to control and monitor BE, but CVs of electrolysed solutions were still obtained in identical fashion to that described above.

On occasions BE was carried out in controlled-potential mode, while monitoring total current passed, but more usually BE was carried out in galvanostatic mode and the total current required calculated before starting, with electrolysis stopped at the appropriate point.

In some instances where a ^{31}P-NMR spectrum was required from an electrolysed solution, most of the solvent was first removed under reduced pressure in order to concentrate the sample. On other occasions a sample was taken from the cyclic voltammetric solution and investigated immediately; in such instances acquisition required a longer time period. Spectra were obtained using a D_2O insert in a glass capillary to provide an external lock signal. Immediately after acquisition of the spectrum, a few transients were obtained from a sample of D_2O containing a 85% orthophosphoric acid insert in a glass capillary, in order to provide a reference for the sample. Spectra were acquired on a Varian XL-300, at 121.45 MHz. If reconstitution of the sample was desirable in order to carry out further investigations, the sample was placed back in the electrochemical cell and diluted to the appropriate level with acetonitrile. ESMS of BE products was carried out on samples which had been dried under reduced pressure, followed by selective dissolution of the compounds of interest in ethyl acetate; this allowed most of the electrolyte to be removed by filtration. The ethyl acetate was then removed under reduced pressure to give the final sample. An appropriate description of ESMS methods can be found in Section 2.3.1, but note that no $AgNO_3$ or NaCl were used for the work described in this Chapter.

5.3.3 Spectroelectrochemistry

The cell used for this work consisted of a flat rectangular quartz vessel with a volume of 0.25 cm^3. A specially modified Pt wire gauze WE and a Pt wire working electrode, with another Pt wire serving as a pseudo-RE, fitted into the cell. Solutions of electrolyte and analyte were made up to the desired concentration in oven-dried volumetric flasks. The

experiments were carried out galvanostatically using a PAR 273 potentiostat, and absorbance at 626 nm monitored against time using a Hewlett Packard 8452A Diode Array Spectrophotometer.

5.3.4 Microelectrode Steady-State Voltammetry

The experimental set-up used for steady-state voltammetry was identical to that used for cyclic voltammetry (Section 5.3.1), with the exception that the WE was a Pt disk microelectrode, of diameter 10 μm. Scanning was carried out at rates of 20 or sometimes 50 mV s^{-1} in order to give the steady-state voltammogram.

5.3.5 Chemical Oxidations

Monitoring of chemical oxidation of **2** by $NOBF_4$ or DDQ using cyclic voltammetry was achieved by step-wise addition of small amounts of the oxidant directly to the electrochemical cell with a period of stirring (in the case of DDQ it was first dissolved in a small amount of acetonitrile). Reaction between **2** and nitrosonium was also monitored using ESMS. For this, AR grade acetonitrile was dried with magnesium sulfate and used to make up 40 ml of 2.1 mM **2**, which was purged and kept under nitrogen. $NOBF_4$ was added gradually to the solution. After each addition, the solution was stirred for one minute before withdrawing a sample for examination by ESMS. Spectra were run in neat acetonitrile with a cone voltage of 20 V. For other details concerning ESMS see Section 2.3.1. The reaction of **2** with DDQ was also carried out in such a way as to allow monitoring by NMR. Compound **2** (5.2 mg, 0.014 mmol) was added to DDQ (2.9 mg, 0.013 mmol) in 0.4 ml of acetonitrile. This resulted in deposition of a large amount of brown precipitate. Dissolution of the brown powder in DMF allowed examination of the products by ^{31}P-NMR, using the same methodology as that described in Section 5.3.2.

Examination of **34** and **35** by NMR was carried out with the equipment and methodology described in Section 2.3.1, although two-dimensional experiments and some other work also was carried out using a Bruker Avance DRX 400 spectrometer, operating at 400.13 MHz for ^{1}H and 100.61 MHz for ^{13}C. ^{19}F spectra were run using the Bruker AC300 at 282.4 MHz, and were referenced to external 1,3,5-trifluorobenzene deemed to be at δ -63.9 ppm with respect to CCl_3F. ESMS spectra of **34** and **35** were run in both acetonitrile/water and neat dichloromethane, and without the use of any further additives, but otherwise were acquired as described in Section 2.3.1.

5.3.6 Reaction of $FcCH_2P(O)(CH_2NEt_2)_2$ **7** with Methyl Iodide

Compound **7** (0.050 g, 0.120 mmol) was reacted with methyl iodide (2 ml, 32 mmol) under reflux in methanol (5 ml) for 20 min. After removal of methyl iodide and solvent under reduced pressure, the residue was dissolved in dichloromethane (5 ml) and $TlPF_6$ (0.083 g, 0.238 mmol) added. After stirring for 15 min the precipitate was filtered off and the supernatant dried under reduced pressure, giving a yellow oil (0.067 g).

5.4 References

1 A. J. Bard, L. R. Faulkner, *Electrochemical Methods, Fundamentals and Applications*, 1980, John Wiley & Sons Inc., New York.

2 G. C. Barris, *Aspects of Group 14 Element-Transition Metal Cluster Chemistry*, 1990, D. Phil. Thesis, University of Waikato, Hamilton, New Zealand, p. 154-157. J. Heinze, *Angew. Chem. Int. Ed. Eng.*, 1984, **23**, 831. G. A. Mabbott, *J. Chem. Ed.*, 1983, **60**, 697. P. T. Kissinger, W. R. Heineman, *J. Chem. Ed.*, 1983, **60**, 702.

3 A. J. Bard, L. R. Faulkner, *Electrochemical Methods, Fundamentals and Applications*, 1980, John Wiley & Sons Inc., New York, p. 370.

4 a) F. Battablini, E. J. Calvo, F. Doctorovich, *J. Organomet. Chem.*, 1997, **547**, 1. b) M. D. Imisides, R. John, G. G. Wallace, *Chemtech*, 1996, May, 19. c) S. Pons, M. Fleischmann, *Anal. Chem.*, 1987, **59**, 1391A.

5 A. J. Bard, L. R. Faulkner, *Electrochemical Methods, Fundamentals and Applications*, 1980, John Wiley & Sons Inc., New York, p. 283.

6 P. Zanello, *Electrochemical and X-ray Structural Aspects of Transition Metal Complexes Containing Redox-Active Ferrocene Ligands*, in *Ferrocenes*, A. Togni, T. Hayashi (Ed.), 1995, VCH Verlagsgesellschaft mbH, Weinheim, p. 317.

7 a) P. Stepnicka, R. Gyepes, O. Lavastre, P. H. Dixneuf, *Organometallics*, 1997, **16**, 5089. b) V. W.-W. Yam, S. W.-K. Choi, K.-K. Cheung, *J. Chem. Soc., Dalton Trans.*, 1996, 3411. c) S. Onaka, M.-A. Haga, S. Takagi, M. Otsuka, K. Mizuno, *Bull. Chem. Soc. Jpn.*, 1994, **67**, 2440. d) A. Louati, M. Huhn, *Inorg. Chem.*, 1993, **32**, 3601. e) L.-T. Phang, S. C. F. Au-Yeung, T. S. A. Hor, S. B. Khoo, Z.-Y. Zhou, T. C. W. Mak, *J. Chem. Soc., Dalton Trans.*, 1993, 165. f) G. Pilloni, B. Corain, M. Dagano, B. Longato, G. Zanotti, *J. Chem. Soc., Dalton Trans.*, 1993, 1777. g) F. Estevan, P. Lahuerta, J. Latorre, E. Peris, S. Garcia-Granda, F. Gomez-Beltran, A. Aguirre, M. A. Salvado, *J. Chem. Soc., Dalton Trans.*, 1993, 1681. h) M. C. Gimeno, A. Laguna, C. Sarroca, P. G. Jones, *Inorg. Chem.*, 1993, **32**, 5926. i) F. Estevan, J. Latorre, E. Peris, *Polyhedron*, 1993, **12**, 2153. j) M. Adachi, M. Kita, K. Kashiwabara, J. Fujita, N. Iitaka, S. Kurachi, S. Ohba, D. Jin, *Bull. Chem. Soc. Jpn.*, 1992, **65**, 2037. k) A. Houlton, R. M. G. Roberts, J. Silver, R. V. Parish, *J. Organomet. Chem.*, 1991, **418**, 269. l) T. M. Miller, K. J. Ahmed, M. S. Wrighton, *Inorg. Chem.*, 1989, **28**, 2347. m) B. Longato, G. Pilloni, G. Valle, B. Corain, *Inorg. Chem.*, 1988, **27**, 956. n) D. A. Clemente, G. Pilloni, B. Corain, B. Longato, M. Tiripicchio-Camallini, *Inorg. Chim. Acta*, 1986, **115**, L9. o) K. R. Mann, W. H. Morrison Jr., D. N. Hendrickson, *Inorg. Chem.*, 1974, **13**, 1180. p) G. Pilloni, B. Longato, *Inorg. Chim. Acta*, 1993, **208**, 17.

8 J. C. Kotz, C. L. Nivert, J. M. Lieber, R. C. Reed, *J. Organomet. Chem.*, 1975, **91**, 87.

9 J. C. Kotz, C. L. Nivert, *J. Organomet. Chem.*, 1973, **52**, 387.

10 A. Gref, P. Diter, D. Guillaneux, H. B. Kagan, *New J. Chem.*, 1997, **21**, 1353.

11 P. Zanello, *Electrochemical and X-ray Structural Aspects of Transition Metal Complexes Containing Redox-Active Ferrocene Ligands,* in *Ferrocenes*, A. Togni, T. Hayashi (Ed.), 1995, VCH Verlagsgesellschaft mbH, Weinheim, p. 333.

12 P. Zanello, G. Opromolla, G. Giorgi, G. Sasso, A. Togni, *J. Organomet. Chem.*, 1996, **506**, 61.

13 B. Corain, B. Longato, G. Favero, D. Ajo, G. Pilloni, U. Russo, F. R. Kreissl, *Inorg. Chim. Acta*, 1989, **157**, 259.

14 G. Pilloni, B. Longato, B. Corain, *J. Organomet. Chem.*, 1991, **420**, 57.

15 W. B. Gara, B. P. Roberts, *J. Chem. Soc., Perkin II*, 1978, 150.

16 J. C. Kotz, C. L. Nivert, J. M. Lieber, R. C. Reed, *J. Organomet. Chem.*, 1975, **84**, 255.

17 J. Podlaha, P. Stepnicka, J. Ludvik, I. Cisarova, *Organometallics*, 1996, **15**, 543.

18 A. Masson-Szymczak, O. Riant, A. Gref, H. B. Kagan, *J. Organomet. Chem.*, 1996, **511**, 193.

19 I. R. Butler, M. Kalaji, L. Nehrlich, M. Hursthouse, A. I. Karaulov, K. M. A. Malik, *J. Chem. Soc., Chem. Commun.*, 1995, 459.

20 A. M. Leiva, L. Rivera, B. Loeb, *Polyhedron*, 1991, **10**, 347. H. Ohmori, H. Maeda, M. Kikuoka, T. Maki, M. Masui, *Tetrahedron*, 1991, **47**, 767. K. S. V. Santhanam, *Electrochemistry of Organophosphorus(III) Compounds*, in *The Chemistry of Organophosphorus Compounds*, F. R. Hartley (Ed.), 1990, John Wiley & Sons Ltd, New York, V. **1**, p. 118. G. Schiavon, S. Zecchin, G. Cogoni, G. Bontempelli, *Electroanalytical Chemistry and Interfacial Electrochemistry*, 1973, **48**, 425. V. H. Matschiner, L. Krause, F. Krech, *Z. anorg. allg. Chem.*, 1970, **373**, 1.

21 Two examples of this kind are also discussed briefly in: M. Emilia, N. P. R. A. Silva, A. J. L. Pombeiro, J. J. R. Frausto da Silva, R. Herrmann, N. Deus, R. E. Bozak, *J. Organomet. Chem.*, 1994, **480**, 81.

22 C. A. Sassano, C. A. Mirkin, *J. Am. Chem. Soc.*, 1995, **117**, 11379.

23 A. Louati, M. Gross, L. Douce, D. Matt, *J. Organomet. Chem.*, 1992, **438**, 167. P. Braunstein, L. Douce, F. Balegroune, D. Grandjean, D. Bayeul, Y. Dusausoy, P. Zanello, *New J. Chem.*, 1992, **16**, 925.

24 DigiSim®, Digital Simulation Software, Bioanalytical Systems Inc., U. S. A.

25 B. Grossmann, J. Heinze, E. Herdtweck, F. H. Köhler, H. Nöth, H. Schwenk, M. Spiegler, W. Wachter, B. Weber, *Angew. Chem. Int. Ed. Engl.*, 1997, **36**, 387. W. H. Morrison Jr., S. Krogsrud, D. N. Hendrickson, *Inorg. Chem.*, 1973, **12**, 1998.

26 A. J. Downard, B. H. Robinson, J. Simpson, *J. Organomet. Chem.*, 1987, **320**, 363.

27 J. E. Cyr, P. H. Rieger, *Organometallics*, 1991, **10**, 2153.

28 L. P. Clarke, J. E. Davies, P. R. Raithby and G. P. Shields, *J. Chem. Soc., Dalton Trans.*, 1996, 4147.

29 P. Lemoine, *Coord. Chem. Rev.*, 1988, **83**, 169.

30 C. J. Jameson, *Flourine*, in *Multinuclear NMR*, J. Mason (Ed.), 1987, Plenum Press, New York, p. 438.

31 S. Ito, N. Morita, T. Asao, *J. Org. Chem.*, 1996, **61**, 5077.

32 G. F. Swiegers, U. T. Mueller-Westerhoff, *Abstracts of the Royal Australian Chemical Institute Inorganic Chemistry Division Conference IC'98*, 1998, Wollongong, Australia, p. 58.

33 U. T. Mueller-Westerhoff, T. J. Haas, G. F. Swiegers, T. K. Leipert, *J. Organomet. Chem.*, 1994, **472**, 229. U. T. Mueller-Westerhoff, *Angew. Chem. Int. Ed. Engl.*, 1986, **25**, 702.

34 U. T. Mueller-Westerhoff, A. Nazzal, W. Prössdorf, J. J. Mayerle, R. L. Collins, *Angew. Chem. Int. Ed. Engl.*, 1982, **21**, 293.

35 S. G. Baxter, R. L. Collins, A. H. Cowley, S. F. Sena, *Inorg. Chem.*, 1983, **22**, 3475.

36 V. I. Boev, *Zh. obshch. khim.*, 1987, **57**, 713.

37 G. Wagner, R. Herrmann, *Chiral Ferrocene Derivatives. An Introduction,* in *Ferrocenes*, A. Togni, T. Hayashi (Ed.), 1995, VCH Verlagsgesellschaft mbH, Weinheim, p. 175.

38 U. Behrens, *J. Organomet. Chem.*, 1979, **182**, 89. R. L. Sime, R. J. Sime, *J. Am. Chem. Soc.*, 1974, **96**, 892.

39 V. I. Boev, L. V. Snegur, V. N. Babin, Yu. S. Nekrasov, *Russ. Chem. Rev.*, 1997, **66**, 613.

40 V. I. Boev, *Zh. obshch. khim.*, 1987, **57**, 633.

41 O. Schmidt, A. Fuchs, D. Gudat, M. Nieger, W. Hoffbauer, E. Niecke, W. W. Schoeller, *Angew. Chem. Int. Ed.*, 1998, **37**, 949.

42 R. Pietschnig, E. Niecke, *Organometallics*, 1996, **15**, 891.

43 M. R. St. J. Foreman, A. M. Z. Slawin, J. D. Woollins, *Chem. Commun.*, 1997, 1269. M. R. St. J. Foreman, A. M. Z. Slawin, J. D. Woollins, *J. Chem. Soc., Dalton Trans.*, 1996, 3653.

44 M. I. Rybinskaya, A. Z. Kreindlin, S. S. Fadeeva, *J. Organomet. Chem.*, 1988, **358**, 363.

45 V. D. Parker, *Anodic Oxidation of Amines,* in *Organic Electrochemistry*, M. M. Baizer (Ed.), 1973, Marcel Dekker Inc., New York, p. 509.

46 R. N. Adams, *Acc. Chem. Res.*, 1969, **2**, 175.

47 W. E. Britton, *Electrochemistry of Amines,* in *The Chemistry of Functional Groups, Suppliment F, Part 1: The Chemistry of Amino, Nitroso and Nitro Compounds and their Derivatives*, S. Patai (Ed.), 1982, John Wiley & Sons, Chichester, p. 350.

48 H. Plenio, D. Burth, *Organometallics*, 1996, **15**, 4054.

49 O. Seidelmann, L. Beyer, *Polyhedron*, 1998, **17**, 1601.

Chapter 6: Synthesis, Characterisation and Electrochemistry of Ferrocenylphosphine Oxide Polymers

6.1 Introduction

6.1.1 Ferrocene-Containing Polymers and Materials

A recent wide-ranging review of ferrocene-containing polymeric materials has been published in book form[1]. A more general review written at a popular level concerning transition-metal containing polymers including ferrocene polymers has also been recently published[2]. This Section offers a condensed account of this area of research as well as other ferrocene-functionalised materials, emphasising points of special relevance to the present study and including more recent references.

A variety of different methods have been used for the production of polymeric materials incorporating ferrocene units. The earliest of these methods to be widely investigated was addition polymerisation of unsaturated monomers such as vinyl ferrocene[3] (Scheme 6.1), following the classical techniques for organic polymer production such as radical, cationic, anionic, and Ziegler-Natta conditions[1].

In recent times, the method for production of ferrocene-containing polymers which has received the most attention is ring-opening polymerisation[4]. In this method a ferrocenophane compound (usually with a strained structure) is reacted in such a way as to produce

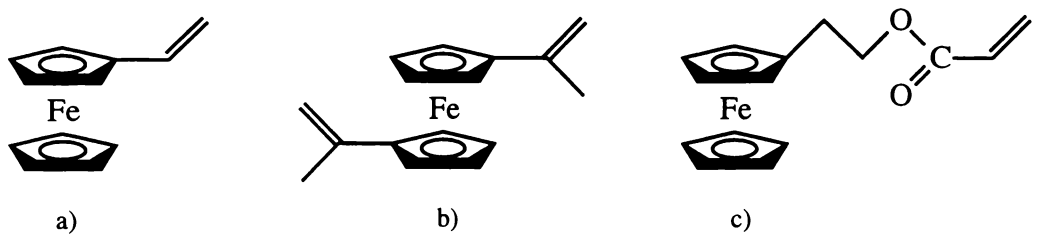

Scheme 6.1: Some examples of unsaturated monomers which can undergo addition polymerisations: a) vinylferrocene[3]; b) 1,1'-diisopropenylferrocene[1]; c) ferrocenylethyl acrylate[1].

polymerisation with cleavage of the bridge. Probably the most prominent example is the production of poly(ferrocenylsilane) polymers from the ring-opening polymerisation of silicon-bridged [1]ferrocenenophanes, which in 1992 became one of the first such polymerisation routes discovered[5]. An example[6] of this process is given in Scheme 6.2. A similar approach to polymer production has been successfully used with [3]trithiaferrocenophanes[7], hydrocarbon-bridged [2]ferrocenophanes[6,8] and a hydrocarbon-bridged [4]ferrocenophane[9], [1]germanaferrocenophanes[6,10], [1]selenaferrocenophanes[7a,11], [1]thiaferrocenophanes[11,12], a [2]carbathioferrocenophane[13], and a [1]boraferrocenophane[14].

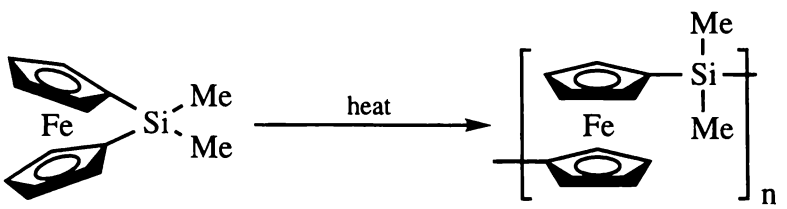

Scheme 6.2: Ring opening polymerisation of *Si,Si*-dimethyl-[1]silaferrocenophane to give the corresponding poly(ferrocenosilane). Polymerisation occurs in the melt of the monomer.

Of more immediate relevance to the present study is the ring-opening polymerisation of *P*-phenyl-[1]phosphaferrocenophane and some closely related species, which results in the production of polymeric ferrocenylphosphines[15]; an example is given in Scheme 6.3. This procedure can be achieved under very mild conditions. The phosphine sulfide derivative of *P*-phenyl-[1]phosphaferrocenophane will also undergo ring-opening to give the

ferrocenylphosphine sulfide polymer; alternatively the ferrocenylphosphine polymers produced by ring-opening polymerisation can be reacted with sulfur to give the corresponding ferrocenylphosphine sulfide materials[15].

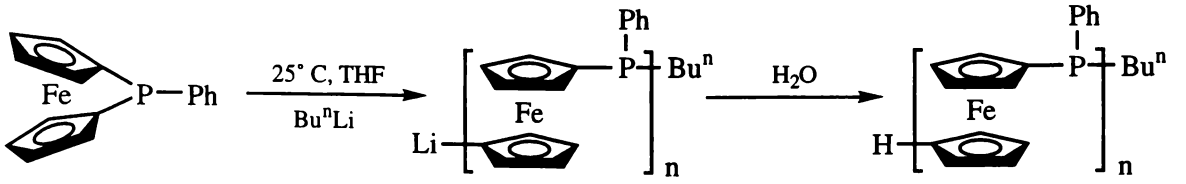

Scheme 6.3: Ring opening polymerisation of a [1]phosphaferrocenophane.

Ring strain can be used in a somewhat different way in order to produce ferrocene-phosphorus polymers from ferrocenylphosphazene compounds[1,16], as illustrated in Scheme 6.4.

A number of different condensation polymers have also been produced containing ferrocenyl groups[1,17], for instance through reaction of 1,1'-bis(2-aminoethyl)ferrocene with the diacid halide $[CH_2C(O)Cl]_2$[18]. In fact, condensation reactions have been used in order to produce rather irregular poly(ferrocenylphosphine) oligomers of a type similar to those which can be made through ring-opening polymerisation[4], through reaction of ferrocene with $PhPCl_2$. These can be further reacted to produce the corresponding phosphine oxides. Another condensation route to poly(ferrocenylphosphine) which gives a better-defined polymer is the reaction of 1,1'-dilithioferrocene with $PhPCl_2$[4]. Both these routes are shown in Scheme 6.5.

Condensation reactions have also been used to attach ferrocenyl pendants to preformed polymers[1,19]. In addition, further reaction of preformed polymers in order to incorporate ferrocene functions has been carried out in other ways. One such reaction has been used to create ferrocene- derived phosphazene polymers similar to those described above[1]. The reaction system is shown in Scheme 6.6, and involves formation of carbanionic centres on the polymer which can then react as nucleophiles with ferrocenyl aldehyde.

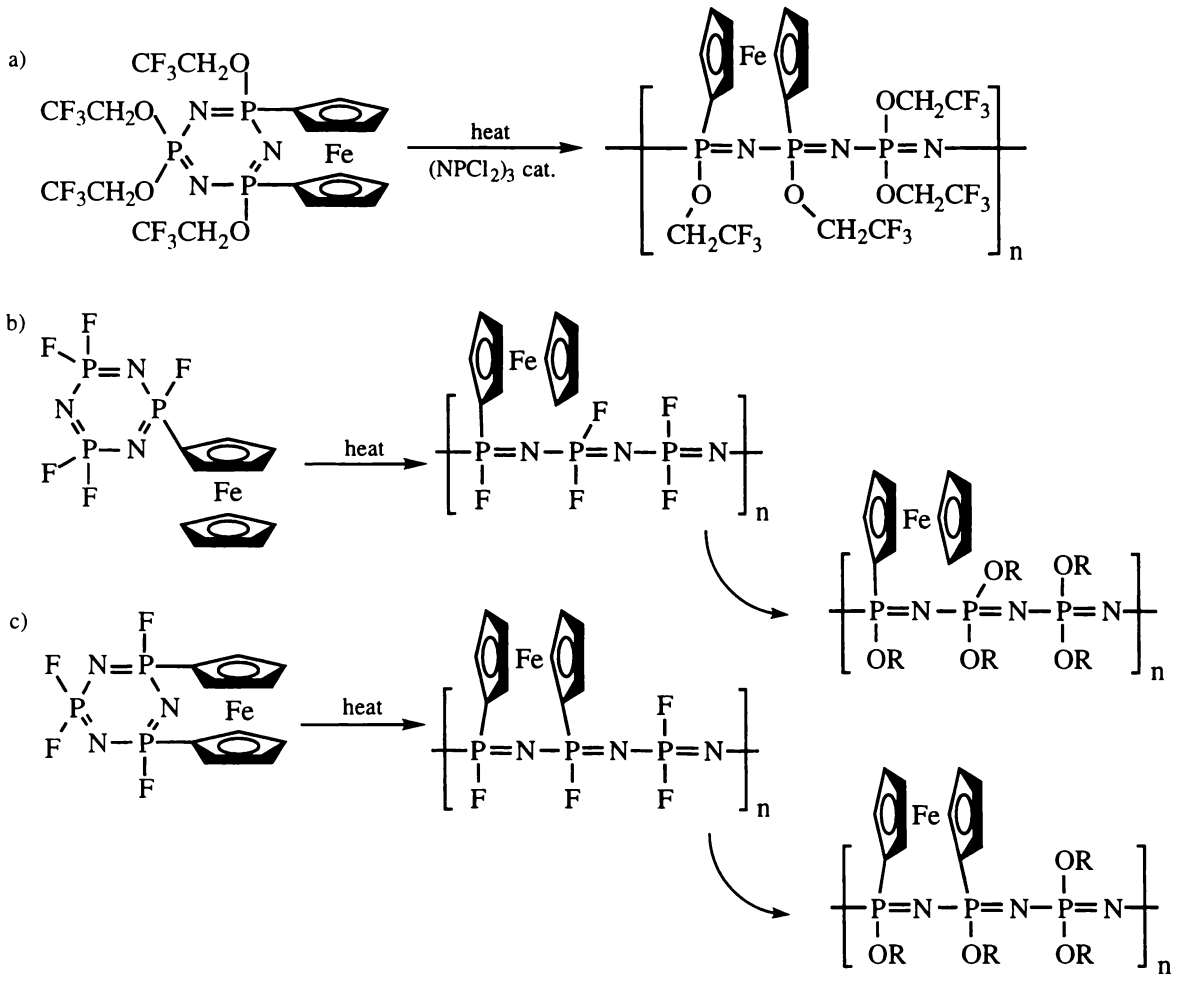

Scheme 6.4: Polymerisation of ferrocenylphosphazenes via ring-opening. a) Here ring strain is the driving force behind the reaction. b), c) Halogen atoms attached to the phosphorus atoms aid progress of these polymerisations and are later removed.

Another method which has been used for the formation of ferrocene-containing polymers is electropolymerisation[1,20]. This is a useful technique where an electrode surface modified with ferrocene groups is desired. It also allows for the production of ultra-thin surface films of the polymer.

Electropolymerisation might be considered as a technique intermediate between polymer formation, and surface modification of a material. Various means of achieving the latter have

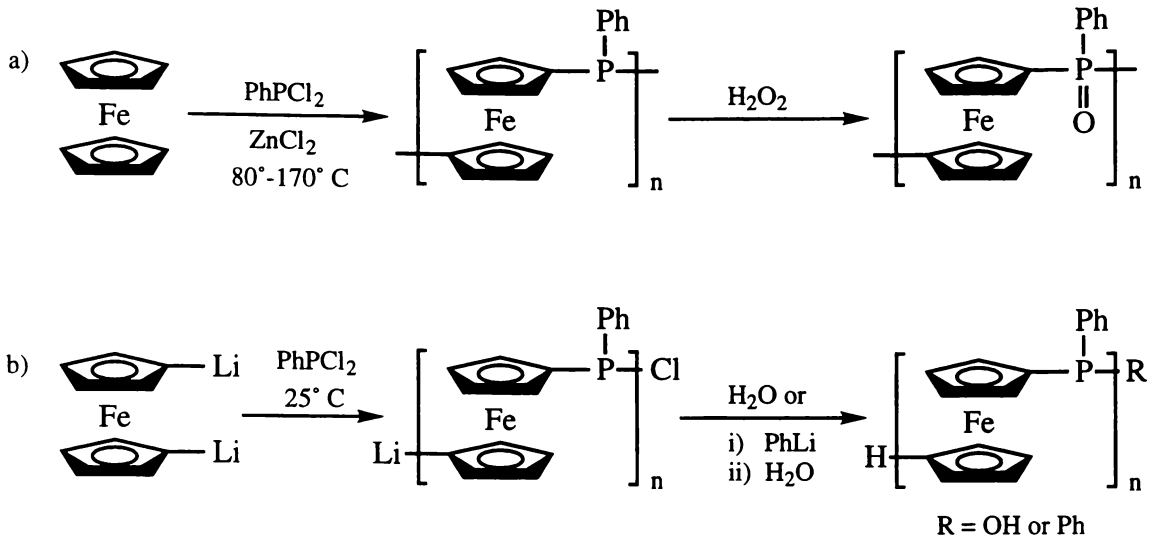

Scheme 6.5: Condensation routes to the production of ferrocenylphosphine and phosphine oxide polymers. a) The products produced by this route, though formally described as depicted here, actually also contained 1,2-, 1,3-, and 1,1'-ferrocenylene linkages. b) It is possible that under certain conditions this reaction takes place partially through the *in situ* formation of the [1]phosphaferrocenophane, which then undergoes ring-opening polymerisation.

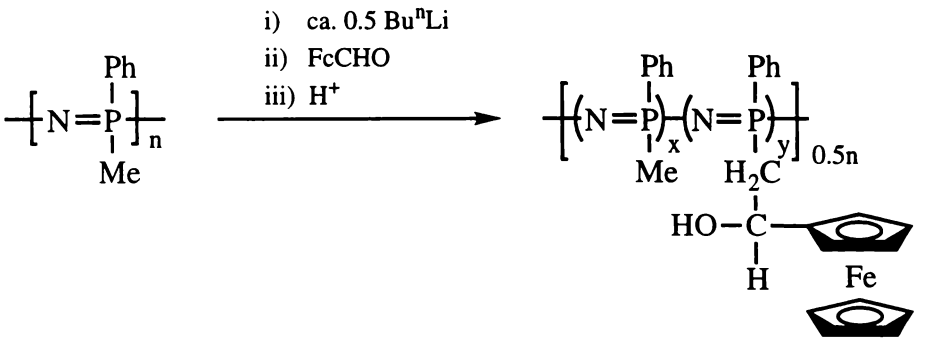

Scheme 6.6: Partial reaction of a phosphazene polymer with *n*-BuLi followed by ferrocenyl aldehyde gives a ferrocenylphosphazene polymer. Both x and y are *ca.* 0.5.

been extensively used to produce monolayers of ferrocene-modified species on electrode surfaces. Perhaps the most widely-used method for surface-modifying electrode surfaces with ferrocene groups has been chemisorption of ferrocene-derivatised thiols (or mercaptans) onto gold electrodes[21]. Fixation of a ferrocenyl oligonucleotide to a gold electrode has also been reported[22].

Not only gold, but also silica[23], a mesoporous silicate[24], and silicon[25] have been surface-derivatised using ferrocenyl-containing species. The last method has in fact been applied to compound **1** in order to produce silicon surfaces derivatised with a ferrocenylphosphine; it is thought that each ferrocene function is bound to the silicon surface through one of the hydroxymethyl groups[26].

6.1.2 The Utility of Ferrocene as a Redox Mediator in Enzyme Electrodes

The 'enzyme electrode'[27] is a system which is designed to allow highly specific detection of the levels of a biologically relevant analyte in solution. The simplest situation requires that a redox enzyme be somehow trapped or immobilised next to an electrode surface. When the electrode is immersed in a solution containing a substrate which the enzyme will recognise, the redox enzyme will catalyse transformation of the substrate into something else, producing a change in oxidation state at the enzyme active site. Usually the charge at the enzyme is detected 'amperometrically', that is, the electrode is held at a particular potential so that as the enzyme undergoes redox reaction, it is regenerated by transfer of charge to the electrode surface. The level of current flowing through the electrode is thus proportional to the level of enzyme activity, which is in turn proportional to the level of analyte in solution. The enzyme electrode is represented schematically in Figure 6.1.

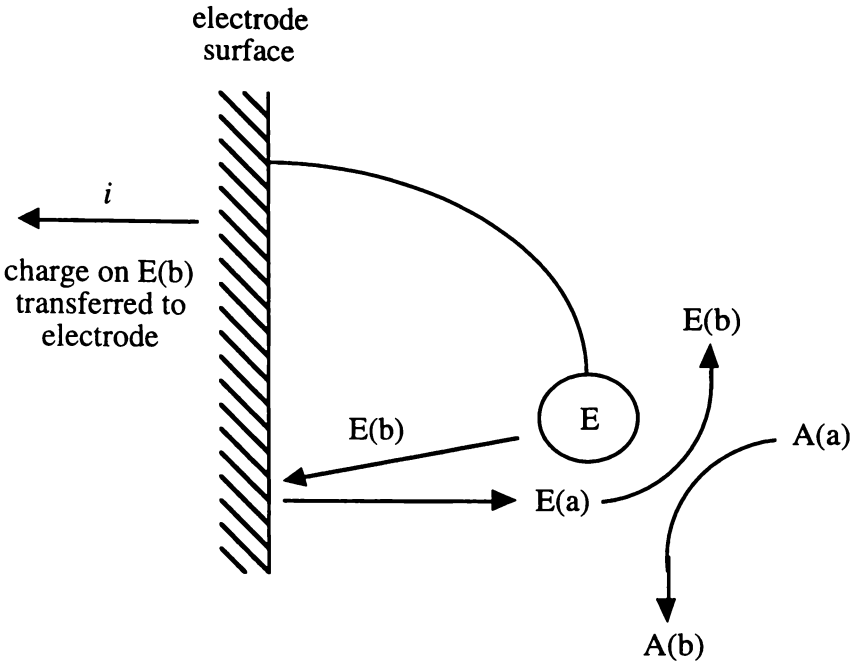

Figure 6.1: Diagram showing the workings of a simple enzyme electrode. E = enzyme, A = analyte in solution. The enzyme is here pictured as 'tethered' to the electrode surface, although enzyme immobilisation can be achieved by a variety of different ways[28]. Reaction between enzyme and analyte leads to the change in oxidation states from A(a) to A(b) and E(a) to E(b). The enzyme is then returned to state E(a) by charge transfer to the electrode surface, producing a detectable current *i*.

Enzyme electrode systems have now been developed for a variety of different analytes, using techniques which can be rather complicated, sometimes necessitating an array of enzymes in order to perform the desired analysis. Some examples of enzyme electrodes are listed in Table 6.1. It will be noted that this table contains a list of mediators. This refers to the fact that most biological molecules, including enzymes, show sluggish kinetics at bare electrode surfaces[29]; many enzyme electrodes therefore incorporate an artificial 'redox shuttle' immobilised with the enzyme in order to facilitate rapid charge transfer to the electrode surface. In fact, recent interest in the development of enzyme electrodes of this kind has been high, since otherwise oxygen or some other suitable reagent needs to be supplied to the

Table 6.1: *Detectable analytes, the enzymes used to detect them, immobilised mediator species where relevant, and recent literature references, for various enzyme electrodes.*

Analyte	Enzyme(s)	Mediator	Reference(s)
glucose	glucose oxidase	ferrocene	21c, 30, 31, 32, 33, 34, 35, 36
		Fe(II) complex	32, 37
		Ru(II) complex	32, 37
		Os(II) complex	38, 39, 40
		tetrathiafulvene	30, 41
		dopamine	42
		pyrroloquinoline quinone	43
		methyl viologen	44
		-	45, 46, 47, 48, 49, 50, 51, 52, 53, 54, 55, 56, 57, 58, 59
glucose, lactate	glucose oxidase, lactate oxidase, horseradish peroxidase	Os(II) complex	60
dinitrophenol antibody	glucose oxidase	ferrocene	61
galactose	galactose oxidase	-	55
fructose	fructose dehydrogenase	-	62
various sugars*	oligosaccharide dehydrogenase	Os(II) complex	63
ethanol	alcohol oxidase	pyrroloquinoline quinone	64
		-	55
lactate	lactate oxidase	Os(II) complex	38
		-	53, 55, 65, 66, 67
	lactate dehydrogenase	pyrroloquinoline quinone	64
L-amino acid	L-amino acid oxidase	-	53
urea	urease	-	54
triolein	lipase	-	54
choline	choline oxidase	-	34

Table 6.1 continued

acetylcholine	acetylcholine esterase, choline oxidase, horseradish peroxidase	Os(II) complex	68
	acetylcholine esterase, choline oxidase	-	34
peroxides	horseradish peroxidase	Os(II) complex	38, 69
		Fe(II) complex	70
		thionine	71
		-	72
	soybean peroxidase	Os(II) complex	73
oxidised glutathione	glutathione reductase	-	58
nitrate	nitrate reductase	methyl viologen	74
nitrite	nitrite reductase	bipyridinium	75
creatinine	creatininase, creatinase, sarcosine oxidase	-	76
linamarin	horseradish peroxidase, linamarase	-	77
cyanide	horseradish peroxidase	-	78
	cytochrome oxidase	-	79
L-phenylalanine	tyrosinase, salicylate hydroxylase, L-phenylalanine dehydrogenase	-	80
azide	tyrosinase	Os(II) complex	81
phenols	tyrosinase	-	72, 82
bilirubin	bilirubin oxidase	-	72
imidazole, histidine	micro-peroxidase	-	83
glutamate	glutamate oxidase	-	84
dopamine	polyphenol oxidase	-	84
riboflavin, FMN, FAD, NADH, NADPH #	flavin reductase	-	85

* Tested for L-arabinose, D-xylose, D-galactose, D-fructose, D-glucose, D-mannose, cellobiose, lactose, maltose, malto-oligosaccharides.

FMN = flavin mononucleotide, FAD = flavin adanine dinucleotide, NADP = nicotinamide adenine dinucleotide phosphate, NADPH = reduced NADP

electrode to keep regenerating the enzyme. For this reason electrodes having such a mediator are commonly called 'reagentless'. As can be seen from the Table 6.1, immobilised osmium complexes[86] continue to be a popular choice as a mediator.

Immobilised ferrocene is also used extensively; the reversible and chemically stable ferrocene/ferrocenium couple, which is easily accessible electrochemically, makes ferrocene well suited to enzyme electrodes where an anodic current is being detected (i.e. when oxidising enzymes are being used). The means by which ferrocene units have been immobilised near the electrode surface in enzyme electrodes are numerous, and include incorporation into hydrogels[32], copolymerisation of vinylferrocene with acrylamides[33,35], binding of ferrocene-thiols to gold electrodes[21c,61], attachment of long-chain ferrocene-carboxylic acid species to the enzymes themselves[34], copolymerisation of (2-aminoethyl)ferrocene with glutaraldehyde[36], simple diffusion of ferrocene species into a gel before use[87], electropolymerisation of ferrocene-modified pyrroles[88], and use of ferrocene-derivatised siloxane polymers[89]. Where an immobilised mediator is not used, soluble ferrocene species are sometimes used as electrode reagents[58,59]. Enzymes with which ferrocene has been used as a mediator or reagent include glucose oxidase[30-36,58,59,87-89,90,91], D-amino acid oxidase[92], and bilirubin oxidase[72]. The gain in efficiency which can be achieved through inclusion of a ferrocene mediator into the electrode matrix is elegantly illustrated by the case of planar-chiral ferrocene systems. Tao *et al.*[21c] have reported that in electrodes formed by the binding of planar-chiral ferrocene-thiols to gold, the anodic current observed in the presence of glucose oxidase and glucose is *ca.* 90% higher for the (*S*)-functionalised electrode than the (*R*)-functionalised electrode. This is in harmony with what is known of planar-chiral ferrocene/enzyme interactions[93]. The ferrocene functions are therefore undoubtedly playing some part in electron transfer from enzyme to electrode. The usefulness of ferrocene mediators is also seen in the fact that large enzymes with well-protected redox centres such as glucose oxidase will show negligible interaction with electrode surfaces; derivatisation of glucose oxidase with up to twelve ferrocene units leads to rapid and effective electron transfer[29].

6.1.3 Enzyme Immobilisation on Copolymers of Amines and Hydroxymethylphosphines

In recent years investigations have been made into the use of hydroxymethylphosphines as cross-linking agents in the production of immobilised enzyme supports. Polymers of this kind were first prepared by the reaction of $P(CH_2OH)_3$ with tetraethyleneglycol diamine; reaction of hydroxyl groups with the amines gave an amorphous cross-linked white product containing phosphine groups capable of acting as ligands[94]. Oxidation of this polymer with hydrogen peroxide gave the air-stable phosphine oxide derivative. A chiral polymeric phosphine ligand was obtained by the reaction of Ph_2PCH_2OH or $MeP(CH_2OH)_2$ with chitosan, an amine-containing biopolymer[95].

Further studies were then carried out on the immobilisation of urease onto hydroxymethylphosphine-amine polymers, such as the reaction of chitosan with $P(CH_2OH)_3$, which was then used as a cross-linking agent for immobilisation of urease[96]. Several alternative systems were developed which show great promise as enzyme immobilisation techniques. For example, reaction of the commercially available polyether triamine Jeffamine® T-403 with the appropriate ratio of $P(CH_2OH)_3$ yields a polymer which contains free hydroxymethyl groups. These groups will react with amine functions in urease in order to achieve immobilisation[97]. A similar polymer was created by the reaction of Jeffamine® T-403 with $P(CH_2OH)_3$ followed by oxidation of the phosphine functions. In this case amine groups were left in excess and the urease bound to the polymer using the cross-linking agent glutaraldehyde[98]. Activity of the immobilised urease in these two Jeffamine T-403 polymers was comparable to activities achieved with other currently used immobilisation techniques. Use of a larger molecular weight Jeffamine® T-3000 also gave a polymer with good urease activity, where glutaraldehyde was used to immobilise the enzyme[99]. A representation of these reactions is given in Scheme 6.7. More recently immobilisation of alcohol dehydrogenase on chitosan using $P(CH_2OH)_3$ as the coupling

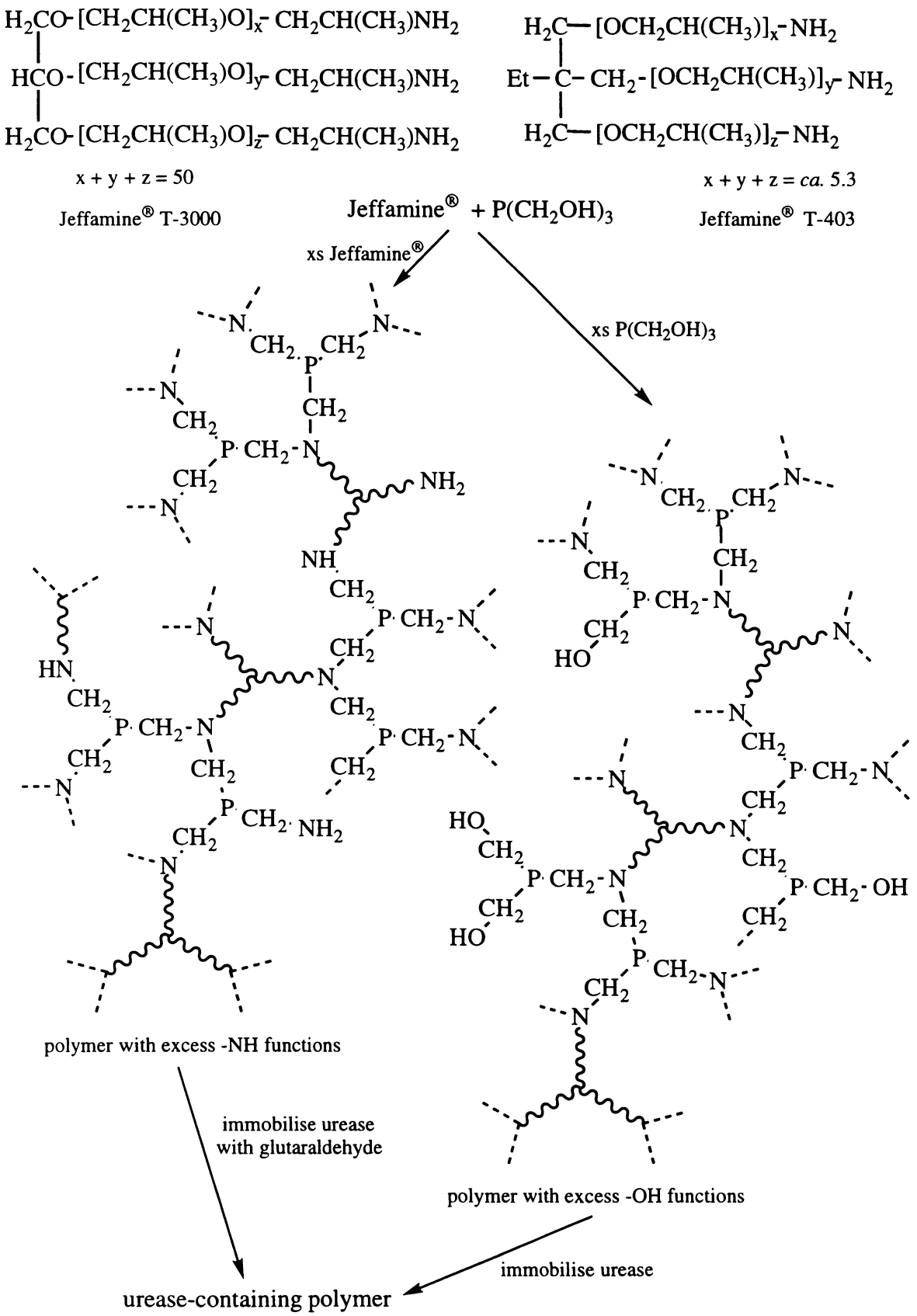

Scheme 6.7: Formation of condensation polymers used for the immobilisation of urease.

agent[100], and likewise β-glucosidase on polyacrylamide-magnetite beads, aminopropyl silica and chitosan[101], were shown to be superior systems to more conventional glutaraldehyde immobilisation methods.

Potential advantages gained from the immobilisation of enzymes using these techniques include high activity due to the fact that enzymes are in some cases "tethered" to the polymer by long-chain molecules[99,102], and the known resistance of polyethers to non-specific protein adsorption[103].

6.2 Results and Discussion

The study outlined here was not intended to be exhaustive, but rather was to function as an exploratory investigation into the synthesis and properties of a variety of ferrocene-containing polymers, and to conduct an initial assessment of their suitability for use as enzyme electrode materials.

6.2.1 Synthesis and Characterisation of Ferrocene-Containing Polymers

On the basis of what has been discussed in Section 6.1, it was reasoned that compound **1** could be cross-linked with multifunctional primary amines in order to produce novel ferrocenylphosphine polymers. Primarily this was seen as a way to produce materials with potential applications in the field of enzyme electrodes, with the ferrocenyl functions acting as mediators as described in Section 6.1.2, and enzymes immobilised on the polymers as described in 6.1.3. However, it should be noted that other applications can be envisaged for such materials. For instance, it was noted in Section 2.1.1 that the reaction of $P(CH_2OH)_3$ with ammonia is used commercially to produce clothing with flame retardant properties[104].

The use of **1** rather than $P(CH_2OH)_3$ in cross-linking reactions with amines may provide a superior product in this regard, as ferrocene has previously been incorporated into fire retardant polymers due to its ability to promote extinction and reduce smoke formation[105].

The feasibility of using cross-linking reactions between the hydroxymethylphosphine groups of **1** and N-H bonds to produce ferrocene-containing materials was initially qualitatively assessed by reaction of **1** with aminopropyl silica. Aminopropyl silica immersed in a methanolic solution of **1** and then rinsed retained a permanent yellow colour, while similar treatment with **3** or **4** led to much less marked staining, as would be expected since hydroxymethyl functionalities of P(V) compounds such as **3** and **4** are inactivated towards this Mannich-type reaction with amine groups.

Huntsman Corporation produce a variety of commercially available amine-functionalised long-chain polyethers such as those discussed in Section 6.1.3. The reaction of **1** with a few of these Jeffamines® was investigated, along with reactions involving $P(CH_2OH)_3$, ammonia and 1,6-diaminohexane. The general synthetic method involved preparation of oxygen-free methanolic solutions of the amine, followed by addition of **1** and stirring overnight at room temperature. A hydrogen peroxide solution was then added in order to produce controlled oxidation of the phosphine centres in the polymer. The polymeric products obtained showed a wide variety of different physical properties; some were soluble in methanol while others were insoluble (none appeared soluble in water); some were powders, others brittle oils, others were viscous or formed flexible films. Systematic characterisation of polymers produced was limited, but in all cases the levels of nitrogen and iron in the polymer was measured, and the ratio of the two corresponded approximately to what was expected on the basis of stoichiometric reaction of **1** with the other reagents. Nitrogen levels were assessed by standard elemental analysis, while iron levels were measured using atomic absorption (AA) spectroscopy. Table 6.2 lists the polymers prepared by number, along with some analytical data. The nature of each of the polymers is described in the following paragraphs.

Table 6.2: *Analytical data for polymers prepared using 1. Experimental percentages of C, H, and N in the polymers were obtained by standard elemental analysis. Experimental percentages of Fe in the polymers were obtained by AA spectroscopy. Theoretical percentages of C, H, N and Fe are those which would be obtained from complete reaction of stoichiometric quantities of the reagents. Calculated mol ratios of ferrocene to amine functions are also given, assuming that all iron and nitrogen in the samples is accounted for by these functionalities.*

	experimental					theoretical				
	C	H	N	Fe	ratio Fc:amine	C	H	N	Fe	ratio Fc:amine
36[a#]	59.7	9.7	1.2	1.8	0.40	63.2	9.7	1.1	4.4	1.00
37[b]	55.7	6.8	2.8	13.2	1.19	58.2	7.0	3.3	13.3	1.00
38[c]	56.3	6.6	4.2	15.6	0.92	55.5	6.3	3.8	15.2	1.00
39[d]*	41.5	4.8	3.9	12.7	0.81	51.2	5.4	5.3	15.9	0.75
40[e]	56.7	6.8	4.2	14.6	0.88	58.2	6.4	4.2	16.9	1.00
41[e]^	55.1	6.6	4.0	14.4	0.90	53.6	6.4	3.7	14.7	1.00

Polymers made with: a = Jeffamine® T-3000, b = Jeffamine® T-403, c = Jeffamine® EDR-192, d = NH_3, e = 1,6-diaminohexane.

Influence of ammonia has been ignored in theoretical calculations.

* Theoretical calculations based on reaction of 3 × **1** with 2 × $P(CH_2OH)_3$ and 4 × NH_3.

^ Theoretical calculations based on full quaternisation of amine groups with MeCl; as described in the experimental section, polymer was reacted with MeI, then exposed to excess NaCl.

Polymer **36** was formed by reaction of **1** with Jeffamine® T-3000, the structure of which has already been described in Scheme 6.7. The two reagents were mixed in a ratio intended to give a small excess of 1.06 OH groups over NH groups, thus meaning the product would contain unreacted OH moieties which could conceivably react with the amine functions of enzymes. After overnight reaction the product remained in solution, so the solvent was removed under vacuum and the product stored in oxygen-free conditions. Analysis of this product by ^{31}P-NMR showed no peak attributable to **1**. The largest collection of peaks was clustered around *ca.* -30 ppm, with other broad signals centred about *ca.* - 36 ppm and -49 ppm. This broad signal at -49 ppm presumably corresponds to reaction of both hydroxymethyl functions of **1**, since the chemical shift for the monomeric diamine **6** is -48.3 ppm (Section 2.3.1). The downfield signals presumably correspond to bonding modes

where the hydroxymethyl functions of **1** have not both reacted, meaning that at this point the average molecular weight of the material is probably not very high. Other sharper and smaller signals were seen at -23.5 ppm, -27.6 ppm, -51.1 ppm, -62.2 ppm and -64.0 ppm. The latter three signals, with upfield chemical shifts, are suggestive of secondary phosphine species. This suggests some migration of formaldehyde from hydroxymethylphosphine moieties into N-H bonds to give the corresponding hydroxymethylamines. ^{1}H-NMR revealed signals in the expected regions for the polyether and ferrocene moieties, with the former heavily predominating by a ratio of *ca.* 70:1, which corresponds to a loading of only about half the available ferrocene groups, consistent with the results obtained by AA.

This product was also examined by ESMS, but this provided little useful information. Neat methanol was used as the eluent, with a cone voltage of 20 V (positive ion mode). Although the baseline produced by this was very dirty from *ca. m/z* 900 up to *m/z* 3000 (the detection limit), a broad signal centred about *ca. m/z* 1500-1600 was evident, with a spread from *ca. m/z* 900 to 1900, although it was impossible to estimate a molecular weight from this, since the level of charge on fragments could not be ascertained. At lower molecular weights a series of fragments of *m/z* 814.6, 756.4, 698.7, 640.3, 582.1, 524.5, 466.5, 408.6, 350.3, 292.4, is seen, with intensities approximately normally distributed about the *m/z* 466.5 peak. The peak at *m/z* 292.4 could be attributed to trace amounts of $[\mathbf{1}]^+$, $[FcCH_2P(CH_2OH)(CH_2NH_2) + H]^+$, or a mixture of both. Other peaks represent stepwise increases by *m/z* 58 at a time, corresponding to units of $CH(CH_3)CH_2O$, so that the peak at *m/z* 814.6 for instance could be attributed to $[FcCH_2P(CH_2OH)CH_2NH_2\{CH(CH_3)CH_2O\}_9 + H]^+$. This is of course consistent with the possibility that the polymer is not fully cross-linked, but in fact predominantly contains phosphines with only one aminomethyl linkage each.

The viscosity of the oily polymer increased over three weeks of storage under nitrogen, suggesting ongoing reaction in the absence of solvent. It was of interest to the author to see if the physical properties of the polymer would be altered dramatically by cross-linking of remaining hydroxymethylphosphine groups with ammonia, and especially to see if its

solubility in methanol would be curtailed. This could potentially provide a useful curing process for the polymer; a solution of polymer could be drop-coated onto an electrode, the solvent dried off, the electrode exposed to ammonia, and the resulting electrode could be used in organic solvents without dissolution. However, exposure of the polymer to an atmosphere of concentrated ammonia in nitrogen for 24 hours did not appear to appreciably change the viscosity or solubility of the polymer. At this point treatment with hydrogen peroxide was used to render the polymer air-stable through oxidation of the phosphine moieties, producing **36**. Interestingly, the viscosity of the polymer continued to increase until it became insoluble in any solvent about three months after first being prepared, forming a flexible film-like material. The reasons why the physical properties of the polymer should have continued to change after inactivation of the hydroxymethyl groups are unclear.

Polymer **37** was produced by reaction of **1** with Jeffamine® T-403, the structure of which has already been described in Scheme 6.7. Reagents were combined in a ratio intended to give a 15% excess of OH groups, reflected in the high experimental Fc:amine mol ratio obtained (Table 6.2). After overnight stirring of the reagents, a viscous oily polymer film had been deposited, although the solvent was still strongly coloured. Addition of hydrogen peroxide to the solution quickly led to re-dissolution of the precipitated polymer. Solvent was removed under vacuum, giving **37** as a brittle oil. As with **36**, it was found that solubility in methanol decreased with time in storage. ^{31}P-NMR showed a broad signal centred around *ca.* 45 ppm, with two sharp and prominent signals at 45.5 ppm and 34.1 ppm. The former signal is comparable with the chemical shifts of **3** and **7**, which are 45.8 ppm and 45.0 ppm respectively (Section 2.3.1). The signal at 34.1 ppm was shown to be attributable to a secondary phosphine oxide by the nondecoupled ^{31}P-NMR spectrum, with the splitting of this signal into a doublet, J = 463 Hz. Little information could be obtained from ^{1}H or ^{13}C spectra. Using the same conditions as described above, ESMS of **37** gave a broad signal centred around *ca. m/z* 900 and with a spread from *ca. m/z* 400 to 1600.

Polymer **38** was prepared by the reaction of **1** with Jeffamine® EDR-192 [formula = $H_2N(CH_2CH_2O)_3CH_2CH_2NH_2$]using the standard method, with the reagents combined in a

ratio intended to give a 22% excess of NH_2 groups, which can react with acid groups in enzymes. The experimental Fc:amine ratio is thus higher than might have been expected. The product was a brittle oil.

Polymer **39** was formed by the reaction of **1** with $[P(CH_2OH)_4]Cl$ and ammonia, in a ratio of 3:2:6.7. It was intended that excess ammonia would convert the $[P(CH_2OH)_4]Cl$ to $P(CH_2OH)_3$, and that the presence of trifunctional $P(CH_2OH)_3$ in the mixture would lead to a more highly cross-linked polymer. Ammonia was present in slight excess. Stirring of the reagents overnight led to precipitation of a yellow powder, which was collected and washed with methanol; no colour remained in the solvent. This product was soluble in DMF, and a small amount of dissolved polymer was spread on a glass slide and dried under vacuum, in order to see if the polymer would re-deposit as a film, but this was unsuccessful. Oxidation of the polymer with hydrogen peroxide gave **39** as a brown powder. Some of the non-oxidised polymer (**39**-R) was retained for later comparisons.

Polymer **40** was prepared by the reaction of **1** with 1,6-diaminohexane in a stoichiometric ratio of 2:1. Stirring of the reagents in solution overnight led to formation of an insoluble oil. The supernatant was removed, and the oil washed with methanol. This product proved to be partly soluble in chloroform, allowing NMR investigation of the soluble fraction. ^{31}P-NMR showed a broad spread of signals from -25 ppm to -50 ppm , with a sharp peak at -34.6 ppm. Two other bands of signals were seen at *ca.* -70 ppm and *ca.* -76 ppm to -80 ppm. Signals in the latter, most upfield, band changed under nondecoupling of the spectrum in a way suggestive of secondary phosphine species. No other signals were affected in this way by nondecoupling. Little information could be ascertained from the ^1H-NMR. Reaction of the polymer with hydrogen peroxide caused the oil to become brittle, though it remained insoluble. In fact, the polymer proved to be insoluble in ether, dichloromethane, acetonitrile, methanol, DMSO and water.

Experience with the electrochemistry of **7** suggested that the electrochemistry of these polymers would not be simple. As explained in Section 5.2.4, it was found that the

electrochemistry of **7** was greatly simplified by sequential reaction with MeI and $TlPF_6$ with the intention of quaternising the amine functions of **7**. Polymer **41** was prepared in similar fashion, starting with overnight stirring of a suspension of **40** with MeI. This was followed by stirring the polymer in a NaCl solution overnight in order to remove most of the iodide which might be present, and which would interfere with electrochemical measurements. Thorough rinsing with NaCl solution and water completed the preparation. Comparison of experimental analytical results with theoretical results (Table 6.2) shows that levels of C, N and Fe did not drop as much as expected upon quaternisation; the observed change is about half that expected, suggesting only half the available sites reacted.

This limited study of polymer preparation indicates that successful polymer formation requires a compromise between conflicting aims. Long-chain 'tethers' for ferrocene, and potentially for enzymes also, are desirable for achieving high enzyme activity and mediator efficiency. However, reaction of the longest-chain Jeffamine®, T-3000, with **1** appears to take too long, and unless the resulting polymer **36** is left to stand for several months the product is probably predominantly oligomeric in nature. Generally speaking, the smaller the molecular weight of the amine used, the greater the impression gained of cross-linked and relatively high molecular weight species in the product. Also, with T-3000 the ferrocene loading in the product was considerably lower than in other cases. Since **36** was not washed, the low levels of iron present are rather inexplicable, but it is possible that extended drying under vacuum led to loss of iron in the form of volatile ferrocene species.

On a positive note, this study has also shown that it should be possible to engineer polymers with a variety of physical properties, from oils to powders and flexible films.

6.2.2 Electrochemistry of Polymer Preparations

The electrochemistry of the polymers was investigated both in solution and when fixed at electrode surfaces, in order to determine whether these polymers were suitable for enzyme electrode applications, and if so, what methods might be best for immobilising the materials at the electrode.

6.2.2.1 Electrochemistry in DMF Solutions

Although the polymers were generally insoluble in low-polarity solvents and water, it was found that some were soluble in DMF. Cyclic voltammetry (see Section 5.1.1.1 for background) was therefore used to investigate DMF solutions of **37**, **38** and **39**-R. Cyclic voltammetric behaviour of **37** and **38** was very similar, and a typical CV for **37** is shown in Figure 6.2. At anodic potentials only one redox wave is seen, which on the cyclic voltammetric timescale is both chemically and electrochemically reversible, in stark contrast to the behaviour of **7** in DMF (see Section 5.2.3). This was an indicator that these polymers may be more stable than was expected on the basis of experiments with **7**. $E_{1/2}$ of ferrocene under the same conditions was 46 mV, with ΔE_P = 65 mV.

The behaviour of polymer **39**-R at anodic potentials was somewhat different, and a CV is shown in Figure 6.3. It can be seen that the redox wave appears to contain at least two partly merged processes, and it is also apparent that these are not chemically reversible. Presumably these chemical complications arise from the fact that the phosphine groups in this polymer had not been chemically oxidised, as was the case for **37** and **38**. For discussion on the electrochemical reactions of $FcCH_2PR_2$ moieties, see Section 5.2.

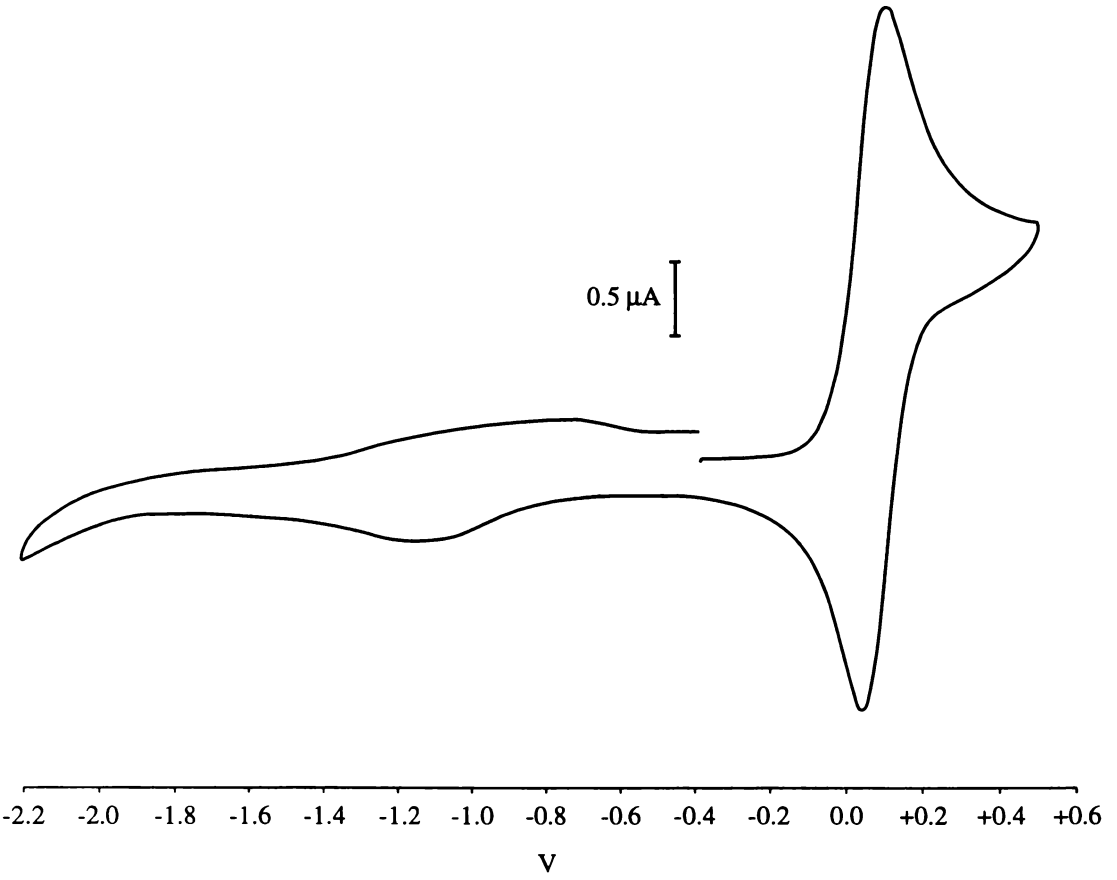

Figure 6.2: CV of 1.0 mg ml^{-1} **37** in DMF, scan rate 100 mV s^{-1}.

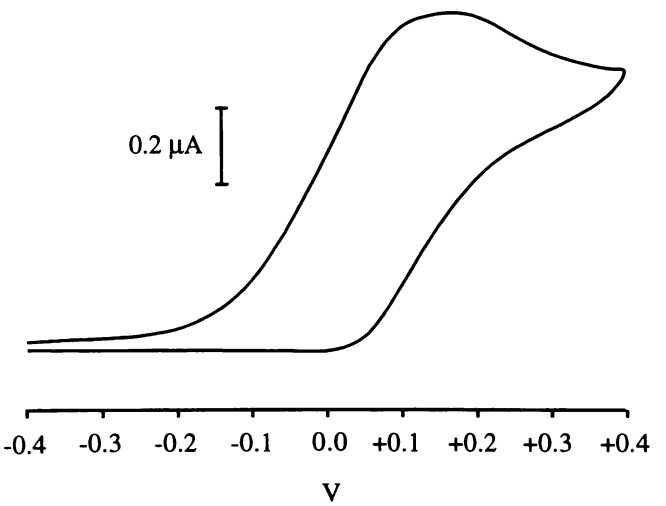

Figure 6.3: CV of 1.0 mg ml^{-1} **39**-R in DMF, scan rate 20 mV s^{-1}.

6.2.2.2 *Electrochemistry of Carbon Paste Electrodes*

Aside from the investigation of DMF solutions of polymers, all methods involved fixing the polymer to an electrode and testing its properties when in contact with an aqueous solution. This was not only because the polymers were insoluble in water, but also because most media in which enzyme electrodes could be used, such as biological fluids, are aqueous solutions, and because enzymes generally function best in aqueous conditions.

A standard method for the incorporation of specialised materials into electrodes is the preparation of carbon paste electrodes. This involves grinding the material with carbon paste and nujol, then pressing the mixture into a depression in an electrode. This method was used to incorporate polymers **37**, **39**-R, **39**, **40** and **41** into electrodes, as well as ferrocene as a reference, and **7** for comparison. The electrolyte used was 0.1 M KCl, the AE was a Pt wire, and the RE was a SCE. After reaching a 'steady-state' response, the ferrocene standard gave the following parameters: E_{PA} = 0.340 V, E_{PC} = 0.172 V, $E_{1/2}$ = 0.256 V vs. SCE, ΔE_p = 0.168 V.

Results obtained using **7** are shown in Figure 6.4. Several scans were required to 'break in' the electrode, as was found to be the case in most other instances also. A series of ten cycles is shown in Figure 6.4a, showing that the electrode is reasonably stable once the induction period is passed, although the pattern observed is not that of a single ferrocene oxidation. Figure 6.4b shows the CV obtained for this electrode after it had been held at a potential of 0.8 V for five minutes, showing some change with time. Holding the electrode at a positive potential in this way amounts to a form of BE, and is an important test of stability since an amperometric enzyme electrode would usually be expected to work in this way; analyte in solution leads to reduction of oxidase enzymes, which are in turn regenerated by ferrocenium species, which are supplied by reaction of ferrocene with the electrode at a constant positive

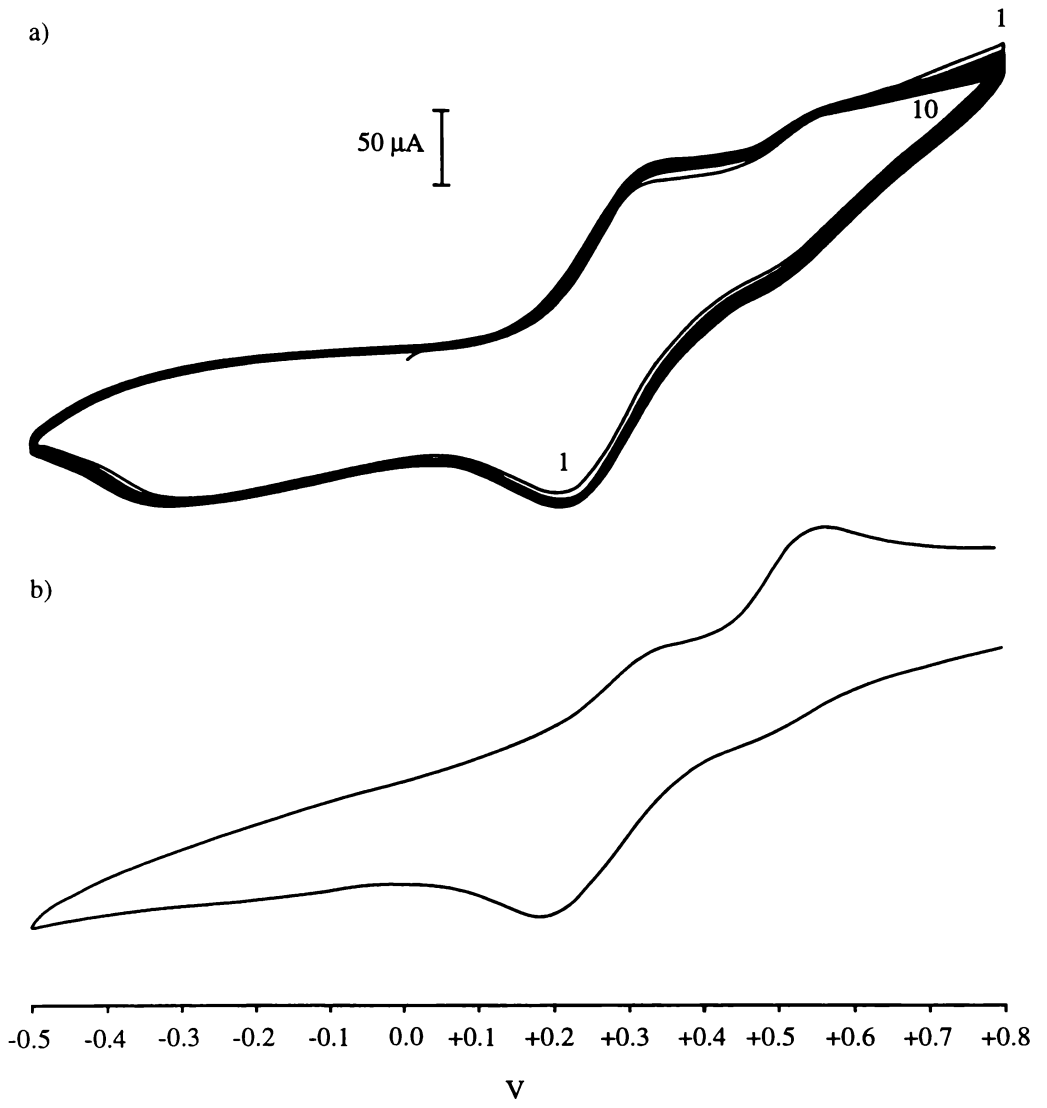

Figure 6.4: a) A CV showing ten cycles of a carbon paste electrode containing 4% by weight of **7**. Scan rate 200 mV s^{-1}. b) A CV of the same electrode after holding the electrode at a potential of 0.8 V for five minutes. Scan rate 200 mV s^{-1}.

potential. Note that while some change was observed in the shape of the CV after holding at positive potentials, the amount of current passed in redox processes did not change greatly.

Polymer **37** gave rather low levels of redox currents, and Figure 6.5 shows a CV of the electrode after eight initial scans. Current fell as scans were continued. Polymer **39** gave greater redox currents, and cyclic voltammetric behaviour appeared reasonably stable after

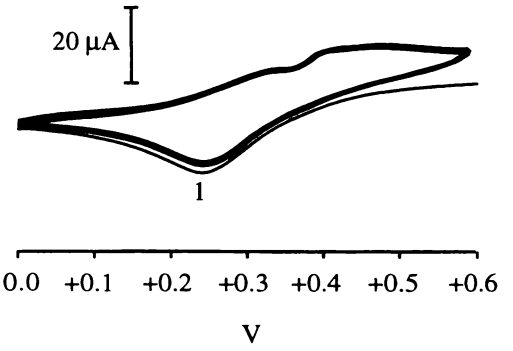

Figure 6.5: CV showing four cycles for a carbon paste electrode containing 4% w/w **37**. Scan rate 100 mV s^{-1}.

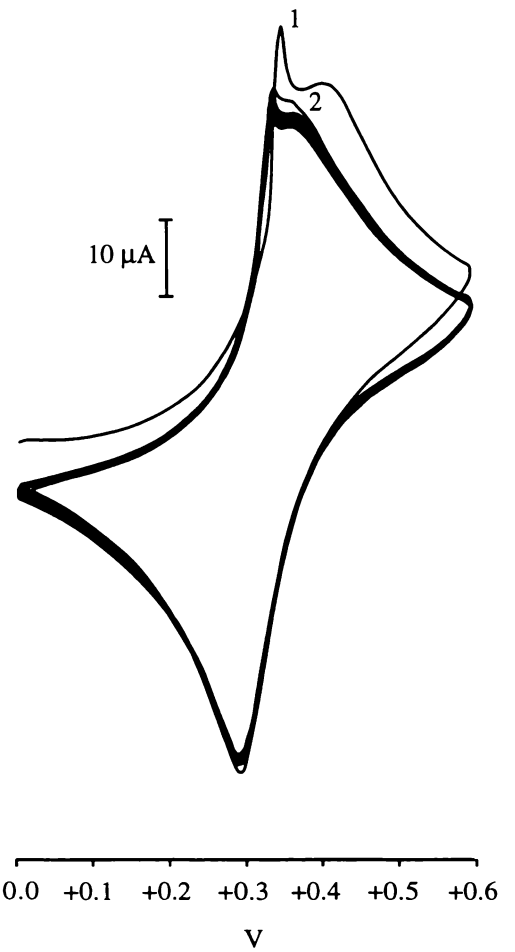

Figure 6.6: A CV showing a series of scans for a carbon paste electrode containing 2% w/w **39**. Scan rate 100 mV s^{-1}.

the break-in period. A series of cycles for this electrode is shown in Figure 6.6. However, this electrode proved to be quite unstable when held at a positive potential. A CV was run after holding the electrode at 0.5 V for five minutes (Figure 6.7), and it can be seen that the shape of the CV was changed. The behaviour of **39**-R provided an interesting contrast. A carbon paste electrode containing this polymer initially showed rather complex redox behaviour, but with time this settled down to give a simple redox wave, as shown in Figure 6.8. This was especially the case after the electrode was held at 0.5 V for five minutes (Figure 6.9a). However, when the electrode was held at a higher potential, the shape of the wave began to change once more (Figure 6.9b). This behaviour suggests that an initial period of oxidation was required for electro-oxidation of the phosphine groups in this polymer, at which point the wave shape of the CV became that of a chemically and electrochemically stable system. Further oxidation led to some form of polymer breakdown. An unfortunate aspect of the behaviour of this polymer was that the level of redox current sustained by the polymer became somewhat less with time, but it is interesting that electrooxidation of **39**-R should produce a polymer which appeared to show different, and in some ways superior, behaviour to **39**, formally the same polymer, but produced by chemical oxidation.

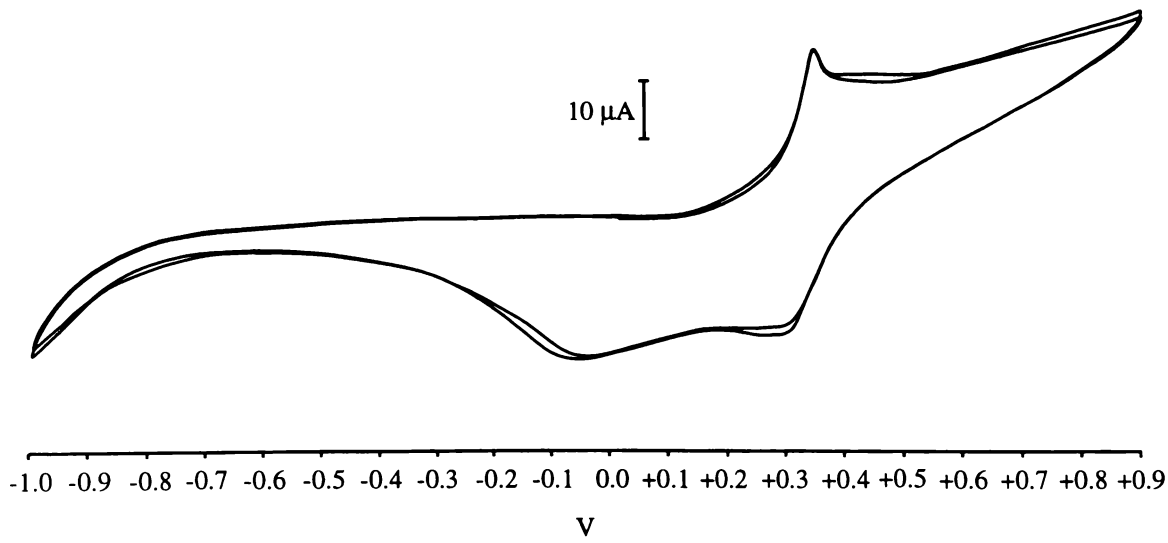

Figure 6.7: A CV of two scans for the carbon paste electrode containing 2% w/w **39**, after holding the electrode at 0.5 V for five minutes. Scan rate 100 mV s^{-1}.

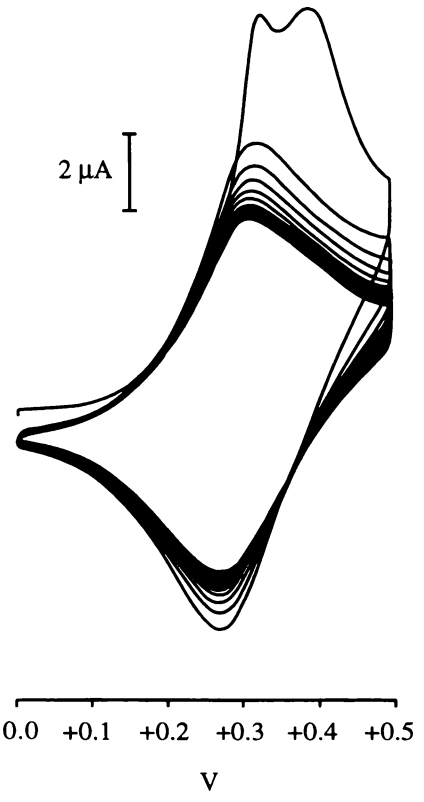

Figure 6.8: A CV showing several scans of a carbon paste electrode containing 2% w/w **39**-R, after the initial break-in period. Scan rate 100 mV s^{-1}.

A CV showing several scans of **40** after the initial curing period is displayed in Figure 6.10. A fairly simple wave pattern was produced, and unlike the other polymers discussed so far, currents *increased* with repeated scanning, at least during the duration of each cyclic voltammetric experiment. However, the shape of the CV changed fairly rapidly with repeated scanning, as is shown in a CV run under identical conditions to that in Figure 6.10, but after a number of cyclic voltammetric experiments (Figure 6.11). No experiments were carried out holding the electrode at positive potentials.

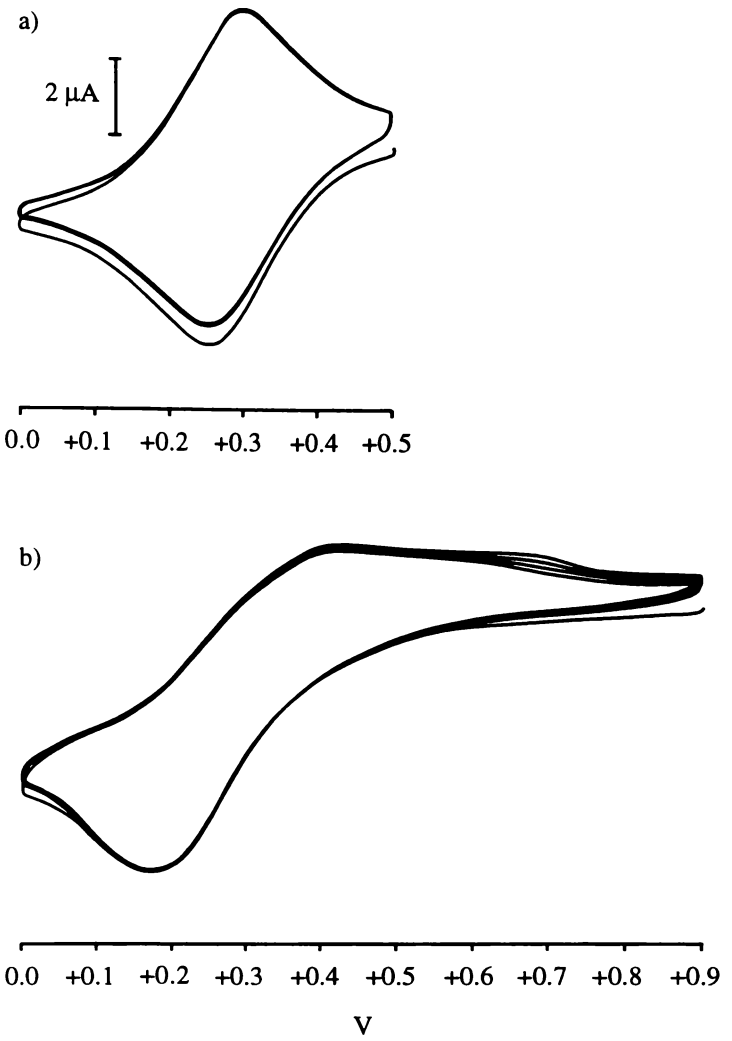

Figure 6.9: a) CV of electrode used to produce Figure 6.8, after holding the electrode at 0.5 V for five minutes. Three scans are shown, with a scan rate of 100 mV s^{-1}. b) The same electrode after holding for a further five minutes, at 0.9 V. Four scans are shown, with a scan rate of 100 mV s^{-1}.

Experimentation with polymer **41** seemed to show no positive benefits from the attempt to quaternise the amine groups in the polymer, as the wave shape was still affected by repeated scanning, and unlike **40**, current intensity fell away rapidly with repeated use. It is possible that stabilisation of the electrochemical behaviour of **7** was achieved by formation of thallium complexes rather than quaternisation of ammonium groups. In addition, partial quaternisation of the amine groups in **41** may have made the polymer more soluble in water and thus had a detrimental rather than positive effect on performance.

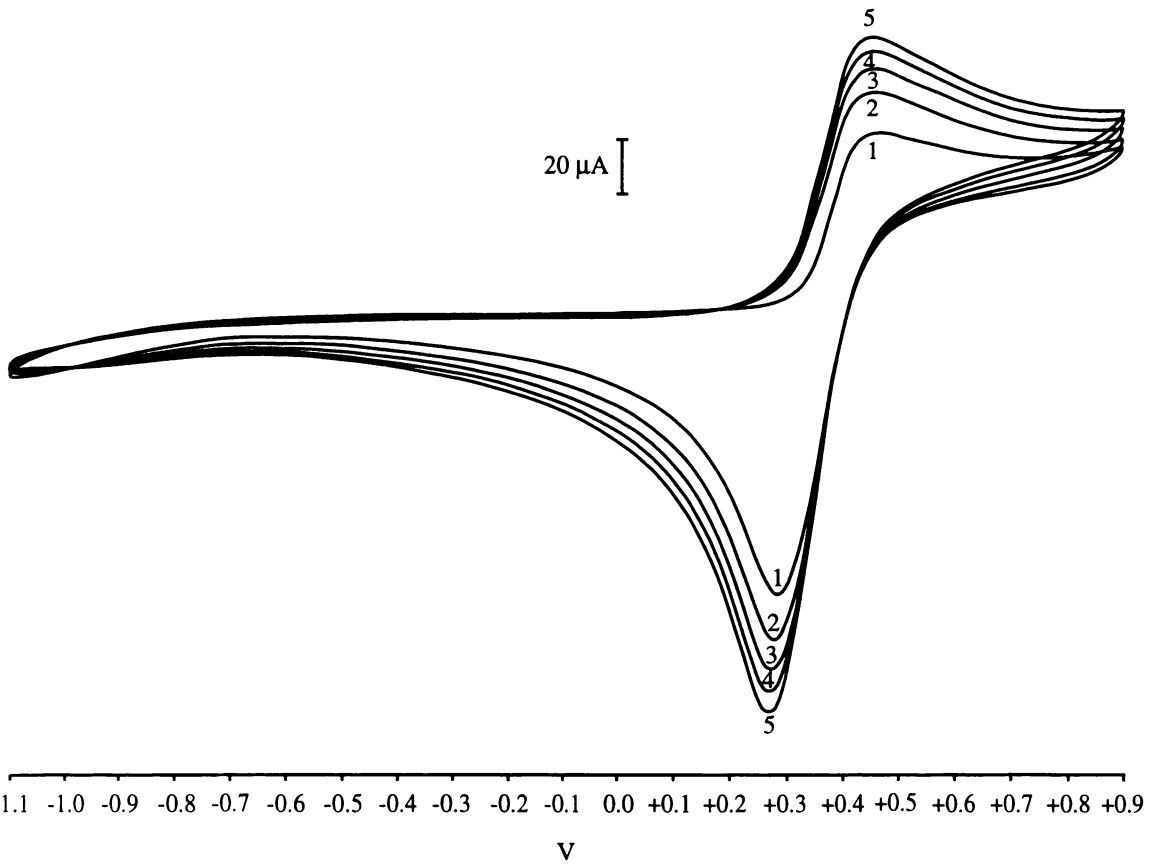

Figure 6.10: A CV showing five scans of a carbon paste electrode containing 10% w/w **40**, scan rate 100 mV s^{-1}.

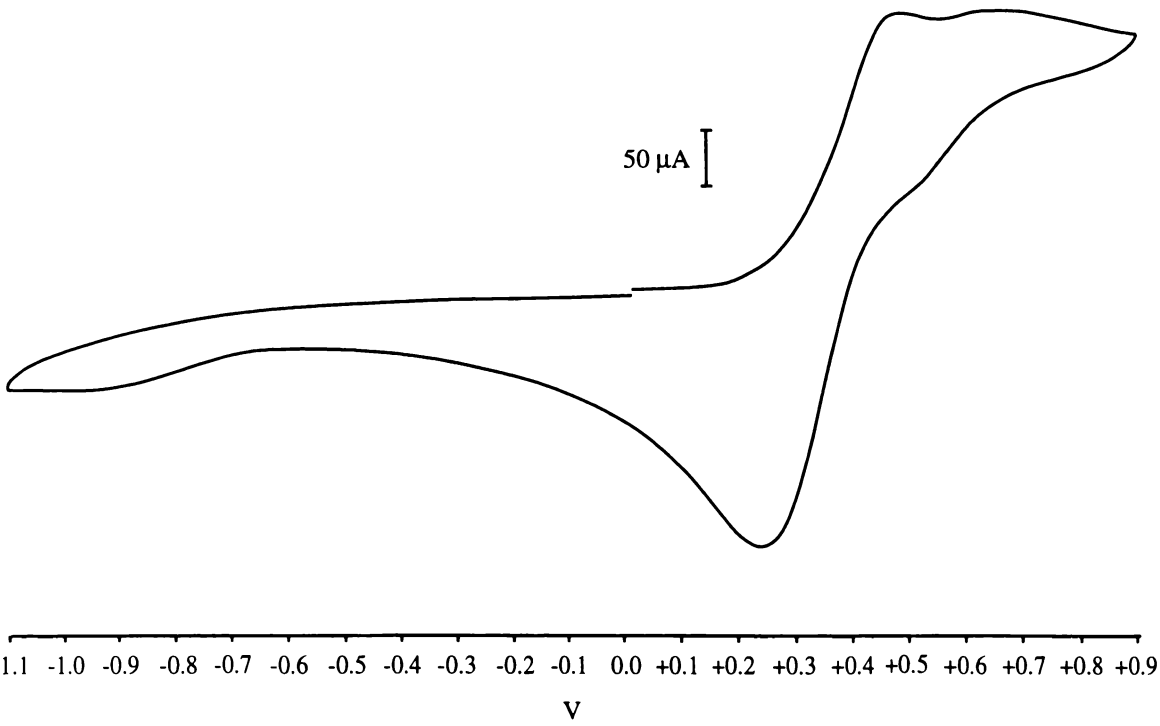

Figure 6.11: A CV of the same electrode as that used to obtain Figure 6.10, under identical conditions a short time later.

6.2.2.3 *Drop-Coating of Electrodes*

The simplest method one might envisage for immobilisation of polymers onto an electrode surface would be removal of solvent from a solution of the polymer deposited on the electrode surface (drop-coating). Drop-coating was used to produce GC electrodes layered with polymers **37**, **38** and **39**-R; a 1 mg ml^{-1} solution of the polymer in DMF was applied to the end of the electrode, and the solvent removed under vacuum.

This proved to be a rather unsuccessful method. Visual inspection showed that the polymers did not seem to have a high affinity for the GC surface, and so as the solvent dried polymer gathered at the edges of the electrode rather than giving an even and reproducible coverage. Once the electrode had undergone an initial 'curing' period similar to that required by the carbon paste electrodes, redox waves were observed, but the shape was unpredictable. The greatest problem seen with this application method, however, was the fact that in each case current intensity was very rapidly lost upon repeated cycling, especially if the electrode was held at a positive potential for a period of time. The electrode showing the best behaviour was that prepared with **38**. Figure 6.12a shows a series of cyclic voltammetric scans of this electrode showing a typical rapid loss of peak intensity with repeated use. The loss of activity is even more pronounced after the electrode is held at a positive potential for a few minutes (Figure 6.12b).

6.2.2.4 *Electrochemical Polymer Deposition*

Claims have been made that amine-containing materials can be covalently bound to carbon electrodes by scanning of the electrodes through positive potentials in the presence of solutions containing the amines[106]. This method was attempted as a means of modifying GC

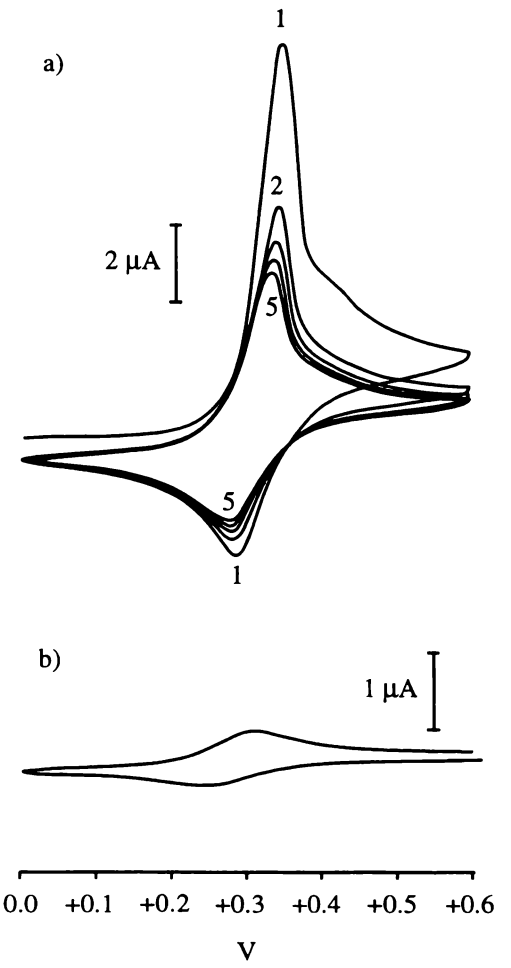

Figure 6.12: a) CV of a GC electrode drop-coated with **38**, showing five consecutive scans at 100 mV s^{-1}. b) After holding the electrode at 0.6 V for five minutes, the loss of electrode activity is very pronounced.

electrodes, using polymer **38**. Slow scanning of a 2.1 mg ml^{-1} DMF solution of **38** was carried out, but after washing the electrode thoroughly with ethanol and water, followed by ultrasonication in ethanol, the expected redox wave due to adsorbed ferrocene groups was almost undetectable. In fact, a better response was given by a control obtained by holding an electrode in the same solution without scanning to positive potentials.

6.2.2.5 General Conclusions

Comparison of the electrochemistry of **7** with various polymers both in DMF and carbon paste electrodes shows that in fact the polymers showed much better electrochemical behaviour than might have been expected on the basis of the behaviour of **7**. Nevertheless, all polymers tested showed limited stability, no matter which method was used in order to immobilise the polymer on the electrode.

Of the three methods tried for polymer immobilisation, use of carbon paste electrodes was the most promising. Results from drop-coating were similar in many ways, but the performance of drop-coated electrodes was much worse than for carbon-paste electrodes. At this stage electrochemical deposition shows little promise for future development as an immobilisation technique with these kinds of materials.

Two main problems were encountered with electrochemical stability of the immobilised polymers; change of cyclic voltammetric wave shape, and loss of current intensity. It is probable that little can be done to remedy the former problem, since it is presumably dependent on the chemical instability of the amine groups in the polymer when subjected to oxidising potentials. The reactive nature of a number of monomeric ferrocenylamines when subjected to electrochemical experiments has already been discussed in Section 5.2.3. However, there was always hope that the polymeric compounds described in this Chapter would prove to be electrochemically stable, since a number of ferrocenylamine polymers and surface modifiers have been reported in the literature as promising and electrochemically stable ferrocene-containing materials[20b,21c,e,f,32,33,34,36,88,107]. In addition, extensive work has been reported involving testing of the electrochemistry of ferrocene[21d,108] or cobaltocenium[108g,h,k,109]-derivatised host molecules containing amine functions. On the cyclic voltammetric time scale the behaviour of these usually macrocyclic compounds appears chemically reversible in solution, although as with the materials described in this Chapter, this may not translate to long-term stability if they were to be immobilised. Why some

amino- and ferrocenyl-containing polymeric materials appear electrochemically stable, while those described in this Chapter are not, is not clear and probably requires a more detailed investigation of the reactions undergone by **7** or other well-defined model compounds.

The ether functions of ferrocene-derivatised polyether molecules or polymers are never described as electrochemically active in the literature[39,108a,b,c,e,k,p,r,s,109d,110] and are therefore probably not involved in electrochemical reactions of the materials described herein.

The problem of decreasing redox currents as the electrodes age obviously stems from loss of ferrocene groups from the electrode surfaces. There are two likely explanations for this. Firstly, the level of cross-linking in the polymers is questionable, particularly in those polymers formed using high molecular weight amines. The problem of products which are possibly largely oligomeric in nature has been discussed in Section 6.2.1. Any molecules of low molecular weight in the polymers are more likely to be soluble in the aqueous medium and simply diffuse away from the electrode surface, particularly where the ferrocene groups have been oxidised, or irreversible oxidation of amine functions has taken place. The faster loss of electrode activity for the carbon paste electrode containing **41** compared with **40** can likewise be ascribed to the more ionic nature of **41**. The second possible reason for loss of electrode activity is breakup of the polymers resulting from chemical reactions stemming from oxidation of the amine groups. The degraded polymer would then diffuse out from the electrode as has just been described. Not enough is known about the reactions involved to be able to postulate how this would take place, if indeed it does. The superior performance of carbon paste electrodes as opposed to drop-coated electrodes presumably stems from: the physical barrier to diffusion provided by the carbon paste; the fact that new molecules of polymer can diffuse from within the electrode to replace activity at the electrode surface; the hydrophobic environment within the carbon paste electrode may provide a superior environment for some polymer fragments than aqueous solution.

6.3 Experimental

6.3.1 Synthesis and Characterisation of Ferrocene-Containing Polymers

For notes on reagents and solvents, as well as NMR, ESMS, and elemental analysis characterisation techniques, see Section 2.3.1.

6.3.1.1 Preparation of Polymers ***36-40***

Preparation of polymers was carried out according to the following method: suitable amounts of **1** and copolymerising agents were dissolved in an oxygen-free methanolic solution (typically 20 ml), which was stirred overnight under nitrogen. At this point some polymers proved insoluble and precipitated overnight (**39**, **40**), in which case the solvent was decanted off and the polymer washed with methanol, in order to remove unreacted starting materials, before adding a methanolic solution of hydrogen peroxide and stirring for several hours under nitrogen. Otherwise, a slight excess of hydrogen peroxide was added to solution and the solution again stirred for several hours under nitrogen (**36**, **38**). Polymer **37** showed intermediate behaviour and was treated in the same fashion as **36** and **38**. Hydrogen peroxide was always added as a 6% aqueous solution, diluted with methanol as required. If after oxidation the polymer proved insoluble the solvent was decanted off and the residue washed with methanol before drying under vacuum (**39**, **40**), otherwise the solution was simply dried down under vacuum (**36**, **37**, **38**). Drying was usually carried out over a period of several days to try and ensure thorough solvent removal from the amorphous materials. Yields by weight were always greater than 80%.

Amounts of starting materials used in preparations:

36: **1** (46.4 mg, 0.159 mmol), Jeffamine® T-3000 (450 mg, *ca.* 0.150 mmol).

37: **1** (143 mg, 0.488 mmol), Jeffamine® T-403 (62.2 mg, *ca.* 0.141 mmol).

38: **1** (158 mg, 0.539 mmol), Jeffamine® EDR-192 (63.4 mg, 0.330 mmol).

39: **1** (101 mg, 0.345 mmol), $[P(CH_2OH)_4]Cl$ (55.1 mg of an 80% aq. soln., 0.231 mmol), ammonia (0.13 ml of 6 M NH_3, 0.78 mmol).

40: **1** (250 mg, 0.857 mmol), 1,6-diaminohexane (50.6 mg, 0.435 mmol).

*6.3.1.2 Preparation of **41***

Polymer **40** (51 mg) was mixed with diethyl ether (5 ml) and methyl iodide (0.5 ml). This was stoppered and stirred overnight, before removing the solvent under vacuum and drying for several hr. The polymer was then stirred overnight in a mixture of sat. aq. NaCl solution (5 ml) and methanol (2 ml), before removing by vacuum filtration and washing thoroughly with sat. aq. NaCl solution, water, and methanol. After drying under vacuum, 46 mg of polymer **41** was obtained.

6.3.1.3 Atomic Absorption Analysis of Iron Content in Polymers

Analysis of the iron content of polymers was carried out as follows: A precisely known weight of polymer, about 10 mg (except in the case of **36**, where about 25 mg was used), was weighed into a 50 ml conical flask. 10 ml of 35% HNO_3 was added and the mixture boiled for 15 min. After cooling, samples were made up to 20 ml with doubly-distilled water. All samples were prepared in duplicate, including blanks. A 1000 ppm stock solution of $FeSO_4$ was prepared and used to produce 0, 4, 10, 20, 50 and 100 ppm standard solutions, containing 17.3% HNO_3. Samples were analysed using a flame AA with an air-acetylene flame, burner angle 0° with optimisation of absorbance, measuring absorbance at a wavelength of 372.0 nm. Readings for all samples were taken in triplicate, and concentration in ppm was automatically calculated by comparison to the external calibration

curve, which in two separate determinations gave values for R^2 of 1.0000 and 0.9998. These concentrations in ppm were used to derive the level of iron as a percentage of the original sample, with adjustment made to account for blank readings (which were small). Values from the two duplicate determinations were averaged. Iron levels were then used in conjuction with commercially obtained nitrogen elemental analysis results to calculate the nitrogen/iron, i.e. amine/ferrocene, mol ratio for the various materials as reported in Table 6.2.

6.3.2 Electrochemistry of Polymers

6.3.2.1 Cyclic voltammetry of DMF Solutions

For a description of cyclic voltammetric equipment and procedures, see Section 5.3.1. Experimental details were identical excepting the use of DMF as the solvent (although acetonitrile was still used for the RE). The DMF was HPLC quality, and no attempt was made to dry it.

6.3.2.2 Cyclic Voltammetry of Modified Electrodes

Experimental details for cyclic voltammetry of modified electrodes are identical to those outlined in Section 5.3.1, with the following exceptions:

1. A perspex cell was used.

2. RE was a SCE.

3. Electrolyte solution was 0.1 M analytical reagent grade KCl in doubly-distilled water.

4. A new electrolyte solution was used for the testing of each new electrode; the solution was initially purged with nitrogen, then kept under nitrogen during experimentation.

Carbon paste electrodes were prepared by manual grinding of the polymer with carbon powder for several minutes, giving a total of 50 mg of material. This was mixed with 1-2 drops of nujol to give a paste, and this was carefully packed into a specially designed electrode consisting of a brass disk electrode of 3 mm diameter depressed into a teflon rod. A smooth finish was given to the electrode by wiping on flat paper.

In order to drop-coat electrodes a 2 mg ml^{-1} solution of the polymer in DMF was prepared. A GC disk electrode with a diameter of 3 mm was positioned vertically so that the minimum amount of solution could be placed on the electrode surface. Electrodes were then dried under vacuum in this upright position. Since a number of electrodes were used in this work, the electrochemical response of these electrodes was compared prior to modification using a standard redox probe, and all electrodes were found to exhibit a similar response.

Attempts to covalently bond **38** to a GC electrode involved slow scanning at 10 mV s^{-1} of a GC electrode in a 2.1 mg ml^{-1} solution of **38** in DMF, from -0.4 V to +1.0 V vs. Ag/Ag^{+} (10 mM) and back; five cycles were used. A control was produced by holding a GC electrode at a potential of -0.4 V for five minutes in the same solution. Before testing for residual electrode activity, both electrodes were thoroughly washed with ethanol and water, and ultrasonicated for 15 minutes in ethanol. Testing of the experimental electrode then showed essentially no activity; the control electrode in fact showed greater activity, with a slight but discernible redox wave visible at *ca.* 0.1 V.

6.4 References

1 K. E. Gonsalves, X. Chen, *Synthesis and Characterisation of Ferrocene-Containing Polymers*, in *Ferrocenes*, A. Togni, T. Hayashi (Ed.), 1995, VCH Verlagsgesellschaft mbH, Weinheim, p. 497.

2 I. Manners, *Chem. Br.*, January 1996, 46.

3 F. S. Arimoto, A. C. Haven Jr., *J. Am. Chem. Soc.*, 1955, **77**, 6295.

4 For a review see: I. Manners, *Adv. Organomet. Chem.*, 1995, **37**, 131.

5 For a review see: I. Manners, *Polyhedron*, 1996, **15**, 4311. See also: J. Rasburn, D. A. Foucher, W. F. Reynolds, I. Manners, G. J. Vancso, *J. Chem. Soc., Chem. Commun.*, 1998, 843. P. Gomez-Elipe, P. M. Macdonald, I. Manners, *Angew. Chem. Int. Ed. Engl.*, 1997, **36**, 762. S. Barlow, A. L. Rohl, D. O'Hare, *J. Chem. Soc., Chem. Commun.*, 1996, 257. R. Rulkens, A. J. Lough, I. Manners, S. R. Lovelace, C. Grant, W. E. Geiger, *J. Am. Chem. Soc.*, 1996, **118**, 12683.

6 J. M. Nelson, H. Rengel, I. Manners, *J. Am. Chem. Soc.*, 1993, **115**, 7035.

7 a) D. L. Compton, P. F. Brandt, T. B. Rauchfuss, D. F. Rosenbaum, C. F. Zukoski, *Chem. Mater.*, 1995, **7**, 2342. b) D. L. Compton, T. B. Rauchfuss, *Organometallics*, 1994, **13**, 4367. c) C. P. Galloway, T. B. Rauchfuss, *Angew. Chem. Int. Ed. Engl.*, 1993, **32**, 1319. d) P. F. Brandt, T. B. Rauchfuss, *J. Am. Chem. Soc.*, 1992, **114**, 1926.

8 J. M. Nelson, P. Nguyen, R. Petersen, H. Rengel, P. M. Macdonald, A. J. Lough, I. Manners, N. P. Raju, J. E. Greedan, S. Barlow, D. O'Hare, *Chem. Eur. J.*, 1997, **3**, 573. M. A. Buretea, T. D. Tilley, *Organometallics*, 1997, **16**, 1507.

9 R. W. Heo, F. B. Somoza, T. R. Lee, *J. Am. Chem. Soc.*, 1998, **120**, 1621.

10 N. P. Reddy, H. Yamashita, M. Tanaka, *J. Chem. Soc., Chem. Commun.*, 1995, 2263.

11 R. Rulkens, D. P. Gates, D. Balaishis, J. K. Pudelski, D. F. McIntosh, A. J. Lough, I. Manners, *J. Am. Chem. Soc.*, 1997, **119**, 10976.

12 J. K. Pudelski, D. Gates, R. Rulkens, A. J. Lough, I. Manners, *Angew. Chem. Int. Ed. Engl.*, 1995, **34**, 1506.

13 R. Resendes, P. Nguyen, A. J. Lough, I. Manners, *Chem. Commun.*, 1998, 1001.

14 H. Braunschweig, R. Dirk, M. Muller, P. Nguyen, R. Resendes, D. P. Gates, I. Manners, *Angew. Chem. Int. Ed. Engl.*, 1997, **36**, 2338.

15 C. H. Honeyman, D. A. Foucher, F. Y. Dahmen, R. Rulkens, A. J. Lough, I. Manners, *Organometallics*, 1995, **14**, 5503. C. H. Honeyman, T. J. Peckham, J. A. Massey, I. Manners, *Chem. Commun.*, 1996, 2589.

16 I. Manners, G. H. Riding, J. A. Dodge, H. R. Allcock, *J. Am. Chem. Soc.*, 1989, **111**, 3067.

17 C. M. Asselin, G. C. Fraser, H. K. Hall Jr., W. E. Lindsell, A. B. Padias, P. N. Preston, *J. Chem. Soc., Dalton Trans.*, 1997, 3765. G. E. Southard, M. D. Curtis, *Organometallics*, 1997, **16**, 5618. K. H. Pannell, H. K. Sharma, *Organometallics*, 1997, **16**, 3077. M. Bochmann, J. Lu, R. D. Cannon, *J. Organomet. Chem.*, 1996, **518**, 97.

18 K. E. Gonsalves, L. Zhan-ru, M. D. Rausch, *J. Am. Chem. Soc.*, 1984, **106**, 3826.

19 A. M. Allgeier, C. A. Mirkin, *Organometallics*, 1997, **16**, 3071.

20 a) A. Deronzier, J.-C. Moutet, *Coord. Chem. Rev.*, 1996, **147**, 339. b) J. G. Eaves, R. Mirrazaei, D. Parker, H. S. Munro, *J. Chem. Soc., Perkin Trans. II*, 1989, 373. c) H. Nishihara, M. Noguchi, K. Aramaki, *Inorg. Chem.*, 1987, **26**, 2862. d) A. Haimerl, A. Merz, *Angew. Chem. Int. Ed. Engl.*, 1986, **25**, 180.

21 a) T. D. McCarley, R. L. McCarley, *Anal. Chem.*, 1997, **69**, 130. b) D. J. Cambell, B. R. Herr, J. C. Hulteen, R. P. Van Duyne, C. A. Mirkin, *J. Am. Chem. Soc.*, 1996, **118**, 10211. c) G. Tao, E. Katz, I. Willner, *Chem. Commun.*, 1997, 2073. d) R. C. Mucic, M. K. Herrlein, C. A. Mirkin, R. L. Letsinger, *Chem. Commun.*, 1996, 555. e) K. S. Alleman, K. Weber, S. E. Creager, *J. Phys. Chem.*, 1996, **100**, 17050. f) G. K. Rowe, S. E. Creager, *J. Phys. Chem.*, 1994, **98**, 5500. g) Y. Sato, B. L. Frey, R. M. Corn, K. Uosaki, *Bull. Chem. Soc. Jpn.*, 1994, **67**, 21. h) J. J. Hickman, D. Ofer, C. Zou, M. S. Wrighton, P. E. Laibinis, G. M. Whitesides, *J. Am. Chem. Soc.*, 1991, **113**, 1128. i) C. E. D. Chidsey, C. R. Bertozzi, T. M.

Putvinski, A. M. Mujsce, *J. Am. Chem. Soc.*, 1990, **112**, 4301. j) C. E. D. Chidsey, *Science*, 1991, **251**, 919. For a review of sulfur-gold monolayers: A. Ulman, *Chem. Rev.*, 1996, **96**, 1533.

22 T. Ihara, M. Nakayama, M. Murata, K. Nakano, M. Maeda, *Chem. Commun.*, 1997, 1609.

23 J.-Z. Yao, Y.-Y. Chen, B.-S. Tian, *J. Organomet. Chem.*, 1997, **534**, 51.

24 S. O'Brien, J. Tudor, S. Barlow, M. J. Drewitt, S. J. Heyes, D. O'Hare, *Chem. Commun.*, 1997, 641.

25 G. Cleland, B. R. Horrocks, A. Houlton, *J. Chem. Soc., Faraday Trans.*, 1995, **91**, 4001.

26 R. D. Eagling, J. E. Bateman, N. J. Goodwin, W. Henderson, B. R. Horrocks, A. Houlton, *J. Chem. Soc., Dalton Trans.*, 1998, 1273.

27 B. R. Eggins, G. McAteer, *Education in Chemistry*, January 1997, 20. V. Moses, R. E. Cape, *Biotechnology: The Science and the Business*, 1991, Harwood Academic Publishers, Chur, p. 355. G. F. Bickerstaff, *Enzymes in Industry and Medicine*, 1987, Edward Arnold, London, p. 21. G. G. Guilbault, M. H. Sodar, *Preparation and Analytical Use of Insolubilised Enzymes*, in *Techniques in the Life Sciences: Techniques in Protein and Enzyme Biochemistry*, H. L. Kornberg, J. C. Metcalfe, D. H. Northcote, C. I. Pogson, K. F. Tipton (Ed.), 1978, Elsevier/North-Holland, Amsterdam, V. **B1/II**, p. B118/7. G. G. Guilbault, *Enzyme Electrodes*, in *Biomedical Applications of Immobilised Enzymes and Proteins*, T. M. S. Cheng (Ed.), 1977, Plenum Press, New York, V. **2**, p. 163.

28 W. Gerhartz (Ed.), *Enzymes in Industry Production and Applications*, 1990, VCH Verlagsgesellschaft, Weinheim. p. 63. C. Bullock, *Education in Chemistry*, November 1989, 179.

29 A. Heller, *Acc. Chem. Res.*, 1990, **23**, 128.

30 J. Svorc, S. Miertus, J. Katrlik, M. Stred'ansky, *Anal. Chem.*, 1997, **69**, 2086.

31 J. Wang, C. Macca, *J. Chem. Ed.*, 1996, **73**, 797.

32 E. J. Calvo, R. Etchenique, C. Danilowicz, L. Diaz, *Anal. Chem.*, 1996, **68**, 4186.

33 H. Z. Bu, A. M. English, S. R. Mikkelsen, *Anal. Chem.*, 1996, **68**, 3951.

34 A. Riklin, I. Willner, *Anal. Chem.*, 1995, **67**, 4118.

35 H.-Z. Bu, S. R. Mikkelsen, A. M. English, *Anal. Chem.*, 1995, **67**, 4071.

36 S. Kuwabata, T. Okamoto, Y. Kajiya, H. Yoneyama, *Anal. Chem.*, 1995, **67**, 1684.

37 G. Du, C. Lin, A. B. Bocarsly, *Anal. Chem.*, 1996, **68**, 796.

38 T. de Lumley-Woodyear, P. Rocca, J. Lindsay, Y. Dror, A. Freeman, A. Heller, *Anal. Chem.*, 1995, **67**, 1332.

39 E. Csöregi, D. W. Schmidtke, A. Heller, *Anal. Chem.*, 1995, **67**, 1240.

40 D. W. Schmidtke, A. Heller, *Anal. Chem.*, 1998, **70**, 2149.

41 B. Wang, B. Li, Q. Deng, S. Dong, *Anal. Chem.*, 1998, **70**, 3170.

42 J.-M. Zen, C.-W. Lo, P.-J. Chen, *Anal. Chem.*, 1997, **69**, 1669.

43 I. Willner, V. Heleg-Shabtai, R. Blonder, E. Katz, G. Tao, *J. Am. Chem. Soc.*, 1996, **118**, 10321.

44 J.-M. Zen, C.-W. Lo, *Anal. Chem.*, 1996, **68**, 2635.

45 J. J. Gooding, V. G. Praig, E. A. H. Hall, *Anal. Chem.*, 1998, **70**, 2396.

46 J. Wang, F. Lu, *J. Am. Chem. Soc.*, 1998, **120**, 1048.

47 J. Wang, J. Liu, G. Cepra, *Anal. Chem.*, 1997, **69**, 3124.

48 B. Liu, R. Hu, J. Deng, *Anal. Chem.*, 1997, **69**, 2343.

49 L. I. Netchiporouk, N. F. Shram, N. Jaffrezic-Renault, C. Martelet, R. Cespuglio, *Anal. Chem.*, 1996, **68**, 4358.

50 A. A. Karyakin, E. E. Karyakina, L. Gorton, O. A. Bobrova, L. V. Lukachova, A. K. Gladilin, A. V. Levashov, *Anal. Chem.*, 1996, **68**, 4335.

51 Z. Zhang, H. Liu, J. Deng, *Anal. Chem.*, 1996, **68**, 1632.

52 S.-K. Jung, G. S. Wilson, *Anal. Chem.*, 1996, **68**, 591.

53 S. Sampath, O. Lev, *Anal. Chem.*, 1996, **68**, 2015.

54 H. Sangodkar, S. Sukkerthi, R. S. Srinivasa, R. Lal, A. Q. Contractor, *Anal. Chem.*, 1996, **68**, 779.

55 M. Mayer, J. Ruzicka, *Anal. Chem.*, 1996, **68**, 3808.

56 G. F. Khan, M. Ohwa, W. Wernet, *Anal. Chem.*, 1996, **68**, 2939.

57 A. A. Karyakin, O. V. Gitelmacher, E. E. Karyakina, *Anal. Chem.*, 1995, **67**, 2419.

58 M. Lion-Dagan, S. Marx-Tibbon, E. Katz, I. Willner, *Angew. Chem. Int. Ed. Engl.*, 1995, **34**, 1604.

59 C. Bourdillon, C. Demaille, J. Moiroux, J.-M. Saveant, *J. Am. Chem. Soc.*, 1995, **117**, 11499.

60 P. G. Osborne, O. Niwa, K. Yamamoto, *Anal. Chem.*, 1998, **70**, 1701.

61 R. Blonder, E. Katz, Y. Cohen, N. Itzhak, A. Riklin, I. Willner, *Anal. Chem.*, 1996, **68**, 3151.

62 K. T. Kinnear, H. G. Monbouquette, *Anal. Chem.*, 1997, **69**, 1771.

63 M. Tessema, E. Csöregi, T. Ruzgas, G. Kenausis, T. Solomon, L. Gorton, *Anal. Chem.*, 1997, **69**, 4039.

64 A. Bardea, E. Katz, A. F. Buckmann, I. Willner, *J. Am. Chem. Soc.*, 1997, **119**, 9114.

65 G. F. Khan, W. Wernet, *Anal. Chem.*, 1997, **69**, 2682.

66 S. A. M. Marzouk, V. V. Cosofret, R. P. Buck, H. Yang, W. E. Cascio, S. S. M. Hassan, *Anal. Chem.*, 1997, **69**, 2646.

67 J. J. Gooding, E. A. H. Hall, *Anal. Chem.*, 1998, **70**, 3131.

68 O. Niwa, T. Horiuchi, R. Kurita, K. Torimitsu, *Anal. Chem.*, 1998, **70**, 1126.

69 E. I. Iwuoha, I. Leister, E. Miland, M. R. Smyth, C. O. Fagain, *Anal. Chem.*, 1997, **69**, 1674.

70 G. Ortiz, M. C. Gonzalez, A. J. Reviejo, J. M. Pingarron, *Anal. Chem.*, 1997, **69**, 3521.

71 C. Ruan, F. Yang, C. Lei, J. Deng, *Anal. Chem.*, 1998, **70**, 1721.

72 Y. Guo, S. Dong, *Anal. Chem.*, 1997, **69**, 1904.

73 M. S. Vreeke, K. T. Yong, A. Heller, *Anal. Chem.*, 1995, **67**, 4247.

74 S. A. Glazier, E. R. Campbell, W. H. Campbell, *Anal. Chem.*, 1998, **70**, 1511.

75 Q. Wu, G. D. Storrier, F. Pariente, Y. Wang, J. P. Shapleigh, H. D. Abruna, *Anal. Chem.*, 1997, **69**, 4856.

76 H. Yamato, M. Ohwa, W. Wernet, *Anal. Chem.*, 1995, **67**, 2776.

77 T. Tatsuma, K. Tani, N. Oyama, *Anal. Chem.*, 1996, **68**, 2946.

78 T. Tatsuma, N. Oyama, *Anal. Chem.*, 1996, **68**, 1612.

79 A. Amine, M. Alafandy, J.-M. Kauffmann, M. N. Pekli, *Anal. Chem.*, 1995, **67**, 2822.

80 T. Huang, A. Warsinke, T. Kuwana, F. W. Scheller, *Anal. Chem.*, 1998, **70**, 991.

81 F. Daigle, D. Leech, *Anal. Chem.*, 1997, **69**, 4108.

82 E. Burestedt, A. Narvaez, T. Ruzgas, L. Gorton, J. Emneus, E. Dominguez, G. Marko-Varga, *Anal. Chem.*, 1996, **68**, 1605.

83 T. Tatsuma, D. A. Buttry, *Anal. Chem.*, 1997, **69**, 887.

84 S. Cosnier, C. Innocent, L. Allien, S. Poitry, M. Tsacopoulos, *Anal. Chem.*, 1997, **69**, 968.

85 S. Cosnier, M. Fontecave, D. Limosin, V. Niviere, *Anal. Chem.*, 1997, **69**, 3095.

86 T. J. Ohara, *Platinum Metals Rev.*, 1995, **39**, 54.

87 P. Audebert, C. Demaille, C. Sanches, *Chem. Mater.*, 1993, **5**, 911.

88 N. C. Foulds, C. R. Lowe, *Anal. Chem.*, 1988, **60**, 2473.

89 P. D. Hale, T. Inagaki, H. I. Kagan, Y. Okamoto, T. A. Skotheim, *J. Am. Chem. Soc.*, 1989, **111**, 3482.

90 W. Schumann, T. J. Ohara, H.-L. Schmidt, A. Heller, *J. Am. Chem. Soc.*, 1991, **113**, 1394.

91 C. Bourdillion, C. Demaille, J. Moiroux, J.-M. Saveant, *Acc. Chem. Res.*, 1996, **29**, 529.

92 Y. Degani, A. Heller, *J. Am. Chem. Soc.*, 1988, **110**, 2615.

93 S. J. Sadeghi, G. Gilardi, G. Nicolosi, A. E. G. Cass, *Chem. Commun.*, 1997, 517. S. Marx-Tibbon, E. Katz, I. Willner, *J. Am. Chem. Soc.*, 1995, **117**, 9925.

94 N. M. Sammes, W. Henderson, *Makromol. Chem., Rapid Commun.*, 1993, **14**, 741.

95 W. Henderson, G. M. Olsen, L. S. Bonnington, *J. Chem. Soc., Chem. Commun.*, 1994, 1863.

96 H. H. Petach, W. Henderson, G. M. Olsen, *J. Chem. Soc., Chem. Commun.*, 1994, 2181.

97 L. S. Bonnington, W. Henderson, H. H. Petach, *Enzyme Microb. Tech.*, 1995, **17**, 746.

98 W. Henderson, H. H. Petach, L. S. Bonnington, *European Polymer Journal*, 1995, **31**, 981.

99 W. Henderson, H. H. Petach, L. S. Bonnington, *Enzyme Microb. Tech.*, 1995, **17**, 804. W. Henderson, H. H. Petach, K. Sarfo, *J. Chem. Soc., Chem. Commun.*, 1994, 245.

100 F. C. Cochrane, H. H. Petach, W. Henderson, *Enzyme Microb. Tech.*, 1996, **18**, 373.

101 P. R. Oswald, R. A. Evans, W. Henderson, R. M. Daniel, C. J. Fee, *Enzyme Microb. Tech.*, 1998, **23**, 14.

102 H. Molinary, F. Montanari, P. Tundo, *J. C. S. Chem. Comm.*, 1977, 639.

103 K. L. Prime, G. M. Whitesides, *J. Am. Chem. Soc.*, 1993, **115**, 10714. C. Pale-Grosdemange, E. S. Simon, K. L. Prime, G. M. Whitesides, *J. Am. Chem. Soc.*, 1991, **113**, 12.

104 E. D. Weil, *Flame Retardants*, in *Handbook of Organophosphorus Chemistry*, R. Engel (Ed), 1992, Marcel Dekker, Inc., New York, p. 707.

105 K. E. Gonsalves, X. Chen, *Synthesis and Characterisation of Ferrocene-Containing Polymers,* in *Ferrocenes*, A. Togni, T. Hayashi (Ed.), 1995, VCH Verlagsgesellschaft mbH, Weinheim, p. 513.

106 R. S. Deinhammer, M. Ho, J. W. Anderegg, M. D. Porter, *Langmuir*, 1994, **10**, 1306. B. Barbier, J. Pinson, G. Desarmot, M. Sanchez, *J. Electrochem. Soc.*, 1990, **137**, 1757.

107 K. Takada, D. J. Diaz, H. D. Abruna, I. Cuadrado, C. Casado, B. Alonso, M. Moran, J. Losada, *J. Am. Chem. Soc.*, 1997, **119**, 10763.

108 a) M. Scherer, J. L. Sessler, A. Gebauer, V. Lynch, *Chem. Commun.*, 1998, 85. b) H. Plenio, C. Aberle, *Organometallics*, 1997, **16**, 5950. c) B. Delavaux-Nicot, A. Bigeard, A. Bousseksou, B. Donnadieu, G. Commenges, *Inorg. Chem.*, 1997, **36**, 4789. d) P. D. Beer, A. R. Graydon, A. O. M. Johnson, D. K. Smith, *Inorg. Chem.*, 1997, **36**, 2112. e) M. C. Grossel, D. G. Hamilton, J. I. Fuller, E. Millan-

Barios, *J. Chem. Soc., Dalton Trans.*, 1997, 3471. f) P. D. Beer, M. G. B. Drew, R. Jagessar, *J. Chem. Soc., Dalton Trans.*, 1997, 881. g) F. P. Schmidtchen, M. Berger, *Chem. Rev.*, 1997, **97**, 1609. h) P. D. Beer, D. K. Smith, *Prog. Inorg. Chem.*, 1997, **46**, 1. i) P. D. Beer, M. G. B. Drew, D. K. Smith, *J. Organomet. Chem.*, 1997, **543**, 259. j) H. Plenio, D. Burth, R. Vogler, *Chem. Ber./Recueil*, 1997, **130**, 1405. k) P. D. Beer, *Chem. Commun.*, 1996, 689. l) M. J. L. Tendero, A. Benito, R. Martinez-Manez, J. Soto, E. Garcia-Espana, J. A. Ramirez, M. I. Burguete, S. V. Luis, *J. Chem. Soc., Dalton Trans.*, 1996, 2923. m) C. D. Hall, T.-K.-U. Truong, *J. Organomet. Chem.*, 1996, **519**, 185. n) P. D. Beer, Z. Chen, M. G. B. Drew, A. O. M. Johnson, D. K. Smith, P. Spencer, *Inorg. Chim. Acta*, 1996, **246**, 143. o) H. Plenio, R. Diodone, *J. Organomet. Chem.*, 1995, **492**, 73. p) P. D. Beer, K. Y. Wild, *Polyhedron*, 1996, **15**, 775. q) M. J. L. Tendero, A. Benito, J. Cano, J. M. Lloris, R. Martinez-Manez, J. Soto, A. J. Edwards, P. R. Raithby, M. A. Rennie, *J. Chem. Soc., Chem. Commun.*, 1995, 1643. r) P. D. Beer, Z. Chen, M. I. Ogden, *J. Chem. Soc., Faraday Trans.*, 1995, **91**, 295. s) P. D. Beer, D. B. Crowe, M. I. Ogden, M. G. B. Drew, B. Main, *J. Chem. Soc., Dalton Trans.*, 1993, 2107. t) P. A. Gale, Z. Chen, M. G. B. Drew, J. A. Heath, P. D. Beer, *Polyhedron*, 1998, **17**, 405.

109 a) P. D. Beer, M. G. B. Drew, D. Hesek, K. C. Nam, *Chem. Commun.*, 1997, 107. b) P. D. Beer, M. G. B. Drew, D. Hesek, R. Jagessar, *J. Chem. Soc., Chem. Commun.*, 1995, 1187. c) P. D. Beer, M. G. B. Drew, J. Hodacova, S. E. Stokes, *J. Chem. Soc., Dalton Trans.*, 1995, 3447. d) P. D. Beer, S. E. Stokes, *Polyhedron*, 1995, **14**, 2631.

110 K. Wang, S. Munoz, L. Zhang, R. Castro, A. E. Kaifer, G. W. Gokel, *J. Am. Chem. Soc.*, 1996, **118**, 6707.

Appendix A

Complete lists of atomic coordinates, bond parameters and tables of thermal parameters and hydrogen atom coordinates for all structures reported in this Thesis are listed in the following tables. Tables are listed by order of compound number.

Table A.1: *Atomic coordinates and equivalent isotropic displacement parameters for 1. U(eq) is defined as one third of the trace of the orthogonalised Uij tensor.*

	x	y	z	U(eq)
Fe(1)	0.0329(1)	0.9109(1)	0.1535(1)	0.019(1)
P(1)	-0.4498(2)	0.9427(1)	0.3649(1)	0.020(1)
O(2)	-0.6807(5)	0.8185(3)	0.4689(2)	0.024(1)
H(2)	-0.7908(74)	0.8393(45)	0.4640(30)	0.029
O(3)	-0.0879(5)	0.8561(3)	0.4366(2)	0.024(1)
H(3)	-0.1301(82)	0.8132(42)	0.4629(28)	0.029
C(1)	-0.3172(7)	0.8778(3)	0.2804(2)	0.023(1)
C(2)	-0.5698(7)	0.8045(3)	0.3984(2)	0.022(1)
C(3)	-0.2257(7)	0.9535(3)	0.4329(2)	0.021(1)
C(11)	-0.1674(7)	0.9565(4)	0.2401(2)	0.019(1)
C(12)	-0.2074(7)	1.0246(3)	0.1739(2)	0.022(1)
C(13)	-0.0186(7)	1.0847(3)	0.1552(2)	0.026(1)
C(14)	0.1382(7)	1.0552(4)	0.2092(2)	0.025(1)
C(15)	0.0468(7)	0.9756(3)	0.2613(2)	0.020(1)
C(21)	-0.0374(9)	0.7437(3)	0.1251(2)	0.031(1)
C(22)	-0.0495(9)	0.8158(3)	0.0600(2)	0.029(1)
C(23)	0.1496(8)	0.8669(4)	0.0492(3)	0.030(1)
C(24)	0.2887(8)	0.8272(4)	0.1072(3)	0.032(1)
C(25)	0.1729(8)	0.7512(4)	0.1540(3)	0.033(1)

Table A.2: *Bond lengths (Å) and angles (°) for 1.*

Fe(1)-C(15)	2.034(4)	C(23)-Fe(1)-C(25)	67.8(2)
Fe(1)-C(23)	2.034(5)	C(13)-Fe(1)-C(25)	163.6(2)
Fe(1)-C(13)	2.035(4)	C(12)-Fe(1)-C(25)	154.4(2)
Fe(1)-C(12)	2.036(4)	C(22)-Fe(1)-C(25)	68.1(2)
Fe(1)-C(22)	2.041(4)	C(11)-Fe(1)-C(25)	119.7(2)
Fe(1)-C(11)	2.042(4)	C(14)-Fe(1)-C(25)	126.5(2)
Fe(1)-C(14)	2.043(4)	C(21)-Fe(1)-C(25)	40.6(2)
Fe(1)-C(21)	2.045(4)	C(15)-Fe(1)-C(24)	120.6(2)
Fe(1)-C(25)	2.046(4)	C(23)-Fe(1)-C(24)	40.6(2)
Fe(1)-C(24)	2.047(5)	C(13)-Fe(1)-C(24)	126.7(2)
P(1)-C(3)	1.851(4)	C(12)-Fe(1)-C(24)	163.7(2)

Table A.2 continued

P(1)-C(1)	1.858(4)	C(22)-Fe(1)-C(24)	68.1(2)
P(1)-C(2)	1.862(4)	C(11)-Fe(1)-C(24)	154.5(2)
O(2)-C(2)	1.429(5)	C(14)-Fe(1)-C(24)	108.7(2)
O(3)-C(3)	1.423(5)	C(21)-Fe(1)-C(24)	68.1(2)
C(1)-C(11)	1.489(6)	C(25)-Fe(1)-C(24)	40.2(2)
C(11)-C(15)	1.417(6)	C(3)-P(1)-C(1)	101.3(2)
C(11)-C(12)	1.424(6)	C(3)-P(1)-C(2)	99.5(2)
C(12)-C(13)	1.415(6)	C(1)-P(1)-C(2)	95.0(2)
C(13)-C(14)	1.410(6)	C(11)-C(1)-P(1)	114.6(3)
C(14)-C(15)	1.419(6)	O(2)-C(2)-P(1)	111.9(3)
C(21)-C(22)	1.415(6)	O(3)-C(3)-P(1)	116.2(3)
C(21)-C(25)	1.421(7)	C(15)-C(11)-C(12)	107.2(4)
C(22)-C(23)	1.399(7)	C(15)-C(11)-C(1)	125.0(4)
C(23)-C(24)	1.417(6)	C(12)-C(11)-C(1)	127.7(4)
C(24)-C(25)	1.406(7)	C(15)-C(11)-Fe(1)	69.3(2)
O(2)-H(2)	0.74(5)	C(12)-C(11)-Fe(1)	69.3(2)
O(3)-H(3)	0.73(5)	C(1)-C(11)-Fe(1)	125.9(3)
C(15)-Fe(1)-C(23)	155.6(2)	C(13)-C(12)-C(11)	108.1(4)
C(15)-Fe(1)-C(13)	68.3(2)	C(13)-C(12)-Fe(1)	69.6(2)
C(23)-Fe(1)-C(13)	108.5(2)	C(11)-C(12)-Fe(1)	69.8(2)
C(15)-Fe(1)-C(12)	68.4(2)	C(14)-C(13)-C(12)	108.3(4)
C(23)-Fe(1)-C(12)	126.0(2)	C(14)-C(13)-Fe(1)	70.1(2)
C(13)-Fe(1)-C(12)	40.7(2)	C(12)-C(13)-Fe(1)	69.7(2)
C(15)-Fe(1)-C(22)	162.7(2)	C(13)-C(14)-C(15)	107.7(4)
C(23)-Fe(1)-C(22)	40.2(2)	C(13)-C(14)-Fe(1)	69.5(2)
C(13)-Fe(1)-C(22)	120.2(2)	C(15)-C(14)-Fe(1)	69.3(2)
C(12)-Fe(1)-C(22)	107.4(2)	C(11)-C(15)-C(14)	108.6(4)
C(15)-Fe(1)-C(11)	40.7(2)	C(11)-C(15)-Fe(1)	70.0(2)
C(23)-Fe(1)-C(11)	162.7(2)	C(14)-C(15)-Fe(1)	70.0(2)
C(13)-Fe(1)-C(11)	68.6(2)	C(22)-C(21)-C(25)	107.6(5)
C(12)-Fe(1)-C(11)	40.9(2)	C(22)-C(21)-Fe(1)	69.6(2)
C(22)-Fe(1)-C(11)	125.3(2)	C(25)-C(21)-Fe(1)	69.7(3)
C(15)-Fe(1)-C(14)	40.7(2)	C(23)-C(22)-C(21)	108.0(4)
C(23)-Fe(1)-C(14)	121.1(2)	C(23)-C(22)-Fe(1)	69.6(3)
C(13)-Fe(1)-C(14)	40.4(2)	C(21)-C(22)-Fe(1)	69.9(2)
C(12)-Fe(1)-C(14)	68.3(2)	C(22)-C(23)-C(24)	108.7(4)
C(22)-Fe(1)-C(14)	155.0(2)	C(22)-C(23)-Fe(1)	70.2(3)
C(11)-Fe(1)-C(14)	68.6(2)	C(24)-C(23)-Fe(1)	70.2(3)
C(15)-Fe(1)-C(21)	125.7(2)	C(25)-C(24)-C(23)	107.4(4)
C(23)-Fe(1)-C(21)	67.9(2)	C(25)-C(24)-Fe(1)	69.8(3)
C(13)-Fe(1)-C(21)	154.5(2)	C(23)-C(24)-Fe(1)	69.2(3)
C(12)-Fe(1)-C(21)	119.5(2)	C(24)-C(25)-C(21)	108.3(4)
C(22)-Fe(1)-C(21)	40.5(2)	C(24)-C(25)-Fe(1)	70.0(3)
C(11)-Fe(1)-C(21)	106.9(2)	C(21)-C(25)-Fe(1)	69.7(2)
C(14)-Fe(1)-C(21)	163.4(2)	H(2)-O(2)-C(2)	113(4)
C(15)-Fe(1)-C(25)	108.0(2)	H(3)-O(3)-C(3)	110(4)

Table A.3: *Anisotropic displacement parameters ($Å^2$) for 1. The anisotropic displacement factor exponent takes the form: $-2\pi^2(h^2a^{*2}U11 + ... + 2hka^*b^*U12)$.*

	U11	U22	U33	U23	U13	U12
Fe(1)	0.0240(3)	0.0143(3)	0.0190(3)	-0.0010(2)	0.0012(3)	0.0013(3)
P(1)	0.0168(5)	0.0189(5)	0.0228(5)	0.0031(4)	-0.0003(5)	-0.0016(5)
O(2)	0.015(2)	0.028(2)	0.030(2)	0.0063(14)	0.004(2)	0.0027(15)
O(3)	0.018(2)	0.026(2)	0.029(2)	0.0087(14)	0.0010(15)	0.0016(14)
C(1)	0.027(3)	0.021(2)	0.021(2)	-0.002(2)	0.003(2)	-0.002(2)
C(2)	0.016(2)	0.022(2)	0.026(2)	0.001(2)	-0.002(2)	-0.003(2)
C(3)	0.020(2)	0.018(2)	0.024(2)	0.002(2)	0.002(2)	-0.003(2)
C(11)	0.019(2)	0.017(2)	0.022(2)	-0.004(2)	0.002(2)	-0.001(2)
C(12)	0.024(2)	0.019(2)	0.023(2)	0.002(2)	-0.002(2)	0.007(2)
C(13)	0.035(2)	0.013(2)	0.031(2)	-0.002(2)	0.011(2)	0.004(2)
C(14)	0.023(2)	0.019(2)	0.033(2)	-0.007(2)	0.008(2)	-0.006(2)
C(15)	0.021(2)	0.024(2)	0.015(2)	-0.004(2)	-0.003(2)	0.004(2)
C(21)	0.044(3)	0.016(2)	0.033(3)	-0.006(2)	-0.002(3)	0.002(2)
C(22)	0.039(3)	0.024(2)	0.023(2)	-0.010(2)	-0.004(3)	0.004(3)
C(23)	0.045(3)	0.027(2)	0.019(2)	-0.007(2)	0.007(2)	0.009(2)
C(24)	0.034(3)	0.031(2)	0.032(3)	-0.016(2)	0.004(2)	0.004(2)
C(25)	0.050(3)	0.017(2)	0.031(3)	-0.005(2)	-0.002(3)	0.016(2)

Table A.4: *Hydrogen coordinates and isotropic displacement parameters for 1.*

	x	y	z	U(eq)
H(2)	-0.7908(74)	0.8393(45)	0.4640(30)	0.029
H(3)	-0.1301(82)	0.8132(42)	0.4629(28)	0.029
H(1A)	-0.2384(7)	0.8081(3)	0.2970(2)	0.028
H(1B)	-0.4276(7)	0.8525(3)	0.2438(2)	0.028
H(2A)	-0.6695(7)	0.7755(3)	0.3591(2)	0.026
H(2B)	-0.4564(7)	0.7460(3)	0.4049(2)	0.026
H(3A)	-0.1400(7)	1.0221(3)	0.4191(2)	0.025
H(3B)	-0.2845(7)	0.9672(3)	0.4845(2)	0.025
H(12)	-0.3380(7)	1.0290(3)	0.1470(2)	0.026
H(13)	-0.0007(7)	1.1361(3)	0.1134(2)	0.031
H(14)	0.2797(7)	1.0836(4)	0.2105(2)	0.030
H(15)	0.1173(7)	0.9409(3)	0.3035(2)	0.024
H(21)	-0.1494(9)	0.6984(3)	0.1457(2)	0.037
H(22)	-0.1714(9)	0.8274(3)	0.0290(2)	0.034
H(23)	0.1855(8)	0.9196(4)	0.0096(3)	0.037
H(24)	0.4335(8)	0.8481(4)	0.1132(3)	0.039
H(25)	0.2261(8)	0.7118(4)	0.1975(3)	0.039

Table A.5: *Atomic coordinates and equivalent isotropic displacement parameters for 2. U(eq) is defined as one third of the trace of the orthogonalised Uij tensor.*

	x	y	z	U(eq)
Fe(1)	0.7582(1)	0.8305(1)	0.0146(1)	0.022(1)
P(1)	0.7453(1)	0.4304(1)	0.3241(1)	0.024(1)
C(1)	0.7152(3)	0.6342(4)	0.2489(3)	0.027(1)
C(11)	0.7947(3)	0.6583(4)	0.1535(3)	0.025(1)
C(12)	0.9079(3)	0.7613(4)	0.1665(3)	0.030(1)
C(13)	0.9512(3)	0.7520(5)	0.0537(3)	0.033(1)
C(14)	0.8664(3)	0.6416(4)	-0.0286(3)	0.030(1)
C(15)	0.7699(3)	0.5827(4)	0.0328(3)	0.024(1)
C(21)	0.6318(4)	0.9973(6)	0.0560(4)	0.049(1)
C(22)	0.7344(4)	1.0759(6)	0.0177(4)	0.044(1)
C(23)	0.7319(4)	1.0263(5)	-0.1041(3)	0.041(1)
C(24)	0.6284(4)	0.9173(5)	-0.1443(3)	0.042(1)
C(25)	0.5641(3)	0.8960(5)	-0.0473(4)	0.051(1)
C(31)	0.6897(3)	0.4670(3)	0.4682(2)	0.022(1)
C(32)	0.7439(3)	0.3771(4)	0.5775(3)	0.028(1)
C(33)	0.6967(3)	0.3959(4)	0.6848(3)	0.034(1)
C(34)	0.5949(3)	0.5055(5)	0.6846(3)	0.035(1)
C(35)	0.5389(3)	0.5922(5)	0.5759(3)	0.033(1)
C(36)	0.5846(3)	0.5723(4)	0.4688(3)	0.027(1)
C(41)	0.9279(3)	0.4313(4)	0.3817(2)	0.023(1)
C(42)	0.9994(3)	0.3491(5)	0.3102(2)	0.029(1)
C(43)	1.1377(3)	0.3442(6)	0.3459(3)	0.035(1)
C(44)	1.2063(3)	0.4213(4)	0.4547(3)	0.032(1)
C(45)	1.1365(3)	0.5057(4)	0.5266(3)	0.031(1)
C(46)	0.9979(3)	0.5120(4)	0.4898(3)	0.028(1)

Table A.6: *Bond lengths (Å) and angles (°) for 2.*

Fe(1)-C(25)	2.027(3)	C(24)-Fe(1)-C(12)	172.22(15)
Fe(1)-C(21)	2.028(4)	C(14)-Fe(1)-C(12)	68.27(13)
Fe(1)-C(22)	2.035(5)	C(13)-Fe(1)-C(12)	40.67(13)
Fe(1)-C(24)	2.040(3)	C(11)-Fe(1)-C(12)	40.79(12)
Fe(1)-C(14)	2.041(3)	C(23)-Fe(1)-C(12)	133.42(15)
Fe(1)-C(13)	2.042(3)	C(25)-Fe(1)-C(15)	109.02(15)
Fe(1)-C(11)	2.044(3)	C(21)-Fe(1)-C(15)	132.57(16)
Fe(1)-C(23)	2.045(3)	C(22)-Fe(1)-C(15)	171.74(14)
Fe(1)-C(12)	2.047(3)	C(24)-Fe(1)-C(15)	116.18(15)
Fe(1)-C(15)	2.048(4)	C(14)-Fe(1)-C(15)	40.84(12)
P(1)-C(41)	1.837(3)	C(13)-Fe(1)-C(15)	68.58(14)
P(1)-C(31)	1.840(3)	C(11)-Fe(1)-C(15)	40.78(12)
P(1)-C(1)	1.860(3)	C(23)-Fe(1)-C(15)	147.23(14)
C(1)-C(11)	1.500(4)	C(12)-Fe(1)-C(15)	68.33(13)
C(11)-C(15)	1.426(4)	C(41)-P(1)-C(31)	103.02(12)
C(11)-C(12)	1.426(4)	C(41)-P(1)-C(1)	100.99(14)
C(12)-C(13)	1.421(4)	C(31)-P(1)-C(1)	100.34(13)

Table A.6 continued

C(13)-C(14)	1.417(5)	C(11)-C(1)-P(1)	111.6(2)
C(14)-C(15)	1.427(4)	C(15)-C(11)-C(12)	107.5(3)
C(21)-C(22)	1.398(6)	C(15)-C(11)-C(1)	126.1(3)
C(21)-C(25)	1.437(6)	C(12)-C(11)-C(1)	126.4(3)
C(22)-C(23)	1.391(6)	C(15)-C(11)-Fe(1)	69.75(17)
C(23)-C(24)	1.382(6)	C(12)-C(11)-Fe(1)	69.73(17)
C(24)-C(25)	1.402(6)	C(1)-C(11)-Fe(1)	125.5(2)
C(31)-C(36)	1.393(4)	C(13)-C(12)-C(11)	108.4(3)
C(31)-C(32)	1.399(4)	C(13)-C(12)-Fe(1)	69.46(17)
C(32)-C(33)	1.393(4)	C(11)-C(12)-Fe(1)	69.49(16)
C(33)-C(34)	1.388(5)	C(14)-C(13)-C(12)	107.9(3)
C(34)-C(35)	1.384(5)	C(14)-C(13)-Fe(1)	69.65(18)
C(35)-C(36)	1.383(4)	C(12)-C(13)-Fe(1)	69.87(17)
C(41)-C(42)	1.385(4)	C(13)-C(14)-C(15)	108.2(3)
C(41)-C(46)	1.390(4)	C(13)-C(14)-Fe(1)	69.73(19)
C(42)-C(43)	1.388(4)	C(15)-C(14)-Fe(1)	69.84(19)
C(43)-C(44)	1.378(5)	C(11)-C(15)-C(14)	107.9(3)
C(44)-C(45)	1.386(5)	C(11)-C(15)-Fe(1)	69.48(19)
C(45)-C(46)	1.391(5)	C(14)-C(15)-Fe(1)	69.3(2)
C(25)-Fe(1)-C(21)	41.51(18)	C(22)-C(21)-C(25)	106.7(3)
C(25)-Fe(1)-C(22)	68.12(17)	C(22)-C(21)-Fe(1)	70.1(2)
C(21)-Fe(1)-C(22)	40.26(18)	C(25)-C(21)-Fe(1)	69.2(2)
C(25)-Fe(1)-C(24)	40.33(17)	C(23)-C(22)-C(21)	108.9(4)
C(21)-Fe(1)-C(24)	68.31(15)	C(23)-C(22)-Fe(1)	70.4(2)
C(22)-Fe(1)-C(24)	67.08(16)	C(21)-C(22)-Fe(1)	69.6(3)
C(25)-Fe(1)-C(14)	133.04(17)	C(24)-C(23)-C(22)	108.6(4)
C(21)-Fe(1)-C(14)	172.70(18)	C(24)-C(23)-Fe(1)	70.0(2)
C(22)-Fe(1)-C(14)	146.62(16)	C(22)-C(23)-Fe(1)	69.7(2)
C(24)-Fe(1)-C(14)	110.53(14)	C(23)-C(24)-C(25)	108.7(3)
C(25)-Fe(1)-C(13)	172.45(17)	C(23)-C(24)-Fe(1)	70.41(19)
C(21)-Fe(1)-C(13)	145.28(17)	C(25)-C(24)-Fe(1)	69.33(19)
C(22)-Fe(1)-C(13)	115.27(16)	C(24)-C(25)-C(21)	107.1(3)
C(24)-Fe(1)-C(13)	133.55(14)	C(24)-C(25)-Fe(1)	70.35(19)
C(14)-Fe(1)-C(13)	40.62(14)	C(21)-C(25)-Fe(1)	69.3(2)
C(25)-Fe(1)-C(11)	114.40(15)	C(36)-C(31)-C(32)	118.0(3)
C(21)-Fe(1)-C(11)	108.00(14)	C(36)-C(31)-P(1)	121.5(2)
C(22)-Fe(1)-C(11)	132.44(15)	C(32)-C(31)-P(1)	120.2(2)
C(24)-Fe(1)-C(11)	146.67(15)	C(33)-C(32)-C(31)	120.9(3)
C(14)-Fe(1)-C(11)	68.75(12)	C(34)-C(33)-C(32)	120.1(3)
C(13)-Fe(1)-C(11)	68.83(12)	C(35)-C(34)-C(33)	119.3(3)
C(25)-Fe(1)-C(23)	67.50(16)	C(36)-C(35)-C(34)	120.7(3)
C(21)-Fe(1)-C(23)	67.70(16)	C(35)-C(36)-C(31)	121.0(3)
C(22)-Fe(1)-C(23)	39.86(16)	C(42)-C(41)-C(46)	118.5(3)
C(24)-Fe(1)-C(23)	39.55(16)	C(42)-C(41)-P(1)	117.2(2)
C(14)-Fe(1)-C(23)	116.35(14)	C(46)-C(41)-P(1)	124.3(2)
C(13)-Fe(1)-C(23)	110.35(15)	C(41)-C(42)-C(43)	121.2(3)
C(11)-Fe(1)-C(23)	171.75(15)	C(44)-C(43)-C(42)	120.0(3)
C(25)-Fe(1)-C(12)	145.99(16)	C(43)-C(44)-C(45)	119.6(3)
C(21)-Fe(1)-C(12)	113.91(15)	C(44)-C(45)-C(46)	120.3(3)
C(22)-Fe(1)-C(12)	109.39(15)	C(41)-C(46)-C(45)	120.4(3)

Table A.7: *Anisotropic displacement parameters ($Å^2$) for 2. The anisotropic displacement factor exponent takes the form: $-2\pi^2(h^2a^{*2}U11 + ... + 2hka^*b^*U12)$.*

	U11	U22	U33	U23	U13	U12
Fe(1)	0.0225(2)	0.0210(2)	0.0234(2)	0.0026(2)	0.0055(1)	0.0023(2)
P(1)	0.0250(3)	0.0237(3)	0.0208(3)	-0.0004(3)	0.0033(3)	-0.0014(3)
C(1)	0.0296(14)	0.0301(15)	0.0224(12)	0.0058(11)	0.0061(11)	0.0034(12)
C(11)	0.0257(13)	0.0259(14)	0.0218(12)	0.0066(11)	0.0026(10)	0.0033(12)
C(12)	0.0249(13)	0.0320(15)	0.0283(14)	0.0027(12)	-0.0008(11)	0.0015(13)
C(13)	0.0237(13)	0.0319(16)	0.0443(17)	0.0079(14)	0.0100(12)	0.0023(13)
C(14)	0.0333(15)	0.0302(16)	0.0295(14)	0.0045(12)	0.0135(12)	0.0097(13)
C(15)	0.0291(15)	0.0191(14)	0.0250(13)	0.0046(12)	0.0076(11)	0.0025(12)
C(21)	0.0055(2)	0.0055(2)	0.0427(19)	0.0104(18)	0.0258(17)	0.0030(2)
C(22)	0.0048(2)	0.0252(19)	0.0053(2)	-0.0051(16)	0.0019(18)	0.0021(17)
C(23)	0.0051(2)	0.0279(17)	0.0469(19)	0.0159(15)	0.0182(16)	0.0110(16)
C(24)	0.0477(19)	0.0364(19)	0.0334(15)	0.0031(15))	-0.0047(14	0.0145(18)
C(25)	0.0238(15)	0.0329(19)	0.0093(3)	0.0019(2)	0.0088(17)	0.0071(14)
C(31)	0.0218(12)	0.0217(14)	0.0221(11)	0.0000(10)	0.0042(9)	-0.0045(10)
C(32)	0.0309(14)	0.0258(15)	0.0263(13)	0.0020(10)	0.0058(11)	0.0005(11)
C(33)	0.0422(18)	0.0322(16)	0.0261(13)	0.0058(12)	0.0079(12)	-0.0015(14)
C(34)	0.0349(16)	0.0406(18)	0.0323(15)	-0.0029(14)	0.0149(13)	-0.0101(15)
C(35)	0.0252(14)	0.0385(18)	0.0371(16)	-0.0027(14)	0.0115(12)	-0.0001(14)
C(36)	0.0222(13)	0.0301(15)	0.0276(13)	0.0024(12)	0.0038(10)	0.0002(12)
C(41)	0.0276(13)	0.0189(12)	0.0216(11)	0.0024(11)	0.0064(10)	0.0000(12)
C(42)	0.0339(13)	0.0304(17)	0.0245(11)	0.0014(13)	0.0105(10)	0.0009(14)
C(43)	0.0359(14)	0.0350(17)	0.0383(14)	0.0001(18)	0.0175(12)	0.0022(18)
C(44)	0.0237(13)	0.0293(16)	0.0446(16)	0.0065(14)	0.0106(12)	0.0013(13)
C(45)	0.0298(14)	0.0280(15)	0.0330(14)	-0.0027(13)	0.0027(12)	-0.0066(13)
C(46)	0.0291(13)	0.0255(14)	0.0292(13)	-0.0035(12)	0.0083(11)	0.0009(12)

Table A.8: *Hydrogen coordinates and isotropic displacement parameters for 2.*

	x	y	z	U(eq)
H(1A)	0.6191	0.6462	0.2070	0.033
H(1B)	0.7396	0.7192	0.3147	0.033
H(12)	0.9476	0.8254	0.2383	0.036
H(13)	1.0241	0.8095	0.0366	0.040
H(14)	0.8728	0.6120	-0.1106	0.036
H(15)	0.7011	0.5066	-0.0009	0.029
H(21)	0.6108	1.0086	0.1350	0.058
H(22)	0.7958	1.1510	0.0669	0.053
H(23)	0.7914	1.0615	-0.1518	0.049
H(24)	0.6047	0.8654	-0.2243	0.050
H(25)	0.4899	0.8274	-0.0495	0.061
H(32)	0.8139	0.3021	0.5787	0.034
H(33)	0.7343	0.3336	0.7582	0.040
H(34)	0.5640	0.5208	0.7582	0.042
H(35)	0.4682	0.6662	0.5747	0.040

Table A.8 continued

H(36)	0.5438	0.6315	0.3946	0.033
H(42)	0.9529	0.2952	0.2352	0.035
H(43)	1.1850	0.2876	0.2954	0.042
H(44)	1.3009	0.4167	0.4801	0.039
H(45)	1.1834	0.5596	0.6014	0.037
H(46)	0.9508	0.5718	0.5388	0.033

Table A.9: *Atomic coordinates and equivalent isotropic displacement parameters for 4. U(eq) is defined as one third of the trace of the orthogonalised Uij tensor.*

	x	y	z	U(eq)
Fe(1)	0.7628(1)	0.1342(1)	0.5798(1)	0.022(1)
P(1)	0.7394(1)	0.5740(1)	0.5721(1)	0.020(1)
S(1)	0.7536(1)	0.6825(1)	0.4110(1)	0.035(1)
C(1)	0.6898(2)	0.4141(2)	0.6089(2)	0.022(1)
C(2)	0.6216(2)	0.6616(2)	0.6512(2)	0.026(1)
O(2)	0.6231(2)	0.6032(2)	0.7701(1)	0.030(1)
C(3)	0.8896(2)	0.5397(2)	0.6339(2)	0.028(1)
O(3)	0.8799(2)	0.4556(2)	0.7491(1)	0.038(1)
C(11)	0.7786(2)	0.3243(2)	0.5565(2)	0.021(1)
C(12)	0.7696(2)	0.3128(2)	0.4509(2)	0.025(1)
C(13)	0.8729(2)	0.2157(2)	0.4342(2)	0.030(1)
C(14)	0.9461(2)	0.1679(2)	0.5281(2)	0.028(1)
C(15)	0.8885(2)	0.2349(2)	0.6034(2)	0.024(1)
C(21)	0.5977(3)	0.0901(3)	0.6746(4)	0.082(2)
C(22)	0.6066(4)	0.0649(4)	0.5718(3)	0.071(1)
C(23)	0.7103(4)	-0.0269(3)	0.5690(2)	0.052(1)
C(24)	0.7686(3)	-0.0641(2)	0.6663(2)	0.041(1)
C(25)	0.7027(4)	0.0065(3)	0.7328(2)	0.052(1)
Fe(1)'	0.2415(1)	0.9063(1)	0.9027(1)	0.022(1)
P(1)'	0.2858(1)	0.4609(1)	0.9167(1)	0.019(1)
S(1)'	0.4279(1)	0.4098(1)	0.8166(1)	0.032(1)
C(1)'	0.2935(2)	0.6009(2)	0.9572(2)	0.026(1)
C(2)'	0.2642(2)	0.3246(2)	1.0512(2)	0.024(1)
O(2)'	0.1605(2)	0.3611(2)	1.1216(1)	0.033(1)
C(3)'	0.1365(2)	0.5017(2)	0.8515(2)	0.023(1)
O(3)'	0.1225(2)	0.4000(2)	0.8134(1)	0.028(1)
C(11)'	0.2542(2)	0.7362(2)	0.8723(2)	0.022(1)
C(12)'	0.3365(3)	0.8188(2)	0.7917(2)	0.033(1)
C(13)'	0.2621(4)	0.9411(3)	0.7339(2)	0.048(1)
C(14)'	0.1343(3)	0.9339(3)	0.7767(2)	0.050(1)
C(15)'	0.1275(2)	0.8078(2)	0.8628(2)	0.034(1)
C(21)'	0.2844(3)	0.8527(3)	1.0636(2)	0.044(1)
C(22)'	0.3759(3)	0.9243(3)	0.9884(3)	0.045(1)
C(23)'	0.3127(3)	1.0506(3)	0.9270(2)	0.043(1)
C(24)'	0.1837(3)	1.0572(3)	0.9641(2)	0.038(1)
C(25)'	0.1654(3)	0.9357(3)	1.0488(2)	0.042(1)

Table A.10: *Bond lengths (Å) and angles (°) for* ***4****.*

Fe(1)-C(22)	2.018(3)	Fe(1)-C(21)	2.021(3)
Fe(1)-C(23)	2.030(3)	Fe(1)-C(25)	2.032(3)
Fe(1)-C(24)	2.039(2)	Fe(1)-C(13)	2.038(2)
Fe(1)-C(15)	2.040(2)	Fe(1)-C(14)	2.042(2)
Fe(1)-C(11)	2.042(2)	Fe(1)-C(12)	2.045(2)
P(1)-C(1)	1.817(2)	P(1)-C(3)	1.821(2)
P(1)-C(2)	1.836(2)	P(1)-S(1)	1.9556(8)
C(1)-C(11)	1.496(3)	C(2)-O(2)	1.413(3)
C(3)-O(3)	1.415(3)	C(11)-C(12)	1.423(3)
C(11)-C(15)	1.424(3)	C(12)-C(13)	1.423(3)
C(13)-C(14)	1.415(3)	C(14)-C(15)	1.417(3)
C(21)-C(25)	1.415(5)	C(21)-C(22)	1.427(6)
C(22)-C(23)	1.347(5)	C(23)-C(24)	1.368(4)
C(24)-C(25)	1.378(4)	Fe(1)'-C(21)'	2.019(2)
Fe(1)'-C(11)'	2.028(2)	Fe(1)'-C(14)'	2.028(2)
Fe(1)'-C(25)'	2.028(2)	Fe(1)'-C(13)'	2.029(2)
Fe(1)'-C(22)'	2.031(3)	Fe(1)'-C(15)'	2.031(2)
Fe(1)'-C(12)'	2.035(2)	Fe(1)'-C(24)'	2.040(2)
Fe(1)'-C(23)'	2.042(3)	P(1)'-C(1)'	1.823(2)
P(1)'-C(3)'	1.825(2)	P(1)'-C(2)'	1.829(2)
P(1)'-S(1)'	1.9614(8)	C(1)'-C(11)'	1.501(3)
C(2)'-O(2)'	1.407(3)	C(3)'-O(3)'	1.423(3)
C(11)'-C(12)'	1.419(3)	C(11)'-C(15)'	1.424(3)
C(12)'-C(13)'	1.413(4)	C(13)'-C(14)'	1.403(5)
C(14)'-C(15)'	1.420(4)	C(21)'-C(22)'	1.402(4)
C(21)'-C(25)'	1.405(4)	C(22)'-C(23)'	1.405(4)
C(23)'-C(24)'	1.390(4)	C(24)'-C(25)'	1.399(4)
C(22)-Fe(1)-C(21)	41.4(2)	C(22)-Fe(1)-C(23)	38.9(2)
C(21)-Fe(1)-C(23)	67.61(14)	C(22)-Fe(1)-C(25)	68.07(13)
C(21)-Fe(1)-C(25)	40.9(2)	C(23)-Fe(1)-C(25)	67.08(11)
C(22)-Fe(1)-C(24)	65.98(13)	C(21)-Fe(1)-C(24)	67.21(12)
C(23)-Fe(1)-C(24)	39.30(11)	C(25)-Fe(1)-C(24)	39.59(12)
C(22)-Fe(1)-C(13)	119.15(14)	C(21)-Fe(1)-C(13)	155.1(2)
C(23)-Fe(1)-C(13)	107.04(11)	C(25)-Fe(1)-C(13)	161.59(13)
C(24)-Fe(1)-C(13)	125.02(10)	C(22)-Fe(1)-C(15)	165.9(2)
C(21)-Fe(1)-C(15)	127.3(2)	C(23)-Fe(1)-C(15)	154.11(12)
C(25)-Fe(1)-C(15)	108.90(10)	C(24)-Fe(1)-C(15)	121.18(10)
C(13)-Fe(1)-C(15)	68.25(9)	C(22)-Fe(1)-C(14)	152.6(2)
C(21)-Fe(1)-C(14)	163.7(2)	C(23)-Fe(1)-C(14)	119.18(12)
C(25)-Fe(1)-C(14)	125.45(13)	C(24)-Fe(1)-C(14)	107.82(11)
C(13)-Fe(1)-C(14)	40.59(10)	C(15)-Fe(1)-C(14)	40.61(9)
C(22)-Fe(1)-C(11)	127.97(13)	C(21)-Fe(1)-C(11)	109.08(11)
C(23)-Fe(1)-C(11)	163.39(11)	C(25)-Fe(1)-C(11)	121.92(10)
C(24)-Fe(1)-C(11)	156.12(10)	C(13)-Fe(1)-C(11)	68.68(9)
C(15)-Fe(1)-C(11)	40.82(8)	C(14)-Fe(1)-C(11)	68.74(9)
C(22)-Fe(1)-C(12)	108.59(11)	C(21)-Fe(1)-C(12)	121.14(13)
C(23)-Fe(1)-C(12)	125.71(10)	C(25)-Fe(1)-C(12)	156.74(12)
C(24)-Fe(1)-C(12)	161.91(10)	C(13)-Fe(1)-C(12)	40.80(9)
C(15)-Fe(1)-C(12)	68.37(9)	C(14)-Fe(1)-C(12)	68.52(9)
C(11)-Fe(1)-C(12)	40.76(8)	C(1)-P(1)-C(3)	105.99(11)
C(1)-P(1)-C(2)	105.19(10)	C(3)-P(1)-C(2)	106.42(11)
C(1)-P(1)-S(1)	116.43(8)	C(3)-P(1)-S(1)	111.66(8)
C(2)-P(1)-S(1)	110.48(8)	C(11)-C(1)-P(1)	113.4(2)
O(2)-C(2)-P(1)	114.3(2)	O(3)-C(3)-P(1)	111.1(2)

Table A.10 continued

C(12)-C(11)-C(15)	107.4(2)	C(12)-C(11)-C(1)	126.6(2)
C(15)-C(11)-C(1)	126.0(2)	C(12)-C(11)-Fe(1)	69.72(12)
C(15)-C(11)-Fe(1)	69.51(12)	C(1)-C(11)-Fe(1)	126.3(2)
C(13)-C(12)-C(11)	107.9(2)	C(13)-C(12)-Fe(1)	69.35(13)
C(11)-C(12)-Fe(1)	69.52(12)	C(14)-C(13)-C(12)	108.3(2)
C(14)-C(13)-Fe(1)	69.85(13)	C(12)-C(13)-Fe(1)	69.85(13)
C(13)-C(14)-C(15)	107.8(2)	C(13)-C(14)-Fe(1)	69.56(14)
C(15)-C(14)-Fe(1)	69.63(13)	C(14)-C(15)-C(11)	108.5(2)
C(14)-C(15)-Fe(1)	69.76(13)	C(11)-C(15)-Fe(1)	69.66(12)
C(25)-C(21)-C(22)	105.8(3)	C(25)-C(21)-Fe(1)	70.0(2)
C(22)-C(21)-Fe(1)	69.2(2)	C(23)-C(22)-C(21)	108.6(3)
C(23)-C(22)-Fe(1)	71.1(2)	C(21)-C(22)-Fe(1)	69.4(2)
C(22)-C(23)-C(24)	108.9(3)	C(22)-C(23)-Fe(1)	70.1(2)
C(24)-C(23)-Fe(1)	70.7(2)	C(23)-C(24)-C(25)	109.6(3)
C(23)-C(24)-Fe(1)	70.0(2)	C(25)-C(24)-Fe(1)	69.9(2)
C(24)-C(25)-C(21)	107.1(3)	C(24)-C(25)-Fe(1)	70.5(2)
C(21)-C(25)-Fe(1)	69.1(2)	C(21)'-Fe(1)'-C(11)'	106.68(10)
C(21)'-Fe(1)'-C(14)'	157.07(14)	C(11)'-Fe(1)'-C(14)'	68.75(9)
C(21)'-Fe(1)'-C(25)'	40.62(12)	C(11)'-Fe(1)'-C(25)'	125.48(11)
C(14)'-Fe(1)'-C(25)'	122.60(13)	C(21)'-Fe(1)'-C(13)'	160.83(14)
C(11)'-Fe(1)'-C(13)'	68.92(9)	C(14)'-Fe(1)'-C(13)'	40.45(13)
C(25)'-Fe(1)'-C(13)'	156.77(12)	C(21)'-Fe(1)'-C(22)'	40.50(12)
C(11)'-Fe(1)'-C(22)'	119.50(10)	C(14)'-Fe(1)'-C(22)'	161.59(14)
C(25)'-Fe(1)'-C(22)'	67.86(11)	C(13)'-Fe(1)'-C(22)'	124.13(14)
C(21)'-Fe(1)'-C(15)'	120.86(12)	C(11)'-Fe(1)'-C(15)'	41.09(9)
C(14)'-Fe(1)'-C(15)'	40.95(11)	C(25)'-Fe(1)'-C(15)'	108.78(11)
C(13)'-Fe(1)'-C(15)'	68.87(12)	C(22)'-Fe(1)'-C(15)'	155.40(11)
C(21)'-Fe(1)'-C(12)'	123.99(11)	C(11)'-Fe(1)'-C(12)'	40.88(9)
C(14)'-Fe(1)'-C(12)'	68.13(12)	C(25)'-Fe(1)'-C(12)'	161.84(11)
C(13)'-Fe(1)'-C(12)'	40.68(11)	C(22)'-Fe(1)'-C(12)'	106.46(11)
C(15)'-Fe(1)'-C(12)'	68.75(11)	C(21)'-Fe(1)'-C(24)'	67.95(11)
C(11)'-Fe(1)'-C(24)'	163.14(11)	C(14)'-Fe(1)'-C(24)'	109.57(10)
C(25)'-Fe(1)'-C(24)'	40.21(11)	C(13)'-Fe(1)'-C(24)'	121.45(11)
C(22)'-Fe(1)'-C(24)'	67.56(10)	C(15)'-Fe(1)'-C(24)'	126.67(10)
C(12)'-Fe(1)'-C(24)'	155.42(11)	C(21)'-Fe(1)'-C(23)'	67.92(12)
C(11)'-Fe(1)'-C(23)'	154.78(11)	C(14)'-Fe(1)'-C(23)'	125.81(12)
C(25)'-Fe(1)'-C(23)'	67.43(11)	C(13)'-Fe(1)'-C(23)'	107.67(12)
C(22)'-Fe(1)'-C(23)'	40.36(11)	C(15)'-Fe(1)'-C(23)'	162.98(11)
C(12)'-Fe(1)'-C(23)'	120.23(11)	C(24)'-Fe(1)'-C(23)'	39.81(11)
C(1)'-P(1)'-C(3)'	106.11(10)	C(1)'-P(1)'-C(2)'	104.59(10)
C(3)'-P(1)'-C(2)'	105.81(11)	C(1)'-P(1)'-S(1)'	117.74(8)
C(3)'-P(1)'-S(1)'	109.99(8)	C(2)'-P(1)'-S(1)'	111.78(8)
C(11)'-C(1)'-P(1)'	116.1(2)	O(2)'-C(2)'-P(1)'	111.45(14)
O(3)'-C(3)'-P(1)'	110.79(14)	C(12)'-C(11)'-C(15)'	107.7(2)
C(12)'-C(11)'-C(1)'	126.4(2)	C(15)'-C(11)'-C(1)'	125.8(2)
C(12)'-C(11)'-Fe(1)'	69.85(12)	C(15)'-C(11)'-Fe(1)'	69.57(12)
C(1)'-C(11)'-Fe(1)'	123.4(2)	C(13)'-C(12)'-C(11)'	108.3(2)
C(13)'-C(12)'-Fe(1)'	69.42(14)	C(11)'-C(12)'-Fe(1)'	69.27(13)
C(14)'-C(13)'-C(12)'	107.9(2)	C(14)'-C(13)'-Fe(1)'	69.7(2)
C(12)'-C(13)'-Fe(1)'	69.90(14)	C(13)'-C(14)'-C(15)'	108.9(2)
C(13)'-C(14)'-Fe(1)'	69.8(2)	C(15)'-C(14)'-Fe(1)'	69.64(13)
C(14)'-C(15)'-C(11)'	107.2(2)	C(14)'-C(15)'-Fe(1)'	69.4(2)
C(11)'-C(15)'-Fe(1)'	69.34(13)	C(22)'-C(21)'-C(25)'	107.7(2)
C(22)'-C(21)'-Fe(1)'	70.2(2)	C(25)'-C(21)'-Fe(1)'	70.04(14)
C(21)'-C(22)'-C(23)'	107.9(2)	C(21)'-C(22)'-Fe(1)'	69.32(14)
C(23)'-C(22)'-Fe(1)'	70.3(2)	C(24)'-C(23)'-C(22)'	108.2(3)
C(24)'-C(23)'-Fe(1)'	70.02(14)	C(22)'-C(23)'-Fe(1)'	69.4(2)

Table A.10 continued

C(23)'-C(24)'-C(25)'	108.2(2)	C(23)'-C(24)'-Fe(1)'	70.17(14)
C(25)'-C(24)'-Fe(1)'	69.45(14)	C(24)'-C(25)'-C(21)'	108.0(2)
C(24)'-C(25)'-Fe(1)'	70.34(14)	C(21)'-C(25)'-Fe(1)'	69.3(2)

Table A.11: *Anisotropic displacement parameters ($Å^2$) for **4**. The anisotropic displacement factor exponent takes the form: $-2\pi^2[h^2a^{*2}U11 + ... + 2hka^*b^*U12)$.*

	U11	U22	U33	U23	U13	U12
Fe(1)	0.032(1)	0.014(1)	0.020(1)	-0.005(1)	-0.004(1)	-0.007(1)
P(1)	0.025(1)	0.015(1)	0.020(1)	-0.006(1)	-0.002(1)	-0.004(1)
S(1)	0.059(1)	0.022(1)	0.021(1)	-0.004(1)	-0.002(1)	-0.005(1)
C(1)	0.023(1)	0.017(1)	0.025(1)	-0.007(1)	-0.002(1)	-0.004(1)
C(2)	0.028(1)	0.018(1)	0.032(1)	-0.012(1)	-0.001(1)	-0.003(1)
O(2)	0.030(1)	0.038(1)	0.028(1)	-0.019(1)	0.000(1)	-0.008(1)
C(3)	0.024(1)	0.035(1)	0.029(1)	-0.013(1)	0.000(1)	-0.011(1)
O(3)	0.026(1)	0.055(1)	0.026(1)	-0.009(1)	-0.007(1)	-0.001(1)
C(11)	0.026(1)	0.015(1)	0.021(1)	-0.004(1)	-0.002(1)	-0.007(1)
C(12)	0.038(1)	0.018(1)	0.020(1)	-0.003(1)	-0.005(1)	-0.010(1)
C(13)	0.047(2)	0.022(1)	0.022(1)	-0.010(1)	0.005(1)	-0.012(1)
C(14)	0.029(1)	0.018(1)	0.036(1)	-0.011(1)	0.003(1)	-0.003(1)
C(15)	0.029(1)	0.018(1)	0.024(1)	-0.006(1)	-0.005(1)	-0.006(1)
C(21)	0.053(2)	0.026(2)	0.146(4)	-0.028(2)	0.061(2)	-0.021(2)
C(22)	0.064(2)	0.050(2)	0.082(3)	0.025(2)	-0.040(2)	-0.042(2)
C(23)	0.099(3)	0.035(2)	0.033(2)	-0.006(1)	-0.008(2)	-0.042(2)
C(24)	0.057(2)	0.017(1)	0.045(2)	-0.001(1)	-0.003(1)	-0.014(1)
C(25)	0.098(3)	0.046(2)	0.024(1)	-0.012(1)	0.010(2)	-0.050(2)
Fe(1)'	0.031(1)	0.015(1)	0.021(1)	-0.009(1)	-0.007(1)	-0.001(1)
P(1)'	0.022(1)	0.015(1)	0.020(1)	-0.006(1)	-0.004(1)	-0.003(1)
S(1)'	0.026(1)	0.032(1)	0.037(1)	-0.016(1)	0.006(1)	-0.006(1)
C(1)'	0.037(1)	0.017(1)	0.027(1)	-0.008(1)	-0.008(1)	-0.006(1)
C(2)'	0.033(1)	0.016(1)	0.021(1)	-0.005(1)	-0.006(1)	-0.004(1)
O(2)'	0.041(1)	0.033(1)	0.026(1)	-0.011(1)	0.002(1)	-0.009(1)
C(3)'	0.025(1)	0.023(1)	0.024(1)	-0.011(1)	-0.006(1)	0.000(1)
O(3)'	0.026(1)	0.032(1)	0.033(1)	-0.018(1)	-0.006(1)	-0.005(1)
C(11)'	0.031(1)	0.017(1)	0.021(1)	-0.011(1)	-0.006(1)	-0.001(1)
C(12)'	0.053(2)	0.023(1)	0.028(1)	-0.016(1)	0.007(1)	-0.009(1)
C(13)'	0.103(3)	0.022(1)	0.020(1)	-0.007(1)	-0.008(1)	-0.009(2)
C(14)'	0.087(2)	0.026(1)	0.048(2)	-0.024(1)	-0.050(2)	0.024(2)
C(15)'	0.035(1)	0.035(1)	0.045(2)	-0.028(1)	-0.017(1)	0.003(1)
C(21)'	0.076(2)	0.033(1)	0.032(1)	-0.014(1)	-0.028(1)	-0.003(1)
C(22)'	0.032(1)	0.055(2)	0.069(2)	-0.046(2)	-0.018(1)	0.004(1)
C(23)'	0.056(2)	0.034(2)	0.050(2)	-0.024(1)	-0.002(1)	-0.019(1)
C(24)'	0.045(2)	0.034(1)	0.048(2)	-0.031(1)	-0.018(1)	0.008(1)
C(25)'	0.044(2)	0.065(2)	0.036(2)	-0.037(1)	0.005(1)	-0.019(1)

Table A.12: *Hydrogen coordinates and isotropic displacement parameters for 4.*

	x	y	z	U(eq)
H(1A)	0.6074(2)	0.4300(2)	0.5824(2)	0.026
H(1B)	0.6811(2)	0.3708(2)	0.6897(2)	0.026
H(2A)	0.5381(2)	0.6668(2)	0.6308(2)	0.031
H(2B)	0.6387(2)	0.7504(2)	0.6279(2)	0.031
H(2)	0.6542(2)	0.5442(2)	0.7996(1)	0.035
H(3A)	0.9118(2)	0.6217(2)	0.6292(2)	0.034
H(3B)	0.9558(2)	0.4994(2)	0.5917(2)	0.034
H(3)	0.9595(2)	0.4156(2)	0.7771(1)	0.046
H(12)	0.7040(2)	0.3613(2)	0.4012(2)	0.030
H(13)	0.8889(2)	0.1875(2)	0.3701(2)	0.036
H(14)	1.0220(2)	0.1025(2)	0.5387(2)	0.034
H(15)	0.9176(2)	0.2218(2)	0.6745(2)	0.028
H(21)	0.5359(3)	0.1492(3)	0.7032(4)	0.098
H(22)	0.5454(4)	0.1077(4)	0.5169(3)	0.085
H(23)	0.7369(4)	-0.0591(3)	0.5076(2)	0.062
H(24)	0.8455(3)	-0.1275(2)	0.6823(2)	0.050
H(25)	0.7273(4)	-0.0014(3)	0.8042(2)	0.063
H(1A)'	0.3794(2)	0.5951(2)	0.9724(2)	0.031
H(1B)'	0.2401(2)	0.5925(2)	1.0266(2)	0.031
H(2A)'	0.3409(2)	0.2967(2)	1.0890(2)	0.028
H(2B)'	0.2474(2)	0.2510(2)	1.0359(2)	0.028
H(2)'	0.1925(2)	0.3935(2)	1.1640(1)	0.040
H(3A)'	0.1330(2)	0.5852(2)	0.7897(2)	0.028
H(3B)'	0.0665(2)	0.5096(2)	0.9068(2)	0.028
H(3)'	0.1863(2)	0.3923(2)	0.7595(1)	0.033
H(12)'	0.4276(3)	0.7968(2)	0.7805(2)	0.040
H(13)'	0.2927(4)	1.0167(3)	0.6762(2)	0.058
H(14)'	0.0633(3)	1.0037(3)	0.7533(2)	0.060
H(15)'	0.0513(2)	0.7774(2)	0.9062(2)	0.040
H(21)'	0.3006(3)	0.7635(3)	1.1164(2)	0.053
H(22)'	0.4654(3)	0.8918(3)	0.9798(3)	0.054
H(23)'	0.3159(3)	1.1202(3)	0.8691(2)	0.064
H(24)'	0.1177(3)	1.1315(3)	0.9363(2)	0.046
H(25)'	0.0858(3)	0.9126(3)	1.0900(2)	0.050

Table A.13: *Atomic coordinates and equivalent isotropic displacement parameters for 8. U(eq) is defined as one third of the trace of the orthogonalised Uij tensor.*

	x	y	z	U(eq)
I(1)	0.1920(1)	0.2500	0.3470(1)	0.030(1)
Fe(1)	0.4901(2)	0.2500	0.6486(2)	0.023(1)
P(1)	0.8775(3)	0.2500	0.4448(4)	0.023(1)
C(1)	0.8085(9)	0.4035(16)	0.4576(14)	0.033(4)
O(1)	0.8639(7)	0.5147(12)	0.4365(11)	0.048(3)
C(2)	0.9611(12)	0.2500	0.5638(16)	0.028(5)

Table A.13 continued

C(3)	0.9332(15)	0.2500	0.2965(18)	0.039(6)
C(11)	0.4205(12)	0.2500	0.8092(17)	0.020(5)
C(12)	0.3980(8)	0.1317(17)	0.7373(12)	0.028(4)
C(13)	0.3631(9)	0.1800(18)	0.6230(12)	0.038(4)
C(21)	0.6204(13)	0.2500	0.6896(18)	0.037(6)
C(22)	0.6009(9)	0.3731(18)	0.6222(12)	0.033(4)
C(23)	0.5676(9)	0.3210(17)	0.5070(12)	0.039(4)

Table A.14: *Bond lengths (Å) and angles (°) for 8.*

Fe(1)-C(21)	1.99(2)	C(12)#1-Fe(1)-C(23)#1	158.3(6)
Fe(1)-C(13)	2.027(14)	C(12)-Fe(1)-C(23)#1	123.1(6)
Fe(1)-C(13)#1	2.027(14)	C(23)-Fe(1)-C(23)#1	39.5(9)
Fe(1)-C(11)	2.03(2)	C(21)-Fe(1)-C(22)	41.5(5)
Fe(1)-C(12)#1	2.032(13)	C(13)-Fe(1)-C(22)	157.3(6)
Fe(1)-C(12)	2.032(13)	C(13)#1-Fe(1)-C(22)	122.1(7)
Fe(1)-C(23)	2.043(13)	C(11)-Fe(1)-C(22)	121.9(6)
Fe(1)-C(23)#1	2.043(13)	C(12)#1-Fe(1)-C(22)	106.0(6)
Fe(1)-C(22)	2.056(14)	C(12)-Fe(1)-C(22)	159.3(6)
Fe(1)-C(22)#1	2.057(14)	C(23)-Fe(1)-C(22)	41.1(5)
P(1)-C(2)	1.79(2)	C(23)#1-Fe(1)-C(22)	68.9(6)
P(1)-C(3)	1.81(2)	C(21)-Fe(1)-C(22)#1	41.5(5)
P(1)-C(1)#1	1.82(2)	C(13)-Fe(1)-C(22)#1	122.1(7)
P(1)-C(1)	1.82(2)	C(13)#1-Fe(1)-C(22)#1	157.3(6)
C(1)-O(1)	1.38(2)	C(11)-Fe(1)-C(22)#1	121.9(5)
C(2)-C(11)#2	1.51(3)	C(12)#1-Fe(1)-C(22)#1	159.3(6)
C(11)-C(12)	1.43(2)	C(12)-Fe(1)-C(22)#1	106.0(6)
C(11)-C(12)#1	1.43(2)	C(23)-Fe(1)-C(22)#1	68.9(6)
C(11)-C(2)#3	1.51(3)	C(23)#1-Fe(1)-C(22)#1	41.1(5)
C(12)-C(13)	1.43(2)	C(22)-Fe(1)-C(22)#1	71.2(10)
C(13)-C(13)#1	1.36(3)	C(2)-P(1)-C(3)	109.0(9)
C(21)-C(22)#1	1.43(2)	C(2)-P(1)-C(1)#1	109.6(6)
C(21)-C(22)	1.43(2)	C(3)-P(1)-C(1)#1	109.1(6)
C(22)-C(23)	1.44(2)	C(2)-P(1)-C(1)	109.6(6)
C(23)-C(23)#1	1.38(3)	C(3)-P(1)-C(1)	109.1(6)
C(21)-Fe(1)-C(13)	159.9(5)	C(1)#1-P(1)-C(1)	110.5(9)
C(21)-Fe(1)-C(13)#1	159.9(5)	O(1)-C(1)-P(1)	107.0(9)
C(13)-Fe(1)-C(13)#1	39.2(9)	C(11)#2-C(2)-P(1)	112.6(12)
C(21)-Fe(1)-C(11)	107.7(8)	C(12)-C(11)-C(12)#1	107(2)
C(13)-Fe(1)-C(11)	69.1(6)	C(12)-C(11)-C(2)#3	126.4(8)
C(13)#1-Fe(1)-C(11)	69.1(6)	C(12)#1-C(11)-C(2)#3	126.4(8)
C(21)-Fe(1)-C(12)#1	123.4(6)	C(12)-C(11)-Fe(1)	69.5(8)
C(13)-Fe(1)-C(12)#1	68.1(6)	C(12)#1-C(11)-Fe(1)	69.5(8)
C(13)#1-Fe(1)-C(12)#1	41.1(5)	C(2)#3-C(11)-Fe(1)	125.7(12)
C(11)-Fe(1)-C(12)#1	41.2(5)	C(13)-C(12)-C(11)	107.2(14)
C(21)-Fe(1)-C(12)	123.4(6)	C(13)-C(12)-Fe(1)	69.2(8)
C(13)-Fe(1)-C(12)	41.1(5)	C(11)-C(12)-Fe(1)	69.3(9)
C(13)#1-Fe(1)-C(12)	68.1(6)	C(13)#1-C(13)-C(12)	109.2(10)
C(11)-Fe(1)-C(12)	41.2(5)	C(13)#1-C(13)-Fe(1)	70.4(5)
C(12)#1-Fe(1)-C(12)	69.0(9)	C(12)-C(13)-Fe(1)	69.6(7)
C(21)-Fe(1)-C(23)	67.6(7)	C(22)#1-C(21)-C(22)	113(2)
C(13)-Fe(1)-C(23)	122.4(6)	C(22)#1-C(21)-Fe(1)	71.8(10)

Table A.14 continued

C(13)#1-Fe(1)-C(23)	108.0(6)	C(22)-C(21)-Fe(1)	71.8(10)
C(11)-Fe(1)-C(23)	159.3(5)	C(21)-C(22)-C(23)	103(2)
C(12)#1-Fe(1)-C(23)	123.1(6)	C(21)-C(22)-Fe(1)	66.7(10)
C(12)-Fe(1)-C(23)	158.3(6)	C(23)-C(22)-Fe(1)	68.9(8)
C(21)-Fe(1)-C(23)#1	67.6(7)	C(23)#1-C(23)-C(22)	110.6(10)
C(13)-Fe(1)-C(23)#1	108.0(6)	C(23)#1-C(23)-Fe(1)	70.2(5)
C(13)#1-Fe(1)-C(23)#1	122.4(6)	C(22)-C(23)-Fe(1)	70.0(7)
C(11)-Fe(1)-C(23)#1	159.3(5)		

Symmetry transformations used to generate equivalent atoms: #1 x,-y+1/2,z #2 x+1/2,-y+1/2,-z+3/2 #3 x-1/2,-y+1/2,-z+3/2

Table A.15: *Anisotropic displacement parameters ($Å^2$) for 8. The anisotropic displacement factor exponent takes the form: $-2\pi^2(h^2a^{*2}U11 + ... + 2hka^*b^*U12)$.*

	U11	U22	U33	U23	U13	U12
I(1)	0.0270(8)	0.0440(11)	0.0201(8)	0.000	-0.0001(6)	0.000
Fe(1)	0.0193(14)	0.033(2)	0.0151(14)	0.000	0.0029(13)	0.000
P(1)	0.019(3)	0.038(4)	0.013(2)	0.000	-0.003(2)	0.000
C(1)	0.022(7)	0.050(12)	0.027(8)	0.012(8)	0.004(7)	-0.007(8)
O(1)	0.048(7)	0.045(8)	0.052(7)	0.000(6)	0.015(7)	-0.005(7)
C(2)	0.012(9)	0.058(16)	0.014(9)	0.000	-0.004(8)	0.000
C(3)	0.033(12)	0.061(18)	0.024(11)	0.000	-0.005(10)	0.000
C(11)	0.011(9)	0.034(14)	0.015(10)	0.000	0.002(8)	0.000
C(12)	0.016(7)	0.048(10)	0.019(7)	0.003(8)	0.009(6)	-0.004(8)
C(13)	0.025(7)	0.071(12)	0.018(7)	0.002(7)	-0.001(6)	0.001(8)
C(21)	0.012(10)	0.080(20)	0.018(10)	0.000	0.014(9)	0.000
C(22)	0.026(8)	0.047(11)	0.028(8)	0.000(8)	0.012(7)	-0.017(8)
C(23)	0.032(8)	0.068(12)	0.018(7)	0.002(7)	0.011(6)	-0.006(8)

Table A.16: *Hydrogen coordinates and isotropic displacement parameters for 8.*

	x	y	z	U(eq)
H(1A)	0.7603(9)	0.4013(16)	0.3974(14)	0.040
H(1B)	0.7821(9)	0.4094(16)	0.5391(14)	0.040
H(1)	0.9148(33)	0.4969(78)	0.4608(173)	0.073
H(2A)	0.9989(12)	0.1694	0.5546(16)	0.033
H(2B)	0.9989(12)	0.3306	0.5546(16)	0.033
H(3A)	0.8889(15)	0.2500	0.2322(18)	0.059
H(3B)	0.9701(15)	0.1694	0.2893(18)	0.059
H(3C)	0.9701(15)	0.3306	0.2893(18)	0.059
H(12)	0.4049(8)	0.0404(17)	0.7608(12)	0.033
H(13)	0.3435(9)	0.1247(18)	0.5586(12)	0.046
H(21)	0.6435(13)	0.2500	0.7692(18)	0.044
H(22)	0.6079(9)	0.4641(18)	0.6469(12)	0.040
H(23)	0.5487(9)	0.3755(17)	0.4416(12)	0.047

Table A.17: *Atomic coordinates and equivalent isotropic displacement parameters for* ***18****. U(eq) is defined as one third of the trace of the orthogonalised Uij tensor.*

	x	y	z	U(eq)
Au(1)	0.3849(1)	0.5631(1)	0.8179(1)	0.023(1)
Fe(1)	0.6573(1)	0.5665(1)	0.9491(1)	0.022(1)
Fe(2)	0.1531(1)	0.0116(1)	0.9132(1)	0.021(1)
P(1)	0.5417(1)	0.7550(2)	0.8286(1)	0.022(1)
P(2)	0.2245(1)	0.3872(2)	0.8048(1)	0.022(1)
Cl(1)	0.5000	0.2794(5)	0.7500	0.050(1)
Cl(2)	0.1527(3)	0.1377(6)	0.6858(1)	0.040(1)
O(1)	0.6157(5)	1.1445(9)	0.8492(2)	0.076(2)
O(2)	0.6741(6)	0.5643(12)	0.7824(2)	0.046(2)
C(2)	0.6272(6)	0.7596(12)	0.7889(2)	0.034(2)
O(2a)	0.7254(19)	0.845(4)	0.7948(6)	0.064(6)
O(4)	0.0868(4)	0.7163(8)	0.7969(1)	0.045(1)
O(5)	0.1374(5)	0.0701(9)	0.7639(1)	0.052(2)
O(6)	-0.1047(6)	0.6207(16)	0.8258(2)	0.093(3)
C(1)	0.5190(6)	1.0345(10)	0.8384(2)	0.031(2)
C(3)	0.6337(5)	0.6631(10)	0.8650(2)	0.024(1)
C(4)	0.1254(6)	0.5389(12)	0.7771(2)	0.034(2)
C(5)	0.2388(6)	0.1509(11)	0.7767(2)	0.034(2)
C(6)	0.1461(5)	0.3043(10)	0.8431(2)	0.026(1)
C(11)	0.5820(5)	0.6571(10)	0.9013(2)	0.024(1)
C(12)	0.5268(5)	0.4821(10)	0.9162(2)	0.027(1)
C(13)	0.4922(5)	0.5394(11)	0.9513(2)	0.029(2)
C(14)	0.5259(5)	0.7504(11)	0.9580(2)	0.030(2)
C(15)	0.5794(5)	0.8251(10)	0.9271(2)	0.025(1)
C(21)	0.8130(5)	0.4982(11)	0.9364(2)	0.032(2)
C(22)	0.7616(6)	0.3183(12)	0.9505(3)	0.047(2)
C(23)	0.7308(6)	0.3697(16)	0.9862(3)	0.057(3)
C(24)	0.7620(6)	0.5794(16)	0.9934(2)	0.047(2)
C(25)	0.8126(6)	0.6571(13)	0.9633(2)	0.038(2)
C(31)	0.2116(5)	0.1754(10)	0.8705(2)	0.023(1)
C(32)	0.2382(5)	-0.0419(10)	0.8679(2)	0.024(1)
C(33)	0.3020(5)	-0.1008(10)	0.8996(2)	0.027(1)
C(34)	0.3144(5)	0.0814(11)	0.9216(2)	0.029(2)
C(35)	0.2589(5)	0.2508(10)	0.9040(2)	0.025(1)
C(41)	-0.0106(6)	0.0541(13)	0.9106(2)	0.038(2)
C(42)	0.0163(6)	-0.1614(12)	0.9060(2)	0.036(2)
C(43)	0.0738(6)	-0.2289(11)	0.9382(2)	0.039(2)
C(44)	0.0843(6)	-0.0556(12)	0.9618(2)	0.034(2)
C(45)	0.0319(5)	0.1206(11)	0.9449(2)	0.031(2)

Table A.18: *Bond lengths (Å) and angles (°) for* ***18****.*

Au(1)-P(2)	2.310(2)	C(42)-Fe(2)-C(34)	159.7(3)
Au(1)-P(1)	2.311(2)	C(32)-Fe(2)-C(34)	68.1(3)
Fe(1)-C(22)	2.034(7)	C(35)-Fe(2)-C(34)	40.5(3)
Fe(1)-C(23)	2.038(7)	C(31)-Fe(2)-C(34)	68.5(3)
Fe(1)-C(14)	2.039(6)	C(41)-Fe(2)-C(34)	159.1(3)

Table A.18 continued

Fe(1)-C(11)	2.038(6)	C(43)-Fe(2)-C(34)	124.9(3)
Fe(1)-C(24)	2.046(7)	C(42)-Fe(2)-C(44)	68.2(3)
Fe(1)-C(12)	2.048(7)	C(32)-Fe(2)-C(44)	157.5(3)
Fe(1)-C(15)	2.049(6)	C(35)-Fe(2)-C(44)	126.2(3)
Fe(1)-C(21)	2.049(7)	C(31)-Fe(2)-C(44)	161.4(3)
Fe(1)-C(25)	2.054(7)	C(41)-Fe(2)-C(44)	67.8(3)
Fe(1)-C(13)	2.057(7)	C(43)-Fe(2)-C(44)	39.9(3)
Fe(2)-C(42)	2.026(7)	C(34)-Fe(2)-C(44)	110.4(3)
Fe(2)-C(32)	2.037(6)	C(42)-Fe(2)-C(33)	122.3(3)
Fe(2)-C(35)	2.040(6)	C(32)-Fe(2)-C(33)	40.9(3)
Fe(2)-C(31)	2.041(6)	C(35)-Fe(2)-C(33)	68.2(3)
Fe(2)-C(41)	2.044(7)	C(31)-Fe(2)-C(33)	68.8(3)
Fe(2)-C(43)	2.050(7)	C(41)-Fe(2)-C(33)	158.6(3)
Fe(2)-C(34)	2.056(6)	C(43)-Fe(2)-C(33)	107.7(3)
Fe(2)-C(44)	2.057(7)	C(34)-Fe(2)-C(33)	40.2(3)
Fe(2)-C(33)	2.057(6)	C(44)-Fe(2)-C(33)	123.2(3)
Fe(2)-C(45)	2.060(7)	C(42)-Fe(2)-C(45)	68.3(3)
P(1)-C(3)	1.821(6)	C(32)-Fe(2)-C(45)	159.1(3)
P(1)-C(1)	1.830(7)	C(35)-Fe(2)-C(45)	109.5(3)
P(1)-C(2)	1.839(7)	C(31)-Fe(2)-C(45)	123.8(3)
P(2)-C(6)	1.822(6)	C(41)-Fe(2)-C(45)	40.3(3)
P(2)-C(5)	1.831(7)	C(43)-Fe(2)-C(45)	67.7(3)
P(2)-C(4)	1.835(7)	C(34)-Fe(2)-C(45)	124.7(3)
O(1)-C(1)	1.428(9)	C(44)-Fe(2)-C(45)	40.4(3)
O(2)-C(2)	1.391(10)	C(33)-Fe(2)-C(45)	159.4(3)
O(4)-C(4)	1.432(9)	C(3)-P(1)-C(1)	105.0(3)
O(5)-C(5)	1.419(9)	C(3)-P(1)-C(2)	103.2(3)
C(3)-C(11)	1.505(9)	C(1)-P(1)-C(2)	103.9(3)
C(6)-C(31)	1.508(8)	C(3)-P(1)-Au(1)	117.0(2)
C(11)-C(12)	1.424(9)	C(1)-P(1)-Au(1)	114.0(2)
C(11)-C(15)	1.427(8)	C(2)-P(1)-Au(1)	112.4(2)
C(12)-C(13)	1.424(9)	C(6)-P(2)-C(5)	105.6(3)
C(13)-C(14)	1.418(10)	C(6)-P(2)-C(4)	102.4(3)
C(14)-C(15)	1.422(9)	C(5)-P(2)-C(4)	101.0(3)
C(21)-C(25)	1.411(10)	C(6)-P(2)-Au(1)	117.3(2)
C(21)-C(22)	1.413(11)	C(5)-P(2)-Au(1)	114.2(2)
C(22)-C(23)	1.424(13)	C(4)-P(2)-Au(1)	114.4(2)
C(23)-C(24)	1.404(13)	O(2)-C(2)-P(1)	112.4(5)
C(24)-C(25)	1.386(11)	O(1)-C(1)-P(1)	113.1(5)
C(31)-C(32)	1.419(9)	C(11)-C(3)-P(1)	112.7(4)
C(31)-C(35)	1.424(8)	O(4)-C(4)-P(2)	110.9(4)
C(32)-C(33)	1.430(9)	O(5)-C(5)-P(2)	112.2(5)
C(33)-C(34)	1.415(9)	C(31)-C(6)-P(2)	112.7(4)
C(34)-C(35)	1.416(9)	C(12)-C(11)-C(15)	107.3(6)
C(41)-C(45)	1.414(10)	C(12)-C(11)-C(3)	126.2(6)
C(41)-C(42)	1.416(11)	C(15)-C(11)-C(3)	126.5(6)
C(42)-C(43)	1.423(11)	C(12)-C(11)-Fe(1)	70.0(4)
C(43)-C(44)	1.402(10)	C(15)-C(11)-Fe(1)	70.0(3)
C(44)-C(45)	1.421(10)	C(3)-C(11)-Fe(1)	125.2(4)
P(2)-Au(1)-P(1)	176.51(6)	C(13)-C(12)-C(11)	108.6(6)
C(22)-Fe(1)-C(23)	41.0(4)	C(13)-C(12)-Fe(1)	70.0(4)
C(22)-Fe(1)-C(14)	161.4(3)	C(11)-C(12)-Fe(1)	69.2(4)
C(23)-Fe(1)-C(14)	125.3(3)	C(14)-C(13)-C(12)	107.5(6)
C(22)-Fe(1)-C(11)	120.5(3)	C(14)-C(13)-Fe(1)	69.1(4)
C(23)-Fe(1)-C(11)	158.0(4)	C(12)-C(13)-Fe(1)	69.4(4)
C(14)-Fe(1)-C(11)	68.9(3)	C(13)-C(14)-C(15)	108.4(6)
C(22)-Fe(1)-C(24)	68.2(4)	C(13)-C(14)-Fe(1)	70.4(4)

Table A.18 continued

C(23)-Fe(1)-C(24)	40.2(4)	C(15)-C(14)-Fe(1)	70.0(4)
C(14)-Fe(1)-C(24)	109.4(3)	C(14)-C(15)-C(11)	108.1(6)
C(11)-Fe(1)-C(24)	158.5(3)	C(14)-C(15)-Fe(1)	69.3(4)
C(22)-Fe(1)-C(12)	107.4(3)	C(11)-C(15)-Fe(1)	69.2(3)
C(23)-Fe(1)-C(12)	123.8(4)	C(25)-C(21)-C(22)	107.6(7)
C(14)-Fe(1)-C(12)	68.2(3)	C(25)-C(21)-Fe(1)	70.1(4)
C(11)-Fe(1)-C(12)	40.8(3)	C(22)-C(21)-Fe(1)	69.2(4)
C(24)-Fe(1)-C(12)	160.1(3)	C(21)-C(22)-C(23)	107.2(8)
C(22)-Fe(1)-C(15)	156.3(3)	C(21)-C(22)-Fe(1)	70.3(4)
C(23)-Fe(1)-C(15)	160.6(4)	C(23)-C(22)-Fe(1)	69.7(4)
C(14)-Fe(1)-C(15)	40.7(3)	C(24)-C(23)-C(22)	107.9(7)
C(11)-Fe(1)-C(15)	40.9(2)	C(24)-C(23)-Fe(1)	70.2(4)
C(24)-Fe(1)-C(15)	123.8(3)	C(22)-C(23)-Fe(1)	69.4(4)
C(12)-Fe(1)-C(15)	68.2(3)	C(25)-C(24)-C(23)	108.3(7)
C(22)-Fe(1)-C(21)	40.5(3)	C(25)-C(24)-Fe(1)	70.6(4)
C(23)-Fe(1)-C(21)	68.0(3)	C(23)-C(24)-Fe(1)	69.6(4)
C(14)-Fe(1)-C(21)	157.3(3)	C(24)-C(25)-C(21)	108.9(7)
C(11)-Fe(1)-C(21)	105.3(3)	C(24)-C(25)-Fe(1)	69.9(4)
C(24)-Fe(1)-C(21)	67.5(3)	C(21)-C(25)-Fe(1)	69.7(4)
C(12)-Fe(1)-C(21)	122.6(3)	C(32)-C(31)-C(35)	107.1(6)
C(15)-Fe(1)-C(21)	120.7(3)	C(32)-C(31)-C(6)	126.8(6)
C(22)-Fe(1)-C(25)	67.8(3)	C(35)-C(31)-C(6)	126.1(6)
C(23)-Fe(1)-C(25)	67.1(3)	C(32)-C(31)-Fe(2)	69.5(4)
C(14)-Fe(1)-C(25)	123.0(3)	C(35)-C(31)-Fe(2)	69.5(4)
C(11)-Fe(1)-C(25)	122.1(3)	C(6)-C(31)-Fe(2)	126.4(4)
C(24)-Fe(1)-C(25)	39.5(3)	C(31)-C(32)-C(33)	108.7(6)
C(12)-Fe(1)-C(25)	158.6(3)	C(31)-C(32)-Fe(2)	69.8(3)
C(15)-Fe(1)-C(25)	107.4(3)	C(33)-C(32)-Fe(2)	70.3(4)
C(21)-Fe(1)-C(25)	40.2(3)	C(34)-C(33)-C(32)	107.3(6)
C(22)-Fe(1)-C(13)	124.5(3)	C(34)-C(33)-Fe(2)	69.8(4)
C(23)-Fe(1)-C(13)	109.8(3)	C(32)-C(33)-Fe(2)	68.8(4)
C(14)-Fe(1)-C(13)	40.5(3)	C(33)-C(34)-C(35)	108.4(6)
C(11)-Fe(1)-C(13)	68.8(3)	C(33)-C(34)-Fe(2)	69.9(4)
C(24)-Fe(1)-C(13)	124.7(3)	C(35)-C(34)-Fe(2)	69.2(4)
C(12)-Fe(1)-C(13)	40.6(3)	C(34)-C(35)-C(31)	108.5(6)
C(15)-Fe(1)-C(13)	68.3(3)	C(34)-C(35)-Fe(2)	70.4(4)
C(21)-Fe(1)-C(13)	159.8(3)	C(31)-C(35)-Fe(2)	69.6(4)
C(25)-Fe(1)-C(13)	159.2(3)	C(45)-C(41)-C(42)	108.3(6)
C(42)-Fe(2)-C(32)	105.1(3)	C(45)-C(41)-Fe(2)	70.4(4)
C(42)-Fe(2)-C(35)	156.7(3)	C(42)-C(41)-Fe(2)	69.0(4)
C(32)-Fe(2)-C(35)	68.2(3)	C(41)-C(42)-C(43)	107.6(6)
C(42)-Fe(2)-C(31)	119.7(3)	C(41)-C(42)-Fe(2)	70.3(4)
C(32)-Fe(2)-C(31)	40.7(2)	C(43)-C(42)-Fe(2)	70.5(4)
C(35)-Fe(2)-C(31)	40.9(2)	C(44)-C(43)-C(42)	108.2(6)
C(42)-Fe(2)-C(41)	40.7(3)	C(44)-C(43)-Fe(2)	70.3(4)
C(32)-Fe(2)-C(41)	121.9(3)	C(42)-C(43)-Fe(2)	68.7(4)
C(35)-Fe(2)-C(41)	122.5(3)	C(43)-C(44)-C(45)	108.3(6)
C(31)-Fe(2)-C(41)	106.2(3)	C(43)-C(44)-Fe(2)	69.7(4)
C(42)-Fe(2)-C(43)	40.9(3)	C(45)-C(44)-Fe(2)	69.9(4)
C(32)-Fe(2)-C(43)	121.2(3)	C(41)-C(45)-C(44)	107.7(6)
C(35)-Fe(2)-C(43)	161.6(3)	C(41)-C(45)-Fe(2)	69.2(4)
C(31)-Fe(2)-C(43)	156.2(3)	C(44)-C(45)-Fe(2)	69.7(4)
C(41)-Fe(2)-C(43)	68.0(3)		

Table A.19: *Anisotropic displacement parameters ($Å^2$) for 18. The anisotropic displacement factor exponent takes the form: $-2\pi^2(h^2a^{*2}U11 + ... + 2hka^*b^*U12)$.*

	U11	U22	U33	U23	U13	U12
Au(1)	0.0209(1)	0.0242(1)	0.0245(1)	0.0005(1)	-0.0005(1)	-0.0027(1)
Fe(1)	0.0171(4)	0.0255(4)	0.0243(4)	0.0018(4)	-0.0016(3)	0.0008(4)
Fe(2)	0.0174(4)	0.0209(4)	0.0240(4)	0.0027(3)	0.0016(4)	-0.0005(3)
P(1)	0.0222(8)	0.0213(8)	0.0217(8)	0.0003(6)	-0.0003(7)	-0.0017(7)
P(2)	0.0243(9)	0.0200(8)	0.0227(8)	0.0009(6)	-0.0015(7)	-0.0039(6)
Cl(1)	0.0579(19)	0.0417(15)	0.0529(16)	0.000	0.0247(15)	0.000
Cl(2)	0.040(2)	0.053(2)	0.0249(16)	0.0025(15)	-0.0096(15)	0.0090(17)
O(1)	0.062(4)	0.032(3)	0.137(6)	-0.032(4)	0.045(4)	-0.025(3)
O(2)	0.051(5)	0.044(4)	0.045(4)	0.002(4)	0.018(4)	0.021(4)
C(2)	0.033(4)	0.040(4)	0.030(4)	-0.006(3)	0.006(3)	-0.007(3)
O(4)	0.045(3)	0.039(3)	0.050(3)	0.004(3)	-0.002(3)	0.014(3)
O(5)	0.055(4)	0.055(4)	0.046(3)	-0.017(3)	0.005(3)	-0.027(3)
O(6)	0.083(6)	0.139(8)	0.058(4)	0.000(5)	0.008(4)	0.019(5)
C(1)	0.036(4)	0.022(3)	0.036(4)	0.005(3)	0.006(3)	0.002(3)
C(3)	0.020(3)	0.027(3)	0.026(3)	0.002(3)	0.000(3)	0.001(3)
C(4)	0.035(4)	0.040(4)	0.026(3)	0.005(3)	-0.010(3)	-0.007(3)
C(5)	0.039(4)	0.030(4)	0.032(4)	0.000(3)	0.009(3)	-0.006(3)
C(6)	0.021(3)	0.029(3)	0.028(3)	0.000(3)	0.000(3)	0.001(3)
C(11)	0.022(3)	0.022(3)	0.027(3)	0.000(3)	-0.007(3)	0.002(3)
C(12)	0.021(3)	0.027(3)	0.031(3)	0.000(3)	-0.002(3)	-0.004(3)
C(13)	0.018(3)	0.041(4)	0.028(3)	0.009(3)	0.001(3)	0.003(3)
C(14)	0.027(4)	0.040(4)	0.023(3)	-0.004(3)	0.001(3)	0.013(3)
C(15)	0.028(4)	0.024(3)	0.024(3)	0.002(3)	-0.003(3)	0.002(3)
C(21)	0.020(3)	0.037(4)	0.038(4)	-0.001(3)	0.003(3)	0.004(3)
C(22)	0.024(4)	0.031(4)	0.086(6)	0.004(4)	-0.007(4)	0.007(3)
C(23)	0.027(4)	0.073(6)	0.069(6)	0.050(5)	0.004(4)	0.017(4)
C(24)	0.024(4)	0.083(7)	0.034(4)	-0.003(4)	-0.010(3)	0.014(4)
C(25)	0.021(4)	0.051(5)	0.043(4)	-0.006(4)	-0.006(3)	-0.002(3)
C(31)	0.019(3)	0.025(3)	0.024(3)	0.001(3)	0.003(3)	-0.006(3)
C(32)	0.019(3)	0.021(3)	0.033(3)	-0.005(3)	0.005(3)	0.000(3)
C(33)	0.020(3)	0.024(3)	0.037(4)	0.003(3)	0.004(3)	0.004(3)
C(34)	0.012(3)	0.044(4)	0.030(3)	0.005(3)	0.001(3)	-0.002(3)
C(35)	0.021(3)	0.024(3)	0.031(3)	0.002(3)	-0.003(3)	-0.003(3)
C(41)	0.019(3)	0.059(5)	0.036(4)	0.014(4)	0.004(3)	0.008(4)
C(42)	0.032(4)	0.041(4)	0.037(4)	-0.005(3)	0.006(3)	-0.015(3)
C(43)	0.034(4)	0.020(3)	0.064(5)	0.009(3)	0.024(4)	-0.003(3)
C(44)	0.025(4)	0.049(4)	0.030(3)	0.004(3)	0.010(3)	0.002(3)
C(45)	0.024(4)	0.031(4)	0.038(4)	0.002(3)	0.011(3)	0.004(3)

Table A.20: *Hydrogen coordinates and isotropic displacement parameters for 18.*

	x	y	z	U(eq)
H(2A)	0.5833	0.8023	0.7674	0.041
H(2B)	0.6844	0.8651	0.7929	0.041

Table A.20 continued

H(1A)	0.4866	1.1026	0.8167	0.037
H(1B)	0.4674	1.0458	0.8578	0.037
H(3A)	0.6592	0.5211	0.8591	0.029
H(3B)	0.6968	0.7567	0.8667	0.029
H(4A)	0.1589	0.5886	0.7550	0.041
H(4B)	0.0644	0.4474	0.7698	0.041
H(5A)	0.2823	0.1856	0.7559	0.040
H(5B)	0.2773	0.0418	0.7910	0.040
H(6A)	0.1180	0.4298	0.8551	0.031
H(6B)	0.0842	0.2204	0.8340	0.031
H(12)	0.5152	0.3507	0.9049	0.032
H(13)	0.4539	0.4531	0.9671	0.035
H(14)	0.5148	0.8278	0.9793	0.036
H(15)	0.6080	0.9612	0.9242	0.030
H(21)	0.8422	0.5099	0.9134	0.038
H(22)	0.7499	0.1888	0.9385	0.056
H(23)	0.6957	0.2793	1.0022	0.068
H(24)	0.7506	0.6542	1.0150	0.057
H(25)	0.8418	0.7934	0.9611	0.046
H(32)	0.2174	-0.1322	0.8486	0.029
H(33)	0.3304	-0.2357	0.9048	0.032
H(34)	0.3529	0.0888	0.9441	0.034
H(35)	0.2542	0.3896	0.9128	0.030
H(41)	-0.0499	0.1384	0.8937	0.046
H(42)	-0.0008	-0.2448	0.8854	0.044
H(43)	0.1002	-0.3659	0.9428	0.047
H(44)	0.1200	-0.0560	0.9848	0.041
H(45)	0.0263	0.2569	0.9548	0.037

Table A.21: *Atomic coordinates and equivalent isotropic displacement parameters for* ***20****. U(eq) is defined as one third of the trace of the orthogonalised Uij tensor.*

	x	y	z	U(eq)
Ru(1)	0.9852(1)	0.2057(1)	0.6594(1)	0.020(1)
Fe(1)	1.3401(1)	0.2983(1)	0.6837(1)	0.029(1)
P(1)	1.0128(2)	0.2435(1)	0.6849(1)	0.020(1)
Cl(1)	1.1605(2)	0.2014(1)	0.7652(1)	0.034(1)
Cl(2)	1.1357(2)	0.2093(1)	0.5516(1)	0.033(1)
C(1)	1.1766(6)	0.2537(1)	0.6850(4)	0.021(1)
C(2)	0.8266(10)	0.1990(2)	0.4644(5)	0.066(3)
C(3)	0.8823(7)	0.1804(1)	0.8365(5)	0.035(2)
C(4)	0.8396(10)	0.1982(2)	0.8950(5)	0.057(3)
C(5)	0.8172(10)	0.1588(2)	0.8540(6)	0.056(3)
C(11)	1.1845(6)	0.2781(1)	0.6779(4)	0.025(1)
C(12)	1.1912(7)	0.2895(1)	0.5972(5)	0.036(2)
C(13)	1.1906(8)	0.3124(2)	0.6154(7)	0.050(2)
C(14)	1.1808(8)	0.3150(2)	0.7047(7)	0.052(2)
C(15)	1.1772(7)	0.2940(1)	0.7437(6)	0.041(2)
C(21)	1.4900(10)	0.2859(3)	0.7523(11)	0.085(5)
C(22)	1.5020(10)	0.2823(3)	0.6680(16)	0.113(7)

Table A.21 continued

C(23)	1.5016(10)	0.3026(4)	0.6269(7)	0.116(8)
C(24)	1.4936(9)	0.3178(2)	0.6902(11)	0.085(5)
C(25)	1.4883(9)	0.3074(3)	0.7651(7)	0.073(4)
C(31)	0.9311(6)	0.2611(1)	0.6042(4)	0.025(1)
C(32)	0.8832(7)	0.2818(1)	0.6229(5)	0.032(2)
C(33)	0.8307(8)	0.2949(1)	0.5573(6)	0.045(2)
C(34)	0.8282(9)	0.2883(2)	0.4729(6)	0.053(2)
C(35)	0.8783(9)	0.2683(2)	0.4530(5)	0.048(2)
C(36)	0.9283(8)	0.2545(1)	0.5185(5)	0.036(2)
C(41)	0.9608(6)	0.2517(1)	0.7890(4)	0.023(1)
C(42)	0.8350(7)	0.2573(1)	0.7994(5)	0.034(2)
C(43)	0.7971(8)	0.2620(2)	0.8804(6)	0.047(2)
C(44)	0.8820(9)	0.2611(2)	0.9526(6)	0.049(2)
C(45)	1.0043(9)	0.2553(2)	0.9434(5)	0.047(2)
C(46)	1.0433(7)	0.2505(1)	0.8620(5)	0.032(2)
C(51)	0.8386(7)	0.1948(2)	0.5594(5)	0.038(2)
C(52)	0.9063(8)	0.1759(1)	0.5930(5)	0.040(2)
C(53)	0.9185(7)	0.1716(1)	0.6804(5)	0.030(2)
C(54)	0.8655(6)	0.1857(1)	0.7412(5)	0.026(2)
C(55)	0.7987(6)	0.2042(1)	0.7087(4)	0.024(1)
C(56)	0.7855(6)	0.2088(1)	0.6191(5)	0.032(2)
Ru(1)'	0.6216(1)	0.0407(1)	0.9813(1)	0.021(1)
Fe(1)'	0.3006(1)	0.1358(1)	0.9736(1)	0.025(1)
P(1)'	0.6111(2)	0.0790(1)	0.9648(1)	0.020(1)
Cl(1)'	0.4415(2)	0.0404(1)	0.8771(1)	0.032(1)
Cl(2)'	0.4795(2)	0.0449(1)	1.0938(1)	0.034(1)
C(1)'	0.4518(6)	0.0908(1)	0.9630(5)	0.027(2)
C(2)'	0.8101(11)	0.0344(2)	1.1674(6)	0.062(3)
C(3)'	0.6834(9)	0.0111(2)	0.8019(5)	0.046(2)
C(4)'	0.7004(13)	0.0288(2)	0.7365(6)	0.077(4)
C(5)'	0.7599(11)	-0.0093(2)	0.7836(7)	0.066(3)
C(11)'	0.4510(6)	0.1149(1)	0.9810(4)	0.021(1)
C(12)'	0.4342(6)	0.1244(1)	1.0616(4)	0.027(2)
C(13)'	0.4452(7)	0.1473(1)	1.0559(5)	0.033(2)
C(14)'	0.4675(7)	0.1525(1)	0.9700(5)	0.034(2)
C(15)'	0.4706(6)	0.1325(1)	0.9237(5)	0.029(2)
C(21)'	0.1551(7)	0.1228(1)	0.8960(5)	0.040(2)
C(22)'	0.1331(8)	0.1206(2)	0.9837(7)	0.058(3)
C(23)'	0.1296(8)	0.1418(2)	1.0192(6)	0.067(3)
C(24)'	0.1507(8)	0.1569(2)	0.9547(7)	0.055(3)
C(25)'	0.1660(7)	0.1453(2)	0.8795(6)	0.043(2)
C(31)'	0.6965(6)	0.0952(1)	1.0490(5)	0.024(1)
C(32)'	0.7525(7)	0.1154(1)	1.0325(5)	0.033(2)
C(33)'	0.8037(7)	0.1280(1)	1.1003(6)	0.040(2)
C(34)'	0.7999(7)	0.1213(1)	1.1848(6)	0.041(2)
C(35)'	0.7437(8)	0.1017(1)	1.2015(5)	0.039(2)
C(36)'	0.6919(7)	0.0886(1)	1.1346(5)	0.030(2)
C(41)'	0.6726(6)	0.0872(1)	0.8634(4)	0.025(1)
C(42)'	0.8022(7)	0.0905(1)	0.8581(5)	0.032(2)
C(43)'	0.8480(8)	0.0947(2)	0.7790(6)	0.045(2)
C(44)'	0.7691(9)	0.0957(2)	0.7045(6)	0.052(2)
C(45)'	0.6413(8)	0.0922(2)	0.7099(5)	0.045(2)
C(46)'	0.5932(7)	0.0881(1)	0.7877(5)	0.033(2)
C(51)'	0.7782(7)	0.0293(1)	1.0731(5)	0.035(2)
C(52)'	0.6993(7)	0.0111(1)	1.0482(5)	0.034(2)
C(53)'	0.6700(6)	0.0054(1)	0.9623(5)	0.029(2)
C(54)'	0.7174(7)	0.0182(1)	0.8943(5)	0.030(2)

Table A.21 continued

C(55)'	0.7955(7)	0.0360(1)	0.9175(5)	0.031(2)
C(56)'	0.8244(7)	0.0418(1)	1.0056(5)	0.036(2)
Ru(1)"	0.1612(1)	0.1251(1)	0.4984(1)	0.020(1)
Fe(1)"	-0.2552(1)	0.0421(1)	0.4452(1)	0.033(1)
P(1)"	0.1103(2)	0.0887(1)	0.4599(1)	0.021(1)
Cl(1)"	0.0211(2)	0.1211(1)	0.6119(1)	0.034(1)
Cl(2)"	-0.0181(2)	0.1349(1)	0.4016(1)	0.033(1)
C(1)"	-0.0586(6)	0.0819(1)	0.4616(5)	0.027(2)
C(2)"	0.3383(9)	0.1239(2)	0.6878(5)	0.055(3)
C(3)"	0.2617(8)	0.1537(1)	0.3285(5)	0.039(2)
C(4)"	0.2782(11)	0.1367(2)	0.2602(5)	0.060(3)
C(5)"	0.3494(11)	0.1734(2)	0.3164(7)	0.071(3)
C(11)"	-0.0845(6)	0.0578(1)	0.4601(4)	0.028(2)
C(12)"	-0.0904(6)	0.0437(1)	0.3866(5)	0.034(2)
C(13)"	-0.1114(7)	0.0218(1)	0.4162(6)	0.046(2)
C(14)"	-0.1201(8)	0.0227(2)	0.5053(6)	0.049(2)
C(15)"	-0.1022(7)	0.0444(1)	0.5331(5)	0.035(2)
C(21)"	-0.3908(8)	0.0655(2)	0.4327(8)	0.061(3)
C(22)"	-0.3980(9)	0.0518(2)	0.3589(7)	0.066(3)
C(23)"	-0.4184(8)	0.0304(2)	0.3870(8)	0.067(3)
C(24)"	-0.4261(8)	0.0309(2)	0.4754(7)	0.057(3)
C(25)"	-0.4091(8)	0.0522(2)	0.5038(7)	0.057(3)
C(31)"	0.1861(6)	0.0677(1)	0.5296(4)	0.026(2)
C(32)"	0.2158(7)	0.0468(1)	0.5004(5)	0.032(2)
C(33)"	0.2699(7)	0.0314(1)	0.5577(6)	0.041(2)
C(34)"	0.2935(9)	0.0367(2)	0.6448(6)	0.051(2)
C(35)"	0.2616(10)	0.0570(2)	0.6746(6)	0.056(3)
C(36)"	0.2080(8)	0.0725(1)	0.6173(5)	0.041(2)
C(41)"	0.1508(6)	0.0822(1)	0.3511(4)	0.023(1)
C(42)"	0.2709(7)	0.0751(1)	0.3345(5)	0.029(2)
C(43)"	0.3021(8)	0.0716(1)	0.2508(5)	0.038(2)
C(44)"	0.2149(8)	0.0755(1)	0.1822(5)	0.039(2)
C(45)"	0.0965(8)	0.0829(1)	0.1969(5)	0.038(2)
C(46)"	0.0636(7)	0.0861(1)	0.2800(4)	0.030(2)
C(51)"	0.3185(7)	0.1307(1)	0.5947(5)	0.035(2)
C(56)"	0.2644(7)	0.1516(1)	0.5743(5)	0.037(2)
C(55)"	0.2466(7)	0.1586(1)	0.4895(5)	0.031(2)
C(54)"	0.2845(6)	0.1451(1)	0.4202(5)	0.026(2)
C(53)"	0.3424(6)	0.1249(1)	0.4404(4)	0.023(1)
C(52)"	0.3588(6)	0.1177(1)	0.5279(5)	0.030(2)
Cl(3)	0.1102(3)	0.0653(1)	0.9331(3)	0.084(1)
Cl(4)	0.0897(3)	0.0241(1)	0.8437(3)	0.107(1)
C(6)	0.1420(9)	0.0377(2)	0.9437(8)	0.071(3)
Cl(3)'	0.4888(3)	0.2242(1)	0.6992(3)	0.090(1)
Cl(4)'	0.4921(3)	0.1785(1)	0.7476(3)	0.094(1)
C(6)'	0.4422(9)	0.1977(2)	0.6696(7)	0.061(3)
Cl(3)"	0.6436(3)	0.1320(1)	0.3913(3)	0.116(2)
Cl(4)"	0.6241(3)	0.1496(1)	0.5658(4)	0.144(2)
C(6)"	0.6974(12)	0.1326(3)	0.4996(9)	0.112(6)

Table A.22: *Bond lengths (Å) and angles (°) for* ***20****.*

Ru(1)-C(56)	2.179(7)	C(51)-C(56)-Ru(1)	72.7(4)
Ru(1)-C(55)	2.187(6)	C(55)-C(56)-Ru(1)	71.4(4)
Ru(1)-C(51)	2.216(7)	C(56)'-Ru(1)'-C(55)'	38.1(3)
Ru(1)-C(52)	2.221(8)	C(56)'-Ru(1)'-C(52)'	67.1(3)
Ru(1)-C(53)	2.230(7)	C(55)'-Ru(1)'-C(52)'	78.8(3)
Ru(1)-C(54)	2.232(6)	C(56)'-Ru(1)'-C(51)'	37.6(3)
Ru(1)-P(1)	2.3507(18)	C(55)'-Ru(1)'-C(51)'	68.2(3)
Ru(1)-Cl(1)	2.4031(18)	C(52)'-Ru(1)'-C(51)'	37.6(3)
Ru(1)-Cl(2)	2.4182(17)	C(56)'-Ru(1)'-C(54)'	68.0(3)
Fe(1)-C(21)	1.998(10)	C(55)'-Ru(1)'-C(54)'	36.8(3)
Fe(1)-C(23)	2.013(10)	C(52)'-Ru(1)'-C(54)'	67.0(3)
Fe(1)-C(22)	2.013(11)	C(51)'-Ru(1)'-C(54)'	80.7(3)
Fe(1)-C(24)	2.019(10)	C(56)'-Ru(1)'-C(53)'	79.3(3)
Fe(1)-C(25)	2.020(10)	C(55)'-Ru(1)'-C(53)'	66.5(3)
Fe(1)-C(14)	2.029(9)	C(52)'-Ru(1)'-C(53)'	36.4(3)
Fe(1)-C(13)	2.034(9)	C(51)'-Ru(1)'-C(53)'	67.3(3)
Fe(1)-C(15)	2.050(8)	C(54)'-Ru(1)'-C(53)'	37.5(3)
Fe(1)-C(11)	2.062(7)	C(56)'-Ru(1)'-P(1)'	91.6(2)
Fe(1)-C(12)	2.067(8)	C(55)'-Ru(1)'-P(1)'	96.72(19)
P(1)-C(41)	1.820(7)	C(52)'-Ru(1)'-P(1)'	151.1(2)
P(1)-C(31)	1.820(7)	C(51)'-Ru(1)'-P(1)'	114.1(2)
P(1)-C(1)	1.854(6)	C(54)'-Ru(1)'-P(1)'	124.5(2)
C(1)-C(11)	1.492(9)	C(53)'-Ru(1)'-P(1)'	161.86(19)
C(2)-C(51)	1.494(11)	C(56)'-Ru(1)'-Cl(1)'	148.0(2)
C(3)-C(4)	1.506(12)	C(55)'-Ru(1)'-Cl(1)'	110.6(2)
C(3)-C(54)	1.512(10)	C(52)'-Ru(1)'-Cl(1)'	123.8(2)
C(3)-C(5)	1.525(11)	C(51)'-Ru(1)'-Cl(1)'	161.2(2)
C(11)-C(15)	1.414(10)	C(54)'-Ru(1)'-Cl(1)'	88.0(2)
C(11)-C(12)	1.441(10)	C(53)'-Ru(1)'-Cl(1)'	94.7(2)
C(12)-C(13)	1.425(12)	P(1)'-Ru(1)'-Cl(1)'	84.67(6)
C(13)-C(14)	1.408(14)	C(56)'-Ru(1)'-Cl(2)'	123.1(2)
C(14)-C(15)	1.422(13)	C(55)'-Ru(1)'-Cl(2)'	160.7(2)
C(21)-C(25)	1.325(18)	C(52)'-Ru(1)'-Cl(2)'	88.8(2)
C(21)-C(22)	1.34(2)	C(51)'-Ru(1)'-Cl(2)'	92.9(2)
C(22)-C(23)	1.39(2)	C(54)'-Ru(1)'-Cl(2)'	147.9(2)
C(23)-C(24)	1.36(2)	C(53)'-Ru(1)'-Cl(2)'	111.18(19)
C(24)-C(25)	1.332(17)	P(1)'-Ru(1)'-Cl(2)'	86.95(6)
C(31)-C(36)	1.388(10)	Cl(1)'-Ru(1)'-Cl(2)'	88.56(7)
C(31)-C(32)	1.400(10)	C(12)'-Fe(1)'-C(22)'	111.5(3)
C(32)-C(33)	1.378(10)	C(12)'-Fe(1)'-C(15)'	67.8(3)
C(33)-C(34)	1.369(13)	C(22)'-Fe(1)'-C(15)'	143.0(4)
C(34)-C(35)	1.380(13)	C(12)'-Fe(1)'-C(23)'	115.4(4)
C(35)-C(36)	1.391(11)	C(22)'-Fe(1)'-C(23)'	40.5(4)
C(41)-C(46)	1.381(10)	C(15)'-Fe(1)'-C(23)'	175.1(5)
C(41)-C(42)	1.404(9)	C(12)'-Fe(1)'-C(13)'	40.4(3)
C(42)-C(43)	1.381(11)	C(22)'-Fe(1)'-C(13)'	137.0(4)
C(43)-C(44)	1.385(13)	C(15)'-Fe(1)'-C(13)'	67.8(3)
C(44)-C(45)	1.369(12)	C(23)'-Fe(1)'-C(13)'	111.8(4)
C(45)-C(46)	1.391(11)	C(12)'-Fe(1)'-C(11)'	40.4(3)
C(51)-C(56)	1.410(11)	C(22)'-Fe(1)'-C(11)'	113.5(3)
C(51)-C(52)	1.436(12)	C(15)'-Fe(1)'-C(11)'	40.8(3)
C(52)-C(53)	1.378(11)	C(23)'-Fe(1)'-C(11)'	144.0(4)
C(53)-C(54)	1.425(10)	C(13)'-Fe(1)'-C(11)'	68.2(3)
C(54)-C(55)	1.407(10)	C(12)'-Fe(1)'-C(21)'	136.5(3)

Table A.22 continued

C(55)-C(56)	1.417(10)	C(22)'-Fe(1)'-C(21)'	40.4(4)
Ru(1)'-C(56)'	2.165(7)	C(15)'-Fe(1)'-C(21)'	113.2(3)
Ru(1)'-C(55)'	2.189(7)	C(23)'-Fe(1)'-C(21)'	67.5(4)
Ru(1)'-C(52)'	2.213(8)	C(13)'-Fe(1)'-C(21)'	176.6(3)
Ru(1)'-C(51)'	2.219(7)	C(11)'-Fe(1)'-C(21)'	110.2(3)
Ru(1)'-C(54)'	2.231(7)	C(12)'-Fe(1)'-C(25)'	175.8(3)
Ru(1)'-C(53)'	2.239(7)	C(22)'-Fe(1)'-C(25)'	67.3(4)
Ru(1)'-P(1)'	2.3483(18)	C(15)'-Fe(1)'-C(25)'	110.5(3)
Ru(1)'-Cl(1)'	2.4109(18)	C(23)'-Fe(1)'-C(25)'	66.6(4)
Ru(1)'-Cl(2)'	2.4137(17)	C(13)'-Fe(1)'-C(25)'	143.2(3)
Fe(1)'-C(12)'	2.019(7)	C(11)'-Fe(1)'-C(25)'	135.9(3)
Fe(1)'-C(22)'	2.030(9)	C(21)'-Fe(1)'-C(25)'	40.0(3)
Fe(1)'-C(15)'	2.036(7)	C(12)'-Fe(1)'-C(24)'	144.4(4)
Fe(1)'-C(23)'	2.039(8)	C(22)'-Fe(1)'-C(24)'	67.6(4)
Fe(1)'-C(13)'	2.045(7)	C(15)'-Fe(1)'-C(24)'	135.6(4)
Fe(1)'-C(11)'	2.046(6)	C(23)'-Fe(1)'-C(24)'	39.7(4)
Fe(1)'-C(21)'	2.047(8)	C(13)'-Fe(1)'-C(24)'	114.6(3)
Fe(1)'-C(25)'	2.048(8)	C(11)'-Fe(1)'-C(24)'	175.0(4)
Fe(1)'-C(24)'	2.051(8)	C(21)'-Fe(1)'-C(24)'	67.2(3)
Fe(1)'-C(14)'	2.053(7)	C(25)'-Fe(1)'-C(24)'	39.5(4)
P(1)'-C(41)'	1.823(7)	C(12)'-Fe(1)'-C(14)'	67.9(3)
P(1)'-C(31)'	1.824(7)	C(22)'-Fe(1)'-C(14)'	176.3(4)
P(1)'-C(1)'	1.843(7)	C(15)'-Fe(1)'-C(14)'	40.5(3)
C(1)'-C(11)'	1.493(9)	C(23)'-Fe(1)'-C(14)'	136.1(4)
C(2)'-C(51)'	1.510(11)	C(13)'-Fe(1)'-C(14)'	40.2(3)
C(3)'-C(4)'	1.502(13)	C(11)'-Fe(1)'-C(14)'	68.6(3)
C(3)'-C(54)'	1.515(11)	C(21)'-Fe(1)'-C(14)'	142.5(3)
C(3)'-C(5)'	1.526(12)	C(25)'-Fe(1)'-C(14)'	113.6(3)
C(11)'-C(12)'	1.403(9)	C(24)'-Fe(1)'-C(14)'	110.7(4)
C(11)'-C(15)'	1.423(9)	C(41)'-P(1)'-C(31)'	106.1(3)
C(12)'-C(13)'	1.404(10)	C(41)'-P(1)'-C(1)'	105.8(3)
C(13)'-C(14)'	1.409(11)	C(31)'-P(1)'-C(1)'	101.9(3)
C(14)'-C(15)'	1.417(10)	C(41)'-P(1)'-Ru(1)'	110.6(2)
C(21)'-C(25)'	1.402(12)	C(31)'-P(1)'-Ru(1)'	116.3(2)
C(21)'-C(22)'	1.407(13)	C(1)'-P(1)'-Ru(1)'	115.2(2)
C(22)'-C(23)'	1.409(15)	C(11)'-C(1)'-P(1)'	113.6(5)
C(23)'-C(24)'	1.389(15)	C(4)'-C(3)'-C(54)'	113.8(8)
C(24)'-C(25)'	1.384(13)	C(4)'-C(3)'-C(5)'	111.4(8)
C(31)'-C(36)'	1.392(10)	C(54)'-C(3)'-C(5)'	108.5(8)
C(31)'-C(32)'	1.402(10)	C(12)'-C(11)'-C(15)'	106.3(6)
C(32)'-C(33)'	1.379(11)	C(12)'-C(11)'-C(1)'	125.1(6)
C(33)'-C(34)'	1.378(12)	C(15)'-C(11)'-C(1)'	128.5(6)
C(34)'-C(35)'	1.373(12)	C(12)'-C(11)'-Fe(1)'	68.8(4)
C(35)'-C(36)'	1.388(11)	C(15)'-C(11)'-Fe(1)'	69.2(4)
C(41)'-C(46)'	1.393(10)	C(1)'-C(11)'-Fe(1)'	128.2(5)
C(41)'-C(42)'	1.404(9)	C(11)'-C(12)'-C(13)'	109.7(6)
C(42)'-C(43)'	1.380(10)	C(11)'-C(12)'-Fe(1)'	70.9(4)
C(43)'-C(44)'	1.377(13)	C(13)'-C(12)'-Fe(1)'	70.8(4)
C(44)'-C(45)'	1.388(12)	C(12)'-C(13)'-C(14)'	107.8(7)
C(45)'-C(46)'	1.372(10)	C(12)'-C(13)'-Fe(1)'	68.8(4)
C(51)'-C(56)'	1.415(11)	C(14)'-C(13)'-Fe(1)'	70.2(4)
C(51)'-C(52)'	1.428(11)	C(13)'-C(14)'-C(15)'	107.3(7)
C(52)'-C(53)'	1.389(11)	C(13)'-C(14)'-Fe(1)'	69.6(4)
C(53)'-C(54)'	1.436(10)	C(15)'-C(14)'-Fe(1)'	69.1(4)
C(54)'-C(55)'	1.398(10)	C(14)'-C(15)'-C(11)'	108.8(6)
C(55)'-C(56)'	1.423(11)	C(14)'-C(15)'-Fe(1)'	70.4(4)
Ru(1)"-C(52)"	2.168(7)	C(11)'-C(15)'-Fe(1)'	70.0(4)

Table A.22 continued

Ru(1)"-C(51)"	2.182(7)	C(25)'-C(21)'-C(22)'	107.1(8)
Ru(1)"-C(53)"	2.193(6)	C(25)'-C(21)'-Fe(1)'	70.0(5)
Ru(1)"-C(54)"	2.222(6)	C(22)'-C(21)'-Fe(1)'	69.1(5)
Ru(1)"-C(56)"	2.234(7)	C(21)'-C(22)'-C(23)'	107.5(9)
Ru(1)"-C(55)"	2.242(7)	C(21)'-C(22)'-Fe(1)'	70.5(5)
Ru(1)"-P(1)"	2.3494(18)	C(23)'-C(22)'-Fe(1)'	70.1(6)
Ru(1)"-Cl(2)"	2.4112(18)	C(24)'-C(23)'-C(22)'	108.3(8)
Ru(1)"-Cl(1)"	2.4113(17)	C(24)'-C(23)'-Fe(1)'	70.6(5)
Fe(1)"-C(23)"	2.026(9)	C(22)'-C(23)'-Fe(1)'	69.4(5)
Fe(1)"-C(21)"	2.028(9)	C(25)'-C(24)'-C(23)'	108.0(9)
Fe(1)"-C(14)"	2.033(8)	C(25)'-C(24)'-Fe(1)'	70.2(5)
Fe(1)"-C(25)"	2.033(9)	C(23)'-C(24)'-Fe(1)'	69.7(5)
Fe(1)"-C(22)"	2.034(10)	C(24)'-C(25)'-C(21)'	109.0(8)
Fe(1)"-C(24)"	2.035(8)	C(24)'-C(25)'-Fe(1)'	70.4(5)
Fe(1)"-C(12)"	2.043(7)	C(21)'-C(25)'-Fe(1)'	69.9(5)
Fe(1)"-C(15)"	2.046(7)	C(36)'-C(31)'-C(32)'	118.3(7)
Fe(1)"-C(13)"	2.048(9)	C(36)'-C(31)'-P(1)'	118.4(5)
Fe(1)"-C(11)"	2.052(7)	C(32)'-C(31)'-P(1)'	122.7(6)
P(1)"-C(41)"	1.821(7)	C(33)'-C(32)'-C(31)'	119.9(7)
P(1)"-C(31)"	1.827(7)	C(34)'-C(33)'-C(32)'	121.5(8)
P(1)"-C(1)"	1.850(7)	C(35)'-C(34)'-C(33)'	119.0(7)
C(1)"-C(11)"	1.493(10)	C(34)'-C(35)'-C(36)'	120.8(8)
C(2)"-C(51)"	1.504(11)	C(35)'-C(36)'-C(31)'	120.6(7)
C(3)"-C(4)"	1.502(13)	C(46)'-C(41)'-C(42)'	118.7(6)
C(3)"-C(54)"	1.518(10)	C(46)'-C(41)'-P(1)'	120.2(5)
C(3)"-C(5)"	1.545(12)	C(42)'-C(41)'-P(1)'	120.8(5)
C(11)"-C(15)"	1.424(10)	C(43)'-C(42)'-C(41)'	119.8(7)
C(11)"-C(12)"	1.428(10)	C(44)'-C(43)'-C(42)'	121.4(8)
C(12)"-C(13)"	1.434(12)	C(43)'-C(44)'-C(45)'	118.7(7)
C(13)"-C(14)"	1.395(13)	C(46)'-C(45)'-C(44)'	121.1(8)
C(14)"-C(15)"	1.397(12)	C(45)'-C(46)'-C(41)'	120.4(7)
C(21)"-C(25)"	1.396(14)	C(56)'-C(51)'-C(52)'	116.7(7)
C(21)"-C(22)"	1.415(15)	C(56)'-C(51)'-C(2)'	122.9(8)
C(22)"-C(23)"	1.400(16)	C(52)'-C(51)'-C(2)'	120.4(8)
C(23)"-C(24)"	1.382(15)	C(56)'-C(51)'-Ru(1)'	69.1(4)
C(24)"-C(25)"	1.381(14)	C(52)'-C(51)'-Ru(1)'	71.0(4)
C(31)"-C(32)"	1.391(10)	C(2)'-C(51)'-Ru(1)'	131.2(6)
C(31)"-C(36)"	1.397(10)	C(53)'-C(52)'-C(51)'	122.4(7)
C(32)"-C(33)"	1.388(11)	C(53)'-C(52)'-Ru(1)'	72.8(4)
C(33)"-C(34)"	1.394(13)	C(51)'-C(52)'-Ru(1)'	71.4(4)
C(34)"-C(35)"	1.371(13)	C(52)'-C(53)'-C(54)'	120.4(7)
C(35)"-C(36)"	1.391(12)	C(52)'-C(53)'-Ru(1)'	70.8(4)
C(41)"-C(42)"	1.397(9)	C(54)'-C(53)'-Ru(1)'	70.9(4)
C(41)"-C(46)"	1.405(10)	C(55)'-C(54)'-C(53)'	117.9(7)
C(42)"-C(43)"	1.383(10)	C(55)'-C(54)'-C(3)'	123.9(7)
C(43)"-C(44)"	1.378(11)	C(53)'-C(54)'-C(3)'	118.1(7)
C(44)"-C(45)"	1.375(11)	C(55)'-C(54)'-Ru(1)'	69.9(4)
C(45)"-C(46)"	1.378(10)	C(53)'-C(54)'-Ru(1)'	71.6(4)
C(51)"-C(52)"	1.401(11)	C(3)'-C(54)'-Ru(1)'	131.5(5)
C(51)"-C(56)"	1.420(12)	C(54)'-C(55)'-C(56)'	121.3(7)
C(56)"-C(55)"	1.384(11)	C(54)'-C(55)'-Ru(1)'	73.2(4)
C(55)"-C(54)"	1.436(10)	C(56)'-C(55)'-Ru(1)'	70.0(4)
C(54)"-C(53)"	1.405(10)	C(51)'-C(56)'-C(55)'	121.2(7)
C(53)"-C(52)"	1.425(10)	C(51)'-C(56)'-Ru(1)'	73.3(4)
Cl(3)-C(6)	1.721(11)	C(55)'-C(56)'-Ru(1)'	71.8(4)
Cl(4)-C(6)	1.809(13)	C(52)"-Ru(1)"-C(51)"	37.6(3)
Cl(3)'-C(6)'	1.740(11)	C(52)"-Ru(1)"-C(53)"	38.1(3)

Table A.22 continued

Cl(4)'-C(6)'	1.740(11)	C(51)"-Ru(1)"-C(53)"	68.2(3)
Cl(3)"-C(6)"	1.734(14)	C(52)"-Ru(1)"-C(54)"	68.0(3)
Cl(4)"-C(6)"	1.691(14)	C(51)"-Ru(1)"-C(54)"	80.4(3)
C(56)-Ru(1)-C(55)	37.9(3)	C(53)"-Ru(1)"-C(54)"	37.1(2)
C(56)-Ru(1)-C(51)	37.4(3)	C(52)"-Ru(1)"-C(56)"	67.1(3)
C(55)-Ru(1)-C(51)	67.8(3)	C(51)"-Ru(1)"-C(56)"	37.5(3)
C(56)-Ru(1)-C(52)	67.2(3)	C(53)"-Ru(1)"-C(56)"	79.0(3)
C(55)-Ru(1)-C(52)	78.8(3)	C(54)"-Ru(1)"-C(56)"	66.7(3)
C(51)-Ru(1)-C(52)	37.8(3)	C(52)"-Ru(1)"-C(55)"	79.2(3)
C(56)-Ru(1)-C(53)	79.0(3)	C(51)"-Ru(1)"-C(55)"	66.8(3)
C(55)-Ru(1)-C(53)	66.5(3)	C(53)"-Ru(1)"-C(55)"	66.8(3)
C(51)-Ru(1)-C(53)	66.9(3)	C(54)"-Ru(1)"-C(55)"	37.5(3)
C(52)-Ru(1)-C(53)	36.1(3)	C(56)"-Ru(1)"-C(55)"	36.0(3)
C(56)-Ru(1)-C(54)	67.8(3)	C(52)"-Ru(1)"-P(1)"	93.2(2)
C(55)-Ru(1)-C(54)	37.1(2)	C(51)"-Ru(1)"-P(1)"	118.1(2)
C(51)-Ru(1)-C(54)	80.3(3)	C(53)"-Ru(1)"-P(1)"	94.70(18)
C(52)-Ru(1)-C(54)	66.7(3)	C(54)"-Ru(1)"-P(1)"	120.91(19)
C(53)-Ru(1)-C(54)	37.2(3)	C(56)"-Ru(1)"-P(1)"	155.4(2)
C(56)-Ru(1)-P(1)	94.0(2)	C(55)"-Ru(1)"-P(1)"	158.42(19)
C(55)-Ru(1)-P(1)	95.02(19)	C(52)"-Ru(1)"-Cl(2)"	153.2(2)
C(51)-Ru(1)-P(1)	118.9(2)	C(51)"-Ru(1)"-Cl(2)"	156.4(2)
C(52)-Ru(1)-P(1)	156.5(2)	C(53)"-Ru(1)"-Cl(2)"	115.17(18)
C(53)-Ru(1)-P(1)	157.80(19)	C(54)"-Ru(1)"-Cl(2)"	89.81(19)
C(54)-Ru(1)-P(1)	120.62(19)	C(56)"-Ru(1)"-Cl(2)"	118.9(2)
C(56)-Ru(1)-Cl(1)	153.5(2)	C(55)"-Ru(1)"-Cl(2)"	92.4(2)
C(55)-Ru(1)-Cl(1)	115.77(18)	P(1)"-Ru(1)"-Cl(2)"	85.35(6)
C(51)-Ru(1)-Cl(1)	156.0(2)	C(52)"-Ru(1)"-Cl(1)"	118.1(2)
C(52)-Ru(1)-Cl(1)	118.2(2)	C(51)"-Ru(1)"-Cl(1)"	90.1(2)
C(53)-Ru(1)-Cl(1)	92.1(2)	C(53)"-Ru(1)"-Cl(1)"	156.23(18)
C(54)-Ru(1)-Cl(1)	89.92(18)	C(54)"-Ru(1)"-Cl(1)"	152.01(19)
P(1)-Ru(1)-Cl(1)	84.99(6)	C(56)"-Ru(1)"-Cl(1)"	89.79(19)
C(56)-Ru(1)-Cl(2)	118.6(2)	C(55)"-Ru(1)"-Cl(1)"	114.63(19)
C(55)-Ru(1)-Cl(2)	156.45(18)	P(1)"-Ru(1)"-Cl(1)"	86.81(6)
C(51)-Ru(1)-Cl(2)	90.6(2)	Cl(2)"-Ru(1)"-Cl(1)"	88.60(7)
C(52)-Ru(1)-Cl(2)	90.0(2)	C(23)"-Fe(1)"-C(21)"	68.0(4)
C(53)-Ru(1)-Cl(2)	114.95(19)	C(23)"-Fe(1)"-C(14)"	123.4(5)
C(54)-Ru(1)-Cl(2)	152.00(19)	C(21)"-Fe(1)"-C(14)"	157.9(5)
P(1)-Ru(1)-Cl(2)	86.97(6)	C(23)"-Fe(1)"-C(25)"	67.2(4)
Cl(1)-Ru(1)-Cl(2)	87.78(7)	C(21)"-Fe(1)"-C(25)"	40.2(4)
C(21)-Fe(1)-C(23)	66.9(5)	C(14)"-Fe(1)"-C(25)"	122.6(4)
C(21)-Fe(1)-C(22)	39.1(6)	C(23)"-Fe(1)"-C(22)"	40.3(5)
C(23)-Fe(1)-C(22)	40.5(7)	C(21)"-Fe(1)"-C(22)"	40.8(4)
C(21)-Fe(1)-C(24)	65.5(5)	C(14)"-Fe(1)"-C(22)"	159.6(5)
C(23)-Fe(1)-C(24)	39.4(6)	C(25)"-Fe(1)"-C(22)"	67.6(4)
C(22)-Fe(1)-C(24)	66.0(5)	C(23)"-Fe(1)"-C(24)"	39.8(4)
C(21)-Fe(1)-C(25)	38.5(5)	C(21)"-Fe(1)"-C(24)"	67.4(4)
C(23)-Fe(1)-C(25)	65.5(5)	C(14)"-Fe(1)"-C(24)"	108.2(4)
C(22)-Fe(1)-C(25)	64.8(5)	C(25)"-Fe(1)"-C(24)"	39.7(4)
C(24)-Fe(1)-C(25)	38.5(5)	C(22)"-Fe(1)"-C(24)"	67.2(4)
C(21)-Fe(1)-C(14)	138.5(6)	C(23)"-Fe(1)"-C(12)"	123.7(4)
C(23)-Fe(1)-C(14)	139.4(8)	C(21)"-Fe(1)"-C(12)"	123.8(4)
C(22)-Fe(1)-C(14)	177.3(6)	C(14)"-Fe(1)"-C(12)"	68.2(4)
C(24)-Fe(1)-C(14)	112.4(5)	C(25)"-Fe(1)"-C(12)"	159.7(4)
C(25)-Fe(1)-C(14)	112.6(5)	C(22)"-Fe(1)"-C(12)"	108.5(4)
C(21)-Fe(1)-C(13)	177.2(6)	C(24)"-Fe(1)"-C(12)"	159.1(4)
C(23)-Fe(1)-C(13)	112.2(5)	C(23)"-Fe(1)"-C(15)"	158.7(4)
C(22)-Fe(1)-C(13)	141.7(8)	C(21)"-Fe(1)"-C(15)"	122.8(4)

Table A.22 continued

C(24)-Fe(1)-C(13)	112.0(4)	C(14)"-Fe(1)"-C(15)"	40.0(3)
C(25)-Fe(1)-C(13)	138.7(5)	C(25)"-Fe(1)"-C(15)"	108.0(4)
C(14)-Fe(1)-C(13)	40.5(4)	C(22)"-Fe(1)"-C(15)"	159.3(5)
C(21)-Fe(1)-C(15)	112.3(5)	C(24)"-Fe(1)"-C(15)"	123.3(4)
C(23)-Fe(1)-C(15)	179.0(5)	C(12)"-Fe(1)"-C(15)"	68.1(3)
C(22)-Fe(1)-C(15)	139.2(7)	C(23)"-Fe(1)"-C(13)"	108.6(4)
C(24)-Fe(1)-C(15)	139.9(6)	C(21)"-Fe(1)"-C(13)"	160.7(4)
C(25)-Fe(1)-C(15)	113.5(4)	C(14)"-Fe(1)"-C(13)"	40.0(4)
C(14)-Fe(1)-C(15)	40.8(4)	C(25)"-Fe(1)"-C(13)"	157.8(4)
C(13)-Fe(1)-C(15)	68.6(4)	C(22)"-Fe(1)"-C(13)"	124.4(4)
C(21)-Fe(1)-C(11)	113.8(4)	C(24)"-Fe(1)"-C(13)"	123.1(4)
C(23)-Fe(1)-C(11)	140.5(7)	C(12)"-Fe(1)"-C(13)"	41.0(3)
C(22)-Fe(1)-C(11)	113.5(5)	C(15)"-Fe(1)"-C(13)"	67.4(3)
C(24)-Fe(1)-C(11)	179.3(4)	C(23)"-Fe(1)"-C(11)"	159.5(4)
C(25)-Fe(1)-C(11)	141.0(4)	C(21)"-Fe(1)"-C(11)"	107.5(4)
C(14)-Fe(1)-C(11)	68.2(3)	C(14)"-Fe(1)"-C(11)"	68.3(3)
C(13)-Fe(1)-C(11)	68.7(3)	C(25)"-Fe(1)"-C(11)"	123.2(4)
C(15)-Fe(1)-C(11)	40.2(3)	C(22)"-Fe(1)"-C(11)"	123.3(4)
C(21)-Fe(1)-C(12)	142.1(6)	C(24)"-Fe(1)"-C(11)"	158.8(4)
C(23)-Fe(1)-C(12)	112.8(4)	C(12)"-Fe(1)"-C(11)"	40.8(3)
C(22)-Fe(1)-C(12)	114.6(5)	C(15)"-Fe(1)"-C(11)"	40.7(3)
C(24)-Fe(1)-C(12)	139.7(5)	C(13)"-Fe(1)"-C(11)"	68.6(3)
C(25)-Fe(1)-C(12)	178.1(4)	C(41)"-P(1)"-C(31)"	105.7(3)
C(14)-Fe(1)-C(12)	68.0(4)	C(41)"-P(1)"-C(1)"	105.4(3)
C(13)-Fe(1)-C(12)	40.7(3)	C(31)"-P(1)"-C(1)"	102.6(3)
C(15)-Fe(1)-C(12)	68.1(3)	C(41)"-P(1)"-Ru(1)"	112.0(2)
C(11)-Fe(1)-C(12)	40.9(3)	C(31)"-P(1)"-Ru(1)"	115.6(2)
C(41)-P(1)-C(31)	106.6(3)	C(1)"-P(1)"-Ru(1)"	114.5(2)
C(41)-P(1)-C(1)	105.0(3)	C(11)"-C(1)"-P(1)"	113.6(5)
C(31)-P(1)-C(1)	101.6(3)	C(4)"-C(3)"-C(54)"	114.0(7)
C(41)-P(1)-Ru(1)	112.1(2)	C(4)"-C(3)"-C(5)"	110.2(8)
C(31)-P(1)-Ru(1)	114.6(2)	C(54)"-C(3)"-C(5)"	109.2(7)
C(1)-P(1)-Ru(1)	115.8(2)	C(15)"-C(11)"-C(12)"	106.7(7)
C(11)-C(1)-P(1)	113.2(5)	C(15)"-C(11)"-C(1)"	126.1(7)
C(4)-C(3)-C(54)	114.8(7)	C(12)"-C(11)"-C(1)"	127.1(7)
C(4)-C(3)-C(5)	110.6(7)	C(15)"-C(11)"-Fe(1)"	69.4(4)
C(54)-C(3)-C(5)	109.7(7)	C(12)"-C(11)"-Fe(1)"	69.2(4)
C(15)-C(11)-C(12)	107.8(7)	C(1)"-C(11)"-Fe(1)"	128.4(5)
C(15)-C(11)-C(1)	128.5(7)	C(11)"-C(12)"-C(13)"	107.7(7)
C(12)-C(11)-C(1)	123.6(6)	C(11)"-C(12)"-Fe(1)"	69.9(4)
C(15)-C(11)-Fe(1)	69.4(4)	C(13)"-C(12)"-Fe(1)"	69.7(4)
C(12)-C(11)-Fe(1)	69.8(4)	C(14)"-C(13)"-C(12)"	107.8(8)
C(1)-C(11)-Fe(1)	129.9(5)	C(14)"-C(13)"-Fe(1)"	69.4(5)
C(13)-C(12)-C(11)	107.5(8)	C(12)"-C(13)"-Fe(1)"	69.3(5)
C(13)-C(12)-Fe(1)	68.5(5)	C(13)"-C(14)"-C(15)"	109.0(8)
C(11)-C(12)-Fe(1)	69.4(4)	C(13)"-C(14)"-Fe(1)"	70.6(5)
C(14)-C(13)-C(12)	108.0(8)	C(15)"-C(14)"-Fe(1)"	70.5(5)
C(14)-C(13)-Fe(1)	69.5(5)	C(14)"-C(15)"-C(11)"	108.8(7)
C(12)-C(13)-Fe(1)	70.9(5)	C(14)"-C(15)"-Fe(1)"	69.5(4)
C(13)-C(14)-C(15)	108.9(8)	C(11)"-C(15)"-Fe(1)"	69.9(4)
C(13)-C(14)-Fe(1)	69.9(5)	C(25)"-C(21)"-C(22)"	107.3(10)
C(15)-C(14)-Fe(1)	70.4(5)	C(25)"-C(21)"-Fe(1)"	70.1(6)
C(11)-C(15)-C(14)	107.9(8)	C(22)"-C(21)"-Fe(1)"	69.9(6)
C(11)-C(15)-Fe(1)	70.3(4)	C(23)"-C(22)"-C(21)"	107.3(10)
C(14)-C(15)-Fe(1)	68.8(5)	C(23)"-C(22)"-Fe(1)"	69.5(6)
C(25)-C(21)-C(22)	108.1(12)	C(21)"-C(22)"-Fe(1)"	69.4(6)
C(25)-C(21)-Fe(1)	71.7(7)	C(24)"-C(23)"-C(22)"	108.2(10)

Table A.22 continued

C(22)-C(21)-Fe(1)	71.1(8)	C(24)"-C(23)"-Fe(1)"	70.4(5)
C(21)-C(22)-C(23)	107.8(12)	C(22)"-C(23)"-Fe(1)"	70.2(6)
C(21)-C(22)-Fe(1)	69.8(6)	C(25)"-C(24)"-C(23)"	108.8(10)
C(23)-C(22)-Fe(1)	69.7(7)	C(25)"-C(24)"-Fe(1)"	70.1(5)
C(24)-C(23)-C(22)	105.9(11)	C(23)"-C(24)"-Fe(1)"	69.8(5)
C(24)-C(23)-Fe(1)	70.6(6)	C(24)"-C(25)"-C(21)"	108.5(9)
C(22)-C(23)-Fe(1)	69.8(7)	C(24)"-C(25)"-Fe(1)"	70.2(5)
C(25)-C(24)-C(23)	108.4(13)	C(21)"-C(25)"-Fe(1)"	69.7(5)
C(25)-C(24)-Fe(1)	70.8(6)	C(32)"-C(31)"-C(36)"	119.1(7)
C(23)-C(24)-Fe(1)	70.1(7)	C(32)"-C(31)"-P(1)"	123.4(5)
C(21)-C(25)-C(24)	109.9(12)	C(36)"-C(31)"-P(1)"	117.4(6)
C(21)-C(25)-Fe(1)	69.8(6)	C(33)"-C(32)"-C(31)"	120.2(7)
C(24)-C(25)-Fe(1)	70.7(6)	C(32)"-C(33)"-C(34)"	119.9(8)
C(36)-C(31)-C(32)	118.6(7)	C(35)"-C(34)"-C(33)"	120.4(8)
C(36)-C(31)-P(1)	117.5(6)	C(34)"-C(35)"-C(36)"	119.9(8)
C(32)-C(31)-P(1)	123.5(5)	C(35)"-C(36)"-C(31)"	120.5(8)
C(33)-C(32)-C(31)	120.2(8)	C(42)"-C(41)"-C(46)"	117.8(6)
C(34)-C(33)-C(32)	120.8(8)	C(42)"-C(41)"-P(1)"	121.8(5)
C(33)-C(34)-C(35)	119.8(8)	C(46)"-C(41)"-P(1)"	120.2(5)
C(34)-C(35)-C(36)	120.1(8)	C(43)"-C(42)"-C(41)"	120.8(7)
C(31)-C(36)-C(35)	120.4(8)	C(44)"-C(43)"-C(42)"	120.2(7)
C(46)-C(41)-C(42)	118.0(6)	C(45)"-C(44)"-C(43)"	120.0(7)
C(46)-C(41)-P(1)	119.8(5)	C(44)"-C(45)"-C(46)"	120.4(7)
C(42)-C(41)-P(1)	122.0(6)	C(45)"-C(46)"-C(41)"	120.7(7)
C(43)-C(42)-C(41)	120.4(8)	C(52)"-C(51)"-C(56)"	119.1(7)
C(42)-C(43)-C(44)	120.6(8)	C(52)"-C(51)"-C(2)"	121.7(8)
C(45)-C(44)-C(43)	119.6(8)	C(56)"-C(51)"-C(2)"	119.1(8)
C(44)-C(45)-C(46)	120.2(8)	C(52)"-C(51)"-Ru(1)"	70.6(4)
C(41)-C(46)-C(45)	121.3(7)	C(56)"-C(51)"-Ru(1)"	73.2(4)
C(56)-C(51)-C(52)	117.6(7)	C(2)"-C(51)"-Ru(1)"	131.1(6)
C(56)-C(51)-C(2)	122.6(9)	C(55)"-C(56)"-C(51)"	120.8(7)
C(52)-C(51)-C(2)	119.8(8)	C(55)"-C(56)"-Ru(1)"	72.3(4)
C(56)-C(51)-Ru(1)	69.9(4)	C(51)"-C(56)"-Ru(1)"	69.3(4)
C(52)-C(51)-Ru(1)	71.3(4)	C(56)"-C(55)"-C(54)"	120.7(7)
C(2)-C(51)-Ru(1)	129.9(6)	C(56)"-C(55)"-Ru(1)"	71.7(4)
C(53)-C(52)-C(51)	121.1(7)	C(54)"-C(55)"-Ru(1)"	70.5(4)
C(53)-C(52)-Ru(1)	72.3(4)	C(53)"-C(54)"-C(55)"	118.6(6)
C(51)-C(52)-Ru(1)	70.9(4)	C(53)"-C(54)"-C(3)"	123.1(7)
C(52)-C(53)-C(54)	121.7(7)	C(55)"-C(54)"-C(3)"	118.2(7)
C(52)-C(53)-Ru(1)	71.6(4)	C(53)"-C(54)"-Ru(1)"	70.3(4)
C(54)-C(53)-Ru(1)	71.5(4)	C(55)"-C(54)"-Ru(1)"	72.0(4)
C(55)-C(54)-C(53)	117.5(6)	C(3)"-C(54)"-Ru(1)"	130.1(5)
C(55)-C(54)-C(3)	122.6(7)	C(54)"-C(53)"-C(52)"	120.2(6)
C(53)-C(54)-C(3)	119.9(7)	C(54)"-C(53)"-Ru(1)"	72.6(4)
C(55)-C(54)-Ru(1)	69.7(4)	C(52)"-C(53)"-Ru(1)"	69.9(4)
C(53)-C(54)-Ru(1)	71.3(4)	C(51)"-C(52)"-C(53)"	120.5(7)
C(3)-C(54)-Ru(1)	130.1(5)	C(51)"-C(52)"-Ru(1)"	71.8(4)
C(54)-C(55)-C(56)	121.4(7)	C(53)"-C(52)"-Ru(1)"	71.9(4)
C(54)-C(55)-Ru(1)	73.2(4)	Cl(3)-C(6)-Cl(4)	108.8(7)
C(56)-C(55)-Ru(1)	70.7(4)	Cl(4)'-C(6)'-Cl(3)'	112.2(6)
C(51)-C(56)-C(55)	120.7(7)	Cl(4)"-C(6)"-Cl(3)"	118.0(8)

Table A.23: *Anisotropic displacement parameters (Å²) for* ***20****. The anisotropic displacement factor exponent takes the form:* $-2\pi^2(h^2 a^{*2}U11 + ... + 2hka^*b^*U12)$.

	U11	U22	U33	U23	U13	U12
Ru(1)	0.0171(3)	0.0235(3)	0.0200(3)	0.0013(2)	0.0033(2)	0.0001(2)
Fe(1)	0.0227(5)	0.0336(6)	0.0311(6)	-0.0022(5)	0.0035(4)	-0.0077(4)
P(1)	0.0172(8)	0.0226(9)	0.0204(8)	0.0021(7)	0.0025(6)	0.0013(6)
Cl(1)	0.0211(8)	0.0406(10)	0.0383(10)	0.0126(8)	-0.0052(7)	-0.0005(7)
Cl(2)	0.0336(9)	0.0332(10)	0.0338(9)	-0.0033(8)	0.0175(8)	-0.0008(7)
C(1)	0.017(3)	0.027(4)	0.019(3)	0.002(3)	0.001(2)	-0.001(3)
C(2)	0.071(7)	0.104(9)	0.023(4)	-0.011(5)	-0.004(4)	-0.027(6)
C(3)	0.026(4)	0.044(5)	0.033(4)	0.013(3)	0.003(3)	-0.007(3)
C(4)	0.076(7)	0.076(7)	0.022(4)	0.006(4)	0.007(4)	-0.006(5)
C(5)	0.068(7)	0.046(6)	0.055(6)	0.024(5)	0.004(5)	-0.016(5)
C(11)	0.018(3)	0.032(4)	0.025(3)	0.001(3)	0.006(3)	-0.004(3)
C(12)	0.031(4)	0.037(4)	0.039(4)	0.010(4)	-0.007(3)	-0.010(3)
C(13)	0.026(4)	0.047(5)	0.075(7)	0.015(5)	-0.006(4)	-0.008(4)
C(14)	0.034(5)	0.037(5)	0.087(7)	-0.020(5)	0.010(5)	-0.008(4)
C(15)	0.029(4)	0.046(5)	0.048(5)	-0.015(4)	0.012(4)	-0.013(4)
C(21)	0.032(6)	0.093(10)	0.128(12)	0.071(10)	-0.008(7)	-0.004(6)
C(22)	0.026(6)	0.100(11)	0.21(2)	-0.100(13)	0.016(9)	0.002(6)
C(23)	0.027(6)	0.29(3)	0.030(5)	0.011(10)	0.010(4)	-0.025(10)
C(24)	0.026(5)	0.075(8)	0.153(14)	0.052(9)	-0.007(7)	-0.023(5)
C(25)	0.037(6)	0.126(12)	0.057(7)	-0.027(7)	0.004(5)	-0.033(6)
C(31)	0.021(3)	0.028(4)	0.026(3)	0.007(3)	-0.002(3)	-0.003(3)
C(32)	0.035(4)	0.023(4)	0.036(4)	0.006(3)	-0.007(3)	0.002(3)
C(33)	0.043(5)	0.032(4)	0.056(6)	0.012(4)	-0.014(4)	0.005(4)
C(34)	0.054(6)	0.048(6)	0.054(6)	0.018(5)	-0.021(5)	-0.003(4)
C(35)	0.051(5)	0.064(6)	0.028(4)	0.006(4)	-0.009(4)	-0.004(5)
C(36)	0.042(4)	0.036(4)	0.030(4)	0.007(3)	-0.003(3)	0.005(3)
C(41)	0.022(3)	0.023(3)	0.026(4)	0.000(3)	0.007(3)	0.001(3)
C(42)	0.022(4)	0.042(4)	0.038(4)	-0.002(4)	0.008(3)	0.005(3)
C(43)	0.040(5)	0.053(5)	0.052(5)	-0.010(4)	0.024(4)	0.007(4)
C(44)	0.056(6)	0.060(6)	0.034(5)	-0.011(4)	0.021(4)	0.002(5)
C(45)	0.049(5)	0.063(6)	0.029(4)	-0.005(4)	0.002(4)	-0.010(4)
C(46)	0.026(4)	0.040(4)	0.028(4)	-0.004(3)	0.002(3)	-0.003(3)
C(51)	0.031(4)	0.055(5)	0.027(4)	-0.005(4)	-0.004(3)	-0.015(4)
C(52)	0.037(4)	0.047(5)	0.037(4)	-0.015(4)	0.011(3)	-0.016(4)
C(53)	0.028(4)	0.023(4)	0.039(4)	-0.002(3)	0.003(3)	-0.004(3)
C(54)	0.017(3)	0.028(4)	0.031(4)	0.007(3)	0.000(3)	-0.007(3)
C(55)	0.018(3)	0.029(4)	0.025(3)	0.003(3)	0.003(3)	-0.002(3)
C(56)	0.019(3)	0.046(5)	0.031(4)	0.008(3)	-0.004(3)	-0.007(3)
Ru(1)'	0.0201(3)	0.0205(3)	0.0217(3)	-0.0007(2)	0.0053(2)	-0.0007(2)
Fe(1)'	0.0209(5)	0.0286(5)	0.0260(5)	-0.0001(4)	0.0020(4)	0.0061(4)
P(1)'	0.0166(8)	0.0215(8)	0.0218(8)	0.0006(7)	0.0033(6)	0.0002(6)
Cl(1)'	0.0252(8)	0.0362(10)	0.0345(9)	-0.0047(8)	-0.0021(7)	-0.0016(7)
Cl(2)'	0.0400(10)	0.0292(9)	0.0358(10)	-0.0047(7)	0.0210(8)	-0.0054(8)
C(1)'	0.020(3)	0.027(4)	0.034(4)	-0.002(3)	0.007(3)	0.001(3)
C(2)'	0.090(8)	0.052(6)	0.039(5)	-0.005(4)	-0.029(5)	0.032(5)
C(3)'	0.052(5)	0.051(5)	0.035(5)	-0.010(4)	0.010(4)	0.012(4)
C(4)'	0.137(11)	0.062(7)	0.034(5)	-0.003(5)	0.014(6)	0.033(7)
C(5)'	0.079(8)	0.067(7)	0.055(6)	-0.026(5)	0.021(6)	0.012(6)
C(11)'	0.014(3)	0.026(3)	0.023(3)	0.000(3)	-0.001(2)	0.006(3)
C(12)'	0.020(3)	0.037(4)	0.022(3)	-0.002(3)	-0.001(3)	0.005(3)

Table A.23 continued

C(13)'	0.026(4)	0.032(4)	0.039(4)	-0.007(3)	-0.005(3)	0.006(3)
C(14)'	0.028(4)	0.024(4)	0.051(5)	0.002(3)	0.003(3)	-0.001(3)
C(15)'	0.021(3)	0.036(4)	0.029(4)	0.004(3)	0.002(3)	0.006(3)
C(21)'	0.030(4)	0.045(5)	0.042(5)	-0.011(4)	-0.011(3)	0.003(4)
C(22)'	0.026(4)	0.068(7)	0.079(7)	0.037(6)	0.002(4)	-0.002(4)
C(23)'	0.026(5)	0.131(11)	0.042(5)	-0.022(6)	0.002(4)	0.025(6)
C(24)'	0.034(5)	0.044(5)	0.084(8)	-0.022(5)	-0.017(5)	0.017(4)
C(25)'	0.029(4)	0.052(5)	0.046(5)	0.012(4)	-0.008(4)	0.007(4)
C(31)'	0.020(3)	0.019(3)	0.033(4)	-0.001(3)	-0.001(3)	0.002(3)
C(32)'	0.029(4)	0.030(4)	0.038(4)	0.002(3)	-0.001(3)	0.000(3)
C(33)'	0.035(4)	0.029(4)	0.053(5)	0.001(4)	-0.008(4)	-0.003(3)
C(34)'	0.031(4)	0.043(5)	0.047(5)	-0.014(4)	-0.015(4)	-0.005(4)
C(35)'	0.043(5)	0.039(5)	0.033(4)	-0.002(4)	-0.004(3)	0.005(4)
C(36)'	0.027(4)	0.030(4)	0.032(4)	0.001(3)	0.003(3)	-0.002(3)
C(41)'	0.021(3)	0.027(4)	0.028(4)	0.002(3)	0.008(3)	0.001(3)
C(42)'	0.023(4)	0.043(5)	0.032(4)	0.007(3)	0.008(3)	-0.001(3)
C(43)'	0.030(4)	0.057(6)	0.050(5)	0.010(4)	0.017(4)	0.000(4)
C(44)'	0.046(5)	0.075(7)	0.037(5)	0.013(5)	0.021(4)	-0.001(5)
C(45)'	0.046(5)	0.067(6)	0.022(4)	0.012(4)	0.005(3)	0.001(4)
C(46)'	0.027(4)	0.043(5)	0.030(4)	0.009(3)	0.005(3)	0.002(3)
C(51)'	0.034(4)	0.034(4)	0.036(4)	-0.003(3)	-0.006(3)	0.018(3)
C(52)'	0.036(4)	0.034(4)	0.033(4)	0.004(3)	0.004(3)	0.006(3)
C(53)'	0.023(4)	0.022(4)	0.044(4)	-0.005(3)	0.005(3)	0.001(3)
C(54)'	0.028(4)	0.031(4)	0.033(4)	-0.005(3)	0.009(3)	0.008(3)
C(55)'	0.029(4)	0.027(4)	0.040(4)	0.003(3)	0.014(3)	0.003(3)
C(56)'	0.019(3)	0.030(4)	0.057(5)	-0.012(4)	-0.003(3)	0.003(3)
Ru(1)"	0.0177(3)	0.0247(3)	0.0193(3)	-0.0013(2)	0.0045(2)	-0.0004(2)
Fe(1)"	0.0208(5)	0.0389(6)	0.0380(6)	0.0035(5)	0.0008(4)	-0.0068(4)
P(1)"	0.0169(8)	0.0255(9)	0.0216(8)	-0.0011(7)	0.0033(6)	-0.0002(7)
Cl(1)"	0.0373(10)	0.0368(10)	0.0314(9)	-0.0064(8)	0.0192(8)	-0.0041(8)
Cl(2)"	0.0215(8)	0.0379(10)	0.0384(10)	0.0036(8)	-0.0027(7)	0.0033(7)
C(1)"	0.024(3)	0.029(4)	0.028(4)	-0.002(3)	0.006(3)	0.000(3)
C(2)"	0.045(5)	0.088(8)	0.028(4)	0.009(5)	-0.008(4)	-0.007(5)
C(3)"	0.034(4)	0.044(5)	0.038(4)	0.013(4)	0.002(3)	0.002(4)
C(4)"	0.091(8)	0.062(7)	0.027(4)	0.009(4)	0.004(5)	-0.026(6)
C(5)"	0.084(8)	0.068(7)	0.063(7)	0.026(6)	0.014(6)	-0.026(6)
C(11)"	0.015(3)	0.041(4)	0.027(4)	0.002(3)	-0.002(3)	-0.002(3)
C(12)"	0.020(4)	0.043(5)	0.039(4)	-0.004(4)	0.006(3)	-0.004(3)
C(13)"	0.026(4)	0.040(5)	0.070(6)	-0.008(4)	0.000(4)	-0.005(3)
C(14)"	0.033(4)	0.045(5)	0.068(6)	0.026(5)	-0.014(4)	-0.003(4)
C(15)"	0.026(4)	0.043(5)	0.034(4)	0.003(3)	-0.009(3)	-0.013(3)
C(21)"	0.028(5)	0.049(6)	0.105(9)	0.004(6)	0.002(5)	0.003(4)
C(22)"	0.033(5)	0.113(10)	0.051(6)	0.014(6)	-0.003(4)	0.012(6)
C(23)"	0.023(5)	0.096(9)	0.081(8)	-0.030(7)	-0.010(5)	-0.009(5)
C(24)"	0.031(5)	0.065(7)	0.076(7)	0.005(6)	0.012(5)	-0.014(4)
C(25)"	0.034(5)	0.080(8)	0.058(6)	-0.008(6)	0.015(4)	0.001(5)
C(31)"	0.024(3)	0.032(4)	0.022(3)	0.006(3)	0.000(3)	-0.005(3)
C(32)"	0.025(4)	0.036(4)	0.035(4)	-0.002(3)	0.001(3)	-0.001(3)
C(33)"	0.029(4)	0.031(4)	0.062(6)	0.000(4)	0.005(4)	0.001(3)
C(34)"	0.055(6)	0.041(5)	0.055(6)	0.017(4)	-0.006(4)	0.006(4)
C(35)"	0.086(7)	0.053(6)	0.026(4)	0.008(4)	-0.008(4)	0.007(5)
C(36)"	0.053(5)	0.038(5)	0.030(4)	0.003(3)	0.003(4)	0.001(4)
C(41)"	0.025(3)	0.023(3)	0.022(3)	-0.007(3)	0.003(3)	-0.001(3)
C(42)"	0.024(4)	0.029(4)	0.033(4)	-0.003(3)	0.002(3)	0.006(3)
C(43)"	0.035(4)	0.044(5)	0.037(4)	-0.007(4)	0.014(3)	0.006(4)
C(44)"	0.047(5)	0.047(5)	0.024(4)	-0.009(3)	0.012(3)	0.002(4)
C(45)"	0.041(5)	0.049(5)	0.024(4)	-0.001(3)	0.002(3)	0.000(4)

Table A.23 continued

C(46)"	0.025(4)	0.038(4)	0.025(4)	-0.004(3)	0.001(3)	0.003(3)
C(51)"	0.029(4)	0.052(5)	0.025(4)	0.000(3)	0.000(3)	-0.008(3)
C(56)"	0.031(4)	0.046(5)	0.034(4)	-0.020(4)	0.008(3)	-0.015(3)
C(55)"	0.029(4)	0.024(4)	0.040(4)	-0.003(3)	0.006(3)	-0.006(3)
C(54)"	0.019(3)	0.029(4)	0.031(4)	0.003(3)	0.005(3)	-0.008(3)
C(53)"	0.018(3)	0.027(4)	0.025(3)	-0.001(3)	0.005(3)	-0.003(3)
C(52)"	0.017(3)	0.036(4)	0.036(4)	0.004(3)	0.000(3)	-0.002(3)
Cl(3)	0.0463(15)	0.0509(16)	0.156(3)	0.0195(18)	0.0123(17)	0.0072(12)
Cl(4)	0.0561(18)	0.086(2)	0.180(4)	-0.026(3)	0.011(2)	0.0157(16)
C(6)	0.037(5)	0.057(7)	0.120(10)	0.019(7)	0.013(6)	0.004(5)
Cl(3)'	0.0429(15)	0.0682(19)	0.158(3)	-0.011(2)	0.0102(17)	0.0101(13)
Cl(4)'	0.072(2)	0.090(2)	0.116(3)	0.029(2)	-0.0132(19)	0.0083(17)
C(6)'	0.043(5)	0.074(7)	0.065(7)	0.004(6)	0.000(5)	0.008(5)
Cl(3)"	0.0422(16)	0.209(5)	0.097(3)	0.016(3)	0.0106(16)	-0.006(2)
Cl(4)"	0.059(2)	0.147(4)	0.234(5)	-0.115(4)	0.063(3)	-0.050(2)
C(6)"	0.049(7)	0.200(18)	0.086(10)	-0.013(11)	0.007(7)	0.036(9)

Table A.24: *Hydrogen coordinates and isotropic displacement parameters for* ***20****.*

	x	y	z	U(eq)
H(1A)	1.2240	0.2490	0.7385	0.026
H(1B)	1.2164	0.2471	0.6365	0.026
H(2A)	0.7835	0.2128	0.4528	0.100
H(2B)	0.7789	0.1872	0.4354	0.100
H(2C)	0.9098	0.1997	0.4432	0.100
H(3)	0.9735	0.1782	0.8514	0.042
H(4A)	0.8790	0.2120	0.8812	0.086
H(4B)	0.8635	0.1944	0.9547	0.086
H(4C)	0.7488	0.1997	0.8867	0.086
H(5A)	0.7275	0.1602	0.8387	0.084
H(5B)	0.8313	0.1551	0.9148	0.084
H(5C)	0.8512	0.1472	0.8196	0.084
H(12)	1.1953	0.2830	0.5426	0.043
H(13)	1.1958	0.3238	0.5749	0.060
H(14)	1.1772	0.3285	0.7338	0.063
H(15)	1.1710	0.2911	0.8027	0.049
H(21)	1.4839	0.2750	0.7948	0.102
H(22)	1.5093	0.2685	0.6415	0.136
H(23)	1.5060	0.3053	0.5676	0.139
H(24)	1.4921	0.3331	0.6824	0.102
H(25)	1.4840	0.3142	0.8190	0.088
H(32)	0.8868	0.2868	0.6803	0.038
H(33)	0.7961	0.3086	0.5707	0.054
H(34)	0.7925	0.2975	0.4287	0.064
H(35)	0.8786	0.2639	0.3950	0.058
H(36)	0.9602	0.2407	0.5047	0.043
H(42)	0.7765	0.2580	0.7509	0.040
H(43)	0.7128	0.2658	0.8867	0.057
H(44)	0.8558	0.2644	1.0074	0.059
H(45)	1.0621	0.2545	0.9923	0.057
H(46)	1.1274	0.2464	0.8567	0.038

Table A.24 continued

H(52)	0.9428	0.1663	0.5548	0.048
H(53)	0.9630	0.1590	0.7005	0.036
H(55)	0.7619	0.2137	0.7473	0.029
H(56)	0.7409	0.2214	0.5991	0.039
H(1'1)	0.4077	0.0881	0.9062	0.032
H(1'2)	0.4051	0.0833	1.0062	0.032
H(2'1)	0.8839	0.0261	1.1885	0.094
H(2'2)	0.7397	0.0304	1.2003	0.094
H(2'3)	0.8271	0.0500	1.1742	0.094
H(3)'	0.5934	0.0069	0.7971	0.055
H(4'1)	0.6598	0.0421	0.7540	0.115
H(4'2)	0.6628	0.0241	0.6805	0.115
H(4'3)	0.7895	0.0315	0.7328	0.115
H(5'1)	0.7358	-0.0145	0.7256	0.099
H(5'2)	0.7436	-0.0207	0.8249	0.099
H(5'3)	0.8488	-0.0057	0.7886	0.099
H(12)'	0.4180	0.1166	1.1118	0.032
H(13)'	0.4387	0.1573	1.1012	0.040
H(14)'	0.4784	0.1667	0.9477	0.041
H(15)'	0.4835	0.1312	0.8648	0.034
H(21)'	0.1612	0.1114	0.8560	0.048
H(22)'	0.1226	0.1073	1.0133	0.069
H(23)'	0.1155	0.1453	1.0766	0.080
H(24)'	0.1540	0.1722	0.9610	0.066
H(25)'	0.1813	0.1516	0.8259	0.051
H(32)'	0.7553	0.1204	0.9754	0.039
H(33)'	0.8419	0.1415	1.0885	0.048
H(34)'	0.8353	0.1301	1.2303	0.050
H(35)'	0.7402	0.0970	1.2590	0.046
H(36)'	0.6535	0.0752	1.1471	0.036
H(42)'	0.8575	0.0900	0.9083	0.039
H(43)'	0.9349	0.0969	0.7760	0.054
H(44)'	0.8013	0.0987	0.6511	0.062
H(45)'	0.5867	0.0926	0.6593	0.054
H(46)'	0.5062	0.0860	0.7900	0.040
H(52)'	0.6659	0.0026	1.0916	0.041
H(53)'	0.6189	-0.0069	0.9487	0.035
H(55)'	0.8297	0.0443	0.8740	0.037
H(56)'	0.8751	0.0541	1.0191	0.043
H(1"1)	-0.0904	0.0882	0.5136	0.032
H(1"2)	-0.1049	0.0887	0.4114	0.032
H(2"1)	0.3507	0.1081	0.6911	0.082
H(2"2)	0.2651	0.1279	0.7177	0.082
H(2"3)	0.4121	0.1313	0.7147	0.082
H(3)"	0.1738	0.1590	0.3209	0.046
H(4"1)	0.3650	0.1318	0.2640	0.090
H(4"2)	0.2568	0.1431	0.2036	0.090
H(4"3)	0.2234	0.1243	0.2688	0.090
H(5"1)	0.4354	0.1683	0.3152	0.107
H(5"2)	0.3440	0.1836	0.3640	0.107
H(5"3)	0.3238	0.1808	0.2624	0.107
H(12)"	-0.0821	0.0479	0.3291	0.041
H(13)"	-0.1181	0.0091	0.3818	0.055
H(14)"	-0.1355	0.0107	0.5409	0.059
H(15)"	-0.1020	0.0493	0.5905	0.042
H(21)"	-0.3763	0.0807	0.4336	0.073
H(22)"	-0.3905	0.0563	0.3016	0.079

Table A.24 continued

H(23)"	-0.4257	0.0178	0.3519	0.081
H(24)"	-0.4405	0.0187	0.5105	0.068
H(25)"	-0.4098	0.0570	0.5613	0.068
H(32)"	0.1992	0.0432	0.4418	0.038
H(33)"	0.2906	0.0174	0.5378	0.049
H(34)"	0.3315	0.0264	0.6833	0.061
H(35)"	0.2759	0.0604	0.7336	0.067
H(36)"	0.1864	0.0864	0.6379	0.049
H(42)"	0.3314	0.0725	0.3808	0.034
H(43)"	0.3830	0.0666	0.2406	0.046
H(44)"	0.2363	0.0732	0.1254	0.047
H(45)"	0.0376	0.0858	0.1499	0.045
H(46)"	-0.0181	0.0909	0.2893	0.035
H(56)"	0.2405	0.1607	0.6190	0.044
H(55)"	0.2093	0.1723	0.4771	0.037
H(53)"	0.3704	0.1161	0.3961	0.028
H(52)"	0.3970	0.1040	0.5409	0.036
H(6A)	0.0981	0.0316	0.9914	0.085
H(6B)	0.2326	0.0355	0.9565	0.085
H(6'1)	0.3502	0.1972	0.6604	0.073
H(6'2)	0.4768	0.1939	0.6149	0.073
H(6"1)	0.6920	0.1177	0.5225	0.134
H(6"2)	0.7867	0.1366	0.5032	0.134

Table A.25: *Atomic coordinates and equivalent isotropic displacement parameters for 21. U(eq) is defined as one third of the trace of the orthogonalised Uij tensor.*

	x	y	z	U(eq)
P(1)	0.4693(2)	0.0872(1)	0.3173(1)	0.023(1)
O(1)	0.6967(4)	0.0631(3)	0.3477(2)	0.027(1)
O(2)	0.2047(4)	-0.0956(3)	0.4325(3)	0.032(1)
C(3)	0.2612(6)	0.0695(5)	0.4222(3)	0.029(1)
C(11)	0.5013(6)	0.2948(5)	0.3028(3)	0.024(1)
C(12)	0.3188(7)	0.3424(5)	0.2648(3)	0.030(1)
C(13)	0.3521(7)	0.5048(5)	0.2585(4)	0.037(1)
C(14)	0.5668(7)	0.6184(5)	0.2905(4)	0.036(1)
C(15)	0.7470(7)	0.5717(5)	0.3282(4)	0.037(1)
C(16)	0.7146(7)	0.4087(5)	0.3350(3)	0.030(1)
C(21)	0.3353(6)	-0.0613(5)	0.1868(3)	0.025(1)
C(22)	0.4791(7)	-0.1121(5)	0.1048(3)	0.035(1)
C(23)	0.3849(8)	-0.2306(6)	0.0039(4)	0.042(1)
C(24)	0.1520(8)	-0.2989(6)	-0.0151(4)	0.045(1)
C(25)	0.0089(8)	-0.2509(6)	0.0679(4)	0.049(1)
C(26)	0.1003(7)	-0.1322(5)	0.1675(4)	0.038(1)

Table A.26: *Bond lengths (Å) and angles (°) for* ***21****.*

P(1)-O(1)	1.497(3)	O(1)-P(1)-C(3)	114.33(16)
P(1)-C(21)	1.803(4)	C(21)-P(1)-C(3)	106.97(18)
P(1)-C(11)	1.813(4)	C(11)-P(1)-C(3)	104.19(18)
P(1)-C(3)	1.816(4)	O(2)-C(3)-P(1)	109.2(3)
O(2)-C(3)	1.421(5)	C(16)-C(11)-C(12)	120.2(3)
C(11)-C(16)	1.383(6)	C(16)-C(11)-P(1)	117.6(3)
C(11)-C(12)	1.388(5)	C(12)-C(11)-P(1)	122.2(3)
C(12)-C(13)	1.390(6)	C(11)-C(12)-C(13)	119.6(4)
C(13)-C(14)	1.388(6)	C(14)-C(13)-C(12)	120.0(4)
C(14)-C(15)	1.371(6)	C(15)-C(14)-C(13)	120.5(4)
C(15)-C(16)	1.397(6)	C(14)-C(15)-C(16)	119.9(4)
C(21)-C(26)	1.381(5)	C(11)-C(16)-C(15)	119.9(4)
C(21)-C(22)	1.389(6)	C(26)-C(21)-C(22)	119.1(4)
C(22)-C(23)	1.392(6)	C(26)-C(21)-P(1)	123.2(3)
C(23)-C(24)	1.366(6)	C(22)-C(21)-P(1)	117.6(3)
C(24)-C(25)	1.387(7)	C(21)-C(22)-C(23)	119.9(4)
C(25)-C(26)	1.379(7)	C(24)-C(23)-C(22)	120.7(4)
O(1)-P(1)-C(21)	111.56(16)	C(23)-C(24)-C(25)	119.4(4)
O(1)-P(1)-C(11)	111.32(16)	C(26)-C(25)-C(24)	120.3(4)
C(21)-P(1)-C(11)	108.02(17)	C(25)-C(26)-C(21)	120.5(4)

Table A.27: *Anisotropic displacement parameters (Å²) for* ***21****. The anisotropic displacement factor exponent takes the form:* $-2\pi^2(h^2a^{*2}U11 + ... + 2hka^*b^*U12)$.

	U11	U22	U33	U23	U13	U12
P(1)	0.0271(7)	0.0142(7)	0.0227(8)	0.0065(6)	0.0087(5)	-0.0024(5)
O(1)	0.0278(15)	0.0210(16)	0.0286(17)	0.0090(14)	0.0092(11)	-0.0017(12)
O(2)	0.0408(17)	0.0227(16)	0.0278(18)	0.0126(14)	0.0099(12)	-0.0084(12)
C(3)	0.032(2)	0.025(2)	0.024(2)	0.0068(19)	0.0108(16)	-0.0011(17)
C(11)	0.034(2)	0.015(2)	0.018(2)	0.0032(19)	0.0122(15)	-0.0008(17)
C(12)	0.035(2)	0.018(2)	0.032(2)	0.005(2)	0.0046(17)	-0.0013(17)
C(13)	0.045(2)	0.023(2)	0.043(3)	0.010(2)	0.0042(19)	0.008(2)
C(14)	0.055(3)	0.015(2)	0.036(3)	0.008(2)	0.011(2)	0.004(2)
C(15)	0.039(2)	0.020(2)	0.042(3)	0.007(2)	0.0085(19)	-0.0099(18)
C(16)	0.030(2)	0.024(2)	0.029(2)	0.006(2)	0.0078(16)	-0.0023(17)
C(21)	0.034(2)	0.017(2)	0.024(2)	0.0080(19)	0.0067(16)	0.0038(17)
C(22)	0.044(2)	0.030(3)	0.027(2)	0.006(2)	0.0128(18)	0.0046(19)
C(23)	0.060(3)	0.037(3)	0.029(3)	0.007(3)	0.016(2)	0.015(2)
C(24)	0.065(3)	0.031(3)	0.030(3)	-0.005(2)	-0.004(2)	0.008(2)
C(25)	0.039(3)	0.040(3)	0.048(3)	-0.006(3)	-0.004(2)	-0.002(2)
C(26)	0.036(2)	0.030(3)	0.037(3)	-0.003(2)	0.0062(19)	0.001(2)

Table A.28: *Hydrogen coordinates and isotropic displacement parameters for 21.*

	x	y	z	U(eq)
H(2)	0.239(7)	-0.089(6)	0.504(4)	0.037(12)
H(3A)	0.3271	0.1499	0.4955	0.034
H(3B)	0.1203	0.0957	0.3994	0.034
H(12)	0.1719	0.2644	0.2433	0.036
H(13)	0.2280	0.5380	0.2323	0.045
H(14)	0.5890	0.7294	0.2862	0.043
H(15)	0.8936	0.6499	0.3498	0.045
H(16)	0.8389	0.3763	0.3617	0.036
H(22)	0.6413	-0.0660	0.1176	0.042
H(23)	0.4836	-0.2644	-0.0522	0.051
H(24)	0.0885	-0.3785	-0.0846	0.055
H(25)	-0.1528	-0.3001	0.0559	0.059
H(26)	0.0008	-0.0989	0.2234	0.046

Table A.29: *Atomic coordinates and equivalent isotropic displacement parameters for 22. U(eq) is defined as one third of the trace of the orthogonalised Uij tensor.*

	x	y	z	U(eq)
S(1)	0.5438(1)	0.6457(1)	-0.0049(1)	0.029(1)
P(1)	0.4662(1)	0.6580(1)	0.1762(1)	0.020(1)
O(1)	0.3866(2)	0.7600(2)	0.3326(3)	0.028(1)
C(3)	0.4230(3)	0.7448(3)	0.1894(4)	0.025(1)
C(11)	0.5361(3)	0.6438(3)	0.3438(4)	0.020(1)
C(12)	0.6257(3)	0.6742(3)	0.3566(4)	0.028(1)
C(13)	0.6804(3)	0.6656(3)	0.4824(4)	0.033(1)
C(14)	0.6465(3)	0.6262(3)	0.5960(4)	0.033(1)
C(15)	0.5571(3)	0.5949(3)	0.5846(4)	0.033(1)
C(16)	0.5012(3)	0.6038(2)	0.4579(4)	0.025(1)
C(21)	0.3622(3)	0.6035(2)	0.1839(3)	0.019(1)
C(22)	0.2759(3)	0.6233(3)	0.2515(4)	0.026(1)
C(23)	0.1970(3)	0.5808(3)	0.2529(4)	0.029(1)
C(24)	0.2022(3)	0.5181(3)	0.1884(4)	0.035(1)
C(25)	0.2878(3)	0.4978(3)	0.1209(5)	0.032(1)
C(26)	0.3666(3)	0.5405(3)	0.1183(4)	0.026(1)

Table A.30: *Bond lengths (Å) and angles (°) for* **22**.

S(1)-P(1)	1.9738(13)	C(21)-P(1)-S(1)	113.00(13)
P(1)-C(21)	1.799(4)	C(11)-P(1)-S(1)	112.75(13)
P(1)-C(11)	1.821(4)	C(3)-P(1)-S(1)	110.36(13)
P(1)-C(3)	1.829(5)	O(1)-C(3)-P(1)	112.1(3)
O(1)-C(3)	1.424(4)	C(12)-C(11)-C(16)	119.9(4)
C(11)-C(12)	1.381(6)	C(12)-C(11)-P(1)	118.5(3)
C(11)-C(16)	1.389(6)	C(16)-C(11)-P(1)	121.7(3)
C(12)-C(13)	1.377(6)	C(13)-C(12)-C(11)	120.4(4)
C(13)-C(14)	1.375(7)	C(14)-C(13)-C(12)	120.2(4)
C(14)-C(15)	1.386(6)	C(13)-C(14)-C(15)	120.2(4)
C(15)-C(16)	1.394(5)	C(14)-C(15)-C(16)	119.8(4)
C(21)-C(26)	1.388(7)	C(11)-C(16)-C(15)	119.6(4)
C(21)-C(22)	1.396(5)	C(26)-C(21)-C(22)	118.6(4)
C(22)-C(23)	1.378(6)	C(26)-C(21)-P(1)	119.4(3)
C(23)-C(24)	1.378(7)	C(22)-C(21)-P(1)	122.0(4)
C(24)-C(25)	1.390(7)	C(23)-C(22)-C(21)	120.4(5)
C(25)-C(26)	1.379(7)	C(22)-C(23)-C(24)	120.6(4)
C(21)-P(1)-C(11)	107.27(18)	C(23)-C(24)-C(25)	119.6(5)
C(21)-P(1)-C(3)	107.72(19)	C(26)-C(25)-C(24)	119.9(5)
C(11)-P(1)-C(3)	105.3(2)	C(25)-C(26)-C(21)	120.9(4)

Table A.31: *Anisotropic displacement parameters (Å²) for* **22**. *The anisotropic displacement factor exponent takes the form:* $-2\pi^2(h^2a^{*2}U11 + ... + 2hka^*b^*U12)$.

	U11	U22	U33	U23	U13	U12
S(1)	0.0240(7)	0.0436(12)	0.0189(7)	-0.0013(5)	0.0059(3)	0.0018(5)
P(1)	0.0168(7)	0.0299(11)	0.0139(7)	0.0001(4)	0.0005(3)	0.0018(5)
O(1)	0.0306(17)	0.033(3)	0.0195(15)	-0.0093(13)	0.0002(10)	0.0044(16)
C(3)	0.024(2)	0.031(3)	0.019(2)	-0.0017(17)	-0.0001(14)	0.002(2)
C(11)	0.018(2)	0.024(3)	0.019(2)	0.0000(17)	-0.0010(13)	0.0060(19)
C(12)	0.024(2)	0.034(3)	0.025(2)	0.004(2)	-0.0018(15)	-0.001(2)
C(13)	0.025(2)	0.036(4)	0.038(2)	-0.009(2)	-0.0094(17)	0.000(2)
C(14)	0.034(2)	0.037(4)	0.028(2)	-0.002(2)	-0.0119(16)	0.012(2)
C(15)	0.033(2)	0.044(4)	0.021(2)	-0.001(2)	-0.0035(15)	0.008(2)
C(16)	0.022(2)	0.033(3)	0.0197(19)	0.0000(18)	-0.0010(15)	0.004(2)
C(21)	0.023(2)	0.023(3)	0.0094(18)	0.0031(16)	-0.0025(12)	0.0039(19)
C(22)	0.020(2)	0.031(3)	0.027(2)	0.0000(18)	0.0008(14)	0.005(2)
C(23)	0.019(2)	0.035(4)	0.031(2)	-0.005(2)	0.0034(14)	-0.002(2)
C(24)	0.028(2)	0.047(4)	0.030(2)	0.007(2)	-0.0061(15)	-0.011(2)
C(25)	0.033(2)	0.028(3)	0.036(2)	-0.005(2)	-0.0042(17)	0.001(2)
C(26)	0.025(2)	0.035(3)	0.0192(19)	-0.002(2)	0.0015(14)	0.001(2)

Table A.32: *Hydrogen coordinates and isotropic displacement parameters for 22.*

	x	y	z	U(eq)
H(1)	0.428(4)	0.785(3)	0.373(7)	0.055(17)
H(3A)	0.4769	0.7758	0.1658	0.030
H(3B)	0.3711	0.7520	0.1156	0.030
H(12)	0.6498	0.7012	0.2782	0.033
H(13)	0.7416	0.6871	0.4908	0.040
H(14)	0.6845	0.6204	0.6825	0.039
H(15)	0.5339	0.5674	0.6629	0.039
H(16)	0.4397	0.5827	0.4496	0.030
H(22)	0.2715	0.6663	0.2968	0.031
H(23)	0.1385	0.5949	0.2988	0.034
H(24)	0.1477	0.4890	0.1901	0.042
H(25)	0.2920	0.4546	0.0767	0.039
H(26)	0.4246	0.5266	0.0709	0.032

Table A.33: *Atomic coordinates and equivalent isotropic displacement parameters for 23. U(eq) is defined as one third of the trace of the orthogonalised Uij tensor.*

	x	y	z	U(eq)
Se(1)	0.5465(1)	0.6431(1)	-0.0061(1)	0.025(1)
P(1)	0.4631(1)	0.6560(1)	0.1856(1)	0.016(1)
O(1)	0.3833(2)	0.7585(1)	0.3375(2)	0.025(1)
C(3)	0.4207(3)	0.7441(2)	0.1980(3)	0.021(1)
C(11)	0.5316(2)	0.6425(2)	0.3501(3)	0.019(1)
C(12)	0.6212(3)	0.6739(2)	0.3628(4)	0.026(1)
C(13)	0.6755(3)	0.6651(2)	0.4880(4)	0.031(1)
C(14)	0.6423(3)	0.6247(2)	0.5987(4)	0.032(1)
C(15)	0.5534(3)	0.5935(2)	0.5872(4)	0.031(1)
C(16)	0.4985(3)	0.6027(2)	0.4629(3)	0.022(1)
C(21)	0.3591(2)	0.6021(2)	0.1922(3)	0.016(1)
C(22)	0.2749(2)	0.6225(2)	0.2610(3)	0.024(1)
C(23)	0.1951(3)	0.5803(2)	0.2616(4)	0.029(1)
C(24)	0.1993(3)	0.5183(2)	0.1952(4)	0.029(1)
C(25)	0.2821(3)	0.4984(2)	0.1270(4)	0.029(1)
C(26)	0.3616(3)	0.5392(2)	0.1245(3)	0.023(1)

Table A.34: *Bond lengths (Å) and angles (°) for* ***23****.*

Se(1)-P(1)	2.1194(8)	C(21)-P(1)-Se(1)	113.20(10)
P(1)-C(21)	1.797(3)	C(11)-P(1)-Se(1)	112.92(11)
P(1)-C(11)	1.803(3)	C(3)-P(1)-Se(1)	109.82(11)
P(1)-C(3)	1.847(3)	O(1)-C(3)-P(1)	111.3(2)
O(1)-C(3)	1.410(4)	C(16)-C(11)-C(12)	119.3(3)
C(11)-C(16)	1.379(5)	C(16)-C(11)-P(1)	122.5(3)
C(11)-C(12)	1.394(5)	C(12)-C(11)-P(1)	118.2(2)
C(12)-C(13)	1.384(5)	C(13)-C(12)-C(11)	119.9(3)
C(13)-C(14)	1.373(5)	C(14)-C(13)-C(12)	120.3(4)
C(14)-C(15)	1.382(5)	C(13)-C(14)-C(15)	120.2(3)
C(15)-C(16)	1.384(5)	C(14)-C(15)-C(16)	119.6(3)
C(21)-C(22)	1.387(4)	C(11)-C(16)-C(15)	120.7(3)
C(21)-C(26)	1.393(4)	C(22)-C(21)-C(26)	119.0(3)
C(22)-C(23)	1.386(5)	C(22)-C(21)-P(1)	121.2(2)
C(23)-C(24)	1.373(5)	C(26)-C(21)-P(1)	119.8(2)
C(24)-C(25)	1.366(5)	C(23)-C(22)-C(21)	119.8(3)
C(25)-C(26)	1.367(5)	C(24)-C(23)-C(22)	120.3(3)
C(21)-P(1)-C(11)	107.81(14)	C(25)-C(24)-C(23)	119.8(3)
C(21)-P(1)-C(3)	107.75(16)	C(24)-C(25)-C(26)	120.9(3)
C(11)-P(1)-C(3)	104.89(14)	C(25)-C(26)-C(21)	120.1(3)

Table A.35: *Anisotropic displacement parameters (Å²) for* ***23****. The anisotropic displacement factor exponent takes the form:* $-2\pi^2(h^2a^{*2}U11 + ... + 2hka^*b^*U12)$.

	U11	U22	U33	U23	U13	U12
Se(1)	0.0212(3)	0.0300(3)	0.0235(2)	-0.0012(1)	0.0066(1)	0.0013(2)
P(1)	0.0154(5)	0.0137(4)	0.0195(4)	-0.0006(3)	0.0006(3)	0.0015(4)
O(1)	0.0239(14)	0.0228(13)	0.0280(12)	-0.0065(10)	-0.0022(10)	0.0047(11)
C(3)	0.024(2)	0.0159(17)	0.0240(15)	0.0011(13)	-0.0061(15)	0.0055(15)
C(11)	0.017(2)	0.0159(18)	0.0238(16)	-0.0030(12)	-0.0024(14)	0.0058(14)
C(12)	0.022(2)	0.0182(18)	0.0368(18)	0.0018(15)	-0.0021(16)	0.0015(15)
C(13)	0.021(2)	0.028(2)	0.045(2)	-0.0088(17)	-0.0123(16)	0.0030(18)
C(14)	0.036(2)	0.029(2)	0.0304(18)	-0.0050(16)	-0.0110(16)	0.0148(19)
C(15)	0.034(2)	0.034(2)	0.0245(17)	0.0001(15)	-0.0012(15)	0.0051(18)
C(16)	0.018(2)	0.0222(19)	0.0263(16)	0.0004(14)	0.0002(15)	0.0001(15)
C(21)	0.0164(18)	0.0150(17)	0.0176(14)	0.0004(12)	-0.0015(13)	-0.0002(14)
C(22)	0.023(2)	0.0211(18)	0.0287(16)	-0.0028(15)	0.0016(15)	0.0019(16)
C(23)	0.016(2)	0.033(2)	0.0379(18)	-0.0025(16)	0.0073(15)	-0.0006(16)
C(24)	0.022(2)	0.027(2)	0.0381(18)	0.0043(16)	-0.0047(16)	-0.0077(17)
C(25)	0.033(2)	0.021(2)	0.0332(18)	-0.0035(14)	-0.0051(16)	-0.0045(17)
C(26)	0.023(2)	0.0192(19)	0.0279(16)	-0.0019(14)	0.0020(14)	0.0018(16)

Table A.36: *Hydrogen coordinates and isotropic displacement parameters for 23.*

	x	y	z	U(eq)
H(1)	0.431(3)	0.782(2)	0.387(4)	0.045(12)
H(3A)	0.4750	0.7751	0.1769	0.026
H(3B)	0.3700	0.7520	0.1238	0.026
H(12)	0.6449	0.7012	0.2857	0.031
H(13)	0.7360	0.6872	0.4974	0.038
H(14)	0.6805	0.6182	0.6835	0.038
H(15)	0.5302	0.5659	0.6642	0.037
H(16)	0.4373	0.5815	0.4552	0.026
H(22)	0.2719	0.6652	0.3076	0.029
H(23)	0.1373	0.5944	0.3080	0.035
H(24)	0.1448	0.4893	0.1967	0.035
H(25)	0.2845	0.4555	0.0806	0.035
H(26)	0.4187	0.5246	0.0766	0.028

Table A.37: *Atomic coordinates and equivalent isotropic displacement parameters for 24. U(eq) is defined as one third of the trace of the orthogonalised Uij tensor.*

	x	y	z	U(eq)
Fe	0.1868(1)	0.0159(1)	0.4348(1)	0.022(1)
P	0.4611(1)	-0.3842(1)	0.6411(1)	0.053(1)
C(1)	0.3897(2)	-0.2161(4)	0.5210(3)	0.043(1)
C(11)	0.2866(2)	-0.1749(3)	0.5335(2)	0.027(1)
C(12)	0.2651(2)	-0.0526(3)	0.6249(2)	0.029(1)
C(13)	0.1577(2)	-0.0541(3)	0.6066(2)	0.029(1)
C(14)	0.1128(2)	-0.1782(3)	0.5045(2)	0.029(1)
C(15)	0.1918(2)	-0.2526(3)	0.4599(2)	0.028(1)
C(21)	0.2530(3)	0.1432(4)	0.3123(4)	0.056(1)
C(22)	0.2333(3)	0.2631(4)	0.4007(3)	0.048(1)
C(23)	0.1289(3)	0.2646(4)	0.3837(3)	0.048(1)
C(24)	0.0825(3)	0.1440(5)	0.2853(4)	0.058(1)
C(25)	0.1595(4)	0.0658(4)	0.2391(3)	0.067(1)

Table A.38: *Bond lengths (Å) and angles (°) for 24.*

Fe-C(25)	2.022(3)	C(24)-Fe-C(11)	160.1(2)
Fe-C(24)	2.028(3)	C(21)-Fe-C(11)	107.35(12)
Fe-C(21)	2.030(3)	C(22)-Fe-C(11)	122.43(12)
Fe-C(22)	2.032(3)	C(15)-Fe-C(11)	40.89(10)
Fe-C(15)	2.036(2)	C(14)-Fe-C(11)	68.98(10)
Fe-C(14)	2.038(2)	C(12)-Fe-C(11)	40.94(10)

Table A.38 continued

Fe-C(12)	2.040(2)	C(23)-Fe-C(11)	158.14(13)
Fe-C(23)	2.041(3)	C(25)-Fe-C(13)	158.6(2)
Fe-C(11)	2.041(2)	C(24)-Fe-C(13)	122.34(14)
Fe-C(13)	2.042(2)	C(21)-Fe-C(13)	158.9(2)
P-C(1)	1.850(3)	C(22)-Fe-C(13)	123.29(13)
C(1)-C(11)	1.492(4)	C(15)-Fe-C(13)	68.65(10)
C(11)-C(15)	1.424(4)	C(14)-Fe-C(13)	40.75(10)
C(11)-C(12)	1.427(3)	C(12)-Fe-C(13)	40.93(10)
C(12)-C(13)	1.427(4)	C(23)-Fe-C(13)	107.89(11)
C(13)-C(14)	1.421(4)	C(11)-Fe-C(13)	69.14(10)
C(14)-C(15)	1.420(4)	C(11)-C(1)-P	113.7(2)
C(21)-C(22)	1.382(5)	C(15)-C(11)-C(12)	107.1(2)
C(21)-C(25)	1.409(6)	C(15)-C(11)-C(1)	126.9(2)
C(22)-C(23)	1.388(5)	C(12)-C(11)-C(1)	126.0(3)
C(23)-C(24)	1.383(5)	C(15)-C(11)-Fe	69.37(13)
C(24)-C(25)	1.417(6)	C(12)-C(11)-Fe	69.50(13)
C(25)-Fe-C(24)	41.0(2)	C(1)-C(11)-Fe	127.5(2)
C(25)-Fe-C(21)	40.7(2)	C(13)-C(12)-C(11)	108.5(2)
C(24)-Fe-C(21)	67.98(14)	C(13)-C(12)-Fe	69.61(13)
C(25)-Fe-C(22)	67.73(14)	C(11)-C(12)-Fe	69.56(13)
C(24)-Fe-C(22)	67.21(13)	C(14)-C(13)-C(12)	107.6(2)
C(21)-Fe-C(22)	39.80(14)	C(14)-C(13)-Fe	69.49(13)
C(25)-Fe-C(15)	107.82(12)	C(12)-C(13)-Fe	69.47(14)
C(24)-Fe-C(15)	124.16(13)	C(15)-C(14)-C(13)	108.1(2)
C(21)-Fe-C(15)	123.16(12)	C(15)-C(14)-Fe	69.51(13)
C(22)-Fe-C(15)	158.54(13)	C(13)-C(14)-Fe	69.77(14)
C(25)-Fe-C(14)	122.87(14)	C(14)-C(15)-C(11)	108.6(2)
C(24)-Fe-C(14)	108.10(12)	C(14)-C(15)-Fe	69.70(13)
C(21)-Fe-C(14)	159.18(14)	C(11)-C(15)-Fe	69.74(13)
C(22)-Fe-C(14)	159.42(13)	C(22)-C(21)-C(25)	108.1(3)
C(15)-Fe-C(14)	40.79(10)	C(22)-C(21)-Fe	70.2(2)
C(25)-Fe-C(12)	159.2(2)	C(25)-C(21)-Fe	69.4(2)
C(24)-Fe-C(12)	158.0(2)	C(21)-C(22)-C(23)	108.7(3)
C(21)-Fe-C(12)	122.90(14)	C(21)-C(22)-Fe	70.0(2)
C(22)-Fe-C(12)	107.77(12)	C(23)-C(22)-Fe	70.4(2)
C(15)-Fe-C(12)	68.49(10)	C(24)-C(23)-C(22)	108.4(3)
C(14)-Fe-C(12)	68.59(10)	C(24)-C(23)-Fe	69.6(2)
C(25)-Fe-C(23)	67.78(14)	C(22)-C(23)-Fe	69.7(2)
C(24)-Fe-C(23)	39.7(2)	C(23)-C(24)-C(25)	108.0(3)
C(21)-Fe-C(23)	67.18(13)	C(23)-C(24)-Fe	70.6(2)
C(22)-Fe-C(23)	39.86(14)	C(25)-C(24)-Fe	69.3(2)
C(15)-Fe-C(23)	159.94(13)	C(21)-C(25)-C(24)	106.8(3)
C(14)-Fe-C(23)	123.77(12)	C(21)-C(25)-Fe	69.9(2)
C(12)-Fe-C(23)	122.70(13)	C(24)-C(25)-Fe	69.7(2)
C(25)-Fe-C(11)	122.9(2)		

Table A.39: *Anisotropic displacement parameters ($Å^2$) for **24**. The anisotropic displacement factor exponent takes the form: $-2\pi^2(h^2a^{*2}U11 + ... + 2hka^*b^*U12)$.*

	U11	U22	U33	U23	U13	U12
Fe	0.0257(2)	0.0194(2)	0.0203(2)	0.0012(1)	0.0062(1)	-0.0006(1)
P	0.0451(5)	0.0550(5)	0.0540(5)	0.0098(4)	0.0059(4)	0.0201(4)
C(1)	0.0368(14)	0.046(2)	0.050(2)	0.0139(13)	0.0199(13)	0.0106(12)
C(11)	0.0280(11)	0.0260(11)	0.0278(11)	0.0047(9)	0.0080(9)	0.0043(9)
C(12)	0.0305(12)	0.0322(12)	0.0206(10)	-0.0009(9)	0.0002(9)	0.0000(9)
C(13)	0.0345(13)	0.0322(11)	0.0219(11)	0.0050(9)	0.0102(9)	0.0075(10)
C(14)	0.0273(11)	0.0277(11)	0.0303(12)	0.0099(9)	0.0052(10)	-0.0024(9)
C(15)	0.0365(13)	0.0200(10)	0.0270(12)	0.0006(8)	0.0069(10)	0.0009(9)
C(21)	0.061(2)	0.047(2)	0.075(2)	0.033(2)	0.047(2)	0.017(2)
C(22)	0.054(2)	0.0295(13)	0.054(2)	0.0095(13)	0.0065(15)	-0.0114(13)
C(23)	0.065(2)	0.0337(14)	0.053(2)	0.0194(13)	0.031(2)	0.0180(14)
C(24)	0.043(2)	0.065(2)	0.052(2)	0.040(2)	-0.0054(15)	-0.009(2)
C(25)	0.148(4)	0.0328(15)	0.0231(14)	0.0047(12)	0.029(2)	-0.006(2)

Table A.40: *Hydrogen coordinates and isotropic displacement parameters for **24**.*

	x	y	z	U(eq)
H(2A)	0.4000	-0.5000	0.6486	0.050
H(2B)	0.5400	-0.3990	0.6310	0.050
H(1A)	0.4303(2)	-0.1052(4)	0.5337(3)	0.051
H(1B)	0.3817(2)	-0.2595(4)	0.4300(3)	0.051
H(12)	0.3141(2)	0.0179(3)	0.6874(2)	0.035
H(13)	0.1225(2)	0.0154(3)	0.6542(2)	0.035
H(14)	0.0421(2)	-0.2066(3)	0.4716(2)	0.035
H(15)	0.1830(2)	-0.3397(3)	0.3923(2)	0.034
H(21)	0.3182(3)	0.1174(4)	0.3026(4)	0.067
H(22)	0.2830(3)	0.3329(4)	0.4629(3)	0.057
H(23)	0.0950(3)	0.3363(4)	0.4315(3)	0.057
H(24)	0.0115(3)	0.1182(5)	0.2540(4)	0.069
H(25)	0.1500(4)	-0.0219(4)	0.1718(3)	0.081

Table A.41: *Atomic coordinates and equivalent isotropic displacement parameters for **27**. U(eq) is defined as one third of the trace of the orthogonalised Uij tensor.*

	x	y	z	U(eq)
Mo	0.7357(1)	0.7172(1)	-0.0018(1)	0.031(1)
P	0.6000(1)	0.6570(1)	0.1791(1)	0.035(1)
C(2)	0.4884(6)	0.7648(4)	-0.0862(4)	0.043(1)
C(3)	0.6982(5)	0.5372(4)	-0.0637(4)	0.043(1)
C(6)	0.8483(6)	0.7709(5)	-0.1438(4)	0.055(1)
C(5)	0.7685(6)	0.8980(4)	0.0699(4)	0.046(1)
O(5)	0.7833(5)	0.9964(3)	0.1126(3)	0.069(1)

Table A.41 continued

O(4)	1.1197(4)	0.6227(4)	0.1140(3)	0.072(1)
O(3)	0.6813(5)	0.4346(4)	-0.0981(3)	0.068(1)
O(2)	0.3517(4)	0.7893(4)	-0.1375(3)	0.068(1)
O(6)	0.9117(6)	0.8000(5)	-0.2257(3)	0.095(2)
C(4)	0.9830(5)	0.6601(4)	0.0749(4)	0.043(1)
Fe	0.7409(1)	0.4198(1)	0.5311(1)	0.023(1)
C(11)	0.6474(4)	0.5459(3)	0.4020(3)	0.027(1)
C(25)	0.9993(4)	0.4131(4)	0.6114(3)	0.037(1)
C(1)	0.7416(4)	0.5763(3)	0.2981(3)	0.030(1)
C(14)	0.5626(4)	0.5487(4)	0.5878(3)	0.033(1)
C(12)	0.5203(4)	0.4450(3)	0.4114(3)	0.029(1)
C(21)	0.9905(5)	0.3694(4)	0.4958(4)	0.038(1)
C(13)	0.4696(4)	0.4471(3)	0.5262(3)	0.032(1)
C(15)	0.6713(4)	0.6105(3)	0.5122(3)	0.029(1)
C(24)	0.8844(5)	0.3331(4)	0.6704(3)	0.039(1)
C(23)	0.8072(5)	0.2411(4)	0.5901(4)	0.042(1)
C(22)	0.8731(5)	0.2642(4)	0.4823(4)	0.042(1)

Table A.42: *Bond lengths (Å) and angles (°) for 27.*

Mo-C(6)	2.007(4)	C(24)-Fe-C(13)	120.91(14)
Mo-C(3)	2.019(4)	C(12)-Fe-C(13)	40.70(15)
Mo-C(4)	2.043(4)	C(22)-Fe-C(25)	68.27(16)
Mo-C(2)	2.048(4)	C(23)-Fe-C(25)	68.63(16)
Mo-C(5)	2.063(5)	C(21)-Fe-C(25)	40.33(16)
Mo-P	2.5056(10)	C(24)-Fe-C(25)	40.97(15)
P-C(1)	1.836(3)	C(12)-Fe-C(25)	163.20(13)
C(2)-O(2)	1.148(5)	C(13)-Fe-C(25)	154.25(16)
C(3)-O(3)	1.143(5)	C(22)-Fe-C(11)	116.84(16)
C(6)-O(6)	1.148(5)	C(23)-Fe-C(11)	152.20(16)
C(5)-O(5)	1.140(6)	C(21)-Fe-C(11)	105.31(15)
O(4)-C(4)	1.137(5)	C(24)-Fe-C(11)	164.25(15)
Fe-C(22)	2.017(4)	C(12)-Fe-C(11)	41.02(13)
Fe-C(23)	2.027(4)	C(13)-Fe-C(11)	68.75(13)
Fe-C(21)	2.027(4)	C(25)-Fe-C(11)	125.07(15)
Fe-C(24)	2.036(3)	C(22)-Fe-C(14)	167.06(16)
Fe-C(12)	2.040(3)	C(23)-Fe-C(14)	129.66(16)
Fe-C(13)	2.043(3)	C(21)-Fe-C(14)	151.86(16)
Fe-C(25)	2.044(3)	C(24)-Fe-C(14)	110.00(15)
Fe-C(11)	2.048(3)	C(12)-Fe-C(14)	68.13(14)
Fe-C(14)	2.055(3)	C(13)-Fe-C(14)	40.34(14)
Fe-C(15)	2.063(3)	C(25)-Fe-C(14)	119.54(15)
C(11)-C(15)	1.431(5)	C(11)-Fe-C(14)	68.39(14)
C(11)-C(12)	1.432(5)	C(22)-Fe-C(15)	150.93(16)
C(11)-C(1)	1.494(4)	C(23)-Fe-C(15)	166.51(17)
C(25)-C(21)	1.403(6)	C(21)-Fe-C(15)	117.15(16)
C(25)-C(24)	1.427(5)	C(24)-Fe-C(15)	128.01(16)
C(14)-C(13)	1.413(5)	C(12)-Fe-C(15)	68.28(13)
C(14)-C(15)	1.416(5)	C(13)-Fe-C(15)	67.97(13)
C(12)-C(13)	1.420(5)	C(25)-Fe-C(15)	107.12(15)
C(21)-C(22)	1.403(6)	C(11)-Fe-C(15)	40.74(14)
C(24)-C(23)	1.409(6)	C(14)-Fe-C(15)	40.22(14)

Table A.42 continued

C(23)-C(22)	1.411(6)	C(15)-C(11)-C(12)	107.1(3)
C(6)-Mo-C(3)	91.49(19)	C(15)-C(11)-C(1)	126.2(3)
C(6)-Mo-C(4)	89.38(18)	C(12)-C(11)-C(1)	126.7(3)
C(3)-Mo-C(4)	87.82(17)	C(15)-C(11)-Fe	70.19(18)
C(6)-Mo-C(2)	89.25(18)	C(12)-C(11)-Fe	69.20(18)
C(3)-Mo-C(2)	88.73(17)	C(1)-C(11)-Fe	124.5(2)
C(4)-Mo-C(2)	176.26(18)	C(21)-C(25)-C(24)	107.4(4)
C(6)-Mo-C(5)	91.71(19)	C(21)-C(25)-Fe	69.22(19)
C(3)-Mo-C(5)	176.80(18)	C(24)-C(25)-Fe	69.22(19)
C(4)-Mo-C(5)	92.01(17)	C(11)-C(1)-P	114.3(2)
C(2)-Mo-C(5)	91.51(17)	C(13)-C(14)-C(15)	108.5(3)
C(6)-Mo-P	177.98(15)	C(13)-C(14)-Fe	69.39(19)
C(3)-Mo-P	90.44(12)	C(15)-C(14)-Fe	70.20(19)
C(4)-Mo-P	90.09(13)	C(13)-C(12)-C(11)	108.2(3)
C(2)-Mo-P	91.39(12)	C(13)-C(12)-Fe	69.77(18)
C(5)-Mo-P	86.36(12)	C(11)-C(12)-Fe	69.79(17)
C(1)-P-Mo	118.84(11)	C(22)-C(21)-C(25)	108.6(4)
O(2)-C(2)-Mo	177.3(4)	C(22)-C(21)-Fe	69.3(2)
O(3)-C(3)-Mo	178.4(4)	C(25)-C(21)-Fe	70.5(2)
O(6)-C(6)-Mo	179.0(5)	C(14)-C(13)-C(12)	108.1(3)
O(5)-C(5)-Mo	177.6(4)	C(14)-C(13)-Fe	70.27(18)
O(4)-C(4)-Mo	176.4(4)	C(12)-C(13)-Fe	69.54(17)
C(22)-Fe-C(23)	40.84(18)	C(14)-C(15)-C(11)	108.2(3)
C(22)-Fe-C(21)	40.60(17)	C(14)-C(15)-Fe	69.58(19)
C(23)-Fe-C(21)	68.51(16)	C(11)-C(15)-Fe	69.07(19)
C(22)-Fe-C(24)	68.37(17)	C(23)-C(24)-C(25)	108.0(3)
C(23)-Fe-C(24)	40.60(17)	C(23)-C(24)-Fe	69.4(2)
C(21)-Fe-C(24)	68.32(15)	C(25)-C(24)-Fe	69.8(2)
C(22)-Fe-C(12)	107.41(15)	C(24)-C(23)-C(22)	107.7(3)
C(23)-Fe-C(12)	119.48(15)	C(24)-C(23)-Fe	70.0(2)
C(21)-Fe-C(12)	126.01(16)	C(22)-C(23)-Fe	69.2(2)
C(24)-Fe-C(12)	154.24(15)	C(21)-C(22)-C(23)	108.4(4)
C(22)-Fe-C(13)	128.53(15)	C(21)-C(22)-Fe	70.1(2)
C(23)-Fe-C(13)	109.92(14)	C(23)-C(22)-Fe	70.0(2)
C(21)-Fe-C(13)	164.99(15)		

Table A.43: *Anisotropic displacement parameters ($Å^2$) for 27. The anisotropic displacement factor exponent takes the form: $-2\pi^2(h^2a^{*2}U11 + ... + 2hka^*b^*U12)$.*

	U11	U22	U33	U23	U13	U12
Mo	0.0335(2)	0.0369(2)	0.0238(1)	0.0035(1)	0.0033(1)	-0.0005(1)
P	0.0322(4)	0.0437(5)	0.0281(5)	0.0109(4)	0.0042(4)	0.0106(4)
C(2)	0.052(2)	0.038(2)	0.039(2)	0.0068(17)	-0.0017(19)	-0.0039(18)
C(3)	0.045(2)	0.052(3)	0.032(2)	-0.0028(18)	0.0117(16)	-0.0028(19)
C(6)	0.053(2)	0.077(3)	0.034(2)	0.008(2)	0.0061(18)	-0.016(2)
C(5)	0.053(2)	0.043(3)	0.041(2)	0.0104(17)	0.0026(18)	-0.0014(19)
O(5)	0.101(3)	0.0369(18)	0.066(2)	-0.0001(16)	-0.0037(19)	-0.0027(18)
O(4)	0.0427(16)	0.097(3)	0.072(3)	-0.038(2)	-0.0135(16)	0.0227(18)
O(3)	0.086(2)	0.059(2)	0.061(2)	-0.0230(19)	0.0230(17)	-0.0140(19)
O(2)	0.059(2)	0.070(2)	0.069(2)	0.0190(19)	-0.0203(17)	0.0087(17)

Table A.43 continued

O(6)	0.090(3)	0.146(4)	0.053(2)	0.020(3)	0.032(2)	-0.026(3)
C(4)	0.040(2)	0.053(2)	0.038(2)	-0.0139(18)	0.0048(17)	0.0024(18)
Fe	0.0214(2)	0.0213(2)	0.0251(2)	0.0030(2)	0.0030(2)	0.0023(2)
C(11)	0.0242(14)	0.0250(16)	0.0302(17)	0.0062(13)	-0.0001(12)	0.0028(12)
C(25)	0.0260(15)	0.0345(19)	0.048(2)	0.0064(19)	-0.0097(14)	0.0052(15)
C(1)	0.0254(15)	0.0334(17)	0.0291(17)	0.0055(14)	0.0013(13)	-0.0001(13)
C(14)	0.0322(17)	0.0346(18)	0.0339(19)	0.0006(15)	0.0062(14)	0.0106(15)
C(12)	0.0217(14)	0.0281(19)	0.0346(18)	0.0016(13)	-0.0014(13)	-0.0003(13)
C(21)	0.0256(15)	0.051(2)	0.040(2)	0.0114(17)	0.0083(14)	0.0111(16)
C(13)	0.0224(15)	0.031(2)	0.043(2)	0.0093(14)	0.0065(13)	0.0016(13)
C(15)	0.0299(16)	0.0197(15)	0.0361(19)	-0.0005(13)	-0.0002(13)	0.0035(13)
C(24)	0.0411(19)	0.045(2)	0.0318(19)	0.0158(16)	0.0046(15)	0.0156(17)
C(23)	0.0343(17)	0.026(2)	0.064(3)	0.0135(17)	0.0049(16)	0.0034(15)
C(22)	0.0390(19)	0.039(2)	0.047(2)	-0.0097(17)	0.0009(16)	0.0175(16)

Table A.44: *Hydrogen coordinates and isotropic displacement parameters for 27.*

	x	y	z	U(eq)
H(2A)	0.4713	0.5808	0.1800	0.050
H(2B)	0.5250	0.7359	0.2400	0.050
H(25)	1.0681	0.4824	0.6439	0.045
H(1A)	0.7872	0.4964	0.2680	0.035
H(1B)	0.8455	0.6310	0.3231	0.035
H(14)	0.5539	0.5714	0.6659	0.040
H(12)	0.4777	0.3874	0.3518	0.034
H(21)	1.0527	0.4046	0.4371	0.046
H(13)	0.3884	0.3908	0.5561	0.038
H(15)	0.7461	0.6817	0.5311	0.035
H(24)	0.8639	0.3405	0.7490	0.047
H(23)	0.7264	0.1762	0.6056	0.050
H(22)	0.8435	0.2171	0.4133	0.050

Table A.45: *Atomic coordinates and equivalent isotropic displacement parameters for 28. U(eq) is defined as one third of the trace of the orthogonalised Uij tensor.*

	x	y	z	U(eq)
Fe	0.1868(1)	0.0159(1)	0.4348(1)	0.022(1)
P	0.4611(1)	-0.3842(1)	0.6411(1)	0.053(1)
C(1)	0.3897(2)	-0.2161(4)	0.5210(3)	0.043(1)
C(11)	0.2866(2)	-0.1749(3)	0.5335(2)	0.027(1)
C(12)	0.2651(2)	-0.0526(3)	0.6249(2)	0.029(1)
C(13)	0.1577(2)	-0.0541(3)	0.6066(2)	0.029(1)
C(14)	0.1128(2)	-0.1782(3)	0.5045(2)	0.029(1)
C(15)	0.1918(2)	-0.2526(3)	0.4599(2)	0.028(1)
C(21)	0.2530(3)	0.1432(4)	0.3123(4)	0.056(1)
C(22)	0.2333(3)	0.2631(4)	0.4007(3)	0.048(1)
C(23)	0.1289(3)	0.2646(4)	0.3837(3)	0.048(1)
C(24)	0.0825(3)	0.1440(5)	0.2853(4)	0.058(1)
C(25)	0.1595(4)	0.0658(4)	0.2391(3)	0.067(1)

Table A.46: *Bond lengths (Å) and angles (°) for* **28**.

Fe-C(25)	2.022(3)	C(24)-Fe-C(11)	160.1(2)
Fe-C(24)	2.028(3)	C(21)-Fe-C(11)	107.35(12)
Fe-C(21)	2.030(3)	C(22)-Fe-C(11)	122.43(12)
Fe-C(22)	2.032(3)	C(15)-Fe-C(11)	40.89(10)
Fe-C(15)	2.036(2)	C(14)-Fe-C(11)	68.98(10)
Fe-C(14)	2.038(2)	C(12)-Fe-C(11)	40.94(10)
Fe-C(12)	2.040(2)	C(23)-Fe-C(11)	158.14(13)
Fe-C(23)	2.041(3)	C(25)-Fe-C(13)	158.6(2)
Fe-C(11)	2.041(2)	C(24)-Fe-C(13)	122.34(14)
Fe-C(13)	2.042(2)	C(21)-Fe-C(13)	158.9(2)
P-C(1)	1.850(3)	C(22)-Fe-C(13)	123.29(13)
C(1)-C(11)	1.492(4)	C(15)-Fe-C(13)	68.65(10)
C(11)-C(15)	1.424(4)	C(14)-Fe-C(13)	40.75(10)
C(11)-C(12)	1.427(3)	C(12)-Fe-C(13)	40.93(10)
C(12)-C(13)	1.427(4)	C(23)-Fe-C(13)	107.89(11)
C(13)-C(14)	1.421(4)	C(11)-Fe-C(13)	69.14(10)
C(14)-C(15)	1.420(4)	C(11)-C(1)-P	113.7(2)
C(21)-C(22)	1.382(5)	C(15)-C(11)-C(12)	107.1(2)
C(21)-C(25)	1.409(6)	C(15)-C(11)-C(1)	126.9(2)
C(22)-C(23)	1.388(5)	C(12)-C(11)-C(1)	126.0(3)
C(23)-C(24)	1.383(5)	C(15)-C(11)-Fe	69.37(13)
C(24)-C(25)	1.417(6)	C(12)-C(11)-Fe	69.50(13)
C(25)-Fe-C(24)	41.0(2)	C(1)-C(11)-Fe	127.5(2)
C(25)-Fe-C(21)	40.7(2)	C(13)-C(12)-C(11)	108.5(2)
C(24)-Fe-C(21)	67.98(14)	C(13)-C(12)-Fe	69.61(13)
C(25)-Fe-C(22)	67.73(14)	C(11)-C(12)-Fe	69.56(13)
C(24)-Fe-C(22)	67.21(13)	C(14)-C(13)-C(12)	107.6(2)
C(21)-Fe-C(22)	39.80(14)	C(14)-C(13)-Fe	69.49(13)
C(25)-Fe-C(15)	107.82(12)	C(12)-C(13)-Fe	69.47(14)
C(24)-Fe-C(15)	124.16(13)	C(15)-C(14)-C(13)	108.1(2)
C(21)-Fe-C(15)	123.16(12)	C(15)-C(14)-Fe	69.51(13)
C(22)-Fe-C(15)	158.54(13)	C(13)-C(14)-Fe	69.77(14)
C(25)-Fe-C(14)	122.87(14)	C(14)-C(15)-C(11)	108.6(2)
C(24)-Fe-C(14)	108.10(12)	C(14)-C(15)-Fe	69.70(13)
C(21)-Fe-C(14)	159.18(14)	C(11)-C(15)-Fe	69.74(13)
C(22)-Fe-C(14)	159.42(13)	C(22)-C(21)-C(25)	108.1(3)
C(15)-Fe-C(14)	40.79(10)	C(22)-C(21)-Fe	70.2(2)
C(25)-Fe-C(12)	159.2(2)	C(25)-C(21)-Fe	69.4(2)
C(24)-Fe-C(12)	158.0(2)	C(21)-C(22)-C(23)	108.7(3)
C(21)-Fe-C(12)	122.90(14)	C(21)-C(22)-Fe	70.0(2)
C(22)-Fe-C(12)	107.77(12)	C(23)-C(22)-Fe	70.4(2)
C(15)-Fe-C(12)	68.49(10)	C(24)-C(23)-C(22)	108.4(3)
C(14)-Fe-C(12)	68.59(10)	C(24)-C(23)-Fe	69.6(2)
C(25)-Fe-C(23)	67.78(14)	C(22)-C(23)-Fe	69.7(2)
C(24)-Fe-C(23)	39.7(2)	C(23)-C(24)-C(25)	108.0(3)
C(21)-Fe-C(23)	67.18(13)	C(23)-C(24)-Fe	70.6(2)
C(22)-Fe-C(23)	39.86(14)	C(25)-C(24)-Fe	69.3(2)
C(15)-Fe-C(23)	159.94(13)	C(21)-C(25)-C(24)	106.8(3)
C(14)-Fe-C(23)	123.77(12)	C(21)-C(25)-Fe	69.9(2)
C(12)-Fe-C(23)	122.70(13)	C(24)-C(25)-Fe	69.7(2)
C(25)-Fe-C(11)	122.9(2)		

Table A.47: *Anisotropic displacement parameters ($Å^2$) for* ***28****. The anisotropic displacement factor exponent takes the form: $-2\pi^2(h^2a^{*2}U11 + ... + 2hka^*b\ U12)$.*

	U11	U22	U33	U23	U13	U12
Fe	0.0257(2)	0.0194(2)	0.0203(2)	0.0012(1)	0.0062(1)	-0.0006(1)
P	0.0451(5)	0.0550(5)	0.0540(5)	0.0098(4)	0.0059(4)	0.0201(4)
C(1)	0.0368(14)	0.046(2)	0.050(2)	0.0139(13)	0.0199(13)	0.0106(12)
C(11)	0.0280(11)	0.0260(11)	0.0278(11)	0.0047(9)	0.0080(9)	0.0043(9)
C(12)	0.0305(12)	0.0322(12)	0.0206(10)	-0.0009(9)	0.0002(9)	0.0000(9)
C(13)	0.0345(13)	0.0322(11)	0.0219(11)	0.0050(9)	0.0102(9)	0.0075(10)
C(14)	0.0273(11)	0.0277(11)	0.0303(12)	0.0099(9)	0.0052(10)	-0.0024(9)
C(15)	0.0365(13)	0.0200(10)	0.0270(12)	0.0006(8)	0.0069(10)	0.0009(9)
C(21)	0.061(2)	0.047(2)	0.075(2)	0.033(2)	0.047(2)	0.017(2)
C(22)	0.054(2)	0.0295(13)	0.054(2)	0.0095(13)	0.0065(15)	-0.0114(13)
C(23)	0.065(2)	0.0337(14)	0.053(2)	0.0194(13)	0.031(2)	0.0180(14)
C(24)	0.043(2)	0.065(2)	0.052(2)	0.040(2)	-0.0054(15)	-0.009(2)
C(25)	0.148(4)	0.0328(15)	0.0231(14)	0.0047(12)	0.029(2)	-0.006(2)

Table A.48: *Hydrogen coordinates and isotropic displacement parameters for* ***28****.*

	x	y	z	U(eq)
H(2A)	0.4000	-0.5000	0.6486	0.050
H(2B)	0.5400	-0.3990	0.6310	0.050
H(1A)	0.4303(2)	-0.1052(4)	0.5337(3)	0.051
H(1B)	0.3817(2)	-0.2595(4)	0.4300(3)	0.051
H(12)	0.3141(2)	0.0179(3)	0.6874(2)	0.035
H(13)	0.1225(2)	0.0154(3)	0.6542(2)	0.035
H(14)	0.0421(2)	-0.2066(3)	0.4716(2)	0.035
H(15)	0.1830(2)	-0.3397(3)	0.3923(2)	0.034
H(21)	0.3182(3)	0.1174(4)	0.3026(4)	0.067
H(22)	0.2830(3)	0.3329(4)	0.4629(3)	0.057
H(23)	0.0950(3)	0.3363(4)	0.4315(3)	0.057
H(24)	0.0115(3)	0.1182(5)	0.2540(4)	0.069
H(25)	0.1500(4)	-0.0219(4)	0.1718(3)	0.081

Table A.49: *Atomic coordinates and equivalent isotropic displacement parameters for* ***30****. U(eq) is defined as one third of the trace of the orthogonalised Uij tensor.*

	x	y	z	U(eq)
Ru(1)	0.1325(1)	0.2168(1)	0.2915(1)	0.023(1)
Ru(2)	0.2398(1)	0.1964(1)	0.4516(1)	0.024(1)
Ru(3)	0.3604(1)	0.0760(1)	0.3349(1)	0.026(1)
Fe(1)	0.6107(1)	0.3495(1)	0.1200(1)	0.026(1)
P(1)	0.3476(1)	0.2269(1)	0.3301(1)	0.022(1)
C(1)	0.1385(4)	0.2198(2)	0.1745(2)	0.033(1)
O(1)	0.1436(3)	0.2213(2)	0.1062(2)	0.054(1)
C(2)	0.0663(3)	0.3384(2)	0.2913(2)	0.031(1)
O(2)	0.0287(3)	0.4114(2)	0.2913(2)	0.048(1)
C(3)	-0.0413(4)	0.1765(2)	0.3184(2)	0.039(1)
O(3)	-0.1423(3)	0.1552(2)	0.3354(2)	0.064(1)
C(4)	0.1722(4)	0.3126(2)	0.4730(2)	0.034(1)

Table A.49 continued

O(4)	0.1336(3)	0.3824(2)	0.4869(2)	0.054(1)
C(5)	0.0951(4)	0.1370(2)	0.5009(2)	0.042(1)
O(5)	0.0125(4)	0.0999(2)	0.5271(2)	0.071(1)
C(6)	0.3701(4)	0.1798(3)	0.5367(2)	0.042(1)
O(6)	0.4464(4)	0.1707(2)	0.5882(2)	0.074(1)
C(7)	0.2988(4)	-0.0394(2)	0.3554(2)	0.041(1)
O(7)	0.2564(3)	-0.1024(2)	0.3672(2)	0.061(1)
C(8)	0.5373(4)	0.0490(2)	0.3818(2)	0.038(1)
O(8)	0.6411(3)	0.0362(2)	0.4113(2)	0.061(1)
C(9)	0.4267(4)	0.0590(2)	0.2262(2)	0.035(1)
O(9)	0.4649(3)	0.0470(2)	0.1627(2)	0.053(1)
C(10)	0.4717(3)	0.2958(2)	0.2879(2)	0.028(1)
C(11)	0.4944(3)	0.2844(2)	0.1996(2)	0.024(1)
C(12)	0.4140(3)	0.3301(2)	0.1338(2)	0.031(1)
C(13)	0.4684(4)	0.2987(3)	0.0559(2)	0.037(1)
C(14)	0.5812(4)	0.2332(2)	0.0804(2)	0.039(1)
C(15)	0.5988(3)	0.2244(2)	0.1662(2)	0.032(1)
C(16)	0.6993(5)	0.4277(3)	0.1855(3)	0.057(1)
C(17)	0.6178(5)	0.4792(3)	0.1255(3)	0.060(1)
C(18)	0.6654(5)	0.4552(3)	0.0498(3)	0.057(1)
C(19)	0.7766(4)	0.3893(3)	0.0628(3)	0.057(1)
C(20)	0.7987(4)	0.3718(3)	0.1466(3)	0.057(1)
Ru(1)'	1.0616(1)	0.3345(1)	0.8589(1)	0.024(1)
Ru(2)'	1.1917(1)	0.1526(1)	0.8426(1)	0.026(1)
Ru(3)'	0.9119(1)	0.1853(1)	0.8853(1)	0.025(1)
Fe(1)'	0.7183(1)	0.3759(1)	0.5569(1)	0.025(1)
P(1)'	1.0164(1)	0.2367(1)	0.7701(1)	0.022(1)
C(1)'	0.9046(4)	0.4219(2)	0.8366(2)	0.034(1)
O(1)'	0.8079(3)	0.4710(2)	0.8273(2)	0.054(1)
C(2)'	1.1728(4)	0.3868(2)	0.7780(2)	0.038(1)
O(2)'	1.2373(3)	0.4121(2)	0.7261(2)	0.060(1)
C(3)'	1.1099(3)	0.3834(2)	0.9588(2)	0.031(1)
O(3)'	1.1324(3)	0.4118(2)	1.0159(2)	0.045(1)
C(4)'	1.3652(4)	0.1667(3)	0.7946(2)	0.043(1)
O(4)'	1.4693(3)	0.1728(2)	0.7684(2)	0.071(1)
C(5)'	1.2469(4)	0.0923(3)	0.9498(2)	0.044(1)
O(5)'	1.2756(4)	0.0542(2)	1.0103(2)	0.075(1)
C(6)'	1.1844(4)	0.0484(3)	0.7949(2)	0.043(1)
O(6)'	1.1813(4)	-0.0143(2)	0.7655(2)	0.073(1)
C(7)'	0.9280(4)	0.1312(2)	0.9981(2)	0.038(1)
O(7)'	0.9355(3)	0.0984(2)	1.0623(2)	0.062(1)
C(8)'	0.8679(4)	0.0843(3)	0.8434(2)	0.041(1)
O(8)'	0.8421(4)	0.0244(2)	0.8174(2)	0.066(1)
C(9)'	0.7289(4)	0.2477(3)	0.8799(2)	0.038(1)
O(9)'	0.6224(3)	0.2864(2)	0.8753(2)	0.061(1)
C(10)'	0.9621(3)	0.2623(2)	0.6632(2)	0.027(1)
C(11)'	0.8400(3)	0.3321(2)	0.6558(2)	0.026(1)
C(12)'	0.8403(4)	0.4236(2)	0.6335(2)	0.034(1)
C(13)'	0.7054(4)	0.4675(2)	0.6382(2)	0.043(1)
C(14)'	0.6210(4)	0.4045(3)	0.6638(2)	0.044(1)
C(15)'	0.7040(3)	0.3204(2)	0.6745(2)	0.033(1)
C(16)'	0.8052(4)	0.3186(3)	0.4591(2)	0.040(1)
C(17)'	0.7785(4)	0.4102(3)	0.4404(2)	0.040(1)
C(18)'	0.6378(4)	0.4369(2)	0.4493(2)	0.041(1)
C(19)'	0.5779(4)	0.3619(3)	0.4737(2)	0.041(1)
C(20)'	0.6812(4)	0.2886(2)	0.4790(2)	0.040(1)

Table A.50: *Bond lengths (Å) and angles (°) for* ***30****.*

Ru(1)-C(2)	1.894(3)	Ru(1)-C(1)	1.926(4)
Ru(1)-C(3)	1.959(4)	Ru(1)-P(1)	2.2828(9)
Ru(1)-Ru(2)	2.8379(5)	Ru(1)-Ru(3)	2.9311(5)
Ru(2)-C(4)	1.888(4)	Ru(2)-C(6)	1.904(4)
Ru(2)-C(5)	1.950(4)	Ru(2)-P(1)	2.2930(8)
Ru(2)-Ru(3)	2.9267(5)	Ru(2)-C(8)	1.907(4)
Ru(3)-C(9)	1.926(4)	Ru(3)-C(7)	1.976(4)
Ru(3)-P(1)	2.3153(9)	Fe(1)-C(16)	2.019(4)
Fe(1)-C(20)	2.024(4)	Fe(1)-C(11)	2.027(3)
Fe(1)-C(15)	2.030(3)	Fe(1)-C(19)	2.034(4)
Fe(1)-C(17)	2.035(4)	Fe(1)-C(12)	2.034(3)
Fe(1)-C(18)	2.045(4)	Fe(1)-C(14)	2.048(4)
Fe(1)-C(13)	2.049(3)	P(1)-C(10)	1.839(3)
C(1)-O(1)	1.124(4)	C(2)-O(2)	1.133(4)
C(3)-O(3)	1.129(4)	C(4)-O(4)	1.134(4)
C(5)-O(5)	1.130(4)	C(6)-O(6)	1.134(5)
C(7)-O(7)	1.122(4)	C(8)-O(8)	1.132(4)
C(9)-O(9)	1.130(4)	C(10)-C(11)	1.494(4)
C(11)-C(12)	1.419(4)	C(11)-C(15)	1.422(4)
C(12)-C(13)	1.425(5)	C(13)-C(14)	1.410(5)
C(14)-C(15)	1.420(5)	C(16)-C(17)	1.393(7)
C(16)-C(20)	1.399(6)	C(17)-C(18)	1.393(7)
C(18)-C(19)	1.386(7)	C(19)-C(20)	1.396(6)
Ru(1)'-C(2)'	1.914(4)	Ru(1)'-C(1)'	1.913(4)
Ru(1)'-C(3)'	1.984(3)	Ru(1)'-P(1)'	2.3168(8)
Ru(1)'-Ru(3)'	2.9377(5)	Ru(1)'-Ru(2)'	2.9463(6)
Ru(2)'-C(6)'	1.883(4)	Ru(2)'-C(4)'	1.920(4)
Ru(2)'-C(5)'	1.958(4)	Ru(2)'-P(1)'	2.2840(8)
Ru(2)'-Ru(3)'	2.8386(5)	Ru(3)'-C(8)'	1.892(4)
Ru(3)'-C(9)'	1.922(4)	Ru(3)'-C(7)'	1.958(4)
Ru(3)'-P(1)'	2.2778(8)	Fe(1)'-C(19)'	2.033(3)
Fe(1)'-C(16)'	2.034(3)	Fe(1)'-C(18)'	2.039(3)
Fe(1)'-C(20)'	2.041(3)	Fe(1)'-C(13)'	2.042(3)
Fe(1)'-C(17)'	2.043(3)	Fe(1)'-C(12)'	2.043(3)
Fe(1)'-C(11)'	2.045(3)	Fe(1)'-C(15)'	2.049(3)
Fe(1)'-C(14)'	2.048(3)	P(1)'-C(10)'	1.839(3)
C(1)'-O(1)'	1.130(4)	C(2)'-O(2)'	1.133(4)
C(2)'-O(3)'	1.122(4)	C(4)'-O(4)'	1.128(5)
C(5)'-O(5)'	1.124(4)	C(6)'-O(6)'	1.136(5)
C(7)'-O(7)'	1.124(4)	C(8)'-O(8)'	1.131(4)
C(9)'-O(9)'	1.132(4)	C(10)'-C(11)'	1.491(4)
C(11)'-C(15)'	1.418(5)	C(11)'-C(12)'	1.429(5)
C(12)'-C(13)'	1.411(5)	C(13)'-C(14)'	1.415(6)
C(14)'-C(15)'	1.425(5)	C(16)'-C(17)'	1.404(5)
C(16)'-C(20)'	1.408(5)	C(17)'-C(18)'	1.406(5)
C(18)'-C(19)'	1.409(6)	C(19)'-C(20)'	1.402(5)
C(2)-Ru(1)-C(1)	94.52(14)	C(2)-Ru(1)-C(3)	96.4(2)
C(1)-Ru(1)-C(3)	102.3(2)	C(2)-Ru(1)-P(1)	95.00(10)
C(1)-Ru(1)-P(1)	105.78(11)	C(3)-Ru(1)-P(1)	148.68(12)
C(2)-Ru(1)-Ru(2)	95.05(10)	C(1)-Ru(1)-Ru(2)	156.36(11)
C(3)-Ru(1)-Ru(2)	98.09(11)	P(1)-Ru(1)-Ru(2)	51.83(2)
C(2)-Ru(1)-Ru(3)	145.38(10)	C(1)-Ru(1)-Ru(3)	100.18(10)
C(3)-Ru(1)-Ru(3)	110.60(11)	P(1)-Ru(1)-Ru(3)	50.89(2)
Ru(2)-Ru(1)-Ru(3)	60.944(9)	C(4)-Ru(2)-C(6)	93.1(2)

Table A.50 continued

C(4)-Ru(2)-C(5)	99.7(2)	C(6)-Ru(2)-C(5)	102.5(2)
C(4)-Ru(2)-P(1)	98.58(10)	C(6)-Ru(2)-P(1)	108.54(12)
C(5)-Ru(2)-P(1)	142.82(11)	C(4)-Ru(2)-Ru(1)	94.74(11)
C(6)-Ru(2)-Ru(1)	159.50(12)	C(5)-Ru(2)-Ru(1)	94.85(12)
P(1)-Ru(2)-Ru(1)	51.51(2)	C(4)-Ru(2)-Ru(3)	148.36(10)
C(6)-Ru(2)-Ru(3)	103.96(12)	C(5)-Ru(2)-Ru(3)	102.28(10)
P(1)-Ru(2)-Ru(3)	50.91(2)	Ru(1)-Ru(2)-Ru(3)	61.100(11)
C(8)-Ru(3)-C(9)	93.6(2)	C(8)-Ru(3)-C(7)	100.6(2)
C(9)-Ru(3)-C(7)	95.2(2)	C(8)-Ru(3)-P(1)	95.29(11)
C(9)-Ru(3)-P(1)	99.56(10)	C(7)-Ru(3)-P(1)	157.54(11)
C(8)-Ru(3)-Ru(2)	97.01(11)	C(9)-Ru(3)-Ru(2)	148.68(10)
C(7)-Ru(3)-Ru(2)	111.53(12)	P(1)-Ru(3)-Ru(2)	50.24(2)
C(8)-Ru(3)-Ru(1)	144.64(11)	C(9)-Ru(3)-Ru(1)	97.91(10)
C(7)-Ru(3)-Ru(1)	111.42(11)	P(1)-Ru(3)-Ru(1)	49.91(2)
Ru(2)-Ru(3)-Ru(1)	57.956(11)	C(16)-Fe(1)-C(20)	40.5(2)
C(16)-Fe(1)-C(11)	106.3(2)	C(20)-Fe(1)-C(11)	123.5(2)
C(16)-Fe(1)-C(15)	119.9(2)	C(20)-Fe(1)-C(15)	106.7(2)
C(11)-Fe(1)-C(15)	41.05(12)	C(16)-Fe(1)-C(19)	67.6(2)
C(20)-Fe(1)-C(19)	40.3(2)	C(11)-Fe(1)-C(19)	161.0(2)
C(15)-Fe(1)-C(19)	124.9(2)	C(16)-Fe(1)-C(17)	40.2(2)
C(20)-Fe(1)-C(17)	67.5(2)	C(11)-Fe(1)-C(17)	120.8(2)
C(15)-Fe(1)-C(17)	155.5(2)	C(19)-Fe(1)-C(17)	67.0(2)
C(16)-Fe(1)-C(12)	124.4(2)	C(20)-Fe(1)-C(12)	160.9(2)
C(11)-Fe(1)-C(12)	40.91(13)	C(15)-Fe(1)-C(12)	68.68(14)
C(19)-Fe(1)-C(12)	157.3(2)	C(17)-Fe(1)-C(12)	108.6(2)
C(16)-Fe(1)-C(18)	67.5(2)	C(20)-Fe(1)-C(18)	67.4(2)
C(11)-Fe(1)-C(18)	156.5(2)	C(15)-Fe(1)-C(18)	162.0(2)
C(19)-Fe(1)-C(18)	39.7(2)	C(17)-Fe(1)-C(18)	39.9(2)
C(12)-Fe(1)-C(18)	122.5(2)	C(16)-Fe(1)-C(14)	155.8(2)
C(20)-Fe(1)-C(14)	121.3(2)	C(11)-Fe(1)-C(14)	68.62(13)
C(15)-Fe(1)-C(14)	40.74(14)	C(19)-Fe(1)-C(14)	109.1(2)
C(17)-Fe(1)-C(14)	162.7(2)	C(12)-Fe(1)-C(14)	68.10(14)
C(18)-Fe(1)-C(14)	126.4(2)	C(16)-Fe(1)-C(13)	162.0(2)
C(20)-Fe(1)-C(13)	156.5(2)	C(11)-Fe(1)-C(13)	68.97(13)
C(15)-Fe(1)-C(13)	68.6(2)	C(19)-Fe(1)-C(13)	122.3(2)
C(17)-Fe(1)-C(13)	126.2(2)	C(12)-Fe(1)-C(13)	40.87(13)
C(18)-Fe(1)-C(13)	109.6(2)	C(14)-Fe(1)-C(13)	40.3(2)
C(10)-P(1)-Ru(1)	132.06(11)	C(10)-P(1)-Ru(2)	138.82(10)
Ru(1)-P(1)-Ru(2)	76.66(3)	C(10)-P(1)-Ru(3)	128.64(11)
Ru(1)-P(1)-Ru(3)	79.20(3)	Ru(2)-P(1)-Ru(3)	78.85(3)
O(1)-C(1)-Ru(1)	179.2(3)	O(2)-C(2)-Ru(1)	178.9(3)
O(3)-C(3)-Ru(1)	177.9(3)	O(4)-C(4)-Ru(2)	178.6(3)
O(5)-C(5)-Ru(2)	177.0(3)	O(6)-C(6)-Ru(2)	179.0(4)
O(7)-C(7)-Ru(3)	176.0(3)	O(8)-C(8)-Ru(3)	177.0(3)
O(9)-C(9)-Ru(3)	178.3(3)	C(11)-C(10)-P(1)	109.5(2)
C(12)-C(11)-C(15)	107.6(3)	C(12)-C(11)-C(10)	126.3(3)
C(15)-C(11)-C(10)	126.2(3)	C(12)-C(11)-Fe(1)	69.8(2)
C(15)-C(11)-Fe(1)	69.6(2)	C(10)-C(11)-Fe(1)	127.0(2)
C(11)-C(12)-C(13)	108.5(3)	C(11)-C(12)-Fe(1)	69.3(2)
C(13)-C(12)-Fe(1)	70.2(2)	C(14)-C(13)-C(12)	107.4(3)
C(14)-C(13)-Fe(1)	69.8(2)	C(12)-C(13)-Fe(1)	69.0(2)
C(13)-C(14)-C(15)	108.7(3)	C(13)-C(14)-Fe(1)	69.9(2)
C(15)-C(14)-Fe(1)	68.9(2)	C(14)-C(15)-C(11)	107.9(3)
C(14)-C(15)-Fe(1)	70.3(2)	C(11)-C(15)-Fe(1)	69.4(2)
C(17)-C(16)-C(20)	107.8(4)	C(17)-C(16)-Fe(1)	70.5(2)
C(20)-C(16)-Fe(1)	70.0(2)	C(18)-C(17)-C(16)	108.3(4)
C(18)-C(17)-Fe(1)	70.4(2)	C(16)-C(17)-Fe(1)	69.3(2)

Table A.50 continued

C(19)-C(18)-C(17)	107.9(4)	C(19)-C(18)-Fe(1)	69.7(2)
C(17)-C(18)-Fe(1)	69.7(2)	C(18)-C(19)-C(20)	108.5(4)
C(18)-C(19)-Fe(1)	70.6(2)	C(20)-C(19)-Fe(1)	69.5(2)
C(19)-C(20)-C(16)	107.5(4)	C(19)-C(20)-Fe(1)	70.3(2)
C(16)-C(20)-Fe(1)	69.6(2)	C(2)'-Ru(1)'-C(1)'	94.5(2)
C(2)'-Ru(1)'-C(3)'	102.07(14)	C(1)'-Ru(1)'-C(3)'	94.17(14)
C(2)'-Ru(1)'-P(1)'	90.46(10)	C(1)'-Ru(1)'-P(1)'	98.09(10)
C(3)'-Ru(1)'-P(1)'	161.73(10)	C(2)'-Ru(1)'-Ru(3)'	139.85(10)
C(1)'-Ru(1)'-Ru(3)'	95.69(11)	C(3)'-Ru(1)'-Ru(3)'	115.73(9)
P(1)'-Ru(1)'-Ru(3)'	49.67(2)	C(2)'-Ru(1)'-Ru(2)'	95.06(11)
C(1)'-Ru(1)'-Ru(2)'	146.35(10)	C(3)'-Ru(1)'-Ru(2)'	115.12(10)
P(1)'-Ru(1)'-Ru(2)'	49.69(2)	Ru(3)'-Ru(1)'-Ru(2)'	57.688(14)
C(6)'-Ru(2)'-C(4)'	93.4(2)	C(6)'-Ru(2)'-C(5)'	94.5(2)
C(4)'-Ru(2)'-C(5)'	101.0(2)	C(6)'-Ru(2)'-P(1)'	96.30(12)
C(4)'-Ru(2)'-P(1)'	111.92(12)	C(5)'-Ru(2)'-P(1)'	144.52(12)
C(6)'-Ru(2)'-Ru(3)'	96.12(12)	C(4)'-Ru(2)'-Ru(3)'	161.62(12)
C(5)'-Ru(2)'-Ru(3)'	93.88(12)	P(1)'-Ru(2)'-Ru(3)'	51.42(2)
C(6)'-Ru(2)'-Ru(1)'	146.58(12)	C(4)'-Ru(2)'-Ru(1)'	103.28(12)
C(5)'-Ru(2)'-Ru(1)'	110.09(11)	P(1)'-Ru(2)'-Ru(1)'	50.67(2)
Ru(3)'-Ru(2)'-Ru(1)'	61.004(9)	C(8)'-Ru(3)'-C(9)'	94.7(2)
C(8)'-Ru(3)'-C(7)'	94.5(2)	C(9)'-Ru(3)'-C(7)'	103.5(2)
C(8)'-Ru(3)'-P(1)'	95.97(11)	C(9)'-Ru(3)'-P(1)'	105.30(10)
C(7)'-Ru(3)'-P(1)'	148.34(11)	C(8)'-Ru(3)'-Ru(2)'	95.20(12)
C(9)'-Ru(3)'-Ru(2)'	155.76(11)	C(7)'-Ru(3)'-Ru(2)'	97.73(11)
P(1)'-Ru(3)'-Ru(2)'	51.62(2)	C(8)'-Ru(3)'-Ru(1)'	146.31(11)
C(9)'-Ru(3)'-Ru(1)'	99.53(12)	C(7)'-Ru(3)'-Ru(1)'	111.40(10)
P(1)'-Ru(3)'-Ru(1)'	50.84(2)	Ru(2)'-Ru(3)'-Ru(1)'	61.308(12)
C(19)'-Fe(1)'-C(16)'	67.9(2)	C(19)'-Fe(1)'-C(18)'	40.5(2)
C(16)'-Fe(1)'-C(18)'	67.66(14)	C(19)'-Fe(1)'-C(20)'	40.3(2)
C(16)'-Fe(1)'-C(20)'	40.4(2)	C(18)'-Fe(1)'-C(20)'	67.7(2)
C(19)'-Fe(1)'-C(13)'	128.0(2)	C(16)'-Fe(1)'-C(13)'	151.8(2)
C(18)'-Fe(1)'-C(13)'	108.0(2)	C(20)'-Fe(1)'-C(13)'	166.1(2)
C(19)'-Fe(1)'-C(17)'	68.1(2)	C(16)'-Fe(1)'-C(17)'	40.3(2)
C(18)'-Fe(1)'-C(17)'	40.3(2)	C(20)'-Fe(1)'-C(17)'	67.9(2)
C(13)'-Fe(1)'-C(17)'	118.1(2)	C(19)'-Fe(1)'-C(12)'	165.1(2)
C(16)'-Fe(1)'-C(12)'	118.4(2)	C(18)'-Fe(1)'-C(12)'	127.1(2)
C(20)'-Fe(1)'-C(12)'	152.7(2)	C(13)'-Fe(1)'-C(12)'	40.4(2)
C(17)'-Fe(1)'-C(12)'	107.4(2)	C(19)'-Fe(1)'-C(11)'	153.0(2)
C(16)'-Fe(1)'-C(11)'	108.16(13)	C(18)'-Fe(1)'-C(11)'	165.0(2)
C(20)'-Fe(1)'-C(11)'	119.19(14)	C(13)'-Fe(1)'-C(11)'	68.44(13)
C(17)'-Fe(1)'-C(11)'	127.33(14)	C(12)'-Fe(1)'-C(11)'	40.93(13)
C(19)'-Fe(1)'-C(15)'	119.6(2)	C(16)'-Fe(1)'-C(15)'	128.3(2)
C(18)'-Fe(1)'-C(15)'	153.2(2)	C(20)'-Fe(1)'-C(15)'	109.1(2)
C(13)'-Fe(1)'-C(15)'	68.4(2)	C(17)'-Fe(1)'-C(15)'	165.44(14)
C(12)'-Fe(1)'-C(15)'	68.40(14)	C(11)'-Fe(1)'-C(15)'	40.53(13)
C(19)'-Fe(1)'-C(14)'	109.0(2)	C(16)'-Fe(1)'-C(14)'	166.5(2)
C(18)'-Fe(1)'-C(14)'	119.17(14)	C(20)'-Fe(1)'-C(14)'	128.9(2)
C(13)'-Fe(1)'-C(14)'	40.5(2)	C(17)'-Fe(1)'-C(14)'	152.2(2)
C(12)'-Fe(1)'-C(14)'	68.0(2)	C(11)'-Fe(1)'-C(14)'	68.25(13)
C(15)'-Fe(1)'-C(14)'	40.70(14)	C(10)'-P(1)'-Ru(3)'	132.97(11)
C(10)'-P(1)'-Ru(2)'	138.32(11)	Ru(3)'-P(1)'-Ru(2)'	76.96(3)
C(10)'-P(1)'-Ru(1)'	127.30(11)	Ru(3)'-P(1)'-Ru(1)'	79.48(3)
Ru(2)'-P(1)'-Ru(1)'	79.64(3)	O(1)'-C(1)'-Ru(1)'	175.7(3)
O(2)'-C(2)'-Ru(1)'	174.1(3)	O(3)'-C(3)'-Ru(1)'	177.5(3)
O(4)'-C(4)'-Ru(2)'	177.5(4)	O(5)'-C(5)'-Ru(2)'	176.4(4)
O(6)'-C(6)'-Ru(2)'	179.2(4)	O(7)'-C(7)'-Ru(3)'	178.1(3)
O(8)'-C(8)'-Ru(3)'	179.2(3)	O(9)'-C(9)'-Ru(3)'	178.0(3)

Table A.50 continued

C(11)'-C(10)'-P(1)'	110.8(2)	C(15)'-C(11)'-C(12)'	107.8(3)
C(15)'-C(11)'-C(10)'	126.1(3)	C(12)'-C(11)'-C(10)'	126.0(3)
C(15)'-C(11)'-Fe(1)'	69.9(2)	C(12)'-C(11)'-Fe(1)'	69.5(2)
C(10)'-C(11)'-Fe(1)'	129.0(2)	C(13)'-C(12)'-C(11)'	108.1(3)
C(13)'-C(12)'-Fe(1)'	69.8(2)	C(11)'-C(12)'-Fe(1)'	69.6(2)
C(12)'-C(13)'-C(14)'	108.2(3)	C(12)'-C(13)'-Fe(1)'	69.8(2)
C(14)'-C(13)'-Fe(1)'	70.0(2)	C(13)'-C(14)'-C(15)'	108.2(3)
C(13)'-C(14)'-Fe(1)'	69.5(2)	C(15)'-C(14)'-Fe(1)'	69.7(2)
C(11)'-C(15)'-C(14)'	107.8(3)	C(11)'-C(15)'-Fe(1)'	69.6(2)
C(14)'-C(15)'-Fe(1)'	69.6(2)	C(17)'-C(16)'-C(20)'	108.4(3)
C(17)'-C(16)'-Fe(1)'	70.2(2)	C(20)'-C(16)'-Fe(1)'	70.1(2)
C(16)'-C(17)'-C(18)'	107.6(3)	C(16)'-C(17)'-Fe(1)'	69.5(2)
C(18)'-C(17)'-Fe(1)'	69.7(2)	C(17)'-C(18)'-C(19)'	108.2(3)
C(17)'-C(18)'-Fe(1)'	70.0(2)	C(19)'-C(18)'-Fe(1)'	69.5(2)
C(20)'-C(19)'-C(18)'	107.9(3)	C(20)'-C(19)'-Fe(1)'	70.2(2)
C(18)'-C(19)'-Fe(1)'	70.0(2)	C(19)'-C(20)'-C(16)'	107.9(3)
C(19)'-C(20)'-Fe(1)'	69.6(2)	C(16)'-C(20)'-Fe(1)'	69.5(2)

Table A.51: *Anisotropic displacement parameters ($Å^2$) for **30**. The anisotropic displacement factor exponent takes the form: $-2\pi^2(h^2a^{*2}U11 + ... + 2hka^*b^*U12)$.*

	U11	U22	U33	U23	U13	U12
Ru(1)	0.024(1)	0.023(1)	0.023(1)	-0.003(1)	-0.002(1)	-0.004(1)
Ru(2)	0.026(1)	0.028(1)	0.019(1)	0.000(1)	0.003(1)	-0.005(1)
Ru(3)	0.027(1)	0.023(1)	0.027(1)	0.000(1)	0.001(1)	-0.003(1)
Fe(1)	0.024(1)	0.030(1)	0.025(1)	0.000(1)	0.003(1)	-0.007(1)
P(1)	0.024(1)	0.024(1)	0.018(1)	-0.001(1)	0.002(1)	-0.005(1)
C(1)	0.037(2)	0.030(2)	0.034(2)	-0.004(2)	-0.006(2)	-0.007(2)
O(1)	0.077(2)	0.066(2)	0.024(1)	-0.006(1)	-0.006(1)	-0.021(2)
C(2)	0.030(2)	0.033(2)	0.031(2)	-0.006(1)	-0.006(1)	-0.006(2)
O(2)	0.058(2)	0.028(2)	0.058(2)	-0.005(1)	-0.009(1)	-0.002(1)
C(3)	0.040(2)	0.035(2)	0.045(2)	-0.016(2)	0.005(2)	-0.010(2)
O(3)	0.045(2)	0.070(2)	0.087(2)	-0.036(2)	0.022(2)	-0.031(2)
C(4)	0.038(2)	0.037(2)	0.028(2)	0.000(2)	0.006(2)	-0.010(2)
O(4)	0.066(2)	0.034(2)	0.060(2)	-0.010(1)	0.010(2)	-0.005(1)
C(5)	0.054(2)	0.038(2)	0.037(2)	-0.013(2)	0.018(2)	-0.013(2)
O(5)	0.079(2)	0.060(2)	0.082(2)	-0.019(2)	0.048(2)	-0.038(2)
C(6)	0.045(2)	0.044(2)	0.034(2)	0.000(2)	-0.004(2)	-0.004(2)
O(6)	0.073(2)	0.088(3)	0.058(2)	0.002(2)	-0.035(2)	-0.007(2)
C(7)	0.038(2)	0.034(2)	0.050(2)	0.005(2)	-0.003(2)	-0.004(2)
O(7)	0.057(2)	0.035(2)	0.090(2)	0.008(2)	-0.001(2)	-0.015(1)
C(8)	0.035(2)	0.034(2)	0.041(2)	0.004(2)	0.000(2)	-0.006(2)
O(8)	0.038(2)	0.066(2)	0.074(2)	0.017(2)	-0.017(2)	-0.008(2)
C(9)	0.034(2)	0.027(2)	0.042(2)	-0.006(2)	-0.002(2)	-0.002(2)
O(9)	0.060(2)	0.060(2)	0.041(2)	-0.023(1)	0.015(1)	-0.011(2)
C(10)	0.033(2)	0.032(2)	0.022(2)	-0.005(1)	0.003(1)	-0.013(1)
C(11)	0.025(2)	0.025(2)	0.024(2)	-0.003(1)	0.005(1)	-0.010(1)
C(12)	0.023(2)	0.041(2)	0.030(2)	-0.002(2)	0.002(1)	-0.010(2)
C(13)	0.038(2)	0.054(2)	0.024(2)	-0.002(2)	-0.001(2)	-0.021(2)
C(14)	0.047(2)	0.039(2)	0.033(2)	-0.014(2)	0.016(2)	-0.014(2)

Table A.51 continued

C(15)	0.034(2)	0.026(2)	0.034(2)	-0.002(1)	0.007(2)	-0.004(1)
C(16)	0.080(3)	0.061(3)	0.043(2)	-0.012(2)	0.004(2)	-0.047(3)
C(17)	0.048(3)	0.029(2)	0.105(4)	-0.010(2)	0.011(3)	-0.013(2)
C(18)	0.060(3)	0.062(3)	0.052(3)	0.021(2)	-0.009(2)	-0.036(2)
C(19)	0.047(3)	0.075(3)	0.059(3)	-0.019(2)	0.023(2)	-0.034(2)
C(20)	0.036(2)	0.052(3)	0.086(4)	0.004(2)	-0.018(2)	-0.017(2)
Ru(1)'	0.029(1)	0.022(1)	0.021(1)	-0.003(1)	0.000(1)	-0.005(1)
Ru(2)'	0.029(1)	0.025(1)	0.022(1)	-0.002(1)	-0.004(1)	0.002(1)
Ru(3)'	0.030(1)	0.029(1)	0.018(1)	0.001(1)	-0.001(1)	-0.010(1)
Fe(1)'	0.027(1)	0.028(1)	0.018(1)	-0.002(1)	-0.003(1)	0.002(1)
P(1)'	0.026(1)	0.022(1)	0.017(1)	0.000(1)	-0.002(1)	-0.002(1)
C(1)'	0.046(2)	0.028(2)	0.025(2)	-0.007(1)	0.001(2)	-0.002(2)
O(1)'	0.063(2)	0.046(2)	0.044(2)	-0.010(1)	-0.004(1)	0.022(2)
C(2)'	0.050(2)	0.029(2)	0.039(2)	-0.009(2)	0.002(2)	-0.017(2)
O(2)'	0.081(2)	0.056(2)	0.052(2)	-0.009(1)	0.027(2)	-0.040(2)
C(3)'	0.033(2)	0.030(2)	0.031(2)	-0.001(2)	0.001(2)	-0.009(2)
O(3)'	0.057(2)	0.050(2)	0.034(1)	-0.012(1)	-0.007(1)	-0.019(1)
C(4)'	0.046(2)	0.047(2)	0.036(2)	-0.010(2)	0.000(2)	-0.004(2)
O(4)'	0.045(2)	0.104(3)	0.070(2)	-0.021(2)	0.021(2)	-0.020(2)
C(5)'	0.048(2)	0.044(2)	0.036(2)	-0.001(2)	-0.007(2)	0.004(2)
O(5)'	0.090(3)	0.081(2)	0.040(2)	0.018(2)	-0.021(2)	0.012(2)
C(6)'	0.051(2)	0.039(2)	0.036(2)	-0.007(2)	-0.001(2)	0.003(2)
O(6)'	0.109(3)	0.041(2)	0.072(2)	-0.028(2)	-0.001(2)	-0.006(2)
C(7)'	0.043(2)	0.044(2)	0.029(2)	0.000(2)	-0.006(2)	-0.017(2)
O(7)'	0.082(2)	0.076(2)	0.028(2)	0.022(1)	-0.007(1)	-0.028(2)
C(8)'	0.053(2)	0.045(2)	0.028(2)	0.003(2)	-0.006(2)	-0.021(2)
O(8)'	0.101(3)	0.052(2)	0.057(2)	-0.008(2)	-0.018(2)	-0.043(2)
C(9)'	0.036(2)	0.059(2)	0.022(2)	-0.003(2)	0.002(2)	-0.012(2)
O(9)'	0.034(2)	0.101(3)	0.040(2)	-0.004(2)	0.002(1)	0.005(2)
C(10)'	0.032(2)	0.031(2)	0.017(2)	-0.002(1)	-0.002(1)	-0.002(1)
C(11)'	0.032(2)	0.031(2)	0.014(1)	-0.001(1)	-0.003(1)	-0.003(1)
C(12)'	0.046(2)	0.029(2)	0.025(2)	-0.002(1)	-0.011(2)	-0.004(2)
C(13)'	0.065(3)	0.033(2)	0.028(2)	-0.011(2)	-0.011(2)	0.012(2)
C(14)'	0.038(2)	0.065(3)	0.020(2)	-0.007(2)	0.001(2)	0.019(2)
C(15)'	0.033(2)	0.046(2)	0.019(2)	0.003(1)	0.001(1)	-0.002(2)
C(16)'	0.040(2)	0.050(2)	0.026(2)	-0.012(2)	-0.004(2)	0.011(2)
C(17)'	0.046(2)	0.049(2)	0.023(2)	0.001(2)	0.004(2)	-0.004(2)
C(18)'	0.053(2)	0.041(2)	0.022(2)	-0.001(2)	-0.010(2)	0.014(2)
C(19)'	0.036(2)	0.056(2)	0.030(2)	-0.012(2)	-0.011(2)	0.001(2)
C(20)'	0.056(2)	0.035(2)	0.030(2)	-0.010(2)	-0.010(2)	-0.005(2)

Table A.52: *Hydrogen coordinates and isotropic displacement parameters for 30.*

	x	y	z	U(eq)
H(1)	0.1941	0.0982	0.2965	0.039(10)
H(2)	0.3029	0.0899	0.4367	0.071(14)
H(10A)	0.5562	0.2788	0.3166	0.034
H(10B)	0.4388	0.3563	0.2944	0.034
H(12)	0.3368	0.3751	0.1387	0.037
H(13)	0.4347	0.3188	0.0060	0.044
H(14)	0.6385	0.2014	0.0423	0.046
H(15)	0.6681	0.1846	0.1965	0.038
H(16)	0.6903	0.4307	0.2432	0.069
H(17)	0.5413	0.5233	0.1347	0.072
H(18)	0.6278	0.4798	-0.0023	0.069
H(19)	0.8291	0.3601	0.0212	0.069
H(20)	0.8698	0.3294	0.1724	0.069
H(3)	1.1887	0.2458	0.8927	0.045(10)
H(4)	0.9591	0.2736	0.9268	0.043(10)
H(10C)	0.9414	0.2102	0.6427	0.033
H(10D)	1.0349	0.2819	0.6309	0.033
H(12)'	0.9188	0.4503	0.6177	0.040
H(13)'	0.6757	0.5295	0.6259	0.052
H(14)'	0.5242	0.4161	0.6716	0.052
H(15)'	0.6737	0.2654	0.6910	0.040
H(16)'	0.8931	0.2828	0.4582	0.048
H(17)'	0.8441	0.4480	0.4247	0.048
H(18)'	0.5905	0.4961	0.4409	0.049
H(19)'	0.4829	0.3610	0.4844	0.049
H(20)'	0.6697	0.2288	0.4942	0.048

Appendix B

Synthesis of $FcCH(Me)P(CH_2OH)_2$ **32**

$FcCH(Me)NMe_2$ (*ca.* 0.1 g, 0.4 mmol) was dissolved in methanol (15 ml), and methyl iodide (1 ml, 16 mmol) added. The solution was heated on a steambath for 5 min before solvent was removed under vacuum. Methanol (20 ml) was then added, and the solution purged and placed under nitrogen. In another flask $[P(CH_2OH)_4]Cl$ (0.917 g, 3.85 mmol) was dissolved in methanol (20 ml), purged, and placed under nitrogen. KOH (0.209 g, 3.72 mmol) was added and the mixture stirred for *ca.* 45 min. This was then added dropwise to the first flask, and the mixture heated at 40° C overnight under nitrogen. Solvent was then removed under vacuum until the product had largely precipitated; at this point water (20 ml), diethyl ether (20 ml), and NEt_3 (10 ml) were added and the mixture stirred for 1 hr. The organic layer was removed, washed with sat. aq. soln. NaCl (10 ml) and water (2 × 10 ml), filtered, and the solvent removed under reduced pressure to give the crude product **32** as a yellow oil (*ca.* quantitative yield). Analysis by NMR showed this to be rather impure, and attempts at crystallisation were unsuccessful. $^{31}P-\{^1H\}$ NMR ($CDCl_3$): δ -2.9 (s).

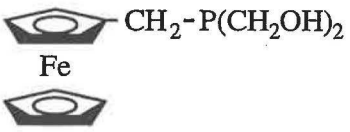

1

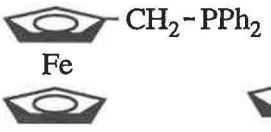

2

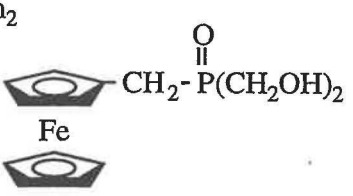

3

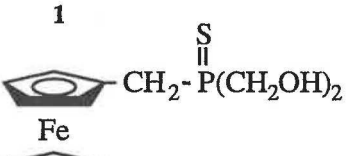

4

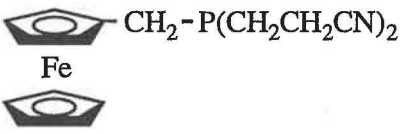

5

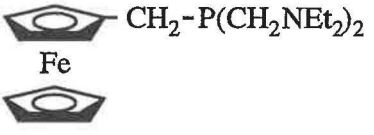

6

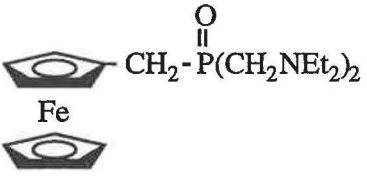

7

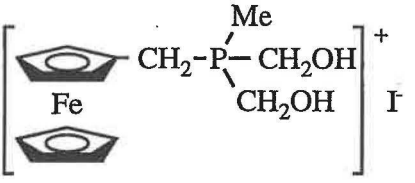

8

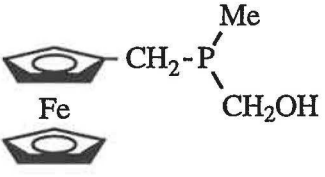

9

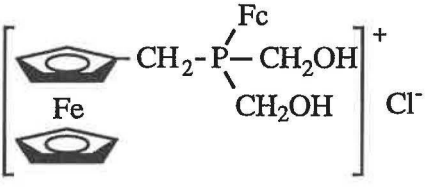

10

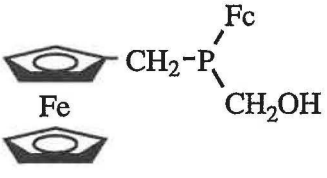

11

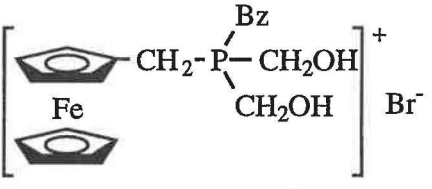

12

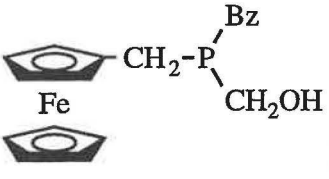

13

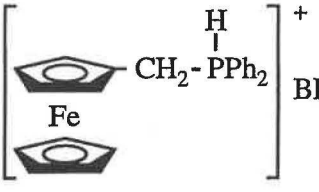

14

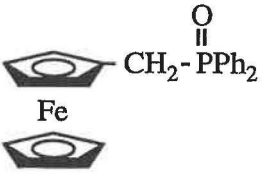

15

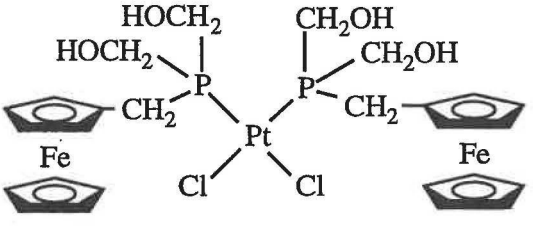

16

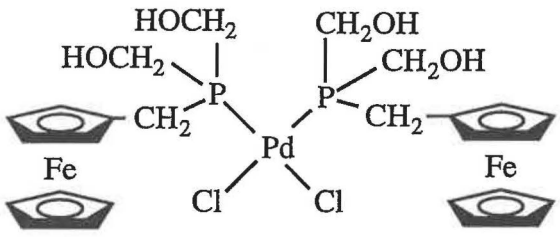

17

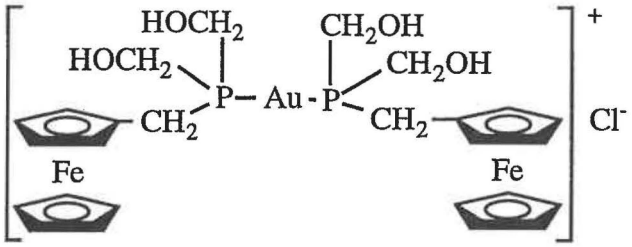

18

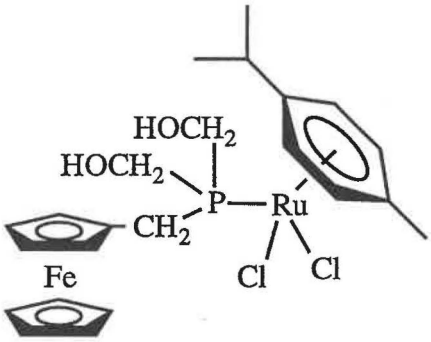

19

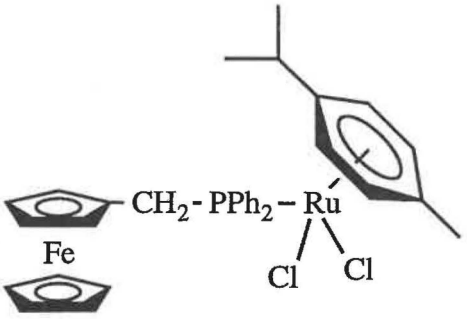

20

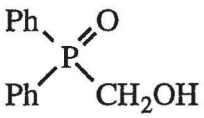

21

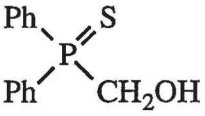

22

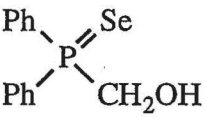

23

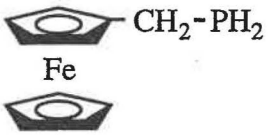

24

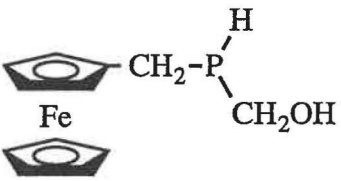

25

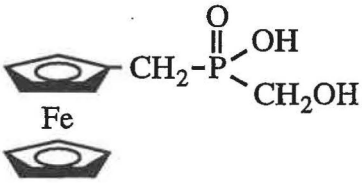

26

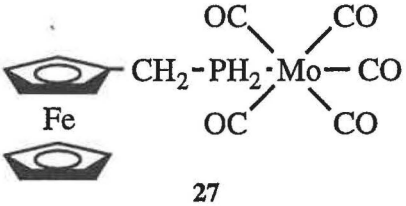

27

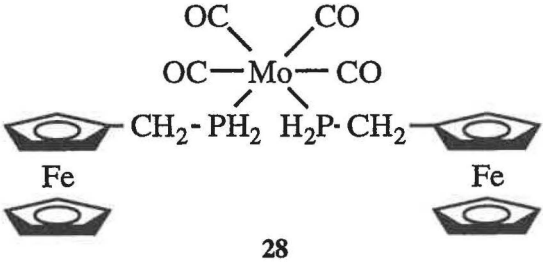

28

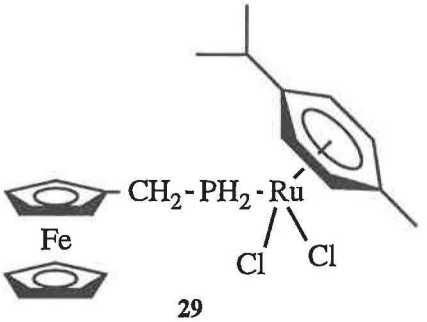

29

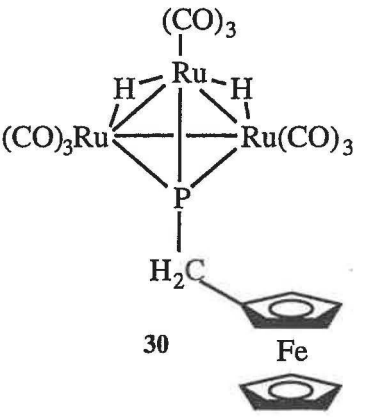

30

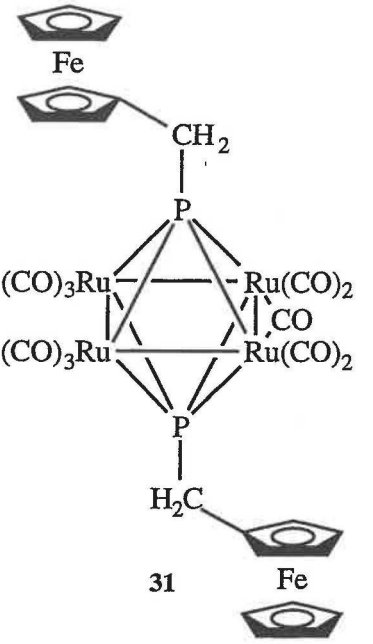

31

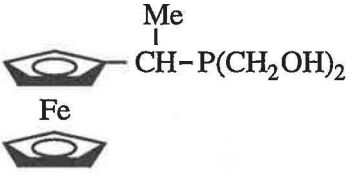

32

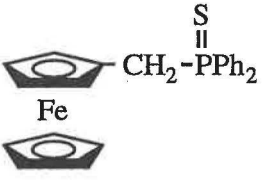

33

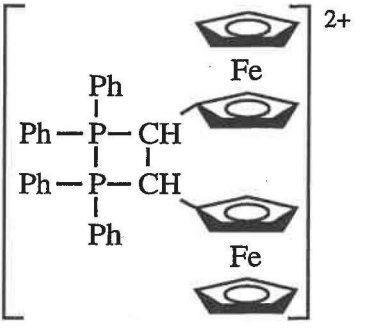

34

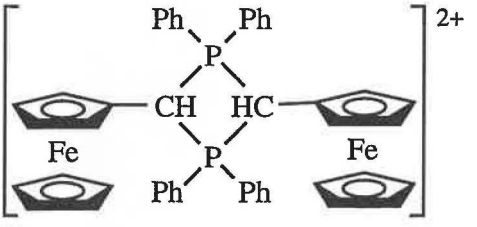

35